The Design and Synthesis of Heteroatom-Containing Small Molecules for the Chemotherapy of Infectious Diseases

by

XIAO LU

(Under the Direction of Timothy E Long)

ABSTRACT

Organic medicinal chemistry is the science dedicated to the development of new synthetic method and their potential usage in drug discovery. It is becoming increasingly clear that heteroatom chemistry plays an important role in lead discovery and modification. In Chapter 2 the preparation and spectral characteristics of olefins through thermal elimination is reported. The reaction of *o*-nitro phenyl sulfoxide precursor under toluene reflux is shown to proceed cleanly and quantitatively via a concerted mechanism; the ratio of *Z*- and *E*-isomers is altered depending on different α- or β- substitution groups. The use of sulfur chemistry in synthetic transformation is further investigated in Chapter 3. An asymmetrical method to synthesize β-lactams using photochemistry as the key in the synthetic steps has been developed. Photooxidation of L-cysteine thiazolidine hydroxamate esters afforded C-5 hydroxylated products which when cyclized and deprotected gave the corresponding 3*R*, 4*R* monocyclic β-lactam platforms. The investigation on a unique antimicrobial platform is next followed in Chapter 4. A group of phosphonium salts were made using atovaquone as lead compound to treat parasitic disease (i.e., malaria). Compound **28k** exhibited moderate in vitro antimalarial activity

(17 ± 4 nM) against chloroquine resistant (W2) *Plasmodium falciparum*. The results demonstrate the advantage of attaching a triphenylphosphonium-based mitochondriotropic group to increase subcellular concentration in the plasmodial mitochondria, within which the drug target is located. Preliminary toxicity and a structure-activity relationship studies of interested compounds are also included.

INDEX WORDS: Olefin
Asymmetrical synthesis
β-lactam antibacterials
Mitochondriotropic lipocations
Sulfoxide elimination
Photochemistry
Phosphonium salt

The Design and Synthesis of Heteroatom-Containing Small Molecules for the Chemotherapy of Infectious Diseases

by

XIAO LU

B.S. Peking University, China, 2005

M.S. Peking University, China, 2008

A Dissertation Submitted to the Graduate Faculty of The University of Georgia in Partial Fulfillment of the Requirements for the Degree

DOCTOR OF PHILOSOPHY

ATHENS, GEORGIA

2012

The Design and Synthesis of Heteroatom-Containing Small Molecules for the Chemotherapy of Infectious Diseases

by

XIAO LU

Major Professor:	Timothy E. Long
Committee:	James V. Bruckner
	Michael G. Bartlett
	Brian S. Cummings
	George F. Majetich

Electronic Version Approved:

Maureen Grasso
Dean of the Graduate School
The University of Georgia
August 2012

DEDICATION

This dissertation is dedicated with love and gratitude to my parents, Xianxiang Lu and Guikuan Sun.

ACKNOWLEDGEMENTS

I am grateful to many people in preparation of this dissertation. First I would like to thank my major advisor, Dr. Timothy E. Long from the bottom of my heart for his always great help, guidance and support during the past five years. I have obtained a vast number of experiences learning and working under his direction in the field of medicinal chemistry and organic chemistry.

I'm also very grateful to my very nice and wonderful committee members: Dr. James V. Bruckner, Dr. Michael G. Bartlett, Dr. Brian S. Cummings and Dr. George F. Majetich, for their knowledge and expertise. Special thanks go to Dr. Quincy Teng for help in NMR, Dr. Dennis Phillips for getting HRMS data. My appreciation also goes to Dr. Roberto Docampo's lab for their help in toxicity test, and Dr. Philip J. Rosenthal's lab for their help in activity test.

I want to recognize many students, faculty, and staff of the School of Pharmacy and particularly: Dr. Shelley B. Hooks, Mary Eubanks, Joy Wilson and Demetrius Smith. I would also like to thank other faculty members and staff I have worked with in the college for their constant support and encouragement.

I would also like to express my gratitude to my lab colleagues especially Sravan K. Patel and Ali I. Altharawi. Finally, many grateful thanks go to my family and all my friends, both new and old, for their believing in me through the years.

TABLE OF CONTENTS

Page

LIST OF TABLES

Page

LIST OF SCHEMES

Page

LIST OF FIGURES

Page

LIST OF ACRONYMS

BEL	bromoenol lactones
BOC	*tert*-butyloxycarbonyl
BPO	benzoyl peroxide
CBz	carboxybenzyl
DIAD	diisopropyl azodicarboxylate
DMAP	4-dimethylaminopyridine
DMSO	dimethyl sulfoxide
DMF	*N*,*N*-dimethylmethanamide
EDC	1-ethyl-3-(3-dimethylaminopropyl)carbodiimide
HIV	human immunodeficiency virus
LDA	lithium di-isopropyl amide
HMPA	hexamethylphosphoramide
HOBt	1-hydroxybenzotriazole
LAH	lithium aluminum hydride
MRSA	methicillin-resistant *Staphylococcus aureus*
MTT	3-(4,5-dimethylthiazol-2-yl)-2, 5-diphenyltetrazolium bromide
NHS	*N*-hydroxysuccinimide
NMM	*N*-methylmorpholine
OBHA	*O*-benzylhydroxylamine
PBP	penicillin-binding protein
S.M.	starting material
TBAI	tetrabutylammonium iodide
TEA	triethylamine
TFA	trifluoroacetic acid
THF	tetrahydrofuran
TLC	thin layer chromatography
TPP	tetraphenylporphyrin

CHAPTER 1

INTRODUCTION AND LITERATURE REVIEW

In organic synthesis, it is important to increase the selectivity of the reaction and the product yield. Among the most widely used types of synthetic transformations is the elimination reaction to introduce a double bond. Conventionally, alkene formation under elimination conditions often requires harsh temperatures that can cause decomposition of the product. A new method to introduce alkenes under mild toluene reflux, which might be suitable to be used in the medicinal chemistry lab to build complex structures, has been described in Chapter 2. The procedure of this reaction utilizes *o*-nitro phenyl sulfoxides as precursors of terminal and substituted alkenes. A discussion of this novel method and results of the study are presented.

The use of sulfur chemistry in synthetic transformation is further examined in Chapter 3. An asymmetrical method to synthesize the β-lactam ring found in penicillins and cephalosporins via the photooxidation of thiazolidines is described. To date, only a limited number of methods have been reported for the synthesis of β-lactams by intramolecular cyclization of intermediates derived from natural α-amino acids. The procedure that has been developed utilizes thiazolidines hydroxamate ester anions that can be readily cyclized to the lactams. The introduction of hydroxyl group at the C-5 position by photooxidation (key step in the synthetic sequence) enables this unique approach to construct highly functionalized, chiral β-lactams that can be employed as platforms in antimicrobial drug discovery.

A specific example of the utilization of platforms for hit-to-lead generation studies of antimicrobials is described in Chapter 4. The chemical modification of phthalimide and 1,4-naphthoquinone to design novel mitochondrion-acting antiparasitic agents was performed. The central hypothesis of this project is that positively-charge antagonists of electron-transport may be used as mitochondriotropic therapies of parasitic diseases including malaria and American Chagas disease. The mitochondriotropic group (i.e., the phosphonium cationic group) were attached to the phthalimide and 1,4-naphthoquinone platforms using classical methods in organic synthesis. The compounds were evaluated for antiparasitic activity and these results are presented in Chapter 4. Calculation of Log *D* values and percent hemolysis values of lead compounds was lastly performed as standard preclinical analyses of experimental therapies.

Chapter 5 summarizes the final conclusions.

CHAPTER 2

PREPARATION OF ALKENES VIA *o*-NITRO PHENYL SULFOXIDE PRECURSOR

Lu, X.; Long, T. E. *J. Org. Chem.* **2010**, *75*, 249-252.

Abstract

Organic medicinal chemistry is the science dedicated to the development of new synthetic method and their potential usage in drug discovery. It is becoming increasingly clear that heteroatom chemistry plays an important role in lead discovery and modification. In Chapter 2 the preparation and spectral characteristics of olefins through thermal elimination is reported. The reaction of *o*-nitro phenyl sulfoxide precursor under toluene reflux is shown to proceed cleanly and quantatively via a concerted mechanism; the ratio of *Z*- and *E*-isomers is altered depending on different α- or β- substitution groups.

2.1 Background

2.1.1 Introduction

Unsaturated hydrocarbons play an important role in biological sciences. Unlike single bonds that possess sp^3 hybridization, the double bond has a higher energy barrier between the *E*- and *Z*-isomers which restrict free rotations around the bond axis. The resulting stable conformation of the isomers may confer unique properties. For example, the chemical transformation of 11-*cis*-retinal, a key photosensitive component of rhodopsin, is generated from its geometric isomer in a typical visual cycle (**Figure 2.01**) [1].

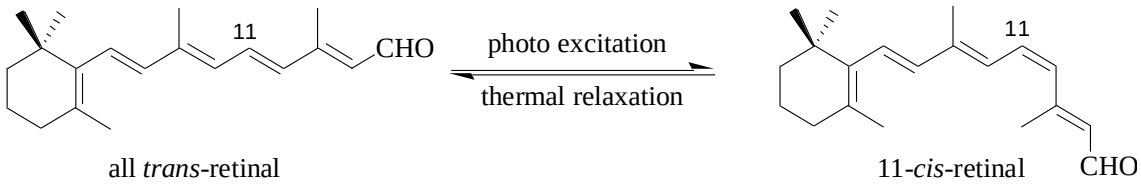

Figure 2.01: 11-*cis*-Retinal isomerizes into its geometric isomer after absorbing a photon in the visible light range.

Substituted double bonds are found in many types of bioactive molecules including steroids (e.g., cholesterol [2]) and antimicrobials (e.g., amphotericin, cephalosporins [3]). As with cephalosporins, the double bond found in haloenol lactones plays an integral role in the deactivation of enzymes. For example, the bromoenol lactone (i.e., BEL; **Figure 2.02**) is suicide substrates of chymotrypsin and related serinases (e.g., phospholipases) [4]. In addition, double bond-containing molecule can also interact noncovalently through hydrophobic

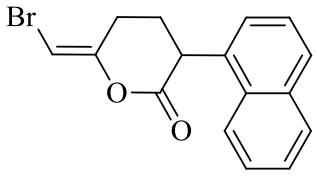

Figure 2.02: The structure of BEL, a haloenol lactone.

interactions with receptors in cell signaling. A brief summary of regular bonding/non-bonding interactions between the drug and the receptor is given below (**Table 2.01**) [5-9].

Table 2.01: Types of interactions between the drug and the receptor.

Type of interaction	Features	Examples
Hydrophobic interaction	non-polar 'like' non-polar, polar 'like' polar	non-nucleotide reverse transcriptase inhibitors to treat HIV-1 [5]
Van der Waals interactions	attractive or repulsive forces exist between molecules	methylene blue to treat malaria [6]
Hydrogen bonding	strong interaction exist between potential donors and acceptors	non-nucleotide reverse transcriptase inhibitors to treat HIV-1 [7]
Ionic bond	strong interaction depends on the pH value in the body and p*K*a value of the drug	positively-charged lysine or arginine residues at physiological pH [8]
Covalent bond	irreversible covalent bonding at the binding site	the β-lactamase inhibitors as antibacterial agents [9]

Currently, there are several different synthetic approaches to make double bonds in molecules. The most common and convenient way is to attach preformed unsaturated hydrocarbons from petroleum and natural gas products to the molecule of interest [10]. Alternatively, the unsaturation may be built indirectly into organic structures from precursors by various well-established methods. For example, the dehydrohalogenation of alkyl halide (in which a base is needed) and the dehydration of alcohols (in which an acid is needed) have been primarily studied due to easy access to the starting materials [11]. Both of these examples are known as eliminations. However, although certain rules can be used to predict the conformation of the products, e.g., the rule of Saytzeff

suggesting the highly substituted olefin is the predominate product [12], many of these classical methods require a further purification step to remove byproduct isomers, thus may not suitable for many large-scale applications in medicinal chemistry.

2.1.2 β-Elimination

Representing an exclusive class of reaction, elimination can be further divided into several types depending on the proton and the leaving group involved. Examples are: (1) the classic method of carbine preparation through the base induced α-elimination from chloroform; (2) β-elimination in unsaturated compound synthesis; and (3) γ- or higher eliminations in ring generation via intracellular nucleophilic displacement (**Scheme 2.01**) [13]. Currently, the most widely used method to introduce double bonds into interested molecule is through β-elimination which involves the removal of the two adjacent atoms or groups from the starting material, e.g., alkyl halides or alkyl alcohol. In the hope of increasing unsaturation in a controlled manner, many other precursors have been previously studied, for example, amine oxides, tertiary ammonium iodides, etc. [14]; however, most of these methods have drawbacks such as the requirement of a high temperature (> 150 °C) or the use of a strong base (*t*-BuOK), thereby limiting their potential usage.

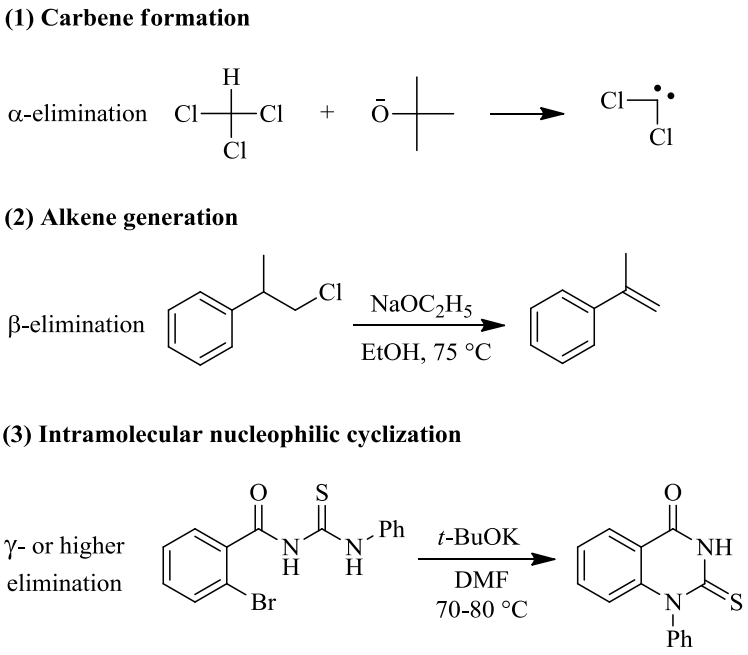

Scheme 2.01: Types of elimination reaction.

In general terms, the β-elimination reaction is brought about by treating the precursor with a base, and proceeds by either the E1 or the E2 mechanism depending on how many molecules and steps are involved. By far, the most common approach of elimination is through the E2 mechanism, which is a concerted, one step process. Here, the research focus in this project is thermal β-elimination, which is a unique example of E2 elimination. As illustrated in **Scheme 2.02**, for instance, induced by heat, the carboxylic acid ester could undergo elimination without adding an external base. It is believed that this type of β-elimination involves a flat cyclic transition state to provide the *syn*-elimination product and the acid byproduct [15].

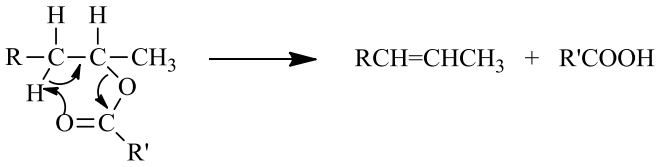

Scheme 2.02: Thermal elimination of carboxylic acid ester.

In spite of the requirement of high temperatures, many successful examples have been reported such as the investigation of the Chugaev elimination [16], and the discovery of the Cope reaction [17] (**Scheme 2.03**). The broad scope of thermal β-elimination has been continuously emphasized and applied in natural product synthesis [18]. However, the need of harsh conditions still make many of these methods unsuitable for building the backbone of complex, biological molecules.

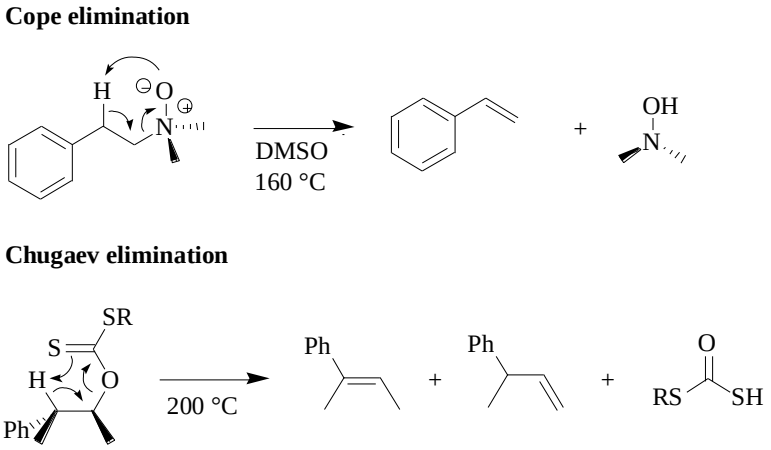

Scheme 2.03: Examples of thermal elimination: Cope elimination and Chugaev elimination.

In 1975, an interesting thermolysis of phenyl selenoxide was reported by Sharpless et al. [19] A typical procedure for this gentle olefin-forming method is shown in **Scheme 2.04**. First of all, the selenide anion was treated with bromide to form selenide, which was then oxidized by hydrogen peroxide. Followingly, without further purification, this newly formed selenoxide was then decomposed readily to provide the alkene product, i.e., 1-dodecene. In this case, the *o*-nitro phenyl selenoxide was astonishingly unstable and can even decompose at room temperature. Due to the high cost and toxicity of

selenium compound, however, this reaction's usage in the pharmaceutical lab or industry is limited [20].

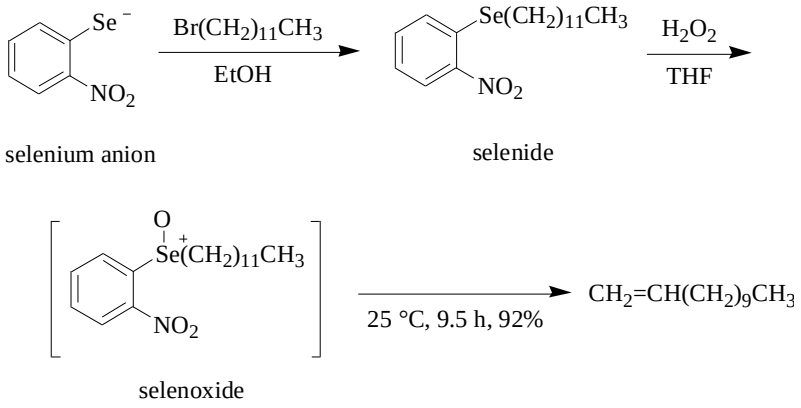

Scheme 2.04: Reported procedure to make alkene via selenoxide [19].

Elimination using phenyl sulfoxide, reminiscent of phenyl selenoxide decomposition, has also been studied. Because sulfur and selenium both possess six valence electrons, the thermolysis of sulfoxide can occur under similar conditions to the reactions of selenoxide, although many reported methods furnish the product in poor yield due to significantly high temperature requirement (**Scheme 2.05)**. Thus, there is still great potential to improve the reaction efficiency by developing milder reaction procedures [21].

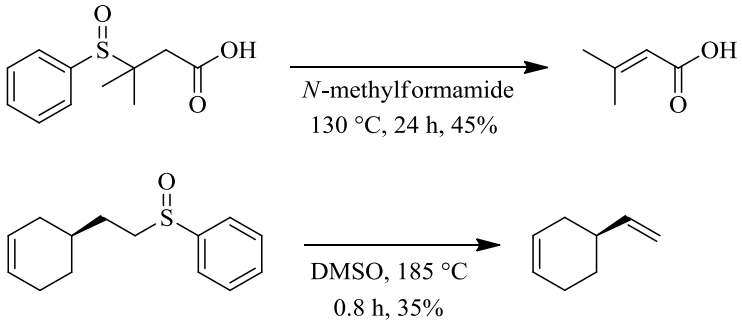

Scheme 2.05: Thermal elimination of phenyl sulfoxide [21f, 21g].

2.1.3 Current precursors

2.1.3.1 Substituted phenyl selenoxides

In a previous study, it was suggested by Sharpless et al. [19] that decomposition of selenoxide to olefin significantly depends on the substitution pattern of the benzene ring. As a result, an electron withdrawing group can greatly increase the reactions outcome. Particularly, a nitro group at the *ortho* position of the benzene ring was found to be optimal for the reaction. Evidence for the effect of substituents can also be seen in Dr. Sayama's study [22]. Using a similar procedure as Sharpless's method, the two steps of continuous synthesis are: (1) the oxidation of selenide to selenoxide, and (2) the *syn*-elimination of the resulting selenoxide to alkene product.

The evaluation of the two-step, one-pot synthesis has also been conducted by a comparison to the formation of selenoxide (the key intermediate) by oxidizing selenide with hydrogen peroxide. It is of some interest to mention that an electron withdrawing group can diminish the electron density of the lone pair of electrons on the benzene ring. As described, selenides with an electron withdrawing group on the benzene ring were oxidized to selenoxides more slowly than selenides with an electron-donating group [22]. However, both above mentioned studies were performed without further purification of the selenoxide (the key intermediate) and had a problem of simultaneously forming impurities still need to be solved.

2.1.3.2 Substituted phenyl sulfoxides

In an earlier publication, Patel et al. [23] examined the thermal β-elimination of various substituted phenyl sulfoxide. The reaction was performed under high temperatures and high vacuum. In this study, the influence of substituent groups on the

benzene ring was also described. Upon heating at 145 °C, the *o*-nitro phenyl sulfoxide precursor can generate alkene product quickly in 1 hour with 36% yield. In comparison, *p*-Cl phenyl, *p*-NO_2 phenyl and *p*-OMe phenyl sulfoxides require longer times (e.g., 18 hours for *p*-Cl phenyl sulfoxide) to produce over 40% yield of the desired products. Meanwhile discovered by chance, the thermolysis of sulfoxide was found can readily occur in refluxing toluene. It was noted when sodium acetate was added into the reaction system, the base and the sulfenic acid byproduct can be removed by simple filtration, producing the final product in high yield and purity.

Undoubtedly, further investigation into different sulfoxide precursors is required to achieve desirable reaction results under milder reaction conditions. In this chapter, the optimization of reaction conditions was continued, followed by a thorough investigation of various substituted phenyl sulfoxide precursors, and a brief examination of the hypothesized mechanism.

2.2 Experimental Design and Results

2.2.1 Design of the substrates

Since earlier studies proved that elimination reactions using sulfoxides as starting materials require harsh conditions (which may cause the decomposition of the starting materials and products), therefore the first aim in this project is to confirm the reaction conditions previously studied in our lab. As been briefly reviewed in section 2.1.3, it is believed the sulfoxide type may have varying degrees of influence on the reaction outcome. Herein, for the first time a preliminary study of the reaction efficiency has been conducted by directly examining different substituted phenyl sulfoxides. The precursors

were with either an electron donating group or an electron withdrawing group on the benzene ring. These carefully designed molecules are described below.

In Study 1, compounds **1a** and **1b** were prepared to continually optimize the reaction conditions (**Figure 2.03**). In order to check the efficiency of *o*-substituted electron withdrawing groups, different phenyl sulfoxide precursors were attached at either end of the alkyl chain. As illustrated in **Figure 2.04**, six different phenyl sulfoxides **1c-h** were designed for screening of optimal precursor in this competition-based assay. At this point, after confirming that the optimal compound has an electron-withdrawing group at the *ortho* position of the benzene ring, *o*-nitro phenyl sulfoxides were continued in the following studies (Study 3-5).

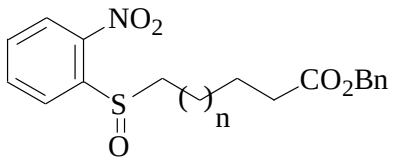

1a n = 7
1b n = 1

Figure 2.03: The designed precursors for Study 1.

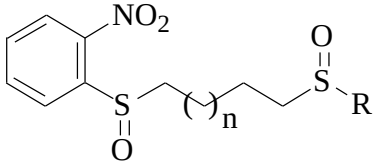

1c n = 8, R = Ph
1d n = 3, R = Ph
1e n = 8, R = *p*-PhMe
1f n = 8, R = *p*-PhCl
1g n = 8, R = *p*-PhNO$_2$
1h n = 3, R = *p*-PhNO$_2$

Figure 2.04: The designed precursors for Study 2.

In Study 3, the preparation of substituted alkene product was assessed. On the branched carbon chain, a phenyl group is located at β position in compound **1k** (**Figure 2.05**). In comparison, smaller groups/atoms (i.e., Me or H) were examined (**1i**, **1j)**. The designs of these precursors (compounds **1i-1k**) were also extended to the analysis of the regioselectivity.

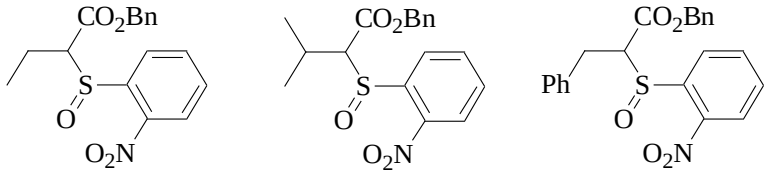

1i **1j** **1k**

Figure 2.05: The designed precursors for Study 3.

Phenyl sulfoxides **1l** and **1m** were designed to further examine the effect of β-H in Study 4. Comparing the two, precursor **1l** has a significantly increase in acidity of β-H due to the attachment of a benzyl ester at that position (**Figure 2.06**). In addition, compound **1n** was specifically designed to examine the possibility of δ-elimination in the molecule containing an alkene at β-position.

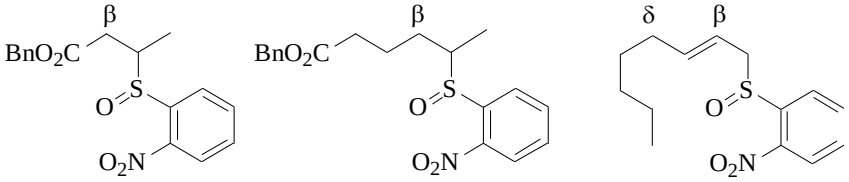

1l **1m** **1n**

Figure 2.06: The designed precursors for Study 4.

In Study 5, compounds **1o-q** were selected to further explore the possibility of utilizing this elimination reaction in the hope of generating α,β-unsaturated aromatic products (**Figure 2.07**).

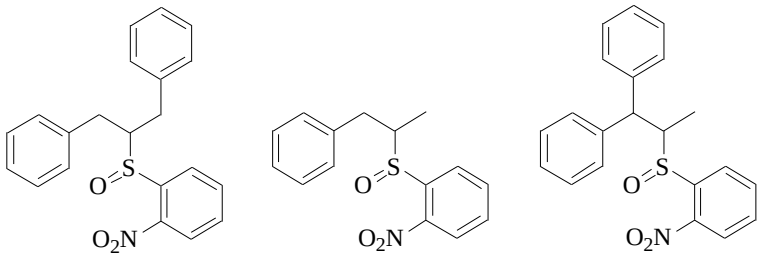

1o **1p** **1q**

Figure 2.07: The designed precursors for Study 5.

2.2.2 Synthesis of the sulfoxide substrates 1a-n

In this project, similar procedures were employed for the preparation of phenyl sulfoxides. For example, the *o*-nitro phenyl precursors were prepared from alkyl halides through two steps of synthesis as illustrated in **Scheme 2.06**. Under the acetone reflux, the treatment of the alkyl bromide or chloride with potassium iodide led to the S_N2 substitution of the halogen and the sulfide. Oxidation of the resulting sulfides to sulfoxides using *meta*-chloroperbenzoic acid (*m*-CPBA) was then performed. For the procedure, only 1.25 equiv per sulfide function group was used and the reaction was carefully monitored to prevent the formation of sulfone (2.5 hours for most substrates). These two steps in combination produced purified yields around 60%.

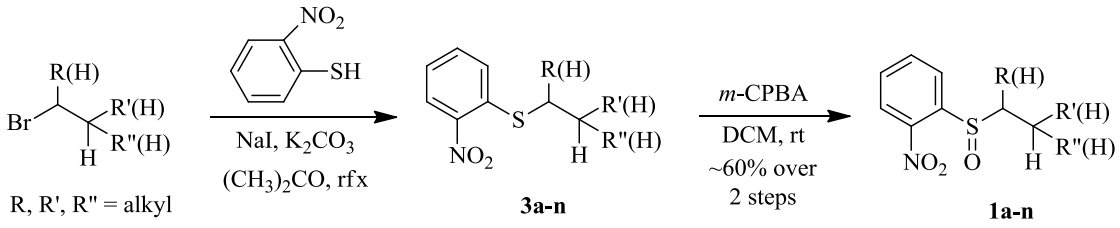

Scheme 2.06: General synthetic route to make the sulfoxide precursors **1a-n**.

2.2.3 Synthesis of the *o*-nitrothiophenol 2

In this project, thiols were obtained from commercial sources or were easily made by simple reduction (**Scheme 2.07**). In the case of preparing *o*-nitrothiophenol **2,** 2-mercaptoethanol was chosen as the reducing agent [24], which is a common tool to cleave disulfide bonds in chemistry labs. Strong phosphorous nucleophile, i.e., triphenylphosphine, was used as well due to its ability to cleave the disulfide bond [25]. Careful column chromatography was followed to ensure the high purity of thiophenol **2**.

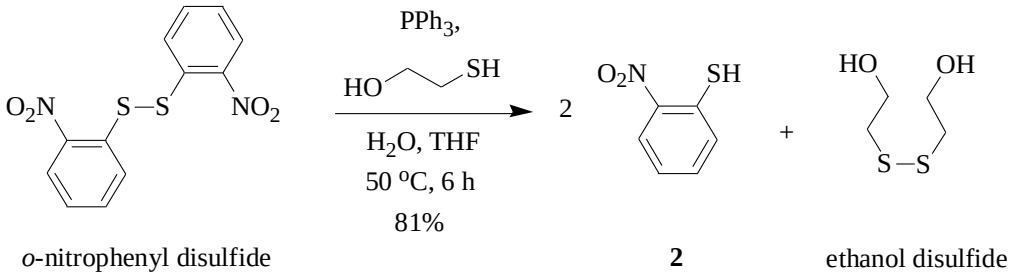

Scheme 2.07: 2-Mercaptoethanol- and triphenylphosphine-mediated disulfide bond cleavage.

2.2.4 The thermal β-elimination: the optimal reaction conditions

Optimal reaction conditions for the elimination reaction were firstly examined on substrates **1a** and **1b** (**Scheme 2.08**). To start with, a qualitative screen was initially performed with different solvent and temperature. Aprotic non-polar solvents with high-medium boiling points were evaluated including 1,4-xylene (bp 139 °C), chlorobenzene (bp 131 °C), toluene (bp 110 °C) and benzene (bp 80 °C). Among them, toluene was found to be the lowest boiling solvent to quantitatively generating alkene products **4a** and **4b** after overnight reflux. In addition, precipitation of the sulfenic acid byproduct can further benefit for use of toluene in this reaction.

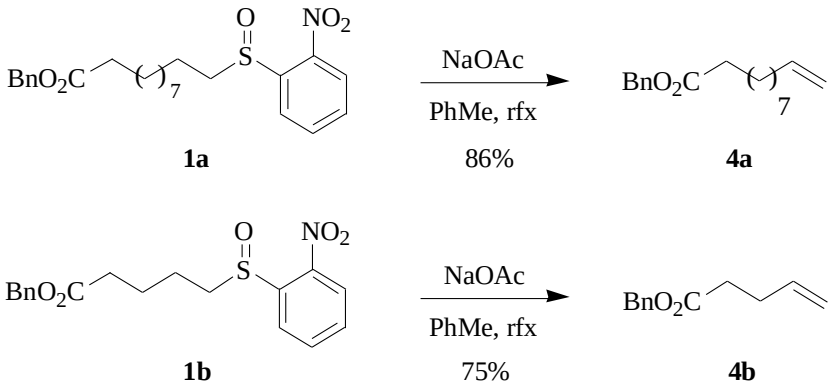

Scheme 2.08: The elimination reaction of sulfoxides **1a** and **1b.**

The next goal in this study was to eliminate the sulfenic acid byproduct **5** (see **Figure 2.08**) without standard aqueous work up or further chromatography purification. Because the sulfenic acid was found to be water-soluble and can precipitate out in non-polar, aprotic solvents, a variety of different bases were tested to neutralize acid byproduct including the usage of K_2CO_3, C_5H_5N (pyridine), $NaHCO_3$, and NaOAc. It was noted that during the process of toluene refluxing, the color of solution changed from bright yellow into lighter yellow or colorless due to the precipitation of sulfenic acid **5**. At the same time, the inorganic base (i.e., NaOAc), that neutralized newly formed byproduct **5**, turned from white solid to pale orange. After reflux, the base with absorbed byproduct as solid residue can be easily removed by Celite filtration and resulted in a high purity product.

Based on the crude ^{1}H NMR of the mixture, when NaOAc was introduced into the reaction system, the alkene products were yielded in highest purity compared to using other bases, no side products were formed. As shown in **Figure 2.08**, the ^{1}H NMR spectrum did not show the presence of sulfoxide, but a group of new peaks which corresponds well to the typical terminal alkene region. The alkenes **4a** (86%) and **4b** (75%) were successfully generated in high yield (**Scheme 2.08**). In other words, the

thermal β-elimination of *o*-nitro phenyl sulfoxide precursor preceded easily under toluene reflux in the presence of NaOAc and did not need any further purification [26].

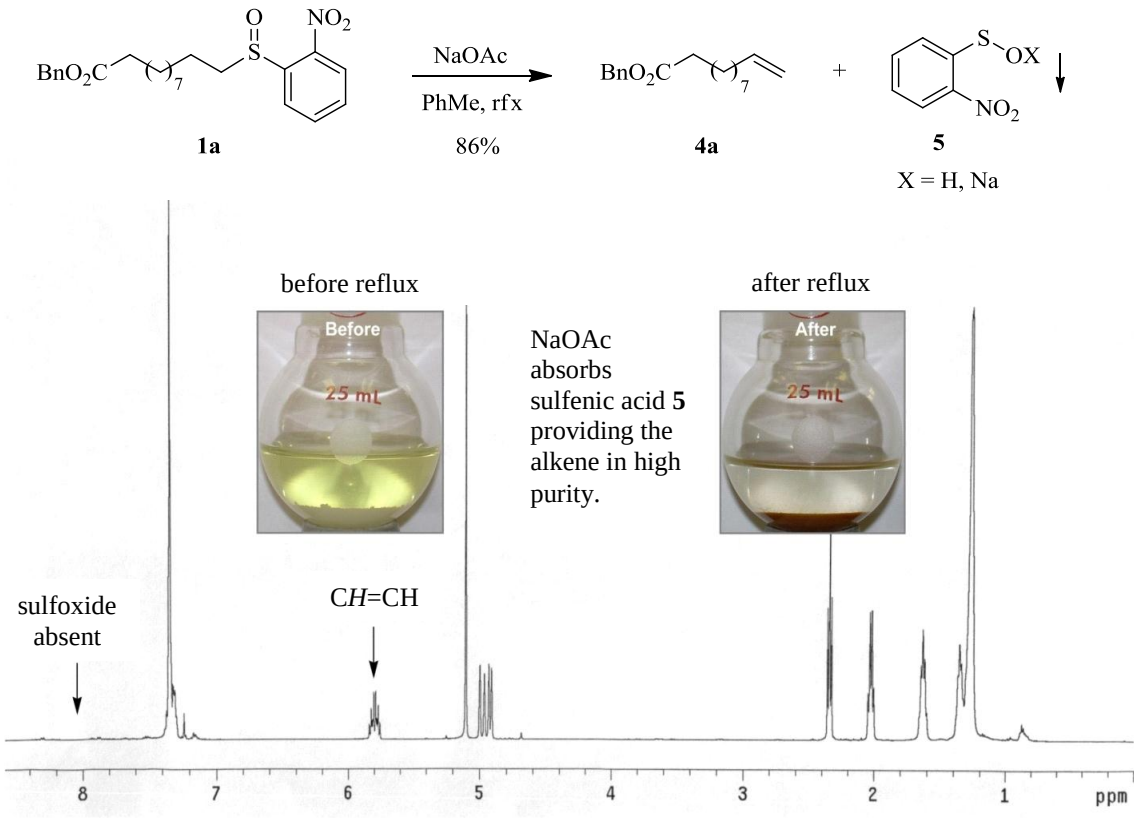

Figure 2.08: ^{1}H NMR of filtered reaction product **4a** prior to purification [26].

2.2.5 The thermal β-elimination: the optimal reaction precursors

Previously, a nitro group has been evidenced to provide higher reaction outcomes for selenoxide compounds [19, 22]. Likewise, it was also shown *o*-nitro phenyl sulfoxide is the best precursor for thermolytic elimination (145 °C, neat) [23]. Based on these findings, each designed substrate in the following sections has the *o*-nitro phenyl sulfoxide at one end as a positive control and has an alternative substituted phenyl group at the other end of the chain. In this study, under the optical reaction conditions, the

importance of an electron withdrawing group on phenyl sulfoxide was performed by a series of competition-based assays.

The first comparison was made between the *o*-nitro phenyl sulfoxide and the unsubstituted phenyl sulfoxide. The unsubstituted phenyl sulfoxide precursor proved to be insufficient since this chemical group did not change after 18 hours toluene reflux. The only acquired product was the olefin with untouched phenyl sulfoxide, giving **4c** and **4d** with 86% and 62% yield, respectively (**Scheme 2.09**). This illustrates that the presence of an electron withdrawing group on the phenyl ring can significantly increase the elimination rate. In contrast, according to the findings from earlier studies, the thermolysis of unsubstituted sulfoxides generally requires a higher temperature [21].

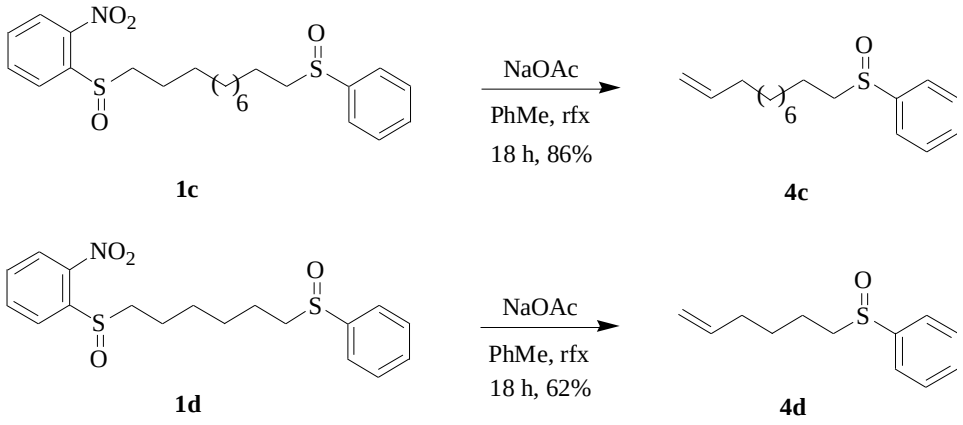

Scheme 2.09: Elimination reaction of compounds **1c** and **1d**.

A second comparison was made between the control precursor (*o*-nitro phenyl sulfoxide) and other substituted phenyl sulfoxides, including an electron-donating group (i.e., Me; **1e**), or an electron-withdrawing group (i.e., Cl; **1f**) at *para*-position on the benzene ring (**Scheme 2.10**). It was hypothesized that the electron-donating group

substituted phenyl sulfoxides are even less efficient precursor than the unsubstituted ones for thermal elimination to generate the alkene.

Similar to previous observations, alkene **4e** was produced with high yield (87%). This confirmed that an electron-donating group such as a methyl group is not able to facilitate the process of elimination. In the case of the *p*-substituted electron-withdrawing phenyl sulfoxides, after 18 hours toluene reflux, olefin **4f** was the only product separated with a yield of 74%. It was also noticed that a weak electron-withdrawing group such as *p*-Cl phenyl sulfoxide group in precursor **1f** can not undergo elimination under toluene reflux. This provided evidence that the optimized precursor may require a strong electron withdrawing group such as a nitro group. On the basis of this analysis, a further investigation on the effects of modification in the substituent position was next followed.

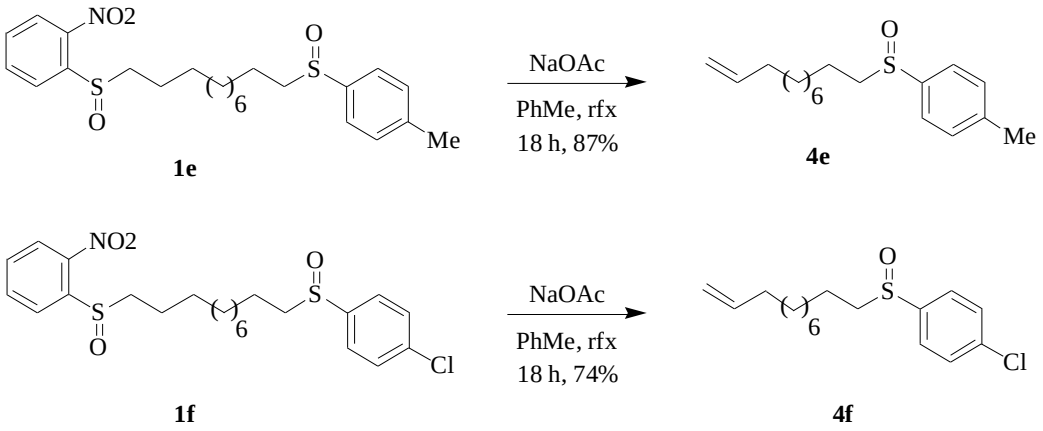

Scheme 2.10: Elimination reaction of sulfoxides **1e** and **1f**.

The final comparison was made to determine if differences in reaction outcome exist between the various positions of the same electron withdrawing group, i.e., a nitro group. After 18 hours heating, alkene products **4g** and **4h** with *p*-nitro phenyl structure untouched were generated in 64% and 61% yield, respectively. In addition, a trace

amount of double eliminated alkenes was also formed (**Scheme 2.11**). This confirmed that only an *ortho* substituted electron withdrawing group can significantly increase the reaction outcome, but not a *para* substituted electron withdrawing one.

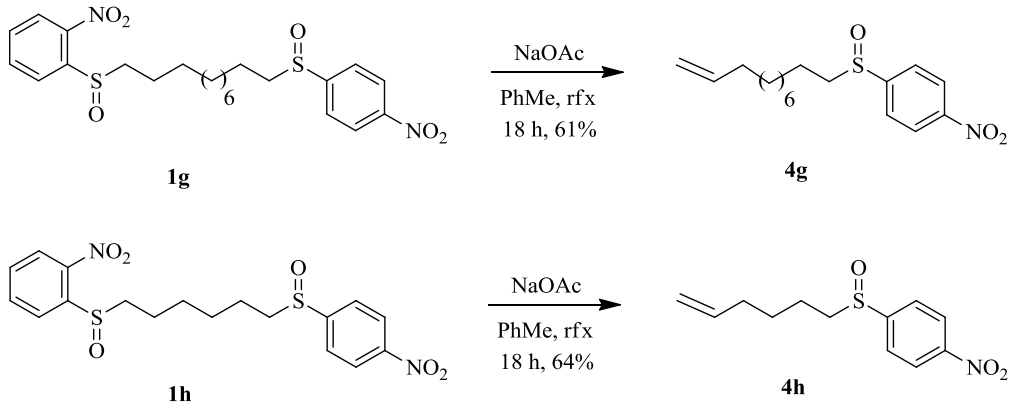

Scheme 2.11: Elimination reaction of compounds **1g** and **1h**.

A possible explanation for these observations was then explored. Since alkene formation via heating involves a concerted *cis* elimination from a five-membered-ring transition state, the enhanced reactivity of *o*-nitro phenyl sulfoxides may be due to the substitution group (in this case a strong electron-withdrawing group, a nitro) at *ortho* positioning which may force the oxygen atom of sulfoxide closer to the leaving proton in the five-membered-ring transition state (**Figure 2.09**).

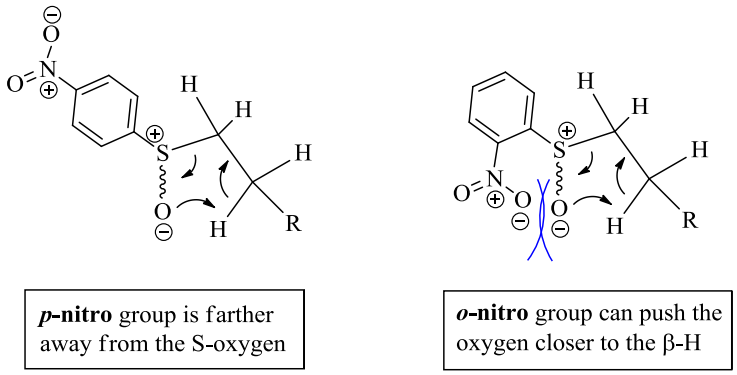

Figure 2.09: Comparison of *ortho*-nitro and *para*-nitro phenyl sulfoxides.

The following figures provide more detailed explanation on how a nitro group can facilitate the elimination and its potential ability to change S=O bond in sulfoxide. Unlike carbonyl structure (the double bond and the other two sp^3 bonds are on the same plane) (**Figure 2.10a**), sulfoxide has its oxygen atom on a different plane (**Figure 2.10b**) and the sulfur atom is more likely to have a pyramidal structure with 1 lone electron pair and 4 bonding pairs (**Figure 2.10c**).

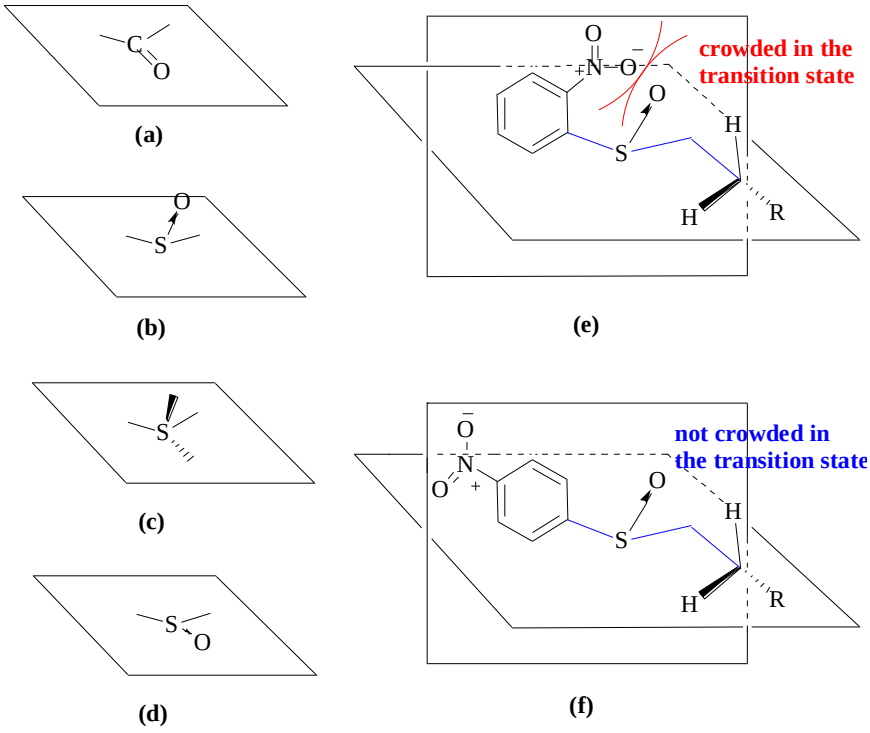

Figure 2.10: Sterically hindered *o*-nitro phenyl sulfoxide vs. less sterically hindered *p*-nitro phenyl sulfoxide.

For convenience of analysis, a pair of sulfoxides with nitro group *ortho-*, or *para-* position to the phenyl are drawn separately. In both figures, single bonds important to the elimination which can rotate freely are highlighted in blue. The rationale behind the increased elimination rate is that the pyramidal sulfur atom is more sterically hindered in

the transition state for *o*-nitro phenyl sulfoxide precursors (**Figure 2.10e**). Pushed by this surrounding nitro group, the oxygen atom is much closer to the leaving proton at β position, giving trigonal bipyramidal geometry around the sulfur atom (**Figure 2.10d**). As a result, this will make the sulfoxide less stable than that of *para* positioning (**Figure 2.10f**). After comparing reaction yields, among all substituted phenyl sulfoxide precursors, *o*-nitro group is the optimal substitution to promote the β-elimination and thus was chosen as the tool to be used in the following investigation. The concept of the proposed mechanism is illustrated in **Figure 2.11** in terms of a concerted *syn*-elimination through a five-membered-ring transition state which is highlighted in red.

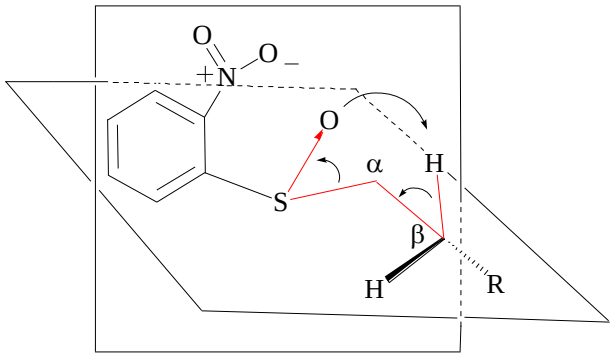

Figure 2.11: Concerted five-membered-ring transition state.

This however does not display the importance of the leaving hydrogen atom since the p*K*a value of this proton can be altered by introducing other substitutions into the hydrocarbon chain. It was thus hypothesized that the more acidic the β-proton, the higher the reaction outcome will result. Moreover, van der Waals repulsion may also exist between the β substitution and the phenyl sulfoxide group. If this steric hindrance is great enough, the formation of *o*-nitro phenyl sulfenic acid (byproduct) and alkene (product)

may require lower energy. Therefore it was also anticipated that the more bulky group at the β-position would require milder reaction conditions for the elimination.

2.2.6 The thermal β-elimination: the importance of van der Waals repulsion

As it became necessary to conduct more research to understand the topic reaction, the optimized procedure was then used to make α,β-unsaturated esters in specially designed hindered substrates (**Scheme 2.12**). Although precursors **1i** and **1j** have a carboxylic ester at α-position, which can cause a slight activation of the α-H, this acidity enhancement does not increase the rate of reaction due to the fact that α-H does not involve in β-elimination.

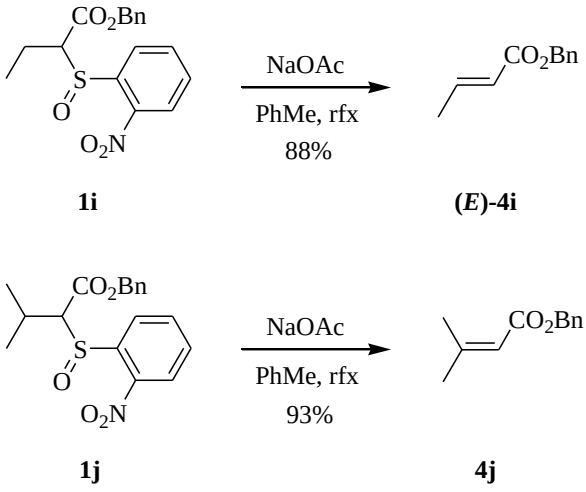

Scheme 2.12: Preparation of substituted alkenes **4i** and **4j**.

At first glance, the precursor **1i** should be able to generate both *E*- and *Z*- isomer products, in fact only alkene **(*E*)-4i** was generated. Surprisingly, prior to this step, a trace amount of the alkene was formed even during the *S*-oxidation of **3i** (**Scheme 2.13**). In other words, the sulfoxide precursor **1i** was unstable and may not require a very high temperature to generate the alkene **4i**.

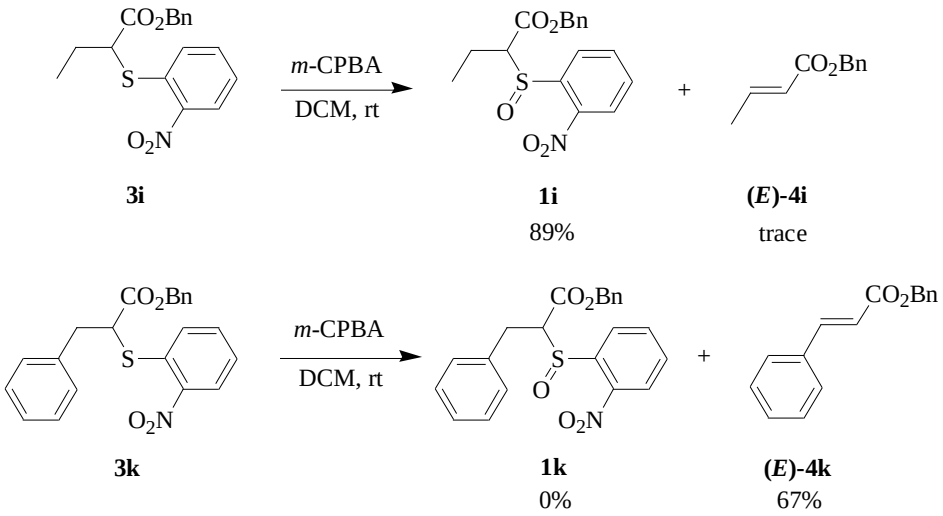

Scheme 2.13: Formation of alkenes **4k** and **4i** with just *m*-CPBA.

More interestingly, in the case of sulfoxide **1k**, workup with 5% $NaHCO_3$ after *S*-oxidation of **3k** was found to form substituted alkenes **4k** sufficiently with a 67% yield. It was further noticed that during the aqueous work up, a unique blue color was observed in the aqueous layer, which was very similar to the water extraction after oxidation of **3k**. This might be because the similar p*K*a value of β-H for both structures **1k** and **1j** (**Scheme 2.13**). However reasons unknown in comparing the two, the sulfoxide **1k** was more unstable, thus decomposed more readily than **1j** at room temperature.

Since the only structure difference between the sulfoxide precursors **1k** and **1i** is the β-substitution, the van der Waals repulsion among the chemical groups may apply to the reason of much higher elimination rate of **1k**. Considering the elimination outcome is highly dependent on the stability of the precursor, a very high van der Waals repulsion may result in minimal energy requirement for the eliminating of the acid byproduct from the alkene. Based on this analysis, it is believed the repulsive force between the β-phenyl and phenyl sulfoxide is essential. In the structure of **1k**, this repulsion is much higher

than that of **1i** or **1j**, hence **1k** is capable of reacting easily at a much low temperature (**Figure 2.12)**.

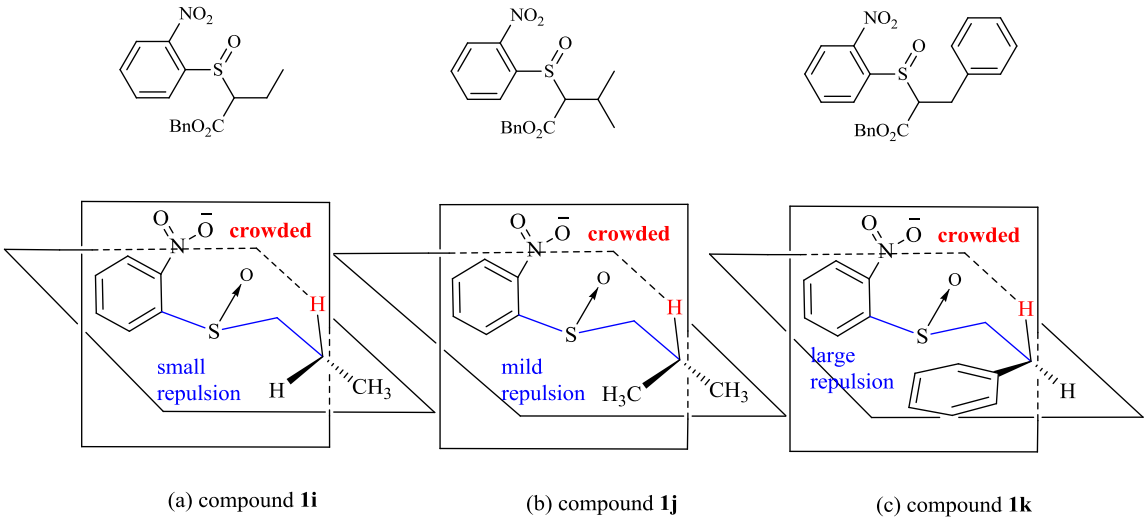

(a) compound **1i** (b) compound **1j** (c) compound **1k**

The estimated strength of repulsive van der Waals force between the sulfoxide and the β-substitution increases when a bigger group is attached, thus: **1i** (1 CH_3 group at β) < **1j** (2 CH_3 group at β) << **1k** (1 Ph group at β). Therefore, the estimated stability of sulfoxide also increases: **1i** < **1j** <<**1k***. (*The compound **1k** is so unstable as to decompose to the alkene at room temperature.)

Figure 2.12: Significance of van der Waals repulsion.

2.2.7 The thermal β-elimination: the importance of β-proton

After considering the results in previous sections, the relevance of β-proton acidities was further investigated by comparing the elimination results of **1l** and **1m**. With benzyl ester attached at different positions of the hydrocarbon chain, there is a large difference in the p*K*a values between the two corresponding β-protons. Assessed by TLC, the elimination of ester **1l** finished within minutes under the toluene reflux condition, as distinct from the elimination of **1m** can only slowly generate multiple products after 20 hours heating (**Scheme 2.14**). Probably, the enhanced reactivity of compound **1l** is conferred by a strong electron withdrawing group (i.e., a nitro group) close to the phenyl

sulfoxide. As a result, in the case of compound **1l**, the benzyl ester can not only make the precursor giving up β-proton more easily, but also expel the sulfenic acid byproduct **5** more quickly.

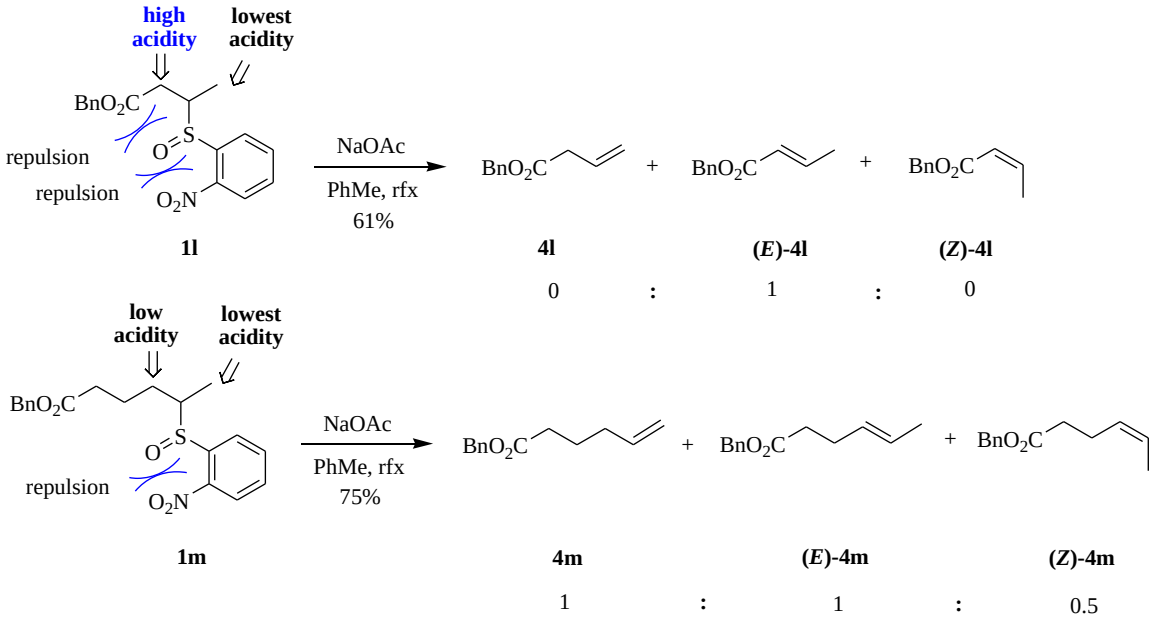

Scheme 2.14: Preparation of substituted alkenes **4l** and **4m**.

Moreover, the β-proton as well plays an important role. It was hypothesized that the elimination reaction will more likely form the five-membered-ring transition state with the β-proton having the lowest p*K*a value. Precursor **1m** produced several products under toluene reflux; however due to the high similarity in polarity between **4m**, **(*E*)-4m** and **(*Z*)-4m**, the mixture of isomers was inseparable.

After analyzing ^{1}H NMR spectrum of this mixture (**Figure 2.13**), peaks of **4m** in typical terminal alkene region were found: δ 5.77 (ddt, 1H, AB*M*, J_{BM} = 17.0 Hz, J_{AM} = 10.5 Hz, J = 7.0 Hz), δ 5.02 (dd, 1H, A*B*M, J_{BM} = 17.0 Hz, J_{AB} = 1.0 Hz), δ 4.98 (dd, 1H, *A*BM, J_{AM} = 10.5 Hz, J_{AB} = 1.0 Hz); a broad overlapped peak between δ 5.52-5.35 was also found which represents both **(*E*)-4m** and **(*Z*)-4m**. The enantiomeric ratio was next

calculated with the corresponding integration values and the ratio of **4m: (*E*)-4m + (*Z*)-4m** was estimated to 2:3. In order to obtain more accurate enantiomeric ratio, the mass spectrometry in combination with capillary column chromatography (GC-MS) was finally used. As illustrated in **Figure 2.13**, the more accurate ratio between **4m**, **(*E*)-4m** and **(*Z*)-4m** was estimated at around 2:2:1. As expected, because the methylene group should be able to give up its proton easier than the methyl, the precursor **1m** generated more substituted alkenes (**(*E*)-4m** and **(*Z*)-4m)** than the terminal one **4m**.

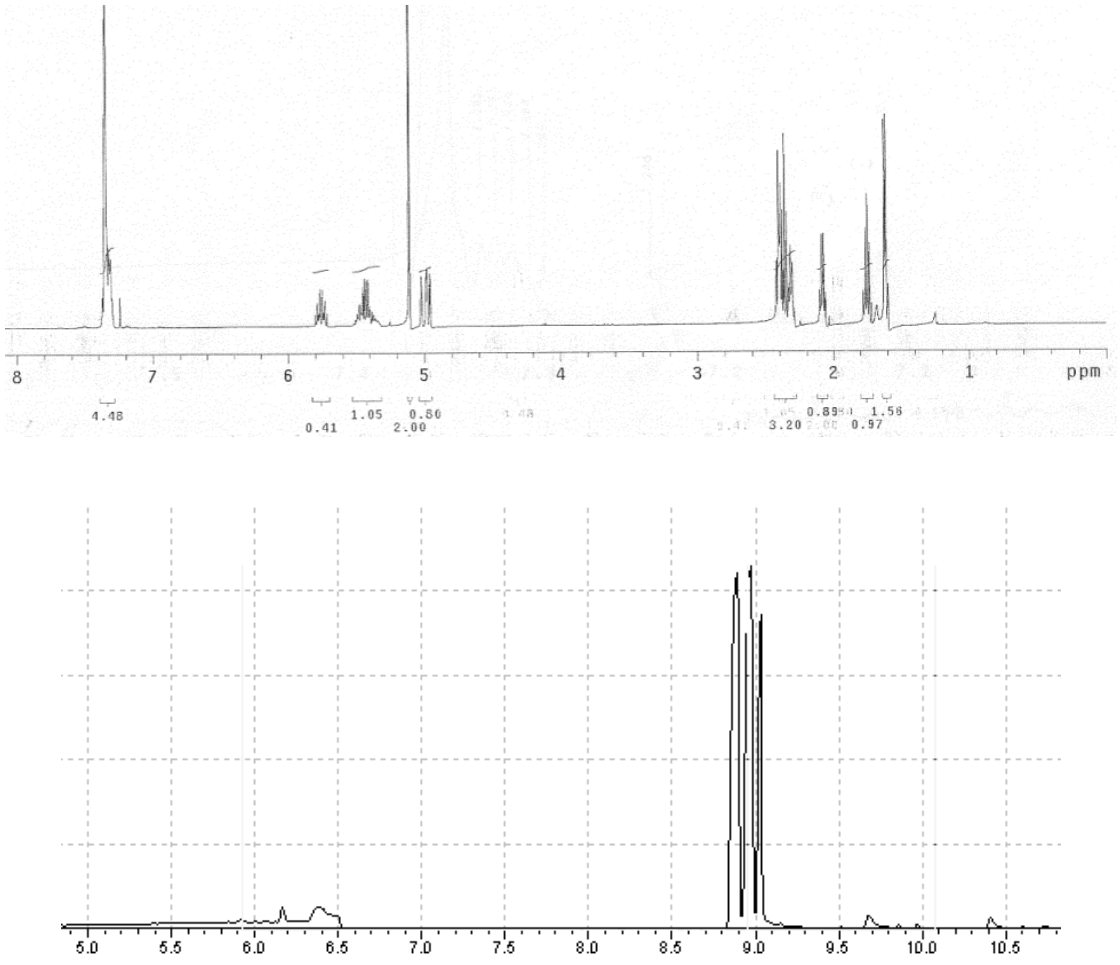

Figure 2.13: ^{1}H NMR and GC-MS graph of **4m** elimination.

2.2.8 The thermal β-elimination: regioselectivity

A proposed mechanism for the observed regioselectivity for product ***(E)*-4i** is illustrated in **Figure 2.14**. When the benzyl ester and the methyl are on the same side of the five-membered-ring plane, this transition state is more favored which produce only **(*E*)-4i**. In comparison, when the benzyl ester and the methyl are not on the same side of the five-membered-ring plane, with free rotation of the C-C bond, the more favored transition state will still be exclusively formed and produces only the (*E*)-isomer.

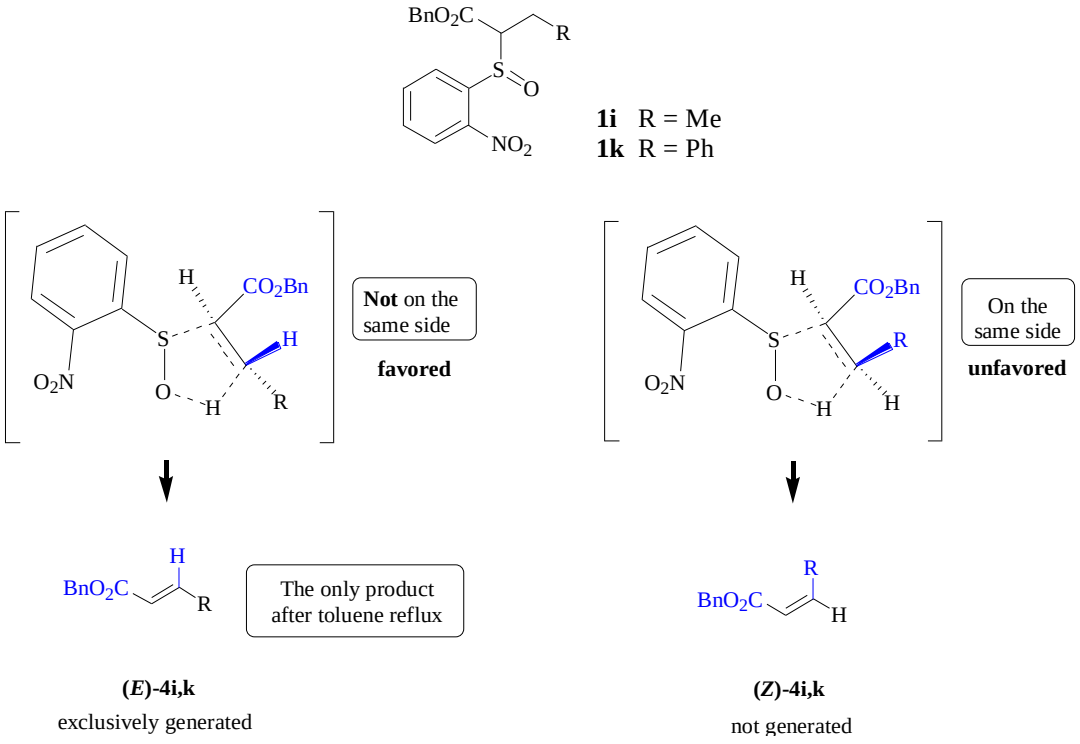

Figure 2.14: Hypothesized transition state for exclusively forming **(*E*)-4i**, **k** from **1i**, **k**.

Having rationalized the reaction of **1i**, the same reasoning can be applied to many other reactions. For example, in the case of precursor **1k**, or as illustrated in **Figure 2.15** precursor **1l**, the less crowded five-membered-ring transition state is more preferred, producing only (*E*)-isomer product.

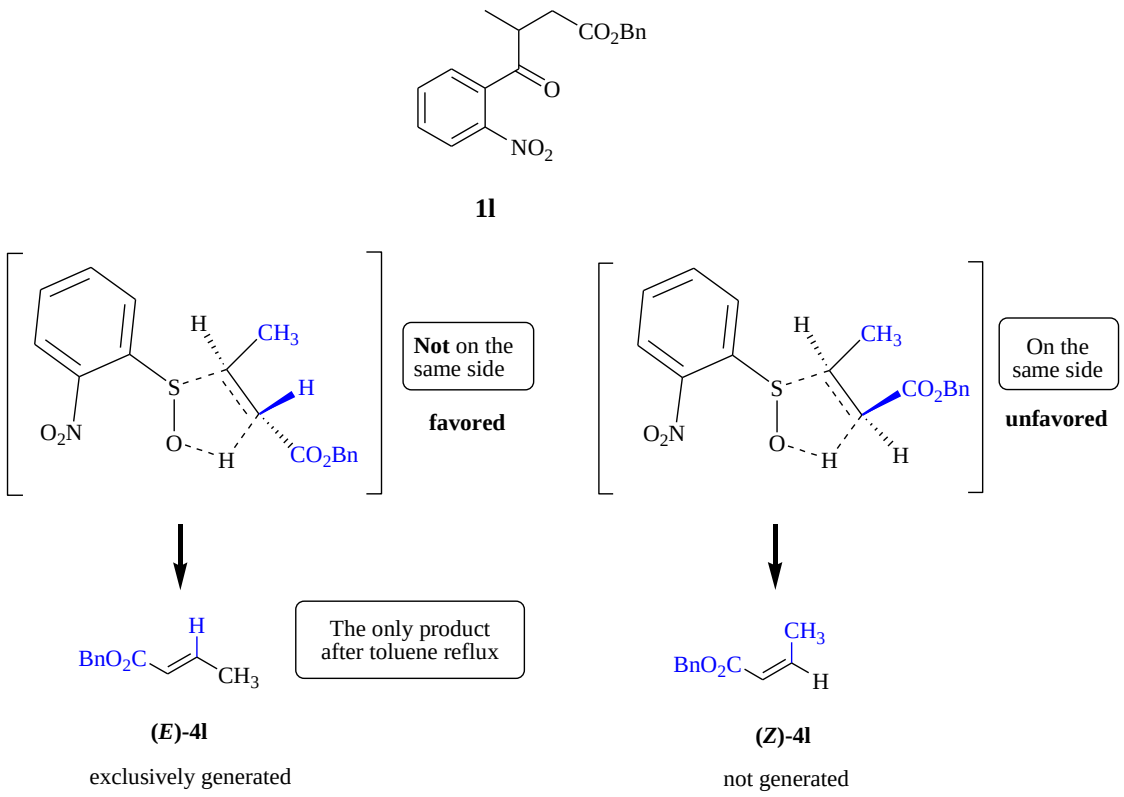

Figure 2.15: Hypothesized transition state for exclusively forming **(*E*)-4l** from **1l**.

At this point, of particular interest is the fact that the ratio between **(*E*)-4m** and **(*Z*)-4m** (mentioned in section 2.2.7). As no bulky group other than phenyl sulfoxide exist in the structure of **1i**, it is believed that in this case, the favorability of one transition state to another is no more significant. As a result, both **(*E*)-4m** and **(*Z*)-4m** were generated, and the (*E*)-isomer is the dominating product between the two.

2.2.9 The thermal β-elimination: additional studies

Further investigation into the possible utilization of this route was attempted as previously described in study 5. However, after several attempts, the alkylation procedure was unable to afford the corresponding sulfide precursors **3o-q** (**Scheme 2.15**). This might be because the conventional alkaline Finkelstein reaction conditions are mostly

suitable for reacting with primary halides [27]. Steric hindrance effects by the phenyl group at β-position were believed to prevent S_N2 attack by the thiol **2**.

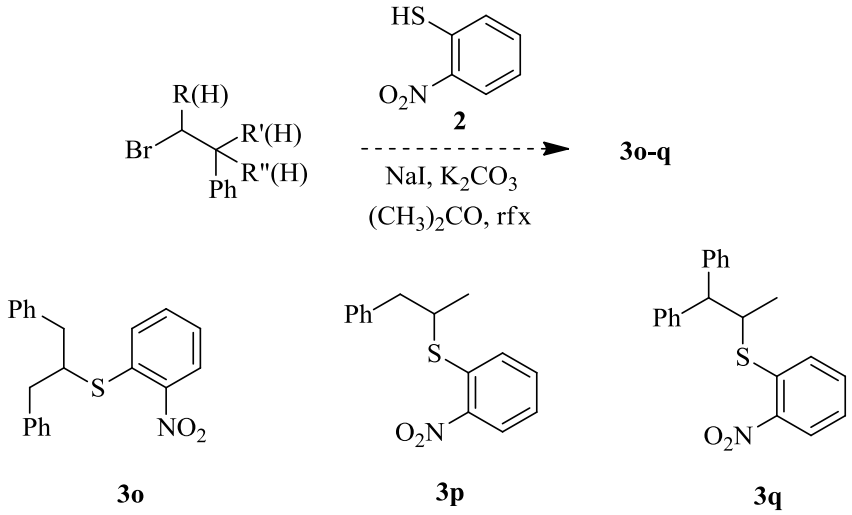

Scheme 2.15: Unsuccessful attempts to make sulfides **3o-q** under Finkelstein reaction conditions.

Further studies also included the unsuccessful attempt of making compound **4n** (**Scheme 2.16**). The alkene structure itself in the sulfoxide precursor **1n** is more likely to act as an electron source and will not give up the β-proton. Thus, the possibility of δ-elimination to generate the diene product **4n** is an interesting topic to study. However, as shown in **Scheme 2.16**, the δ-H might be too far away for the oxygen atom of sulfoxide in the transition state [28] and extraction of β-H was not possible. As a result, the desired compound can not be generated neither in refluxing chloroform nor in refluxing toluene.

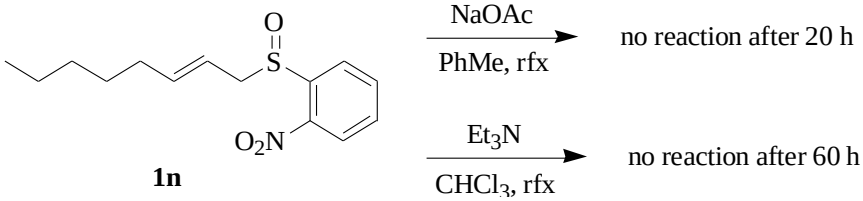

Scheme 2.16: Unsuccessful elimination reaction of sulfoxide **1n**.

Scheme 2.16 (con.)

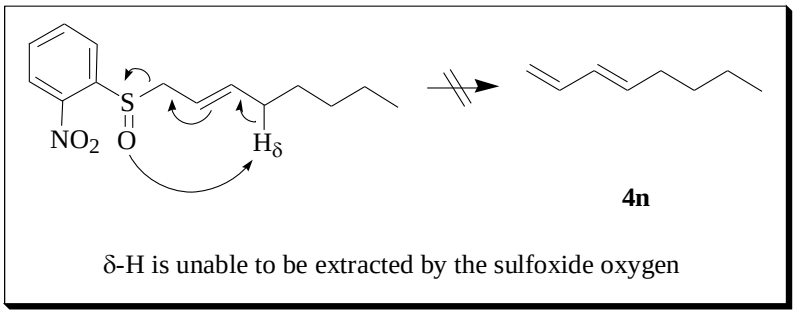

2.3 Conclusions

Compared with using traditional selenoxides to prepare alkenes, using phenyl sulfoxides has several advantages including lower cost and lower toxicity. Several phenyl sulfoxides **1a-n** were prepared and the chemistry of the precursors was investigated. It was found that the effects of nitro group proved to be essential for the reaction, and the optical precursor is the *o*-nitro phenyl sulfoxide. A typical procedure includes the addition of NaOAc which can absorb the sulfenic acid **5** during the toluene reflux. Confirmed by ^{1}H NMR, the alkene product was obtained with high purity before performing further chromatography purification.

The stereoselectivity of these reactions were also examined on several branched precursors and it is noticed the elimination tends to occur at the more acidic β-H. While the acidity was increased by an adjacent benzyl ester group, only highly substituted alkene product was obtained. Further, when bulky groups were present in the five-membered-ring transition state, it was discovered that the regioselectivity of the thermal β-elimination will generate only (*E*)-isomer product as less crowded isomers are more favored.

It was also shown that precursor **1k** can undergo elimination at room temperature. The mechanism of this reaction was rationalized. It is believed that the repulsion between the *o*-nitro group can push the oxygen atom on the sulfoxide more closely to the β-H atom in the transition state. In addition, the repulsion between the bulky β-substitution and the phenyl sulfenic group can facilitate the leaving of the byproduct. Lastly, it is likely the increase in acidity of β-H also enhanced the elimination rate.

The optimized synthetic sequence (2-3 steps) has several general features including: (1) similar to selenoxide precursors, the unique yellow color of intermediate (sulfide) observed on the silica gel column and ease of purification; (2) the *o*-nitro phenyl sulfoxide can undergo with high yield under toluene reflux; and (3) the thermal β-elimination provide the olefin products in high purity after simple filtration. The *o*-nitro phenyl sulfoxide precursor can be used as effective precursors to introduce unsaturated bond into the structure of interest.

2.4 Alkenes as Potential Anti-Cancer Agents

2.4.1 Bromoenol lactones to inhibit $iPLA_2$

The haloenol lactone family is known by many researchers as suicide substrates of chymotrypsin and related serine proteases [4]. Bromoenol lactones (BEL), a subset of the haloenol lactone family, are suicide substrates of other enzymes including group VI Ca^{2+}-independent phospholipase A_2 ($iPLA_2$) [29]. It has been reported that $iPLA_2$ can cause apoptosis through a series of biochemical reactions, leading to the increased interest to design novel BEL analogues as anticancer agents [30]. In this project, a series of bromoenol lactones (BEL) analogues were designed for testing as inhibitors of $iPLA_2$ phospholipases in prostate cell lines, including substituted aryl analogues and the

anthracene derivative **7** which we hope could be useful to identify the target of lactones via its unique fluorescent properties (**Figure 2.16**).

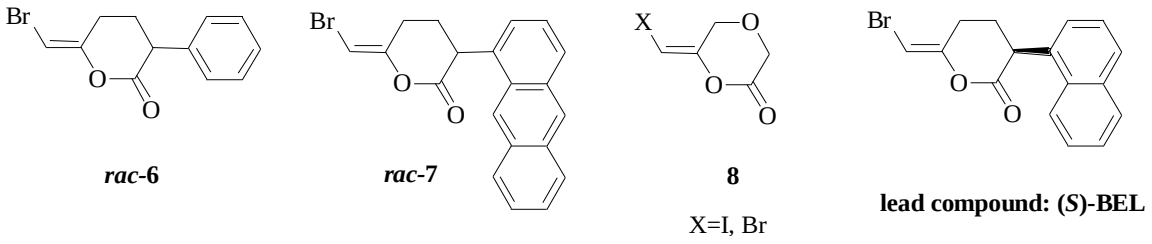

Figure 2.16: Chemical structures of BEL analogues.

2.4.2 Mechanism-based inhibition

Mechanism based inhibition of $iPLA_2$ has been proposed in previous studies of BEL [29]. As illustrated in **Figure 2.17**, at the active site, the haloenol lactone is first hydrolyzed by the protease enzyme causing an acyl transfer to the serine's hydroxyl group [31]. The released highly electrophilic intermediate finally alkylates the nucleophilic residue. As a result, the enzyme is irreversibly deactivated.

2.4.3 The synthetic route to make phenyl analogue 6

The synthesis of phenyl analogue was accomplished via a two-step process. At first, the acid precursor *rac*-**9** was prepared from phenyl acetic acid via classical, base-generated metal enolate chemistry [32]. With the help of LDA, the 4-bromo-but-1-yne tends to react at α-carbon instead of the carbonyl oxygen. In this reaction, 2 equiv of LDA was used since phenyl acetic acid starting material requires 1 extra equiv of lithium base [33]. The low yield (11%) may be because the reaction temperature was not low enough and unwanted self condensation may occur. The designed phenyl analogue *rac*-**6** was finally formed by a standard *E*-specific haloenol lactonization procedure [34]. The

stereoselective halolactonization of the acetylenic acid took place with *N*-halosuccinimides in the presence of aqueous potassium carbonate in dichloromethane (**Scheme 2.17**).

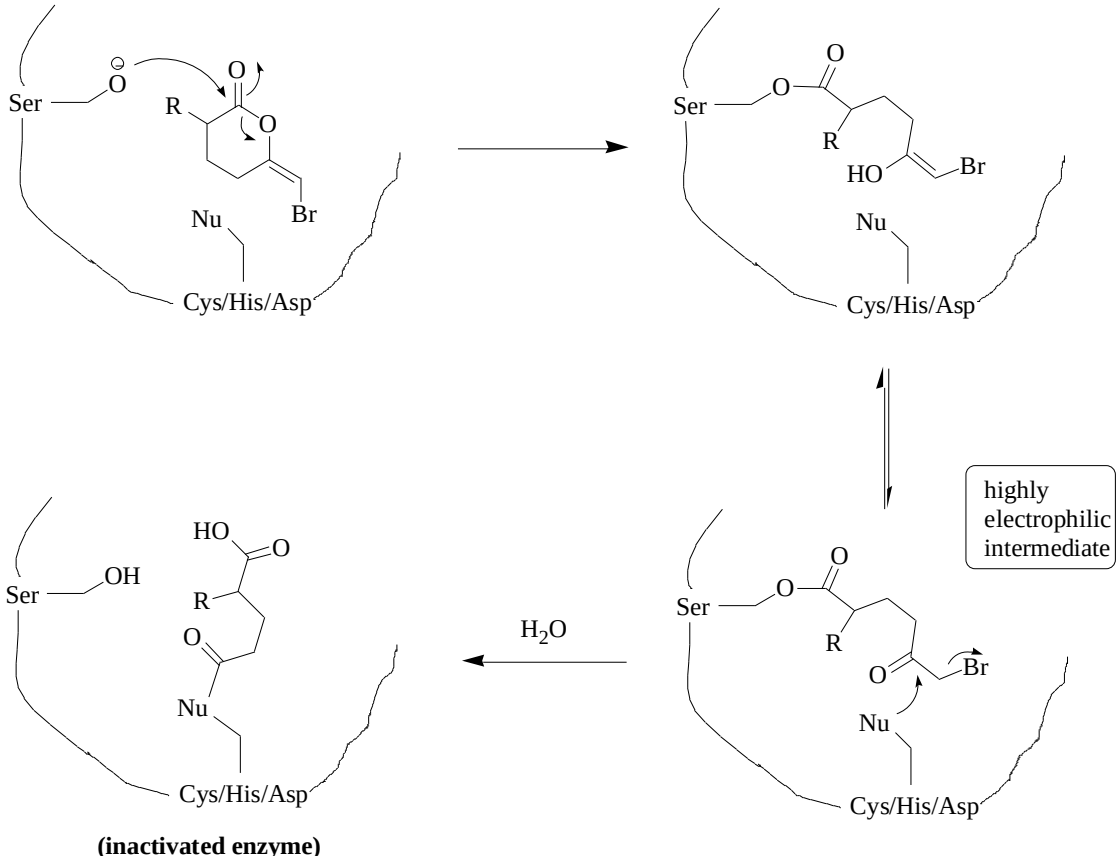

Figure 2.17: Mechanism-based serinase (Ser) inhibition of haloenol pyran-2-ones: suitably-positioned nucleophilic (Nu) residues are located near the active site, which can be covalent attachment by the powerful alkylating agent, i.e., lactone. These nuleophiles can be divideded into two classes: irreversible (e.g., -SH of Cys, -NH of His) and reversible (e.g., -CO_2H of Asp).

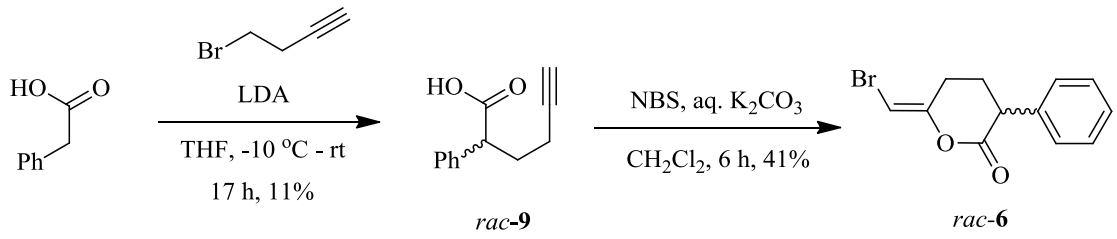

Scheme 2.17: Synthetic route to make phenyl analogue **6**.

2.4.4 The synthetic route to make anthracene bromoenol lactone analogue 7

After obtaining the phenyl analogue, the attachment of a luminescent group to the bromoenol lactone for bio-imaging applications was attempted. As illustrated in **Scheme 2.18**, the sulfate salt of anthroquinoyl diazonium **10** was prepared via nitrosation of 1-aminoanthroquinone with nitrous acid (which was in situ generated by mixing concentrated sulfuric acid and finely ground sodium nitrite powder below 10 °C) [35]. The resulting intermediate **10** was then diazotized and reacted with 1,1-dichloroethene in MeOH to give methyl anthraquinone-1-acetate **11**. Hydrolysis was followed with 2N aqueous NaOH giving anthraquinone-1-acetic acid **12** in quantitative yield [36]. Finally, anthracene-1-acetic acid **13** was formed by Zn reduction [37].

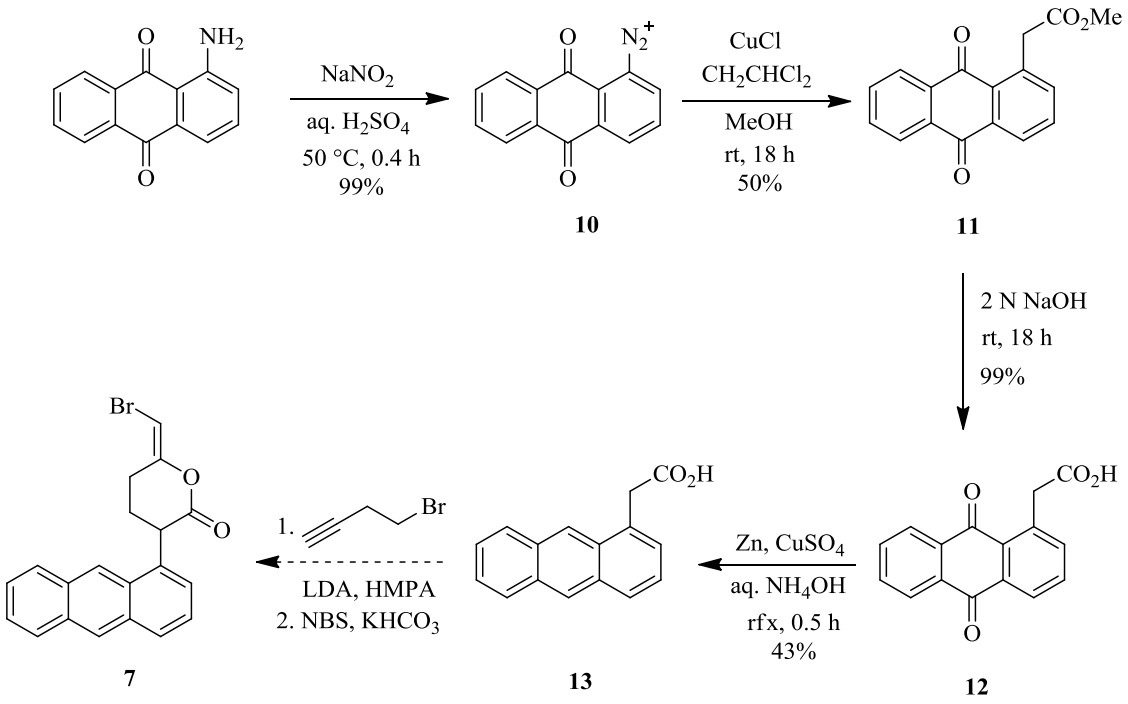

Scheme 2.18: Designed synthetic route to make anthracene BEL analogue **7**.

Notably, during the preparation of the anthraquinone-1-acetic acid **13**, besides visualization of product spot under short-wavelength (254 nm) as a black-brown dot, a very strong blue fluorescence can also be seen under long-wavelength (365 nm) (**Figure 2.18**) [38]. At the longer wavelength, the fused anthracene ring system conferred the illuminescence due to the large degree of conjugation found in molecule.

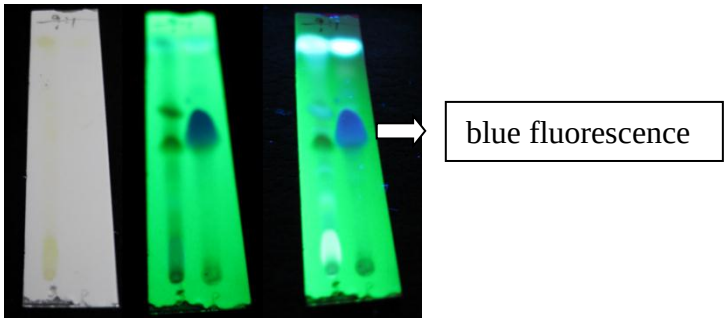

Figure 2.18: The TLC plate of reaction to make compound **13**.

As illustrated in **Table 2.02**, many reaction conditions have been studied, including the similar procedure to make *rac*-**6** (1 equiv S.M., 2 equiv LDA, 0.58 equiv HMPA, 1.04 equiv bromide, 0 °C – rt). The unique purple color was observed when a THF solution of *n*-BuLi was cannulated slowly into the reaction flask containing starting material (entry 2 and 3); however none produced the designed product **14**. The reaction failure may be due to the decomposition of the chemical before using in the reaction. It is believed the reagent used in this reaction may have decomposed. Neither LDA [39] nor *n*-BuLi [40] was as reactive as they were purchased over a year prior.

Table 2.02: Attempts to make compound **14**.

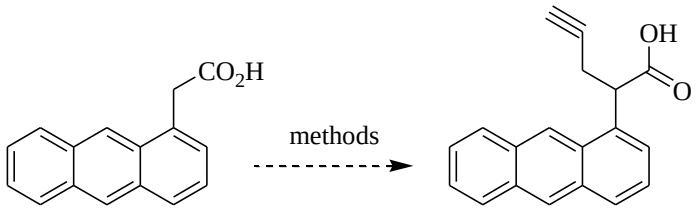

13 **14**

entry	reaction conditions	reaction time	Results
1	2 equiv LDA, 3 equiv HMPA, THF	0 °C – rt	0%
2	2 equiv *n*-BuLi, THF, 4 Å M.S.	0 °C – rt	0%
3	2 equiv *n*-BuLi, THF, 4 Å M.S., N_2	0 °C – rt	0%
4	2.5 equiv LDA, 0.52 equiv HMPA, THF, Ar	0 °C – rt	0%

2.4.5 The synthetic route to make analogue 8

The analogue with an additional oxygen atom in the lactone ring was also designed. The synthesis used a similar *E*-specific haloenol lactonization procedure to generate the pyranone analogues (*N*-iodosuccinimides for **8b**, *N*-bromosuccinimides for **8a**). The acid precursor **16** was prepared from propargyl alcohol and the bromoacetic acid *tert*-butyl ester via traditional Williamson synthesis [41]. Several conditions were tried and the best reaction result was obtained with NaH after stirring at room temperature for 48 hours.

The following cleavage of the *tert*-butoxycarbonyl (*t*-BOC) protecting group proceeded in excellent yields with the triethylsilane and trifluoroacetic acid (Et_3SiH/TFA) system in dichloromethane solution [42]. However, the attempt to make the final compound was not successful. Although some new, less polar spots were observed on $KMnO_4$ staining TLC, no product was obtained after chromatography. It is believed the designed compounds **8a** and **8b** may be too unstable to survive the silica gel column

which is acidic enough to cause the decomposition of the lactone during the purification (**Scheme 2.19**).

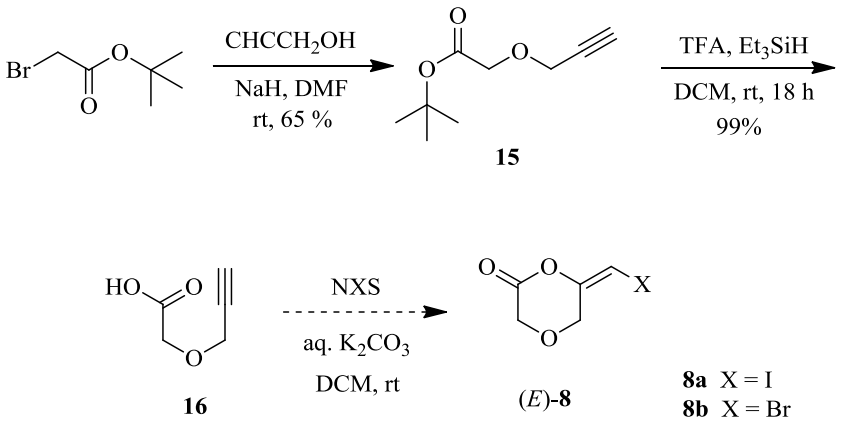

Scheme 2.19: Synthetic route to make haloenol lactones **8.**

2.4.6 Haloenol lactone as potential inhibitor against human prostate cancers.

Haloenol pyran-2-one (**BEL** and **6**) were evaluated as inhibitors of cell growth in two different prostate human cancer cell lines (PC-3 and LNCaP) in the laboratory of Dr. Brian S. Cummings (University of Georgia, Department of Pharmaceutical and Biomedical Science) by Jason N. Mock. Minimum inhibitory concentrations (IC_{50}s) were determined by MTT staining for the haloenol pyranones (*rac*-BEL, *rac*-**6**) against LNCaP cells, and the more resistant PC-3 human prostate cancer cell line. Activity comparisons of BEL to the substituted aryl analogue *rac*-**6** showed slightly enhanced activities with IC_{50}s ranging from 6-27 µM against PC-3 (**Table 2.03**) [32]. With this result, the usage of haloenol pyranones and morpholinones may serve as valuable research tools in the study of mammalian tumorigenesis.

Table 2.03: IC_{50}s (μM) against human prostate cancers after 24, 48, and 72 h exposure to haloenol inhibitors [a,b].

compd	LNCaP			PC-3		
	24 h	48 h	72 h	24 h	48 h	72 h
rac-BEL	13	5	9	34	26	14
rac-**6**	31	5	4	27	10	6

[a] Data represent the calculated IC_{50} using data assessed 3-5 experiments ran in duplicate using separate passages of cells assessing alteration in MTT staining;
[b] Testing performed by Jason N. Mock in the laboratory of Dr. Brian S. Cummings.

2.5 Experimental

In general, reagents and solvents were used as purchased without further purification. Reaction products were purified by column chromatography on silica gel (60-100 mesh) and visualized by UV on TLC plates (silica gel 60 F_{254}). Melting points were determined with a melting point apparatus and were left uncorrected. Mass spectrometry was performed by electrospray ionization (ESI). ^{1}H and ^{13}C NMR spectra were recorded on a Varian Inova 500 MHz spectrometer. Chemical shifts were expressed in δ (ppm) values with tetramethylsilane or residual $CHCl_3$/DMSO as an internal standard. The designation "ABq" for a ^{1}H NMR peak indicates that a peak was one partner of an AB quartet; if additional splitting was observed, they are noted after the ABq designation (e.g., ABqd). Copies of NMR spectra may be found in APPENDIX A.

Preparation of *o*-nitrothiophenol 2. To a suspension of *o*-nitro phenyl disulfide (0.805 g, 2.61 mmol) in 20 mL of degassed THF was added PPh_3 (1.03 g, 3.92 mmol), 2-mercaptoethanol (184 μL, 2.61 mmol), and 470 μL of H_2O (26.1 mmol). The solution was stirred at 50 °C for 6 hours. After cooling to room temperature, the mixture was concentrated, redissolved in DCM, washed with brine, and then, the organic layer was

dried over Na_2SO_4, filtered, and evaporated. The crude orange oil was separated by flash chromatography on silica gel (9:1 hexanes:EtOAc) to give pure *o*-nitrothiophenol (bright yellow band, 653 mg, 4.21 mmol) in 80.5% yield. mp 40-42 °C.

Preparation of sulfides 3; general procedure. To a suspension of NaI (0.4 mmol), K_2CO_3 (1 mmol), and bromide **1** (1 mmol) in dry acetone (10 mL) was added 1.05 mmol equiv of *o*-nitrothiophenol **2**. The mixture was heated under reflux until the reaction was complete (checked by TLC). The solution was then filtered, evaporated, redissolved in DCM, washed with brine, and then, the organic layer was dried over Na_2SO_4, filtered, and evaporated. The sulfides **3** were separated by flash chromatography on silica gel in accordance to product R_f values.

Benzyl 11-(2-nitrophenylthio)undecanoate (3a): Yield: 670 mg, 88%; yellow oil; TLC (SiO_2) R_f 0.48 (6:1 hexanes:EtOAc); ^{1}H NMR (500 MHz, $CDCl_3$) δ 8.17 (dd, 1H, *J* = 7.0, 1.5 Hz), 7.52 (dt, 1H, *J* = 8.0, 1.5 Hz), 7.38 (d, 1H, *J* = 8.0 Hz), 7.34-7.29 (m, 5H), 7.21 (dt, 1H, *J* = 8.0, 1.0 Hz), 5.09 (s, 2H), 2.92 (t, 2H, *J* = 7.5 Hz), 2.33 (t, 2H, *J* = 7.5 Hz), 1.71 (qnt, 2H, *J* = 7.5 Hz), 1.62 (qnt, 2H, *J* = 7.5 Hz), 1.45 (qnt, 2H, *J* = 7.5 Hz), 1.30-1.26 (m, 10H); ^{13}C NMR (125 MHz, $CDCl_3$) δ 173.7, 146.0, 138.4, 136.2, 133.5, 128.6, 128.2, 126.7, 126.2, 124.3, 66.1, 34.4, 32.4, 29.4, 29.3, 29.2, 27.9, 25.0; ESI-HRMS calcd. for $C_{24}H_{31}NO_4S$ $[M+H]^+$ 430.2052, found 430.2041.

Benzyl 5-(2-nitrophenylthio)pentanoate (3b): Yield: 74 mg, 80%; yellow oil; TLC (SiO_2) R_f 0.23 (6:1 hexanes:EtOAc); ^{1}H NMR (500 MHz, $CDCl_3$) δ 8.18 (d, 1H, *J* = 8.5 Hz), 7.52 (t, 1H, *J* = 7.5 Hz), 7.37-7.31 (m, 4H), 7.25-7.20 (m, 3H), 5.10 (s, 2H), 2.94 (t, 2H, *J* = 7.0 Hz), 1.82 (qnt, 2H, *J* = 7.5 Hz), 1.76 (qnt, 2H, *J* = 7.5 Hz); ESI-HRMS calcd. for $C_{18}H_{20}NO_4S$ $[M+H]^+$ 346.1180, found 346.1112.

1-(11-(2-Nitrophenylthio)undecylthio)benzene (3c): Yield: 664 mg, 93%; yellow solid, mp 38-39 °C; TLC (SiO_2) R_f 0.47 (9:1 hexanes:EtOAc); ^{1}H NMR (500 MHz, $CDCl_3$) δ 8.16 (d, 1H, *J* = 8.5 Hz), 7.51 (t, 1H, *J* = 7.5 Hz), 7.37 (d, 1H, *J* = 8.0 Hz), 7.29-7.19 (m, 5H), 7.13 (t, 1H, *J* = 7.5 Hz), 2.91 (t, 2H, *J* = 7.5 Hz), 2.88 (t, 2H, *J* = 7.5 Hz), 1.71 (qnt, 2H, *J* = 7.5 Hz), 1.61 (qnt, 2H, *J* = 7.5 Hz), 1.48-1.42 (m, 2H), 1.41-1.36 (m, 2H), 1.32-1.24 (m, 10H); ^{13}C NMR (125 MHz, $CDCl_3$) δ 137.3, 133.5, 129.1, 129, 126.8, 126.4, 125.8, 124.4, 33.8, 32.6, 29.6, 29.4, 29.3, 29, 28.1.

1-(6-(Phenylthio)hexylthio)-2-nitrobenzene (3d): Yield: 253 mg, 72%; yellow solid, mp 39-40 °C; R_f 0.49 (9:1 hexanes:EtOAc); ^{1}H NMR (500 MHz, $CDCl_3$) δ 8.21 (dd, 1H, *J* = 10.0, 2.0 Hz), 7.54 (dt, 1H, *J* = 10.5, 2.0 Hz), 7.40-7.15 (m, 7H), 2.96-2.91 (m, 4H), 1.76-1.65 (m, 4H), 1.51-1.48 (m, 4H); ^{13}C NMR (125 MHz, $CDCl_3$) δ133.6, 129.2, 129, 126.7, 126.4, 125.9, 124.5, 33.7, 32.4, 29.1, 28.8, 28.5, 27.9; ESI-HRMS calcd. for $C_{18}H_{21}NO_2S_2$ $[M+H]^+$ 348.1086, found 348.1095.

1-(11-(2-Nitrophenylthio)undecylthio)-4-methylbenzene (3e): Yield: 96.5 mg, 56%; yellow solid, mp 66-67 °C; TLC (SiO_2) R_f 0.51 (9:1 hexanes:EtOAc); ^{1}H NMR (500 MHz, $CDCl_3$) δ 8.18 (d, 1H, *J* = 8.0 Hz), 7.53 (t, 1H, *J* = 7.0 Hz), 7.39 (d, 1H, *J* = 8.5 Hz), 7.25-7.20 (m, 3H), 7.08-7.07 (m, 2H), 2.94 (t, 2H, *J* = 7.5 Hz), 2.86 (t, 2H, *J* = 7.5 Hz), 2.30 (s, 3H), 1.72 (qnt, 2H, *J* = 7.5 Hz), 1.60 (qnt, 2H, *J* = 7.5 Hz), 1.50-1.42 (m, 2H), 1.41-1.36 (m, 2H), 1.36-1.22 (m, 10H); ^{13}C NMR (125 MHz, $CDCl_3$) δ 138.5, 136.0, 133.5, 133.3, 129.9, 129.8, 126.8, 126.3, 124.4, 34.5, 32.6, 29.6, 29.5, 29.4, 29.4, 29.3, 29.2, 29.0, 28.0, 21.2.

1-(11-(2-Nitrophenylthio)undecylthio)-4-chlorobenzene (3f): Yield: 343 mg, 76% (over 2 steps); yellow solid, mp 83-84 °C; TLC (SiO_2) R_f 0.5 (9:1 hexanes:EtOAc); ^{1}H

NMR (500 MHz, $CDCl_3$) δ 8.20 (d, 1H, *J* = 8.5 Hz), 7.54 (t, 1H, *J* = 7.5 Hz), 7.40 (d, 1H, *J* = 8.5 Hz), 7.26-7.22 (m, 5H), 2.95 (t, 2H, *J* = 7.5 Hz), 2.88 (t, 2H, *J* = 7.5 Hz), 1.74 (qnt, 2H, *J* = 7.5 Hz), 1.63 (qnt, 2H, *J* = 7.5 Hz), 1.48 (qnt, 2H, *J* = 7.5 Hz), 1.41 (qnt, 2H, *J* = 7.5 Hz), 1.36-1.26 (m, 10H); ^{13}C NMR (125 MHz, $CDCl_3$) δ 138.5, 135.8, 133.5, 131.8, 130.4, 129.1, 126.8, 126.3, 124.5, 34.1, 32.6, 29.6, 29.4, 29.3, 29.2, 28.9, 28.1.

1-(11-(2-Nitrophenylsulfinyl)undecylsulfinyl)-4-nitrobenzene (3g): Yield: 96.5 mg, 53% (over 2 steps); yellow solid, mp 66-67 °C; TLC (SiO_2) R_f 0.26 (9:1 hexanes:EtOAc); ^1H NMR (500 MHz, $CDCl_3$) δ 8.18 (d, 1H, *J* = 8.0 Hz), 8.09 (d, 2H, *J* = 9.0 Hz), 7.52 (t, 1H, *J* = 8.0 Hz), 7.38 (d, 1H, *J* = 8.5 Hz), 7.28 (d, 1H, *J* = 9.0 Hz), 7.22 (t, 1H, *J* = 8.0 Hz), 7.18, (t, 1H, *J* = 8.0 Hz), 2.95 (t, 2H, *J* = 7.5 Hz), 2.89 (t, 2H, *J* = 7.5 Hz), 1.71-1.63 (m, 4H), 1.45-1.37 (m, 4H), 1.26-1.19 (m, 10H); ^{13}C NMR (125 MHz, $CDCl_3$) δ 148.4, 133.6, 126.9, 126.8, 126.3, 126.2, 124.5, 124.1, 32.6, 32.1, 29.6, 29.3, 29.2, 29, 28.7, 28.0.

1-(6-(4-Nitrophenylthio)hexylthio)-2-nitrobenzene (3h): Yield: 156.7 mg, 98%; yellow solid, mp 83-84 °C; TLC (SiO_2) R_f 0.68 (1:1 hexanes:EtOAc); ^1H NMR (500 MHz, $CDCl_3$) δ 8.18 (d, 1H, *J* = 8.0 Hz), 8.10 (d, 2H, *J* = 8.5 Hz), 7.52 (t, 1H, *J* = 7.5 Hz), 7.37 (d, 1H, *J* = 8.5 Hz), 7.29 (d, 2H, *J* = 8.0 Hz), 7.21 (m, 1H), 2.99 (t, 2H, *J* = 7.0 Hz), 2.95 (t, 2H, *J* = 7.0 Hz), 1.76-1.72 (m, 4H), 1.54 (m, 4H); ESI-HRMS calcd. for $C_{18}H_{20}N_2O_4S_2$ $[M+H]^+$ 393.0937, found 393.0943.

Benzyl 2-(2-nitrophenylthio)butanoate (3i): Yield: 166 mg, 78%; yellow oil; TLC (SiO_2) R_f 0.34 (9:1 hexanes:EtOAc); ^1H NMR (500 MHz, $CDCl_3$) δ 8.07 (dd, 1H, *J* = 8.0, 1.0 Hz), 7.51 (d, 1H, *J* = 8.0 Hz), 7.39 (dt, 1H, *J* = 8.0, 1.0 Hz), 7.31-7.21 (m, 6H), 5.17 and 5.09 (ABq, 2H, Δ*v* = 40.0 Hz, *J* = 12.0 Hz), 3.87 (t, 1H, *J* = 7.5 Hz), 2.09-2.00 (m,

1H), 1.96-1.87 (m, 1H), 1.06 (t, 3H, J = 7.5 Hz); ^{13}C NMR (125 MHz, $CDCl_3$) δ 171.7, 147.0, 135.4, 135.1, 133.5, 132.2, 132.1, 128.8, 128.7, 128.5, 125.9, 125.8, 67.3, 50.6, 25.2, 12.1.

Benzyl 2-(2-nitrophenylthio)-3-methylbutanoate (3j): Yield: 489 mg, 56%; yellow solid, mp 54-55 °C; TLC (SiO_2) R_f 0.50 (9:1 hexanes:EtOAc); ^{1}H NMR (500 MHz, $CDCl_3$) δ 7.99 (dd, 1H, J = 8.0, 1.0 Hz), 7.46 (d, 1H, J = 8.0 Hz), 7.33 (dt, 1H, J = 8.0, 1.0 Hz), 7.26-7.21 (m, 5H), 7.16 (t, 1H, J = 7.5 Hz), 5.13 and 5.05 (ABq, 2H, Δv = 40.0 Hz, J = 12.0 Hz). 3.72 (d, 1H, J = 8.5 Hz), 2.24 (oct, 1H, J = 7.0 Hz). 1.12 (d, 3H, J = 7.0 Hz), 1.04 (d, 3H, J = 7.0 Hz); ^{13}C NMR (125 MHz, $CDCl_3$) δ 185.4, 135.5, 133.5, 129.0, 128.8, 128.7, 126.0, 125.8, 67.4, 56.9, 31.0, 20.8.

Benzyl 2-(2-nitrophenylthio)-3-phenylpropanoate (3k): Yield: 199 mg, 83%; yellow oil; TLC (SiO_2) R_f 0.50 (7:1 hexanes:EtOAc); ^{1}H NMR (500 MHz, $CDCl_3$) δ 8.06 (d, 1H, J = 8.5 Hz), 7.53 (d, 1H, J = 8.0 Hz), 7.38 (dt, 1H, J = 7.5, 1.5 Hz), 7.27-7.21 (m, 7H), 7.18-7.17 (m, 2H), 7.13-7.11 (m, 2H), 5.07 and 4.98 (ABq, 2H, Δv = 45.0 Hz, J = 12.0 Hz), 4.18 (dd, 1H, AB*X*, J_{AX} = 9.0 Hz, J_{BX} = 6.0 Hz), 3.29 (ABdq, 1H, A*B*X, J_{AB} = 14.0 Hz, J_{BX} = 6.0 Hz), 3.13 (ABdq, 1H, *A*BX, J_{AB} = 14.0 Hz, J_{AX} = 9.0 Hz); ^{13}C NMR (125 MHz, $CDCl_3$) δ 171.2, 136.9, 135.2, 133.6, 129.2, 128.9, 128.7, 128.6, 128.5, 127.4, 126.2, 126, 67.5, 50.7, 37.9. ESI-HRMS calcd. for $C_{22}H_{19}NO_4S$ $[M+Na]^+$ 416.0932, found 416.0920.

Benzyl 3-(2-nitrophenylthio)butanoate (3l): Yield: 179 mg, 66%; yellow oil; TLC (SiO_2) R_f 0.52 (25:1 hexanes:EtOAc); ^{1}H NMR (500 MHz, $CDCl_3$) δ 8.08 (d, 1H, J = 8.0 Hz), 7.54-7.49 (m, 2H), 7.36-7.29 (m, 5H), 7.26 (t, 1H, J = 6.5 Hz), 5.13 (s, 2H), 3.88 (m, 1H), 2.76 (A*B*dq, 1H, J_{AB} = 16.0 Hz, J = 5.0 Hz), 2.54 (*A*Bdq, 1H, J_{AB} = 16.0 Hz, J = 8.5

Hz), 1.41 (d, 3H, *J* = 6.5 Hz); ^{13}C NMR (125 MHz, $CDCl_3$) δ 170.9, 147.5, 135.6, 135.1, 133.5, 128.7, 128.5, 128.4, 126.1, 125.5, 66.8, 41.1, 37.1, 20.4.

Benzyl 5-(2-nitrophenylthio)hexanoate (3m): Yield: 250 mg, 99%; yellow oil; TLC (SiO_2) R_f 0.62 (3:1 hexanes:EtOAc); ^{1}H NMR (500 MHz, $CDCl_3$) δ 8.08 (d, 1H, *J* = 8.5 Hz), 7.50 (dt, 1H, *J* = 7.0, 1.0 Hz), 7.41 (d, 1H, *J* = 8.0 Hz), 7.33-7.29 (m, 5H), 5.09 (s, 2H), 3.38 (m, 1H), 2.37 (t, 2H, *J* = 7.0 Hz), 1.85-1.79 (m, 2H), 1.75-1.68 (m, 1H), 1.64-1.56 (m, 1H), 1.35 (d, 3H, *J* = 6.5 Hz); ^{13}C NMR (125 MHz, $CDCl_3$) δ 173.2, 136.1, 133.2, 128.8, 128.5, 126.1, 125.2, 66.5, 40.9, 25.7, 34.1, 22.7, 20.5; ESI-HRMS calcd. for $C_{19}H_{21}NO_4S$ $[M+Na]^+$ 382.1083, found 382.1082.

Preparation of sulfoxides 1; general procedure. To a stirring solution of sulfides **3a-n** (1 mmol) in DCM (10 mL) was added *m*-CPBA (1.25 mmol equiv) in 5 mL of DCM while the reaction temperature was maintained at 0 °C (or in the case of making disulfides **3c-h**, 2.50 equiv of peroxide was used). The reaction mixture was then stirred at room temperate for 2.5 hours. After quenching of the solution with 5% $NaHCO_3$ (20 mL), the mixture was extracted twice with DCM. The combined organic layer was dried over Na_2SO_4, filtered, and evaporated. The crude sulfoxides **1** were separated by flash chromatography on silica gel in accordance to product R_f values.

Benzyl 11-(2-nitrophenylsulfinyl)undecanoate (1a): Yield: 532 mg, 74%; yellow solid, mp 37-38 °C; TLC (SiO_2) R_f 0.43 (3:1 hexanes:EtOAc); ^{1}H NMR (500 MHz, $CDCl_3$) δ 8.31-8.28 (m, 2H), 7.93 (t, 1H, *J* = 7.5 Hz), 7.68 (t, 1H, *J* = 7.5 Hz), 7.32-7.28 (m, 5H), 5.09 (s, 2H), 3.15 (ddd, 1H, *J* = 13.0, 9.5, 7.0 Hz), 2.72 (ddd, 1H, *J* = 13.0, 9.5, 4.5 Hz), 2.32 (t, 2H, *J* = 7.5 Hz), 2.02-1.95 (m, 1H), 1.73-1.66 (m, 1H), 1.63-1.58 (qnt, 2H, *J* = 7.5 Hz), 1.51-1.46 (m, 1H), 1.41-1.35 (m, 1H), 1.30-1.24 (m, 10H); ^{13}C NMR (125 MHz,

$CDCl_3$) δ 173.8, 144.8, 144.0, 136.3, 135.5, 131.4, 128.7, 128.3, 126.9, 125.3, 66.2, 57.2, 34.4, 29.4, 29.4, 29.3, 29.2, 28.6, 25.2, 23.3; ESI-HRMS calcd. for $C_{24}H_{32}NO_5S$ $[M+H]^+$ 446.1996, found 446.2004.

Benzyl 5-(2-nitrophenylsulfinyl)pentanoate (1b): Yield: 85.5 mg, 86%; yellow solid, mp 60-61 °C; TLC (SiO_2) R_f 0.25 (1:1 hexanes:EtOAc); ^1H NMR (500 MHz, $CDCl_3$) δ 8.28 (d, 1H, *J* = 8.0 Hz), 8.25 (d, 1H, *J* = 8.0 Hz), 7.91 (t, 1H, *J* = 7.5 Hz), 7.67 (t, 1H, *J* = 7.5 Hz), 7.34-7.27 (m, 5H), 5.07 (s, 2H), 3.17 (ddd, 1H, AA'M*X*, J_{MX} = 13.5 Hz, J_{AX} = 9.0 Hz, $J_{A'X}$ = 7.0 Hz), 2.73 (ddd, 1H, AA'*M*X, J_{MX} = 13.5, J_{AM} = 9.0 Hz, $J_{A'M}$ = 4.5 Hz), 2.38 (t, 2H, *J* = 7.0 Hz), 2.02 (m, 1H, A*A'*MX), 1.86 (m, 1H, *A*A'MX), 1.75 (m, 2H); ^{13}C NMR (125 MHz, $CDCl_3$) δ 172.9, 144.7, 143.6, 136, 135.5, 131.5, 128.7, 128.4, 128.3, 126.9, 125.4, 66.4, 56.5, 33.8, 23.8, 22.7; ESI-HRMS calcd. for $C_{18}H_{20}NO_5S$ $[M+H]^+$ 362.1057, found 362.1067.

1-(11-(2-Nitrophenylsulfinyl)undecylsulfinyl)benzene (1c): Yield: 128 mg, 86%; yellow solid, mp 65-66 °C; TLC (SiO_2) R_f 0.05 (1:1 hexanes:EtOAc); ^1H NMR (500 MHz, $CDCl_3$) δ 8.23 (t, 2H, *J* = 9.0 Hz), 7.88 (t, 1H, *J* = 7.5 Hz), 7.63 (t, 1H, *J* = 7.5 Hz), 7.55-7.53 (m, 2H), 7.45-7.39 (m, 3H), 3.10 (ddd, 1H, *J* = 13.0, 10.0, 7.0 Hz), 2.71 (t, 2H, *J* = 8.0 Hz), 2.66 (ddd, 1H, *J* = 13.0, 9.5, 5.0 Hz), 1.99-1.87 (m, 1H), 1.70-1.59 (m, 2H), 1.57-1.49 (m, 1H), 1.47-1.38 (m, 1H), 1.36-1.26 (m, 3H), 1.26-1.16 (m 10H); ^{13}C NMR (125 MHz, $CDCl_3$) δ 144.6, 144.0, 143.8, 135.4, 131.4, 130.9, 129.2, 126.8, 125.2, 124.0, 57.3, 57.1, 29.3, 29.2, 29.1, 28.6, 28.4, 23.2; ESI-HRMS calcd. for $C_{23}H_{31}NO_4S_2$ 450.1773 $[M+H]^+$, found 450.1773.

1-(6-(Phenylsulfinyl)hexylsulfinyl)-2-nitrobenzene (1d): Yield: 92.7 mg, 70%; yellow solid, mp 104-105 °C; TLC (SiO_2) R_f 0.26 (1:1 hexanes:EtOAc); ^1H NMR (500 MHz,

$CDCl_3$) δ 8.26 (d, 1H, *J* = 8.0 Hz), 8.22 (d, 1H, *J* = 8 Hz), 7.89 (t, 1H, *J* = 7.5 Hz), 7.65 (t, 1H, *J* = 7.5 Hz), 7.56-7.54 (m, 2H), 7.47-7.41 (m, 3H), 3.14-3.07 (m, 1H), 2.72 (t, 2H, *J* = 7.5 Hz), 2.69-2.64 (m, 1H), 1.99-1.90 (m, 1H), 1.76-1.62 (m, 2H), 1.60-1.54 (m, 1H), 1.52-1.37 (m, 4H); ^{13}C NMR (125 MHz, $CDCl_3$) δ 144.7, 144.0, 143.7, 135.5, 131.5, 131.1, 129.3, 126.8, 125.3, 124.1, 57.0, 56.9, 28.4, 28.1, 23.1, 22.0; ESI-HRMS calcd. for $C_{18}H_{21}NO_4S_2$ $[M+H]^+$ 380.0985, found 380.0990.

1-(11-(2-Nitrophenylsulfinyl)undecylsulfinyl)-4-methylbenzene (1e): Yield: 61 mg, 62%; yellow oil; TLC (SiO_2) R_f 0.20 (1:1 hexanes:EtOAc); ^{1}H NMR (500 MHz, $CDCl_3$) δ 8.24 (t, 2H, *J* = 8.5 Hz), 7.89 (t, 1H, *J* = 7.5 Hz), 7.64 (t, 1H, *J* = 7.5 Hz), 7.43 (d, 2H, *J* = 7.5 Hz), 7.25 (d, 2H, *J* = 7.5 Hz), 3.12 (ddd, 1H, *J* = 12.5, 9.5, 7.0 Hz), 2.74-2.65 (m, 3H), 1.98-1.89 (m, 1H), 1.69-1.59 (m, 2H), 1.57-1.50 (m, 1H), 1.49-1.39 (m, 1H), 1.37-1.28 (m, 3H), 1.25-1.17 (m, 10H); ^{13}C NMR (125 MHz, $CDCl_3$) δ 144.7, 143.8, 141.4, 140.8, 135.4, 131.4, 129.9, 126.8, 125.2, 124.1, 57.4, 57.1, 29.4, 29.3, 29.1, 28.7, 28.5, 23.2, 22.2, 21.5; ESI-HRMS calcd. for $C_{24}H_{34}NO_4S_2$ 464.1924 $[M+H]^+$, found 464.1910.

1-(11-(2-Nitrophenylsulfinyl)undecylsulfinyl)-4-chlorobenzene (1f): Yield: 130.1 mg, 70%; yellow oil; TLC (SiO_2) R_f 0.20 (1:1 hexanes:EtOAc); ^{1}H NMR (500 MHz, $CDCl_3$) δ 8.27 (t, 2H, *J* = 8.5 Hz), 7.92 (t, 1H, *J* = 7.5 Hz), 7.67 (t, 1H, *J* = 7.5 Hz), 7.52 (d, 2H, *J* = 8.5 Hz), 7.46 (d, 2H, *J* = 8.0 Hz), 3.17-3.11 (m, 1H), 2.74-2.67 (m, 3H), 1.99-1.92 (m, 1H), 1.71-1.64 (m, 2H), 1.59-1.51 (m, 1H), 1.50-1.43 (m, 1H), 1.40-1.31 (m, 2H), 1.29-1.20 (m, 11H); ^{13}C NMR (125 MHz, $CDCl_3$) δ 144.8, 144.0, 142.7, 137.2, 135.5, 131.4, 129.6, 126.9, 125.6, 125.3, 57.5, 57.3, 29.5, 29.4, 29.3, 29.2, 28.8, 28.5, 23.4, 22.2; ESI-HRMS calcd. for $C_{23}H_{30}ClNO_4S_2$ 484.1383 $[M+H]^+$ found 484.1383.

1-(11-(2-Nitrophenylsulfinyl)undecylsulfinyl)-4-nitrobenzene (1g): Yield: 87.5 mg, 86%; yellow solid, mp 82-83 °C; TLC (SiO_2) R_f 0.12 (1:1 hexanes:EtOAc); ^{1}H NMR (500 MHz, $CDCl_3$) δ 8.32 (d, 2H, *J* = 7.5 Hz), 8.27 (d, 1H, *J* = 8.0 Hz), 8.24 (d, 1H, *J* = 8.0 Hz), 7.91 (t, 1H, *J* = 7.5 Hz), 7.76 (d, 2H, *J* = 8.5 Hz), 7.66 (t, 1H, *J* = 7.5 Hz), 3.12 (dt, 1H, *J* = 13.0, 6.5 Hz), 2.86-2.80 (m, 1H), 2.78-2.73 (m, 1H), 2.71-2.67 (m, 1H), 1.99-1.90 (m, 1H), 1.80-1.73 (m, 1H), 1.70-1.63 (m, 1H), 1.58-1.51 (m, 1H), 1.48-1.43 (m, 1H), 1.40-1.31 (m, 3H), 1.29-1.19 (m, 10H); ^{13}C NMR (125 MHz, $CDCl_3$) δ 151.9, 149.5, 144.7, 143.9, 135.5, 131.4, 126.9, 125.3, 125.2, 124.3, 57.3, 57.2, 29.4, 29.3, 29.2, 28.7, 28.5, 23.3, 22.0; ESI-HRMS calcd. for $C_{23}H_{30}N_2O_6S_2$ 495.1624 $[M+H]^+$ found 495.1624.

1-(6-(4-Nitrophenylsulfinyl)hexylsulfinyl)-2-nitrobenzene (1h): Yield: 89 mg, 77%; yellow solid, mp 86-88 °C; TLC (SiO_2) R_f 0.26 (1:1 hexanes:EtOAc); ^{1}H NMR (500 MHz, $CDCl_3$) δ 8.37 (d, 2H, *J* = 8.5 Hz), 8.30 (d, 1H, *J* = 8.0 Hz), 8.27 (d, 1H, *J* = 8.5 Hz), 7.94 (t, 1H, *J* = 7.5 Hz), 7.78 (d, 2H, *J* = 8.5 Hz), 7.69 (t, 1H, *J* = 7.5 Hz), 3.19-3.12 (m, 1H), 2.89-2.83 (m, 1H), 2.80-2.77 (m, 1H), 2.74-2.69 (m 1H), 2.06-1.98 (m, 1H), 1.90-1.81 (m, 1H), 1.77-1.69 (m, 1H), 1.65-1.44 (m, 5H); ^{13}C NMR (125 MHz, $CDCl_3$) δ 151.7, 149.7, 144.8, 143.8, 135.7, 131.6, 126.9, 125.4, 125.3, 124.5, 57.1, 56.9, 28.4, 28, 23.2, 21.9; ESI-HRMS calcd. for $C_{18}H_{21}N_2O_6S_2$ 450.1773 $[M+H]^+$ 425.0836, found 425.0837.

Benzyl 2-(2-nitrophenylsulfinyl)butanoate (1i): Yield: 140 mg, 89%; yellow oil; TLC (SiO_2) R_f 0.29 (3:1 hexanes:EtOAc); ^{1}H NMR (500 MHz, $CDCl_3$) δ 8.26 (dd, 1H, *J* = 8.0, 1.0 Hz), 8.04 (dd, 1H, *J* = 8.0, 1.5 Hz), 7.69 (dt, 1H, *J* = 8.0, 1.0 Hz), 7.55 (dt, 1H, *J* = 8.0, 1.5 Hz), 7.28-7.26 (m, 3H), 7.08-7.06 (m, 2H), 4.86 and 4.65 (ABq, 2H, Δ*v* = 105.0

Hz, *J* = 12.5 Hz), 3.94 (dd, 1H, *J* = 9.0, 7.0 Hz), 2.34-2.17 (m, 2H), 1.22 (t, 3H, *J* = 7.5 Hz); ^{13}C NMR (125 MHz, $CDCl_3$) δ 166.1, 164.9, 145.1, 141.4, 135.1, 131.8, 128.7, 128.6, 128.5, 127.8, 125.2, 67.7, 67.0, 21.1, 11.8; ESI-HRMS calcd. for $C_{17}H_{18}NO_5S$ $[M+H]^+$ 348.0900, found 348.0893.

Benzyl 2-(2-nitrophenylsulfinyl)-3-methylbutanoate (1j): Yield: 68.4 mg, 77% (an inseparable mixture of diastereomers); yellow solid, mp 101-102 °C; TLC (SiO_2) R_f 0.33 (3:1 hexanes:EtOAc); ESI-HRMS calcd. for $C_{18}H_{20}NO_5S$ $[M+H]^+$ 362.1057, found 362.1050; **(±) *anti*-1j** (major) ^{1}H NMR (500 MHz, $CDCl_3$) δ 8.27 (d, 1H, *J* = 8.0 Hz), 8.20 (d, 1H, *J* = 8.0 Hz), 7.85 (t, 1H, *J* = 7.5 Hz), 7.63 (t, 1H, *J* = 7.5 Hz), 7.30-7.23 (m, 4H), 7.01 (m, 1H), 4.98 and 4.87 (ABq, 2H, Δ*v* = 55.0 Hz, *J* = 12.0 Hz), 3.42 (d, 1H, AA'B*C*, J_{BC} = 7.0 Hz), 2.56 (app sxt, 1H, AA'*B*C, *J* = 7.0 Hz), 1.09 (d, 3H, A*A'*BC, $J_{A'B}$ = 7.0 Hz), 1.05 (d, 3H, *A*A'BC, J_{AB} = 7.0 Hz); **(±) *syn*-1j** (minor) ^{1}H NMR (500 MHz, $CDCl_3$) 8.23 (d, 1H, *J* = 8.0 Hz), 8.10 (d, 1H, *J* = 8.0 Hz), 7.76 (t, 1H, *J* = 7.5 Hz), 7.60 (t, 1H, *J* = 7.5 Hz), 7.30-7.23 (m, 4H), 7.01 (m, 1H), 4.77 and 4.46 (ABq, 2H, Δ*v* = 155.0 Hz, *J* = 12.0 Hz), 3.70 (d, 1H, *J* = 11.5 Hz), 2.66 (app spt, 1H, AA'*B*, *J* = 6.5 Hz), 1.41 (d, 3H, A*A'*B, $J_{A'B}$ = 6.5 Hz), 1.03 (d, 3H, *A*A'B, J_{AB} = 6.5 Hz); mixture of **1j**: ^{13}C NMR (125 MHz, $CDCl_3$) δ 168.1, 165.7, 144.9, 143.1, 141.5, 135.1, 135.0, 134.9, 131.9, 131.8, 128.7, 128.6, 128.5, 128.4, 127.8, 127.4, 125.2, 79.5, 76.7, 72.2, 67.4, 66.6, 27.3, 26.9, 21.6, 21.3, 21.2, 20.1, 19.7.

Benzyl 3-(2-nitrophenylsulfinyl)butanoate (1l): Yield: 75 mg, 73% (mixture of diastereomers); orange solid, mp 108-109 °C; ESI-HRMS calcd. for $C_{17}H_{17}NO_5S$ $[M+H]^+$ 348.0900, found 348.0910; **(±) *anti*-1l** (major): yellow oil; TLC (SiO_2) R_f 0.30 (5:1 hexanes:EtOAc); ^{1}H NMR (500 MHz, $CDCl_3$) δ 8.31 (d, 1H, *J* = 8.5 Hz), 8.12 (dd,

1H, *J* = 8.0, 1.5 Hz), 7.89 (dt, 1H, *J* = 8.0, 1.0 Hz), 7.68 (dt, 1H, *J* = 8.0, 1.0 Hz), 7.43-7.31 (m, 5H), 5.17 and 5.13 (ABq, 2H, $\Delta\nu$ = 20.0 Hz, *J* = 12.5 Hz), 3.58 (m, 1H), 3.15 (dd, 1H, *J* = 16.0, 6.0 Hz), 2.73 (dd, 1H, *J* = 16.0, 9.5 Hz), 0.97 (d, 3H, *J* = 7.0 Hz); **(±) *syn*-1l** (minor): yellow oil; TLC (SiO_2) R_f 0.44 (5:1 hexanes:EtOAc); ^{1}H NMR (500 MHz, $CDCl_3$) δ 8.26 (d, 1H, *J* = 8.0 Hz), 8.06 (dd, 1H, *J* = 8.0, 1.0 Hz), 7.72 (dt, 1H, *J* = 8.0, 1.0 Hz), 7.60 (dt, 1H, *J* = 8.0, 1.0 Hz), 7.43-7.31 (m, 5H), 4.77 and 4.73 (ABq, 2H, $\Delta\nu$ = 20.0 Hz, *J* = 12.5 Hz), 3.72 (m, 1H), 2.73 (dd, 1H, *J* = 17.5, 7.0 Hz), 2.31 (dd, 1H, *J* = 17.5, 6.0 Hz), 1.61 (d, 3H, *J* = 7.5 Hz); Mixture of **1l**: ^{13}C NMR (125 MHz, $CDCl_3$) δ 170.8, 170.4, 145.5, 145.0, 141.0, 140.9, 135.0, 128.8, 128.7, 128.6, 128.3, 128.1, 127.3, 125.7, 125.6, 76.2, 66.7, 66.2, 54.1, 53.1, 37.8, 31.4, 18.8, 17.9, 10.3.

Benzyl 5-(2-nitrophenylsulfinyl)hexanoate (1m): Yield: 320 mg, 79% (a mixture of diastereomers); yellow oil; ESI-HRMS calcd. for $C_{19}H_{21}NO_5S$ $[M+H]^+$ 376.1213, found 376.1218; **(±) *anti*-1m**: yellow oil; TLC (SiO_2) R_f 0.16 (3:1 hexanes:EtOAc); ^{1}H NMR (500 MHz, $CDCl_3$) δ 8.30 (d, 1H, *J* = 8.0 Hz), 8.16 (dd, 1H, *J* = 7.5 Hz), 7.86 (t, 1H, *J* = 7.5 Hz), 7.65 (td, 1H, *J* = 8.0 Hz), 7.35-7.26 (m, 5H), 4.99 (s, 2H), 3.00 (m, 1H), 2.19 (t, 2H, *J* = 7.5 Hz), 1.69-1.63 (m, 1H), 1.56 (d, 3H, *J* = 7.5 Hz), 1.54-1.50 (m, 1H), 1.36-1.27 (m, 2H); ^{13}C NMR (125 MHz, $CDCl_3$) δ 172.8, 145.1, 142.2, 136.0, 135.0, 131.5, 128.8, 128.5, 128.4, 128.0, 125.6, 66.4, 57.8, 34.1, 26.0, 22.0, 16.6; **(±) *syn*-1m**: yellow oil; TLC (SiO_2) R_f 0.11 (3:1 hexanes:EtOAc); ^{1}H NMR (500 MHz, $CDCl_3$) δ 8.31 (dd, 1H, *J* = 8.0, 0.5 Hz), 8.16 (dd, 1H, *J* = 7.5, 1.5 Hz), 7.90 (td, 1H, *J* = 8.0, 1.0 Hz), 7.67 (td, 1H, *J* = 7.5, 1.5 Hz), 7.35-7.28 (m, 5H), 5.12 (s, 2H), 3.07 (sxt, 1H, *J* = 7.0 Hz), 2.47 (td, 2H, *J* = 7.0, 3.0 Hz), 2.10-1.93 (m, 3H), 1.79-1.72 (m, 1H), 0.91 (d, 3H, *J* = 6.5 Hz);

^{13}C NMR (125 MHz, $CDCl_3$) δ 173.1, 145.0, 142.2, 136.2, 134.9, 131.4, 128.8, 128.4, 125.6, 66.5, 57.3, 34.1, 32.6, 22.5, 10.2.

Preparation of alkenes 4; general procedure. A solution of sulfoxide **1** (1 mmol equiv) and NaOAc (10 mmol equiv) in toluene (10 mL) was heated under for 1-18 hours. The mixture was then cooled to room temperature. After the precipitate was removed by filtration through Celite, the reaction flask was rinsed with toluene, filtered, and the solvent was evaporated to provide alkene **4**. Decolorization of the concentrated product was achieved by vacuum filtration of the oil through a plug of silica with 3:1 hexanes:EtOAc. If the starting material was still present, the mixture can be heated again with 10 mmol equiv of NaOAc in toluene until the reaction is complete.

Benzyl undec-10-enoate (4a): Yield: 28.2 mg, 86%; colorless oil; TLC (SiO_2) R_f 0.40 (20:1 hexanes:EtOAc); ^{1}H NMR (500 MHz, $CDCl_3$) δ 7.34-7.30 (m, 5H), 5.79 (ddt, 1H, AB*M*, J_{BM} = 16.5 Hz, J_{AM} = 10.5, 6.5 Hz), 5.10 (s, 2H), 4.98 (dd, 1H, A*B*M, J_{BM} = 16.5 Hz, J_{AB} = 1.5 Hz), 4.92 (dd, 1H, *A*BM, J_{AM} = 10.5 Hz, J_{AB} = 1.5 Hz), 2.34 (t, 2H, *J* = 7.5 Hz), 2.02 (m, 2H), 1.63 (qnt, 2H, *J* = 7.0 Hz), 1.36 (qnt, 2H, *J* = 7.0 Hz), 1.28-1.25 (m, 8H); ^{13}C NMR (125 MHz, $CDCl_3$) δ 173.7, 139.2, 136.2, 128.6, 128.2, 128.2, 114.2, 66.1, 34.4, 33.8, 29.3, 29.2, 29.1, 28.9, 24.0; ESI-HRMS calcd for $C_{18}H_{26}O_2$ $[M+Na]^+$ 297.1825, found 297.1826.

Benzyl pent-4-enoate (4b): Yield: 19 mg, 75%; colorless oil; TLC (SiO_2) R_f 0.48 (20:1 hexanes:EtOAc); ^{1}H NMR (500 MHz, $CDCl_3$) δ 7.35-7.30 (m, 5H), 5.81 (ddt, 1H, AB*M*, J_{BM} = 17.0 Hz, J_{AM} = 10.5 Hz, *J* = 7.5 Hz), 5.11 (s, 2H), 5.03 (dd, 1H, A*B*M, J_{BM} = 17.0 Hz, J_{AB} = 1.5 Hz), 4.98 (dd, 1H, *A*BM, J_{AM} = 10.5 Hz, J_{AB} = 1.5 Hz), 2.47-2.44 (m, 2H),

2.41-2.36 (m, 2H); ^{13}C NMR (125 MHz, $CDCl_3$) δ 173.1, 136.8, 136.2, 128.7, 128.4, 115.8, 66.4, 33.7, 29.0.

1-(Undec-10-enylsulfinyl)benzene (4c): Yield: 28.5 mg, 86%; colorless oil; TLC (SiO_2) R_f 0.18 (7:1 hexanes:EtOAc); ^{1}H NMR (500 MHz, $CDCl_3$) δ 7.59-7.57 (m, 2H), 7.49-7.43 (m, 3H), 5.75 (ddt, 1H, AB*M*, J_{BM} = 17.0 Hz, J_{AM} = 10.5, J = 6.5 Hz), 4.95 (dd, 1H, *AB*M, J_{BM} = 17.0 Hz, J_{AB} = 1.5 Hz), 4.88 (dd, 1H, *A*BM, J_{AM} = 10.5 Hz, J_{AB} = 1.5 Hz), 2.76 (app t, 2H, J = 7.0 Hz), 2.00 (m, 2H), 1.75-1.66 (m, 1H), 1.64-1.54 (m, 1H), 1.41-1.30 (m, 2H), 1.29-1.21 (m, 10H); ^{13}C NMR (125 MHz, $CDCl_3$) δ 144.3, 139.3, 131.1, 129.4, 124.2, 114.3, 57.6, 33.9, 29.5, 29.4, 29.3, 29.2, 29.1, 29.0, 28.8, 22.3.

1-(Hex-5-enylsulfinyl)benzene ((*Z*)-4d): Yield: 22 mg, 62%; colorless oil; TLC (SiO_2) R_f 0.32 (3:1 hexanes:EtOAc); ^{1}H NMR (500 MHz, $CDCl_3$) δ 7.59-7.58 (m, 2H), 7.50-7.45 (m, 3H), 5.71 (ddt, 1H, AB*M*, J_{BM} = 17.0 Hz, J_{AM} = 10.0 Hz, J = 6.5 Hz), 4.95 (dd, 1H, A*B*M, J_{BM} = 17.0 Hz, J_{AB} = 1.5 Hz), 4.91 (dd, 1H, *A*BM, J_{AM} = 10.0 Hz, J_{AB} = 1.5 Hz), 2.76 (t, 2H, J = 8.0 Hz), 2.02 (m, 2H), 1.76-1.71 (m, 1H), 1.64-1.58 (m, 1H), 1.54-1.48 (m, 2H); ^{13}C NMR (125 MHz, $CDCl_3$) δ 150.2, 144.2, 138, 131.1, 124.2, 115.3, 110.2, 57.4, 33.4, 28.1, 21.9.

1-Methyl-4-(undec-10-enylsulfinyl)benzene (4e): Yield: 33.8 mg, 87%; colorless oil; TLC (SiO_2) R_f 0.30 (4:1 hexanes:EtOAc); ^{1}H NMR (500 MHz, $CDCl_3$) δ 7.74 (d, 2H, J = 8.5 Hz), 7.28 (d, 2H, J = 8.0 Hz), 5.77 (ddt, 1H, AB*M*, J_{BM} = 17.0 Hz, J_{AM} = 10.0 Hz, J = 7.0 Hz), 4.95 (d, 1H, A*B*M, J_{BM} = 17.0 Hz), 4.89 (d, 1H, *A*BM, J_{AM} = 10.0 Hz), 2.78-2.67 (m, 2H), 2.38 (s, 3H), 1.98 (q, 2H, J = 7.0 Hz), 1.72-1.63 (m, 1H), 1.60-1.53 (m, 1H), 1.41-1.31 (m, 4H), 1.22 (m, 8H); ^{13}C NMR (125 MHz, $CDCl_3$) δ 141.5, 141.0, 139.3,

130.0, 124.2, 114.3, 57.6, 33.9, 29.5, 29.4, 29.3, 29.2, 29.0, 28.8, 22.4, 21.6; ESI-HRMS calcd. for $C_{18}H_{28}O$ $[M+H]^+$ 293.1934, found 293.1933.

1-Chloro-4-(undec-10-enylsulfinyl)benzene (4f): Yield: 12.9 mg, 74%; colorless oil; TLC (SiO_2) R_f 0.23 (7:1 hexanes:EtOAc); ^{1}H NMR (500 MHz, $CDCl_3$) δ 7.54 (m, 2H), 7.49-7.47 (m, 2H), 5.78 (ddt, 1H, AB*M*, J_{BM} = 17.0 Hz, J_{AM} = 10.5 Hz, J = 6.5 Hz), 4.95 (dd, 1H, *AB*M, J_{BM} = 17.0 Hz, J_{AB} = 1.5 Hz), 4.90 (dd, 1H, *A*BM, J_{AM} = 10.5 Hz, J_{AB} = 1.5 Hz), 2.74 (t, 2H, J = 8.0 Hz), 2.00 (m, 2H), 1.75-1.65 (m, 1H), 1.61-1.52 (m, 1H), 1.43-1.31 (m, 3H), 1.23 (m, 9H); ^{13}C NMR (125 MHz, $CDCl_3$) δ 142.8, 139.4, 137.3, 129.7, 125.7, 114.4, 57.6, 34.0, 29.5, 29.3, 29.2, 29.1, 28.8, 22.2; ESI-HRMS calcd. for $C_{17}H_{25}ClO$ $[M+H]^+$ 313.1387, found 313.1387.

1-Nitro-4-(undec-10-enylsulfinyl)benzene (4g): Yield: 15.3 mg, 64%; colorless oil; TLC (SiO_2) R_f 0.47 (3:1 hexanes:EtOAc); ^{1}H NMR (500 MHz, $CDCl_3$) δ 8.35 (d, 2H, J = 8.0 Hz), 7.78 (d, 2H, J = 8.0 Hz), 5.76 (ddt, 1H, AB*M*, J_{BM} = 17.5 Hz, J_{AM} = 10.0 Hz, J = 6.5 Hz) 4.95 (dd, 1H, *AB*M, J_{BM} = 17.5 Hz, J_{AB} = 1.5 Hz), 4.90 (dd, 1H, *A*BM, J_{AM} = 10.0 Hz, J_{AB} = 1.5 Hz), 2.88-2.75 (m, 2H). 2.00 (m, 2H), 1.84-1.75 (m, 1H), 1.60-1.52 (m, 1H), 1.45-1.38 (m, 1H), 1.37-1.30 (m, 3H), 1.27-1.22 (m, 8H); ^{13}C NMR (125 MHz, $CDCl_3$) δ 152.0, 139.3, 125.3, 124.4, 114.4, 57.4, 34.0, 29.5, 29.4, 29.3, 29.2, 29.1, 28.8, 22.1; ESI-HRMS calcd. for $C_{17}H_{26}NO_3S$ $[M+H]^+$ 324.1628, found 324.1622.

1-(Hex-5-enylsulfinyl)-4-nitrobenzene (4h): Yield: 13.4 mg, 61%; yellow oil; TLC (SiO_2) R_f 0.27 (3:1 hexanes:EtOAc); ^{1}H NMR (500 MHz, $CDCl_3$) δ 8.35 (d, 2H, J = 8.5 Hz), 7.77 (d, 2H, J = 8.5 Hz), 5.71 (ddt, 1H, AB*M*, J_{AM} = 17.0 Hz, J_{BM} = 10.5 Hz, J = 7.0 Hz), 4.97-4.91 (m, *AB*M, 2H), 2.84 (m, 1H), 2.78 (m, 1H), 2.04 (m, 2H), 1.86-1.79 (m, 1H), 1.64-1.44 (m, 3H); ^{13}C NMR (125 MHz, $CDCl_3$) δ 151.9, 150.2, 149.6, 137.7,

125.3, 124.4, 115.6, 57.1, 33.3, 27.9, 21.6; ESI-HRMS calcd. for $C_{12}H_{15}NNaO_3S$ 276.0665 $[M+Na]^+$, found 276.0673.

(*E*)-Benzyl but-2-enoate ((*E*)-4i): Yield: 24.7 mg, 88%; colorless oil; TLC (SiO_2) R_f 0.55 (9:1 hexanes:EtOAc); ^1H NMR (500 MHz, $CDCl_3$) δ 7.35-7.29 (m, 5H), 7.06 (dq, 1H, AM*X*, J_{MX} = 16.0 Hz, J_{AX} = 7.0 Hz), 5.87 (d, 1H, A*M*X, J_{MX} = 16.0 Hz), 5.16 (s, 2H), 1.86 (d, 3H, *A*MX, J_{AX} = 7.0 Hz); ^{13}C NMR (125 MHz, $CDCl_3$) δ 166.5, 145.3, 136.4, 128.7, 122.7, 66.1, 18.2; MS (*m/z*): 176(25), 158(48), 147(5), 131(96), 117(8), 107(50).

Benzyl 3-methylbut-2-enoate (4j): Yield: 20 mg, 93%; colorless oil; TLC (SiO_2) R_f 0.60 (9:1 hexanes:EtOAc); ^1H NMR (500 MHz, $CDCl_3$) δ 7.38-7.29 (m, 5H), 5.72 (s, 1H), 5.12 (s, 2H), 2.17 (s, 3H), 1.88 (s, 3H); ^{13}C NMR (125 MHz, $CDCl_3$) δ 166.6, 157.5, 136.7, 128.7, 128.3, 128.2, 116.0, 65.6, 27.6, 20.5; MS (*m/*z): 190(48), 175(27), 145(95), 144(42), 131(10), 117(5), 107(33).

(*E*)-Benzyl cinnamate ((*E*)-4k): Yield: 74 mg, 67%; yellow solid, mp 32-33 °C; TLC (SiO_2) R_f 0.77 (7:1 hexanes:EtOAc); ^1H NMR (500 MHz, $CDCl_3$) δ 7.74 (d, 1H, A*X*, J_{AX} = 16.0 Hz), 7.52-7.51 (m, 2H), 7.44-7.33 (m, 8H), 6.50 (d, 1H, *A*X, J_{AX} = 16.0 Hz), 5.27 (s, 2H); ^{13}C NMR (125 MHz, $CDCl_3$) δ 185.3, 166.9, 136.2, 134.5, 129.0, 128.7, 128.4, 128.3, 118, 66.5. (*Elimination occurred during the S-oxidation reaction)

Benzyl hexenoate 4m: Yield: 71 mg, 75%; colorless oil; TLC (SiO_2) R_f 0.52 (25:1 hexanes:EtOAc; a mixture of diastereomers); Ratio of isomers was determine by GC/MS;

Benzyl hex-5-enoate (4m): ^1H NMR (500 MHz, $CDCl_3$) δ 7.38-7.29 (m, 5H), 5.77 (ddt, 1H, AB*M*, J_{BM} = 17.0 Hz, J_{AM} = 10.5 Hz, *J* = 7.0 Hz), 5.11 (s, 2H), 5.02 (dd, 1H, A*B*M,

J_{BM} = 17.0 Hz, J_{AB} = 1.0 Hz), 4.98 (dd, 1H, *A*BM, J_{AM} = 10.5 Hz, J_{AB} = 1.0 Hz), 2.37 (t, 2H, *J* = 7.5 Hz), 2.09 (q, 2H, *J* = 7.5 Hz), 1.75 (qnt, 2H, *J* = 7.5 Hz);

(*E*)-Benzyl hexenoate ((*E*)-4m): ^{1}H NMR (500 MHz, $CDCl_3$) δ 7.38-7.29 (m, 5H), 5.52-5.35 (m, 2H), 5.11 (s, 2H), 2.41 (t, 2H, *J* = 7.5 Hz), 2.32 (q, 2H, *J* = 7.0 Hz), 2.32 (q, 2H, *J* = 7.0 Hz), 1.62 (t, 3H, *J* = 7.5 Hz).

Preparation of 2-phenylhex-5-ynoic acid (9): 2-Phenylacetic acid (0.68 g, 5 mmol) was dissolved in anhydrous THF (8.4 mL). LDA (10 mmol) was then added slowly when the temperature was maintained at 0 °C. The reaction mixture was stirred at 0 ºC for 1 hour. The yellow precipitate that was formed was dissolved with the addition of HMPA (0.5 mL). To this, 3-bromoprop-1-yne (0.49 mL, 5.2 mmol) was added dropwise. The solution was then warmed to room temperature and stirred for 16 hours. The reaction mixture was acidified with 3N HCl, extracted with ether. The organic layer was then washed 3 times with distilled water and dried over $MgSO_4$, filtered, and evaporated. The product was separated by flash chromatography on silica gel using 3:1 hexanes:EtOAc in accordance to product R_f values. Yield: 11%; colorless oil; TLC (SiO_2) R_f 0.70 (1:1 hexanes:EtOAc); ^{1}H NMR (500 MHz, $CDCl_3$) δ 7.34-7.26 (m, 5H), 3.82 (t, 1H, *J* = 7.5 Hz), 2.33-3.26 (m, 1H), 2.25-2.19 (m, 1H), 2.11-2.06 (m, 1H), 2.03-1.96 (m, 1H).

Preparation of (*E*)-6-(bromomethylene)-tetrahydro-3-phenylpyran-2-one (6): To a stirring reaction mixture of K_2CO_3 (14.7 mg, 0.106 mmol) in dry dichloromethane (2 mL) was added 2-phenylhex-5-ynoic acid (20 mg, 0.106 mmol). After 10 minutes, *N*-bromosuccinimide (18.9 mg, 0.106 mmol) was added, followed by addition of H_2O (7.56 μL, 0.425 mmol). The reaction mixture was stirred at room temperature for 6 hours. After

that, the mixture was then diluted with dichloromethane (5 mL). The organic layer was then dried over $MgSO_4$, filtered, and evaporated. The product was separated by flash chromatography on silica gel using 4:1 hexanes:EtOAc. Yield: 41%; yellow oil; TLC (SiO_2) R_f 0.73 (1:1 hexanes:EtOAc); ^{1}H NMR (500 MHz, $CDCl_3$) δ 7.49-7.32 (m, 5H), 3.89 (q, 1H, *J* = 5.5 Hz), 3.01-2.95 (m, 1H), 2.85-2.79 (m, 1H), 2.39-2.27 (m, 2H); ^{13}C NMR (125 MHz, $CDCl_3$) δ 168.7, 151.7, 137.2, 129.1, 128.2, 128.2, 91.6, 47.5, 26.0, 23.9.

Preparation of anthraquinone-1-diazonium salt (10): 3.4 g (50.0 mmol) of finely ground sodium nitrite was added slowly into 30 mL of concentrated sulfuric acid at 0 °C. 10 g (45.0 mmol) of 1-aminoanthroquinone was then added at room temperature. The reaction mixute was then heated to 50 °C and kept at that temperature for 30 minutes. After cooling to room temperature, the mixture was mixed with 70 g of chopped ice and the final producet was collected as dark red solid after filtration and washing with water (10 mL) and acetone (10 mL). Yield: 99%; mp 140-143 °C. The diazonium sulfate salt was used directly in the next step.

Preparation of methyl 2-(9,10-dihydro-9,10-dioxoanthracen-5-yl)acetate (11): Cuporous chloride (0.7 mmol) was added slowly into a mixture of anthraquinone-1-diazonium salt (15.8 mmol), 1,1-dichloroethylene (157.8 mmol) and MeOH (30 mL) at 30 °C. The reaction was stirred at that temperature for 30 minutes, and then was genetly reflux for several minutes. The final product was collected as yellow solid after simple filtration. Yield: 50%; mp 184-185 °C; ^{1}H NMR (500 MHz, $CDCl_3$) δ 8.33 (d, 1H, *J* =

7.5 Hz), 8.24 (m, 2H), 7.76-7.71 (m, 3H), 7.55 (d, 1H, *J* = 7.5 Hz), 4.19 (s, 2H), 3.73 (s, 3H). The ester was used directly in the next step.

Preparation of 2-(9,10-dihydro-9,10-dioxoanthracen-5-yl)acetic acid (12): 20 mL of 2N NaOH was added into a solution of 10 mL H_2O containing 550 mg of ester at 0 °C. The mixture was then stirred at room temperature for 18 hours and acidified with 6N HCl until the pH value decreased from 13 to 2. The final product was collected as yellow-pink solid after simple filtration. Yield: 99%; mp 232 °C. The acid was used directly in the next step.

Preparation of 2-(anthracen-5-yl)acetic acid (13): A mixture of anthraquinone-1-acetic acid (1.3 g, 4.9 mmol), concentrated NH_4OH (25 mL), water (25 mL), excess Zn powder and a trace of $CuSO_4$ was heated under reflux for 30 min, the solids were filtered off, and the solution and acidified to pH value reach to 2 using 6N HCl. The final compound was filted as yellow solid. Yield: 0.5 g, 43%; TLC (SiO_2) R_f 0.32 (2:1 hexanes:EtOAc + 1 drop of acetic acid); ^{1}H NMR (500 MHz, $CDCl_3$) δ 9.62 (bs, 1H), 8.34-7.00 (m, 9H), 3.97 (s, 2H).

Preparation of *tert*-butyl 2-(prop-2-ynyloxy)acetate (15): NaH (23 mg, 0.51 mmol) was added slowly into a THF:DMF (5 mL:1 mL) solution of bromoacetic acid *tert*-butyl ester (100 mg, 0.51 mmol) and propagyl alcohol (29 mg, 0.51mmol) with molecular sieves. The resulting grey solution was stirred at room temperature for 16 hours. The solid was then filtered, and the filtrate was concentrated and redissolved in EtOAc (10 mL). The organic layer was extracted three times with water, two times with 5% citric acid, one time with brine, and then dried over $MgSO_4$. The final product was separated by

flash chromatography on silica gel in accordance to product R_f values. The final product is a colorless oil; Yield: 57 mg, 65%; R_f 0.40 (15:1 hexanes:EtOAc); ^{1}H NMR (500 MHz, $CDCl_3$) δ 4.25 (d, 2H, *J* = 2.0 Hz), 4.02 (s, 2H), 2.43 (m, 1H), 1.43 (s, 9H); ^{13}C NMR (125 MHz, $CDCl_3$) δ 169.7, 81.9, 78.9, 75.5, 66.8, 58.2, 28.2.

Preparation of 2-(prop-2-ynyloxy)acetic acid (**16):** Triethylsilane (91 mg, 0.78 mmol) was added into a DCM solution (16 mL) of *tert*-butyl 2-(prop-2-ynyloxy)acetate (95 mg, 0.56 mmol). Trifluoroacetic acid (1.8 mL) was next added. The solution was then stirred at room temperature for 16 hours. After that, the solvent was evaporated. The final product was collected as a colorless oil. Yield: 64 mg, 99%; R_f 0.50 (1:1 hexanes:EtOAc); ^{1}H NMR (500 MHz, $CDCl_3$) δ 4.24 (s, 2H), 4.19 (s, 2H), 2.49 (s, 1H); ^{13}C NMR (125 MHz, $CDCl_3$) δ 174.5, 78.1, 76.3, 65.8, 58.4.

CHAPTER 3

PREPARATION OF β-LACTAM ANALOGUES

Lu, X.; Long, T. E. *Tetrahedron Lett.* **2011**, *52*, 5051-5054.

Abstract

The use of sulfur chemistry in synthetic transformation is further investigated in Chapter 3. An asymmetrical method to synthesize β-lactams using photochemistry as the key in the synthetic steps has been developed. Photooxidation of L-cysteine thiazolidine hydroxamate esters afforded C-5 hydroxylated products which when cyclized and deprotected gave the corresponding 3*R*, 4*R* monocyclic β-lactam platforms.

3.1 Background

3.1.1 Introduction

Many species of bacteria are human pathogens. For over 100 years, chemotherapy is the first choice for many patients, either by selective kill (bactericidal activity) or by slowing growth of bacteria (bacteriostatic activity) [1]. A variety structures have been identified to treat infections, and currently these medications can be divided into several groups based on their unique modes of actions. For example, β-lactams (e.g., penicillins) can inhibit bacterial cell wall synthesis [2], tetracyclines (e.g., doxycycline) can interfere with protein synthesis [3], fluoroquinolones (e.g., ciprofloxacin) can inhibit DNA gyrase [4]. Among them, penicillin is one of the most widely used for many years.

This powerful antibacterial targets the synthesis of bacterial cell wall by binding to cellular receptors which is now identified as transpeptidation enzymes (PBPs) that catalyze the cross-linking reaction of the cell wall (**Figure 3.01**) [5]. The high similarity with the backbone of the D-Ala-D-Ala sidechain permits penicillin to bind with PBPs interrupting the final stages of the synthesis of cell wall peptidoglycan. The resulting defective bacterial cell wall allows water to enter, and the cell swells resulting in membrane lysis and cell death.

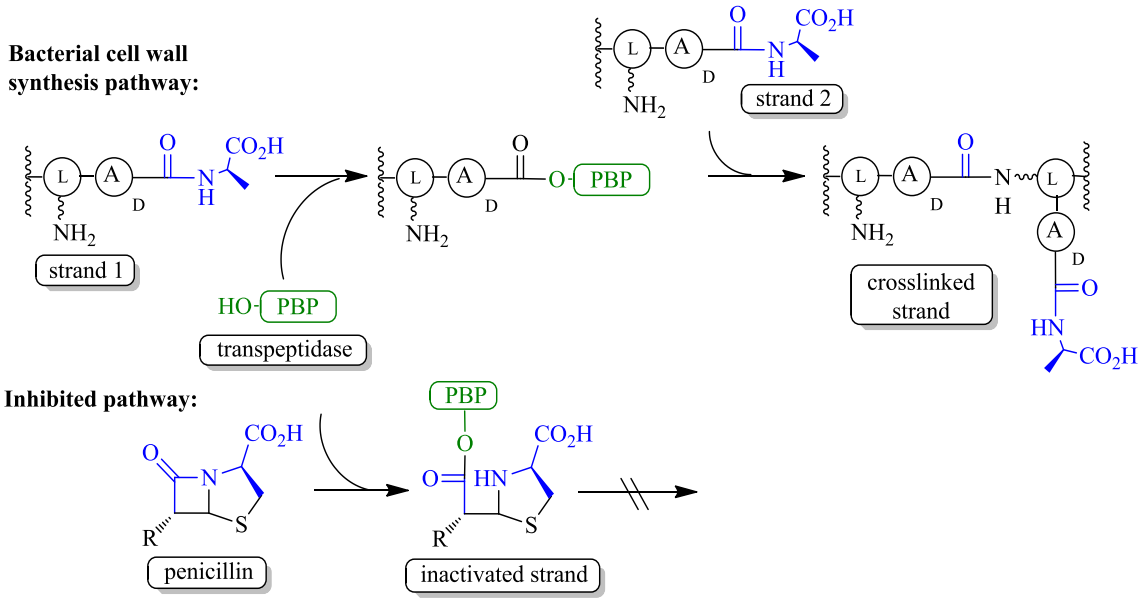

Figure 3.01: The mechanism of action of penicillin.

General features of this binding process include: (1) penicillin interferes with daughter cells during the formation of cell walls (i.e., prevents new cross-links but does not disrupt those established); (2) penicillin shows superior selectivity since animal cells do not possess cell walls; and (3) penicillin does not work against all kinds of bacteria, as Gram-negative bacteria have relatively less peptidoglycan and are generally much less sensitive to penicillin compared to Gram-positive bacteria [6].

3.1.2 β-Lactam antibacterials

Penicillins and cephalosporins are classified as β-lactam antibacterials because they share a similar chemical structure (i.e., β-lactam ring). Sharing similar mechanisms to block bacterial cell wall synthesis, many different scaffolds have also been explored (**Figure 3.02**). However, even back in the 1940s, resistance to β-lactams quickly emerged as a problem in therapy [7]. Different strategies have been used by various bacterial

pathogens to survive antibiotic exposure. For example, β-lactamases produced by bacteria can hydrolyze β-lactams antibacterials [8], or most recently, the modification of transpeptidase can cause a decreased affinity for binding β-lactams in methicillin-resistant *Staphylococcus aureus* (MRSA) [9]. For this reason, the modification and substitution to treat resistance strains have been one of the ongoing focuses in the discovery of new effective antibacterial agents.

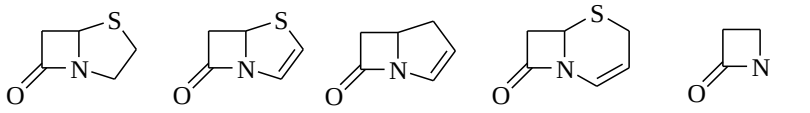

Figure 3.02: Examples of heterocyclic scaffolds of β-lactam antibacterials.

3.1.3 The traditional route to make β-lactam drugs

After its first discovery by Sir Alexander Fleming in 1928 [10], the isolation of penicillin proved to be problematic until the 1940s. The first reported synthetic work was performed in 1957 but, the total yield was only 1% and thus was not practical for use in industry [11]. In the following years, several synthetic routes have been reported to prepare semisynthetic β-lactam antibacterials. For instance, the synthesis of ampicillin was accomplished by using benzaldehyde as the overall starting material (**Scheme 3.01**) through six steps, using 6-aminopenicillanic acid (6-APA, which has β-lactam ring and derived from mold) condensation as the key step [12]. Besides indirectly obtained from nature, it is also practical to make the β-lactam via amino acid pool. To this extent, the aim of this project is to build the β-lactam scaffold using L-cysteine as the overall starting material.

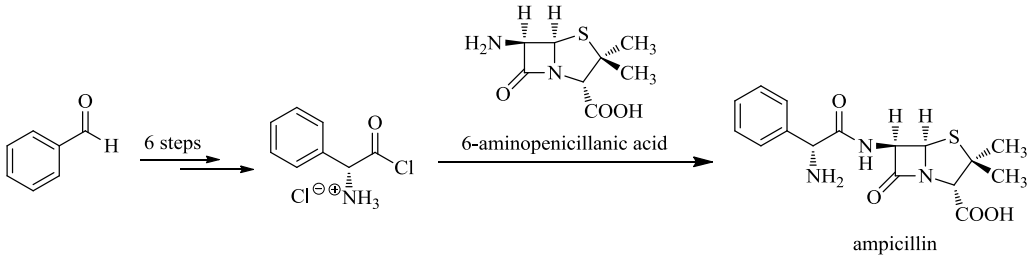

Scheme 3.01: Semisynthesis of ampicillin.

3.2 Experimental Design and Results

3.2.1 The route to build designed molecule

Numerous articles can be found throughout the literature describing the preparation of β-lactam rings. However, the lactam ring formation typically requires harsh conditions thus, giving rise to the problem of relatively low reaction yield due to decomposition of the starting material or product [13]. The goal of the new design is to impart a practical advantage to the synthetic procedure by mild reaction conditions, including a beneficial use of green chemistry. The optimized route using photochemistry as a key step is illustrated in **Scheme 3.02**. The corresponding 3*R*, 4*R* monocyclic β-lactam was obtained via cyclization, cleavage of the thiazolidine ring, the following deprotection of the lactam ring nitrogen [14].

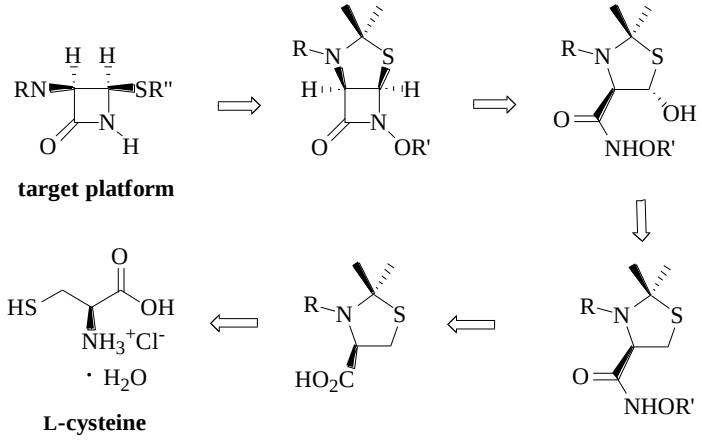

Scheme 3.02: Retrosynthesis of monocyclic β-lactam platform.

3.2.2 Synthesis of *N*-protected thiazolidine esters

The synthetic sequence commenced with the preparation of *N*-protected thiazolidines **2** by refluxing L-cysteine in dry acetone to afford corresponding 2,2-dimethylthiazolidine hydrochloride salt **1** (**Scheme 3.03**). As shown below, the reaction may proceed in both directions. When water is present, the product will go through hydrolysis to regenerate cysteine (L-cys) and acetone [15]. In order to make sure the reaction moves towards the products instead of the reactants, the solvent (acetone) was first pre-treated with Drierite™. Meanwhile, considering water molecules (which will cause the reaction to shift to the left) can also be generated during the process of condensation, 10 mol% Drierite™ was used during the reflux. Finally after two hours reflux, the reaction residue (compound **1**) was collected as white solid after simply filtrating and washing with dry acetone.

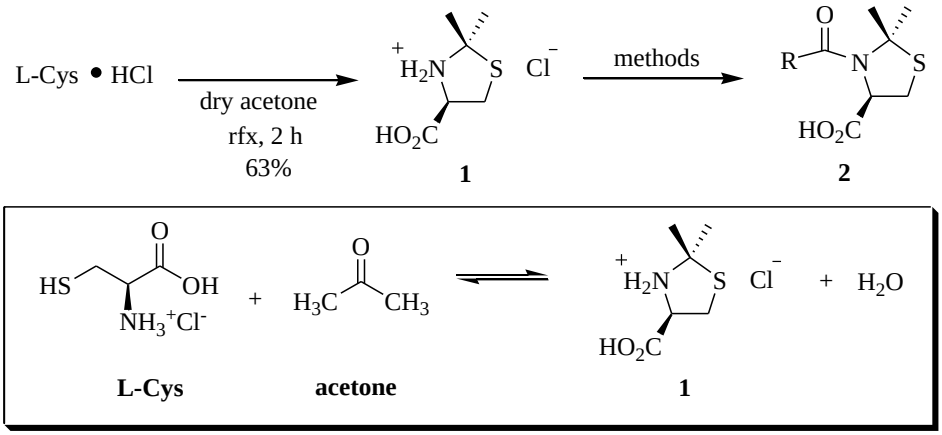

Scheme 3.03: Synthesis of *N*-protected thiazolidines.

The attachment of a carbonyl protecting group onto the ring nitrogen was the second step of the synthesis. In order to study the effect of different *N*-protecting group on the outcome of photochemical reaction (the key step in the synthetic sequence), five different analogs (**2a-e**) were synthesized (**Scheme 3.04**). Firstly, a formyl group was introduced

by mixed-anhydride method to provide the *N*-protected thiazolidine **2a** in 83% yield [16]. Next, the amide linkage between *tert*-butyloxycarbonyl (*t*-BOC) and amino group in the thiazolidine was achieved by acid anhydride condensation via $(t\text{-Boc})_2O$, giving compounds **2b** in moderate yield (48%) [17]. Since the reaction to introduce *t*-BOC resulted in only moderate yield, a more direct synthetic procedure using tert-butyloxycarbonyl chloride should be considered in the future optimization procedures. Lastly, carboxybenzyl (Cbz), phenoxyacetyl and benzoyl were attached by stirring 2,2-dimethylthiazolidine-4-carboxylic acid **1** in pyridine with corresponding chloride, giving **2c**, **2d**, and **2e** in yields of 90%, 63% and 67% respectively [18]. In general, carbamate and amide bond formation reactions do not require a strong base, thus pyridine (C_5H_5N) was selected serving both as a solvent and as a base.

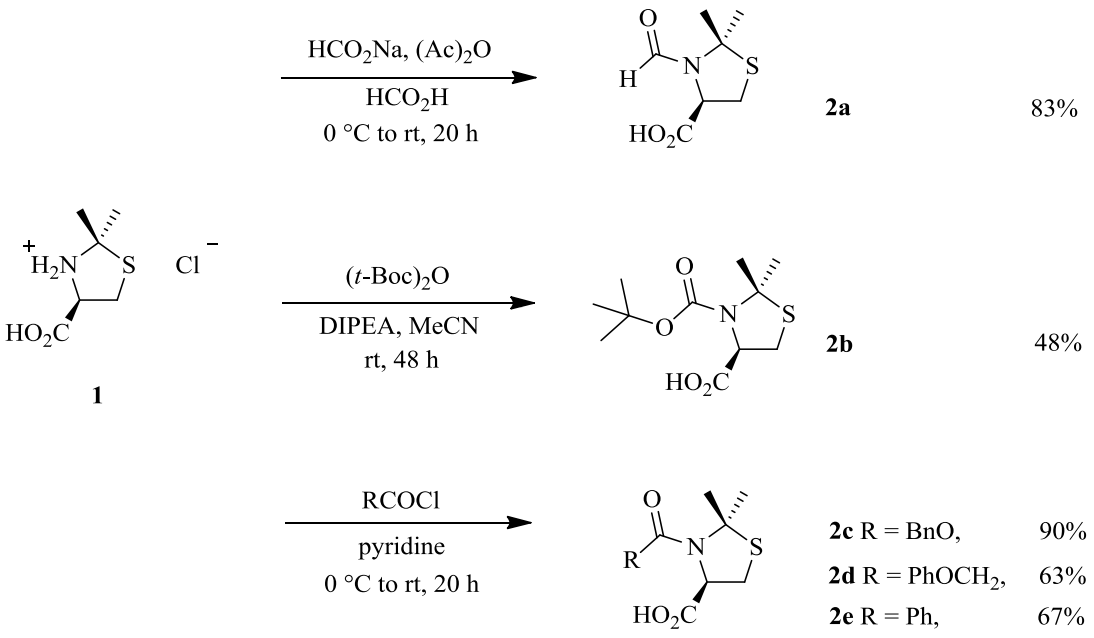

Scheme 3.04. The protection of thiazolidine **1**.

3.2.3 Synthesis of hydroxamate esters

Conversion of the carboxylic acid **2** to the hydroxamate esters **9** was performed using common procedures widely adopted in peptide chemistry. In order to further study the effect of different C-5 ester groups on the photochemistry (the key step of the synthetic sequence), a range of *O*-substituted hydroxylamine were separately prepared (e.g., **5**, **8**). Among them, the preparation of the two most widely studied substrates is illustrated in **Scheme 3.05** [19]. The preparation of *O*-benzyl hydroxylamine hydrochloride salt **5** (H_2NOBn, OBHA) was achieved in three steps: Williamson ether synthesis followed by hydrazinolysis to provide the primary amine **4**, which was later converted into its hydrochloride salt **5** by stirring with concentrated hydrochloric acid [20]. This final product **5** was kept at a low temperature and was generally stable for several months.

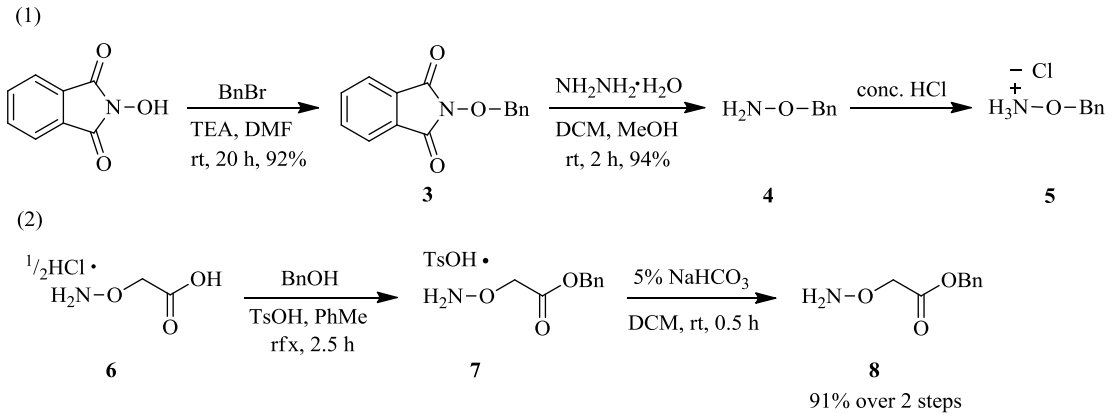

Scheme 3.05: Synthesis of aminooxy-acetic acid ester **8** and *O*-benzyl hydroxylamine **5**.

The preparation of aminooxy-acetic acid benzyl ester **8** involved the substitution of 2-(aminooxy) acetic acid **6** with benzyl alcohol. The ester intermediate **7** was formed through toluene reflux in the presence of a mild acid, i.e., *p*-toluenesulfonic acid. Similar to the condensation of the L-cysteine in dry acetone, because water molecule can be

generated as a byproduct, the Dean-Stark apparatus was used for continuous removal of newly formed water. The *p*-toluenesulfonic acid can easily be removed later from the stable salt **7** by simply stirring with 5% sodium bicarbonate in dichloromethane at room temperature.

In peptide chemistry, the most commonly used approach to make amides from amines typically requires two steps: first, the generation of carbonyl intermediate from the carboxylic acid, and then the substitution reaction between this activated intermediate and the corresponding amine. In this project, the hydroxamate ester synthesis was performed via a similar manner. It was initiated by the utilization of the mixed anhydride method or the carbodiimide mediated coupling amidation, which was followed by *N*-acylation of different alkoxyamines (e.g., compounds **4** and **8**). The reaction conditions have been successfully applied and are as follows.

Carbodiimide mediated coupling (method A) was used to introduce the OBHA into the thiazolidine molecule **2**. Specifically, 1-ethyl-3(3-dimethyl amino) propyl carbodiimide hydrochloride (EDC salt, a water soluble carbodiimide) was reacted with the starting material in a carefully controlled acidic environment (pH 4-5) [21]. This carboxyl activated structure was then coupled with the primary amine, i.e., OBHA **4**.

As illustrated in **Scheme 3.06**, this amine-reactive intermediate **2c'** can easily react with OBHA to generate a stable amide bond, forming the final compound **9a**. Also, this *O*-acylisourea structure is highly susceptible to potential hydrolysis, making amine-reactive intermediate **2c'** very unstable in the THF/H_2O solution. For this reason, it was noted that a longer reaction time did not increase the reaction yield of product **9a**. To

solve this problem, one more equivalent of EDC was added after 0.5 hour into the reaction mixture, however a typical yield for this reaction was only around 50%.

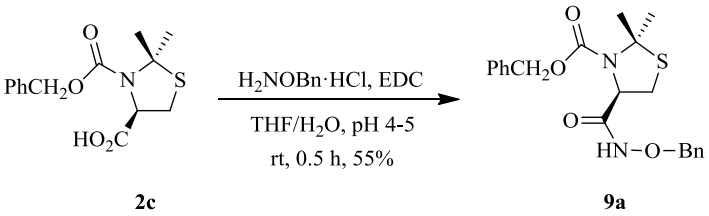

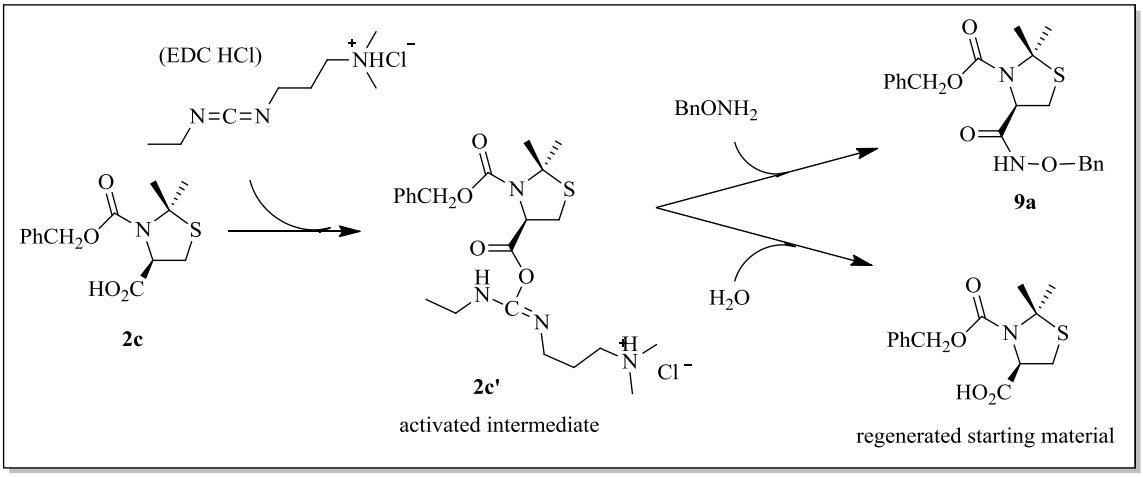

Scheme 3.06: EDC-mediated synthesis of hydroxamate ester **9a** (method A).

Another powerful coupling method was also performed with the use of alkyl chloroformate [22]. Activation of the acid starting material **2c** with isobutyl chloroformate in THF at a low temperature in the presence of *N*-methylmorpholine (NMM) provided corresponding activated mixed anhydride **2c"**. As illustrated in **Scheme 3.07**, the free amine can be used directly (method B). An alternative approach has also been studied by using the ammonium salt, which requires larger amount of base for the transformation (method C). The *N*-hydroxy-acetamide intermediate **9d'** was produced upon the addition of hydroxylamine, which was then converted to the hydroxamate ester **9d** by treatment with corresponding chloride in the presence of triethylamine in

dichloromethane for 1.5 hours. However, neither method was able to achieve a desired result (yields were mostly less than 50%; see **Table 3.02**).

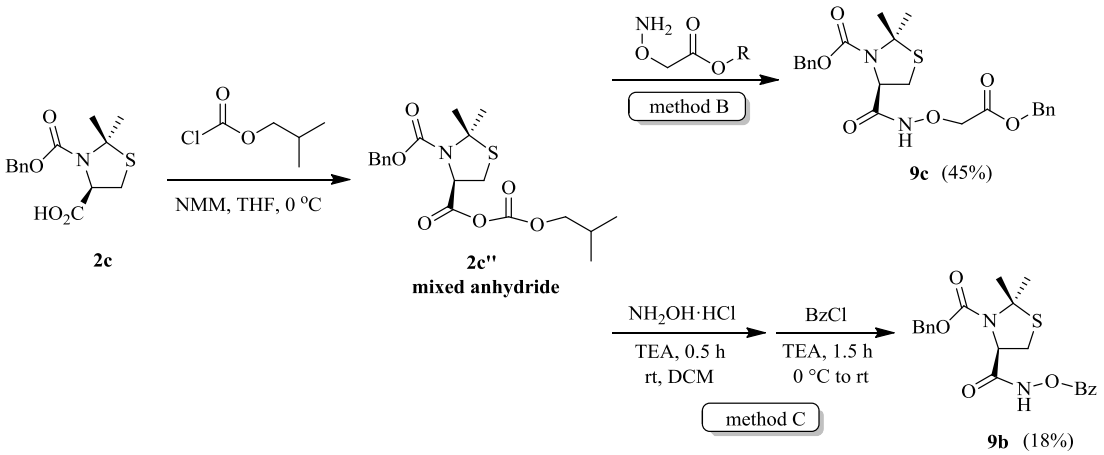

Scheme 3.07: Preparation of hydroxamate ester via mixed anhydride (method B and C).

The moderate yield in the mixed anhydride method might be due to the regioselectivity of the reaction [23]. The mixed anhydride **2c''** is attacked by the nucleophilic amine in which the attack direction highly depends on the electrophilicity and the steric substitution surrounding of the two competing carboxyl groups. The desired path a, as shown in **Scheme 3.08,** can generate product **9d** together with carbon dioxide and *tert*-butyl alcohol. Following the undesired path b, the acid starting material will also be regenerated and this can greatly reduce the reaction yield. **Scheme 3.08** may also explain that when making more sterically hindered hydroxamate, the reaction outcome was poorest (e.g., Cbz).

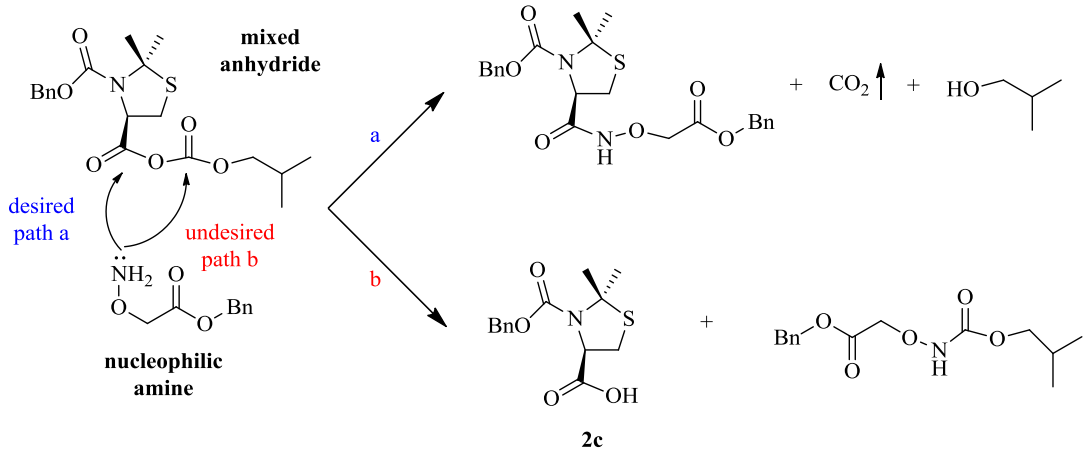

Scheme 3.08: Regeneration of starting material **2c**.

3.2.4 Synthesis of hydroxamate esters: the substituents effects

Conversion of *N*-protected thiazolidine carboxylic acid **2** to hydroxamate esters **9** was achieved by the *N*-acylation of different alkoxyamines via method A-C. The results are summarized in **Table 3.01**. When R is benzyl, the highest yield resulted from the reaction with the least hindered group (71%, H_2NOMe in entry 13). In comparison, a more hindered substrate can only generate compound with moderate yields (51%, $H_2NOCH_2CO_2Bn$ in entry 11 and 50%, H_2NOBn in entry 12). It was also found that when the HOBt and NHS esters of acid **2** were used, multiple products of similar polarities resulted and the purified yields were less than 30%. Additionally, methyl esters **9d** were made as a standard control for photochemistry. Simple refluxing of compound **2** for 16 hours, in presence of anhydrous potassium carbonate and acetone, with excess amount of methyl iodide, provided methyl ester **9d** in good yield (80% in entry 4) [24].

Table 3.01: Synthesis of hydroxamate esters **9**.

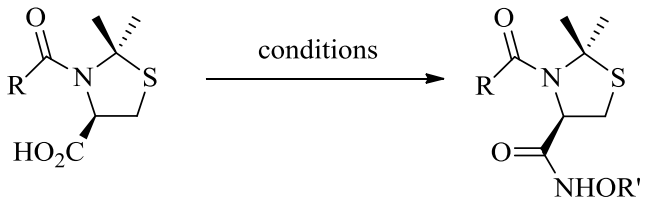

2 **9**

entry	R	R'	reaction conditions	compd	yield (%)
1	$PhCH_2O$	Bn	$H_2NOBn{\cdot}HCl$, method A	**9a**	55
2	$PhCH_2O$	CH_2CO_2Bn	H_2NOR', method B	**9b**	45
3	$PhCH_2O$	Bz	BzCl, method C	**9c**	18
4	$PhCH_2O$	Me	MeI, K_2CO_3	**9d**	80
5	H	Bn	$H_2NOBn{\cdot}HCl$, method A	**9e**	45
6	^tBuO	Bz	BzCl method C	**9f**	14
7	^tBuO	Ac	AcCl, method C	**9g**	38
8	^tBuO	CH_2CO_2Bn	H_2NOR', method B	**9h**	42
9	$PhOCH_2$	Ac	AcCl, method C	**9i**	10
10	$PhOCH_2$	$CH_2CO_2{}^tBu$	H_2NOR', method B	**9j**	30
11	Ph	CH_2CO_2Bn	H_2NOR', method B	**9k**	51
12	Ph	Bn	H_2NOR', method B	**9l**	50
13	Ph	Me	$H_2NOMe{\cdot}HCl$, method A	**9m**	71

Method A: EDC mediated coupling method (**Scheme 3.06)**
Method B and C: mixed anhydride method (**Scheme 3.07)**

3.2.5 Photo-oxidation of thiazolidine esters 9

Pummerer rearrangement has been widely studied and its mechanism is illustrated in **Scheme 3.09** [25]. Adopting a similar mechanism, the photooxidation of 3-acyl-2,2-dimethyl-4-substituted thiazolidine derivatives was first discovered by Takata et al. [26], which can provide C-5 hydroxy derivative in excellent yield (**Scheme 3.10**). However, comparing with Pummerer rearrangement, no activating agent such as a mineral acid is required.

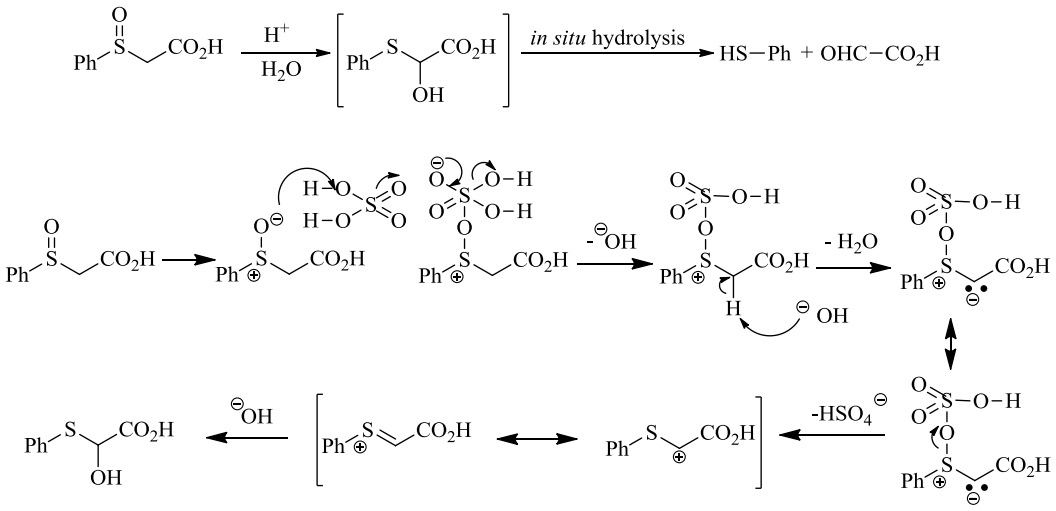

Scheme 3.09: The mechanism of Pummerer rearrangement: phenylsulfinyl acetic can generate α-hydroxyl sulfide when heating with mineral acid (e.g., sulfuric acid). This α-substituted sulfide can then be easily hydrolyzed to form the thiol (thiophenol) and carbonyl compound (glycoxylic acid).

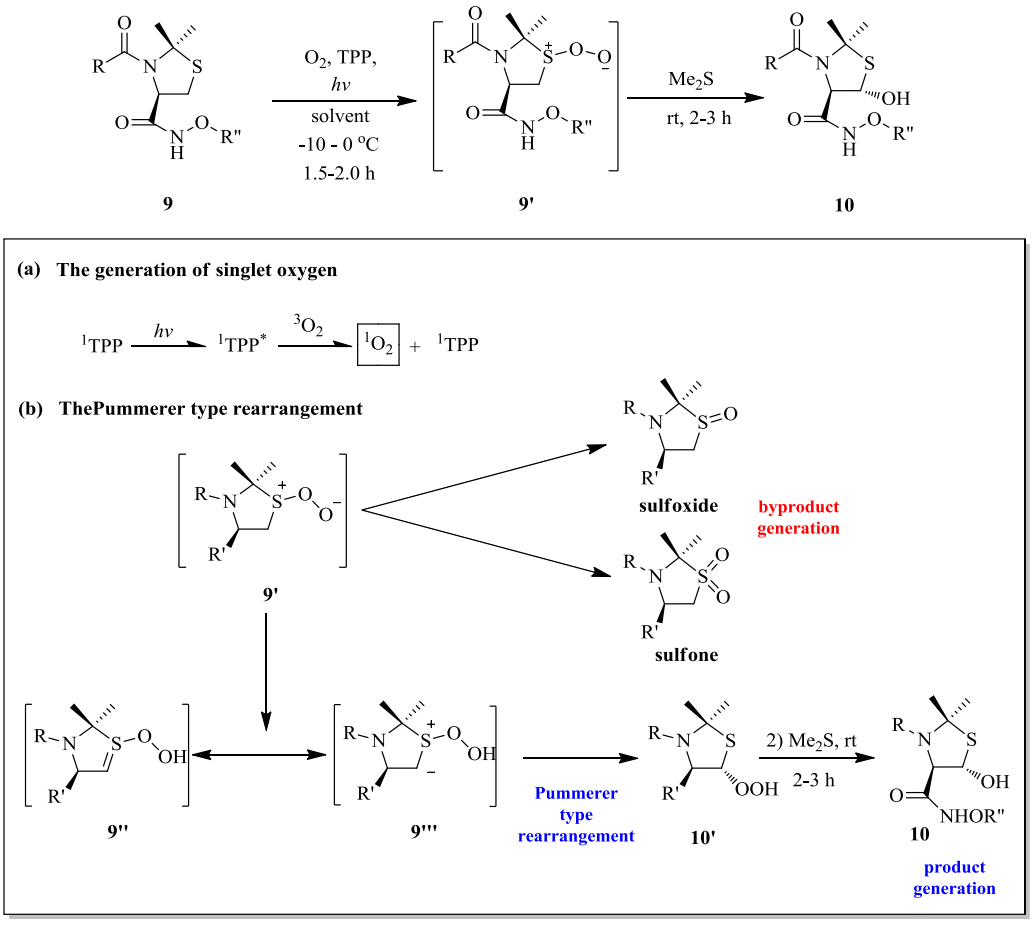

Scheme 3.10: The photo-oxidation key step, the modified mechanism: C-5 H was extracted by the oxygen in persulfoxide of intermediate **9'**.

In an aprotic solvent at low temperature, the persulfoxide **9'** was generated during the first step. The resulting persulfoxide **9'** (S-O-O$^-$) then underwent a Pummerer type rearrangement to yield **10'**. Initiated by treatment with excess amount of dimethyl sulfide, the cleavage of hydroperoxide bond leads to quantitative generation of C-5 oxidized thiazolidine **10** and dimethylsulfoxide. Of note, the sulfone or sulfoxide (byproducts) can also be generated through *S*-oxidation [27].

Herein, this unique photochemical approach, i.e., the photo-oxidation, was chosen as the key step of the synthetic sequence to make the β-lactam ring. During the reaction performance, tetraphenylporphyrin (TPP) was employed as the sensitizer to irradiate the ground state of oxygen to singlet oxygen at a low temperature. The effects of temperature, lamp, and substitutions were also been tested and discussed in the following sections [28].

3.2.6 Photo-oxidation: the reaction setup

The reaction setup is illustrated in **Figure 3.03**. The photo-oxidation to produce the C-5 oxidized thiazolidine products was performed using a 250 or 500 watt halogen portable bulb and photosensitizer at a low temperature. The most important consideration is how to sufficiently maintain the reaction solution at a low temperature. This is because the stability of singlet oxygen at room temperature is poor and a high temperature can also cause the decomposition of the starting material compound **9**, resulting in more impurities and low yield. In addition, a 250 watt halogen bulb can generate a lot of heat. If coolant circulating system is not utilized, the solution temperature can reach 70 ºC, resulting a quickly loss of reaction solvent. Generally, in the first part of the procedure,

iced water or chilled acetone was circulating through the jacketed beaker, and the reaction progress was carefully monitored by TLC

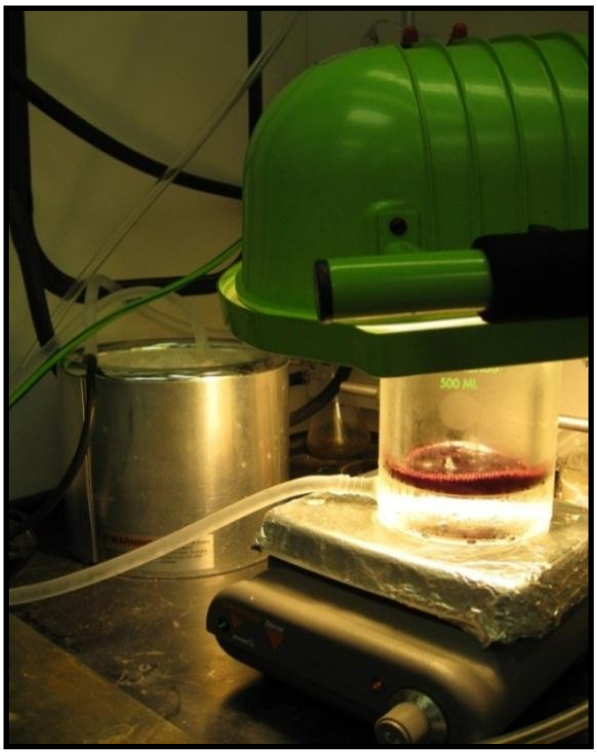

Figure 3.03: Set up for photo-oxidation reaction.

On TLC plate, spot having hydroxamate molecules stained brown by $FeCl_3$ after heating. Research has shown that most substrates (see **Table 3.02**) require 1.5 to 2 hours to have quantitative conversion of the starting material **9** into the hydroperoxide **9'** [29]. However, due to the high similarity in the structures' polarity, hydroperoxide intermediates **9'** (or **10'**) and starting materials **9** are too close to each other on TLC. In order to confirm the full conversion from starting material **9** into hydroperoxide **9' (**or **10'**), a co-spotting was performed with a trace amount of Me_2S in the reaction mixture co-spotting on the same lane of the TLC plate. By doing so, hydroperoxide **10'** can quantitatively convert to chemically stable C-5 hydroxy product **10** with a lower R_f value.

In the second part of the procedure, Me_2S was added after the complete disappearance of the starting material, the reaction solution was then left stirring at room temperature.

3.2.7 Photo-oxidation: the influence of solvent

Various aprotic solvents were studied. This is because protic solvents might be possible to extract the proton at C-5 position and therefore mainly form the sulfoxide (conversion of hydroperoxide **9'** to **9'''**, **Scheme 3.10**). Among all solvents tested as shown in **Scheme 3.11**, THF gave product at least 20% higher than MeCN and PhH after column purification. Interestingly, the study also showed temperatures lower than 0 ºC may not be required in the transformation. When the experiment was performed in *p*-dioxane (mp 11.8 ºC), the product **10a** was generated in 56% yield. In this case, instead of circulating cold acetone (< -10 ºC), the reaction solution was chilled by cold water and the temperature was just above 12 ºC.

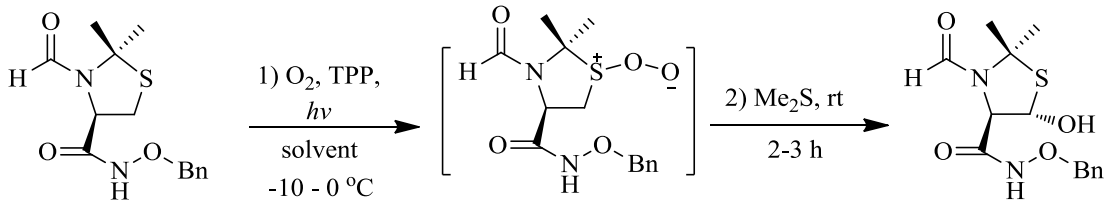

solvent of choice	yield (%)
THF	59
PhH	37
MeCN	35
p-dioxane*	56

* reaction temperature is above 12 ºC

Scheme 3.11: The effect of the solvent on photochemistry.

3.2.8 Photo-oxidation: the influence of reaction substrate

As described in section 3.2.5, various analogues with different R and R' groups were examined. The effect of R' was negligible in the reaction yield; however, it was noted that less hindered R substituents gave rise to the corresponding product at a higher yield. In many instances (**Table 3.02**), the yields after purification were above 60% with the highest observed for thiazolidines consistently having an *N*-benzoyl protecting group (entry 8-9). Generally, the reaction scales ranged from 0.4 to 2.0 g with a slight to moderate decrease in the resulting yields. When greater than 1.0 g of hydroxamate ester **9** was used, a decrease in reaction yield was observed which might be due to the insufficient cooling in upper part of the solution.

Table 3.02: Photo-oxidation of thiazolidine hydroxamate esters **9**.

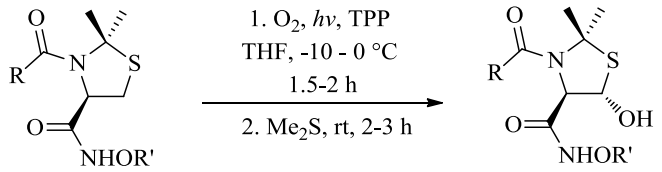

9 **10**

entry	R	R'	compd	yield (%)
1	H	Bn	**10a**	59
2	$PhCH_2O$	Bn	**10b**	65
3	$PhCH_2O$	Me	**10c**	42
4	$PhCH_2O$	CH_2CO_2Bn	**10d**	53
5	^tBuO	CH_2CO_2Bn	**10e**	58-73
6	$PhOCH_2$	Ac	**10f**	44
7	$PhOCH_2$	$CH_2CO_2{}^tBu$	**10g**	60-68
8	Ph	CH_2CO_2Bn	**10h**	67-84
9	Ph	Bn	**10i**	68-73
10	Ph	Me	**10j**	80

The optimized reaction concentration was around 0.05 M. It was noticed that a higher concentration can generate more impurities. Additionally, in order to maintain this

optimized concentration (0.05 M), when more anhydrous THF is needed, the volume of currently used jacked beaker (100 mL) became a major limitation of the present setup as shown in **Figure 3.03**.

Interestingly the hydroperoxide is very stable at room temperature. Only adding Me_2S can generate the rearranged product **10**. Trace amount of impurities were also detected: the two very polar spots (R_f < 0.05, not stain browned by $FeCl_3$) were formed before adding dimethylsulfide. In the first part of procedure, when the reaction time lengthens, the two impurities spots started to gather over time. As illustrated in **Scheme 3.10**, these two byproducts might be the sulfoxide and sulfone. The slow formation of these impurities may explain why the yields of product **10** were always less than 80%.

3.2.9 Photo-oxidation: the influence of ring platform

Different scaffolds (**Scheme 3.12**) were also been attempted. The first example has R as a phenyl (**12a, 12b)** and the second example has a benzyl group (**12c**). The 4,5-dihydrothiazole ring was synthesized via methanol refluxing of L-cysteine in the presence of TEA, followed by creation of carboxylic hydroxamate ester **12**. However, the photochemistry step was not able to generate the corresponding C-5 hydroxy product. The first part of the reaction was very slow and no further change was observed on TLC after adding Me_2S. As further illustrated in **Scheme 3.12,** it is believed that the desired proton extraction step can not occur on both imidazole analogues, because oxygen in persulfoxide and nitrogen in imidazole are both good proton acceptors. As a result, the key intermediate **11'''** can not be generated thus will not undergo Pummerer type rearrangement. Interestingly, the unique property of azole structure also play an important role in biological structure and function. Azole structure as proton acceptor can

be found at several enzymes' active site. For example, the lead compound molecule form a hydrogen-bonded pair through the (azole) N···H···O (hydroxy) interaction (**Figure 4.02**, Chapter 4).

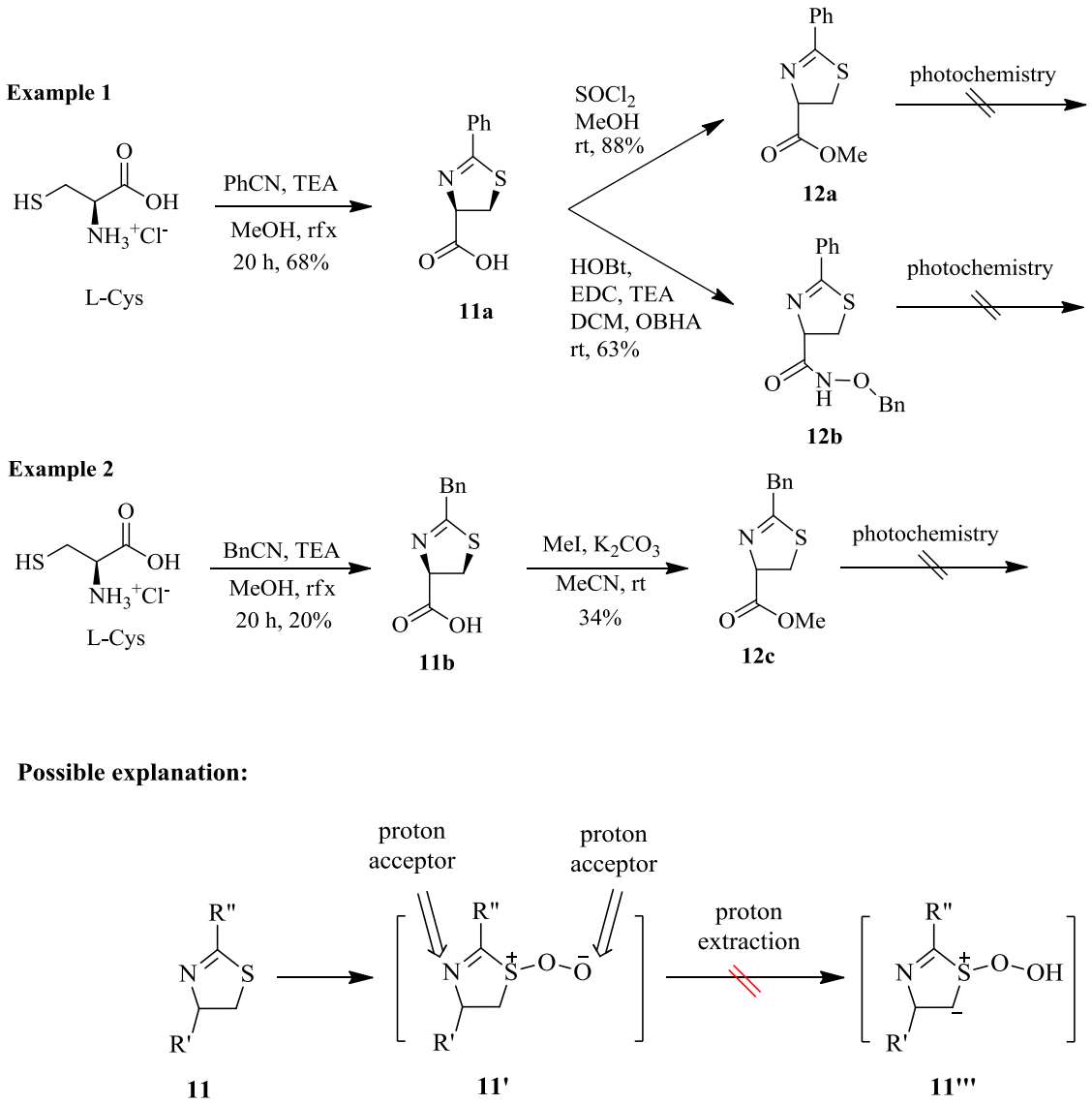

Scheme 3.12: The photochemistry attempts on compounds **12a-c**.

3.2.10 Photo-oxidation: the application of green chemistry

During the course of this work, even though using a reduced amount (e.g., 0.1 equiv) of sensitizer, chromatography purification was still a problem. In the case of

tetraphenylporphyrin (TPP), which proved very difficult to remove from the product because of its extremely low polarity. It was hypothesized that by using the resin bound sensitizer [31], the sensitizer can be more easily removed from the reaction solution through simple filtration. This process is adopted widely in solid-phase peptide chemistry.

The synthetic route involves ether bond formation between the chloride of the Merrifield resin, and the hydroxyl group of the sensitizer. Listed in **Scheme 3.13** are the designed structures that have been included in the study. The Merrifield resin-bound rose bengal, methylene blue, and fluorescein were simply obtained by heating the resin and photosensitizer in DMF at 80 °C. The final product was simply washed by methanol to provide clean particles in unique color, e.g., Merrifield resin bound acid red as a red solid, Merrifield resin bound methylene blue as a blue solid, and Merrifield resin bound fluorescein as a yellow solid.

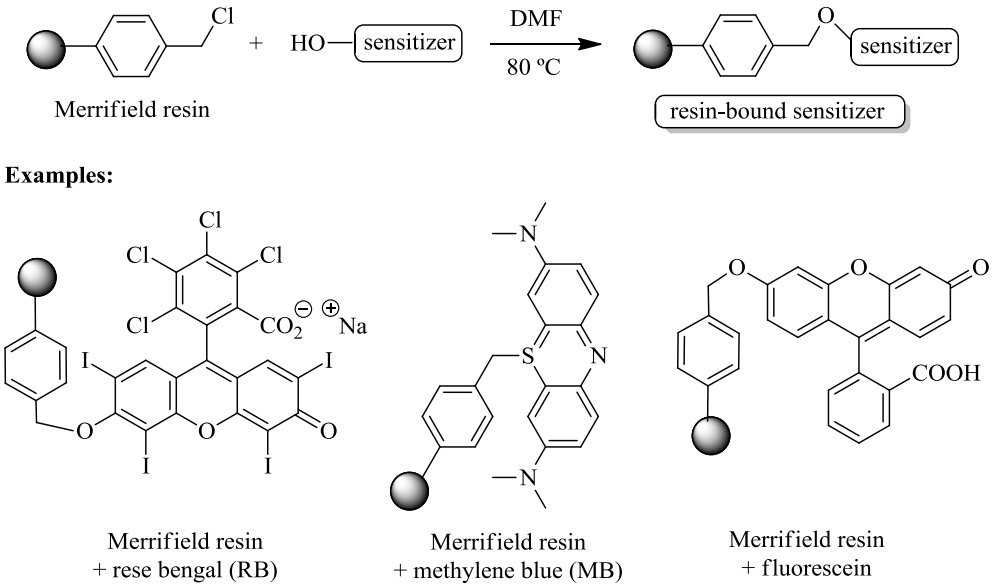

Scheme 3.13: Synthesis of the resin-bound sensitizers.

Merrifield resin bound tetraphenylporphyrin was also prepared. The TPP was made by refluxing benzaldehyde and pyrrole in propanoic acid for one hour followed by cold filtration with a methanol wash. The synthetic sequence was completed by Dr. Long. Illustrated as retrosynthesis in **Scheme 3.14**, nitration was continually performed by directly adding concentrated nitric acid, followed by reduction and *N*-alkylation of the resin.

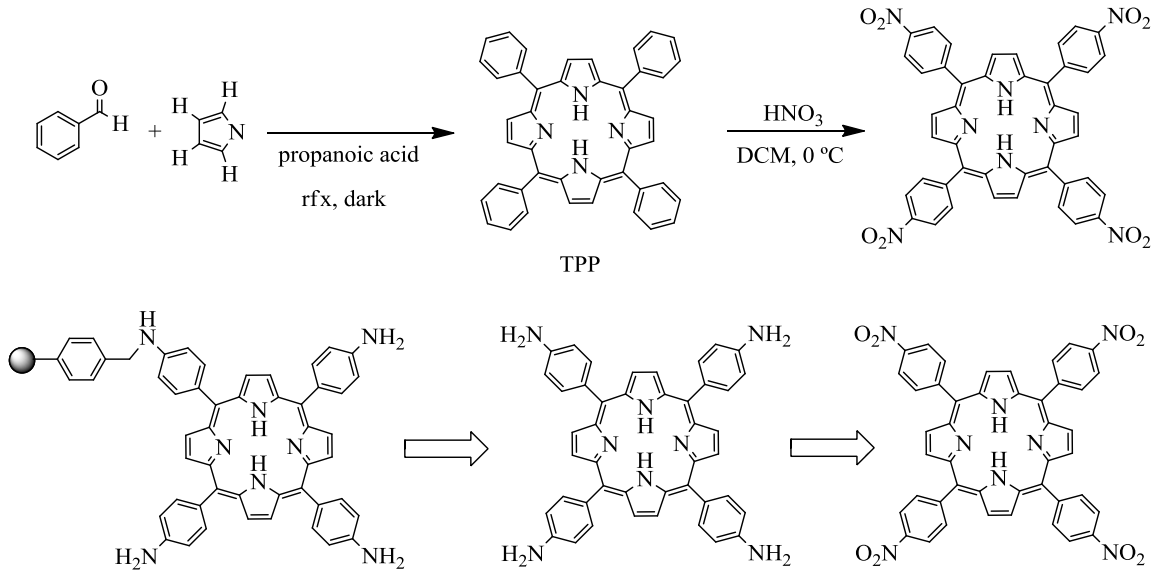

Scheme 3.14: Retrosynthesis of the resin-bound tetraphenylporphyrin.

It is expected that the designed resin bound sensitizer should to be stable and very easy to remove. Using compound **9e** as starting material and resin bounded tetraphenylporphyrin as sensitizer, the photochemistry was performed by the same procedure (**Table 3.03**). The resin bound sensitizer can be removed easily by simple filtration before the following column purification. Using the reaction of compound **9e** with unbound TPP as a control, a small increase in reaction outcome was observed (63% in entry 2). This might be due to the easier purification procedure compared to the

original design. This application has also been tested in other form of sensitizers (i.e., resin bound rose bengal and resin bound methylene blue), providing the corresponding product in good yield (59% in entry 3, 53% in entry 4).

Table 3.03: Photo-oxidation with resin attached sensitizer.

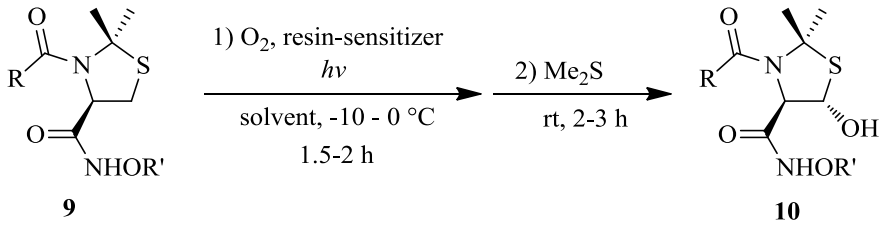

entry	R	R'	sensitizer	solvent	compd	yield (%)
1	H	Bn	TPP	THF	**10a**	59
2	H	Bn	TPP resin	THF	**10a**	63
3	H	Bn	MB resin	MeCN	**10a**	59
4	H	Bn	RB resin	THF	**10a**	53
5	^{t}BuO	Bz	TPP resin	THF	**10k**	33

3.2.11 An alternative approach: the oxidation with benzoyl peroxide (BPO)

An alternative method that utilized benzoyl peroxide was also studied. The reaction was performed by refluxing hydroxamate ester **9c** with $(PhCO_2)_2$ in toluene [32]. Afterwards, the benzoyl ester **13** was deprotected by basic hydrolysis. However the complicated purification limited its further use and the overall yield of two-steps synthesis was only 35% (not higher than the photochemistry, **Scheme 3.15**). Thus, the photo-oxidation approach was preferred in the synthetic route design.

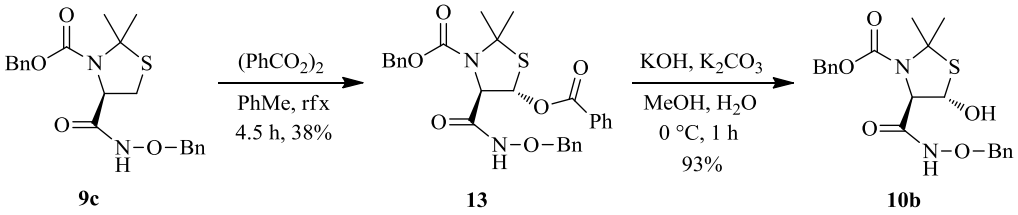

Scheme 3.15: Reaction of hydroxamate ester with benzoyl peroxide.

3.2.12 Cyclization of thiohemiacetals 10

The key ring-forming step was easily accomplished by combining MsCl, Et_3N and C-5 hydroxy thiazolidine **10** in DCM and left overnight in a -20 °C freezer [33]. Yields obtained by this method were in the range of 25-58%. Interestingly, for the cyclization of *O*-methyl lactam **14j**, the reaction was complete in less than 10 min at 0 °C while several hours were needed for the more sterically hindered *O*-benzyl analogue **14i** (**Table 3.04**). The low yield of many substrates was attributed to the formation of byproducts and decomposition of the lactam ring during the chromatography purification. Evidence for this was that the crude ^{1}H NMR spectrum contained only trace amounts of impurities prior to silica gel purification.

Table 3.04: The cyclization reaction

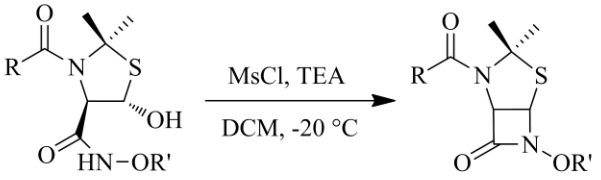

10 **14**

entry	R	R'	compd	yield
1	$PhCH_2O$	Bn	**14a**	58
2	$PhCH_2O$	Bz	**14b**	49
3	$PhCH_2O$	CH_2CO_2Bn	**14c**	48
4	H	Bn	**14d**	36
5	^{t}BuO	Bz	**14e**	25
6	^{t}BuO	CH_2CO_2Bn	**14f**	45
7	$PhOCH_2$	$CH_2CO_2{}^t$Bu	**14g**	46
8	Ph	CH_2CO_2Bn	**14h**	42
9	Ph	Bn	**14i**	41
10	Ph	Me	**14j**	51

Methods to introduce other leaving groups (X = Br, Cl, etc.) have also been studied, including Mitsunobu esterification procedure initiated with diisopropyl azodicarboxylate (DIAD) and triphenylphosphine (PPh_3) [34], and phosphorus tribromide (PBr_3) mediated bromination [35]. As summarized in **Table 3.05**, however, the only successful reaction was performed by using MsCl and TEA. Since the hydroxamate ester anions (p*K*a < 10)

are more basic than typical amides (p*K*a > 20). A weak base, i.e., TEA, was sufficient to facilitate the ring closure.

Table 3.05: Intramolecular cyclization of thiohemiacetal **10g**.

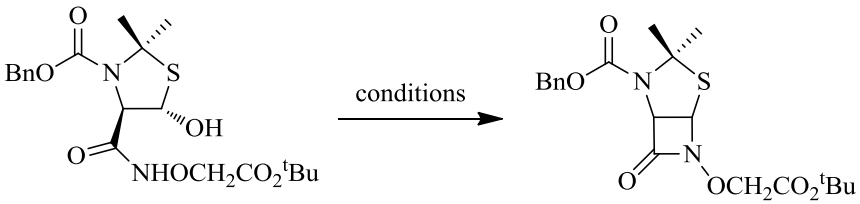

10g **14g**

entry	conditions	results
1	MsCl, TEA, DCM, -20 °C	46% product
2	PBr_3, DCM, 0 °C to rt	S.M.
3	PBr_3, K_2CO_3, DCM, 0 °C to rt	poor yield
4	PBr_3, pyridine, 0 °C to rt	S.M.
5	PPh_3, DIAD, MeCN, 0 °C to rt	S.M.
6	PPh_3, I_2, imidazole, DCM, rt	many spots
7	PPh_3, Br_2, MeCN	no reaction
8	PPh_3, TEA, CCl_4	no reaction

3.2.13 Synthesis of *N*-alkoxy monocyclic β-lactams 15a

The thiazolidine ring cleavage was the next step. The product **15a** was efficiently formed by direct reaction with methoxycarbonylsulfenyl chloride (ScmCl), which has been previously used in peptide chemistry to cleave the thiazolidine ring of the parent compounds [36]. During the reaction, AcOH was chosen as reaction solvent, DMF was used as a cosolvent to solubilize the starting material, water was introduced since it can promote the hydrolysis of enamine intermediate back to acetone, and NaOAc was used as a chloride ion scavenger. However, the original procedure provide very slow yield.

Finally, when co-administered with a stronger acid catalyst (i.e., TFA), the monocyclic β-lactam **15a** was formed after 1.5 hours in higher yield (70%) (**Table 3.06**).

Table 3.06: Solvent effect on ring cleavage.

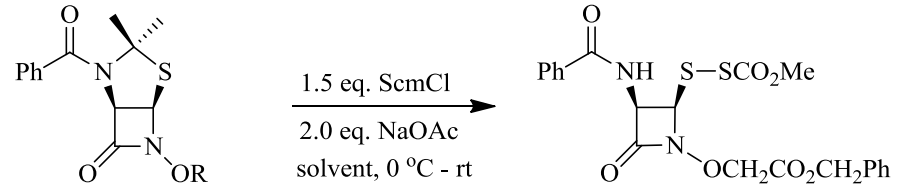

14h R = $CH_2CO_2CH_2Ph$ **15a**

entry	AcOH	DMF	H_2O	TFA	yield (%)
1	12	2	1	1	34.1
2	0	2	1	10	trace
3	12	2	0	1	70.0

It is believed during the reaction, due to the large dipole moment of methoxycarbonylsulfenyl chloride (ScmCl), the protonation is expected to be difficult. It is believed that the TFA can both accelerated this process and promoted hydrolysis of enamine intermediate as resulting in significantly increase the reaction yield (**Scheme 3.16**).

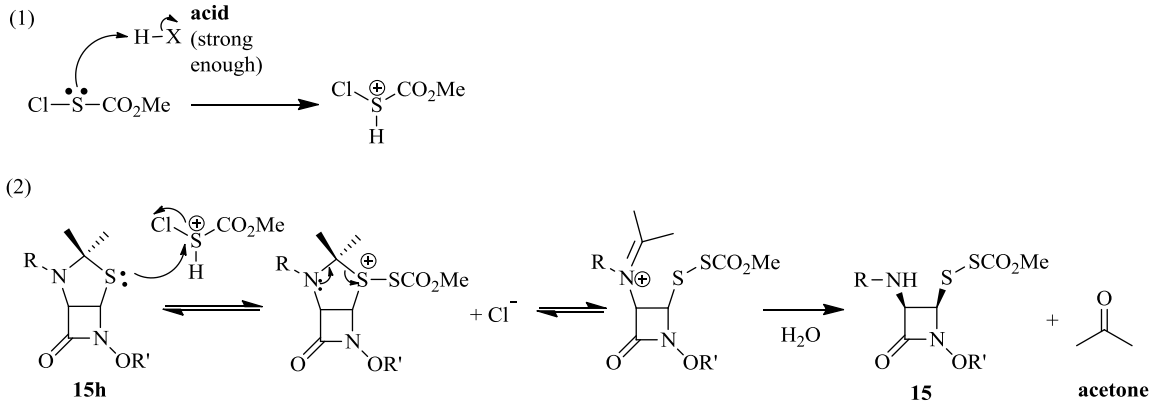

Scheme 3.16: Mechanism of thiazolidine cleavage.

3.2.14 Thiazolidine cleavage and *N*-deprotection

The cleavage of the benzyloxy group was attempt next on compound **16**. However, in model reactions, many reducing agents (e.g., LAH; $NaBH_4$; Zn dust; SmI_2 [37]) were found to be too harsh for the N-1/C-4 bond of the β-lactam nucleus (**Table 3.07**).

Table 3.07: Cleavage of thiazolidine ring.

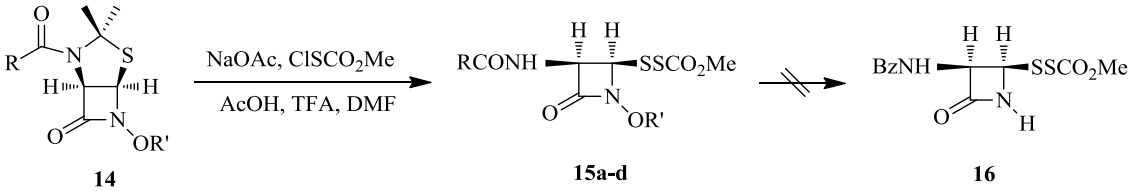

entry	R	R'	compd	yield (%)
1	Ph	CH_2CO_2Bn	**15a**	49-55
2	Ph	Bn	**15b**	47-65
3	$PhCH_2O$	Bn	**15c***	32
4	^tBuO	CH_2CO_2Bn	**15d***	38

*** 15c**, **15d** were obtained without adding TFA

As shown in **Table 3.08**, the screening of milder reaction conditions were continued on bicyclic analogues **14d** and **14i**, including acid hydrolysis (entry 1-3), palladium/carbon catalyzed reduction (entry 4) and reduction in liquid ammonia with alkali-metal (entry 5). None of tested reactions resulted in desirable product, which may have been due to instability of the starting material.

Table 3.08: Unsuccessful cleavage reactions.

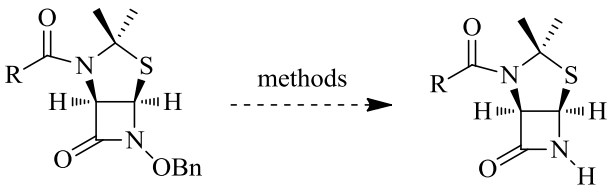

14 **17**

entry	starting material	reaction condition		results
1	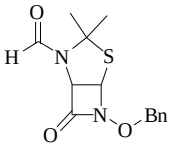 **14d**	Clay, MeOH	rt/reflux 24 h	no change on TLC
2		1N HCl, MeOH	reflux 1h	S.M. all decomposed
3		1N HCl, AcOH	reflux 0.1h	S.M. all decomposed
4	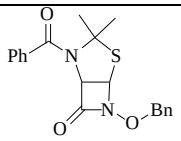 **15i**	Pd/C, MeOH, H_2	rt 3h	one new more polar spot no more S.M., (^{1}H NMR: still showing 2 CH_3 groups)
5		1) Na, anh. NH_3 2) NH_4Cl	-40 °C 0.25 h	no more S.M. (^{1}H NMR: not correct)

Assuming that the synthetic sequence required the removal of the alkoxy group before the ring conversion, the N-O bond cleavage was initially conducted via SmI_2-mediated reaction [38]. Upon ring opening with ScmCl, the *N*-protio monocyclic β-lactam **16** possessing the *cis*-configured azetidinone nucleus of penicillins and cephalosporins was obtained (**Scheme 3.17**).

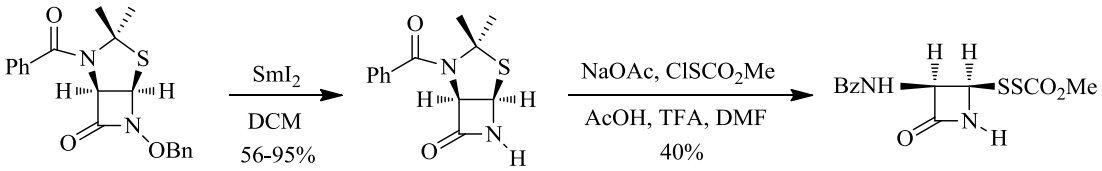

14i **17** **16**

Scheme 3.17: Synthesis of monocyclic β-lactams **16**.

As illustrated in **Scheme 3.18**, one more reaction using inorganic salt was attempted. Mercury salts were screened to cleave the thiazolidine ring [39]. When $Hg(OAc)_2$ was

used, the first part of the reaction produced nice white solid with 55% yield. This mercury salt intermediate **9a** directly reacted with acetyl chloride after simple filtration. The resulting *S*-acetyl final product **19** has a diagnostic CH_3 peak found in the ^1H NMR graph. However, the overall yield of this two-steps sequence was very poor and was not continued in this study.

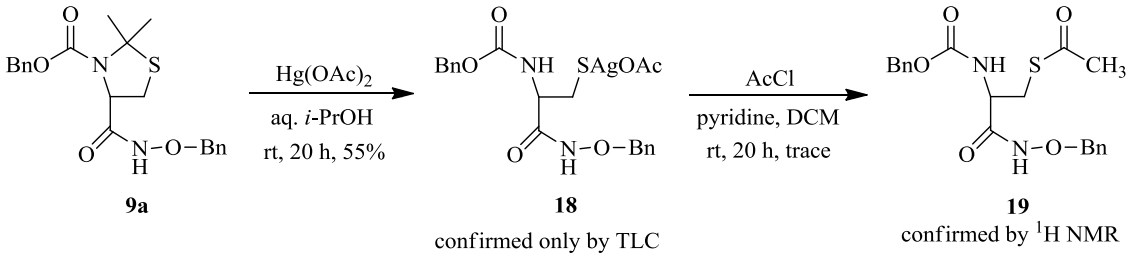

9a **18** confirmed only by TLC **19** confirmed by ^1H NMR

Scheme 3.18: Cleavage reaction using $Hg(OAc)_2$.

3.2.15 Other studies

Alternatively, the synthetic sequence on a different scaffold (i.e., 2-*tert*-butyl-thiazolidine) was attempted. As illustrated in **Scheme 3.19**, through condensation and protection on the thiazolidine nitrogen atom, EDC coupling followed. The resulting hydroxamate ester **22** later went through photo-oxidation or BPO oxidation; however this approach proved to have a lower yield compared with 2,2-dimethyl thiazolidines and thus was not continued.

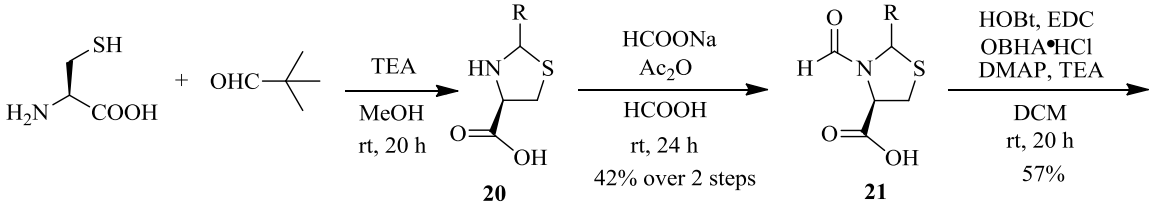

20 **21**

Scheme 3.19: Preparation of bicyclic 2-*tert*-butyl-thiazolidine **24**.

Scheme 3.19 (con.)

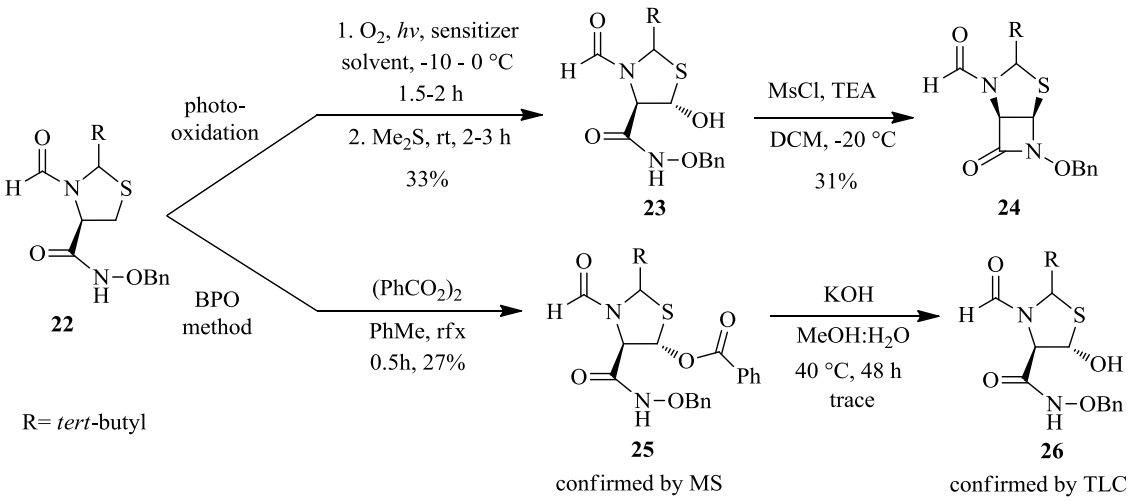

3.3 Conclusion and Future Directions

In summary, a new method to synthesize β-lactams, using photochemistry as one of the key steps in the final stages of the synthetic sequence, was developed.

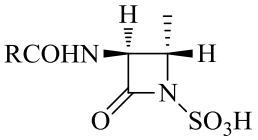

monobactams

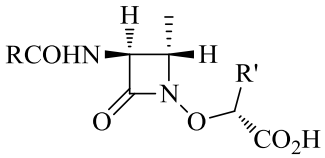

oxamazins

Figure 3.04: Structure of monobactams.

The stereoselective introduction of hydroxyl group at C-5 by photooxidation enables an alternative approach to formation of the azetidinone ring. It was found the thiazolidine starting material react readily with singlet oxygen (generated in the presence of 0.1 equiv of tetraphenylporphyrin with the help of 250 Watt halogen lamp at 12 °C). However for the first time it was discovered a temperature lower than -10 °C was not required. During the photooxidation a practical study of resin-bound sensitizer was also examined, which may offer advantages in ease of silica gel chromatography purification. Other interests in this

study include the direct usage of sunlight as light source, which should have no limitation on the solution volume for photo-oxidation.

Subsequent cyclization of C-5 hydroxy thiazolidine **10** to bicyclic β-lactams was found to be clean and facile. Although mild conditions (i.e., TEA, MsCl) would facilitate the ring closure of the the hydroxamate ester, the stability of the constrained rings likely had an adverse effect on the isolated yields. Evidence for this was observed during the efforts to deprotect lactam **14** which frequently resulted in regeneration of the starting material (i.e., hydroxamate **9**).

Cleavage of the thiazolidine ring was achieved by using methoxycarbonylsulfenyl chloride. It was found the addition of a stronger acid catalyst can increase the yield from 35% to 70%. Lastly, the removal of the *N*-alkoxy group prior to thiazolidine ring cleavage successfully afforded the *N*-protio monocyclic β-lactam, which is capable of further elaboration into biologically active antibacterials (**Figure 3.04**) (e.g., oxamazins [40]). Additional work will also include the activity test of the synthesized compounds in the future.

3.4 Experimental

In general, reagents and solvents were used as purchased without further purification. Reaction products were purified by column chromatography on silica gel (60-100 mesh) and visualized by UV on TLC plates (silica gel 60 F_{254}). Methoxycarbonylsulfenyl chloride was purchased from Oakwood Products, Inc (West Columbia, SC) and SmI_2 (0.7-0.12 M in THF; lot # K22W038) was obtained from Alfa Aesar (Ward Hill, MA). Melting points were determined with a melting point apparatus and were left uncorrected. Optical rotations were recorded on a Bellingham & Stanley Digital Polarimeter ADP220

with the values given in 10^{-1} deg cm^2 g^{-1}. Mass spectrometry was performed by electrospray ionization (ESI). ^1H and ^{13}C NMR spectra were recorded on a Varian Inova 500 MHz spectrometer. Chemical shifts were expressed in δ (ppm) values with tetramethylsilane or residual solvent (e.g., $CHCl_3$ or DMSO) as an internal standard. Abbreviations used in the description of resonances are as follow: s (singlet); d (doublet); t (triplet); q (quartet); qnt (quintet); sxt (sextet); spt (septet); oct (octet), m (multiplet); app (apparent); bs (broad singlet), bm (broad multiplet). The designation "ABq" for a ^1H NMR peak indicates that a peak was one partner of an AB quartet; if additional splitting was observed, they are noted after the ABq designation (e.g., ABqd). Copies of NMR spectra may be found in APPENDIX B.

Synthesis of (*R*)-2,2-dimethylthiazolidine-4-carboxylic acid (1): Acetone (150 mL) was firstly dried over Drierite™ (1.5 g), and was refluxed for 1 hour and distilled. The L-cysteine HCl (5.05 g) was then refluxed in this pre-treated acetone for two hours under nitrogen, the product was collected by simple filtration. Yield: 63%; white solid, mp 165-167 °C.

Synthesis of *N*-benzyl-2,2-dimethyl thiazolidine-4-carboxylic acid (2e): Benzoyl chloride (3.93 g, 28 mmol) was slowly added into a pyridine solution (30 mL) of (*R*)-2,2-dimethylthiazolidine-4-carboxylic acid (5.5 g, 28 mmol). The reaction mixture was then stirred overnight. After that, the solvent was concentrated and was redissolved in EtOAc. This organic layer was washed four times with 0.5 N HCl, dried over Na_2SO_4. The white solid was finally triturated in a 1:1 solution of hexanes:EtOAc to provide the *N*-benzyl-2,2-dimethyl thiazolidine-4-carboxylic acid **2e**. Yield: 67%; white solid, mp 181-183 °C;

TLC (SiO_2) R_f 0.37 (9:1 DCM:MeOH); ^{1}H NMR (500 MHz, DMSO-d_6) δ 7.74-7.34 (m, 5H), 4.72 (bs, 1H), 3.48 (dd, 1H, J = 12.0, 6.5 Hz), 3.13 (dd, J = 12.0, 5.0 Hz), 1.94-1.92 (m, 6H).; ^{13}C NMR (125 MHz, DMSO-d_6) δ 172.1, 169.1, 142.34, 142.33, 129.6, 128.8, 126.3, 72.8, 67.7, 31.2, 29.7, 28.3.

Preparation of thiazolidine hydroxamate esters (9); general procedure. Thiazolidine carboxylate **2** (26 mmol) and *N*-methylmorpholine (3.17 mL, 28.6 mmol) were combined in anhydrous THF (105 mL) when the temperature was maintained at 0 °C. Isobutyl chloroformate (3.39 mL, 26 mmol) was added and the cloudy solution was stirred at 0 ºC for 0.5 hours. A THF solution of alkoxyamine (25 mmol, 5 mL) was next added slowly over a 5 minutes period. The reaction flask was sealed and left in a -20 °C freezer overnight. After warming to room temperature, the reaction solution was t filtered, evaporated, redissolved in EtOAc, and then, the organic layer was dried over $MgSO_4$, filtered, and evaporated. The hydroxamate ester **9** was separated by flash chromatography on silica gel using a 6-50% gradient of EtOAc in hexanes**.**

(***R*)-Benzyl 4-((2-(benzyloxy)-2-oxoethoxy)carbamoyl)-2,2-dimethylthiazolidine-3-carboxylate (9b):** Yield: 45%; colorless oil; TLC (SiO_2) R_f 0.17 (4:1 hexanes:EtOAc); ^{1}H NMR (500 MHz, $CDCl_3$) δ 9.78 (s, 1H), 7.36-7.30 (m, 10H), 5.21-5.09 (m, 4H), 4.83 (s, 1H), 4.47 (s, 2H), 3.24 (s, 2H), 1.89 (s, 3H), 1.77 (s, 3H).

(*R*)-*N*-(Benzyloxy)-3-formyl-2,2-dimethylthiazolidine-4-carboxamide (9e): Yield: 43%; white solid, mp 130-132 ºC; TLC (SiO_2) R_f 0.25 (2:1 hexanes:EtOAc); $[\alpha]^{26}_D$: -96 (*c* 1, $CHCl_3$); ^{1}H NMR (500 MHz, $CDCl_3$) δ 10.07 (s, 1H), 8.17 (s, 1H), 7.42-7.40 (m, 2H), 7.36-7.33 (m, 3H), 4.90 (s, 2H), 4.77 (t, 1H, *J* = 6.0 Hz), 3.48 (dd, 1H, *J* = 12.5, 5.0 Hz), 3.16 (dd, 1H, *J* = 12.5, 7.5 Hz), 1.77 (s, 3H), 1.73 (s, 3H); ^{13}C NMR (125 MHz,

$CDCl_3$) δ 185.2, 167.0, 159.8, 135.1, 129.2, 128.5, 128.4, 77.9, 70.5, 60.9, 31.3, 30.1, 29.8.

(*R*)-*tert*-Butyl 4-(((benzyloxy)carbonyl)methoxycarbamoyl)-2,2-dimethylthiazolidine-3-carboxylate (9h): Yield: 61%; colorless oil; TLC (SiO_2) R_f 0.55 (1:1 hexanes:EtOAc); ^{1}H NMR (500 MHz, $CDCl_3$) δ 7.39-7.33 (m, 5H), 5.22 and 5.16 (ABq, 2H, Δ*v* = 31.5 Hz, *J* = 12.5 Hz), 4.73 (bs, 1H), 4.55 and 4.49 (ABq, 2H, Δ*v* = 22.0 Hz, *J* = 17.5 Hz), 3.21 (s, 2H), 2.35 (s, 1H), 1.87-1.74 (m, 6H), 1.46 (s, 9H).

(*R*)-*tert*-Butyl 2-((2,2-dimethyl-3-(2-phenoxyacetyl)thiazolidine-4-carboxamido)oxy)-acetate (9i): Yield: 30%; pale solid, mp 128-130 ºC; TLC (SiO_2) R_f 0.32 (2:1 hexanes:EtOAc); ^{1}H NMR (500 MHz, $CDCl_3$) δ 7.28-7.25 (m, 2H), 6.98 (t, 1H, *J* = 7.5 Hz), 6.91 (d, 2H, *J* = 7.5 Hz), 4.95 (s, 1H), 4.62-4.53 (m, 2H), 4.35 and 4.26 (ABq, 2H, Δ*v* = 45.5 Hz, *J* = 16.5 Hz), 3.30-3.24 (m, 2H), 1.99 (s, 3H), 1.83 (s, 3H), 1.46 (s, 9H); ^{13}C NMR (125 MHz, $CDCl_3$) δ 168.7, 167.9, 166.5, 157.5, 129.7, 121.9, 114.6, 83.2, 74.9, 72.4, 68.9, 65.2, 32.6, 28.5, 28.1, 27.4.

(*R*)-Benzyl 2-((3-benzoyl-2,2-dimethylthiazolidine-4-carboxamido)oxy)acetate (9k): Yield: 51%; colorless oil; TLC (SiO_2) R_f 0.32 (1:1 hexanes:EtOAc); $[\alpha]^{26}_D$: -54 (*c* 1, $CHCl_3$); ^{1}H NMR (500 MHz, $CDCl_3$) δ 9.65 (s, 1H), 7.38-7.25 (m, 10H), 5.19 (m, 3H), 4.70 (s, 1H), 4.41 (m, 1H), 4.27 (m, 1H), 3.17 (s, 2H), 1.98-1.86 (m, 6H); ^{13}C NMR (125 MHz, $CDCl_3$) δ 171.1, 169.3, 167.9, 137.6, 134.7, 129.6, 128.8, 128.7, 128.6, 128.5, 126.1, 73.8, 72.1, 67.1, 60.3, 31.4, 29.6.

(*R*)-3-Benzoyl-*N*-(benzyloxy)-2,2-dimethylthiazolidine-4-carboxamide (9l): Yield: 51%; colorless oil; TLC (SiO_2) R_f 0.68 (1:1 hexanes:EtOAc); $[\alpha]^{27}_D$: -112 (*c* 1, $CHCl_3$); ^{1}H NMR (500 MHz, DMSO-d_6) δ 11.04 (s, 1H), 7.46-7.27 (m, 10H), 4.60 (d, 2H, *J* =

10.0 Hz), 4.40 (d, 1H, *J* = 10.0 Hz), 3.36 (s, 2H), 1.96-1.90 (m, 6H); ^{13}C NMR (125 MHz, DMSO-d_6) δ 169.1, 167.1, 142.3, 138.8, 136.0, 129.6, 129.4, 128.9, 128.8, 128.7, 126.7, 77.3, 66.4, 60.2, 32.3, 28.9.

(*R*)-3-Benzoyl-*N*-methoxy-2,2-dimethylthiazolidine-4-carboxamide (9m): Yield: 70%; pale solid, mp 165-169 ºC; TLC (SiO_2) R_f 0.31 (1:1 hexanes:EtOAc); $[\alpha]^{26}_D$: -132 (*c* 1, $CHCl_3$); ^{1}H NMR (500 MHz, $CDCl_3$) δ 10.38 (s, 1H), 7.34-7.27 (m, 5H), 4.59 (bs, 1H), 3.26 (s, 3H), 3.03 (m, 2H), 2.02-1.87 (m, 6H); ^{13}C NMR (125 MHz, $CDCl_3$) δ 170.1, 167.6, 137.6, 129.7, 128.5, 126.5, 66.4, 63.8, 60.5, 32.1, 28.3.

Photo-oxidation of thiazolidines 9; general procedure. To a 500 mL jacketed beaker equipped with a circulating -10 - 0 ºC bath was added tetraphenylporphyrin (17 mg, 28 μmol) and hydroxamate ester **9** (2.8 mmol) in anhydrous THF (55 mL). A 500 W halogen lamp was illuminated approximately one inch above the beaker for 1.5 h while a stream of purified oxygen was bubbled into the solution. Methyl sulfide (520 μL, 7.0 mmol) was next added and the solution was left at room temperature until conversion to the thiohemiacetal was complete (2-3 h). The mixture was then concentrated and the crude oil was purified by silica gel chromatography on silica gel using a 10-70% gradient of EtOAc in hexanes to provide the product **10**.

(4*R*,5*S*)-*N*-(Benzyloxy)-3-formyl-5-hydroxy-2,2-dimethylthiazolidine-4-carboxamide (10a): Yield: 48%; white solid, mp 68-70 ºC; TLC (SiO_2) R_f 0.42 (1:1 hexanes:EtOAc); $[\alpha]^{26}_D$: -84 (*c* 1, $CHCl_3$); ^{1}H NMR (500 MHz,CD_3OD) δ 8.49 (s, 1H), 7.46-7.44 (m, 2H), 7.40-7.36 (m, 3H), 5.49 (s, 1H), 4.95 (s, 1H), 4.86 (s, 2H), 1.97 (s, 3H), 1.86 (s, 3H); ^{13}C NMR (125 MHz, CD_3OD) δ 181.6, 161.5, 135.3, 129.2, 128.3, 128.1, 79.3, 77.5, 71.1, 70.3, 30.2, 29.3.

(4*R*,5*S*)-Benzyl 4-((2-(benzyloxy)-2-oxoethoxy)carbamoyl)-5-hydroxy-2,2-dimethylthiazolidine-3-carboxylate (10d): Yield: 53%; pale oil; TLC (SiO_2) R_f 0.23 (2:1 hexanes:EtOAc); ^{1}H NMR (500 MHz, $CDCl_3$) δ 9.95 (s, 1H), 7.36-7.27 (m, 10H), 5.54 (s, 1H), 5.16 (s, 4H), 5.03 (s, 1H), 4.52 (s, 1H), 4.37 (s, 2H), 1.95 (s, 3H), 1.90 (s, 3H).

(4*R*,5*S*)-*tert*-Butyl 4-(((benzyloxy)carbonyl)methoxycarbamoyl)-5-hydroxy-2,2-dimethylthiazolidine-3-carboxylate (10e): Yield: 58-73%; pale oil; TLC (SiO_2) R_f 0.46 (3:1 hexanes:EtOAc); ^{1}H NMR (500 MHz, $CDCl_3$) δ 7.36-7.33 (m, 5H), 5.55 (bs, 1H), 5.22 and 5.15 (ABq, 2H, $\Delta\nu$ = 30.0 Hz, J = 12.5 Hz), 4.93 (bs, 1H), 4.52 (s, 2H), 1.96 (s, 3H), 1.82 (s, 3H), 1.48 (s, 9H); ^{13}C NMR (125 MHz, $CDCl_3$) δ 169.4, 167.1, 149.9, 134.7, 128.7, 128.4, 82.0, 74.4, 72.2, 67.1, 55.3, 33.2, 28.3.

(4*R*,5*S*)-*N*-Acetoxy-5-hydroxy-2,2-dimethyl-3-(2-phenoxyacetyl)thiazolidine-4-carboxamide (10f): Yield: 44%; colorless oil; TLC (SiO_2) R_f 0.24 (1:1 hexanes:EtOAc); ^{1}H NMR (500 MHz, $CDCl_3$) δ 7.26-7.20 (m, 2H), 6.94-6.87 (m, 3H), 5.57 (s, 1H), 5.02 (s, 1H), 4.50 (s, 2H), 2.10 (s, 3H), 1.99 (s, 3H), 1.92 (s, 3H); ^{13}C NMR (125 MHz, $CDCl_3$) δ 168.5, 167.7, 165.5, 157.5, 129.6, 121.9, 114.9, 79.6, 76.4, 72.2, 67.4, 32.1, 27.8, 18.0, 14.2.

***tert*-Butyl 2-(((4*R*,5*S*)-5-hydroxy-2,2-dimethyl-3-(2-phenoxyacetyl)thiazolidine-4-carboxamido)oxy)-acetate (10g):** Yield: 60-68%; pale oil; TLC (SiO_2) R_f 0.30 (1:1 hexanes:EtOAc); ^{1}H NMR (500 MHz, $CDCl_3$) δ 10.17 (s, 1H), 7.28-7.24 (m, 2H), 6.96 (t, 1H, J = 7.5 Hz), 6.90 (d, 2H, J = 7.5 Hz), 5.61 (s, 1H), 5.01 (s, 1H), 4.59 and 4.31 (ABq, 2H, $\Delta\nu$ = 40.0 Hz, J = 13.0 Hz), 4.34-4.26 (m, 2H), 2.05 (s, 3H), 1.96 (s, 3H), 1.44 (s, 9H); ^{13}C NMR (125MHz, $CDCl_3$) δ 168.7, 167.0, 166.2, 157.5, 129.7, 121.9, 114.7, 83.3, 79.5, 76.9, 76.5, 72.6, 68.6, 32.0, 28.0.

Benzyl 2-(((4*R*,5*S*)-3-benzoyl-5-hydroxy-2,2-dimethylthiazolidine-4 carboxamido)-oxy)acetate (10h): Yield: 67-84%; pale solid, mp 170-172 °C; TLC (SiO_2) R_f 0.13 (1:1 hexanes:EtOAc); ^{1}H NMR (500 MHz, $CDCl_3$) δ 9.89 (s, 1H), 7.38-7.24 (m, 10H), 5.33 (s, 1H), 5.16 (s, 2H), 4.80 (s, 1H), 4.38-4.26 (m, 2H), 2.09-1.96 (m, 6H); ^{13}C NMR (125 MHz, $CDCl_3$) δ 171.4, 170.5, 169.3, 137.7, 134.7, 129.5, 128.9, 128.8, 128.6, 128.5, 125.9, 75.4, 74.9, 72.1, 67.3, 60.5, 32.3, 28.9.

(4*R*,5*S*)-3-Benzoyl-*N*-(benzyloxy)-5-hydroxy-2,2-dimethylthiazolidine-4-carbox-amide (10i): Yield: 68-73%; pale solid, mp 64-66 °C; TLC (SiO_2) R_f 0.28 (1:1 hexanes:EtOAc); $[\alpha]^{28}_D$: -58 (*c* 1, $CHCl_3$); ^{1}H NMR (500 MHz, DMSO- d_6) δ 11.20 (s, 1H), 7.46-7.28 (m, 10H), 6.64 (d, 1H, J = 3.0 Hz), 5.27 (d, 1H, J = 3.0 Hz), 4.72 and 4.62(ABq, 2H, $\Delta\nu$ = 40.5 Hz, J = 11.0 Hz), 4.52 (s, 1H), 2.08-1.93 (m, 6H); ^{13}C NMR (125 MHz, DMSO- d_6) δ 169.4,165.4, 142.3, 139.4, 136.1, 129.5, 129.4, 128.9, 128.8, 128.7, 125.9, 78.9, 77.0, 75.2, 73.7, 32.3, 28.5.

(4*R*,5*S*)-3-Benzoyl-5-hydroxy-*N*-methoxy-2,2-dimethylthiazolidine-4-carboxamide (10j): Yield: 80%; colorless oil; TLC (SiO_2) R_f 0.20 (1:1 hexanes:EtOAc); $[\alpha]^{25}_D$: -50 (*c* 1, $CHCl_3$); ^{1}H NMR (500 MHz, $CDCl_3$) δ 9.92 (s, 1H), 7.36-7.30 (m, 5H), 5.38 (s, 1H), 4.77 (s, 1H), 3.05 (s, 3H), 2.19 (s. 1H), 2.06-1.86 (m, 6H).

Cyclization of thiohemiacetals; general procedure. Thiohemiacetal **10** (2.0 mmol), mesyl chloride (318 μL, 4.0 mmol) and Et_3N (1.14 mL, 8.2 mmol) were combine in 16 mL of DCM while the reaction temperature was maintained at 0 °C. The reaction flask was sealed and kept in a -20 ºC freezer overnight. The brown solution was diluted with DCM (10 mL) and washed with brine, and then, the organic layer was dried over $MgSO_4$,

filtered, and evaporated. The bicyclic β-lactam product **14** was separated by flash chromatography on silica gel in accordance to product R_f values.

(1*R*,5*R*)-Benzyl 6-(2-(benzyloxy)-2-oxoethoxy)-3,3-dimethyl-7-oxo-4-thia-2,6-diazabi-cyclo[3.2.0]heptane-2-carboxylate (14c): Yield: 48%; pale oil; TLC (SiO_2) R_f 0.27 (4:1 hexanes:EtOAc); ^{1}H NMR (500 MHz, $CDCl_3$) δ 7.44-7.30 (m, 10H), 5.68 (d, 1H, *J* = 4.5 Hz), 5.60 (s, 1H), 5.27 and 5.22 (ABq, 2H, Δ*v* = 36.5 Hz, *J* = 12.0 Hz), 5.20(m, 2H), 4.64 (q, 2H, *J* = 16.5 Hz), 1.91 (s, 3H), 1.83 (s, 3H); ^{13}C NMR (125 MHz, $CDCl_3$) δ 168.2, 163.2, 153.8, 134.7, 128.9, 128.8, 128.7, 128.6, 128.3, 128.0, 72.9, 70.8, 69.1, 67.8, 67.4, 60.4, 31.7, 30.3.

(1*R*,5*R*)-6-(Benzyloxy)-3,3-dimethyl-7-oxo-4-thia-2,6-diazabicyclo[3.2.0]heptane-2-carbaldehyde (14d): Yield: 36%; colorless oil; TLC (SiO_2) R_f 0.55 (1:1 hexanes:EtOAc); ^{1}H NMR (500 MHz, $CDCl_3$) δ 8.33 (s, 1H), 7.40-7.37 (m, 5H), 5.92 (d, 1H, *J* = 4.0 Hz), 5.13 (d, 1H, *J* = 4.0 Hz), 5.06 and 5.02 (ABq, 2H, Δ*v* = 17.0 Hz, *J* = 11.0 Hz), 1.84 (s, 3H), 1.73 (s, 3H); ^{13}C NMR (125 MHz, $CDCl_3$) δ 161.7, 158.2, 134.5, 129.4, 129.3, 128.9, 78.6, 73.6, 69.9, 67.1, 35.6, 29.2.

(1*R*,5*R*)-*tert*-Butyl 6-(2-(benzyloxy)-2-oxoethoxy)-3,3-dimethyl-7-oxo-4-thia-2,6-di-azabicyclo[3.2.0]heptane-2-carboxylate (14e): Yield: 38-45%; orange oil; TLC (SiO_2) R_f 0.43 (4:1 hexanes:EtOAc); ^{1}H NMR (500 MHz, $CDCl_3$) δ 7.38-7.35 (m, 5H), 5.62 (m, 1H), 5.49 (m, 1H), 5.25 and 5.17 (ABq, 2H, Δ*v* = 37.5 Hz, *J* = 12.5 Hz), 4.65 and 4.57 (ABq, 2H, Δ*v* = 31.0 Hz, *J* = 16.0 Hz), 1.84 (s, 3H), 1.77 (s, 3H), 1.49 (s, 9H); ^{13}C NMR (125 MHz, $CDCl_3$) δ 168.2, 164.4, 163.5, 151.7, 134.7, 128.8, 128.7, 128.7, 81.9, 75.0, 72.9, 71.2, 68.7, 67.3, 31.7, 30.4, 28.2.

***tert*-Butyl 2-(((1*R*,5*R*)-3,3-dimethyl-7-oxo-2-(2-phenoxyacetyl)-4-thia-2,6-diazabicyclo[3.2.0]heptan-6-yl)oxy)-acetate (14f):** Yield: 43-46%; orange oil; TLC (SiO_2) R_f 0.73 (2:1 hexanes:EtOAc); ^{1}H NMR (500 MHz, $CDCl_3$) δ 7.31-7.26 (m, 2H), 7.01-6.96 (m, 3H), 5.88 (d, 1H, *J* = 4.5 Hz), 5.69 (d, 1H, *J* = 4.5 Hz), 4.88 and 4.75 (ABq, 2H, Δ*v* = 62.5 Hz, *J* = 14.5 Hz), 4.51 and 4.45 (ABq, 2H, Δ*v* = 34.0 Hz, *J* = 16.0 Hz), 1.92 (s, 3H), 1.90 (s, 3H), 1.50 (s, 9H); ^{13}C NMR (125 MHz, $CDCl_3$) δ 167.3, 166.5, 162.2, 157.7, 129.7, 121.9, 114.6, 83.3, 78.3, 73.3, 70.7, 69.0, 68.7, 31.3, 29.8, 28.1.

Benzyl 2-(((1*R*,5*R*)-2-benzoyl-3,3-dimethyl-7-oxo-4-thia-2,6-diazabicyclo[3.2.0]heptan-6-yl)oxy)acetate (14h): Yield: 40-43%; white solid, mp 111-113 ºC; TLC (SiO_2) R_f 0.56 (2:1 hexanes:EtOAc); $[\alpha]^{24}_D$: -8 (*c* 1, $CHCl_3$); ^{1}H NMR (500 MHz, $CDCl_3$) δ 7.57-7.56 (m, 2H), 7.42- 7.41 (m, 3H), 7.37- 7.35 (m, 5H), 5.68 (d, 1H, *J* = 4.5 Hz), 5.25 (d, 1H, *J* = 5.0 Hz), 5.20 and 5.15 (ABq, 2H, Δ*v* = 30.0 Hz, *J* = 12.5 Hz), 4.57 and 4.54 (ABq, 2H, Δ*v* = 18.5 Hz, *J* = 17.0 Hz), 2.04 (s, 3H), 1.94 (s, 3H); ^{13}C NMR (125 MHz, $CDCl_3$) δ 169.1, 167.9, 163.0, 136.8, 134.6, 129.9, 128.7, 128.6, 128.5, 126.7, 76.5, 72.7, 72.0, 71.9, 70.1, 31.4, 29.8.

(1*R*,5*R*)-2-Benzoyl-6-(benzyloxy)-3,3-dimethyl-4-thia-2,6-diazabicyclo[3.2.0]heptan-7-one (14i): Yield: 34-41%; white solid, mp 104-106 °C; TLC (SiO_2) R_f 0.26 (4:1 hexanes:EtOAc); $[\alpha]^{28}_D$: -122 (*c* 1, $CHCl_3$); ^{1}H NMR (500 MHz, $CDCl_3$) δ 7.60-7.56 (m, 2H), 7.46- 7.39 (m, 8H), 5.27 (d, 1H, *J* = 5.0 Hz), 5.17 (d, 1H, *J* = 5.0 Hz), 5.09 and 5.03 (ABq, 2H, Δ*v* = 40.5 Hz, *J* = 11.0 Hz), 2.05 (s, 3H), 1.97 (s, 3H); ^{13}C NMR (125 MHz, $CDCl_3$) δ 169.2, 162.6, 136.9. 134.0, 130.0, 129.2, 129.0, 128.8, 128.6, 126.8, 78.5, 76.8, 72.2, 69.3, 31.4, 29.9.

(1*R*,5*R*)-2-Benzoyl-6-methoxy-3,3-dimethyl-4-thia-2,6-diazabicyclo[3.2.0]heptan-7-one (14j): Yield: 38-51%; pale white solid, mp 129-141 ºC; TLC (SiO_2) R_f 0.29 (4:1 hexanes:EtOAc); $[\alpha]^{26}_D$: -196 (*c* 1, $CHCl_3$); ^{1}H NMR(500 MHz, $CDCl_3$) δ 7.60-7.58 (m, 2H), 7.44-7.42 (m, 3H). 5.63 (d, 1H, *J* = 5.0 Hz), 5.34 (d, 1H, *J* = 5.0 Hz), 3.92(s, 3H), 2.07 (s, 3H), 2.02 (s, 3H); ^{13}C NMR (125 MHz, $CDCl_3$) δ 169.4, 161.7, 136.9, 130.1, 128.7, 126.9, 76.9, 72.2, 68.2, 64.3, 31.7, 30.0.

Thiazolidine ring cleavage of β-Lactam 14i. Methoxycarbonylsulfenyl chloride (57 μL, 0.69 mmol) was added dropwise into a mixture solution of β-lactam (169 mg, 0.46 mmol) and NaOAc (76 mg, 0.92 mmol) in a 12:2:1 solution of AcOH:DMF:TFA (2.25 mL) while the reaction temperature was maintained at 0 °C. The solution was then stirred at that temperature for 1.5 hours. After quenching of the solution with distilled water, the yellow mixture was diluted with EtOAc (10 mL). The organic layer was then washed 3 times with distilled water and dried over $MgSO_4$, filtered, and evaporated. The yellow solid was finally triturated in a 4:1 solution of hexanes:EtOAc to provide the monocyclic β-lactam product **15b** (125 mg, 0.29 mmol).

***SS*-((2*R*,3*R*)-3-Benzamido-1-(benzyloxy)-4-oxoazetidin-2-yl) *O*-methyl carbon-(dithioperoxoate) (15b):** Yield: 65%; white solid, mp 139-141 °C; TLC (SiO_2) R_f 0.12 (2:1 hexanes:EtOAc); $[\alpha]^{28}_D$: -16 (*c* 1, $CHCl_3$); ^{1}H NMR (500 MHz, $CDCl_3$) δ 7.82 (d, 2H, *J* = 7.5 Hz), 7.69 (1H, d, *J* = 7.0 Hz), 7.54-7.43 (m, 7H), 7.30 (s, 1H), 5.43 (m, 1H), 5.15 (s, 2H), 4.99 (d, 1H, *J* = 4.5 Hz), 3.85 (s, 3H); ^{13}C NMR (125 MHz, $CDCl_3$) δ 169.3, 167.8, 161.7, 134.1, 132.9, 132.2, 129.5, 129.4, 128.8, 128.6, 127.5.

***N*-Deprotection of the β-lactam 14i.** To a stirring solution lactam **14i** (48 mg, 0.13 mmol) in dry DCM (1 mL) was added SmI_2 in THF (4.6 mL, 0.32 mmol) under Ar. determined by TLC, the reaction was complete after 15 minutes. After quenching of the solution with 5% $Na_2S_2O_3$ (1 mL), the reaction mixture was added 5% $NaHCO_3$ (5 mL) and extracted with DCM (3 x 10 mL). The organic layer was dried over $MgSO_4$, filtered, and evaporated. The *N*-protio β-lactam **17** was separated by flash chromatography on silica gel using an 8-66% gradient.

(1*R*,5*R*)-2-Benzoyl-3,3-dimethyl-4-thia-2,6-diazabicyclo[3.2.0]heptan-7-one (17): Yield: 56-95% (the higher yields were observed when fresh SmI_2 was used in an unopened bottle from Alfa Aesar); colorless oil; TLC (SiO_2) R_f 0.29 (2:1 hexanes:EtOAc); $[\alpha]^{25}_D$: -98 (*c* 1, $CHCl_3$); ^{1}H NMR (500 MHz, $CDCl_3$) δ 7.63-7.61 (m, 2H), 7.45-7.37 (m, 3H), 5.53 (dd, 1H, *J* = 5.0, 1.5 Hz), 5.38 (d, 1H, *J* = 5.0 Hz), 2.07 (s, 3H), 2.03 (s, 3H); ^{13}C NMR (125 MHz, $CDCl_3$) δ 169.1, 167.5, 137.2, 130.2, 129.3, 128.8, 127.0, 126.3, 77.7, 77.6, 60.8, 31.8, 30.1.

Thiazolidine ring cleavage of β-lactam 17. Methoxycarbonylsulfenyl chloride (12 μL, 0.145 mmol) was added dropwise into an ice-chilled solution of β-lactam (25.5 mg, 0.096 mmol) and NaOAc (15.8 mg, 0.192 mmol) in a 12:2:1 solution of AcOH:DMF:TFA (1 mL). The mixture was stirred at room temperature for 15 minutes. Distilled water (2 mL) was then added and the cloudy solution was extracted with EtOAc (2 x 5 mL). The organic layer was washed with distilled water (3 x 5 mL), and then dried over $MgSO_4$, filtered, and evaporated. The monocyclic β-lactam **16** (12 mg, 0.04 mmol) was separated by flash chromatography on silica gel using an 8-66% gradient afforded.

***SS*-((2*R*,3*R*)-3-Benzamido-4-oxoazetidin-2-yl) *O*-methyl carbon-(dithioperoxoate) (16):** Yield: 40%; white solid, mp 161-163 °C; TLC (SiO_2) R_f 0.18 (1:1 hexanes:EtOAc); $[\alpha]^{22}_D$: -16 (*c* 0.5, MeOH); ^{1}H NMR (500 MHz, CD_3OD) δ 7.90 (d, 2H, *J* = 7.5 Hz), 7.57 (d, 1H, *J* = 7.5 Hz), 7.49 (t, 2H, *J* = 7.5 Hz), 5.49 (d, 1H, *J* = 4.5 Hz), 5.16 (d, 1H, *J* = 4.5 Hz), 3.87 (s, 3H); ^{13}C NMR (125 MHz, CD_3OD) δ 170.8, 170.7, 168.8, 134.8, 133.4, 129.8, 128.8, 69.8, 63.2, 56.6.

CHAPTER 4

PHOSPHONIUM LIPOCATIONS AS POTENTIAL AS POTENTIAL ANTI-PARASITIC AGENTS

Lu, X.; Altharawi, A.; Hansen, E. N.; Long, T. E. Submitted to *Synthesis*, 05/24/2012

Abstract

The investigation on a unique antimicrobial platform is next followed in Chapter 4. A group of phosphonium salts were made using atovaquone as lead compound to treat parasitic disease (i.e., malaria). Compound **28k** exhibited moderate in vitro antimalarial activity (17 ± 4 nM) against chloroquine resistant (W2) *Plasmodium falciparum*. The results demonstrate the advantage of attaching a triphenylphosphonium-based mitochondriotropic group to increase subcellular concentration in the plasmodial mitochondria, within which the drug target is located. Preliminary toxicity and a structure-activity relationship studies of interested compounds are also included.

4.1 Background

4.1.1 Introduction

As concluded in Chapter 3, a synthetic precursor to β-lactam ring system has been introduced through a six-step synthetic sequence. However, even the interested molecule have a plausible site-specific mode of action against its target (e.g., structures having β-lactam moiety which can the bacterial cell wall growth), it may still have low in vivo activity [1]. In other words, several limitations may greatly reduce the efficacy such as undesirable physiochemical properties (e.g., low aqueous solubility) and low bioavailability due to poor absorption, high metabolism, etc. In order to counter these problems, outside of simply making a pharmaceutical salt (e.g., sodium or potassium salts of β-lactam antibacterials) [2] or easily preparation of a prodrug (e.g., paclitaxel prodrug of taxol) of the designed molecule, further modification through chemical approaches is also preferred [3]. In this chapter, the modification of a FDA-approved anti-parasitic drug has been performed in the hope of increasing its specificity for *Plasmodium*-infected cells.

4.1.2 Malaria as a disease

To date, malaria affects millions of humans, particularly in Latin-America, sub-Saharan Africa and Southeast Asia [4]. Of those affected, about 1 million die each year. The specific protozoan organisms causing this disease is a parasite called *Plasmodium*. It was found that there are over one hundred *Plasmodium* species globally but only four of them can cause malaria in humans [5] via infected female *Anopheles* mosquitos [6]. The major cause of malaria in humans is *P. falciparum. P vivax*, *P. ovale* and *P. malariae* are also known to cause infection.

After the parasites enter the human body by a mosquito bite, the initial symptoms include chills, shaking and fever. If untreated, coma and death will follow due to organ failure [7]. In general terms, malaria has two stages inside the human body, the primary liver stage and the successively red blood cell stage. The former one in the life cycle usually has no symptoms, but in the second stage daughter cells are reproduced and released from red blood cells. As the number increases, they can invade more host cells and cause symptoms [8]. Typically in order to treat this disease, medication must at least target the blood cell stage infection.

4.1.3 Medications for anti-malarial treatment

Chemotherapy plays an important role in killing parasites. Several medications are used in the clinic to treat malaria. Considering the latency period of the parasite, the regimen usually takes one or two weeks [9]. The ideal medication should effectively treat both blood-stage and latent parasites. New strategies for preventive treatment of malaria have also been undergoing development [10].

To date, depending on the difference in chemical structures, there are three main types of drugs to prevent or cure malaria: quinine analogues, artemisinin analogues, or pyrimidine analogues [11]. Currently, the artemisinin-based combination therapy is one of the most effective and widely used treatments. Some newer drugs have also been approved by the FDA, such as atovaquone, the overall lead compound in this project (**Figure 4.01**).

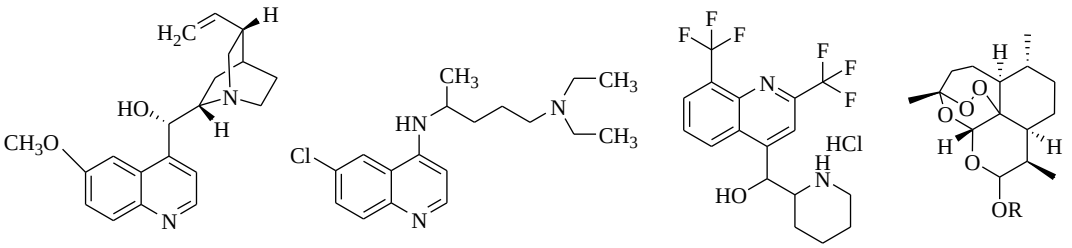

Figure 4.01: Medications to treat malaria.

4.1.4 The discovery of atovaquone (ATV)

In the 1940s, hydroxynaphthoquinones were found to have greater activity than quinine against *Plasmodium lophurae* [12]. It was later discovered 2-cyclohexyl-3-hydroxy-1,4-naphthoquinone (parvaquone) is effective against different protozoan infections including malaria. However the therapeutic efficacy was limited by metabolism problems [13]. In 1993, atovaquone, the orally and metabolically stable form of parvaquone was reported [14]. Interestingly, atovaquone target both liver stage and red blood cell stage infection and it is effective against all *Plasmodium* species [15]. This is partially due to atovaquone's action on the cytochrome bc_1 complex (in which electrons are transferred from ubiquinol to cytochrome *c*) to block either ubiquinol oxidation or ubiquinone reduction (**Figure 4.02**) [16]. The target selectivity of atovaquone is high as plasmodial and eukaryotic mitochondria have evolutionary dissimilarities [17]. Due to its structural similarity to plasmodian ubiquinones, atovaquone can inhibit the respiration of plasmodial mitochondria 1000-fold more selective than mammalian and avian mitochondria [18].

Although effective and nontoxic, the use of atovaquone is limited by high cost, poor absorption, and the need of combination therapy to avoid the problem of developing resistance [19]. It has been concluded that atovaquone treatment is more effective when combined with proguanil hydrochloride. The commercially available co-formulated (i.e., Malarone™) is generally prescribed as a prophylaxis, and due to its high cost is not affordable to persons where malaria is often most prevalent [20]. In this project, chemical modification was made on the atovaquone platform in an effort to increase its mitochondrial bioavailability.

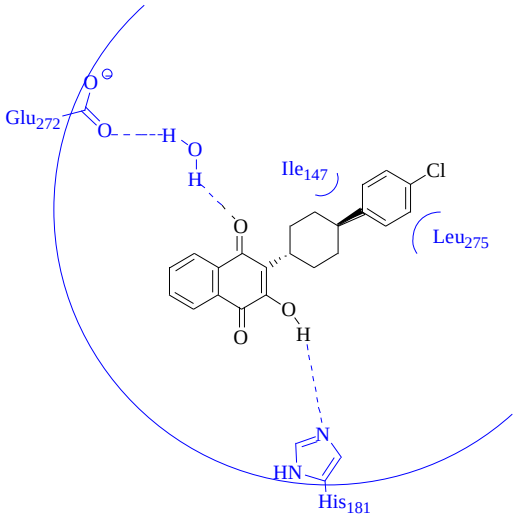

Figure 4.02: Docking of atovaquone to oxidation inside yeast bc_1 complex.

4.1.5 Cationic group to increase subcellular concentration

So far, lipocations have been used extensively as molecular probes for studying cellular activity and mitochondrial function (i.e., Mitotracker Red™, rhodamine 123) [21]. A similar strategy has also been adopted in making cationic nanoparticles for target delivery. The attachment of the cationic group to the liposomal surface can effectively attract molecules to the target, e.g., mitochondria. However, the disadvantages include high toxicity and poor stability [22].

Examples of the direct attachment of mitochondriotropic residue to the drug molecule have already advanced into clinical trials. Mitoquinone ($MitoQ_{10}$ mesylate™) [23], a synthetic phosphonium cationic analogue of ubiquinone, has progressed to phase II trials

in the US for the management of Parkinson's disease, hepatitis C, and fatty liver disease (**Figure 4.03**). Its increased therapeutic efficacy is conferred by the hydrocarbon side chain being attached by a triphenylphosphonium group, resulting in a 100-500 fold increase in the concentration of the target molecule inside negatively-charged mitochondria.

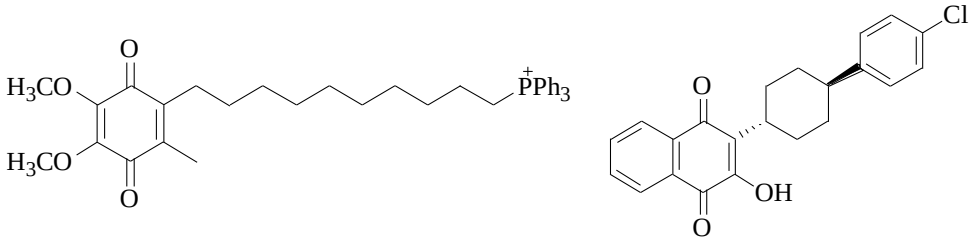

mitoquinone atovaquone (ATV)

Figure 4.03: Structure of mitoquinone and atovaquone.

4.2 Experimental Design and Results

4.2.1 Rationale of design and hypothesis

The uniqueness of malaria parasite is its host red blood cells lack many organelles including mitochondria. Also, the reduction of the potential across the membrane (**Figure 4.04**) is ideal for the use of drug targeting strategies: red blood cells $\Delta\psi_p \leq$ -35 mV [24a]; *Plasmodium* $\Delta\psi_p$ -95 mV [24b], *Plasmodium* $\Delta\psi_m$est. $\geq$ -150 mV [24c]. It is hypothesized that if a cationic moiety were bound to the lipid substituent of antimalarial agents that inhibit electron transport, drug concentrations would increase inside the *Plasmodium* mitochondrion, leading to increased antiplasmodial effects. It is anticipated cationic mitochondrion antagonists would concentrate where the negative charge is highest, namely the *Plasmodium* mitochondrial matrix.

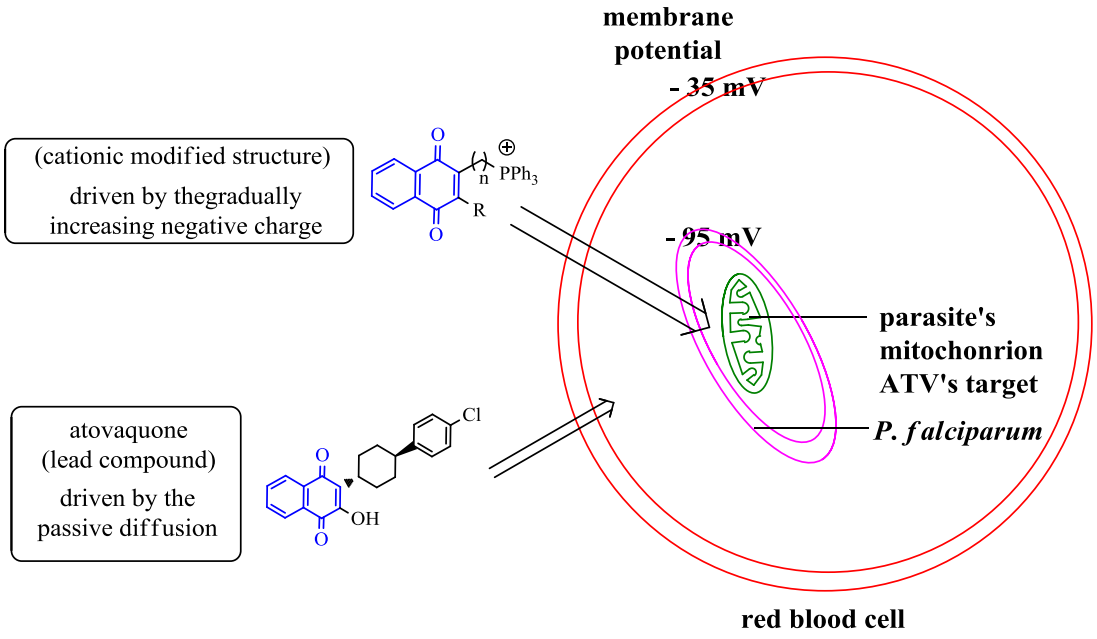

Schematic depiction of a mitochondriotropic triphenylphosphonium attached to the lead compound via an alkyl residue (not drawn to molecular scale): a lipophilic cation should be able to rapidly accumulate inside the negatively charged mitochondrion and thus the subcellular concentration is increased.

Figure 4.04: Subcellular targeting to the parasite's mitochondrion.

4.2.2 Design of the target molecules

As illustrated in **Figure 4.05**, a hydrocarbon chain is designed to connect between the ring platform of atovaquone (overall lead compound in Chapter 4) and the cationic moiety. There are several general features that have been included in the original design. Firstly, in order to distinguish the best ring platform, five different ring systems were designed including 1,4-naphthoquinone ring of the atovaquone. Secondly, phosphonium groups (with different Y substitutions) were chosen as mitochondriotropic residues. Thirdly, since the correlation between the chemical natures of the linker and the antiplasmodial activity is unknown, different chain length has been included. Lastly,

different connections via the formation of various bonds (e.g. amine, ether) have been studied in the hope of reducing of the current high manufacturing cost of the lead compound.

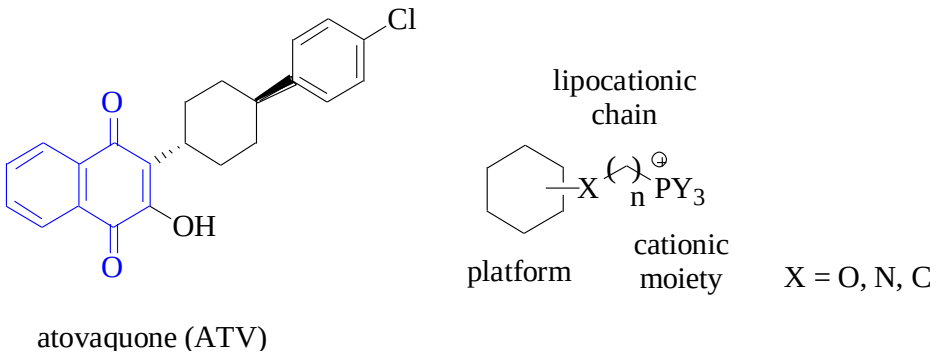

Figure 4.05: Designed target molecules.

4.2.3 The key steps in the synthetic route

To be able to introduce the cationic moiety on to the ring platform via 2-3 straightforward steps, synthetic routes were developed using a diverse range of chemistry. In the process of making atovaquone, the conventional radical decarboxylation of carboxylic ester with 1,4-naphthoquinone requires 1 equiv silver nitrate ($AgNO_3$), which is a very expensive chemical. It was proposed in an earlier paper that a reduction in the amounts of $AgNO_3$ (from 1 equiv to 0.5 equiv) will not have a major impact on the reaction outcome [25]. In other words, smaller amounts of $AgNO_3$ can still generate the radical and product efficiently (**Scheme 4.01**).

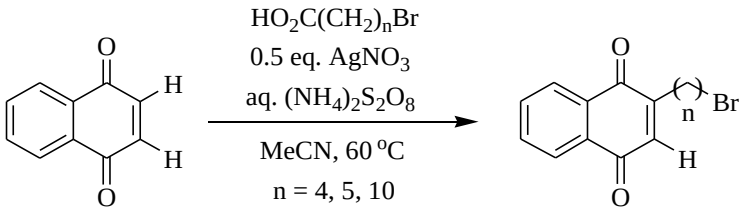

Scheme 4.01: Kochi-Anderson reaction.

During the last step of the synthetic sequence, the tertiary phosphine was coupled with halogen–substituted or *O*-mesylated intermediate through a conventional heating method. As expected, reaction conditions (**Scheme 4.02**) did not eliminate triphenylphosphine to generate alkene byproduct. The less time consuming microwave irradiation was also employed [26].

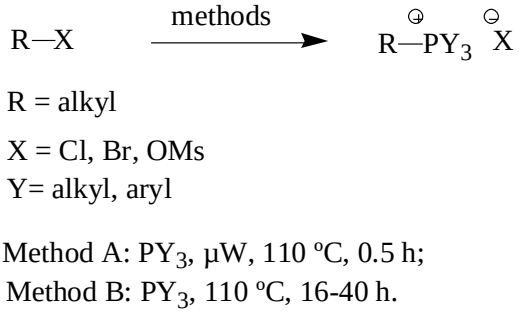

Scheme 4.02: Preparation of phosphonium salt.

4.2.4 1-Alkoxybenzotriazole cation 3

1-Hydroxybenzotriazole (HOBt) was chosen as the first platform as it is widely used in peptide chemistry to activate carboxylic acid. Interestingly, alkyl benzotriazole analogues as ligands for some serotonin and dopamine receptor have been studied before [27]. In our project, the synthetic sequence is first reacting HOBt with 10-bromodecan-1-ol at room temperature in the presence of TEA to form the ether bond. The use of organic

bases as additives (i.e., Et_3N) at room temperature can not generate the potential byproduct by forming the ether bond between the two hydroxyl groups. The mesylation was later performed by a similar routine procedure (Chapter 3) with the hope that primary alcohol **1** can quantitatively generate the desired *O*-mesylated compound. This intermediate **2** was then treated with triphenylphosphine under microwave irradiation (**Scheme 4.03**).

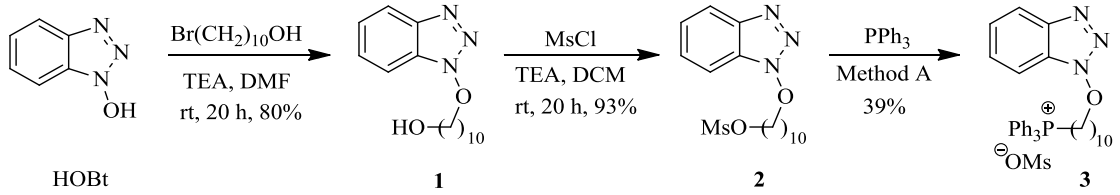

Scheme 4.03: Synthesis of alkoxybenzotriazole cation **3**.

4.2.5 *N*-Alkyoxysuccinimide cation 7

Previously, a *N*-hydroxysuccinimide (NHS) analogue has been studied as new anticonvulsants [28]. In this project, due to its structural similarity to 1,4-naphthoquinone, this widely used activating reagent for carboxylic acids was also included. Since the compound is only slightly acidic, the synthetic sequence began with the preparation of potassium salt instead of using NHS directly to react with the bromide (i.e., 10-bromodecan-1-ol). The potassium salt **4** was then treated with 10-bromo-1-decanol in the presence of TEA. It was found, however, that without adding the organic base no reaction can occur. The introduction of *O*-mesylated group and the following formation of phosphonium salt **7** were achieved using similar procedures for the preparation of the HOBt cation (**Scheme 4.04**).

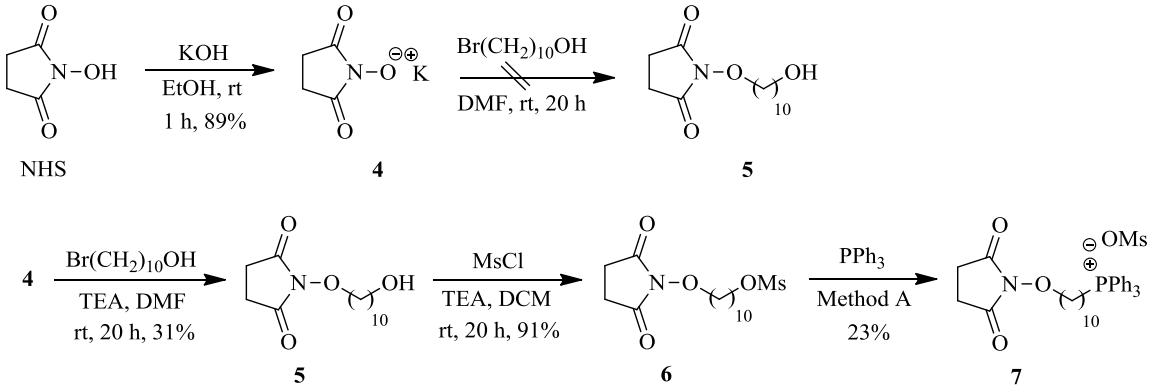

Scheme 4.04: Synthesis of alkyoxysuccinimide cation **7**.

4.2.6 *N*-Alkylphthalimide cation 12

Phthalimide was next studied since its structure is more similar to the 1,4-naphthoquinone platform than *N*-hydroxysuccinimide. Interestingly, using phthalimide derivatives as lead compounds can also be found in other drug discovery projects, e.g., pyridinone reverse transcriptase inhibitors to treat HIV [29]. In the course of synthetic investigation of phthalimide analogue, the potassium salt **8** was formed by reacting phthalimide with potassium hydroxide in ethanol with a good yield (82%). However the following formation of *N*-alkyl imide **9a** at room temperature only resulted in a poor yield (20%). This low rate of substitution was finally overcome by the use of a higher reaction temperature and an appropriate choice of solvent. The reaction of potassium phthalimide **8** with bromide was carried out in dry dimethylformamide (DMF) by reflux under nitrogen, in which potassium phthalimide was able to partially solubilize in the solution and this can facilitate the displacement of halogen by phthalimide ion. The alkylated intermediate **9a** was then subjected to *O*-mesylation, and the resulting intermediate **10a** was later converted to the corresponding phosphonium salt **11a, d-g** (see **Table 4.04**) via microwave irradiation method.

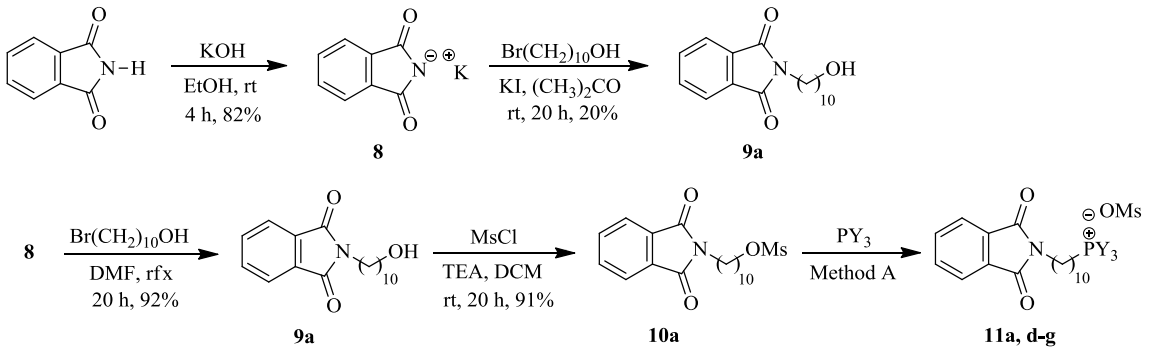

Scheme 4.05: Synthesis of phthalimide cation **11a**, **d-g**.

In cases when 4-bromobutanol and 6-bromohexanol were not available, the preparation of tertiary amine was also studied under DMF reflux conditions using dibromoalkane which resulted in a very poor yield. In dihalogenated systems the bromide was able to generate the alkene byproduct through elimination. As a result, an equal amount of alkene (**9b'** or **9c')** was finally obtained when using 1,4-dibromobutane or 1,6-dibromohexane at a high temperature (153 ºC) (**Scheme 4.06(a)**) [30]. Since the synthesis mentioned previously (see **Scheme 4.05**) was too long to be practical, a shorter alternative has been adopted without forming the imide anion with KOH. With the help a weak base, i.e., Cs_2CO_3, the preparation of the *N*-alkyl phthalimide bromide **9b** commenced with the direct substitution of a dibromide. In acetonitrile solution, the nucleophilic substitution on the alkyl halide was achieved at a lower temperature (80 ºC) after 9 hours in 52% yield (**Scheme 4.06(b)**) [31].

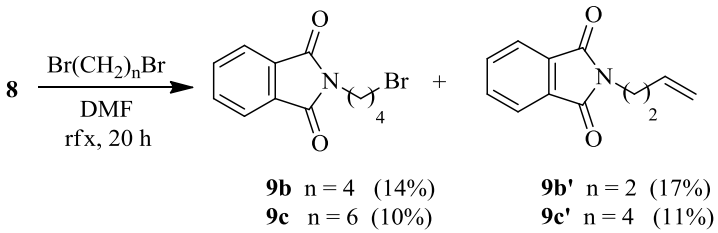

Scheme 4.06(a): Preparation of alkylated phthalimide with dibromide.

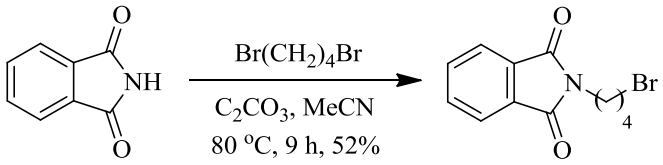

9b

Scheme 4.06(b): Preparation of alkylated phthalimide with dibromide.

4.2.7 1,4-Naphthoquinone cation

The analogues having 1,4-naphthoquinone platform with different substitutions at C-3 position have been designed (**Figure 4.06**). The original design of the analogues contains different hydrocarbon chains between the platform and the phosphonium cationic group. The research interest was eventually to evaluate the antiplasmodial activity of the 2-hydroxyl or 2-alkoxy 1,4-naphthoquinone-based lipocations, since the hydroxyl group in atovaquone is thought to be essential in binding to cytochrome bc_1 complexes [13]. Comparing the IC_{50} values may provide useful clue as to whether the designed analogue plays its role at the same binding pocket of the lead compound.

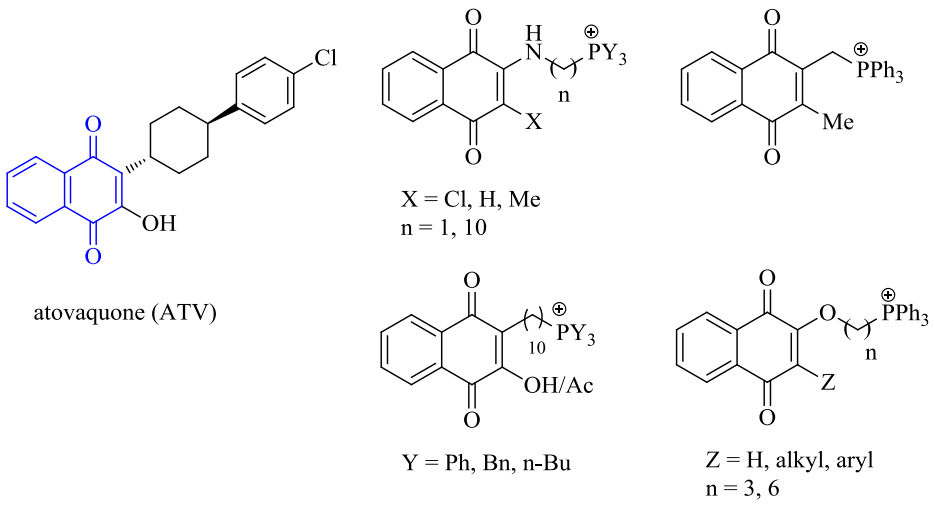

Figure 4.06: 1,4-Naphthoquinone analogues.

4.2.8 PART I: 1,4-naphthoquinone cation with NH- connection

As illustrated in **Scheme 4.07**, the original designed route could not be fully adapted for the large-scale preparation due to the difficulty in the purification. Similar to the Gabriel synthesis briefly discussed in section 4.2.6, the phthalimide was heated under EtOH reflux to generate the phosphonium salt [32]. In this part of study, the imide protecting group was cleaved through the reduction reaction with hydrazine to provide the free primary amine. However, because the chromatographic separation of phosphonium salt can be very unsatisfactory due to its high polarity, the effort was then directed towards an alternative route yielding the phosphonium salt (intermediate or product) only at the very end of the synthetic sequence.

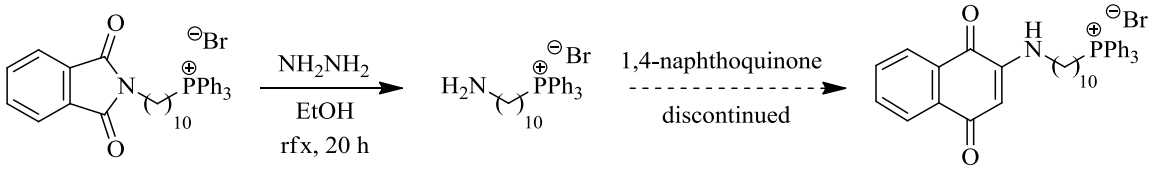

Scheme 4.07: The original designed route to make phosphonium intermediate for later alkylation.

Many successful examples have been made by this new modified strategy: starting from the commercially available 2-aminoethanol, or 10-aminodecan-1-ol (**12**, **Scheme 4.08**) which was generated from conventional Gabriel synthesis, the nucleophilic addition of the amino alcohols to 1,4-naphthoquinone was achieved easily at room temperature [33]. The *O*-mesylated intermediate have been made in a similar way (with MsCl and TEA) and converted to the final compounds with the help of microwave irradiation. Interestingly, when preparing the short-chain analogue **14a**, the synthetic sequence yielded more alkylation (87%) and mesylation (85%) products.

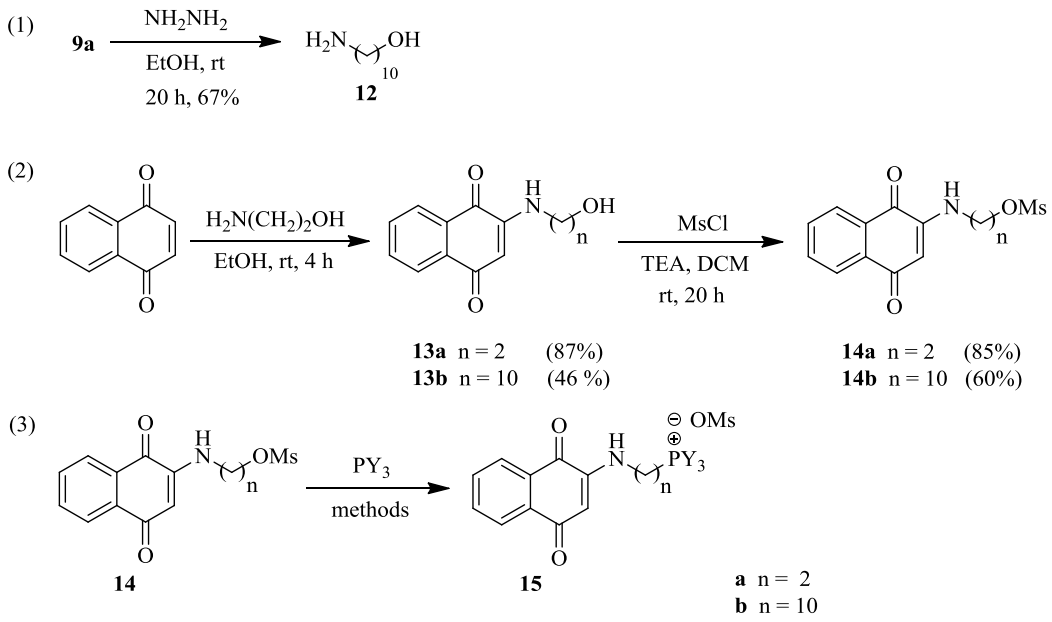

Scheme 4.08: The redesigned route to make 1,4-naphthoquinone analogues **15**.

The synthetic route is superior to the predecessor (**Scheme 4.07**) as its high efficiency allows a general synthesis of 1,4-naphthoquinone-based lipocationic analogues via direct substitution of the same key intermediate, methanesulfonate **14b**. Reaction of this common intermediate **14** with different trisubstituted phosphine proceeds rapidly under microwave irradiation, providing a library of Y-substituted phosphonium salts **15** as final products (**Scheme 4.08**).

Potential halogen bonding, which is somewhat similar to hydrogen bonding, was also considered in this project. In order to understand the potential halogen bonding between the designed lipocationic compound and the amino acid residue at the binding pocket of the bc_1 complex, the 2-Cl 1,4-naphthoquinone based lipocations were designed and the synthesis was carried out in a similar manner. The alkylation reaction condition was first tested by exposing 2,3-dichloro-1,4-naphthoquinone to undecan-1-amine at room temperature for 48 hours, which gave rise to the corresponding mono alkylated

compound **16** in 80% yield. The similar synthetic sequence to make 2-chloro-1,4-naphthoquinone analogue **19** was created as illustrated in **Scheme 4.09**. It was also noted that the nucleophilic addition of 10-aminodecan-1-ol yielded in a fair outcome, around 45% for **17**, which is a similar result for compound **13b** (46%).

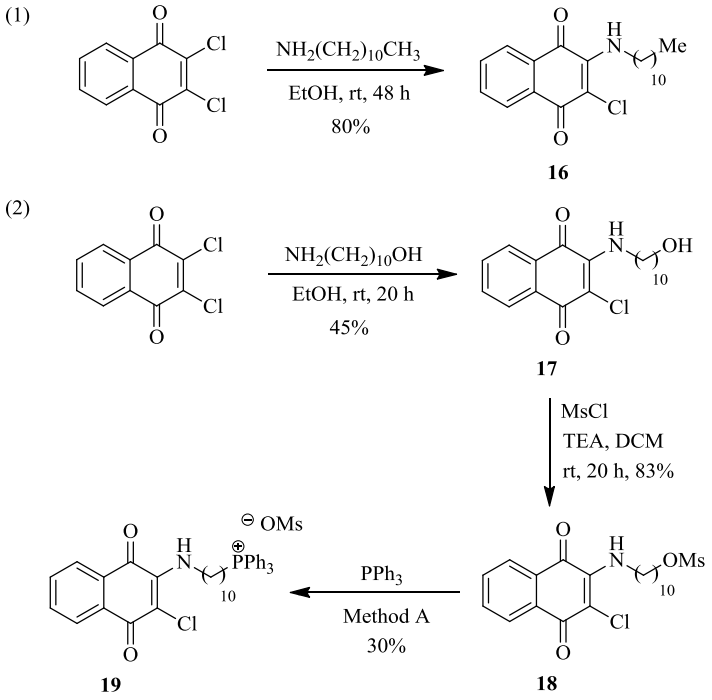

Scheme 4.09: Generation of 2-chloro-1,4-naphthoquinone analogue.

4.2.9 PART II: 1,4-naphthoquinone cation with CH_2- connection

The connection by non-polar hydrocarbon chains, including production of vitamin K analogues, has been the focus of PART II of this research. This approach featured a radical decarboxylation to construct the alkylated 1,4-naphthoquinone **22**, which was later transformed to the corresponding final product via a two-step sequence. In order to distinguish between the effects of distance between the 1,4-naphthoquinone platform and the phosphonium cationic group on potential antiplasmodial activity, various attempts were made to introduce short- and long-chain hydrocarbons.

Unfortunately, it was found that the reaction outcomes of radical alkylation of 1,4-naphthoquinone with various fatty acids highly depends on the chain length. The alkylation to make the short-chain alkyl bromide intermediate **22a** and **22b** resulted in very poor reaction yields (10% yield for the 5-hydrocarbon chain and 5% for 4-hydrocarbon chain) and were not further used.

Research was also focused on the chloroalkylation reaction to introduce the shortest 1-hydrocarbon chain, which took place according to **Scheme 4.10** with formaldehyde (37% formalin solution) and hydrochloric acid (by directly bubbling HCl gas into the mixture [34]). The subsequent conversion into triphenyl phosphonium salt **21** was carried out by microwave irradiation.

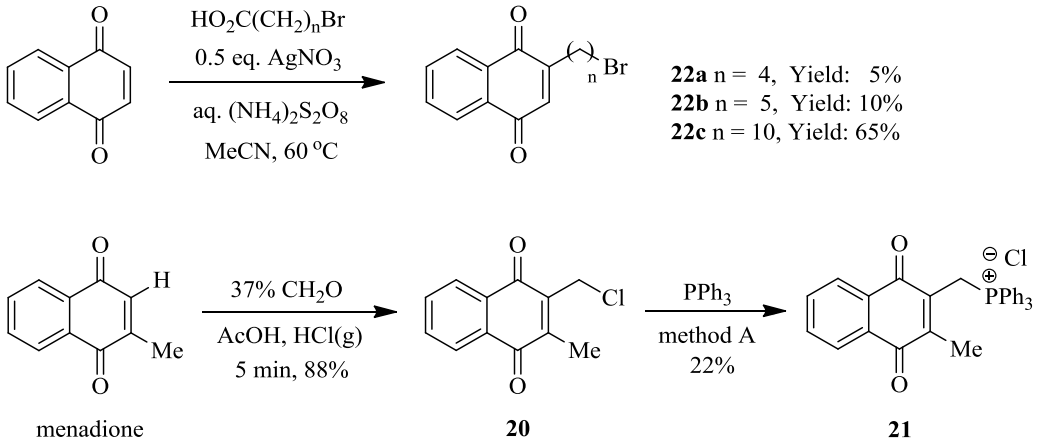

Scheme 4.10: Generation of 2-alkyl-1,4-naphthoquinone analogue, all three longer chain phosphonium salts (10-, 5-, 4-hydrocarbon chain) were ultimately made by Dr. Long.

4.2.10 PART III: 1,4-naphthoquinone cation with OH or *O*-ester linkage

Since the binding to the cytochrome bc_1 complex plays a central role in the atovaquone's anti-parasitic activity, in part because of the presence of the hydrogen bonding between the C-2 hydroxyl on the naphthoquinone ring and the histamine residue,

it is important to determine whether or not the activity of the designed compounds fit well into the same binding pocket as atovaquone and show the potential anti-parasitic activity.

Numerous attempts have been made to prepare the lipocationic analogues with a hydrogen bond donor, i.e., OH, at C-2 position of 1,4-naphthoquinone, but seemingly without success due to the formation of a complex mixture of polar products. It thus became necessary to modify the original designed route. Consequently, the improvement in chemical purity before chromatography purification was achieved by minimization of side reactions through protecting the hydroxyl group via acetylation. As discussed in previous sections, the phosphonium salts were generated from the naphthoquinone bromide **25c** under a conventional heating method in mixed solution of isopropanol and toluene (3:1). Finally, the acetyl protecting group was cleavable by acid-catalyzed hydrolysis to give a clean cationic product **27** (**Scheme 4.11**) [35].

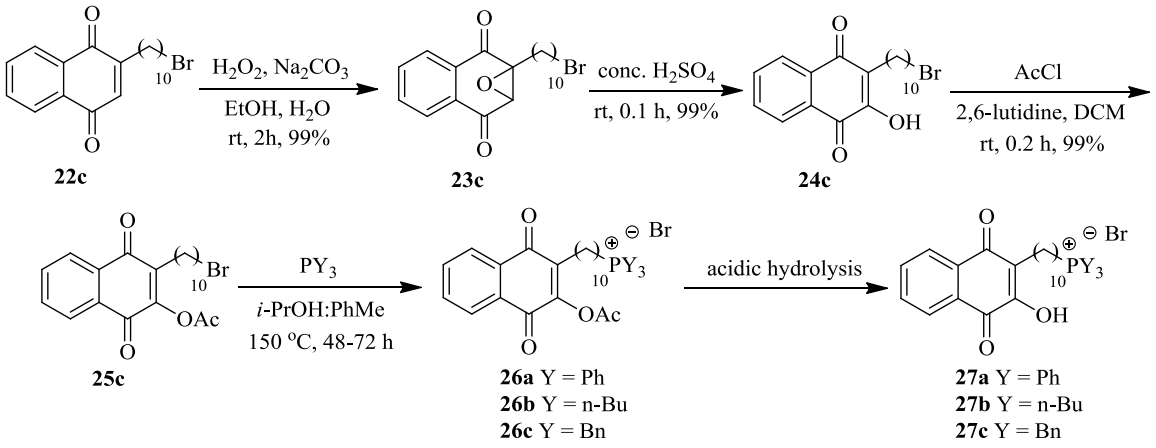

Scheme 4.11: Generation of 2-hydroxyl 1,4-naphthoquinone analogues **27**.

This approach was initially tested to create the control compound **31**. Started from the preparation of the epoxidized 1,4-naphthoquinone **29** with a yield of 99%, the synthetic sequence was continued by treatment with concentrated sulfuric acid to give the 2-hydroxynaphthoquinone **31** with a yield of 61%. The purified compound (also chosen as a control in activity testing) was then protected by the acetyl in the final step (**Scheme 4.12**).

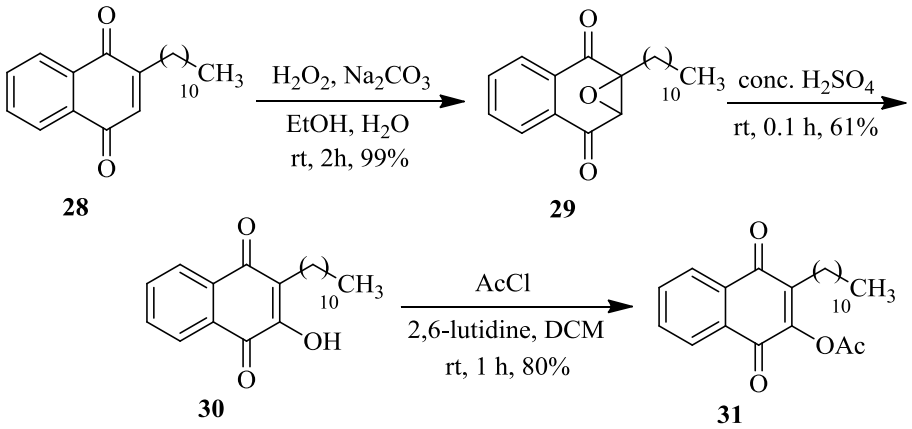

Scheme 4.12: Preparation of 2-OAc 1,4-naphthoquinone control **31**.

Acid-catalyzed hydrolysis of the ester protecting group was carefully studied to minimize the byproduct generation during the sufficient transformation. A series of trial reactions were performed by using the acetic acid ester of 2-hydroxyl 1,4-naphthoquinone **32** as starting material. The precursor was exposed to a range of acidic environments by using various types of acids at different temperatures (**Table 4.01**).

First, the temperature was carefully increased. It was found that when the reaction was performed at a higher temperature (i.e., above 56 ºC), the starting material disappeared after one hour, but the generation of impurities was also observed. For this reason it seemed plausible to attempt to use a different acid to suppress the generation of the impurities. Finally, a rapid, efficient and high yield method for the deprotection was

found. It was noticed that reflux with 5N HCl in acetone can also generate pure product **32** sufficiently (entry 10), but the highest yield was obtained when treating the ester with 5N hydrochloric acid in *i*-PrOH (entry 14).

Table 4.01: The deprotection of 2-acetoxy in 1,4-naphthoquinone.

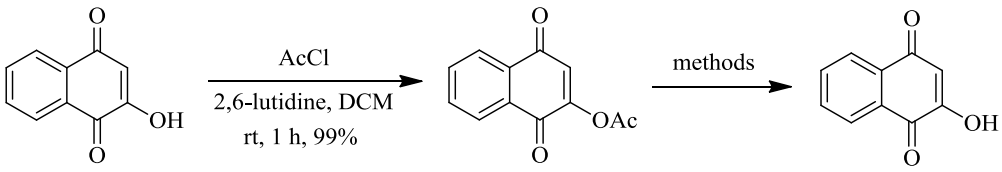

lawsone **32**

entry	methods	temperature	results
1	HBr (aq.), $CHCl_3$	20 ºC	very slow
2	HBr (33% HOAc), $CHCl_3$	20 ºC	very slow
3	TFA, $CHCl_3$	20 ºC	18 h
4	K_2CO_3, MeOH	20 ºC	0.5 h
5	1N HCl, DCM	40 ºC	very slow
6	5N HCl, DCM	40 ºC	very slow
7	5N HBr, DCM	40 ºC	very slow
8	10N HCl, DCM	40 ºC	very slow
9	9N HCl, DCM	40 ºC	very slow
10	5N HCl, acetone	56 ºC	0.5 h
11	9N HBr, acetone	56 ºC	1 h (more impurities formed)
12	5N HCl, THF	65 ºC	1 h (impurity formed)
13	5N HCl, MeOH	65 ºC	1 h (impurity formed)
14	5N HCl, *i*-PrOH	65 ºC	1 h

Surprisingly, when efforts were made to prepare the designed cationic compound, the conventional heating method generated both the protected form **26** and unprotected form **27** of the products. When a series of substrates was examined, it was noted that the stability of protected form final compound was dependent on the substituents of the phosphonium cationic group. As depicted in **Scheme 4.13 (1)**, comparing with bulky

phosphonium substituted derivative **25a**, it was noted that the less bulky derivative **25b** resulted in a higher rate of hydrolysis. However, the applicability of this reaction is very limited, since the unprotected form **27a** is difficult to isolated from the protected form **26a**, thus in many cases the hydrolysis procedure (entry 14, **Table 4.01**) was separately performed.

For example, in the effort to deprotect the acetyl group in compound **26a**, simply heating in the presence of 5N HCl in *i*-PrOH (optimal condition stated in **Table 4.01**) can remove the acetyl group readily. However the reaction must be carefully monitored since hydrochloric acid may generate chloride salt product **27a'** which requires extra effort in purification (**Scheme 4.13 (2)**).

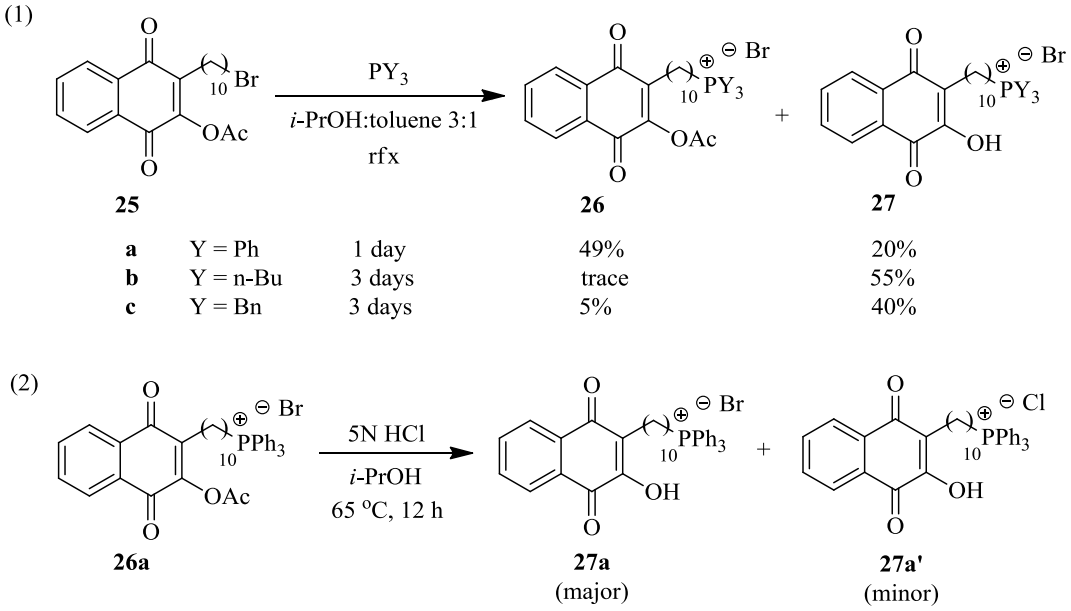

Scheme 4.13: Preparation of 2-hydroxyl 1,4-naphthoquinone analogues **27**.

In order to distinguish the nature of the linker, further mimicking of the hydrocarbon chain to the platform of atovaquone was investigated. With an aromatic ring in between the 1,4-naphthoquinone ring and the hydrocarbon chain, the aryl moiety was introduced

into ester-protected bromide intermediate **28** (made by Dr. Long). The target **30** was obtained by sequential application of the conventional heating method and deprotection of acetyl group (**Scheme 4.14**).

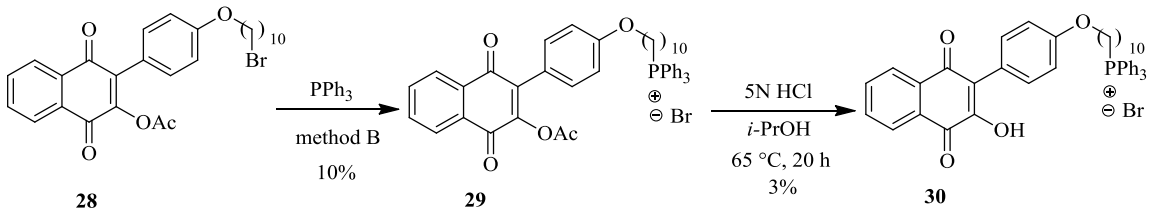

Scheme 4.14: Preparation of 2-hydroxyl 3-aryl 1,4-naphthoquinone analogue **30**.

4.2.11 PART I: 1,4-naphthoquinone cation with *O*-ether linkage

Unexpectedly, the 2-hydroxyl 1,4-naphthoquinone **27a-c** and 2-acetoxy 1,4-naphthoquinone **26a-c** demonstrated weak antiplasmodial (IC_{50} > 3 μM), which may be due to the undesirable physiochemical properties of the designed compound. The goal in this section thus became to prevent the possible decomposition of the OAc by forming a stronger linkage, i.e. ether bond. Since the Ag^{2+}-mediated radical decarboxylation method (see section 4.2.9) is not applicable to a wide range of compounds due to high cost and significantly low yield, the preparation of *O*-alkylated derivatives may also potentially reduce the manufacturing cost in the effort to connect the cationic moiety and the quinone platform.

The *O*-alkylated bromide intermediates **31** were made by the procedure as illustrated in **Scheme 4.15**, and were finally converted to the corresponding phosphonium cationic compounds **32** via conventional heating method. However, C-2 hydroxyl group alkylation is problematic because chelated 1,4-naphthoquinones do not dissolve in aprotic organic solvents result in poor yields of intermediates **31a** and **31b**. It has been reported,

though without explanation, that the combination a crown ether and a TBA salt can increase the yield [36b]. Thus this modified procedure (introducing both TBAI and crown ether) was employed in the preparation of intermediate **34a**. In this part of study, a possible explanation on catalysts' function was examined after performing a series of control reactions in the following sections.

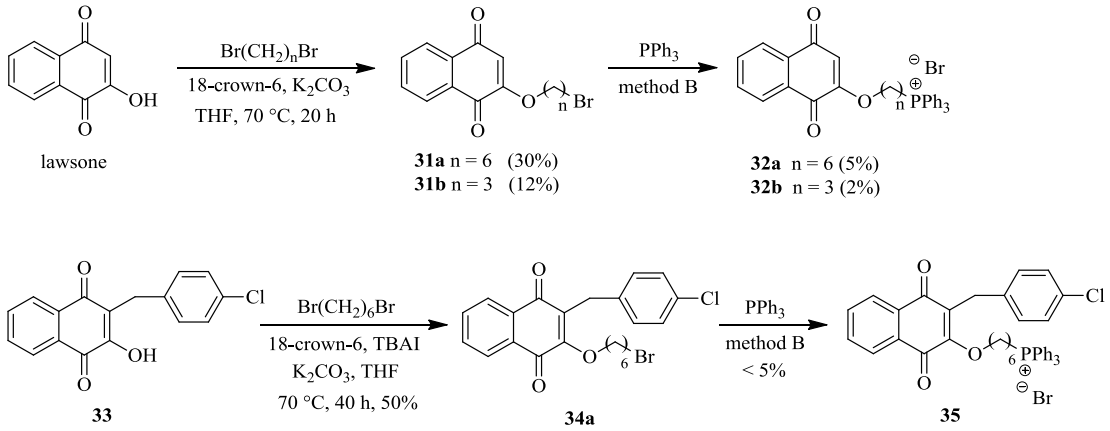

Scheme 4.15: Preparation of *O*-alkylated 1,4-naphthoquinone analogue **32a, 32b** and **35**.

4.2.12 The *O*-alkylation reaction: the optimal reaction conditions

Generally the addition of a phase transfer catalyst can increase the reaction outcomes. For example, the use of tetrabutylammonium iodide (TBAI) as an additive can facilitate the migration of a reactant from one phase into another, such as in a liquid/solid reaction system [36]. Another example is the usage of another kind of phase transfer catalyst, i.e., crown ether, whose unique chemical property can allow it to bind metal cation such as potassium (K^+) and sodium (Na^+). The counterions thereby become highly reactive naked nucleophile [37].

Using phthiocol as starting material, four control reactions were performed to examine the *O*-alkylation of 2-hydroxynaphthoquinones (**Scheme 4.16**). The choice of

salt was potassium carbonate, which is sufficiently basic to deprotonated the 2-hydroxyl group of phthiocol (pK_a = 5.08) [38]. The choice of crown ether was 18-crown-6 because of its unique capability to chelate potassium cations.

As illustrated in **Scheme 4.16**, in the first reaction, 0% of final product 3-decyloxymenadione was isolated. The reaction solution is red in color with large precipitates, which was identified after filtration as the potassium salt of phthiocol that was insoluble in THF. In the second reaction, it was noticed that 18-crown-6 can effectively dissolve the K^+ metal complexes and resulted a dense violet-purple color in THF, the aprotic solvent of choice. The crown ether itself was found to enhance the isolated yield of *O*-alkylated product from 0 to 11 %. In the third reaction, the TBAI was found to significantly increase the reaction yield from 0% to 49%, and the color of reaction solution changed into orange-red. In the fourth reaction, the combination of the two catalysts (18-crown-6 and TBAI) was found to have the highest product yield (68%) of the four reaction conditions screened.

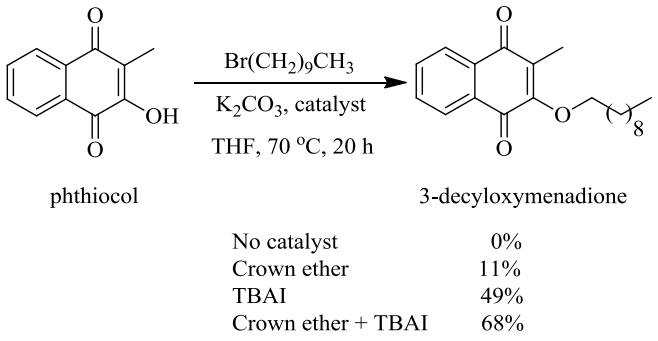

Scheme 4.16: *O*-Alkylation of 2-hydroxy-3-methyl-1,4-naphthoquinone (phthiocol) in the presence and absence of 18-crown-6 and TBAI.

The question remained as to whether the combination of the two catalysts has a synergistic effect. In order to further explore the mechanism and its possible usage in *O*-

alkylation reactions, a group of substrates were studied. Comparing to the reaction results using only 18-crown-6 (**Table 4.02**), the reaction yields were consistently low (< 30 %). The reaction conditions were also optimized by varying temperatures, solvents, bases, and amounts of catalyst. Highest yields were found when THF was used instead of acetone, acetonitrile or toluene. From here, a further investigation was initiated into the effect of the R group on the naphthoquinone substrates, as well the effect of alkylating agent in section 4.2.13.

Table 4.02: *O*-Alkylation of 2-hydroxy-3- methyl-1,4-naphthoquinone (phthiocol) in the absence of TBAI.

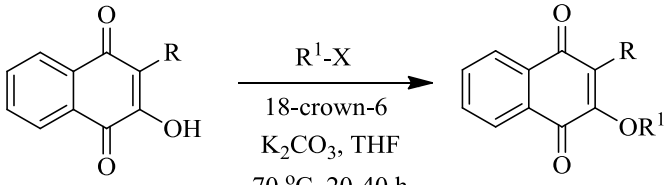

31

entry	compd	R	R^1	X	time (h)	yield (%)[a]
1	**31a**	H	$(CH_2)_6Br$	Br	20	31
2	**31b**	H	$(CH_2)_3Br$	Br	20	12
3	**31c**	H	$H_2C(p\text{-}C_6H_4)CH_2Br$	Br	20	19
4	**31d**	H	$(CH)_5Me$	I	48	20
5	**31e**	*p*-ClBn	$(CH_2)_3Br$	Br	20	47

[a] isolated yield.

4.2.13 The *O*-alkylation reaction: the influence of substrate and alkylating agent

Using the optimized reaction conditions, a variety of 2-hydroxy-3-methyl-1,4-naphthoquinone were tested. The results of the reactions are summarized in **Table 4.03**. The substrates were prepared generally by two steps: the epoxidation and the following acid-catalyzed cleavage (**Scheme 4.12**, the same procedure used to prepare compound

24c). Various alkylating agents with different types of leaving groups were included. The reaction outcomes depended greatly on the nature of the leaving group/atom. Among I, Br, Cl and OMs, reaction yields were higher when X is Br. In addition to this, among different R_1-X, secondary alkyl halide equates to very poor electrophiles. Moreover, tertiary substituted alkylating reagents (e.g., $(CH_3)_3CCl$) did not form any product. It is believed that these results follow a similar order of reactivity in Williamson ether synthesis, in which the tertiary alkyl structure is the worst substrate since the bulky group may prevent the S_N2 attack.

Table 4.03: *O*-Alkylation of 2-hydroxynaphthoquinones.

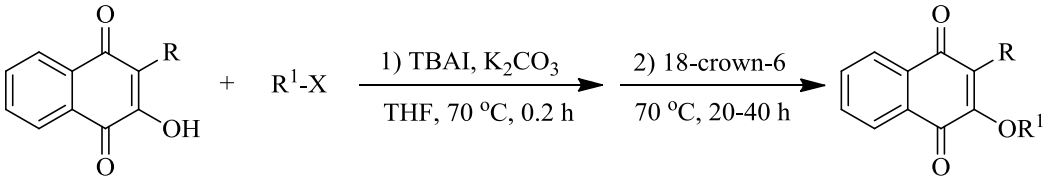

34a-m

entry	compd	R	R^1	X	time (h)	yield (%)[a]
1	**34b**	Me	$(CH_2)_2Me$	I	20	37
2	**34c**	Me	$(CH_2)_3Me$	OMs	20	49
3	**34d**	Me	$CH(CH_3)_2$	OMs	20	0
4	**34d**	Me	$CH(CH_3)_2$	I	40	22
5	**34e**	Me	cyclopropyl	Br	20	0
6	**34f**	Me	$C(CH_3)_3$	Cl	20	0
7	**34g**	C_6H_{11}	$(CH_2)_3Br$	Br	40	82
8	**34h**	C_6H_{11}	$(CH_2)_6Br$	Br	40	72
9	**34i**	CH_2Ph	$(CH_2)_2Me$	I	20	44
10	**34j**	CH_2Ph	$(CH_2)_6Br$	Br	20	57
11	**34a**	*p*-ClBn	$(CH_2)_6Br$	Br	40	51
12	**34k**	Cl	$(CH_2)_3Br$	Br	40	56
13	**34l**	Cl	$(CH_2)_6Br$	Br	40	59
14	**34m**	H	$(CH_2)_2Me$	I	20	20

[a] isolated yield.

Additional research was pursued after evaluating the R substituent effects on the reaction outcomes (**Table 4.03**). It was found that the reaction yield was highly affected by the substituents attached at C-3 position. When benzyl is attached, the yield is only between 44-57% (entry 9 and 10). If R is electron withdrawing (Cl), it was possible to obtain the desired ether compound in fair yield although longer reaction times were required (56% in entry 12, 59% in entry 13).

Conversely, an electron donating group can further increase the yield (R = Me, 68%; not included in the table, made by lab colleague Ali Altharawi), and a secondary alkyl group (stronger electron donating group) can generate the desired compound with the highest yield, 72% or 82% (entry 7 and 8). These observations might be due to the change of delocalization of the negative charge as the conversion rate is highest when the electron density on the oxygen atom of the 2-hydroxyl is greatest. For example, the increased reactivity of cyclohexyl analogue might be attributed to the cyclohexane ring's ability to depress electron delocalization of the oxygen anion. In contrast, when an electron withdrawing is bound, the delocalization may be augmented which could result in a reduced anionic character on the oxygen (lowering the reaction outcome).

Among the results summarized in **Table 4.03**, the yields vary significantly with different R groups. As well as the poor reactivity, the low yield might also be due to the poor regioselectivity for the reaction. When there is no R group at C-3 position, the reaction yield is low (20% in entry 14). Confirmed by ^{1}H NMR after chromatography purification, several products were constructed under the optimized condition including the desired 1,4-quinone **34m** together with 1,2-quinone **34m'** (**Scheme 4.17**). Based on

the above mentioned observation, the rationale for this result was further explored in the following section.

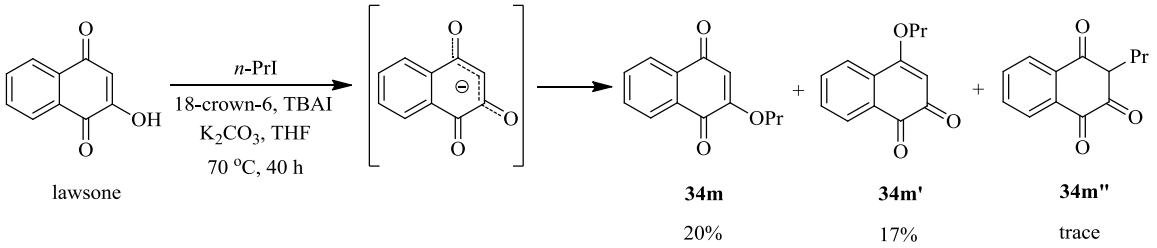

Scheme 4.17: *O*-Alkylation of lawsone.

4.2.14 The *O*-alkylation reaction: a proposed explanation

The mechanism of *O*-alkylation involves the formation of naked anionic structure **26a'** with the help of adding crown ether. Even through crown ether can solubilize the substrate **26a**, the nucleophilicity of the hydroxyl group in the 'naked' anionic structure is possibly decreased, which requires a counterion to stabilize the C-2 oxygen anion. $(n\text{-}Bu)_4N^+$ from the TBAI may be able to stabilize the negative charge and hence, greatly enhance the product yields. As just concluded, the effect of R group may further facilitate this process. For example, the electron donating group such as cyclohexyl group may prevent the delocalization of the electron through the quinone ring. Without adding a counterion to stabilize the negative charge on the oxygen of the C-2 hydroxyl, the electron delocalizes into the quinone ring which will not continually be attacked by the alkylating agent due to reducing the nucleophilicity of the oxygen anion. Consequently, yields were consistently below 20% when 18-crown-6 was used alone.

The possible synergetic role of the catalysts in the reaction was illustrated in **Figure 4.07**: The initial step would be extraction of K^+ from complex by 18-crown-6. The naked resonance-stabilized anion has considerably increased solubility in THF, giving the dark

violet-purple color in the solution. Secondly, the bulky $(n\text{-Bu})_4N^+$ from TBAI is thought to stabilize the oxygen anion. The new formed loose ionic bond would facilitate the reaction and displays the greatest yield up to 68%. In comparison, the TBAI itself can also facilitate the reaction, but the poor solubility of K^+ complex may prevent the further interaction with TBAI. The unique purple color was observed only after adding 18-crown-6 [39].

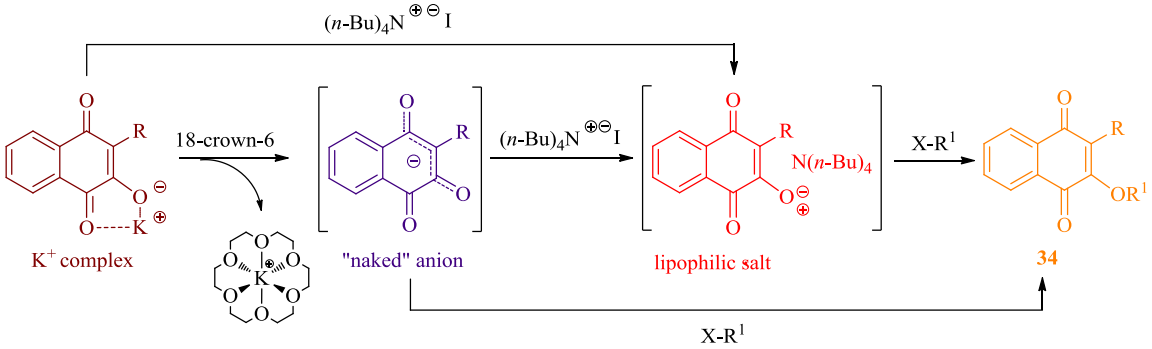

Figure 4.07: Proposed explanation: a synergistic effect of the two catalysts.

4.2.15 Evidence: the solution color change and red shift in UV-Vis spectrum

The analyzing of phthiocol's change during the reaction process was followed by identifying the color difference [40] and light absorption (detected by UV-Vis spectrometer). It was concluded that 2-hydroxynaphthoquinone under neutral conditions has typical peaks in the wavelength range 245-250 nm ($\pi\rightarrow\pi^*$) and 330 nm ($n\rightarrow\pi^*$) for the benzenoid transition, and at 285 nm ($\pi\rightarrow\pi^*$) and 380 ($n\rightarrow\pi^*$) nm for the quinoid transition [41]. Evidence of electron delocalization was seen since the peak shifts as a consequence of delocalization of the negative charge into the quinone ring (**Figure 4.08**). The phthiocol THF solution as a yellow color and the emission bands for benzenoid were detected at 247 and 326 nm, while absorbances for the quinoid transitions were at 268

and 374 nm. In addition to this, although the concentrated suspension of K^+ phthiocol is red in color, the UV-Vis spectrum was unable to obtain due to the poor solubility. When the K^+ complex was combined with just 1 equiv of 18-crown-6 in THF, a violet colored solution resulted. During the same time a broad peak was displayed at 525 nm (the red shift indicating an increase in π electron delocalization) along with the enhancement of color intensity. For the K^+ complex with just 1 equiv of TBAI resulted in a red chestnut solution and revealed a broad band at 364 nm representing the quinoid n→π* transition. Note, that broad bands did not peak above 510 nm which, is the evidence of decreased electron delocalization due to the possible ionic bond forming between $(n\text{-Bu})_4N^+$ and the C-2 oxygen anion (which favors the substitution reaction). In the spectrum of K^+ phthiocol containing both 1 equiv of crown ether and 1 equiv of TBAI, the medium red-violet solution was observed. Peaks can be found at both 362 and 525 nm (almost identical to the one with just 18-crown-6), suggesting both the "naked" anion and stabilized anion exist in the THF solution.

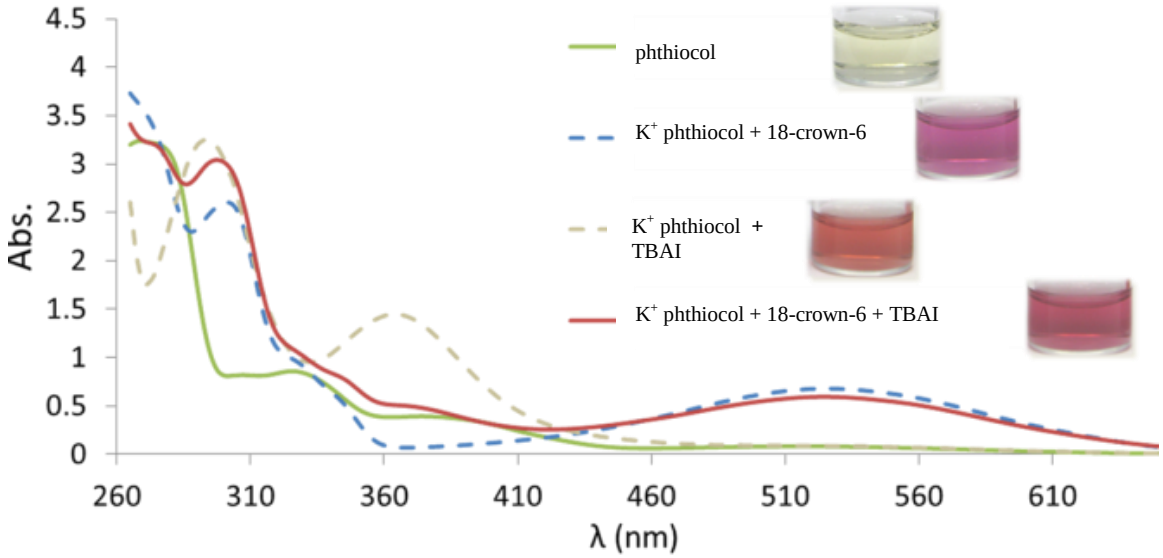

Figure 4.08: The solution color change and red shift in UV-Vis Spectrum.

In summary, each catalyst (18-crown-6 and TBAI, both as phase transfer catalysts) was able to solubilize the K^+ phthiocol complex in THF and act synergistically to greatly increase the reaction outcome. The optimized reaction condition in this study was also repeated in additional attempts to make 5-alkoxy-1,4-naphthoquinone, but no reaction occurred after 20 hours (**Scheme 4.18**). It is believed that the deprotonation of phenol may require a stronger base, e.g., aqueous hydroxides, thus a further investigation will be conducted in future studies.

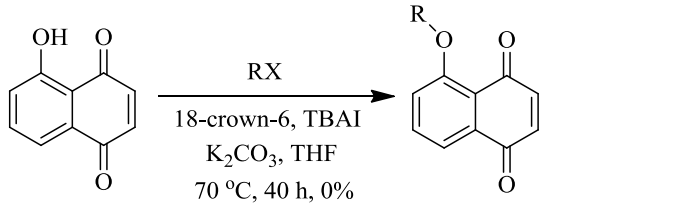

36a RX = $CH_3(CH_2)_3OTs$

36b RX = $Br(CH_2)_4Br$

36c RX = CH_2CHCH_2Cl

36d RX = $MeOSO_3Me$

Scheme 4.18: Attempts to synthesize 5-alkoxy-1,4-naphthoquinone.

4.2.16 Cationic analogue: preliminary study of structure activity relationship

Comparison of antiplasmodial activities was performed by minimum inhibitory concentrations against the chloroquine-resistant *P. falciparum* (W2 strain) in Dr. Rosenthal's lab [42]. Among the first series of non-naphthoquinone derivatives, studies showed the control compound (without cationic group) has an IC_{50} value over than 10 µM, compared to the positive control chloroquine (IC_{50} = 67 nM). As illustrated in **Table 4.04**, when n = 10, the activities of the resulting phosphonium lipocations are similar. It was further noticed the IC_{50} values was greatly depend on the length of the hydrocarbon

chain. Although it fails to reveal any correlation between IC_{50} values of compound **11d** and **11e**, the similarities were noticed in the IC_{50} values of phosphonium salts **11a**, **11f**, **11g** and **11h**. The other two analogues (HOBt and NHS forms) have IC_{50} values both above 800 nM. All of them were less active than the positive control. Thus it was concluded that the phthalimide group, HOBt group and NHS group were not serving as a mitochondrion antagonist.

Table 4.04: Comparisons of IC_{50}s for *P. falciparum* growth: compound **11a-g [43]**.

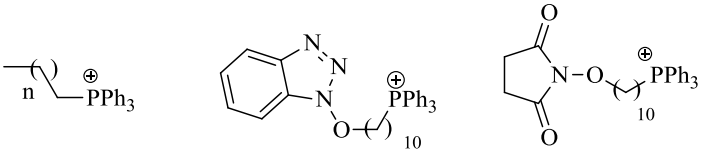

(n = 8) 141.6 ± 3.5 nM
(n = 2) 3.5 ± 0.5 μM

3
831.9 nM

7
1.5 μM

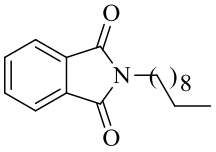

11h
>10.0 μM

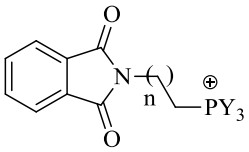

11a-g

entry	compd	n	Y	IC_{50} (nM)[a]	Log *D*[b]	MW[c]
1	**11b**	3*	Ph	>3,000	0.01	464.5
2	**11c**	5*	Ph	1021 ± 93.2	1.14	492.6
3	**11d**	9*	4-PhF	345.6 ± 15.3	2.13	602.6
4	**11e**	9	Bn	288.5 ± 35.2	1.37	590.8
5	**11a**	9	Ph	172.7 ± 4.0	1.67	548.7
6	**11f**	9	C_6H_{11}	140.6 ± 0.7	4.50	566.8
7	**11g**	9	4-PhOMe	134.0 ± 1.7	3.19	638.7
8	**CQ**[d]	-	-	66.93 ± 2.3	-	319.9

* made by Dr. Long
[a] testing performed by Jiri Gut in the laboratory of Dr. Philip J. Rosenthal
[b] measured by 1-octanol–water partition at pH 7.4
[c] molecular weights of lipocations **11** minus the counterion
[d] chloroquine (CQ)

Alternatively, the analogues with 1,4-naphthoquinone platform were tested. The amino carbon chain with 1,4-naphthoquinone platform **15a-g**, proved to have very similar activity compared to the control and similar to the phthalimide analogues. The chain length seemingly has moderate effects on the activity. The shorter chain analogue results in poor activity. In contrast, for the analogue without the amino group in the hydrocarbon chain, shorter chain analogues (**37b** and **37c**) demonstrate 4-15 fold increased activity compared to the 10-carbon chain analogue **37a**. However, compound **21** with only one methylene in the chain had very poor activity (**Table 4.05**). The interesting feature found in the structure is that the P-substituent could be either alkyl (e.g. Y = cyclohexyl) or aromatic (e.g., Y = Ph) with only a moderate effect on the IC_{50} values (both were made by Dr. Long). The only exception is trimethyl derivative (made by Dr. Long) which has much less activity compared to analogues of equal chain length.

Table 4.05: Comparisons of IC_{50}s for *P. falciparum* growth: compound **15**, **21**, **31 [43]**.

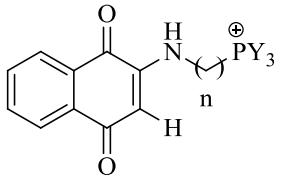

15

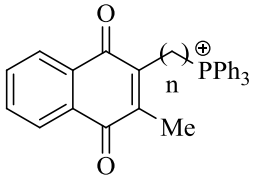

21, **37**

entry	compd	n	Y	IC_{50} (nM)[a]	Log *D*[b]	MW[c]
1	**15a**	2	Ph	519.9 ± 61.2	-1.08	462.5
2	**15b**	10	4-PhF	292.0 ± 53.2	1.67	628.7
3	**15c**	10	Bn	214.6 ± 0.5	2.80	616.8
4	**15d**	10	4-PhOMe	134.2 ± 10.5	4.37	664.8
5	**15e**	10	Ph	113.9 ± 7.6	3.60	574.7
6	**15f**	10	C_6H_{11}	94.4 ± 35.2	3.41	592.9
7	**37a**	10*	Ph	143.4 ± 6.3	3.97	573.7

Table 4.05 (con.)

8	**37b**	5*	Ph	48.3 ± 1.5	2.15	503.6
9	**37c**	4*	Ph	18.7 ± 0.3	1.91	489.6
10	**21**	1	Ph	543.4 ± 79.2	1.89	447.5
11	**ART**[d]			7.31 ± 0.14		262.3
12	**ATV**[d]			0.28 ± 0.19		366.3

* made by Dr. Long
[a] testing performed by Jiri Gut in the laboratory of Dr. Philip J. Rosenthal
[b] measured by 1-octanol–water partition at pH 7.4
[c] molecular weights of lipocations minus the counterion
[d] artemisinin (ART), atovaquone (ATV)

The above findings warrant further investigation, although these compounds were still relatively weak compared to the control. With a postulated mechanism that these compounds might interfere with the integrity of the mitochondrion membrane, the study was continued to investigate the possible mechanism of action.

In order to obtain evidence whether the designed molecules act at the binding site of the lead compound (atovaquone), the 2-hydroxyl naphthoquinone-based lipocations were made and tested (**Figure 4.09**). *O*-acetyl (**26**, **29**) and hydroxyl analogues (**27**, **30**) with different R groups at 2-position of 1,4-naphthoquinone were also included. But surprisingly, the activity of this series is very poor.

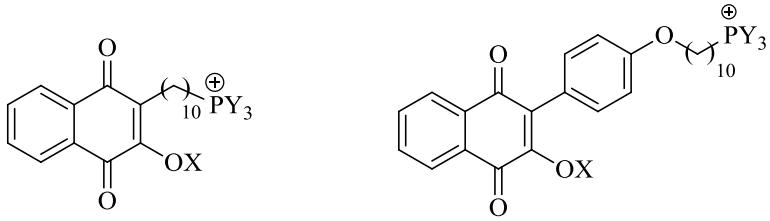

26, 29 $IC_{50} > 3$ μM X = Ac; Y = Bn, *n*-Bu, Ph
27, 30 $IC_{50} > 3$ μM X = H; Y = Bn, *n*-Bu, Ph

Figure 4.09: 2-Hydroxynaphthoquinone and the ester form prodrug.

Each of the 2-hydroxy 1,4-naphthoquinone lipocations possessed weak activity in the medium-low μM range. The activity data for the uncharged controls revealed that hydroxyl moiety had a largely adverse effect. With these unexpected results, an investigation was performed by using UV-Vis spectrometer. It was also anticipated that the ester prodrug might have been cleaved resulting in similar poor antiplasmodial activity.

Light absorption (detected by UV-Vis spectrometer, similar to section 4.2.15) has been shown to be a reliable method for detecting the chemical change in the structure, thereby giving rise to reasonable explanation of poor activity. In order to ascertain whether the poor results were due to the deprotonation and possibly further delocalization due to the weak acidity of the 2-hydroxyl under physiological pH, the UV-Vis graph of compound **37b** was obtained in pH = 7.4 buffer at room temperature (**Figure 4.10**). This was confirmed by the appearance of red shift peak above 480 nm. In comparison, the compound without C-2 hydroxyl (**38**) has no red peak observed above 480 nm. As a consequence, cationic charge is lost which is neutualized by the negative charge. This overall neutral charge on the molecules will cause the decrease of specificity for the parasite infected red blood cells, thus all the compounds with 2-hydroxyl group have only poor activity. Moreover, it was believed in the case of the pro-drug form phosphonium lipocations 2-acetoxy derivatives **26** and **29**, deprotection might first occur followed by deprotonation in the neutral medium. The negative charge then delocalized into the quinone ring and again resulted in poor activity.

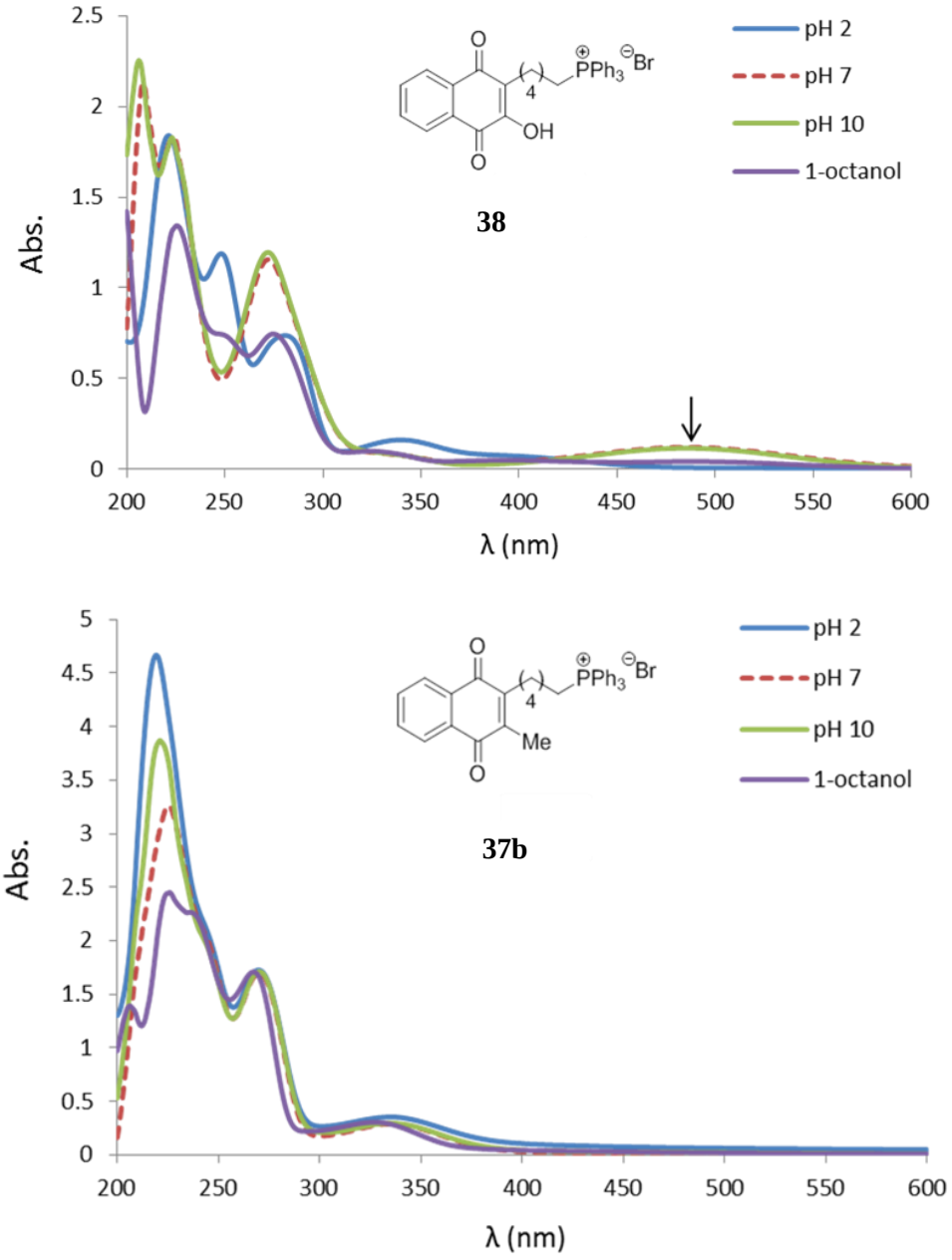

Figure 4.10: UV-Vis spectra of compound **37b.**

The continuing study on *O*-alkyl analogues has led to advanced understanding of designed cationic species (**Table 4.06**). When the carbon chain length increases to ten, the IC_{50} value is highest. Between 3-6 methylene groups, similar antiplasmodial activity was observed. It was anticipated that the more stable ether bond can not only prevent

potential cleavage of the *O*-substituted chain, but also provide the hydrogen bonding at the pocket. Additional data of compound **47** (whose uniqueness is especially striking) shows when the R is 4-PhOMe, the activity is highest. This slight increase in activity is possibly subject to the introduction of the aromatic ring; however, since only this one 2-*O*-alkyl 3-aryl 1,4-naphthoquinone base lipocations were made, more examples are needed to confirm this speculation. The most logical conclusion is that the good activity of designed cationic derivatives might bind to the same binding site as atovaquone.

Table 4.06: Comparisons of IC_{50}s for *P. falciparum* growth: compound **32a-b**, **35**, **40-47**.

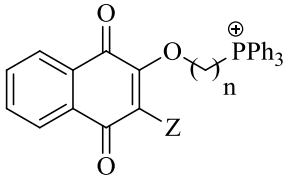

compd	n	Z	IC_{50} (nM)[a]	MW[b]
40	10	Me	119.3 ± 11.3	589.7
35	6	4-ClBn	49.5 ± 7.8	644.2
41	6	Bn	49.1 ± 6.3	609.7
42	3	Bn	46.7 ± 4.4	601.7
43	6	C_6H_{11}	47.9 ± 6.3	567.6
44	3	C_6H_{11}	42.3 ± 0.0	559.7
45	6*	Me	42.7 ± 1.4	553.6
46	3*	Me	41.9 ± 4.0	491.5
32b	3	H	40.0 ± 0.8	477.5
32a	6	H	28.5 ± 3.0	519.6
47	3	4-PhOMe	17.4 ± 4.1	583.6
CQ[c]			139.6 ± 4.9	
ATV[c]			0.5 ± 0.2	

* made by Dr. Long
[a] testing performed by Jiri Gut in the laboratory of Dr. Philip J. Rosenthal
[b] molecular weights of lipocations minus the counterion
[c] chloroquine (CQ), atovaquone (ATV)

One may tentatively conclude that 1,4-naphthoquinone-based triphenyl phosphonium with a proper chain length (n = 3-6) has the most promising activity. The additional aromatic moiety and further introduction of H bonding donor/receptor will be the next steps for this research topic.

4.3 Conclusions and Future Studies

The current lead compound (**Figure 4.11**) has demonstrated an outstanding therapeutic index. In addition to this, the Log *D* values were obtained by the shaking flask method at 25 ºC [44]. It was found with a log *D* = 1.91 at pH 7.4 that this new lead should be lipophilic enough to penetrate the lipid bilayer of the red blood cell membrane, as well as outer membrane and inner membrane of mitochondria where the electron transport chain is located.

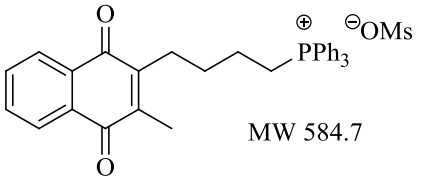

compound **37c**
lead compound

Plasmodium falciparum IC_{50} 18.9 nM[a]
Vero (kidney) cell IC_{50} 53,200 nM[b]

therapeutic index = 2,818
{TI = [IC_{50}(Vero)]/[IC_{50}(*P. falciparum*)]}

Log *D* 1.91
(pH 7.4, octanol:buffer partition)

[a] testing performed by Jiri Gut in the laboratory of Dr. Philip J. Rosenthal
[b] testing performed by Melina Galizzi in the laboratory of Dr. Roberto Docampo

percent hemolysis (%)

concentration	compound **19c**	atovaquone	artemisinin
12.5 µM	0.06 ± 0.10%	0.13 ± 0.18%	0.05 ± 0.05%
25.0 µM	0.27 ± 0.11%	0.09 ± 0.15%	0.22 ± 0.21%

Figure 4.11: New lead compound for the following studies.

Since the lower number of host cells may result in false test result, preliminary toxicity test was also performed to confirm the designed compound will not harm the red blood cell [45]. After incubation with red blood cells at 37 ºC after 1 hour, using atovaquone and artemisinin as controls, the percent hemolysis was below 0.06% at 12.5 µM, and below 0.27% at 25 µM. The low values indicate the designed compound **37c** show no or little in vitro toxicity on human red blood cell membrane.

In summary, the selectively delivering strategy based on triphenyl phosphonium may facilitate passive transport of the lipophilic cations across the plasma membranes, and further penetrate into the negatively-charged parasite mitochondrion membrane. During this process, electrostatic attraction is rationalized as the driving force for movement into the parasite mitochondrion. It is expected the 1,4-naphthoquinone based lipocations continue to accumulate inside the mitochondrion until the membrane collapses.

However, whether these compounds act as an analogue of ubiquinone at the bc_1 complex is still unknown. Because the structural similarity between the designed molecule the atovaquone is only the 1,4-naphthoquinone platform and the hydrocarbon side chain, the IC_{50} values were still not in the range of the control (atovaquone). The mechanism of the lower IC_{50} in *O*-alkylated analogues for growth inhibition of the plasmodium is still need to be rationalized.

As the preliminary study has shown, the phosphonium cationic derivatives of the lead compound, i.e., atovaquone, are accessible from common naphthoquinone precursors in 3-4 simple steps. Although more evidence is required, a further study may lead to a workable synthetic route to attach a cationic group onto various target therapeutic agent.

Besides antiparasitic therapy, it is anticipated this development would presumably lend itself to such applications as potential mitochondriotropic agents to treat other diseases.

During procedure using two phase-transfer the same time, a mild catalysts (crown ether and tetrabutylammonium salt) to enhance the *O*-alkylation of 2-hydroxy 1,4-naphthoquinones was developed. These findings demonstrate a unique application in which a two phase-transfer catalyst system can enhance a reaction involving a resonance-stabilized nucleophile. Groups of substrates (with either an electron donating group or an electron withdrawing group at C-3 position) presented in **Table 4.03** may lead to more fruitful explanation of this reaction.

4.4 Experimental

In general, reagents and solvents were used as purchased without further purification. Reaction products were purified by column chromatography on silica gel (60-100 mesh) and visualized by UV on TLC plates (silica gel 60 F_{254}). Reactions conducted under microwave irradiation were performed in a Biotage™ Initiator reactor. IR spectra were recorded and reported in cm^{-1}. Melting points were determined with a melting point apparatus and were left uncorrected. Mass spectrometry was performed by electrospray ionization (ESI). ^{1}H and ^{13}C NMR spectra were recorded on a Varian Inova 500 MHz spectrometer. Chemical shifts were expressed in δ (ppm) values with tetramethylsilane or residual solvent (e.g., $CHCl_3$ or DMSO) as an internal standard. The designation "ABq" for a ^{1}H NMR peak indicates that a peak was one partner of an AB quartet; if additional splitting was observed, they are noted after the ABq designation (e.g., ABqd). Copies of NMR spectra may be found in APPENDIX C.

Preparation of *N*-alkyl phthalimide phosphonium salts 11; general procedure. Trisubstituted phosphine (1.5 mol equiv) and phthalimide (1 mol equiv) were mixed in a 5 mL conical-shaped reaction tube. The mixture was then stirred at 110 °C for 40 h under an argon atmosphere. After cooling to room temperature, the phosphonium mesylated phthalimide product **11** was separated by flash chromatography on silica gel using acetone to elute nonpolar impurities followed by DCM:MeOH. This method was also used to prepare tri-substituted phosphonium cationic compound **3** and **7**.

(10-(1,3-Dioxoisoindolin-2-yl)decyl)triphenylphosphonium methanesulfonate (11a): Yield: 42%; colorless oil; TLC (SiO_2) R_f 0.36 (9:1 DCM:MeOH); ^{1}H NMR (500 MHz, $CDCl_3$) δ 7.83-7.79 (m, 9H), 7.78-7.75 (m, 2H), 7.75-7.69 (m, 8H), 3.64 (t, 2H, J = 7.5 Hz), 3.56-3.48 (m, 2H), 2.70 (s, 3H), 1.65-1.57 (m, 6H), 1.28-1.18 (m, 10H); ^{13}C NMR (125 MHz, $CDCl_3$) δ 168.4, 135.1, 135.0, 133.9, 133.6, 133.5, 132.1, 130.6, 130.5, 123.1, 118.7, 118.1, 37.9, 30.4, 30.2, 29.3, 29.1, 29.0, 28.5, 26.7, 22.6, 21.8.

(10-(1,3-Dioxoisoindolin-2-yl)decyl)*tris*(4-fluorophenyl)phosphonium methanesulfonate (11d): Yield: 55%; hazy white oil; TLC (SiO_2) R_f 0.44 (9:1 DCM:MeOH); ^{1}H NMR (500 MHz, $CDCl_3$) δ 7.95-7.90 (m, 6H), 7.83-7.81 (m, 2H), 7.74-7.72 (m, 2H), 7.44 (t, 6H, J = 6.0 Hz), 3.65-3.63 (m, 4H), 2.65 (s, 3H), 1.64-1.58 (m, 6H), 1.26-1.20 (m, 10H); ^{13}C NMR (125 MHz, $CDCl_3$) δ 168.5, 166.7 (dd, app $J_{C\text{-}F}$ = 259.0, 3.4 Hz), 136.6 (dd, app $J_{C\text{-}F}$ = 11.5, 9.5 Hz), 133.9, 132.1, 123.1, 118.5 (m), 114.0 (dd, app $J_{C\text{-}F}$ = 90.0, 3.4 Hz), 39.5, 37.9, 30.4, 30.2, 29.7, 29.2, 29.04, 29.95, 28.4, 29.7, 22.5, 22.1.

Tribenzyl(10-(1,3-dioxoisoindolin-2-yl)decyl) phosphonium methanesulfonate (11e): Yield: 63%; colorless oil; TLC (SiO_2) R_f 0.51 (9:1 DCM:MeOH); ^{1}H NMR (500 MHz,

$CDCl_3$) δ 7.84-7.82 (m, 2H), 7.73-7.71 (m, 2H), 7.34-7.26 (m, 15H), 4.02 (d, 6H, *J* = 15.0 Hz), 3.66 (t, 2H, *J* = 7.5 Hz), 2.91 (s, 3H), 1.92-1.88 (m, 2H), 1.69-1.63 (m, 2H), 1.35-1.07 (m, 14H); ^{13}C NMR (125 MHz, $CDCl_3$) δ 168.5, 134.0, 132.1, 130.6, 130.4, 130.3, 129.6, 128.6, 128.2, 128.1, 127.8, 123.2, 39.9, 38.0, 30.9, 30.8, 29.2, 29.1, 29.0, 28.7, 28.6, 26.9, 26.8, 26.5, 21.7, 18.7.

Tricyclohexyl(10-(1,3-dioxoisoindolin-2-yl)decyl) phosphonium methanesulfonate (11f): Yield: 82%; colorless oil; TLC (SiO_2) R_f 0.48 (9:1 DCM:MeOH); ^{1}H NMR (500 MHz, $CDCl_3$) δ 7.85-7.83 (m, 2H), 7.74-7.72 (m, 2H), 3.67 (t, 2H, *J* = 7.5 Hz), 2.74 (s, 3H), 2.48 (q, 3H, *J* = 12.5 Hz), 2.29-2.24 (m, 2H), 2.01-1.95 (m, 6H), 1.85-1.81 (m, 4H), 1.70-1.63 (m, 2H), 1.56-1.29 (m, 34H); ^{13}C NMR (125 MHz, $CDCl_3$) δ 168.6, 134.0, 132.1, 123.2, 50.5, 38.0, 31.3, 31.2, 30.0 ,29.7, 29.3, 29.2, 29.1, 29.0, 28.6, 27.2, 27.1, 26.8, 26.6, 26.5, 25.5, 22.8, 15.6, 15.3.

(10-(1,3-Dioxoisoindolin-2-yl)decyl)*tris*(4-methoxyphenyl)phosphonium methanesulfonate (11g): Yield: 87%; colorless oil; TLC (SiO_2) R_f 0.23 (9:1 DCM:MeOH); ^{1}H NMR (500 MHz, $CDCl_3$) δ 7.83-7.81 (m, 2H), 7.74-7.72 (m, 2H), 7.63 (dd, 6H, *J* = 11.5 , 8.5 Hz), 7.19 (dd, 6H, *J* = 8.5 , 2.5 Hz), 3.93 (s, 9H), 3.65 (t, 2H, *J* = 7.5 Hz), 3.24-3.19 (m, 2H), 1.63 (qnt, 2H, *J* = 7.0 Hz), 1.60-1.54 (m, 4H), 1.28-1.21 (m, 10H); ^{13}C NMR (125 MHz, $CDCl_3$) δ 168.3, 164.6, 164.5, 135.3, 135.2, 133.9, 131.9, 123.0, 116.2, 116.1, 109.3, 108.6, 55.9, 55.8, 39.3, 37.8, 30.4, 30.3, 29.2, 29.0, 28.9, 28.8, 28.4, 26.6, 23.3, 22.4.

10-(1-Decyloxy-1H-benzotriazole)triphenylphosphonium bromide (3): Yield: 19%; pale oil; TLC (SiO_2) R_f 0.37 (9:1 DCM:MeOH); ^{1}H NMR (500 MHz, $CDCl_3$) δ 7.99 (d, 1H, *J* = 8.0 Hz), 7.83-7.71 (m, 15H), 7.69 (d, 1H, *J* = 8.5 Hz), 7.53 (t, 1H, *J* = 8.5 Hz),

7.38 (t, 1H, *J* = 8.5 Hz), 4.52 (t, 2H, *J* = 6.5 Hz), 3.58-3.55 (m, 2H), 1.83 (qnt, 2H, *J* = 7.5 Hz), 1.52 (qnt, 2H, *J* = 7.5 Hz), 1.31-1.24 (m, 12H); ^{13}C NMR (125 MHz, $CDCl_3$) δ 165.1, 164.9, 143.5, 135.0, 134.9, 133.7, 133.6, 130.5, 130.4, 128.0, 127.4, 124.6, 120.2, 118.9, 118.2, 108.8, 81.0, 39.6, 30.4, 30.3, 29.2, 29.0, 29.5, 28.0, 25.5, 22.6.

10-(1-Decyloxy-pyrrolidine-2,5-dione)triphenylphosphonium bromide (7): Yield: 23%; pale oil; TLC (SiO_2) R_f 0.38 (9:1 DCM:MeOH); ^{1}H NMR (500 MHz, $CDCl_3$) δ 7.81-7.71 (m, 15H), 4.06 (t, 2H, *J* = 6.5 Hz), 3.55-3.49 (m, 2H), 2.72-2.69 (m, 4H), 1.69 (qnt, 2H, *J* = 7.0 Hz), 1.59 (m, 4H), 1.39 (qnt, 2H, *J* = 7.0 Hz), 1.26-1.21 (m, 8H); ^{13}C NMR (125 MHz, $CDCl_3$) δ 171.4, 153.1, 135.0, 133.6, 133.6, 130.6, 130.5, 118.8, 118.1, 77.4, 39.53, 30.4, 30.2, 29.2, 29.0, 28.97, 28.94, 27.9, 25.5, 25.3, 22.6.

Preparation of 2-((hydroxyalkyl)amino)naphthalene-1,4-dione 13; general procedure. Suspension of quinone (0.2 mmol) in EtOH (2 mL) and amine (0.2 mmol) was stirred at room temperature for 18 hours or until the reaction was complete (checked by TLC). The mixture was concentrated and the product **15** was separated by flash chromatography on silica gel using 2:1 hexane:EtOAc.

2-(2-Hydroxyethylamino)naphthalene-1,4-dione (13a): Yield: 87%; red oil; TLC (SiO_2) R_f 0.40 (1:1 hexanes:EtOAc); ^{1}H NMR (500 MHz, $CDCl_3$) δ 8.10 (d, 1H, *J* = 7.5 Hz), 8.05 (d, 1H, *J* = 7.5 Hz), 7.73 (t, 1H, *J* = 7.5 Hz), 7.62 (t, 1H, *J* = 7.5 Hz), 6.22 (bs, 1H), 5.77 (s, 1H), 3.95-3.91 (m, 2H), 3.39-3.35 (m, 2H); MS (*m*/z): 216.1 (12), 215.1 (86), 200.1 (100), 160.1 (35), 132.1(13).

2-(10-Hydroxydecylamino)naphthalene-1,4-dione (13b): Yield: 76%; red solid, mp 117-118 ºC; TLC (SiO_2) R_f 0.38 (1:1 hexanes:EtOAc); ^{1}H NMR (500 MHz, $CDCl_3$) δ

8.05 (d, 1H, *J* = 7.5 Hz), 7.98 (d, 1H, *J* = 7.5 Hz), 7.67 (t, 1H, *J* = 7.5 Hz), 7.56 (t, 1H, *J* = 7.5 Hz), 5.92-5.88 (m, 1H), 5.68 (s, 1H), 3.59 (t, 2H, *J* = 6.5 Hz), 3.13 (q, 2H, *J* = 6.5 Hz), 1.64 (qnt, 2H, *J* = 7.0 Hz), 1.52 (qnt, 2H, *J* = 7.0 Hz), 1.39-1.33 (m, 12H); ^{13}C NMR (125 MHz, $CDCl_3$) δ 183.2 182.0, 148.2, 134.9, 133.8, 132.1, 130.6, 126.4, 126.3, 100.7, 63.1, 42.7, 32.9, 29.6, 29.5, 29.4, 29.3, 28.4, 27.1, 25.8; MS (*m*/z): 329.3 (33), 228.2 (41), 214.2 (10), 200.2 (10), 186.1 (100), 174.1 (81).

Preparation of 2-aminoalkyl naphthoquinone mesylates 14; general procedure. Naphthoquinone (0.44 mmol), mesyl chloride (39 µL, 0.49 mmol) and Et_3N (129 µL, 0.89 mmol) were mixed in dry DCM (10 mL) while the reaction temperature was maintained at 0 °C. The reaction mixture was then stirred at room temperature for 18 hours. The solution was then washed with distilled water (10 mL) and 5% $NaHCO_3$ (10 mL), dried over $MgSO_4$, filtered, and evaporated. The final compound **16** was finally obtained by trituration in a 1:1 solution of hexanes:EtOAc and used without further purification.

2-((1,4-Dioxo-1,4-dihydronaphthalen-2-yl)amino)ethyl methanesulfonate (14a): Yield: 85%; orange solid, mp 160 ºC (decomp.); TLC (SiO_2) R_f 0.19 (1:1 hexanes:EtOAc); ^{1}H NMR (500 MHz, DMSO-d_6) δ 8.03 (d, 1H, *J* = 7.5 Hz), 7.97 (d, 1H, *J* = 7.5 Hz), 7.87 (t, 1H, *J* = 7.5 Hz), 7.77 (t, 1H, *J* = 7.5 Hz), 7.65 (s, 1H), 5.87 (s, 1H), 4.42 (t, 2H, *J* = 5.0 Hz), 3.61-3.58 (m, 2H), 3.22 (s, 3H); ^{13}C NMR (125 MHz, DMSO-d_6) δ 182.6, 181.6, 161.7, 135.8, 133.9, 133.3, 131.3, 126.9, 126.3, 68.3, 41.9, 37.7.

10-(1,4-Dihydro-1,4-dioxonaphthalen-3-ylamino)decyl methanesulfonate (14b): Yield: 97%; red solid, mp 102-104 ºC; TLC (SiO_2) R_f 0.53 (3:1 hexanes:EtOAc); ^{1}H NMR (500 MHz, $CDCl_3$) δ 8.01 (d, 1H, *J* = 7.5 Hz), 7.95 (d, 1H, *J* = 7.5 Hz), 7.65 (t, 1H,

J = 7.5 Hz), 7.53 (t, 1H, *J* = 7.5 Hz), 7.92-7.89 (m, 1H), 5.65 (s, 1H), 4.15 (t, 2H, *J* = 7.0 Hz), 3.10 (q, 2H, *J* = 7.0 Hz), 2.95 (s, 3H), 1.67 (qnt, 2H, *J* = 7.0 Hz), 1.59 (qnt, 2H, *J* = 7.0 Hz), 1.35-1.22 (m, 12H); ^{13}C NMR (125 MHz, $CDCl_3$) δ 182.8, 181.9, 148.0, 134.7, 133.7, 131.9, 130.5, 126.3, 126.2, 70.3, 42.6, 37.4, 37.3, 29.5, 29.3, 29.1, 28.9, 28.2, 27.0, 25.4; MS (*m*/z): 311.3 (26), 242.2 (12), 228.2 (36), 214.1 (10), 200.2 (11), 186.1 (100).

Preparation of 2-amino naphthoquinones phosphonium mesylates 15; general procedure. Trisubstituted phosphine (0.26 mmol) and methanesulfonate (0.13 mmol) were combined in a 5 mL conical-shaped microwave with a stir rod. The tube was capped and the mixture was heated at 110 °C in a sand bath for 2 minutes. The tube was then placed in microwave reactor (Biotage^{TM}) and was irradiated on high absorption at 150 °C for 30 minutes. After cooling to room temperature, the phosphonium mesylated phthalimide product **15** was directly separated by flash chromatography on silica gel using acetone to elute nonpolar impurities followed by 9:1 DCM:MeOH.

(2-(1,4-Dihydro-1,4-dioxonaphthalen-3-ylamino)ethyl)triphenylphosphonium methanesulfonate (15a): Yield: 20%; red oil; TLC (SiO_2) R_f 0.11 (9:1 DCM:MeOH); ^{1}H NMR (500 MHz, $CDCl_3$) δ 8.03 (m, 1H), 7.69 (d, 1H, *J* = 7.5 Hz), 7.87-7.72 (m, 16H), 7.65 (t, 1H, *J* = 7.5 Hz), 7.56 (t, 1H, *J* = 7.5 Hz), 5.17 (s, 1H), 4.15-4.08 (m, 2H), 3.68-3.60 (m, 2H), 2.88 (s, 3H); ^{13}C NMR (125 MHz, $CDCl_3$) δ 183.2, 180.8, 165.8, 135.6, 135.6, 134.5, 133.8, 133.7, 133.3, 132.2, 131.0, 130.9, 130.8, 126.6, 125.9, 118.1, 39.7, 36.3, 29.8.

(10-(1,4-Dihydro-1,4-dioxonaphthalen-3-ylamino)decyl)*tris*(4-fluorophenyl)-phosphonium methanesulfonate (15b): Yield: 14%; red oil; TLC (SiO_2) R_f 0.35 (9:1 DCM:MeOH); ^{1}H NMR (500 MHz, $CDCl_3$) δ 8.08 (d, 1H, *J* = 7.0 Hz), 8.04 (d, 1H, *J* =

7.0 Hz), 7.94-7.88 (m, 6H), 7.72 (t, 1H, *J* = 7.0 Hz), 7.61 (t, 1H, *J* = 7.0 Hz), 7.41 (t, 6H, *J* = 7.0 Hz), 5.95 (bs, 1H), 5.71 (s, 1H), 3.86 (m, 2H), 3.16 (q, 2H, *J* = 6.5 Hz), 2.73 (s, 3H), 1.67-1.55 (m, 6H), 1.35-1.23 (m, 10H); ^{13}C NMR (125 MHz, $CDCl_3$) δ 183.2, 182.1, 167.9, 165.8, 136.8, 136.7, 136.6, 134.9, 133.9, 132.1, 130.7, 126.5, 126.3, 118.6, 118.5, 114.6, 42.7, 30.4, 29.9, 29.6, 29.4, 29.3, 29.2, 28.3, 27.0, 22.8.

(10-(1,4-Dihydro-1,4-dioxonaphthalen-3-ylamino)decyl)tribenzyl-phosphonium methanesulfonate (15c): Yield: 28%; red oil; TLC (SiO_2) R_f 0.33 (9:1 DCM:MeOH); ^{1}H NMR (500 MHz, $CDCl_3$) δ 8.09 (d, 1H, *J* = 7.0 Hz), 8.04 (d, 1H, *J* = 7.0 Hz), 7.73 (t, 1H, *J* = 7.0 Hz), 7.62 (t, 1H, *J* = 7.0 Hz), 7.34-7.25 (m, 15H), 5.94 (bs, 1H), 5.72 (s, 1H), 4.08 (d, 6H, *J* = 15.0 Hz), 3.19-3.16 (m, 2H), 1.99-1.92 (m, 2H), 1.70-1.66 (m, 2H), 1.38-1.10 (m, 14H); ^{13}C NMR (125 MHz, $CDCl_3$) δ 183.1, 182.1, 165.6, 134.9, 132.1, 130.5, 129.6, 128.6, 128.3, 128.2, 126.4, 126.3, 42.6, 31.1, 29.4, 29.2, 28.9, 28.3, 27.1, 27.0, 26.7, 21.8, 18.9.

(10-(1,4-Dihydro-1,4-dioxonaphthalen-3-ylamino)decyl)*tris*(4-methoxyphenyl)phosphonium methanesulfonate (15d): Yield: 78%; red oil; TLC (SiO_2) R_f 0.22 (9:1 DCM:MeOH); ^{1}H NMR (500 MHz, $CDCl_3$) δ 8.06 (d, 1H, *J* = 7.5 Hz), 8.02 (d, 1H, *J* = 7.5 Hz), 7.71 (t, 1H, *J* = 7.5 Hz), 7.62 (m, 6H), 6.07 (bs, 1H), 5.69 (s, 1H), 3.92 (s, 9H), 3.34-3.20 (m, 2H), 3.19-3.15 (q, 2H, *J* = 6.5 Hz), 2.73 (s, 3H), 1.68-1.63 (qnt, 2H, *J* = 7.0 Hz), 1.62-1.54 (m, 2H), 1.40-1.35 (m, 2H), 1.34-1.05 (m, 10H); ^{13}C NMR (125 MHz, $CDCl_3$) δ 182.9, 181.8, 164.6, 164.6, 135.3, 135.2, 134.7, 133.6, 131.9, 130.5, 126.2, 126.0, 116.2, 116.1, 109.0, 108.6, 56.0, 55.9, 42.5, 39.5, 30.6, 30.4, 29.0, 28.0, 26.9, 23.4, 23.0, 22.5.

(10-(1,4-Dihydro-1,4-dioxonaphthalen-3-ylamino)decyl)triphenylphosphonium methanesulfonate (15e): Yield: 40%; red oil; TLC (SiO_2) R_f 0.24 (9:1 DCM:MeOH); ^1H NMR (500 MHz, $CDCl_3$) δ 8.03 (dd, 1H, *J* = 8.0, 1.0 Hz), 7.98 (dd, 1H, *J* = 8.0, 1.0 Hz), 7.76-7.64 (m, 16H), 7.56 (dt, 1H, *J* = 7.5 Hz, 1.0 Hz), 5.95 (bs, 1H), 5.66 (s, 1H), 3.52-3.46 (m, 2H), 3.12 (q, 2H, *J* = 6.5 Hz), 2.66 (s, 3H), 1.64-1.55 (m, 4H), 1.32-1.27 (m, 2H), 1.26-1.20 (m, 10H); ^{13}C NMR (125 MHz, $CDCl_3$) δ 183.1, 182.1, 148.2, 135.2, 135.2, 134.9, 133.9, 133.8, 133.7, 132.1, 130.7, 130.6, 130.5, 126.4, 126.3, 118.9, 118.3, 42.7, 39.6, 30.6, 30.4, 29.4, 29.2, 29.1, 28.2, 27.0, 22.8, 21.8.

(10-(1,4-Dihydro-1,4-dioxonaphthalen-3-ylamino)decyl)tricyclohexyl-phosphonium methanesulfonate (15f): Yield: 47%; red oil; TLC (SiO_2) R_f 0.27 (9:1 DCM:MeOH); ^1H NMR (500 MHz, $CDCl_3$) δ 8.10 (d, 1H, *J* = 7.5 Hz), 8.04 (d, 1H, *J* = 7.5 Hz), 7.73 (t, 1H, *J* = 7.5 Hz), 7.62 (t, 1H, *J* = 7.5 Hz), 5.96 (bs, 1H), 5.73 (s, 1H), 3.18 (q, 2H, *J* = 6.5 Hz), 2.75 (s, 3H), 2.56 (q, 3H, *J* = 12.0 Hz), 2.44-2.39 (m, 2H), 1.83-1.80 (m, 4H), 1.72-1.65 (m, 2H), 1.54-1.31 (m, 40H); ^{13}C NMR (125 MHz, $CDCl_3$) δ 185.7, 185.5, 150.1, 134.9, 132.1, 126.4, 126.3, 42.7, 39.8, 31.4, 30.2, 29.9, 29.5, 29.4, 29.2, 28.3, 27.3, 27.1, 26.7, 26.6, 25.7.

((3-Methyl-1,4-dioxo-1,4-dihydronaphthalen-2-yl)methyl)triphenylphosphonium chloride (21): Yield: 22%; brown solid, mp 198-200 ºC; TLC (SiO_2) R_f 0.22 (9:1 DCM:MeOH); ^1H NMR (500 MHz, $CDCl_3$) δ 7.98-7.46 (m, 19H), 5.42 (d, 2H, *J* = 16.5 Hz), 2.19 (s, 3H); ^{13}C NMR (125 MHz, $CDCl_3$) δ 185.3, 185.0, 136.2, 136.1, 135.2, 134.8, 134.3, 134.27, 134.24, 133.9, 132.1, 132.0, 131.5, 130.8, 130.3, 130.2, 128.5, 126.7, 126.2, 118.4, 117.7, 29.7, 15.3.

Preparation of 2-(chloromethyl)-3-methylnaphthalene-1,4-dione 20. To 2-methyl-1,4-naphthoquinone (500 mg, 2.9 mmol) was added formaldehyde (1.5 mL, 14.5 mmol, 37% w/w in H_2O) in glacial AcOH (2.5 mL). HCl gas was then passed through the mixture and after 5 minutes, the color of solution turned dark red. The mixture was extracted with EtOAc (3 x 5 mL), and then, the organic layer was washed with distilled water (10 mL), dried over $MgSO_4$, filtered, and evaporated. The product was separated by flash chromatography on silica gel using 9:1 hexanes:EtOAc. Yield: 88%; light yellow solid, mp 94-96 ºC; TLC (SiO_2) R_f 0.34 (19:1 hexanes:acetone); ^{1}H NMR (500 MHz, $CDCl_3$) δ 8.11-8.06 (m, 2H), 7.75-7.72 (m, 2H), 4.61 (s, 2H), 2.31 (s, 3H); ^{13}C NMR (125 MHz, $CDCl_3$) δ 184.9, 182.6, 146.7, 141.3, 134.0, 133.9, 132.0, 131.7, 126.7, 126.6, 35.9, 12.8.

Preparation of 2-alkylated 1,4-naphthoquinones 22; general procedure. Naphthoquinone (3.2 mmol), 1-bromoalkylcarboxylic acid (3.5 mmol), and $AgNO_3$ (1.6 mmol) were combined in 30 mL of anhydrous MeCN at room temperature. The reaction mixture was heated 60 °C and 30 mL ammonium persulfate aqueous solution (6.1 mmol) was then slowly added (over a 2.5 hours period). The reaction mixture was heated at 60 °C for 20 hours. After cooling to room temperature, the mixture was redissolved in EtOAc (15 mL) and washed with brine, and then, the organic layer was dried over Na_2SO_4, filtered, and evaporated. The final compound **22** was separated by flash chromatography on silica gel using 9:1 hexanes:EtOAc in accordance to product R_f values.

2-(5-Bromopentyl)naphthalene-1,4-dione (22b): Yield: 11%; yellow solid, mp 56-58 ºC; TLC (SiO_2) R_f 0.50 (7:1 hexanes:EtOAc); ^{1}H NMR (500 MHz, $CDCl_3$) δ 8.12-8.03 (m, 2H), 7.95-7.70 (m, 2H), 6.79 (s, 1H), 3.45-3.41 (m, 2H), 2.64-2.57 (m, 2H), 1.95-

1.89 (m, 2H), 1.70-1.51 (m, 4H); ^{13}C NMR (125 MHz, $CDCl_3$) δ 185.2, 185.1, 151.4, 134.8, 133.7, 133.6, 132.2, 132.0, 126.6, 126.0, 35.5, 32.3, 29.4, 27.8, 27.2.

2-(10-Bromodecyl)naphthalene-1,4-dione (22c): Yield: 75%; yellow solid, mp 43-45 ºC; TLC (SiO_2) R_f 0.36 (7:1 hexanes:EtOAc); ^{1}H NMR (500 MHz, $CDCl_3$) δ 8.10-8.07 (m, 1H), 8.05-8.03 (m, 1H), 7.74-7.71 (m, 2H), 6.78 (s, 1H), 3.40 (t, 2H, *J* = 7.0 Hz), 2.56 (t, 2H, *J* = 7.5 Hz), 1.84 (qnt, 2H, *J* = 7.0 Hz), 1.58 (qnt, 2H, *J* = 7.5 Hz), 1.43-1.29 (m, 12H); ^{13}C NMR (125 MHz, $CDCl_3$) δ 185.2, 185.1, 151.9, 134.7, 133.6, 132.3, 132.1, 126.6, 126.0, 34.0, 32.8, 29.6, 29.4, 29.4, 29.3, 28.7, 28.2, 27.1.

Preparation of 1α-(bromoalkyl)naphtho[2,3-β]oxirene-2,7(1α*H*,7α*H*)-dione 23c; general procedure. A mixture of 30% H_2O_2 (1.5 mL), Na_2CO_3 (60 mg, 0.57 mmol) and H_2O (0.6 mL) was added to a stirring mixture of 1,4-naphthoquinone (4.4 mmol) in 3 mL EtOH at room temperature. The suspension was stirred at that temperature for 1 hour, after that, 3 mL H_2O was added. The reaction mixture was extracted three times with DCM (6 mL). The combined organic layer was dried over $MgSO_4$, filtered, and concentrated. The final product was then collected and used without further purification.

1α-(10-Bromodecyl)naphtho[2,3-β]oxirene-2,7(1α*H*,7α*H*)-dione (23c): Yield: 82%; white semi-solid; TLC (SiO_2) R_f 0.48 (7:1 hexanes:EtOAc); ^{1}H NMR (500 MHz, $CDCl_3$) δ 8.03-8.01 (m, 1H), 7.96-7.94 (m, 1H), 7.78 (m, 2H), 3.87 (s, 1H), 3.41 (t, 2H, *J* = 6.5 Hz), 2.31-2.05 (m, 1H), 1.91-1.82 (m, 3H), 1.52-1.47 (m, 2H), 1.42-1.38 (m, 4H), 1.29 (m, 8H); ^{13}C NMR (125 MHz, $CDCl_3$) δ 192.2, 191.9, 134.7, 134.5, 132.6, 132.0, 127.6, 126.9. 64.2, 60.4, 34.3, 32.9, 29.8, 29.6, 29.5, 29.4, 28.9, 28.4, 28.3, 24.7.

Preparation of 2-(bromoalkyl)-3-hydroxynaphthalene-1,4-dione 24; general procedure. Concentrated H_2SO_4 (1.4 mL) was mixed with epoxide **21** (1.3 mmol) and was stirred at room temperature for 10 minutes. The mixture was then chilled to 0 °C and was added 10 mL of saturated aqueous $NaHCO_3$ solution. The resulting mixture was then extracted twice with DCM (10 mL), dried over $MgSO_4$, filtered and concentrated. The final product was separated by flash chromatography on silica gel in accordance to product R_f values.

2-(Bromodecyl)-3-hydroxynaphthalene-1,4-dione (24c): Yield 65%; yellow solid; TLC (SiO_2) R_f 0.43 (7:1 hexanes:EtOAc); ^{1}H NMR (500 MHz, $CDCl_3$) δ 8.11 (d, 1H, *J* = 7.5 Hz), 8.06 (d, 1H, *J* = 7.5Hz), 7.76-7.73 (m, 1H), 7.69-7.65 (m, 1H), 7.38 (s, 1H), 3.41-3.38 (t, 2H, *J* = 7.0 Hz), 2.61 (t, 2H, *J* = 7.5 Hz), 1.84 (qnt, 2H, *J* = 7.0 Hz), 1.55 (qnt, 2H, *J* = 7.0 Hz), 1.40-1.25 (m, 12H); ^{13}C NMR (125 MHz, $CDCl_3$) δ 184.9, 181.6, 153.2, 134.9, 134.7, 134.5, 133.1, 133.0, 132.6, 129.6, 127.6, 126.93, 129.91, 126.2, 124.9, 34.3, 33.0, 29.9, 29.7, 29.6, 29.5, 28.9, 28.4, 28.3, 23.5.

Preparation of 3-(10-bromoalkyl)-1,4-dioxo-1,4-dihydronaphthalen-2-yl acetate 25c; general procedure. Quinone (0.375 mmol) was added into a chloroform (5 mL) solution of acetyl chloride (54 μl, 0.75 mmol) and 2,6-lutidine (70 μL, 0.68 mmol). The reaction was stirred at 0 °C for 5 minutes. 0.5 M HCl (5 mL) was then added and the aqueous layer was extracted five times with DCM (1 mL). The combined organic layer was washed five times with brine (1 mL), dried over $MgSO_4$, filtered and concentrated. The product was isolated as white solid and was used without further purification.

3-(10-Bromodecyl)-1,4-dioxo-1,4-dihydronaphthalen-2-yl acetate (25c): Yield 98%; yellow solid, mp 52-54 °C; TLC (SiO_2) R_f 0.48 (7:1 hexanes:EtOAc); ^{1}H NMR (500

MHz, $CDCl_3$) δ 8.13-8.09 (m, 2H), 7.75-7.73 (m, 2H), 3.04 (t, 2H, *J* = 6.5 Hz), 2.55 (t, 2H, *J* = 8.0 Hz), 2.41 (s, 3H), 1.85 (qnt, 2H, *J* = 7.0 Hz), 1.51 (t, 2H, *J* = 7.0 Hz), 1.42-1.29 (m, 12H); ^{13}C NMR (125 MHz, $CDCl_3$) δ 184.8, 178.3, 168.2, 151.3, 140.0, 134.3, 134.0, 132.3, 131.1, 126.9, 126.8, 34.3, 33.0, 29.9, 29.6, 29.4, 28.9, 28.7, 28.3, 24.5, 20.6.

Preparation of (3-acetoxy-1,4-dioxo-1,4-dihydronaphthalen-2-yl)alkyl phosphonium bromide 26.

General procedure was same as the preparation of phosphonium salts **11**. The conventional heating method was followed by silica gel chromatography purification using acetone to elute the nonpolar impurities followed by 10:1 $CHCl_3$:MeOH to afford the phosphonium bromide product. However because many product was very difficult to purify, thus only the purist fraction was collected.

(10-(3-Acetoxy-1,4-dioxo-1,4-dihydronaphthalen-2-yl)decyl)triphenylphosphonium bromide (26a): Yield: 30%; pale yellow oil; TLC (SiO_2) R_f 0.27 (10:1 $CHCl_3$:MeOH); ^{1}H NMR (500 MHz, $CDCl_3$) δ 8.09-8.06 (m, 2H), 7.85-7.73 (m, 17H), 3.68 (s, 2H), 2.53 (t, 2H, *J* = 7.5 Hz), 2.40 (s, 3H), 2.17 (s, 2H), 1.62 (s, 4H), 1.48-1.45 (m, 2H), 1.32-1.21 (m, 8H); ^{13}C NMR (125 MHz, $CDCl_3$) δ. 185.7, 184.6, 178.1, 168.1, 151.1, 139.8, 135.1, 134.1, 133.9, 133.7, 133.6, 132.0, 130.8, 130.6, 130.5, 126.7, 126.6, 118.6, 117.5, 30.5, 30.4, 29.6, 29.3, 29.2, 29.1, 28.5, 24.3, 22.9, 22.6, 20.5.

(4-(10-(3-acetoxy-1,4-dioxo-1,4-dihydronaphthalen-2-yl) phenyl)bromodecyloxy)triphenylphosphonium bromide (29): Yield: 10**%;** orange red oil; TLC (SiO_2) R_f 0.18 (9:1 $CHCl_3$:MeOH);^{1}H NMR (500 MHz, $CDCl_3$) δ 8.17-8.13 (m, 2H), 7.86-7.78 (m, 10H), 7.72-7.70 (m, 7H), 7.31 (d, 2H, *J* = 8.0 Hz), 7.96 (d, 2H, *J* = 8.0 Hz), 3.98 (t, 2H, *J*= 6.0 Hz), 3.79-3.75 (m, 2H), 2.27 (s, 3H), 1.77 (qnt, 2H, *J* = 6.5 Hz),

1.41 (qnt, 2H, *J* = 6.5 Hz), 1.29-1.24 (m, 12H); ^{13}C NMR (125 MHz, $CDCl_3$) δ 184.2, 178.6, 168.4, 160.3, 149.6, 137.1, 135.0, 135.0, 134.3, 134.0, 133.8, 133.7, 132.1, 131.6, 130.9, 130.6, 130.5, 127.1, 126.5, 120.9, 118.8, 118.1, 114.2, 68.1, 29.4, 29.3, 29.2, 29.2, 29.1, 26.0, 22.7, 20.5.

(10-(3-Hydroxy-1,4-dioxo-1,4-dihydronaphthalen-2-yl)decyl)triphenylphosphonium bromide (27a): red oil; TLC (SiO_2) R_f 0.14 (10:1 $CHCl_3$:MeOH); ^{1}H NMR (500 MHz, $CDCl_3$) δ 8.08 (d, 1H, *J* = 7.5 Hz), 8.02 (d, 1H, *J* = 7.5 Hz), 7.84-7.77 (m, 9H), 7.72-7.67 (m, 7H), 7.62 (t, 1H, *J* = 7.5 Hz), 3.74-3.70 (m, 2H), 2.55 (t, 2H, *J* = 7.5 Hz), 1.62-1.58 (m, 4H), 1.50-1.46 (m, 2H), 1.31-1.19 (m, 10H); ^{13}C NMR (125 MHz, $CDCl_3$) δ 184.8, 181.4, 153.2, 135.0, 134.8, 133.8, 133.7, 133.0, 132.9, 130.67, 130.5, 129.6, 126.7, 126.1, 124.8 118.8, 118.2, 30.4, 30.3, 29.6, 29.3, 29.2, 29.1, 29.1, 28.2, 23.3, 22.6.

(10-(3-Hydroxy-1,4-dioxo-1,4-dihydronaphthalen-2-yl)decyl)tributylphosphonium bromide (27b): orange red oil; TLC (SiO_2) R_f 0.23 (9:1 $CHCl_3$:MeOH); ^{1}H NMR (500 MHz, $CDCl_3$) δ 8.81 (d, 1H, *J* = 7.5 Hz), 8.07 (d, 1H, *J* = 7.5 Hz), 7.75 (t, 1H, *J* = 7.5 Hz), 7.67 (t, 1H, *J* = 7.5 Hz), 2.59 (t, 2H, *J* = 8.0 Hz), 2.44-2.33 (m, 10H), 1.53-1.35 (m, 22H), 1.27-1.19 (m, 18H), 0.97-0.93 (12H); ^{13}C NMR (125 MHz, $CDCl_3$) δ 184.8, 150.0, 134.8, 133.0, 132.9, 129.6, 126.7, 126.1, 124.7, 32.2?, 32.0?, 30.8, 30.7, 29. 7, 29.29, 29.27, 29.22, 28.9, 28.2, 26.4, 24.1, 24.0, 23.9, 23.8, 23.4, 22.0, 19.6, 19.4, 19.2, 19.0, 14.2, 13.5

(10-(3-Hydroxy-1,4-dioxo-1,4-dihydronaphthalen-2-yl)decyl)tribenzylphosphonium bromide (27c): orange red oil; TLC (SiO_2) R_f 0.22 (9:1 $CHCl_3$:MeOH); ^{1}H NMR (500 MHz, $CDCl_3$) δ 8.10 (d, 2H, *J* = 7.0 Hz), 8.07 (d, 2H, *J* = 7.0 Hz), 7.35-7.27 (m, 15H), 4.18 (d, 6H, *J* = 15.0 Hz), 2.61-2.58 (m, 2H), 1.99-1.95 (m, 2H), 1.55-1.51 (m, 2H), 1.37-

1.31 (m, 2H), 1.28-1.21 (m, 10H); ^{13}C NMR (125 MHz, $CDCl_3$) δ 185.4, 185.3, 165.5, 161.8, 134.9, 132.9, 130.3, 129.6, 128.6, 128.0, 127.9, 126.7, 126.1, 124.7, 103.3, 30.8, 29.6, 29.2, 29.0, 28.7, 28.2, 26.5, 23.3, 21.6

Deprotection of acetyl group: phosphonium bromide **30** was added into a mixture of 5N of HCl and *i*-PrOH (1:1), the mixture was heated at 65 °C for 12 hours. After that, the solution was cooled down to room temperature and was purified by silica gel chromatography using acetone to elute the nonpolar impurities followed by 10:1 $CHCl_3$:MeOH. The final product was obtained in accordance to product R_f value.

(4-(10-(3-Hydroxy-1,4-dioxo-1,4-dihydronaphthalen-2-yl)-phenyl)bromodecyloxy)triphenylphosphonium bromide (30): Yield: 3**%;** orange red oil; TLC (SiO_2) R_f 0.12 (9:1 $CHCl_3$:MeOH); ^{1}H NMR (500 MHz, $CDCl_3$) δ 8.18 (d, 1H, *J* = 7.5 Hz), 8.13 (d, 1H, *J* = 7.5 Hz), 7.87-7.73 (m, 16H), 7.48 (d, 2H, *J* = 8.0 Hz), 6.96 (d, 2H, *J* = 8.0 Hz), 3.99 (t, 2H, *J* = 5.5 Hz), 1.79-1.75 (m, 2H), 1.69-1.65 (m, 4H), 1.45-1.40 (m, 2H), 1.31-1.23 (m, 10H); ^{13}C NMR (125 MHz, $CDCl_3$) δ 184.1, 181.8, 159.5, 151.9, 150.0, 135.2, 134.3, 134.2, 133.1, 132.9, 132.3, 130.9, 130.8, 129.4, 127.3, 126.1, 122 .0, 121.9, 118.9, 118.2, 114.1, 68.0, 32.6, 31.0, 29.5, 29.4, 29.3, 29.2, 26.0, 22.9.

Preparation of O-alkylated 2-hydroxy-1,4-naphthoquinones 34; general procedure. In 8 mL of dry THF was combined quinone(1 equiv), alkylating agent (2.2 equiv), K_2CO_3 powder (1.1 equiv), and tetrabutylammonium iodide (0.1 equiv). The solution was stirred at 70 ºC for 15 minutes, then was added 18-crown-6 (21 μl, 0.1 equiv). The solution was stirred at that temperature for 2-40 hours. After cooling to room temperature, the reaction mixture was concentrated, redissolved in EtOAc and washed twice with 5% Na_2CO_3. The

aqueous layer was extracted once more with EtOAc, and then, the combined organic layer was dried over $MgSO_4$, filtered, and evaporated. The product **27** was separated by flash chromatography on silica gel using hexanes to elute nonpolar impurities followed by 10-15% EtOAc in hexanes.

2-(4-Chlorobenzyl)-3-(6-bromohexyloxy)naphthalene-1,4-dione (34a): Yield: 29%; yellow oil; TLC (SiO_2) R_f 0.25 (7:1 hexanes:EtOAc); ^{1}H NMR (500 MHz, $CDCl_3$) δ 8.04 (d, 1H, *J* = 6.5 Hz), 8.01 (d, 1H, *J* = 6.5 Hz), 7.70-7.65 (m, 2H), 7.25-7.20 (m, 4H), 4.41 (t, 2H, *J* = 6.0 Hz), 3.90 (s, 2H), 3.41 (t, 2H, *J* = 6.0 Hz), 1.88-1.84 (m, 2H), 1.78-1.75 (m, 2H), 1.49-1.46 (m, 4H); ^{13}C NMR (125 MHz, $CDCl_3$) δ 185.13, 181.92, 157.53, 137.8, 134.1, 133.5, 132.9, 132.1, 131.9, 131.6, 130.5, 128.6, 126.4, 126.3, 73.8, 33.9, 32.7, 30.5, 28.9, 27.9, 25.2.

2-Methyl-3-propoxynaphthalene-1,4-dione (34b): Yield: 37%; yellow oil; TLC (SiO_2) R_f 0.46 (5:1 hexanes:EtOAc); IR (neat) (ν_{max}, cm^{-1}): 1674, 1590, 1563, 1250, 1211, 1044, 1015; ^{1}H NMR (500 MHz, $CDCl_3$) δ 8.08-8.03 (m, 2H), 7.70-7.68 (m, 2H), 4.32 (t, 2H, *J* = 6.5 Hz), 2.12 (s, 3H), 1.80 (sxt, 2H, *J* = 7.0 Hz), 1.04 (t, 3H, *J* = 7.5 Hz); ^{13}C NMR (125 MHz, $CDCl_3$) δ 186.1, 181.6, 157.8, 133.9, 133.4, 132.2, 132.1,131.7, 126.3, 75.5, 24.1, 10.6, 9.6; EI MS (*m*/*z*): 230(M, 38%), 201 (72), 188 (88), 172 (57), 160 (100), 132 (77).

2-Butoxy-3-methylnaphthalene-1,4-dione (34c): Yield: 49%; yellow oil; TLC (SiO_2) R_f 0.50 (9:1 hexanes:EtOAc); IR (neat) (ν_{max}, cm^{-1}): 1670, 1597, 1326, 1265, 1197, 1082; ^{1}H NMR (500 MHz, $CDCl_3$) δ 8.06-8.03 (m, 2H), 7.69-7.68 (m, 2H), 4.35 (t, 2H, *J* = 6.5 Hz), 2.11 (s, 3H), 1.77-1.47 (qnt, 2H, *J* = 7.5 Hz), 1.52-1.47 (sxt, 2H, *J* = 7.5 Hz), 0.98 (t, 3H, *J* = 7.5 Hz); ^{13}C NMR (125 MHz, $CDCl_3$) δ 186.9, 181.4, 157.6, 133.7, 133.2, 132.0,

131.9, 131.5, 126.1, 73.5, 32.6, 19.1, 13.8, 9.4; EI MS (*m*/*z*): 244 (M, 14%), 201 (45), 188 (100), 172 (42), 160 (81), 132 (56).

2-Isopropoxy-3-methylnaphthalene-1,4-dione (34d): Yield: 22%; yellow oil; TLC (SiO_2) R_f 0.47 (5:1 hexanes:EtOAc); IR (neat) (ν_{max}, cm^{-1}): 1669,1597, 1335, 1265, 1200, 1099; ^1H NMR (500 MHz, $CDCl_3$) δ 8.09-8.05 (m, 2H), 7.70-7.69 (m, 2H), 5.00 (qnt, 1H, *J* = 6.0 Hz), 2.12 (s, 3H), 1.37 (s, 3H), 1.34 (s, 3H); ^{13}C NMR (125 MHz, $CDCl_3$) δ 186.1, 181.7, 157.0, 133.9, 133.8, 133.4, 132.3, 131.8, 126.4, 76.5, 23.3, 9.9; EI MS (*m*/*z*): 230 (M, 9%), 188 (100), 172 (9), 132 (42).

2-(3-Bromopropoxy)-3-cyclohexylnaphthalene-1,4-dione (34g): Yield: 114 mg, 82%; bright yellow oil; TLC (SiO_2) R_f 0.50 (9:1 hexanes:EtOAc); IR (neat) (ν_{max}, cm^{-1}): 1668, 1596, 1329, 1292, 1239, 1192; ^1H NMR (500 MHz, $CDCl_3$) δ = 8.06 (d, 1H, *J* = 7.0 Hz), 8.02 (d, 1H, *J* = 7.5 Hz), 7.72-7.66 (m, 2H), 4.39 (t, 2H, *J* = 5.0 Hz), 3.68 (t, 2H, *J* = 5.5 Hz), 3.11 (t, 1H, *J* = 12.0 Hz), 2.39 (t, 2H, *J* = 5.5 Hz), 1.98-1.91 (m, 2H), 1.84-1.82 (m, 2H), 1.73-1.74 (m, 1H), 1.62-1.60 (m, 2H), 1.41-1.25 (m, 5H); ^{13}C NMR (125 MHz, $CDCl_3$) δ = 185.7, 181.9, 157.5, 140.3, 133.9, 133.3, 132.5, 131.5, 126.6, 126.1, 71.2, 36.3, 33.5, 30.3, 29.9, 27.1, 26.2; MS (*m*/z): 376 (M, 46), 378 (45), 255 (100), 187 (43).

2-Benzyl-3-propoxynaphthalene-1,4-dione (34i): Yield: 44%; yellow oil; TLC (SiO_2) R_f 0.67 (7:1 hexanes:EtOAc); IR (neat) (ν_{max}, cm^{-1}): 1670, 1652, 1597, 1331, 1264, 1216; ^1H NMR (500 MHz, $CDCl_3$) δ 8.06 (d, 1H, *J* = 5.5 Hz), 8.02 (d, 1H, *J* = 5.5 Hz), 7.75-7.68 (m, 2H), 7.40-7.16 (m, 5H), 4.37 (t, 2H, *J* = 5.0 Hz), 3.96 (s, 2H), 1.79 (dd, 2H, *J* = 13.0, 7.0 Hz), 1.04-1.02 (t, 3H, *J* = 7.0 Hz); ^{13}C NMR (125 MHz, $CDCl_3$) δ 185.4, 182.2, 157.6, 139.4, 134.0, 133.7, 133.4, 132.1, 131.7, 129.3, 128.6, 126.5, 126.3, 75.6, 29.6, 24.1, 10.6; EI MS (*m*/*z*): 306 (M, 78%), 263 (100), 247 (52).

2-((6-Bromohexyl)oxy)-3-cyclohexylnaphthalene-1,4-dione (34h): Yield: 50 mg, 72%; yellow oil; TLC (SiO_2) R_f 0.34 (19:1 hexanes:EtOAc); IR (neat) (ν_{max}, cm^{-1}): 1668, 1596, 1267, 1196; ^1H NMR (500 MHz, $CDCl_3$) δ 8.05 (d, 1H, *J* = 7.0 Hz), 8.00 (d, 1H, *J* = 6.5 Hz), 4.28-4.27 (m, 2H), 3.45-3.43 (m, 2H), 3.12 (t, 1H, *J* = 12.5 Hz), 2.00-1.55 (m, 14H), 1.37-1.26 (m, 4H); ^{13}C NMR (125 MHz, $CDCl_3$) δ 185.7, 182.2, 158.0, 139.7, 133.9, 133.2, 132.6, 131.6, 126.5, 126.0, 73.8, 36.2, 34.0, 32.9, 30.3, 30.2, 28.1, 27.1, 26.3, 25.3; MS (*m*/z): 420 (M + 2, 13), 418 (M, 13), 256 (100).

2-Benzyl-3-((6-bromohexyl)oxy)naphthalene-1,4-dione (34j): Yield: 46 mg, 57%; yellow oil; TLC (SiO_2) R_f 0.47 (9:1 hexanes:EtOAc); IR (neat) (ν_{max}, cm^{-1}): 1669, 1597, 1217; ^1H NMR (500 MHz, $CDCl_3$) δ 8.06 (d, 1H, *J* = 6.5 Hz), 8.02 (d, 1H, , *J* = 6.5 Hz), 7.68-7.67 (m, 2H), 7.32-7.31 (m, 2H), 7.26-7.24 (m, 2H), 7.18-7.16 (m, 1H), 4.38 (t, 2H, *J* = 6.5 Hz), 3.95 (s, 2H), 3.41 (t, 2H, *J* = 6.5 Hz), 1.87 (t, 2H, *J* = 6.5 Hz), 1.77 (t, 2H, *J* = 6.5 Hz), 1.48 (m, 4H); ^{13}C NMR (125 MHz, $CDCl_3$) δ 185.3, 182.0, 157.6, 139.4, 134.0, 133.8, 133.4, 132.1, 131.7, 129.2, 128.6, 126.5, 126.3, 73.8, 33.9, 32.8, 30.5, 29.6, 28.0, 25.2; MS (*m*/z): 428 (M + 2, 4), 426 (M, 4), 263 (40), 247 (10).

2-(3-Bromopropoxy)-3-chloronaphthalene-1,4-dione (34k): Yield: 56%; yellow solid, mp 58-60 °C; TLC (SiO_2) R_f 0.49 (5:1 hexanes:EtOAc); IR (neat) (ν_{max}, cm^{-1}): 1673, 1590, 1563, 1312, 1250, 1211, 1140; ^1H NMR (500 MHz, $CDCl_3$) δ 8.15 (dd, 1H, *J* = 4.5, 3.0 Hz), 8.08 (dd, 1H, *J* = 5.0, 2.5 Hz), 7.77-7.75 (m, 2H), 4.71 (dt, 2H, *J* = 7.0, 1.5 Hz), 3.69 (t, 2H, *J* = 6.5 Hz), 2.47 (qnt, 2H, *J* = 6.0 Hz); ^{13}C NMR (125 MHz, $CDCl_3$) δ 179.8, 178.7, 156.5, 134.6, 134.2, 131.3, 130.9, 129.5, 127.2, 127.1, 72.2, 33.4, 29.7; EI MS (*m*/z): 250 (M - 79, 1%), 207 (100).

2-(6-Bromohexyloxy)-3-chloronaphthalene-1,4-dione (34l): Yield: 59%; yellow solid,

mp 36-38 °C; TLC (SiO_2) R_f 0.44 (5:1 hexanes:EtOAc); IR (neat) (ν_{max}, cm^{-1}): 1672, 1655, 1590, 1560, 1311, 1252, 1206 ; ^1H NMR (500 MHz, $CDCl_3$) δ 8.10 (m, 1H), 8.04 (m, 1H), 7.74 (m, 2H), 4.57 (t, 2H, *J* = 4.5 Hz), 3.43 (t, 2H, *J* = 6.5 Hz), 1.90 (m, 2H), 1.83 (m, 2H), 1354 (m, 4H); ^{13}C NMR (125 MHz, $CDCl_3$) δ 179.8, 178.6, 156.7, 134.4, 133.9, 131.1, 130.8, 129.0, 127.0, 126.9, 74.7, 33.9, 32.7, 30.3, 27.8, 25.0; EI MS (*m*/*z*): 221 (M - 149, 49%), 133 (100).

2-Propoxynaphthalene-1,4-dione (34m): Yield: 20%; yellow solid, mp 80-81 °C; TLC (SiO_2) R_f 0.33 (5:1 hexanes:EtOAc); IR (neat) (ν_{max}, cm^{-1}) 1655, 1604, 1248, 1016; ^1H NMR (500 MHz, $CDCl_3$) δ 8.13 (d, 1H, *J* = 7.5 Hz), 8.08 (d, 1H, *J* = 7.5 Hz), 7.76-7.70 (m, 2H), 6.16 (s, 1H), 3.98 (t, 2H, *J* = 5.5 Hz), 1.94 (dd, 2H, *J* = 13.0, 7.0 Hz), 1.08 (t, 3H, *J* = 5.5 Hz); ^{13}C NMR (125 MHz, $CDCl_3$) δ 185.3, 180.4, 160.1, 134.4, 133.5, 132.2, 131.4, 126.9, 126.3, 110.4, 71.2, 21.9, 10.6; EI MS (*m*/*z*): 216 (M, 48%), 187 (32), 173 (23), 158 (52).

Preparation of naphthoquinones 31; general procedure. The compounds were made without adding TBAI. In 8 mL of dry THF was combined quinone (1.0 mmol, 1 equiv), alkylating agent (1.5 equiv), K_2CO_3 powder (1.1 equiv) and 18-crown-6 (0.1 equiv). The solution was stirred at 70 ºC for 2-40 hours. After cooling to room temperature, the reaction mixture was concentrated, redissolved in EtOAc and washed twice with 5% Na_2CO_3. The aqueous layer was extracted once with EtOAc, and then, the combined organic layer was dried over $MgSO_4$, filtered, and evaporated. The product **27** was separated by flash chromatography on silica gel using hexanes to elute nonpolar impurities followed by 10-15% EtOAc in hexanes.

2-(3-Bromopropoxy)naphthalene-1,4-dione (**31b**): Yield: 20 mg, 12%; yellow solid, mp 102-104 °C; TLC (SiO_2) R_f 0.22 (5:1 hexanes:EtOAc); ^{1}H NMR (500 MHz, $CDCl_3$) δ 8.12 (d, 1H, *J* = 7.0 Hz), 8.08 (d, 1H, *J* = 7.0 Hz), 7.77-7.72 (m, 2H), 4.17 (t, 2H, *J* = 5.0 Hz), 3.63 (t, *J* = 5.5 Hz), 2.49-2.43 (m, 2H); ^{13}C NMR (125 MHz, $CDCl_3$) δ 185.0, 180.6, 159.6, 134.5, 133.5, 132.1, 131.3, 126.8, 126.4, 110.7, 110.6, 66.9, 31.4, 29.5.

2-(6-Bromohexyloxy)naphthalene-1,4-dione (**31a**): Yield: 38 mg, 20%; yellow oil; TLC (SiO_2) R_f 0.60 (5:1 hexanes:EtOAc); ^{1}H NMR (500 MHz, $CDCl_3$) δ 8.12 (d, 1H, *J* = 7.0 Hz), 8.07 (d, 1H, *J* = 7.0 Hz), 7.74-7.71 (m, 2H), 4.01 (t, 2H, *J* = 6.5 Hz), 3.44-3.42 (m, 2H), 1.92-1.91 (m, 4H), 1.53 (s, 4H); ^{13}C NMR (125 MHz, $CDCl_3$) δ 185.2, 180.3, 159.9, 134.4, 133.5, 132.2, 131.3, 126.8, 126.3, 110.4, 69.6, 33.8, 32.7, 28.3, 27.9, 25.3.

2-(4-(Bromomethyl)benzyloxy)naphthalene-1,4-dione (**31c**): Yield: 65 mg, 31%; yellow solid, mp 151-153 °C; TLC (SiO_2) R_f 0.27 (5:1 hexanes:EtOAc); ^{1}H NMR (500 MHz, $CDCl_3$) δ 8.14 (d, 1H, *J* = 7.0 Hz), 8.07 (d, 1H, *J* = 7.0 Hz), 7.76-7.70 (m, 2H), 7.43 (m, 4H), 6.21 (s, 1H), 5.12 (s, 2H), 4.49 (s, 2H); ^{13}C NMR (125 MHz, $CDCl_3$) δ 185.1, 180.2, 159.4, 138.6, 137.6, 134.5, 133.6, 132.1, 131.3, 129.4, 128.2, 126.9, 126.4, 111.4, 70.8, 32.9.

2-(3-Bromopropoxy)-3-(4-chlorobenzyl)naphthalene-1,4-dione (**31e**): Yield: 66mg, 47%; yellow oil; TLC (SiO_2) R_f 0.45 (9:1 hexanes:EtOAc); ^{1}H NMR (500 MHz, $CDCl_3$) δ 8.05-8.02 (m, 2H), 7.67 (m, 2H), 7.23 (m, 4H), 4.53 (m, 2H), 3.90 (m, 2H), 3.55 (m, 2H), 3.32 (t, 2H, *J* = 7.0 Hz); ^{13}C NMR (125 MHz, $CDCl_3$) δ 185.1, 181.7, 157.1, 137.6, 134.2, 133.6, 133.3, 132.3, 131.8, 131.5, 130.4, 128.8, 126.5, 126.4, 71.4, 33.5, 29.7, 29.0.

Preparation of 2-O-alkylated naphthoquinones phosphonium bromide 32a-b, 35, 40-47; general procedure. Triphenylphosphine (1 equiv) and naphthoquinone (**31**, **34**) were combined in a 5 mL conical-shaped tube and reacted under conventional heating method. After cooling to room temperature, the phosphonium salt product was directly separated by flash chromatography on silica gel using acetone to elute nonpolar impurities followed by 9:1 DCM:MeOH.

10-(2-Oxy-3-methylnaphthalene-1,4-dione)decyl triphenylphosphonium bromide (40): Yield: 3%; orange oil**;** TLC (SiO_2) R_f 0.30 (9:1 DCM:MeOH); ^{1}H NMR (500 MHz, $CDCl_3$) δ 8.06-8.04 (m, 2H), 7.86-7.71 (m, 17H), 4.33-4.31 (m, 2H), 3.74 (m, 2H), 2.09 (s, 3H), 1.82-1.22 (m, 16H); ^{13}C NMR (125 MHz, $CDCl_3$) δ 185.7, 185.5, 181.6, 157.7, 150.6, 135.2, 133.9, 133.8, 133.4, 132.1, 131.7, 130.7, 130.6, 126.3, 118.9, 118.3, 81.5, 73.9, 48.7, 34.3, 30.6, 29.6, 29.4, 29.3, 28.8, 28.2, 25.9, 22.8, 9.6.

3-(2-Oxy-3-(4-chlorobenzyl)naphthalene-1,4-dione)propyl triphenylphosphonium bromide (35): Yield: 5.5 mg, 10%; green oil; TLC (SiO_2) R_f 0.32 (9:1 DCM:MeOH); ^{1}H NMR (500 MHz, $CDCl_3$) δ 8.04-8.02 (m, 1H), 7.97-7.96 (m, 1H), 7.80-7.70 (m, 17H), 7.18 (d, 2H, *J* = 5.5 Hz), 7.06 (d, 2H, *J* = 5.5 Hz), 4.01-3.62 (m, 7H), 2.20-1.93 (m, 2H); ^{13}C NMR (125 MHz, $CDCl_3$) δ 184.9, 181.5, 157.0, 137.5, 135.2, 135.1, 134.1, 133.8, 133.7, 133.68, 133.65, 133.2, 131.9, 131.7, 131.4, 130.7, 130.6, 130.5, 130.2, 128.5, 126.4, 126.3, 118.6, 118.3, 117.9, 117.7, 71.9, 53.7, 53.6, 28.9, 23.9, 23.2, 22.8, 22.2.

6-(2-Oxy-3-benzylnaphthalene-1,4-dione)hexyl triphenylphosphonium bromide (41): Yield: 44 mg, 62%; orange oil; TLC (SiO_2) R_f 0.31 (9:1 DCM:MeOH); ^{1}H NMR (500 MHz, $CDCl_3$) δ 8.03-8.02 (m, 1H), 7.98-7.97 (m, 1H), 7.85-7.79 (m, 9H), 7.70 (m, 8H), 7.26 (m, 2H), 7.18 (m, 2H), 7.08 (m, 1H), 4.30(m, 2H), 3.89 (s, 2H), 3.77 (m, 2H),

1.72-1.65 (m, 6H), 1.45 (m, 2H); ^{13}C NMR (125 MHz, $CDCl_3$) δ 185.2, 181.8, 157.4, 139.2, 135.1, 133.9, 133.7, 133.7, 133.4, 131.8, 131.5, 130.6, 130.5, 129.0 ,128.4, 126.3, 126.2, 118.6, 117.9, 77.4, 73.6, 30.1, 30.0, 29.7, 29.4, 25.5, 22.7.

3-(2-Oxy-3-benzylnaphthalene-1,4-dione)propyl triphenylphosphonium bromide (42): Yield: 7.4 mg, 78%; yellow oil; TLC (SiO_2) R_f 0.32 (9:1 DCM:MeOH); ^{1}H NMR (500 MHz, $CDCl_3$) δ 8.05 (d, 1H, *J* = 7.0 Hz), 7.96 (d, 1H, *J* = 7.0 Hz), 7.87-7.81 (m, 3H), 7.79-7.75 (m, 7H), 7.71-7.66 (m, 7H), 7.21 (d, 2H, *J* = 7.0 Hz), 7.09 (t, 2H, *J* = 7.0 Hz), 6.99 (t, 1H, *J* = 7.0 Hz), 4.69 (m, 2H), 4.08-4.05 (m, 2H), 3.93 (s, 2H), 1.19-1.18 (m, 2H); ^{13}C NMR (125 MHz, $CDCl_3$) δ 185.1, 181.7, 157.1, 146.7, 139.0, 135.2, 134.2, 133.9, 133.8, 133.7, 133.5, 131.9, 131.6, 130.7, 130.6, 128.8, 128.6, 126.6, 126.4, 118.6, 117.9, 72.5, 48.7, 29.6, 24.1, 23.4, 23.1.

6-(2-Oxy-3-cyclohexylnaphthalene-1,4-dione)hexyl triphenylphosphonium bromide (43): Yield: 3%; red oil; TLC (SiO_2) R_f 0.42 (9:1 DCM:MeOH); ^{1}H NMR (500 MHz, $CDCl_3$) δ 8.03 (d, 1H, *J* = 7.0 Hz), 7.97 (d, 1H, *J* = 7.0 Hz), 7.88-7.78 (m, 9H), 7.72-7.64 (m, 8H), 4.18 (t, 2H, *J* = 6.0 Hz), 3.89-3.83 (m, 2H), 3.05 (t, 1H, *J* = 12.5 Hz), 1.94-1.86 (m, 4H), 1.79-1.74 (m, 6H), 1.71-1.68 (m, 4H), 1.55-1.52 (m, 4H), 1.33-1.26 (m, 2H); ^{13}C NMR (125 MHz, $CDCl_3$) δ 185.7, 185.5, 185.4, 182.1, 166.0, 157.9, 150.1, 139.8, 135.2, 133.9, 133.8, 133.2, 132.5, 131.6, 130.7, 130.6, 126.5, 125.9, 118.9, 118.2, 110.1, 73.8, 36.2, 30.2, 30.0, 27.0, 26.2, 25.7, 22.9.

3-(2-Oxy-3-cyclohexylnaphthalene-1,4-dione)propyl triphenylphosphonium bromide (44): Yield: 32 mg, 68%; yellow oil; TLC (SiO_2) R_f 0.33 (9:1 DCM:MeOH); ^{1}H NMR (500 MHz, $CDCl_3$) δ 8.02 (d, 1H, *J* = 7.0 Hz), 7.75 (d, 1H, *J* = 7.0 Hz), 7.92-7.87 (m, 5H), 7.82-7.80 (m, 4H), 7.74- 7.68 (m, 8H), 4.44 (m, 2H), 4.16-4.10 (m, 2H), 3.00 (t, 1H,

J = 11.0 Hz), 1.85 (q, 2H, *J* = 12.5 Hz), 1.75 (d, 2H, *J* = 12.5 Hz), 1.67 (d, 1H, *J* = 12.0 Hz), 1.56 (d, 2H, *J* = 12.0 Hz), 1.30-1.22 (m, 3H), 1.19-1.18 (m, 2H); ^{13}C NMR (125 MHz, $CDCl_3$) δ 185.6, 181.2, 157.3, 140.6, 135.3, 134.1, 134.0, 133.9, 133.8, 133.4, 132.5, 131.3, 130.8, 130.7, 126.5, 126.1, 118.7, 117.9, 72.9, 72.8, 36.5, 30.4, 26.9, 26.0, 24.0, 23.3, 22.9.

3-(2-Oxynaphthalene-1,4-dione)propyl triphenylphosphonium bromide (32b): Yield: 3%; yellow solid; TLC (SiO_2) R_f 0.61 (9:1 DCM:MeOH); ^{1}H NMR (500 MHz, $CDCl_3$) δ 8.08-8.06 (m, 2H), 7.95-7.91 (m, 5H), 7.81-7.79 (m, 3H), 7.75-7.73 (m, 9H), 6.24 (s, 1H), 4.44 (m, 2H), 4.23 (m, 2H), 2.34 (m, 2H); ^{13}C NMR (125 MHz, $CDCl_3$) δ 184.6, 180.3, 159.1, 150.1, 135.3, 134.6, 134.2, 134.1, 133.4, 132.3, 131.2, 130.9, 130.8, 126.5, 118.7, 117.9, 48.7, 30.1, 22.9.

6-(2-Oxynaphthalene-1,4-dione)hexyl triphenylphosphonium bromide (32a): Yield: 3 mg, 5%; orange oil; TLC (SiO_2) R_f 0.26 (19:1 DCM:MeOH); ^{1}H NMR (500 MHz, $CDCl_3$) δ 8.06 (m, 2H), 7.87-7.80 (m, 10H), 7.72-7.71 (m, 7H), 6.14 (s, 1H), 3.39 (m, 2H), 3.79 (m, 2H), 1.86 (m, 2H), 1.78 (m, 2H), 1.69 (m, 2H), 1.54 (m, 2H); ^{13}C NMR (125 MHz, $CDCl_3$) δ 185.1, 180.4, 159.9, 150.1, 135.2, 134.4, 133.9, 133.8, 133.4, 132.2, 131.2, 130.7, 130.6, 126.7, 126.3, 118.8, 118.1, 110.5, 110.4, 69.6, 31.1, 30.0, 29.8, 27.9, 25.6, 22.6.

3-(2-Oxy-3-(4-methoxyphenyl)naphthalene-1,4-dione)propyl triphenylphosphonium bromide (47): Yield: 3%; red oil; TLC (SiO_2) R_f 0.31 (9:1 DCM:MeOH); ^{1}H NMR (500 MHz, $CDCl_3$) δ 8.09-8.05 (m, 2H), 7.79-7.68 (m, 17H), 7.32 (d, 2H, *J* = 6.5 Hz), 6.81 (d, 2H, *J* = 6.5 Hz), 4.48 (s, 2H), 3.74 (s, 2H), 3.67 (s, 3H), 1.98 (s, 2H); ^{13}C NMR (125 MHz, $CDCl_3$) δ 184.9, 182.0, 159.8, 156.2, 135.2, 134.4, 134.2, 133.9, 133.8, 133.7,

133.6, 132.6, 132.3, 132.0, 131.5, 130.6, 130.5, 126.8, 126.3, 122.9, 118.5, 118.4, 117.9, 113.7, 72.9, 72.8, 55.4, 23.9.

CHAPTER 5

CONCLUSIONS

Conventionally, alkene formation under elimination conditions often requires harsh temperatures that can cause decomposition of the product. A new method to introduce alkenes under mild toluene reflux, which might be suitable to be used in the medicinal chemistry lab to build complex structures, has been described in Chapter 2. Several phenyl sulfoxides **1a-n** were prepared and the chemistry of the precursors was investigated. A typical procedure includes the addition of NaOAc which can absorb the sulfenic acid **5** during the toluene reflux. Confirmed by ^{1}H NMR, the alkene product was obtained with high purity before performing further chromatography purification. It was found that the effects of nitro group proved to be essential for the reaction, and the optical precursor is the *o*-nitro phenyl sulfoxide. The *o*-nitro phenyl sulfoxide precursor can be used as effective precursors to introduce unsaturated bond into the structure of interest.

The use of sulfur chemistry in synthetic transformation is further examined in Chapter 3. A new method to synthesize β-lactams, using photochemistry as one of the key steps in the final stages of the synthetic sequence, was developed. The procedure that has been developed utilizes thiazolidines hydroxamate ester anions that can be readily cyclized to the lactams. The introduction of hydroxyl group at the C-5 position by photooxidation (key step in the synthetic sequence) enables this unique approach to construct highly functionalized, chiral β-lactams that can be employed as platforms in antimicrobial drug discovery.

A specific example of the utilization of platforms for hit-to-lead generation studies of antimicrobials is described in Chapter 4. The chemical modification of phthalimide and 1,4-naphthoquinone to design novel mitochondrion-acting antiparasitic agents was performed. The central hypothesis of this project is the selectively delivering strategy based on triphenyl phosphonium may facilitate passive transport of the lipophilic cations across the plasma membranes, and further penetrate into the negatively-charged parasite mitochondrion membrane.

The compounds were evaluated for antiparasitic activity and these results are presented in Chapter 4. Calculation of Log *D* values and percent hemolysis values of lead compounds was lastly performed as standard preclinical analyses of experimental therapies.

REFERENCES

CHAPTER 2

[1] Granit, R. *Annu. Rev. Physiol.* **1950**, *12*, 485.

[2] Olson, R. E. *J. Nutr.* **1998**, *128*, 439S.

[3] Mascaretti, A. S. *Am. Soc. Microb.* **2003**, 144.

[4] (a) Rai, R.; Katzenellenbogen, J. A. *J. Med. Chem.* **1992**, *35*, 4150. (b) Reed, P. E.; Katzenellenbogen, J. A. *J. Biol. Chem.* **1991**, *266*, 13. (c) Sofia, M. J.; Katzenellenbogen, J. A. *J. Med. Chem.* **1986**, *29*, 230. (d) Daniels, S. B.; Katzenellenbogen, J. A. *Biochemistry* **1986**, *25*, 1436. (e) Daniels, S. B.; Cooney, E.; Sofia, M. J.; Chakravarty, P. K.; Katzenellenbogen, J. A. *J. Biol. Chem.* **1983**, *258*, 15046. (f) Chakravarty, P. K.; Krafft, G. A.; Katzenellenbogen, J. A. *J. Biol Chem.* **1982**, *257*, 610. (g) Krafft, G. A.; Katzenellenbogen, J. A. *J. Am. Chem. Soc.* **1981**, *103*, 5459. (h) Rando, R. R. *Science* **1974**, *185*, 320.

[5] Ren, J.; Milton, J.; Weaver, K. L.; Short, S. A.; Stuart, D. I.; Stammers, D. K. *Structure* **2000**, *8*, 1089.

[6] Farbera, P. M.; Arscottb, L. D.; Williams C. H. Jr.; Beckera, K.; Schirmera, R. H. *FEBS Lett.* **1998**, *422*, 311.

[7] Wang, X.; Zhang, J.; Huang, Y.; Wang, R.; Zhang, L.; Qiao, K.; Li, L.; Liu, C.; Ouyang, Y.; Xu, W.; Zhang, Z.; Zhang, L.; Shao, Y.; Jiang, S.; Ma, L.; Liu, J. *J. Med. Chem.* **2012**, *55*, 2242.

[8] Whitehouse, M. W.; Skidmore, I. F. *J. Pharm. Pharmac.* **1965**, *17*, 668.

[9] Wong, C. S. *Clin. Microbiol. Newsl.* **1988**, *10*, 177.

[10] Wade, L. G. *Organic* Chemistry (Prentice Hall, 6th edition)

[11] Carey, F. A.; Sundberg, R. J. *Advanced Organic Chemistry: Structure and Mechanisms* (Springer, 5th edition)

[12] Saytzeff, A. *Liebigs Ann. der Chemie* **1875**, *179*, 296.

[13] von E. Doering, W.; Hoffmann, A. K. *J. Am. Chem. Soc.* **1954**, *76*, 6162.

[14] (a) Cope, A. C.; Foster, T. T.; Towle, P. H. *J. Am. Chem. Soc.* **1949**, *71*, 3929. (b) DePuy, C. H.; King, R. W. *Chem. Rev* . **1960**, *60*, 431. (c) Hofmann, A. W. *Ber. Dtsch. Chem. Ges.* **1881**, *14*, 494. (d) Hofmann, A. W. *Ber. Dtsch. Chem. Ges.* **1881**, *14*, 659. (e) Cope, A. C.; Trumbell, E. R. *Org. React.* **1960**, *11*, 317. (f) Bamford, W. R.; Stevens, T. S. *J. Chem. Soc*. **1952**, 4735. (g) Shapiro, R. H. *Org. React.* **1976**, *23*, 405. (h) Adlington, R. M.; Barrett, A. G. M. *Acc. Chem. Res.* **1983**, *16*, 55. (i) Chugaev, L. *Ber. Dtsch. Chem. Ges.* **1899**, *32*, 3332. (j) Nace, H. R. *Org. React.* **1962**, *12*, 57. (k) Grieco, P. A.; Sydney, G.; Mugio, N. *J. Org. Chem.* **1976**, *41*, 1485. (l) Sharpless, K. B.; Young, M. W. *J. Org. Chem.* **1975**, *40*, 947. (m) Field, L. *Synthesis* **1972**, 101.

[15] Komaromi, I.; Tronchet , J. M. J. *J. Phys. Chem.* **1997**, *101*, 3554.

[16] Tschugaeff, L. *Ber. Dtsch. Chem. Ges.* **1900**, *33*, 3118.

[17] Cope, C.; Trumbull, E. R. *Org. React.* **1960**, *11*, 317.

[18] Holton, R. A.; Kim, H. B.; Somoza, C.; Liang, F.; Biediger, R.J.; Boatman, P. D.; Shindo, M.; Smith, C. C.; Kim, S. *J. Am. Chem. Soc.* **1994**, *116*, 1599.

[19] Sharpless, K. B.; Young, M. W. *J. Org. Chem.* **1975**, *40*, 947.

[20] "Dietary Supplement Fact Sheet: Selenium". National Institutes of Health **2009**

[21] (a) Field, L. *Synthesis* **1972**, 101. (b) Field, L. *Synthesis* **1978**, 713. (c) Trost, B. M.; Salzman, T. N.; Hiroi, K. *J. Am. Chem. Soc.* **1976**, *98*, 4887. (d) Trost, B. M. *Acc. Chem. Res.* **1978**, *11*, 453. (e) Trost, B. M. *Chem. Rev.* **1978**, *78*, 363. (f) Moghaddam, F. M.; Ghaffarzadeh, M. *Tetrahedron Lett.* **1996**, *37*, 1855. (g) Mash, E. A.; Gregg, T. M. *J. Org. Chem.* **1995**, *60*, 6180.

[22] Sayama, S.; Onami, O. *Tetrahedron Lett.* **2000**, *41*, 5557.

[23] Patel, S. K.; Long, T. E. *Tetrahedron Lett.* **2009**, *50*, 5067.

[24] Burns, J. A.; Butler, J. V.; Moran, J.; Whitesides, G. M. *J. Org. Chem.* **1991**, *56*, 2648.

[25] Dmitrenko, O.; Thorpe, C.; Bach, R. D. *J. Org. Chem.* **2007**, *72*, 8298.

[26] Lu, X.; Long, T. E. *J. Org. Chem.* **2010**, *75*, 249.

[27] Finkelstein, H. *Ber. Dtsch. Chem. Ges.* **1910**, *43*, 1528.

[28] Ishibashi, H.; Komatsu, H.; Ikeda, M. *J. Chem. Res.* **1987**, 296.

[29] (a) Sun, B.; Zhang, X. L.; Yonz, C.; Cummings, B. S. *Biochem. Pharmacol.* **2010**, *79*, 1727. (b) Sun, B.; Zhang, X.; Talathi, S.; Cummings, B. S. *J. Pharmacol. Exp. Ther.* **2008**, *326*, 59.

[30] Mock, J. N.; Taliaferro, J. P.; Lu, X.; Patel, S. K.; Cummings, B. S.; Long, T. E. *Bioorg. Med. Chem. Lett.* **2012**, *22*, 4854.

[31] Daniels, S. B.; Cooney, E.; Sofia, M. J.; Chakravarty, P. K.; Katzenellenbogen, J. A. *J. Biol. Chem.* **1983,** *258*, 15046.

[32] Krafft, G. A.; Katzenellenbogen, J. A. *J. Am. Chem. Soc.* **1981**, *103*, 5459.

[33] Roydhouse, M. D.; Walton, J. C. *Eur. J. Med. Chem.* **2007**, *27*, 1059.

[34] Dai, W.; Katzenellenbogen, J. A. *J. Org. Chem.* **1991**, *56*, 6893.

[35] (a) Ribaldone, G.; Borsotti, G. German Patent, **1973**, 2,323,543. (b) *Chem. Abstr.* **1974**, *80*, 61068b.

[36] Rewcastle, G. W.; Atwell, G. J.; Palmer, B. D.; Boyd, P. D. W.; Baguley, B. C.; Denny, W. A. *J. Med. Chem.* **1991**, *34*, 491.

[37] Newman, M.S.; Otsuka. S. *J. Org. Chem.* **1958**, *23*, 797.

[38] Wagner, H.; Bladt, S. *Plant Drug Analysis: A Thin Layer Chromatography Atlas* (Springer, 2nd edition)

[39] Rai, R.; Katzenellenbogen, J. A. *J. Med. Chem.* **1992**, *35*, 4297.

[40] Zupan, L. A.; Weiss, R. H.; Hazen, S. L.; Parnas, B. L.; Aston, K. W.; Lennon, P. J.; Getman, D. P.; Gross, R. W. *J. Med. Chem.* **1993**, *36*, 95.

[41] Kita, M.; Kitamura, M.; Koyama, T.; Teruya, T.; Matsumoto, H.; Nakano, Y.; Uemura, D. *Tetrahedron Lett.* **2005**, *46*, 8583.

[42] Seiser, T.; Kamena, F.; Cramer, N. *Angew. Chem. Int. Edit.* **2008**, *47*, 6483.

CHAPTER 3

[1] Pankey, G. A.; Sabath, L. D. *Clin. Infect. Dis.* **2004**, *38*, 864.

[2] Waxman, D. J.; Strominger, L. J. *Annu. Rev. Biochem.* **1983**, *52*, 825.

[3] Day, L. E. *J. Bacteriol.* **1966**, *91*, 1917.

[4] Hooper, D. C. *Clin. Infect. Dis.* **2000**, *31*, S24.

[5] Tomasz, A. *Annu. Rev. Microbiol.* **1979**, *33*, 113.

[6] Popescu, S.; Doyle. R. J. *Biotech. Histochem.* **1996**, *71*, 145.

[7] Brown, D. F.; Reynolds, P. E. *FEBS Lett.* **1980**, *122*, 275.

[8] Simpson, I. N.; Harper, P. B.; O'Callaghan, C. H. *Antimicrob. Agents Chemother.* **1980**, *17*, 929.

[9] Vaudaux, P.; Waldvogel F. A. *J. Infect. Dis.* **1979**, *139*, 547.

[10] Flemming, A. *Br. Med. Bull.* **1944**, *2*, 4.

[11] Sheehan, J. C.; Henery-Logan, K. R. *J. Am. Chem. Soc.* **1957**, *79*, 1262.

[12] (a) Svedas, V. K.; Margolin, A. L.; Berezin, I. V. *Enz. Microb. Tech.* **1980**, *2*, 138. (b) Hatanaka, M.; Ishimaru T. *J. Med. Chem.* **1973**, *16*, 978.

[13] Durham, T. B.; Miller, M. J. *Org. Lett.* **2002**, *4*, 135.

[14] Lu, X.; Long, T. E. *Tetrahedron Lett.* **2011**, *52*, 5051.

[15] (a) Iwakawa, M.; Pinto, B. M.; Szarek, W. A. *Can. J. Chem*. **1978**, *56*, 329. (b) Sheehan, J. C.; Yang, D. H. *J. Am. Chem. Soc.* **1958**, *80*, 1158. (c) Suaifan, G. A. R.; Mahon, M. F.; Arafat, T.; Threadgill, M. D. *Tetrahedron* **2006**, *62*, 11245.

[16] (a) Shepherd, A.; Miller, M. J. *J. Chem. Soc., Perkin Trans. 1* **1990**, 2519; (b) Shin, I.; Park, K. *Org. Lett.* **2002**, *4*, 869. (c) Lee, H. S.; Kim, D. H. *Bull. Korean Chem. Soc.* **2002**, *23*, 593.

[17] Hanessian, S.; Bayrakdarian, M. *Tetrahedron Lett.* **2002**, *43*, 967.

[18] King, J. A.; McMillan, F. H. *J. Am. Chem. Soc.* **1951**, *73*, 4911.

[19] Falborg, L.; Jørgensen, K. A. *J. Chem. Soc., Perkin Trans. 1* **1996**, 2823.

[20] English, A. R.; Girard, D.; Jasys, V. J.; Martingano, R. J.; Kellogg, M. S. *J. Med. Chem.* **1990**, *33*, 344.

[21] Neya, M.; Hagiwara, D.; Miyazaki, Y.; Nakamura, T.; Hemmi, K.; Hashimoto, M. *J. Chem. Soc. Perkin Trans. 1* **1989**, 2187.

[22] (a) Dong, Y.; Tang, Y.; Chollet, J.; Matile, H.; Wittlin, S.; Charman, S. A.; Charman, W. N.; Tomas, J. S.; Scheurer, C.; Snyder, C.; Scorneaux, B.; Bajpai, S.; Alexander, S. A.; Wang, X.; Padmanilayam, M.; Cheruku, S. R.; Brun, R.; Vennerstrom, J. L. *Bioorg. Med. Chem.* **2006**, *14*, 6368. (b) Miller, M. J.; Zhao, G.; Vakulenko, S.; Franzblau, S.; Mollmann, U. *Org. Biol. Chem.* **2006**, *4*, 4178.

[23] Han S.; Kim, Y. *Tetrahedron* **2004**, *60*, 2447.

[24] (a)Sparks, S. M.; Chow, C. P.; Zhu, L.; Shea, K. J. *J. Org. Chem.* **2004**, *69*, 3025. (b) Falck, J. R.; Kumar, P. S.; Reddy, Y. K.; Zou, G.; Capdevila, J. H. *Tetrahedron Lett.* **2001**, *42*, 7211.

[25] (a) Pummerer, R. *Ber.* **1909**, *42*, 2282. (b) Pummerer, R. *Ber.* **1910**, *43*, 1401.

[26] (a) Takata, T.; Tamura, Y.; Ando, W. *Tetrahedron* **1985**, *41*, 2133. (b) Takata, T.; Ishibashi, K.; Ando, W. *Tetrahedron Lett.* **1985**, 26, 4609. (c) Takata, T.; Huang, L.; Ando, W. *Chem. Lett.* **1985**, 1705. (d) Takata, T.; Ando, W. *Tetrahedron Lett.* **1986**, *27*, 1591. (e) Takata, T.; Ando, W. *Bull. Chem. Soc. Jpn.* **1986**, *59*, 1275.

[27] Takata, T.; Hoshino, K.; Takeuchi, E.; Tamura, Y.; Ando, W. *Tetrahedron Lett.* **1984**, *25*, 4767.

[28] Akasaka, T.; Sakurai, A.; Ando, W. *J. Am. Chem. Soc.* **1991**, *113*, 2696.

[29] Thouin, E.; Lubell , W. D. *Tetrahedron Lett.* **2000**, *41*, 457.

[30] (a) Emtenas, H.; Alderin, L.; Almqvist, F. *J Org. Chem.* **2001**, *66*, 6756. (b) Chen, H.; O'Connor, S.; Cane D. E.; Walsh C. T. *Chem. Biol.* **2001**, *8*, 899.

[31] Prat, F.; Foote, C. S. *Photochem. Photobiol.* **1998**, *67*, 626.

[32] (a) Wasserman, H. H.; Adickes, H. W.; Espejo de Ochoa, P. *J. Am. Chem. Soc.* **1971**, *93*, 5586. (b) Koppel, G. A.; McShane, L.; Jose, F.; Cooper, R. D. G. *J. Am. Chem. Soc.* **1978**, 100, 3933.

[33] Maeda, H.; Kikui, T.; Nakatsuji, Y.; Okahara, M. *J. Org. Chem.* **1982**, *47*, 5167.

[34] Dolle, R. E.; Li, C. S.; Novelli, R.; Kruse, L. I.; Eggleston, D. *J. Org. Chem.* **1992**, *57*, 128.

[35] Nakatsuka, S.; Tanino, H.; Kishi, Y. *J. Am. Chem. Soc.* **1975**, *97*, 5008.

[36] Kemp, D. S.; Carey, R. I. *J.Org. Chem.* **1989**, *54*, 3640.

[37] Keck, G. E.; McHardy, S. F.; Wager, T. V. *Tetrahedron Lett.* **1995**, *36*, 7419.

[38] (a) Keck, G. E.; Wager, T. T.; McHardy, S. F. *Tetrahedron* **1999**, *55*, 11755. (b) Nielsen, S. D.; Smith, G.; Begtrup, M.; Kristensen, J. L. *Chem. Eur. J.* **2010**, *16*, 4557.

[39] Sheehan, J. C.; Yang, D. H. *J. Am. Chem. Soc.* **1958**, *80*, 1158.

[40] (a) Woulfe, S. R.; Miller, M. J. *Tetrahedron Lett.* **1984**, *25*, 3293. (b) Woulfe, S. R.; Miller, M. J. *J. Med. Chem.* **1985**, *28*, 1447. (c) Boyd, D. B.; Eigenbrot, C.; Indelicato, J. M.; Miller, M. J.; Pasini, C. E.; Woulfe, S. R. *J. Med. Chem.* **1987**, *30*, 528.

CHAPTER 4

[1] Yamanaka, H; Chiba, T; Kawabata, K; Takasugi, H; Masugi, T; Takaya, T *J. Antibiot. (Tokyo)* **1985**, *38*, 1738.

[2] Deutsch, H. M.; Glinski, J. A.; Hernandez, M.; Haugwitz, R. D.; Narayanan, V. L.; Suffness, M.; Zalkow L. H. *J. Med. Chem.* **1989**, *32*, 788.

[3] Berge, S. M.; Bighley, L. D.; Monkhouse, D. C. *J. Pharm. Sci.* **1977**, *66*, 1.

[4] Snow, R. W.; Guerra, C. A.; Noor, A. M.; Myint, H. Y.; Hay, S. I. *Nature* **2005**, *434*, 214.

[5] Snounou, G.; Viriyakosol, S.; Jarra, W.; Thaithong, S.; Brown, K. N. *Mol. Biochem. Parasitol.* **1993**, *58*, 283.

[6] Vlachou, D.; Schlegelmilch, T.; Runn, E.; Mendes A.; Kafatos, F. C. *Curr. Opin. Genet. Dev.* **2006**, *16*, 384.

[7] Weber, R.; Schlagenhauf, P.; Amsler, L.; Steffen. R. *J. Trav. Med.* **2003**, *10*, 219.

[8] Dockrell, H. M.; de Souza, J. B.; Playfair, J. H. *Immunology* **1980**, *41*, 421.

[9] Guidelines for Treatment of Malaria in the United States, CDC, **2011**.

[10] Backmund, M.; von Zielonka, M.; Hartmann, W. J.; Hesse J.; Eichenlaub, D. *Fortschr. Med.* **1999**, *117*, 24.

[11] Craft, J. C. *Curr. Opin. Microb.* **2008**, *11*, 428.

[12] Clarke, D.H.; Theiler, M. *J. Infect. Dis.* **1948**, *82*, 138.

[13] Hudson, A. T.; Randall, A. W.; Fry, M.; Ginger, C. D.; Hill, B.; Latter, V. S.; McHardy, N.; Williams, R. B. *Parasitology* **1985**, *90*, 45.

[14] DeAngelis, D. V.; Long, J. D.; Kanics, L. L.; Woolley, J. L. *J. Chromatogr. B Biomed. Sci. Appl.* **1994**, *652*, 211.

[15] Biagini, G. A.; Fisher, N.; Shone, A. E.; Mubaraki, M. A.; Srivastava, A.; Hill, A.; Antoine, T.; Warman, A. J.; Davies, J.; Pidathala, C.; Amewu, R. K.; Leung, S. C.; Sharma, R.; Gibbons, P.; Hong, D. W.; Pacorel, B.; Lawrenson, A. S.; Charoensutthivarakul, S.; Taylor, L.; Berger, O.; Mbekeani, A.; Stocks, P. A.; Nixon, G. L.; Chadwick, J.; Hemingway, J.; Delves, M. J.; Sinden, R. E.; Zeeman, A.; Kocken, C.

H. M.; Berry, N. G.; O'Neill, P. M.; Ward, S. A. *P. Natl. Acad. Sci. USA* **2012**, *109*, 8298.

[16] (a) Rodrigues, T.; Lopes, F.; Moreira, R. *Curr. Med. Chem.* **2010**, *17*, 929. (b) Porter, T. H.; Folkers, K. *Angew. Chem. Int. Edit.* **1974**, *13*, 559.

[17] Vaidya, A. B.; Mather, M. W. *Annu. Rev. Microb.* **2009**, *63*, 249.

[18] Kessl, J. J.; Lange, B. B.; Merbitz-Zahradnik, T.; Zwicker, K.; Hill, P.; Meunier, B.; Palsdottir, H.; Hunte, C.; Meshnick, S; Trumpower, B. L. *J. Bio. Chem.* **2003**, *278*, 31312.

[19] Vaidya, A. B.; Mather, M. W. *Drug Resist. Updat.* **2000**, *3*, 283.

[20] Patel, S. N.; Kain, K. C. *Expert Rev. of Anti Infect. Ther.* **2005**, *3*, 849.

[21] Martin, P.; Lisa, L. G.; Victoria, L. S. *Cytometry* **1997**, *27*, 358–364.

[22] (a) Andrew, D. M. *Angew. Chem. Int. Edit.* **1998**, *37*, 1768. (b) Mikkelsen, R. B.; Tanabe, K.; Wallach, D. H. F. *J. Cell. Biol.* **1982**, *93*, 685. (c) Allen, R. J.; Kirk, K. *J. Biol. Chem.* **2004**, *279*, 11264.

[23] (a) Smith, R. A. J.; Murphy, M. P. *Ann. N.Y. Acad. Sci.* **2010**, *1201*, 96. (b) Asin-Cayuela, J.; Manas, A. R.; James, A. M.; Smith, R. A.; Murphy, M. P. *FEBS Lett.* **2004**, *571*, 9. (c) Kelso, G. F.; Porteous, C. M.; Coulter, C. V.; Hughes, G; Porteous, W. K.; Ledgerwood, E. C.; Smith, R. A. J.; Murph, M. P. *J. Biol. Chem.* **2001**, *276*, 4588. (d) James, M. A.; Cochemé, H. M.; Smith, R. J.; Murphy, M. P. *J. Biol. Chem.* **2005**, *280*, 21295.

[24] (a) Mikkelsen, R.B.; Tanabe, K.; Wallach, D. F. *J. Cell Biol.* **1982**, *93*, 685. (b) Allen, R. J.; Kirk, K. *J. Biol. Chem.* **2004**, *279*, 11264. (c) Uyemura, S. A.; Luo, S.; Moreno, S. N.; Docampo, R. *J. Biol. Chem.* **2000**, *275*, 9709.

[25] (a) Commandeur, C.; Chalumeau, C.; Dessolin, J.; Laguerre, M. *Eur. J. Org. Chem.* **2007**, 3045. (b) Yan, G.; Lin, L. *Molecules* **2011**, *16*, 2714.

[26] (a) Kiddle, J. J. *Tetrahedron Lett.* **2000**, *41*, 1339. (b) Cvengros, J.; Toma, S.;Marque, S.; Loupy, A. *Can. J. Chem.* **2004**, *82*, 1365.

[27] Boido, A.; Boido, C. C.; Sparatore, F. *Il Farmaco* **2001**, *56*, 263.

[28] Byun, A; Kim, M; Choi, J; Moon, K. H.; Lee, C. K.; Park, M. *Arch. Pharm. Res.* **2004**, *27*, 273.

[29] Saari, W. S.; Hoffman, J. B.; Wai, J. S.; Fisher, T. E.; Rooney, C. S.; Smith, A. M.; Thomas, C. M.; Goldman, M. E.; O'Brien. J. A. *J. Med. Chem.* **1991**, *34*, 2922.

[30] Lu, J.; Cheng, C.; Zhao, X.; Liu, Q.; Yang, P.; Wang, Y.; Luo, G. *Eur. J. Med. Chem.* **2010**, *45*, 1731.

[31] Escudero, M. I.; Kremenchuzky, L. D.; Perillo, I. A.; Blanco, M. M.; Cerecetto, H. *Synthesis* **2011**, *4*, 571 .

[32] Heikki, J.; Pekka, L. *Phys. Chem. Chem. Phys.* **1999**, *1*, 4003.

[33] Bruno, O.; Romussi, A.; Spallarossa, A.; Brullo, C.; Schenone, S.; Bondavalli, F.; Vanthuyne, N.; Roussel, C. *J. Med. Chem.* **2009**, *52*, 6546.

[34] Lipshutz, B. H.; Kim, S. K.; Mollard, P.; Stevens, K. L. *Tetrahedron* **1998**, *54*, 1241.

[35] Madej, M. G.; Nasiri, H. R.; Hilgendorff, N. S.; Schwalbe, H.; Unden, G.; Lancaster, C. R. *Biochemistry* **2006**, *45*, 15049.

[36] (a) Starks, C. M. *J. Am. Chem. Soc.* **1971**, *93*, 195. (b) Dueno, E. E.; Chu, F.; Kim, S.; Jung, K. W. *Tetrahedron Lett.* **1999**, *40*, 1843.

[37] Pedersen, C. J. *J. Am. Chem. Soc.* **1967**, *89*, 2495.

[38] Ball, E. B. *J. Bio. Chem*. **1934**, *106*, 515.

[39] Lu, X.; Altharawi, A.; Hansen, E. N.; Long, T. E. *Synthesis* **2012**, under revision.

[40] (a) Singh, I.; Ogata, R. T.; Moore, R. E.; Chang, C. W. J.; Scheuer, P. J. *Tetrahedron* **1968**, *24*, 6053. (b) Crowe, M. O. *J. Biol. Chem.* **1936**, *115*, 479.

[41] (a) Juster, N. J. *J. Chem. Ed*. **1962**, *39*, 596. (b) Ossowski, T.; Goulart, M. O. F.; de Abreu, F. C.; Sant'Ana, A. E. G.; Zarzeczanska, D.; Miranda, P. R. B.; Costa, C. D.; Liwo, A.; Falkowski, P. *J. Braz. Chem. Soc.* **2008**, *19*, 175. (c) Amro, B. I. N.; James, K. C.; Turner, T. D. *J. Soc. Cosmet. Chem.* **1994**, *45*, 159.

[42] Coteron, J. M.; Catterick, D.; Castro, J.; Chaparro, M. J.; Diaz, B.; Fernandez, E.; Ferrer, S.; Gamo, F. J.; Gordo, M.; Gut, J.; de las Heras, L.; Legac, J.; Marco, M.; Miguel, J.; Munoz, V.; Porras, E.; de la Rosa, J. C.; Ruiz, J. R.; Sandoval, E.; Ventosa, P.; Rosenthal, P. J.; Fiandor, J. M. *J. Med. Chem.* **2010**, *53*, 6129.

[43] Long, T. E.; Lu, X.; Galizzi, M.; Docampo, R.; Gut, J.; Rosenthal, P. J. *Bioorg. Med. Chem.***2012**, *22*, 2976.

[44] Appendix D

[45] Appendix E

APPENDIX A

Benzyl 11-(2-nitrophenylthio)undecanoate (3a)

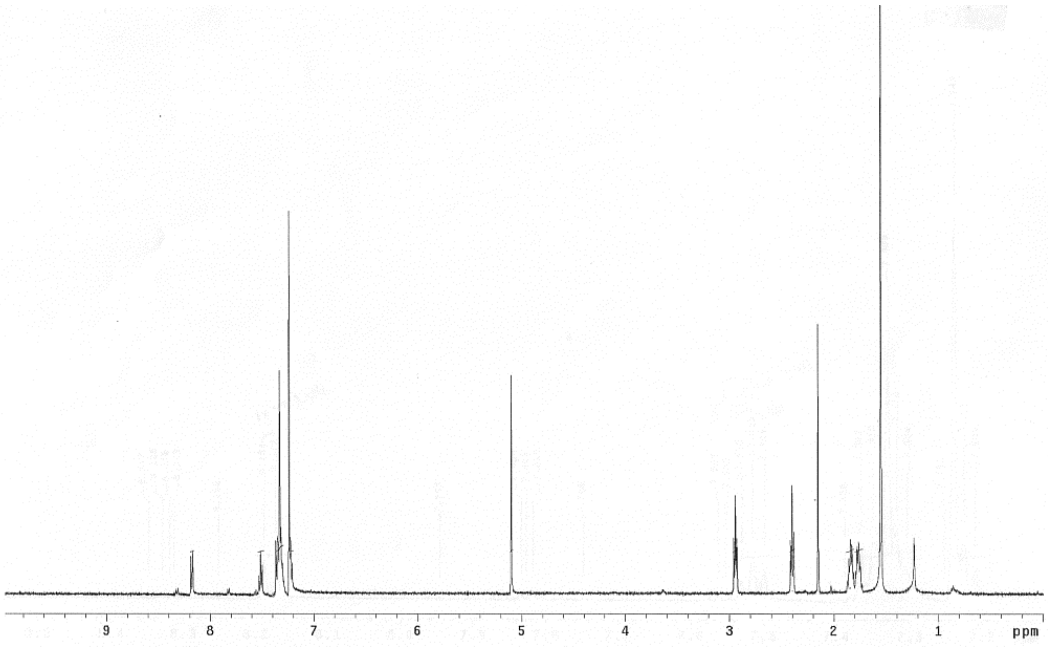

Benzyl 5-(2-nitrophenylthio)pentanoate (3b)

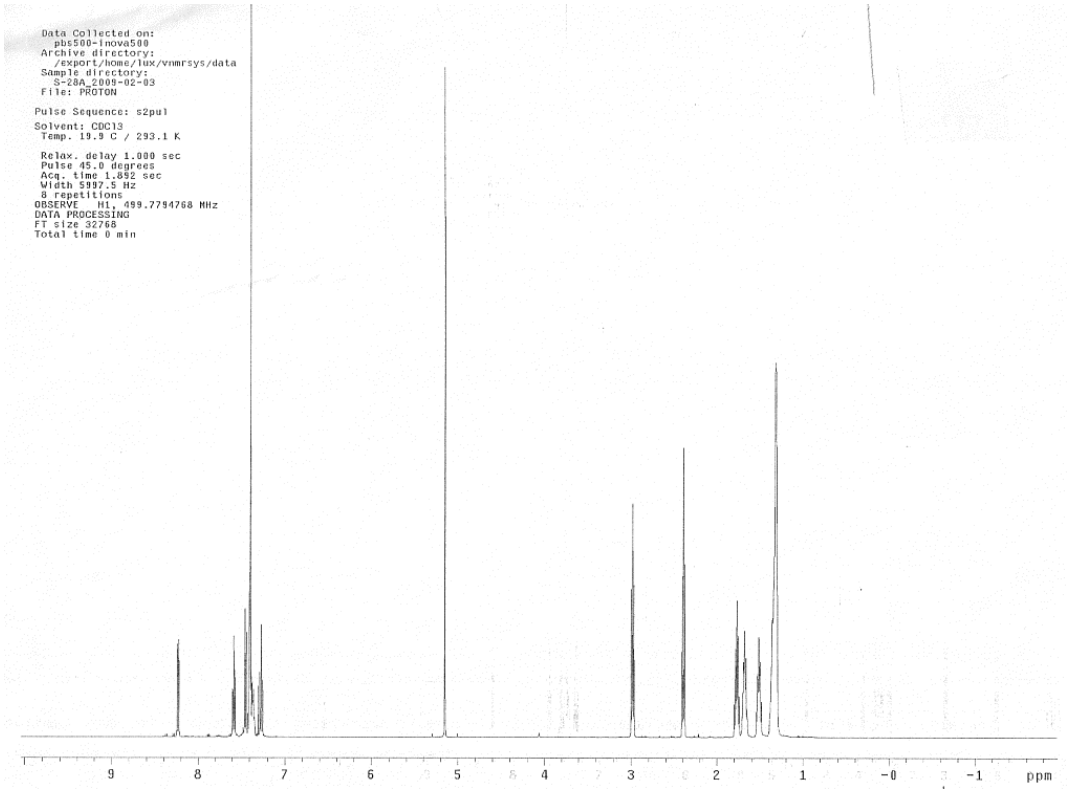

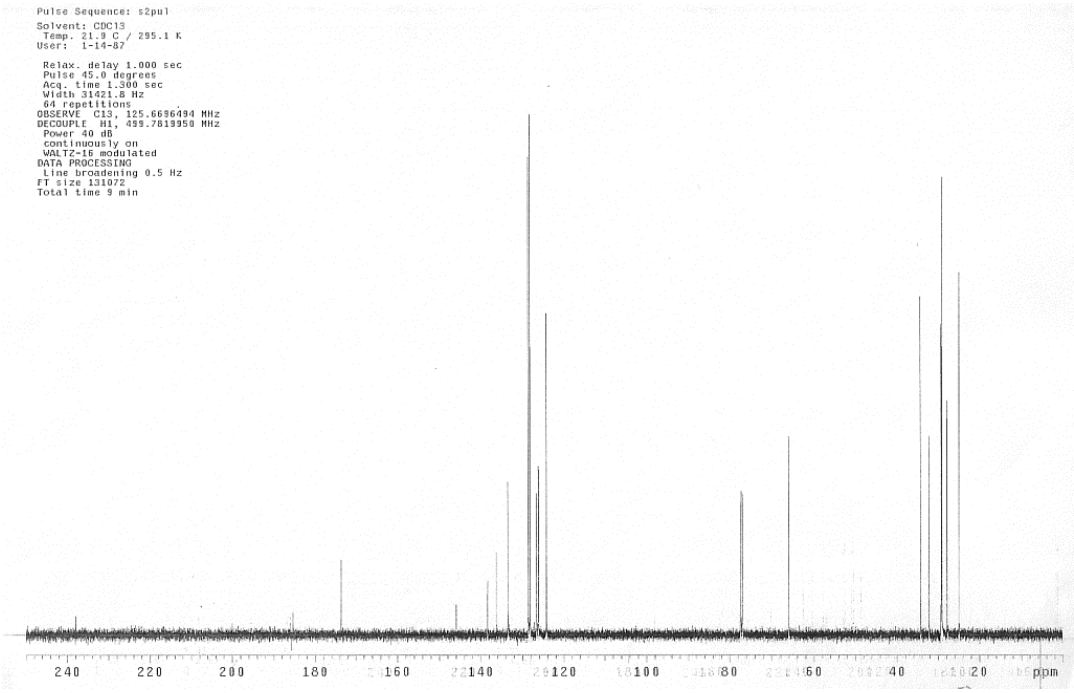

1-(11-(2-Nitrophenylthio)undecylthio)benzene (3c)

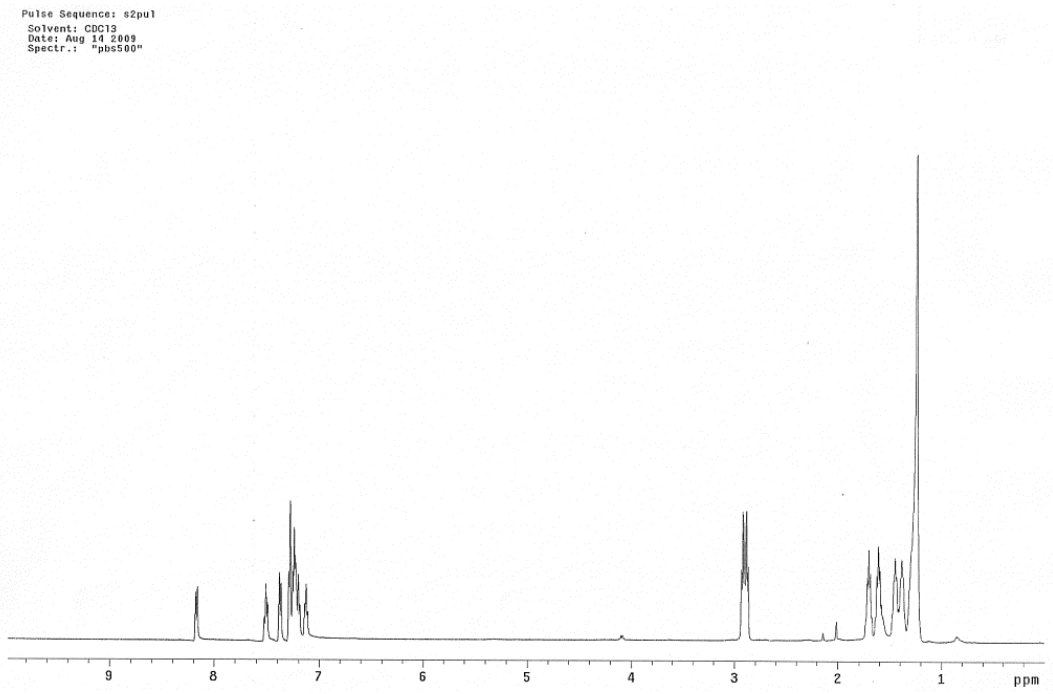

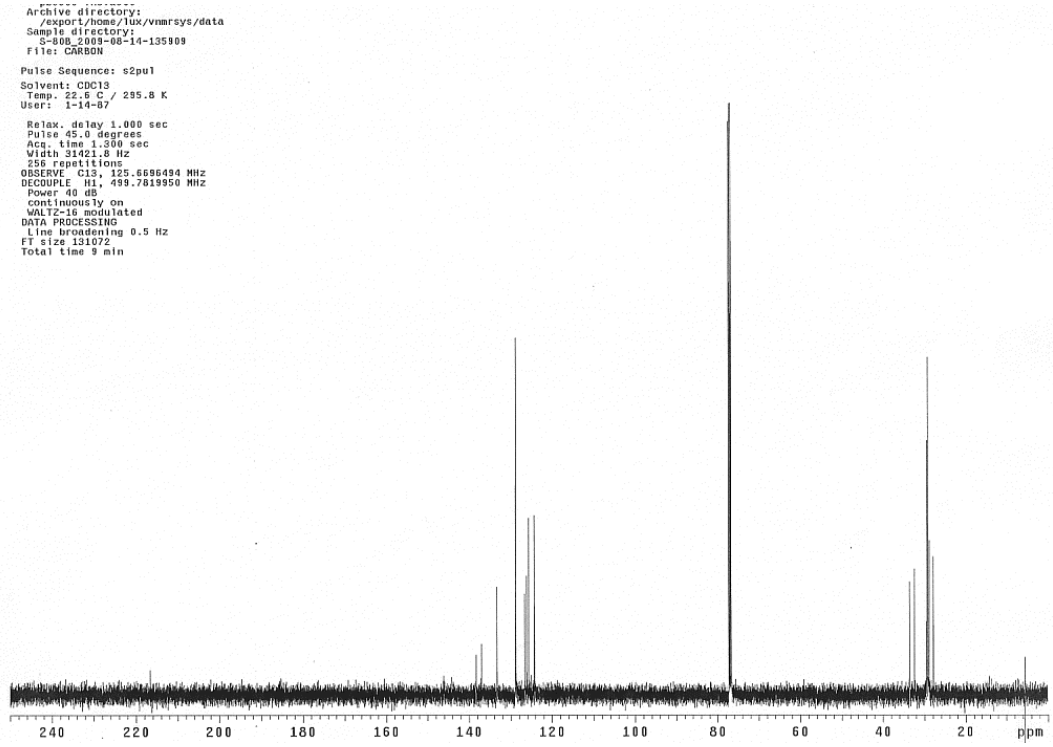

1-(6-(Phenylthio)hexylthio)-2-nitrobenzene (3d)

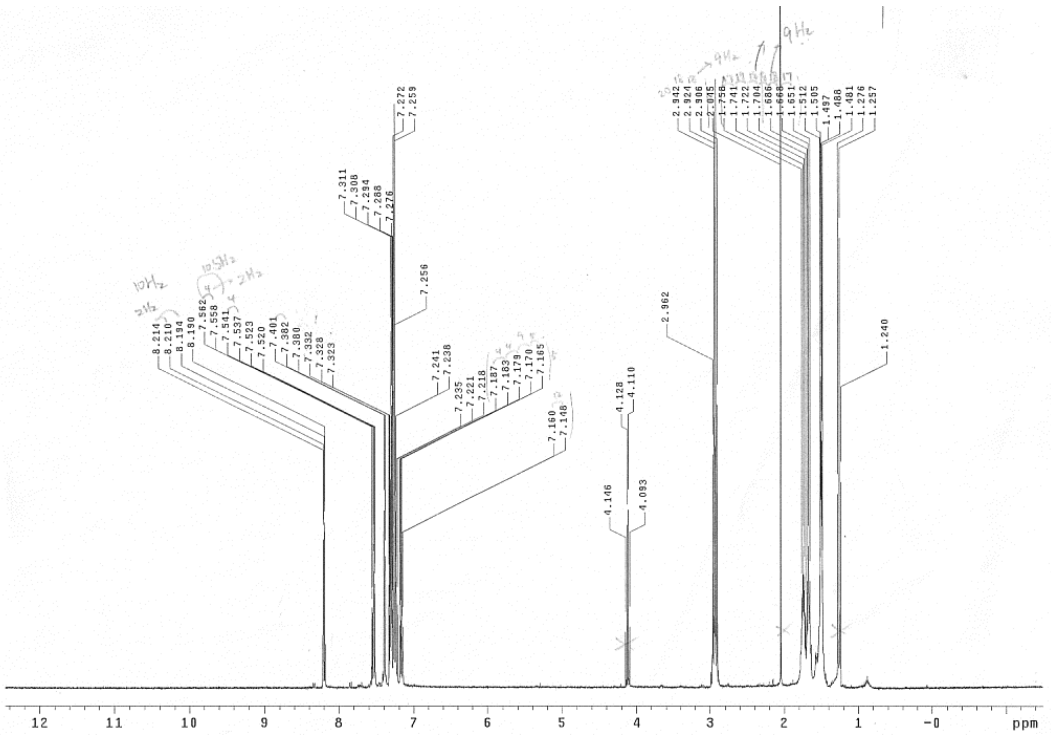

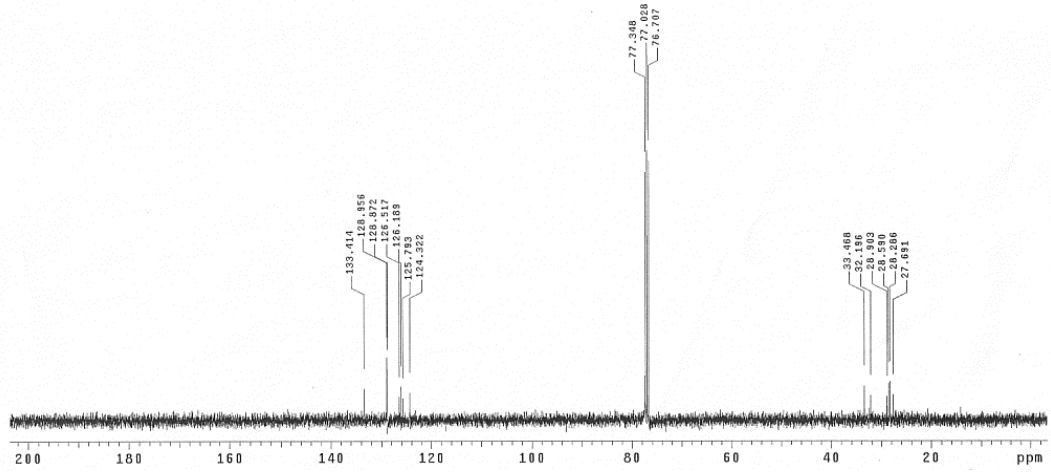

1-(11-(2-Nitrophenylthio)undecylthio)-4-methylbenzene (3e)

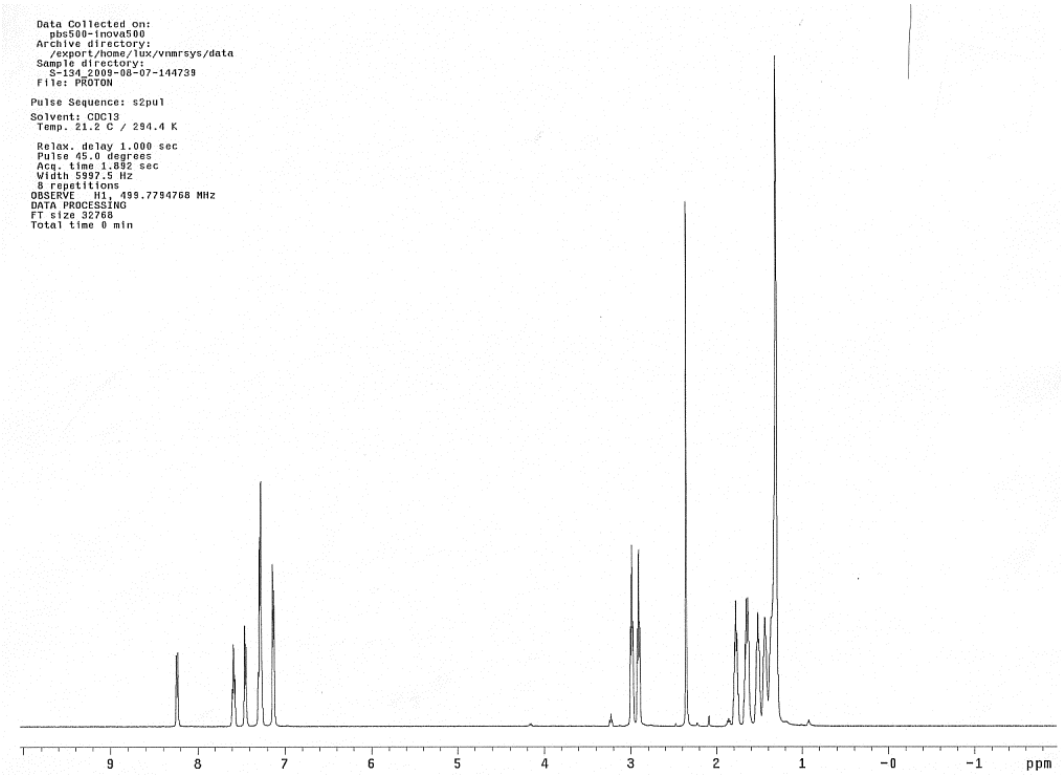

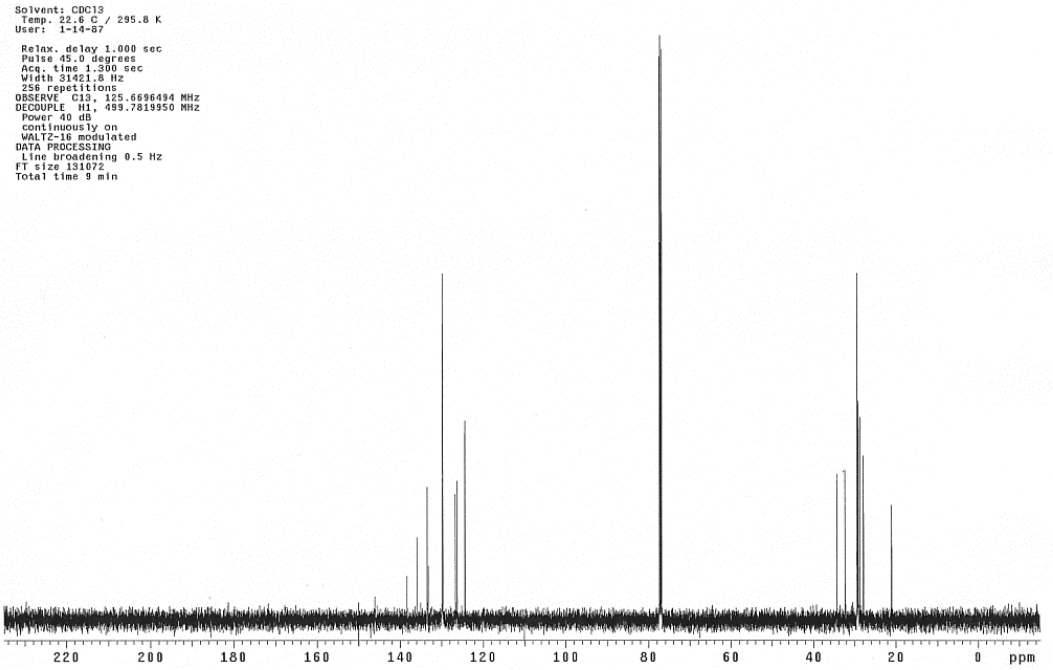

1-(11-(2-Nitrophenylthio)undecylthio)-4-chlorobenzene (3f)

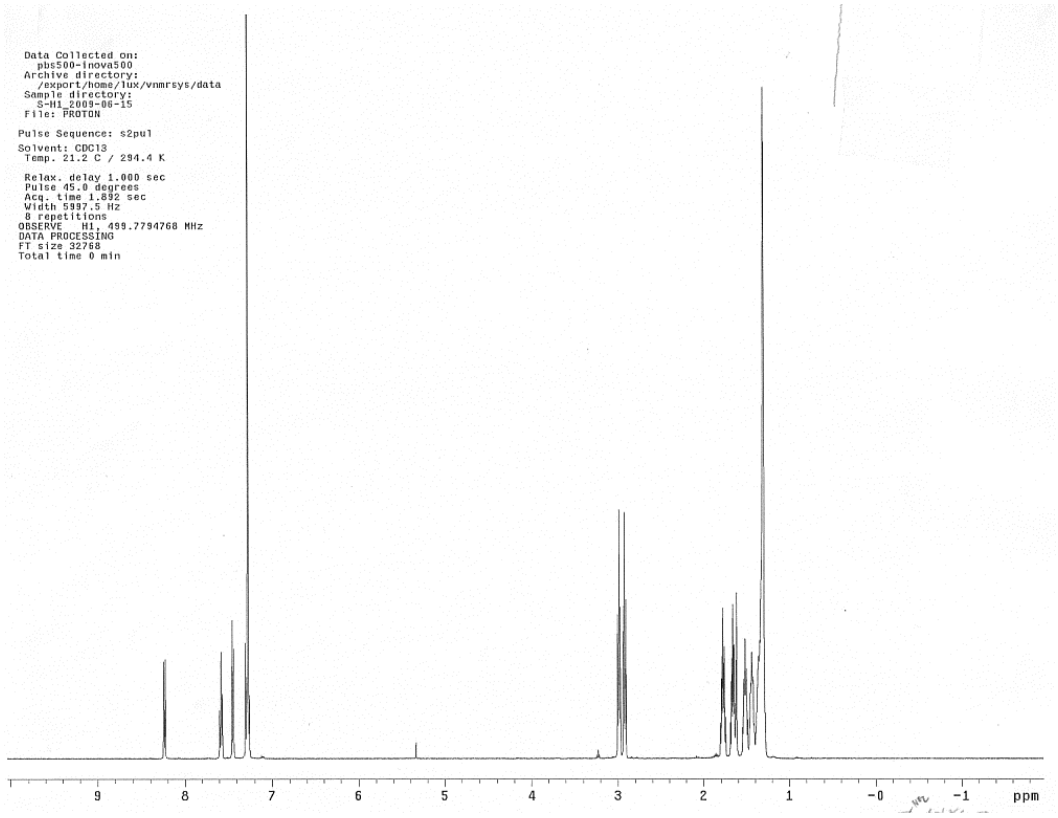

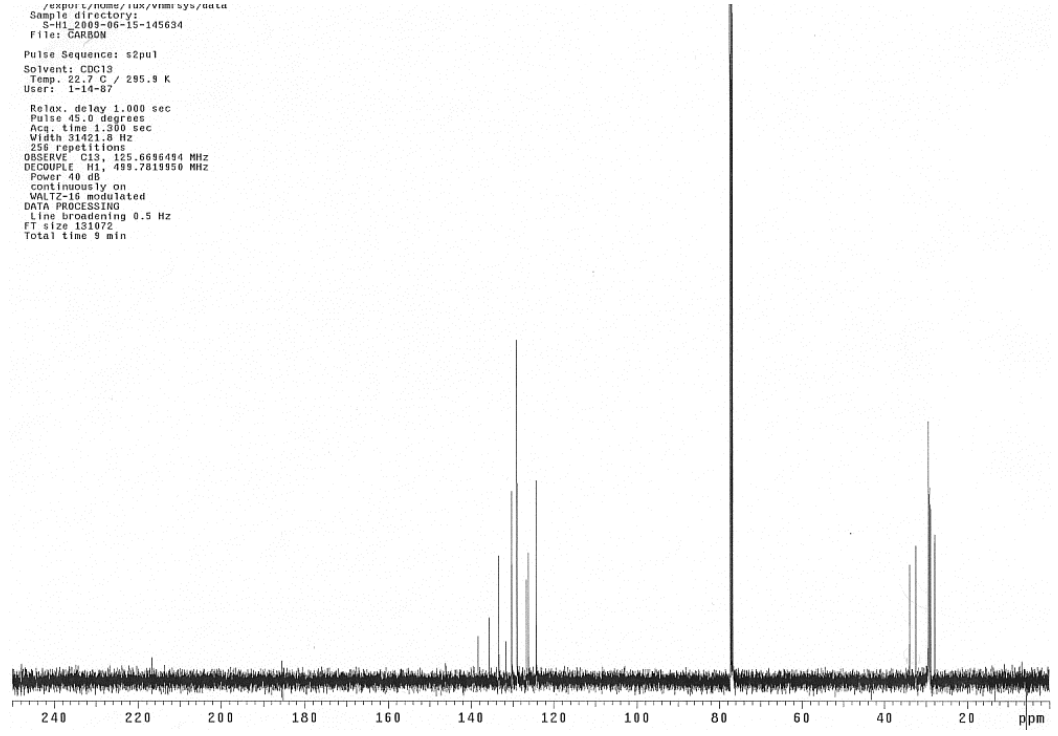

1-(11-(2-Nitrophenylsulfinyl)undecylsulfinyl)-4-nitrobenzene (3g)

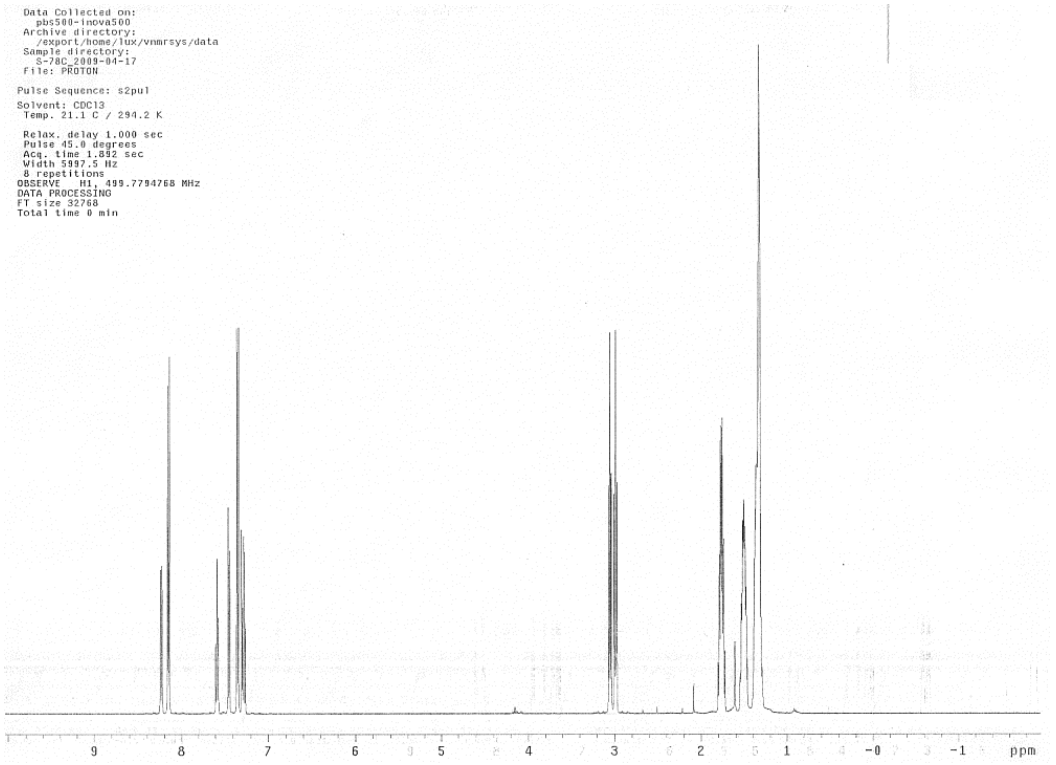

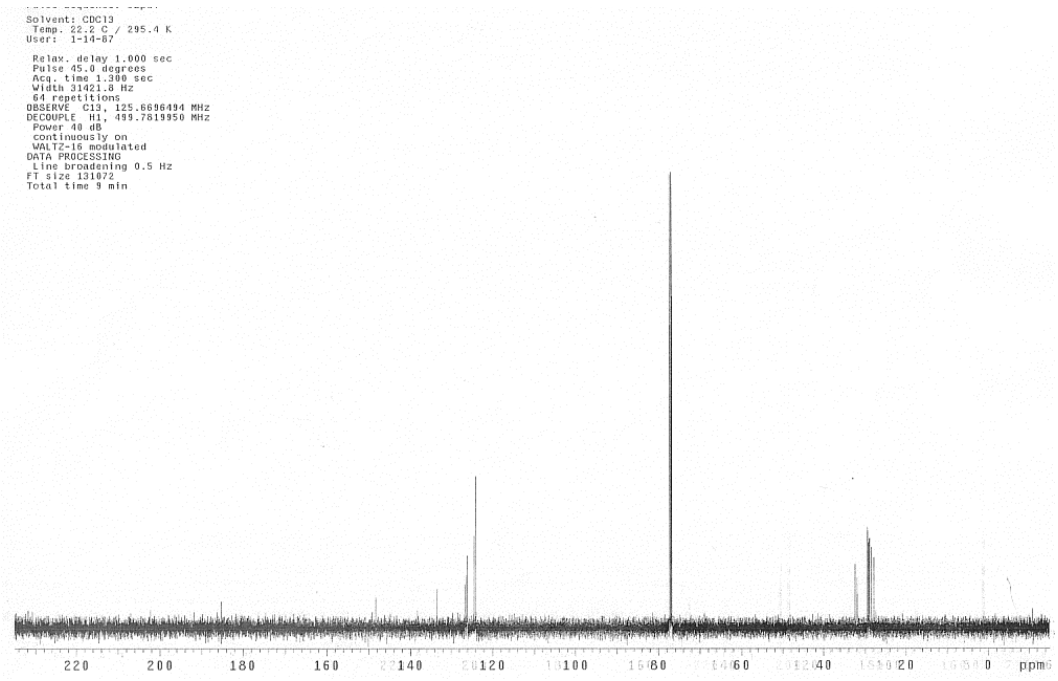

1-(6-(4-Nitrophenylthio)hexylthio)-2-nitrobenzene (3h)

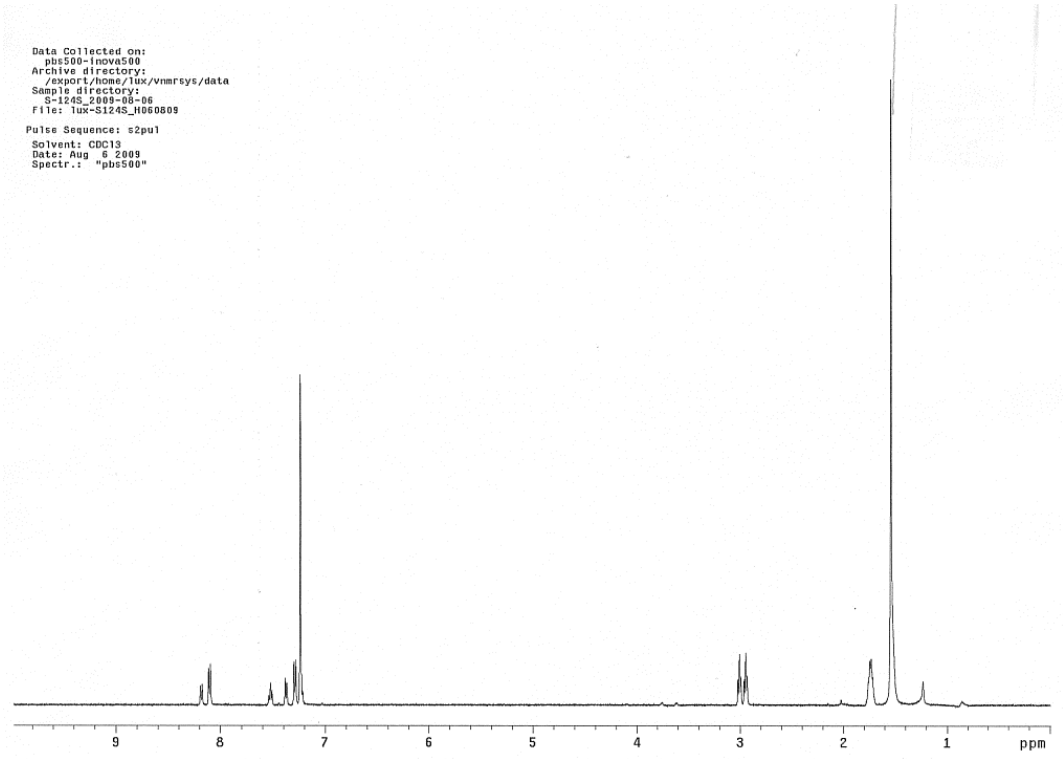

Benzyl 2-(2-nitrophenylthio)butanoate (3i)

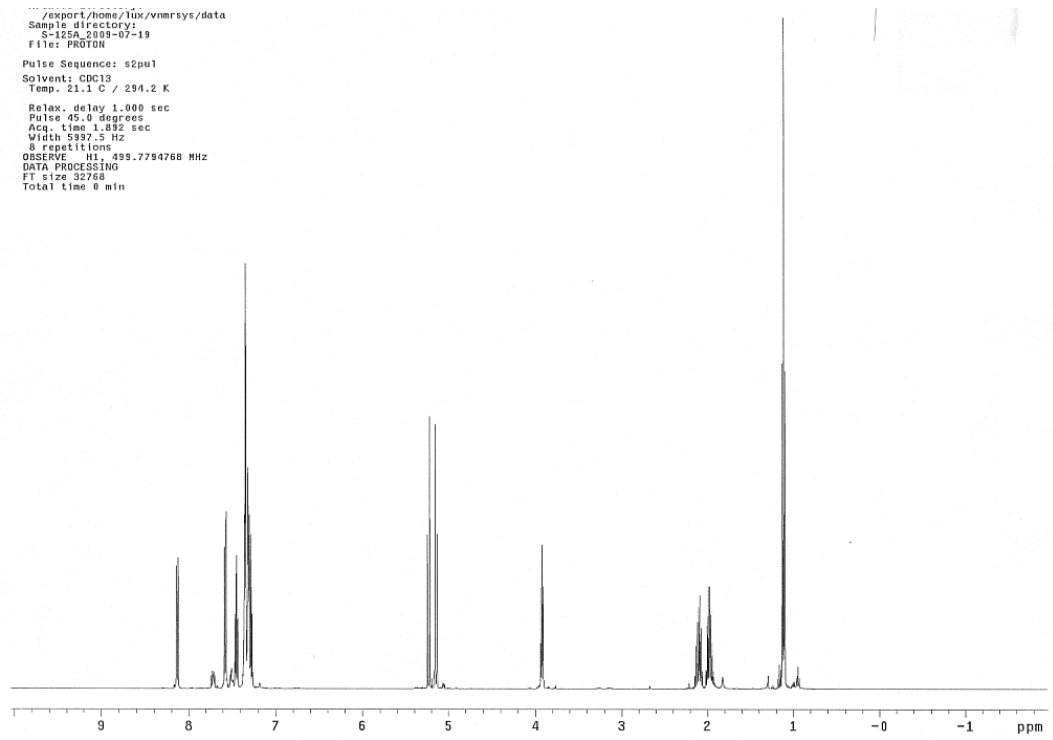

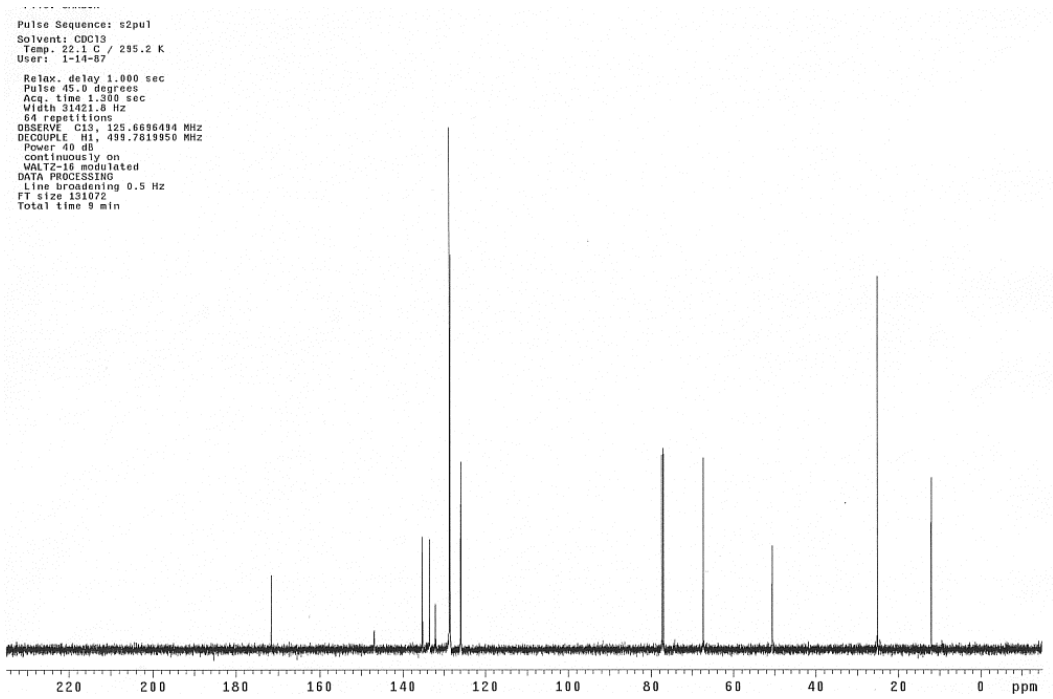

Benzyl 2-(2-nitrophenylthio)-3-methylbutanoate (3j)

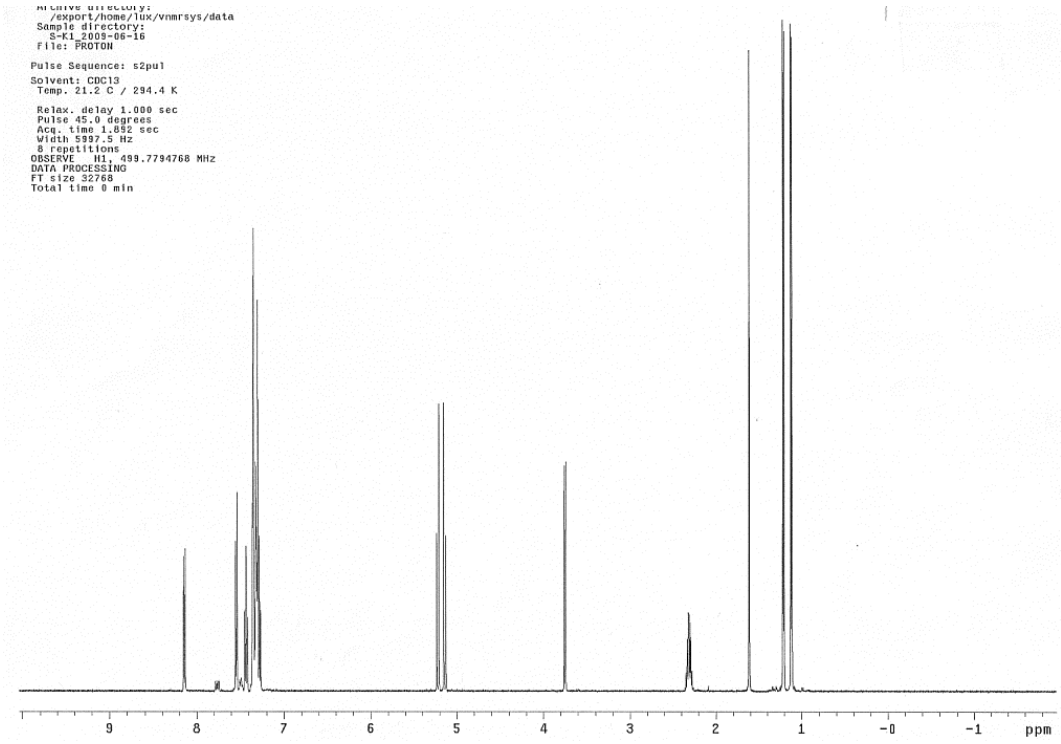

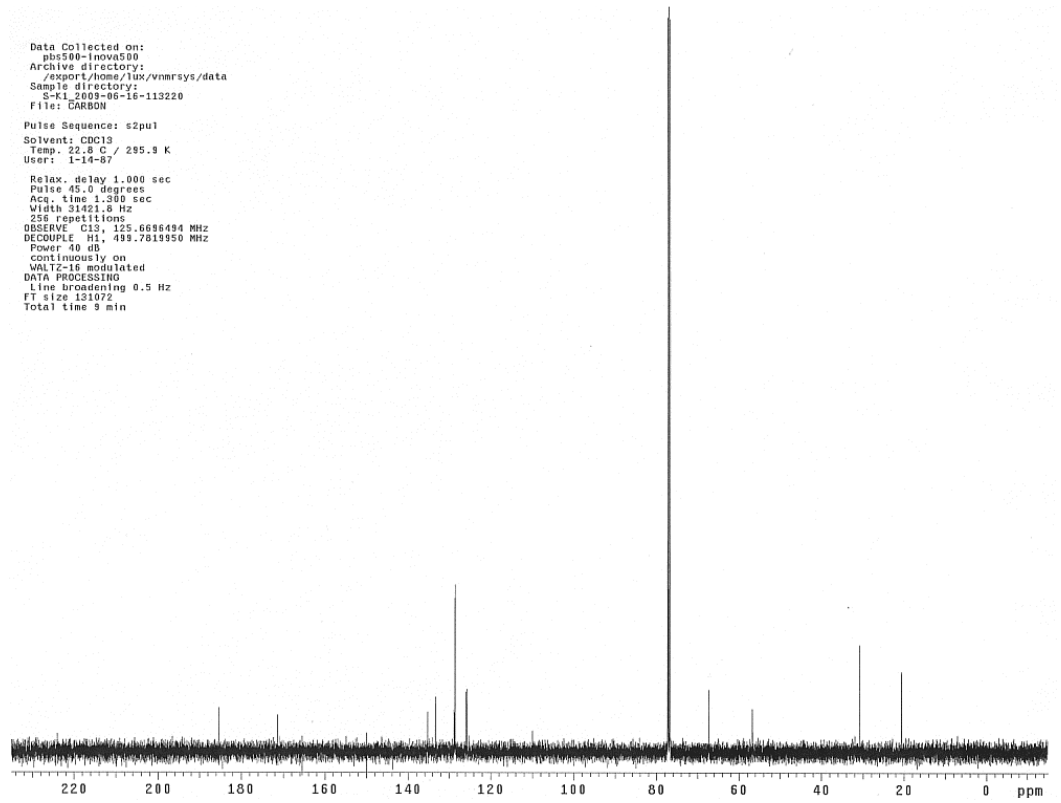

Benzyl 2-(2-nitrophenylthio)-3-phenylpropanoate (3k)

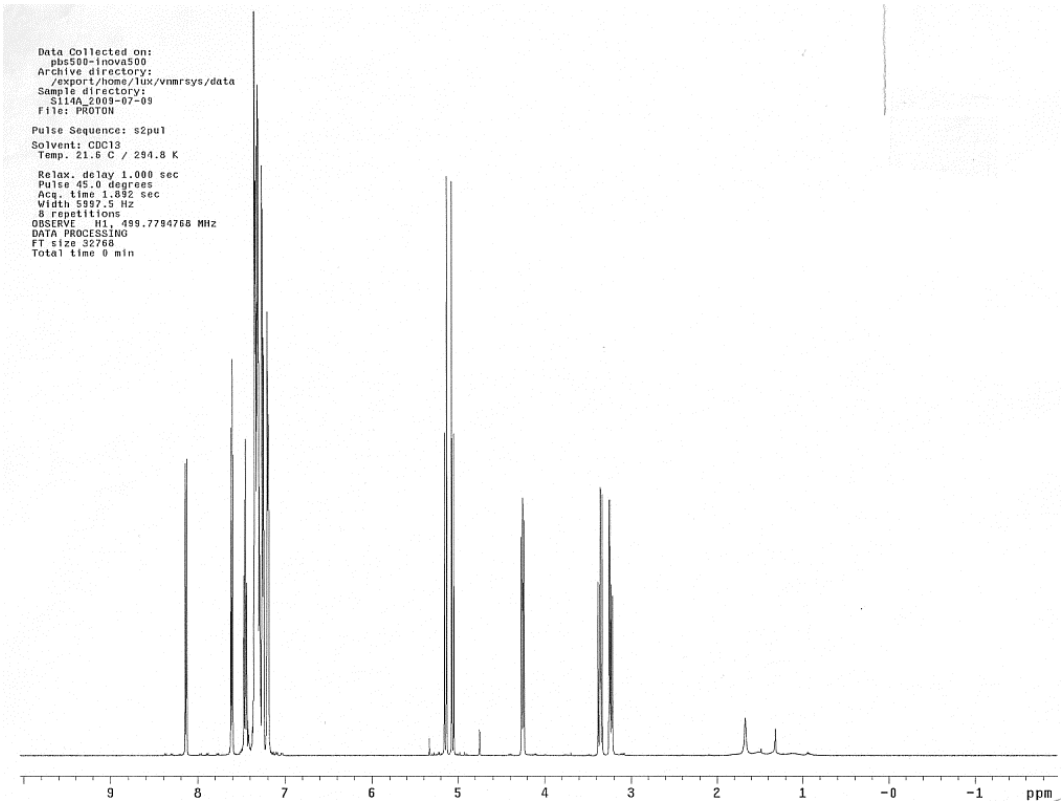

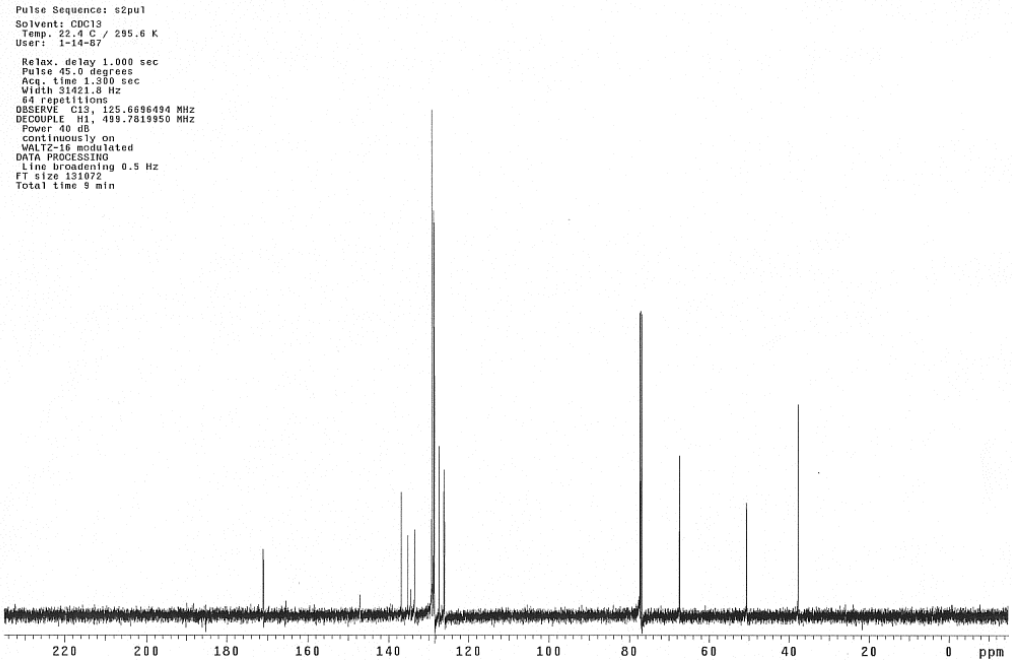

Benzyl 3-(2-nitrophenylthio)butanoate (3l)

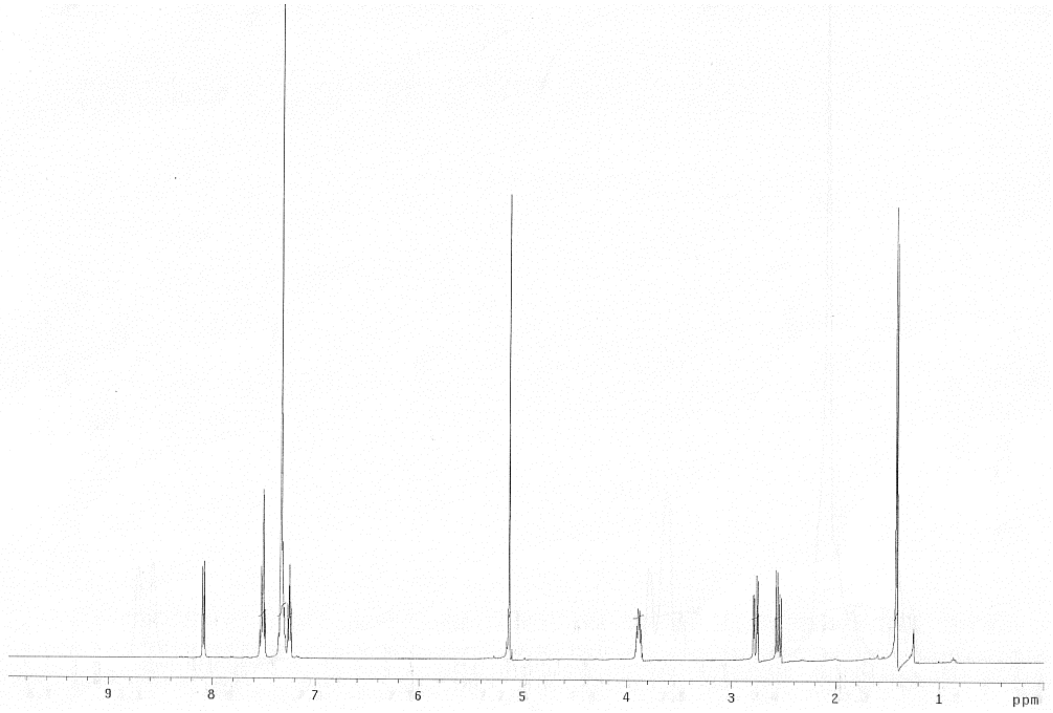

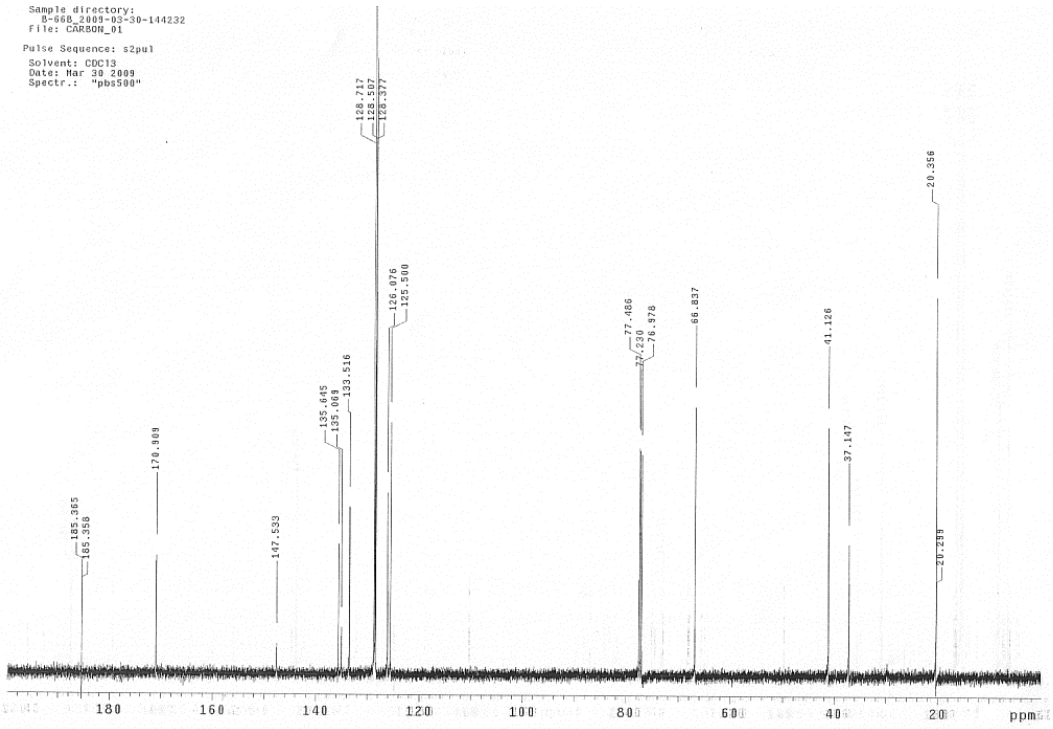

Benzyl 5-(2-nitrophenylthio)hexanoate (3m)

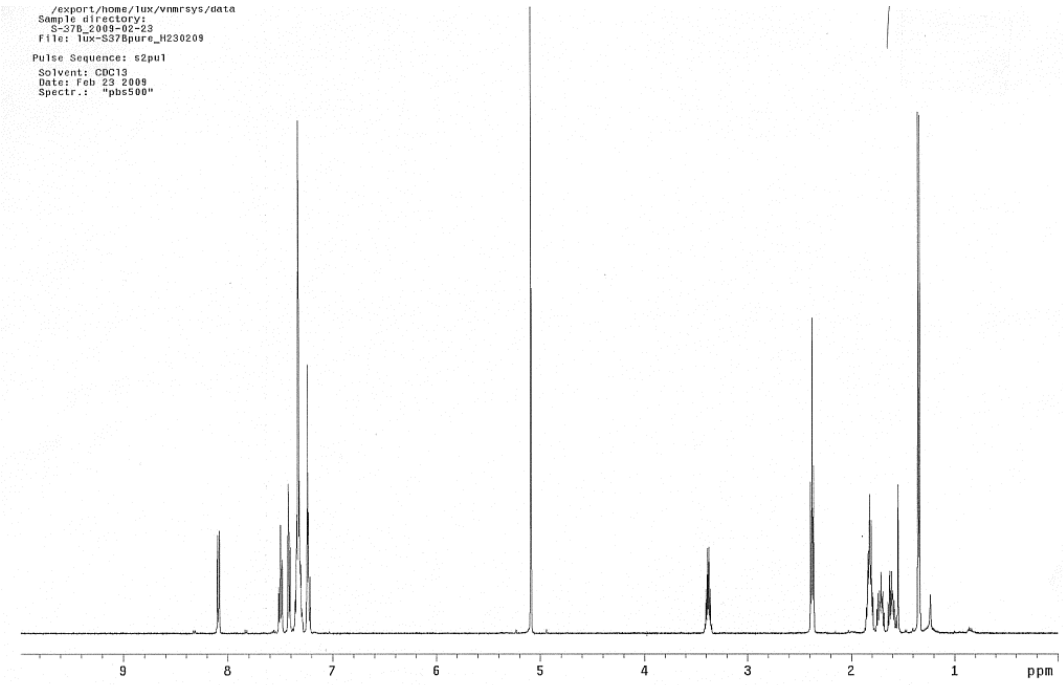

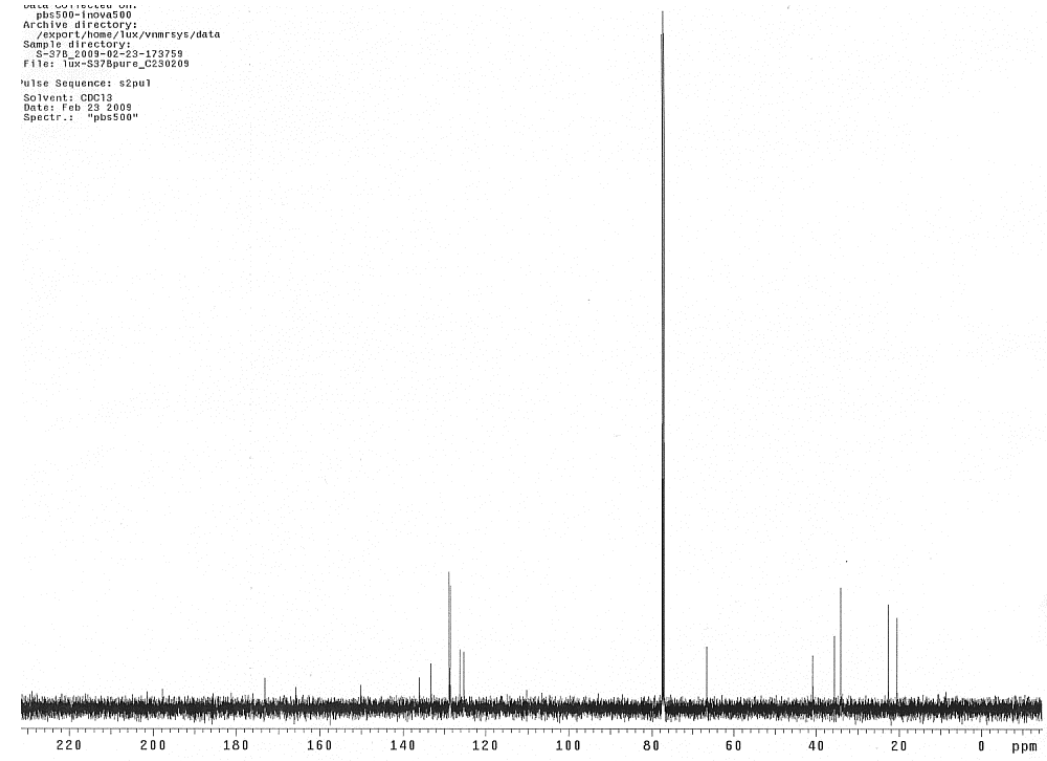

Benzyl 11-(2-nitrophenylsulfinyl)undecanoate (1a)

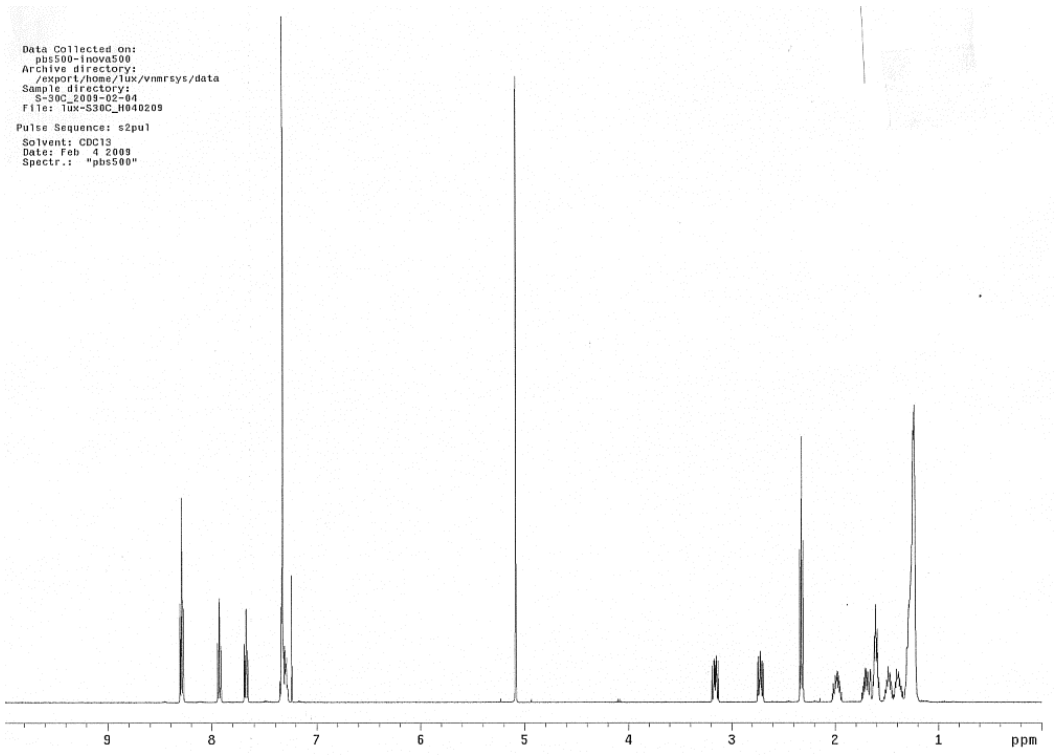

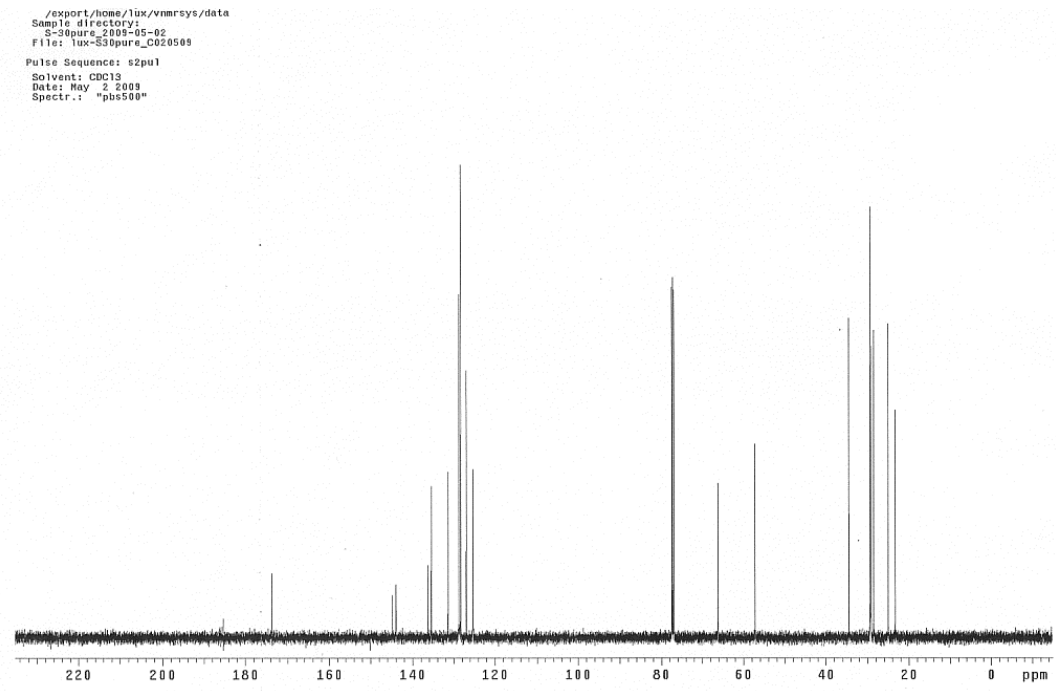

Benzyl 5-(2-nitrophenylsulfinyl)pentanoate (1b)

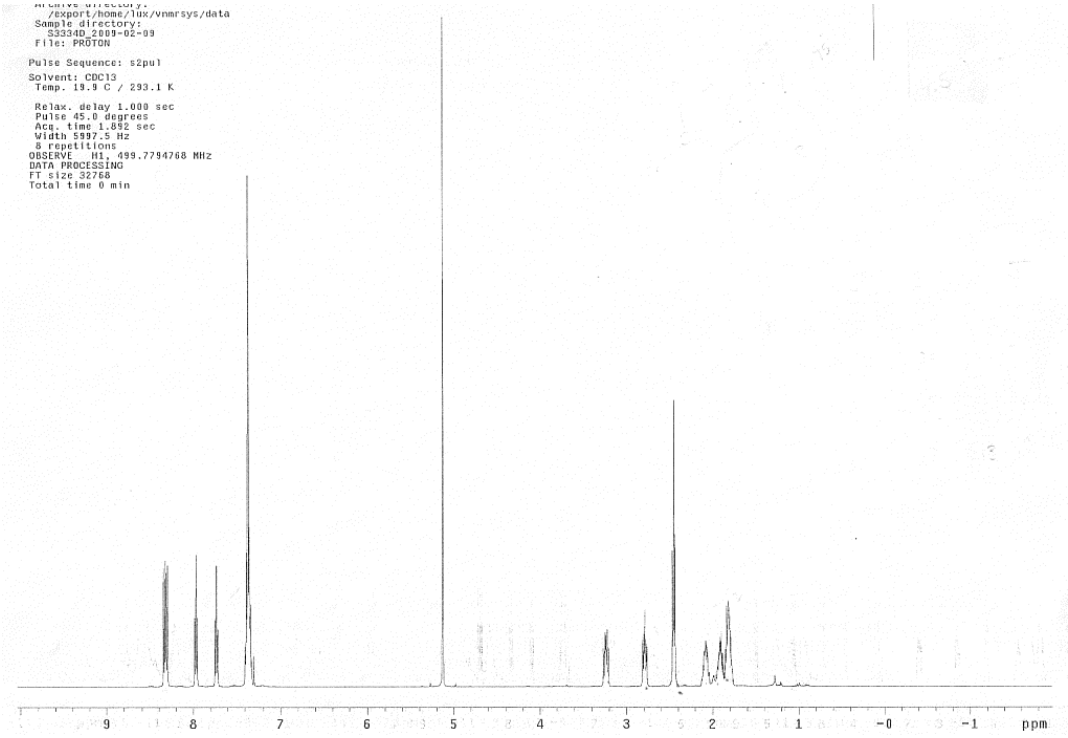

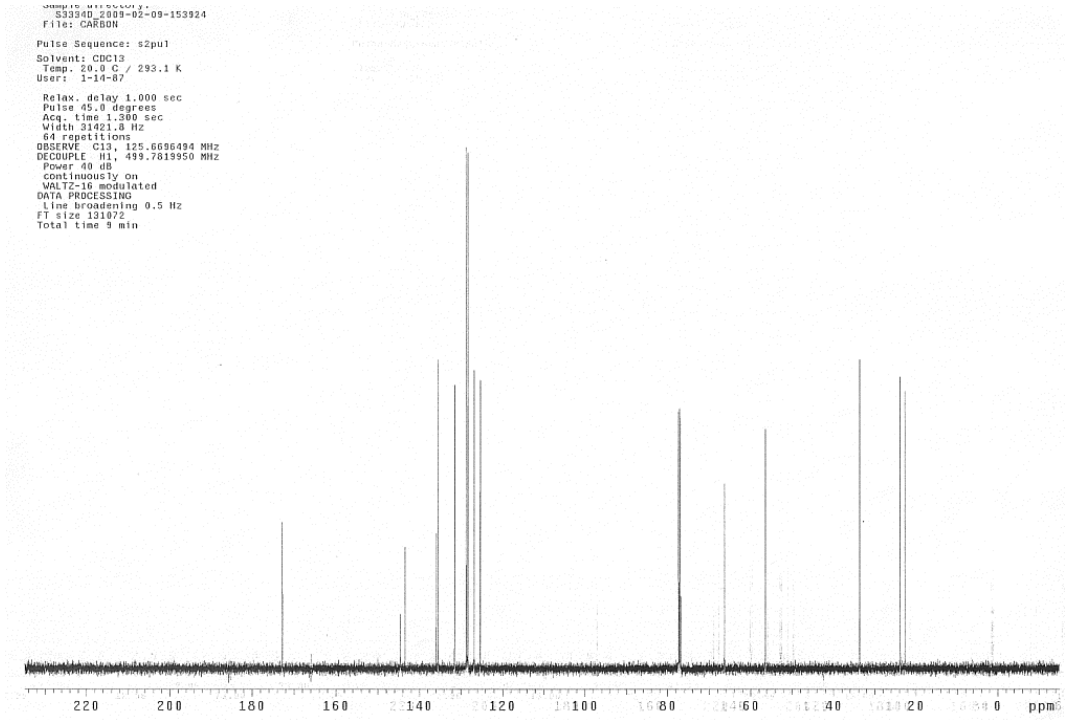

1-(11-(2-Nitrophenylsulfinyl)undecylsulfinyl)benzene (1c)

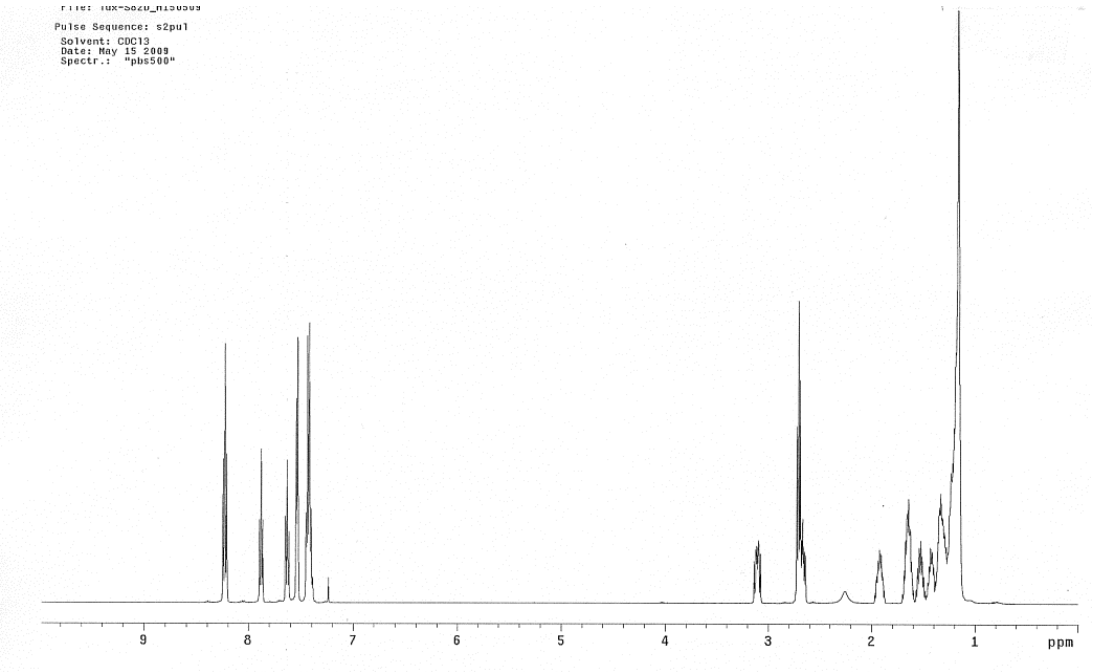

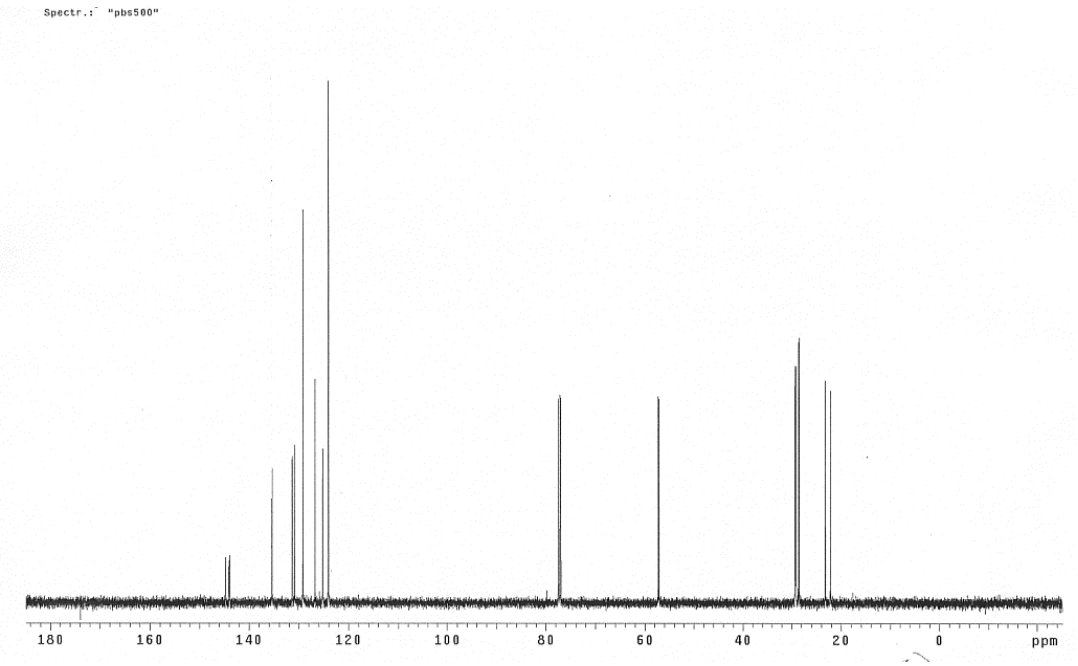

1-(6-(Phenylsulfinyl)hexylsulfinyl)-2-nitrobenzene (1d)

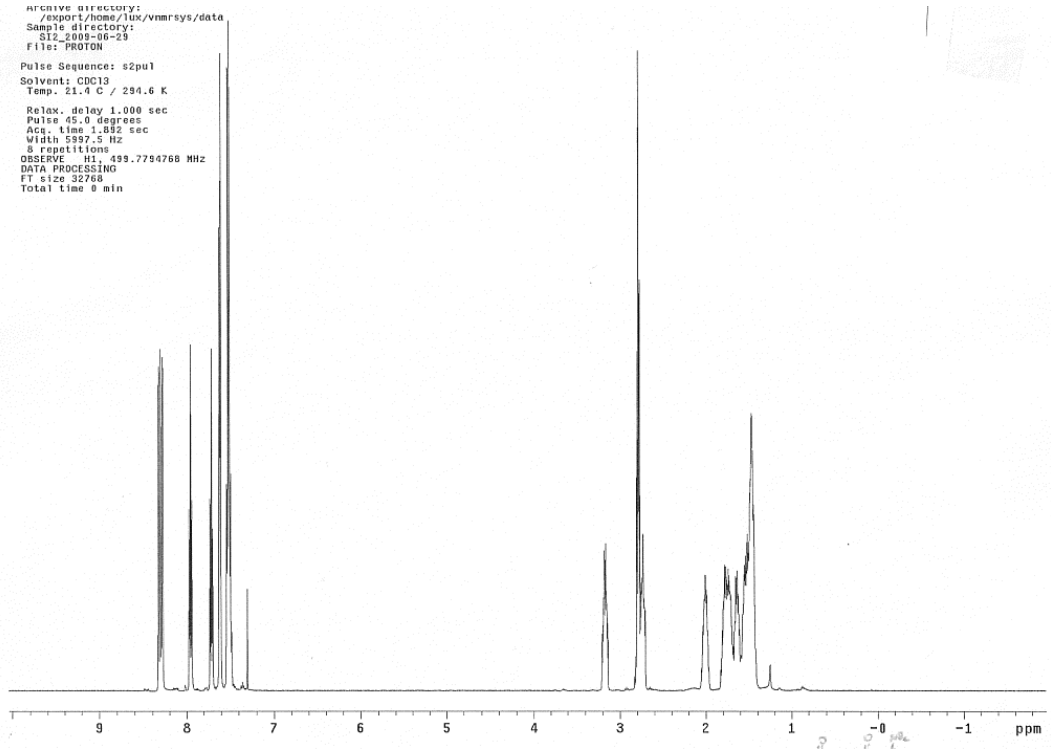

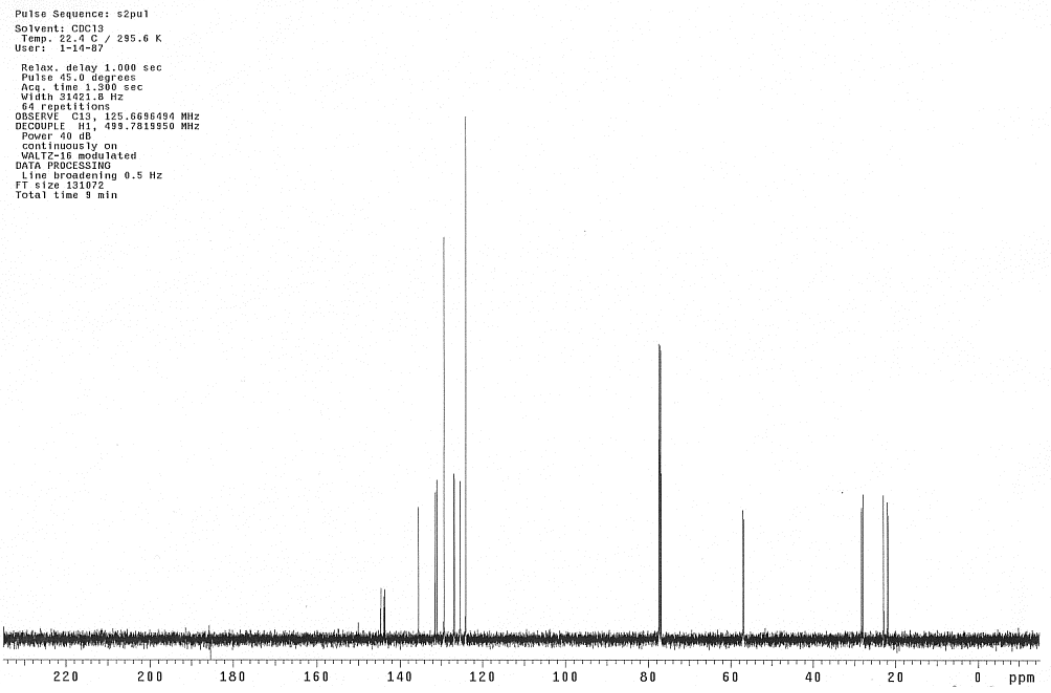

1-(11-(2-Nitrophenylsulfinyl)undecylsulfinyl)-4-methylbenzene (1e)

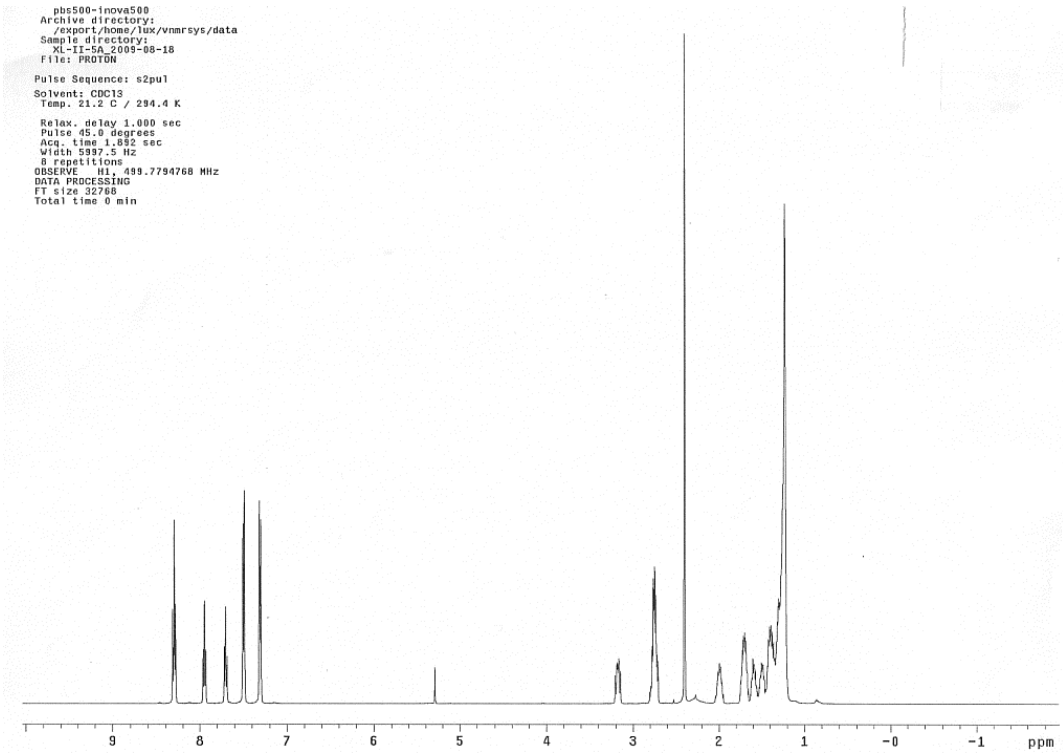

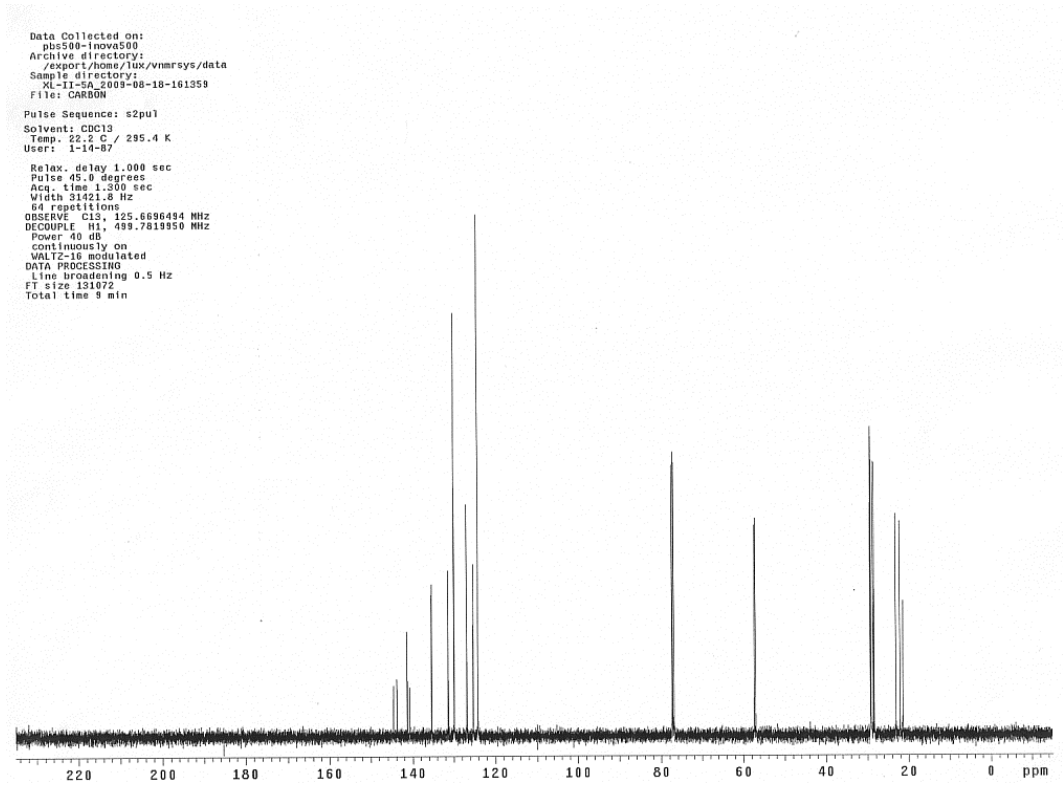

1-(11-(2-Nitrophenylsulfinyl)undecylsulfinyl)-4-chlorobenzene (1f)

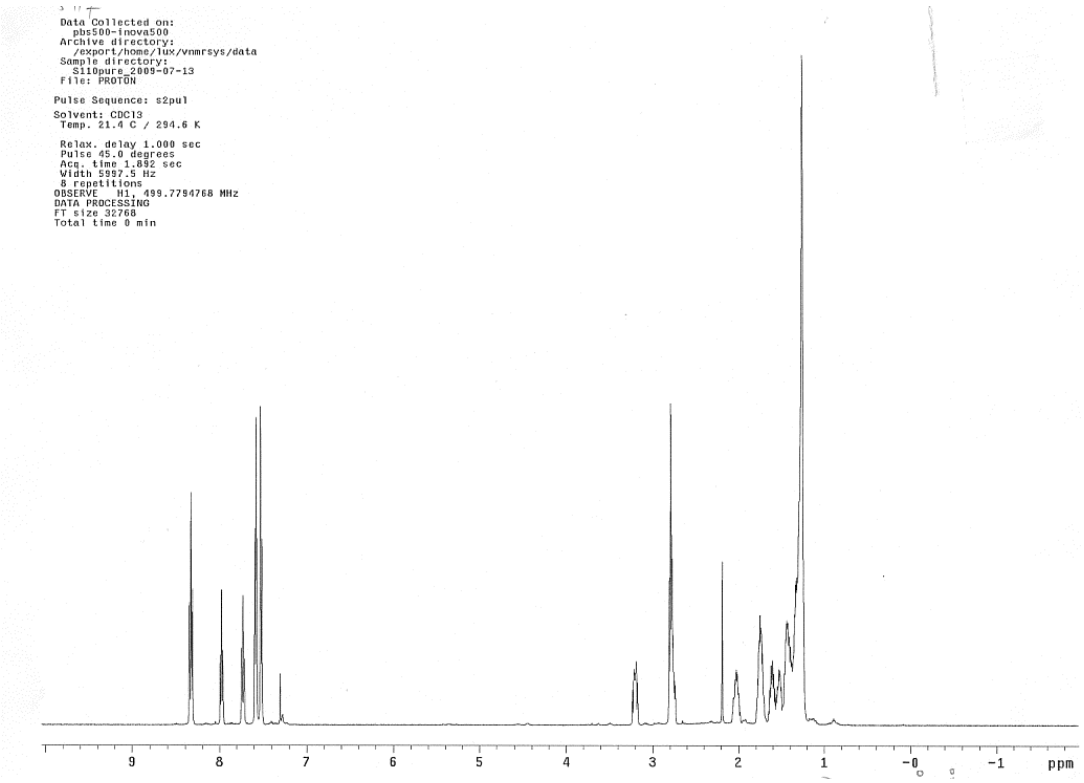

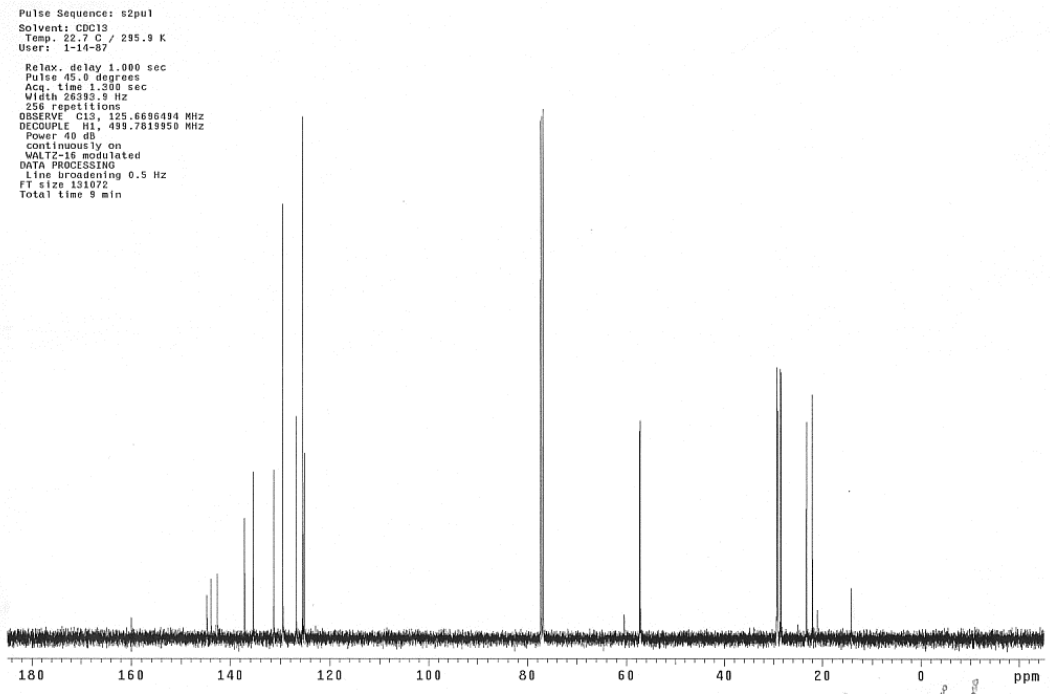

1-(11-(2-Nitrophenylsulfinyl)undecylsulfinyl)-4-nitrobenzene (1g)

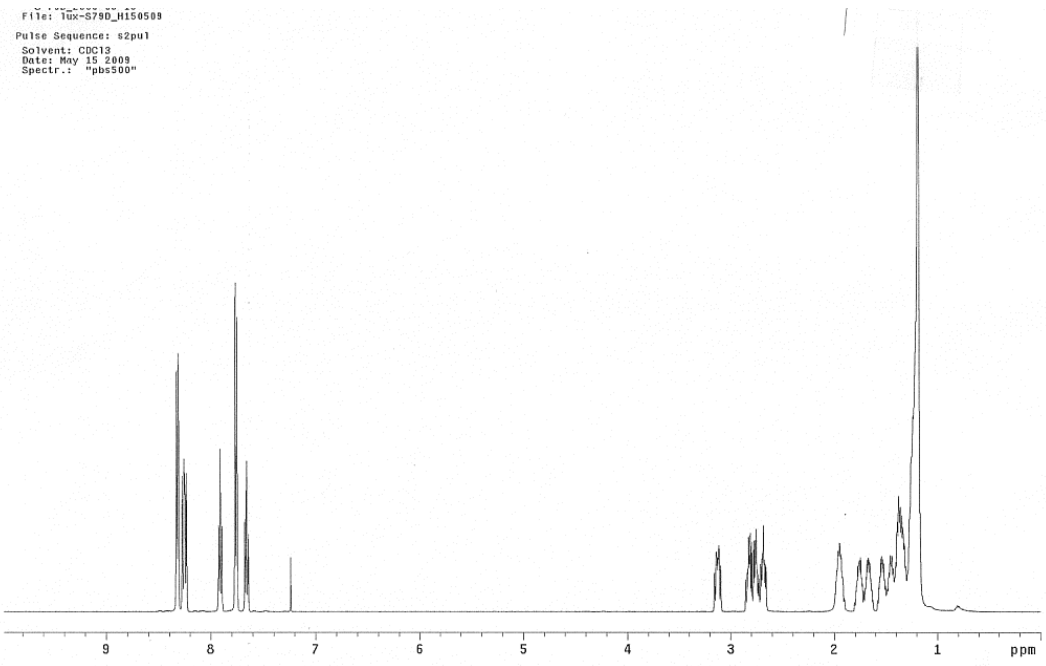

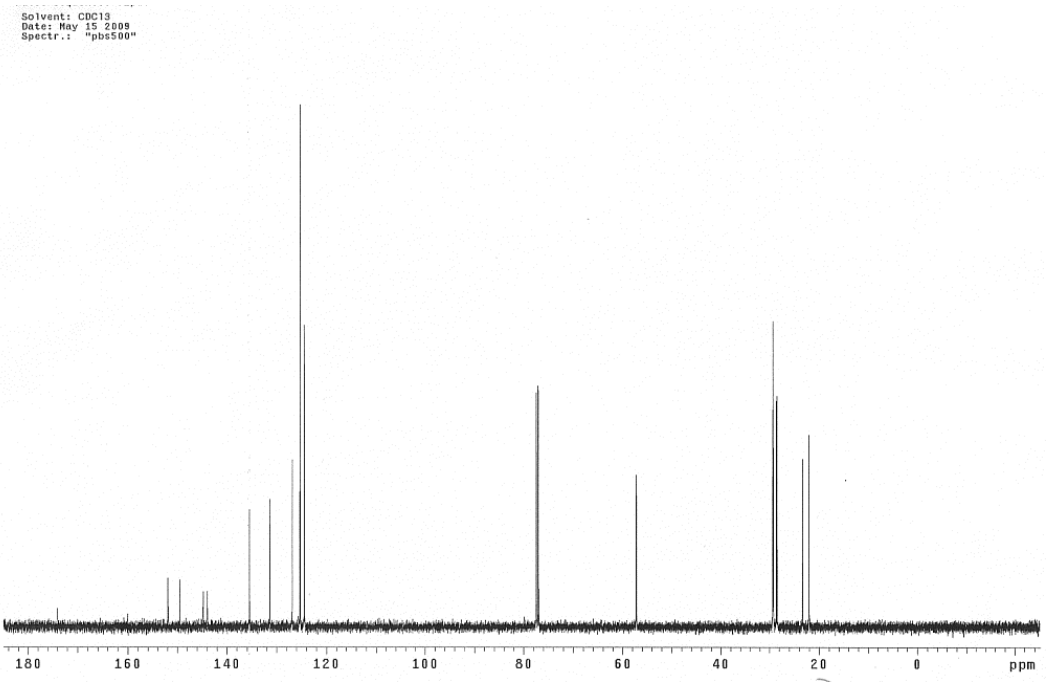

1-(6-(4-Nitrophenylsulfinyl)hexylsulfinyl)-2-nitrobenzene (1h)

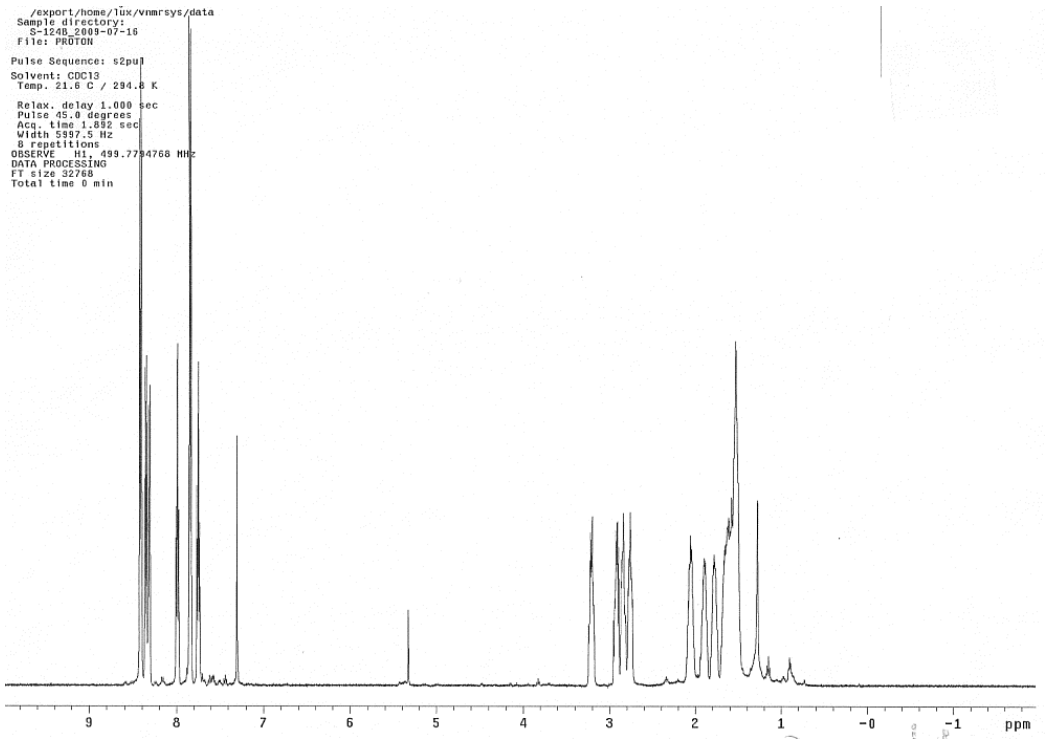

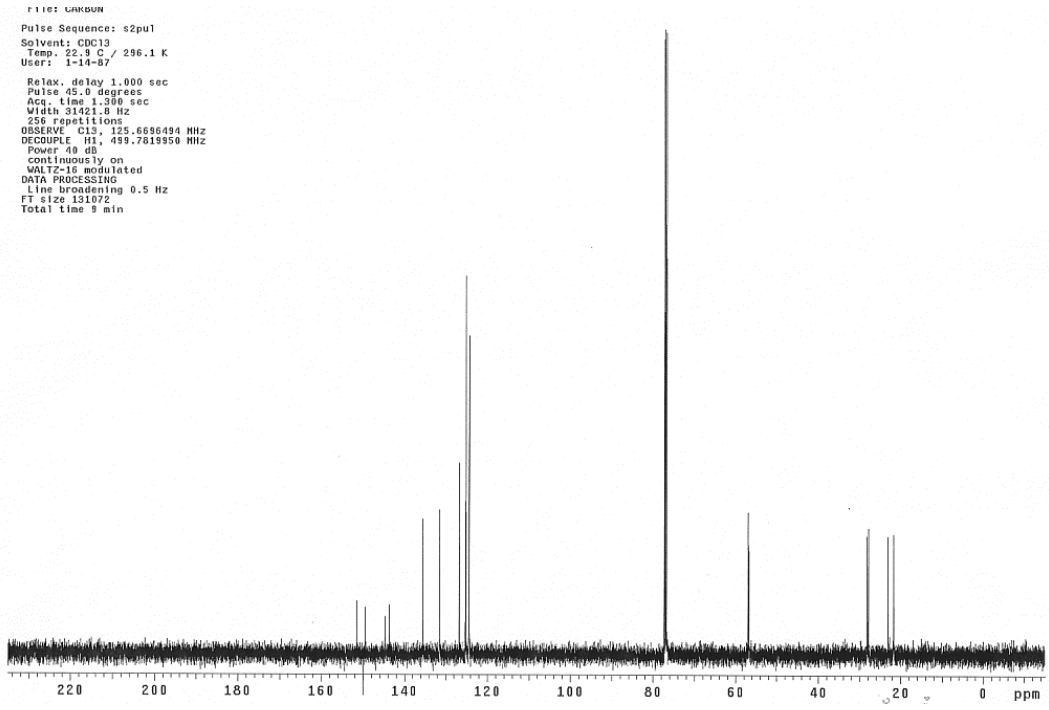

Benzyl 2-(2-nitrophenylsulfinyl)butanoate (1i)

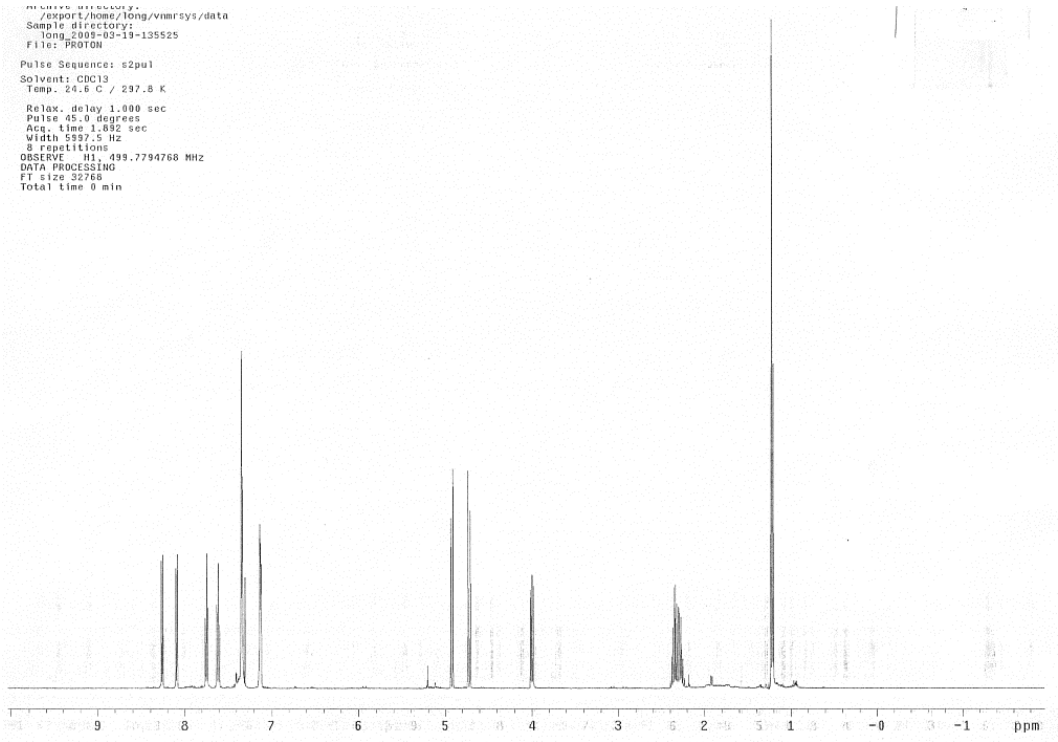

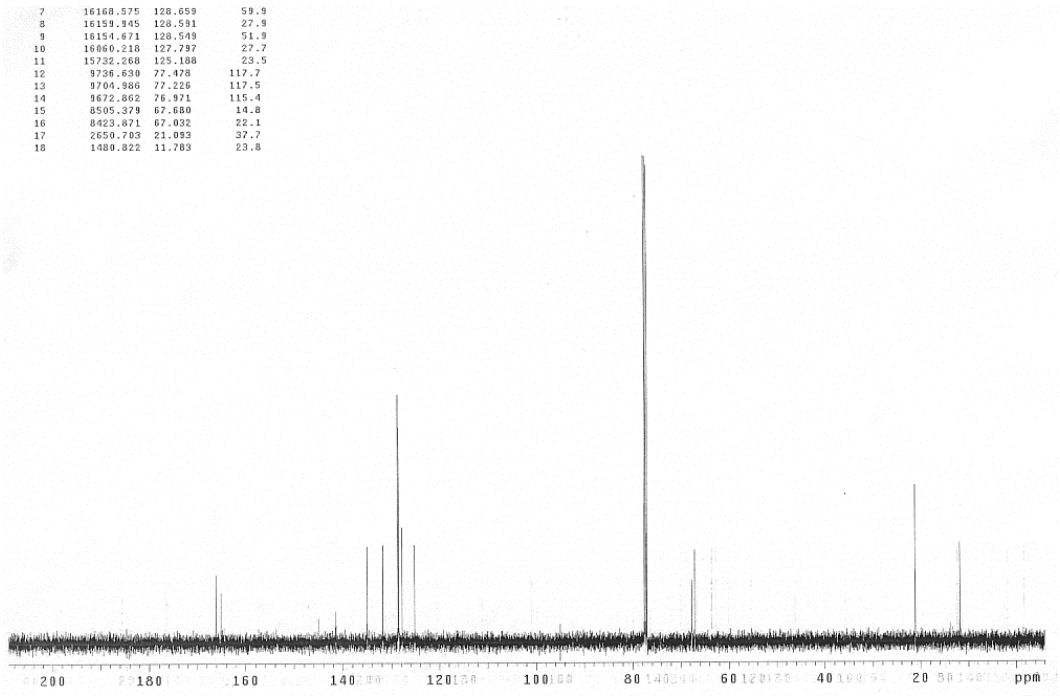

Benzyl 2-(2-nitrophenylsulfinyl)-3-methylbutanoate (1j)

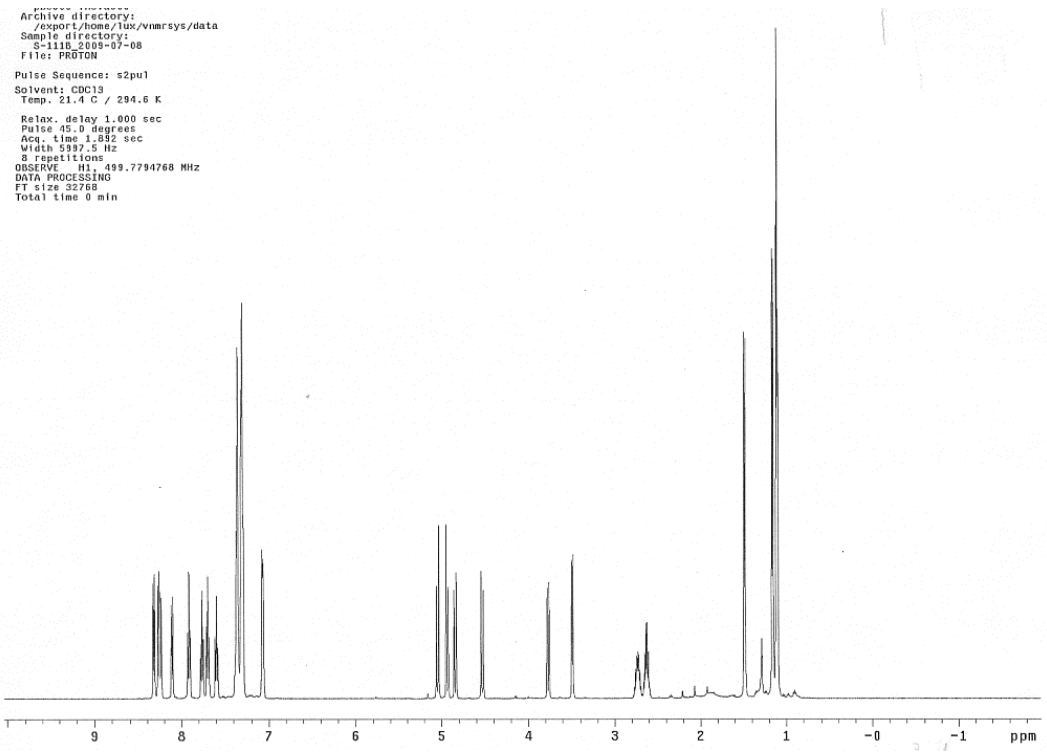

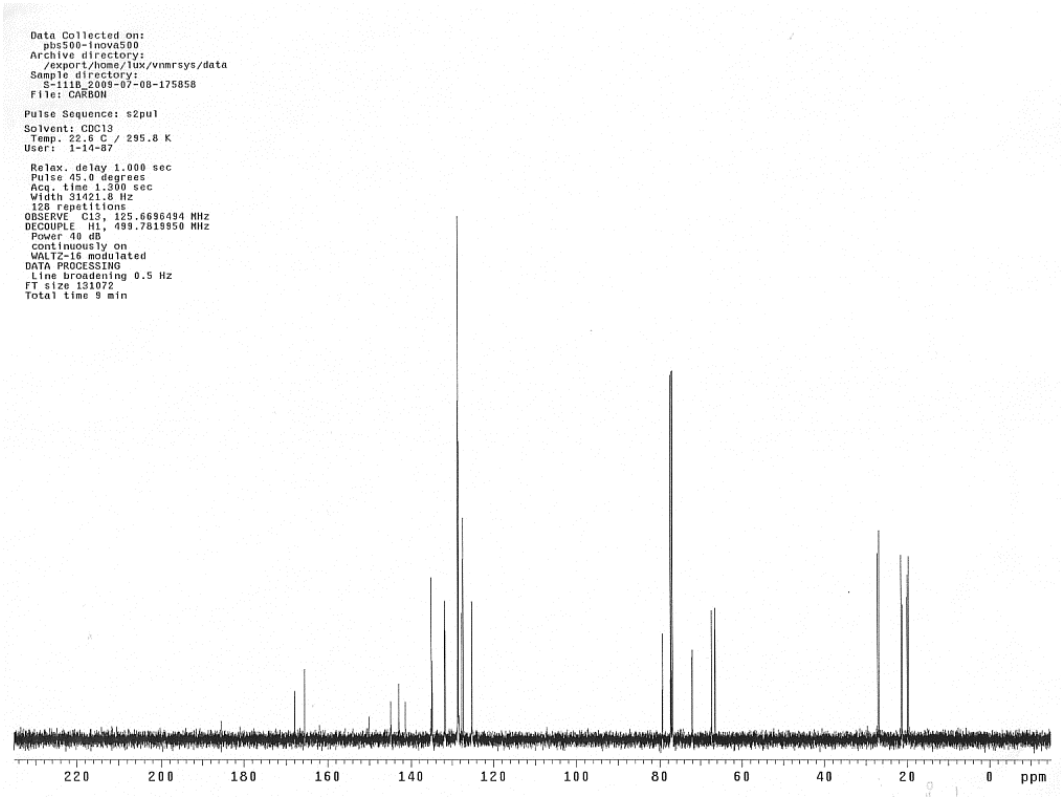

Benzyl 3-(2-nitrophenylsulfinyl)butanoate (1l)

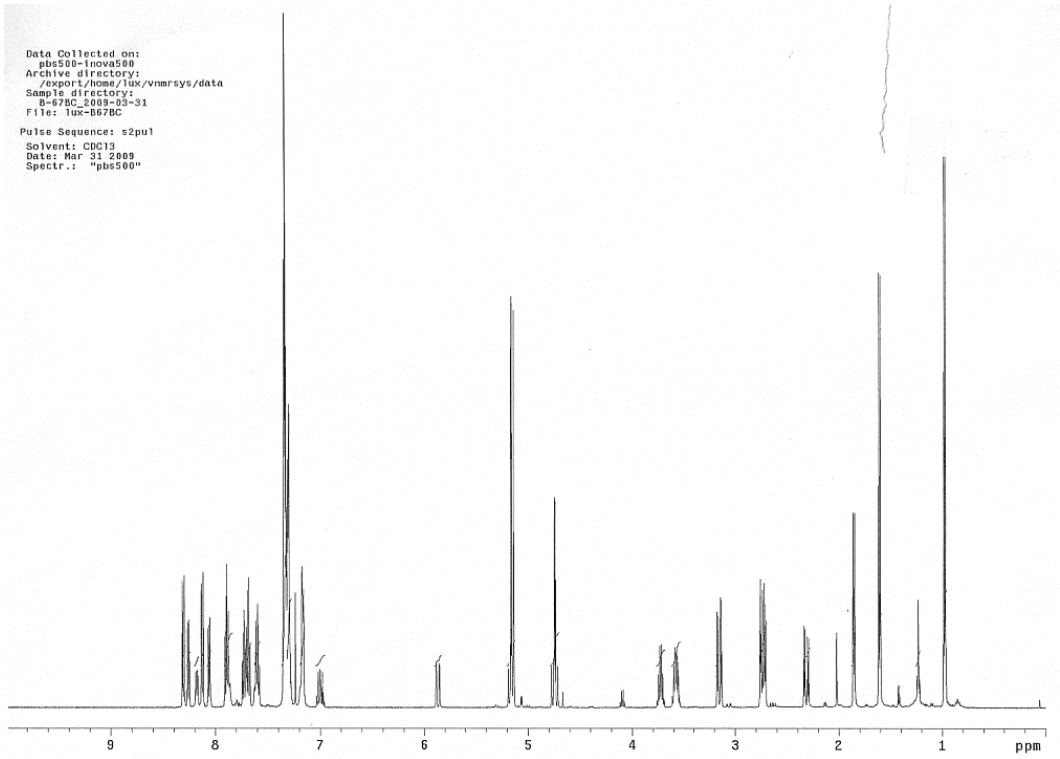

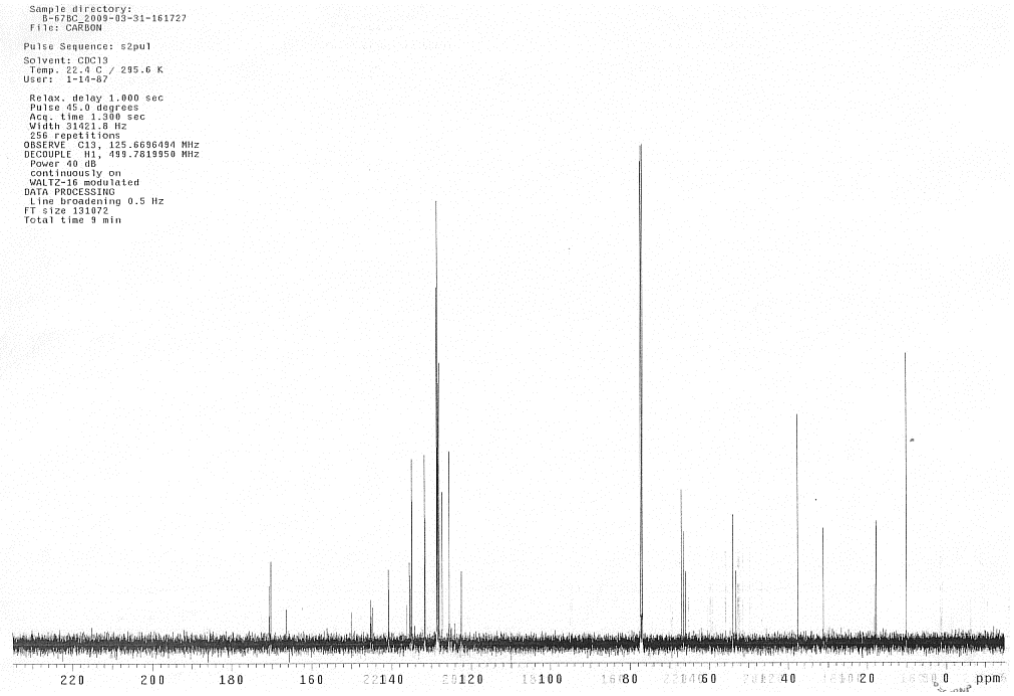

Benzyl 5-(2-nitrophenylsulfinyl)hexanoate (1m)

(±) *anti*-1m

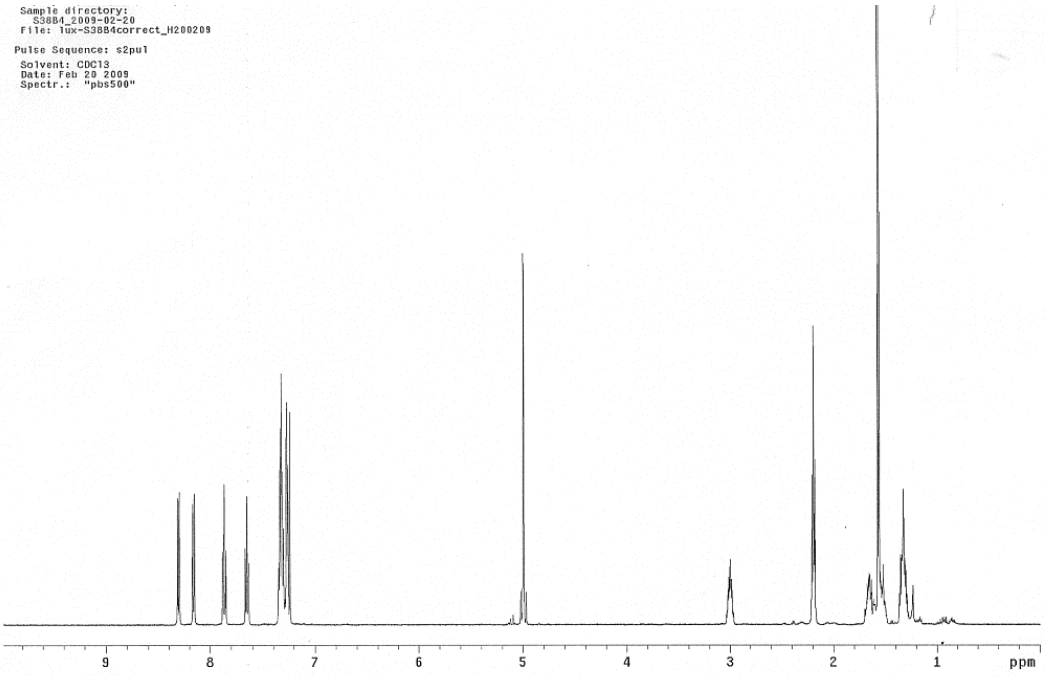

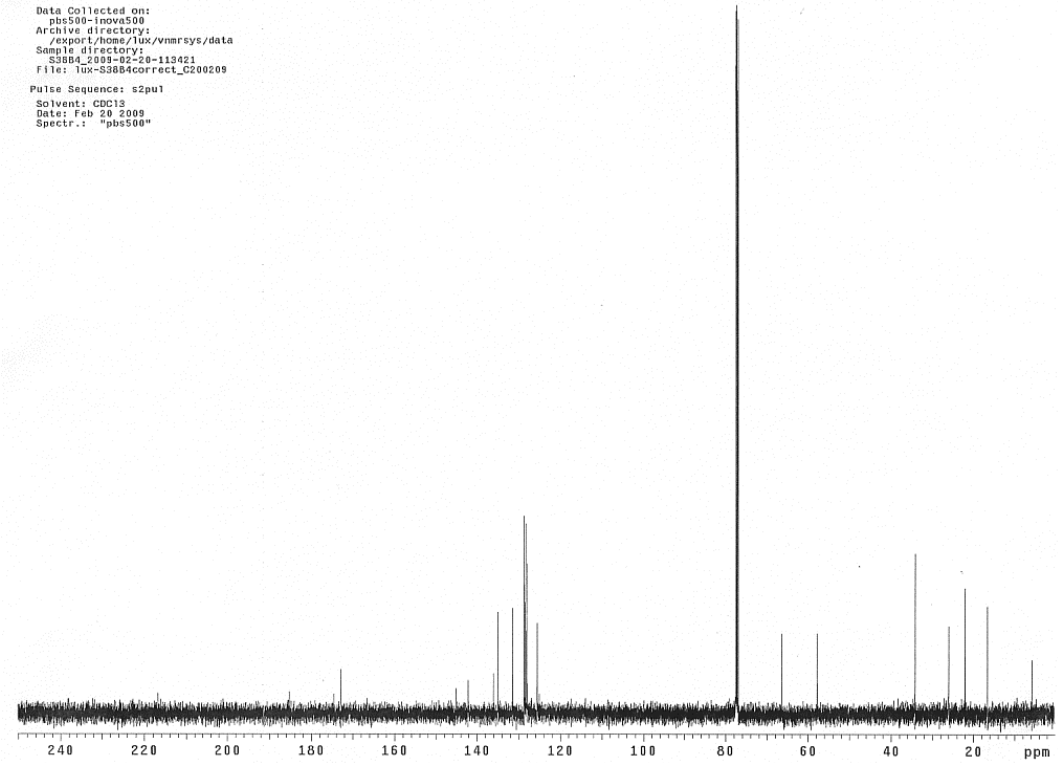

(±) *syn*-1m

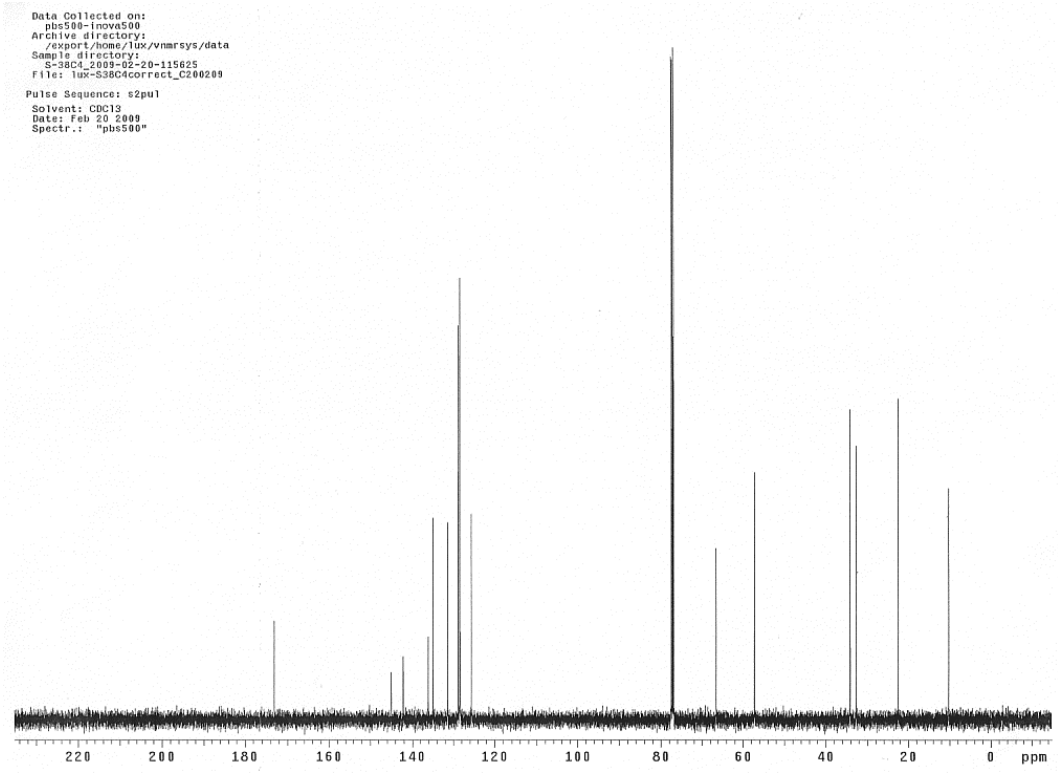
Data Collected on:
pbs500-inova500
Archive directory:
/export/home/lux/vnmrsys/data
Sample directory:
S-38C4_2009-02-20-115625
File: lux-S38C4correct_C200209
Pulse Sequence: s2pul
Solvent: CDCl3
Date: Feb 20 2009
Spectr.: "pbs500"
220
200
180
160
140
120
100
80
60
40
20
0
ppm

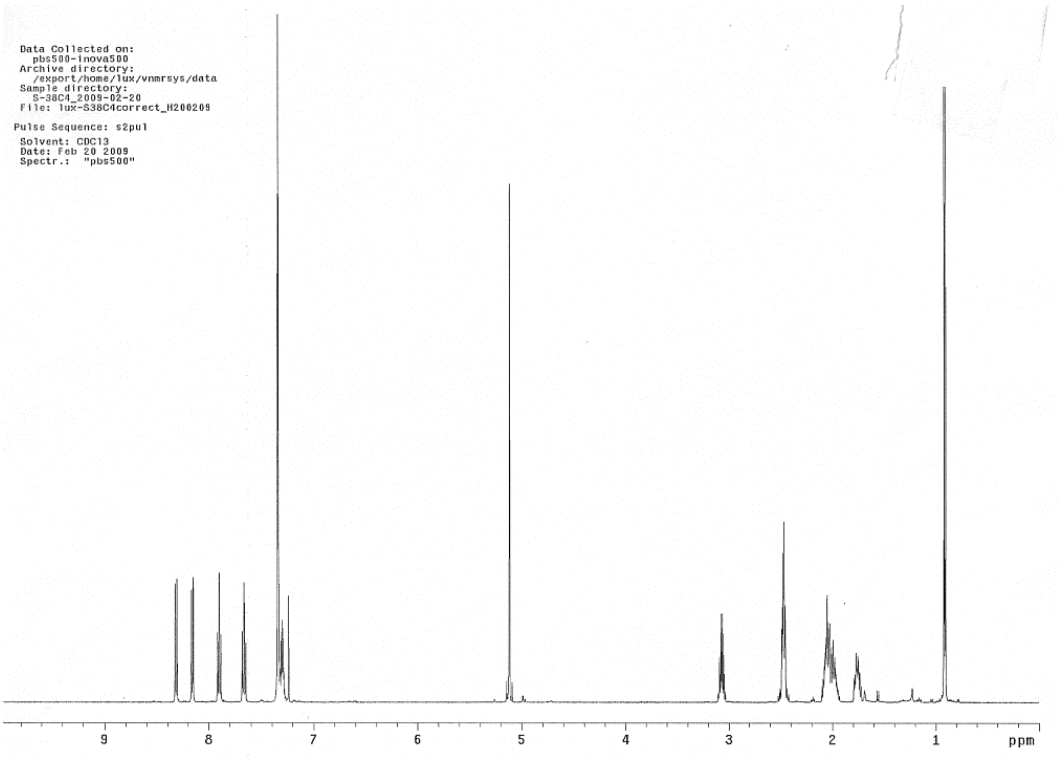
Data Collected on:
pbs500-inova500
Archive directory:
/export/home/lux/vnmrsys/data
Sample directory:
S-38C4_2009-02-20
File: lux-S38C4correct_H200209
Pulse Sequence: s2pul
Solvent: CDCl3
Date: Feb 20 2009
Spectr.: "pbs500"
9
8
7
6
5
4
3
2
1
ppm

Benzyl undec-10-enoate (4a)

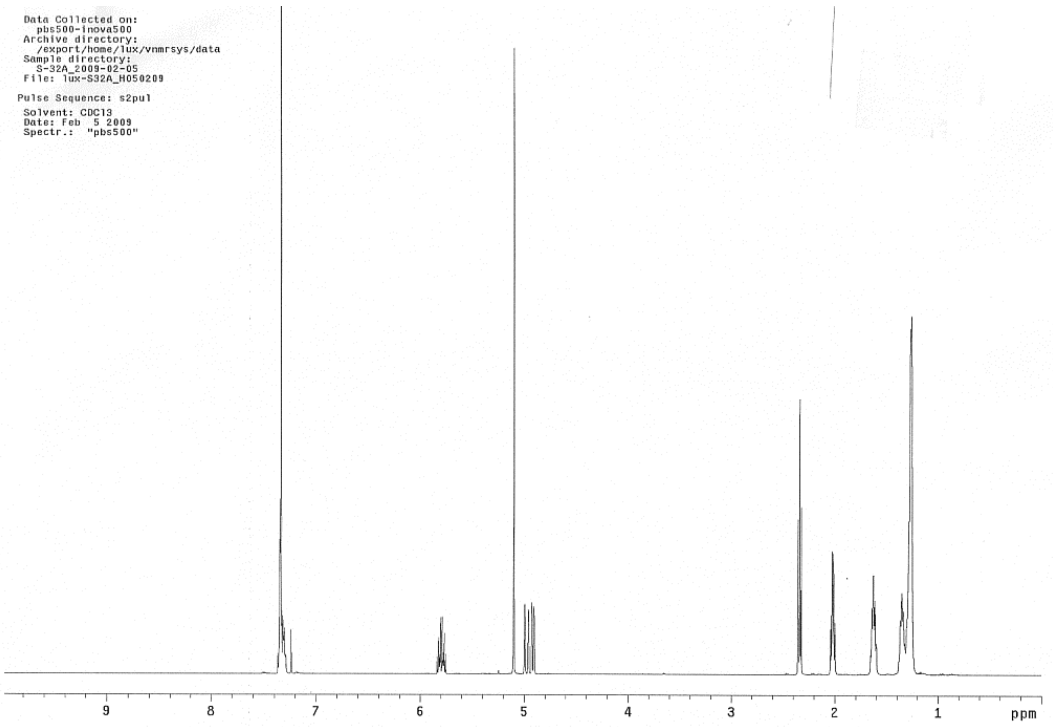

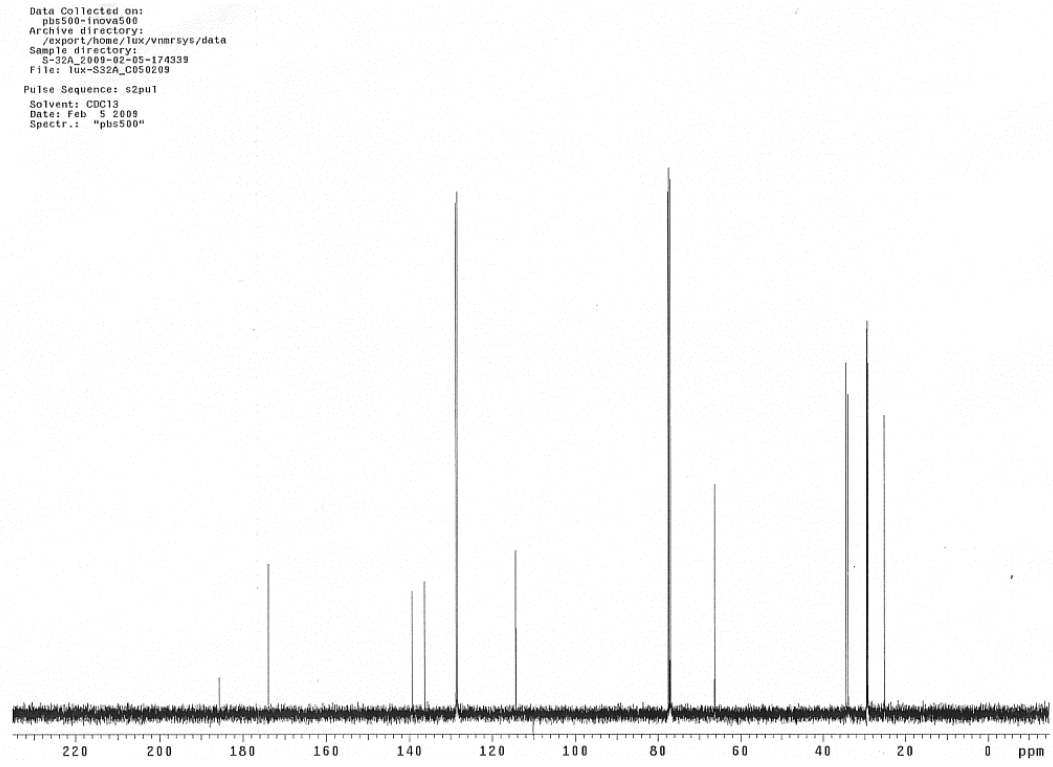

Benzyl pent-4-enoate (4b)

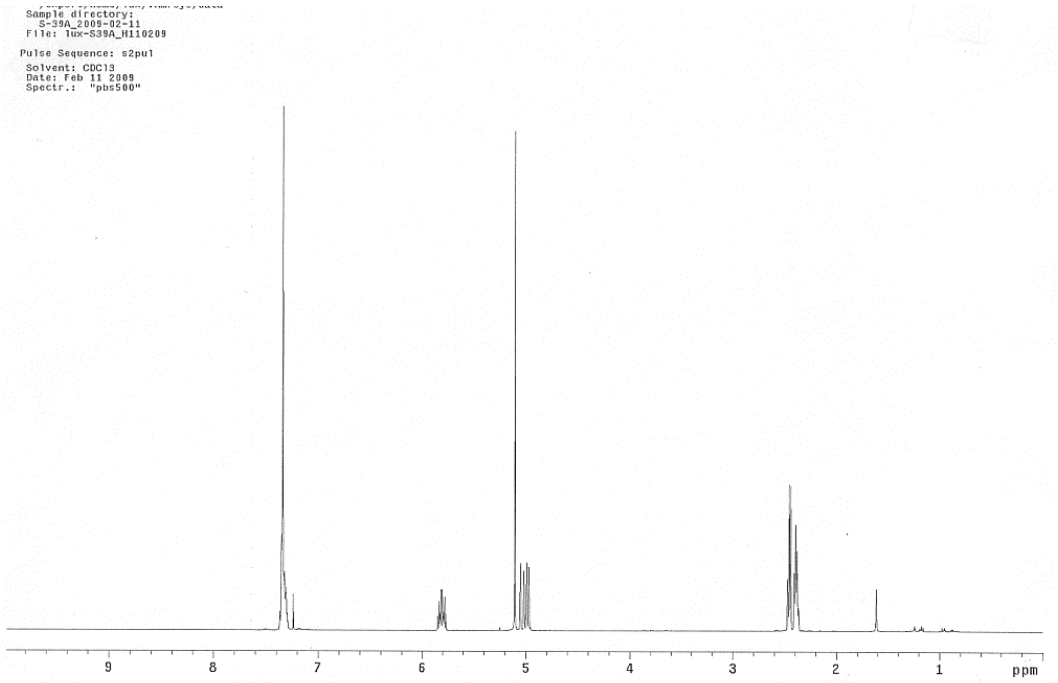

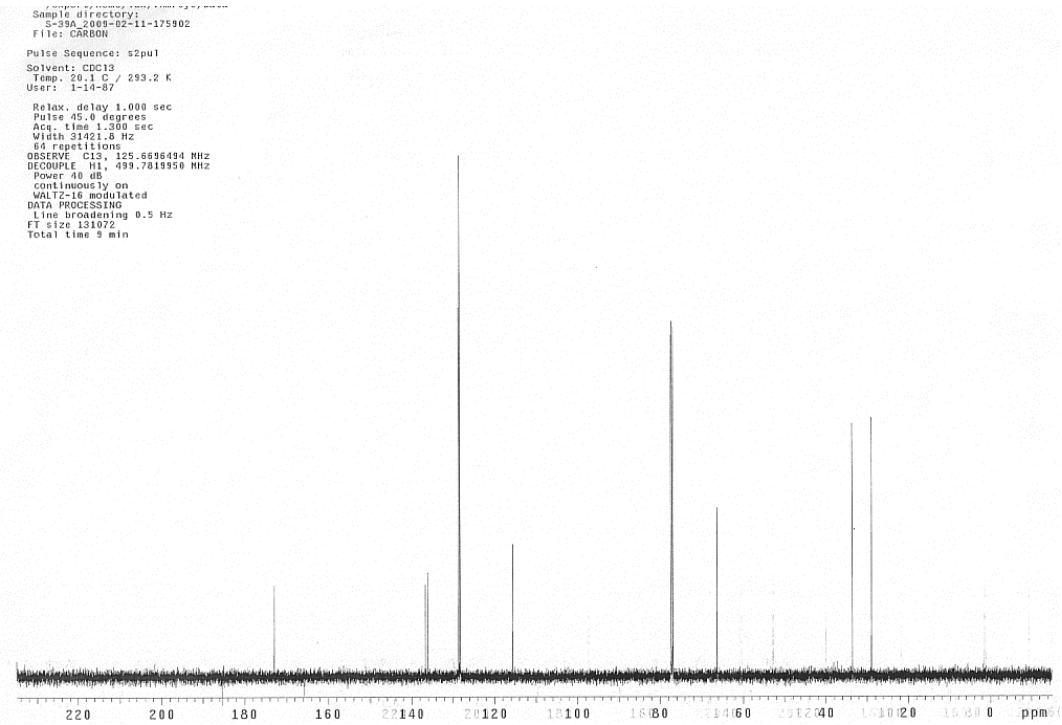

1-(Undec-10-enylsulfinyl)benzene (4c)

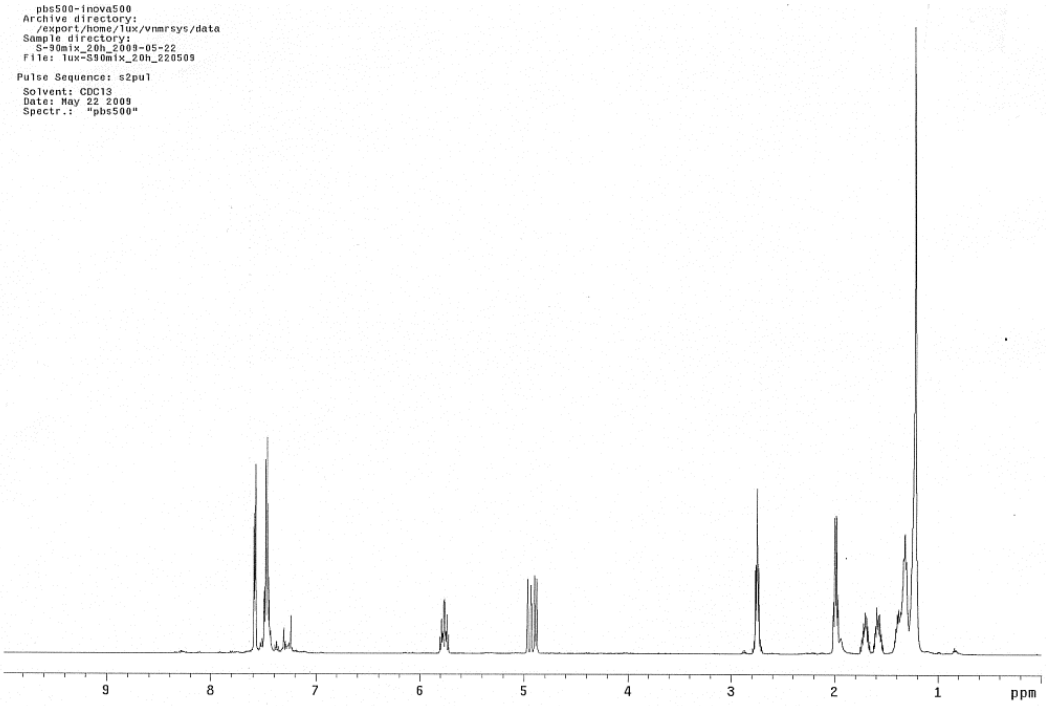

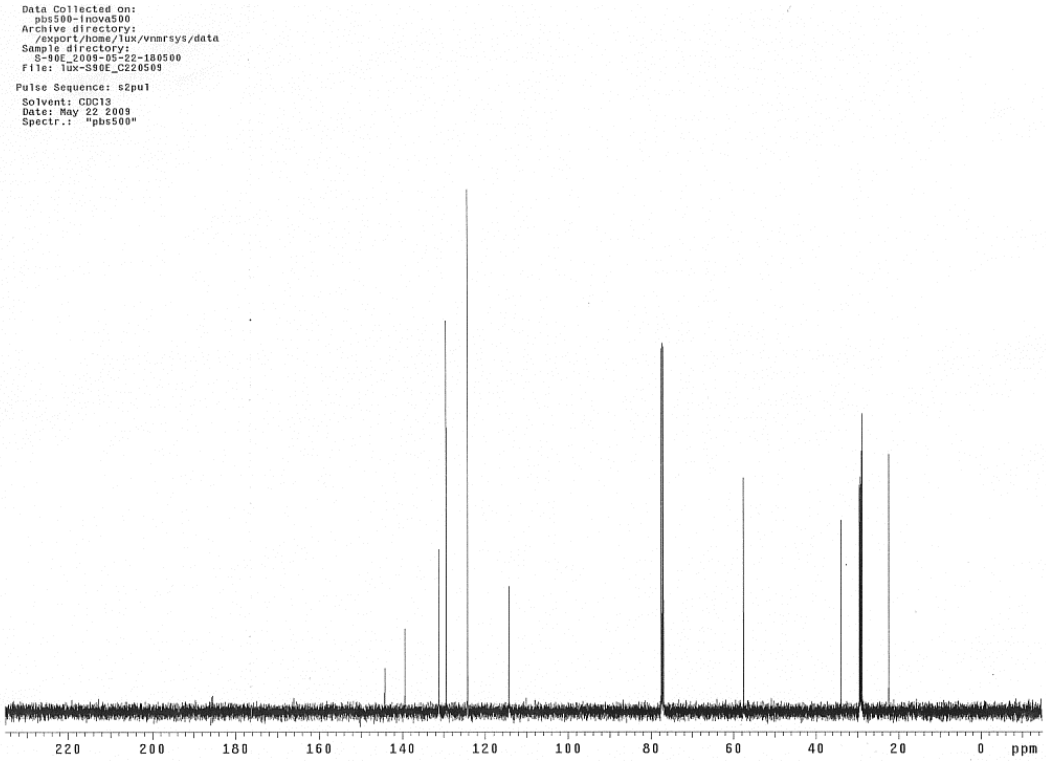

1-(Hex-5-enylsulfinyl)benzene ((*Z*)-4d)

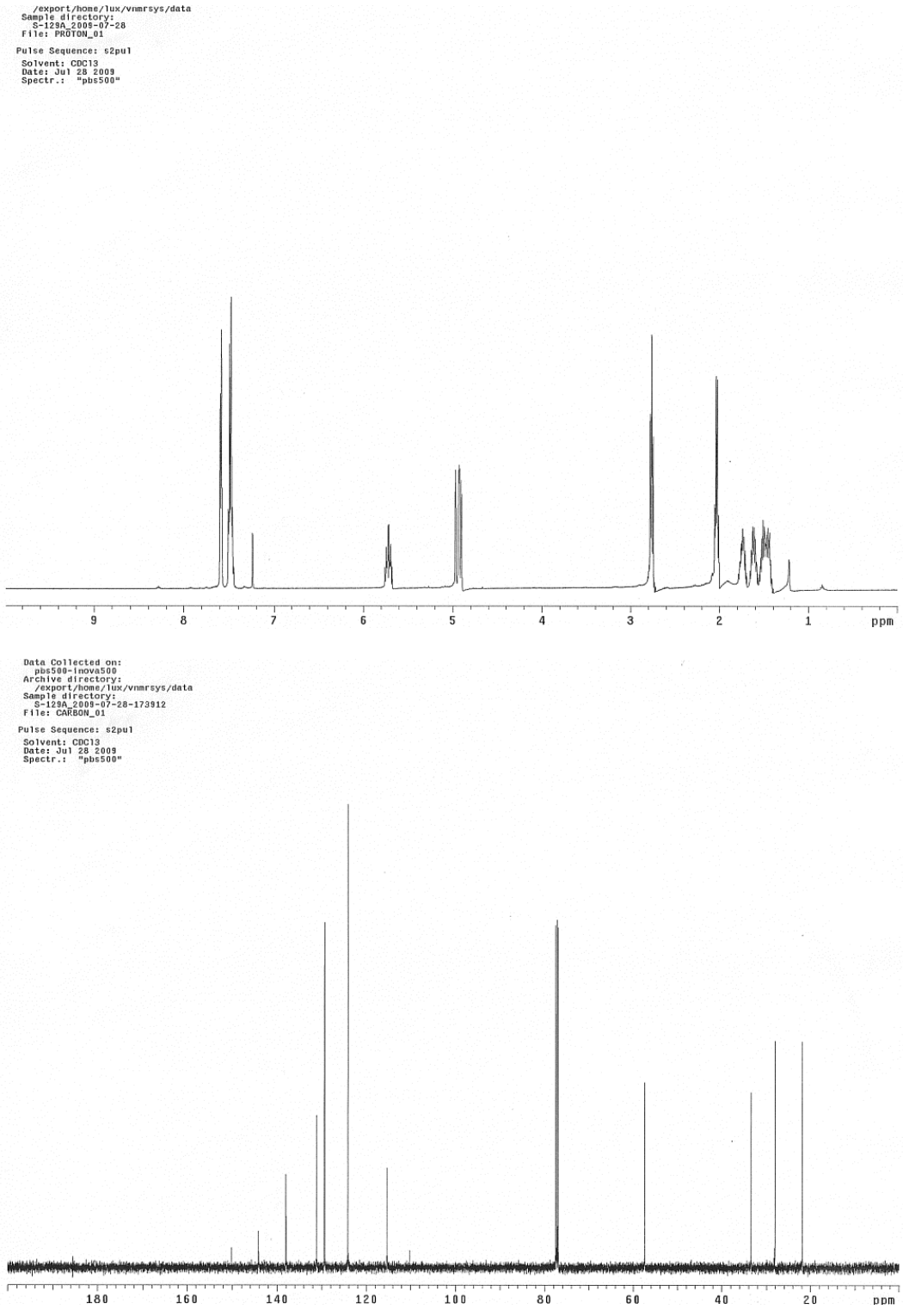

1-Methyl-4-(undec-10-enylsulfinyl)benzene (4e)

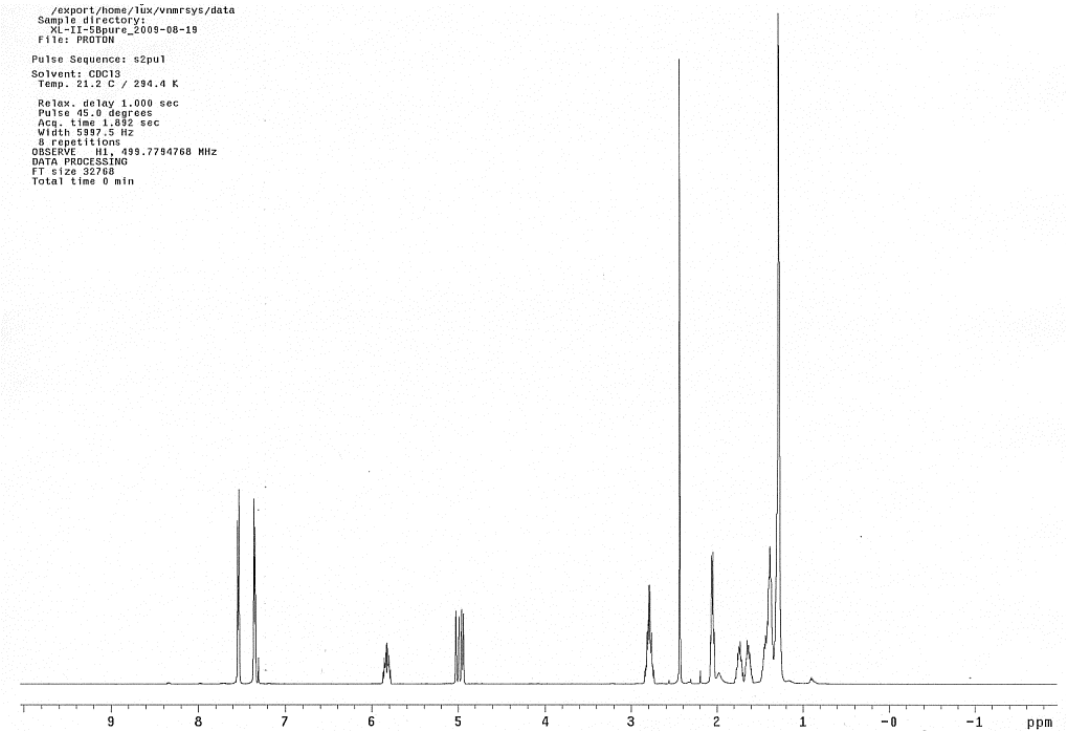

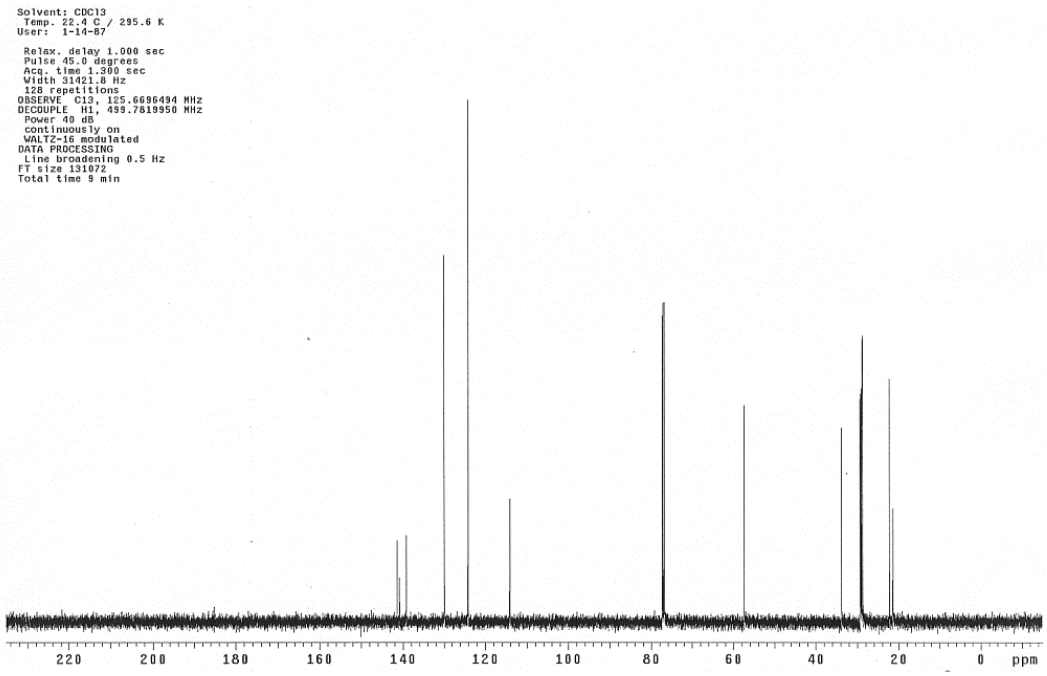

1-Chloro-4-(undec-10-enylsulfinyl)benzene (4f)

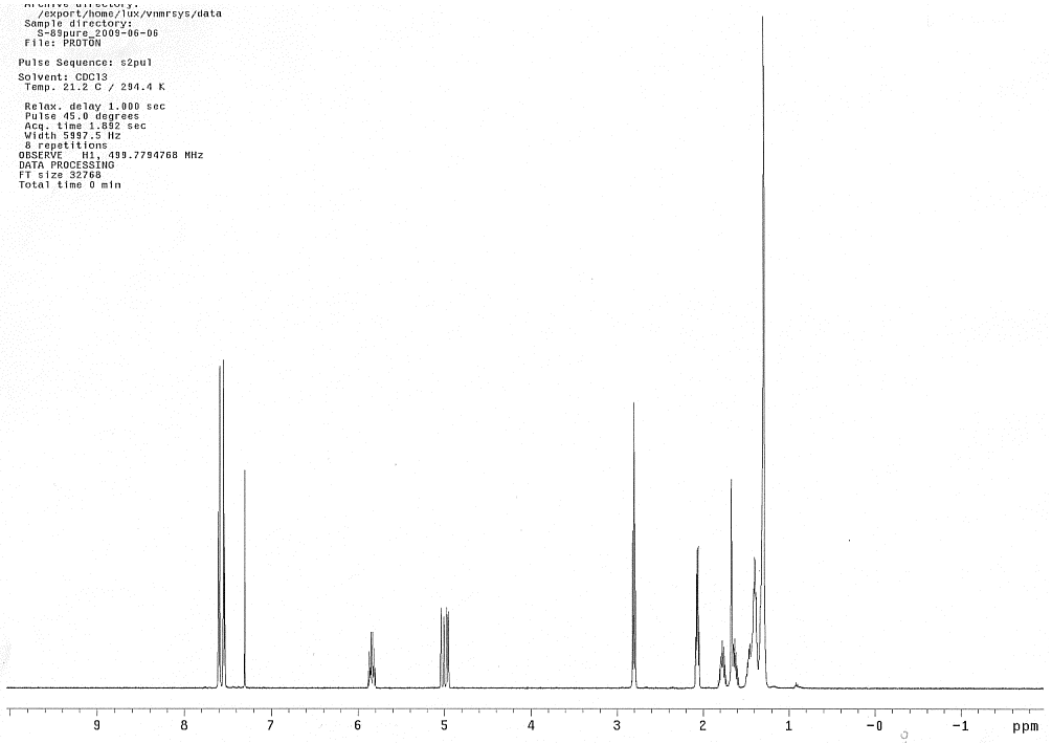

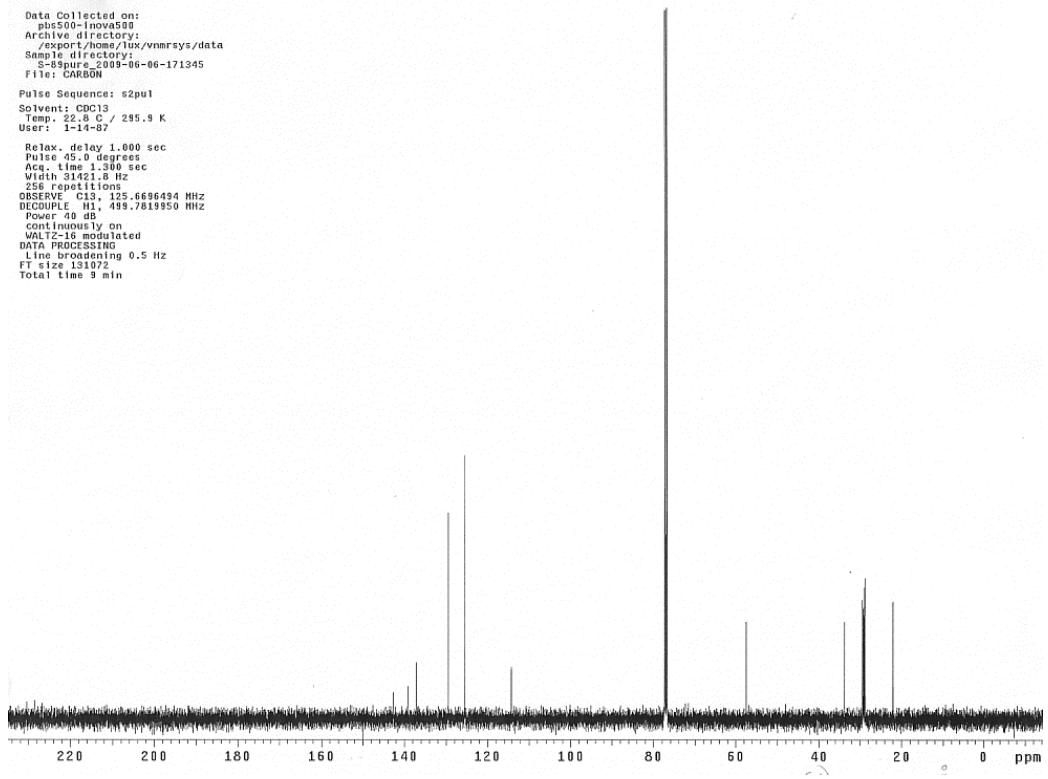

1-Nitro-4-(undec-10-enylsulfinyl)benzene (4g)

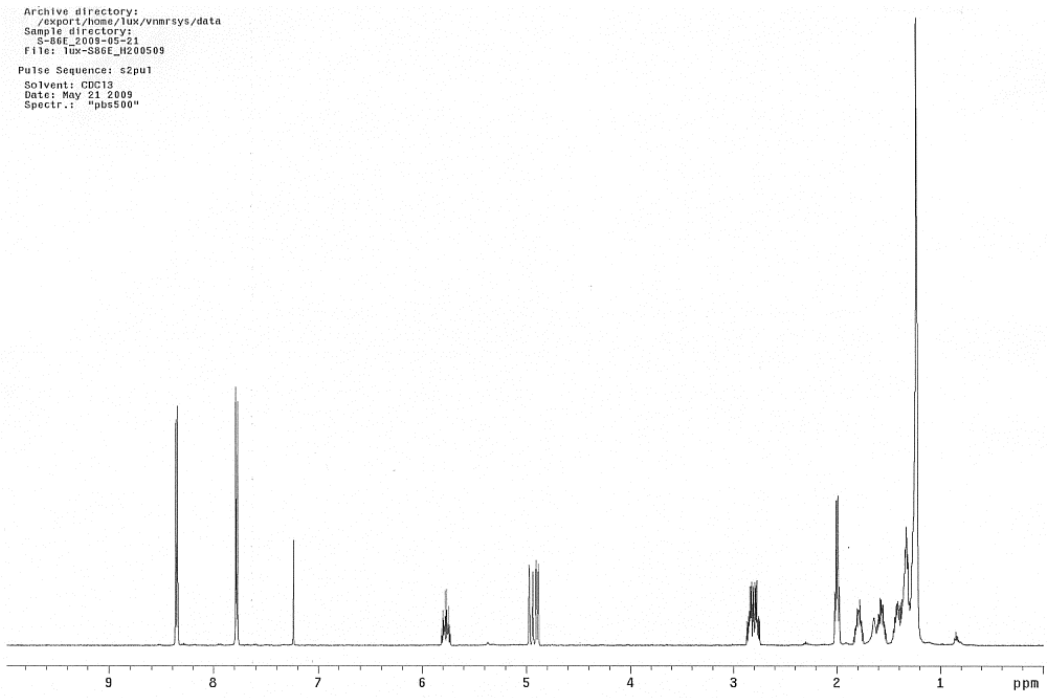

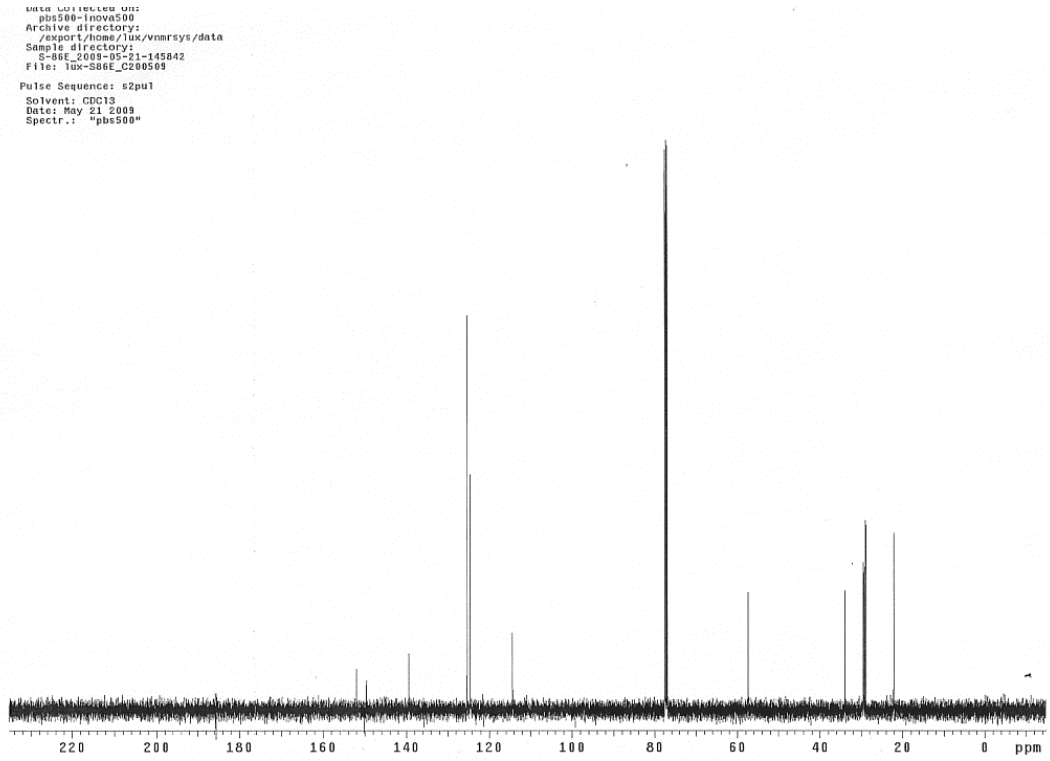

1-(Hex-5-enylsulfinyl)-4-nitrobenzene (4h)

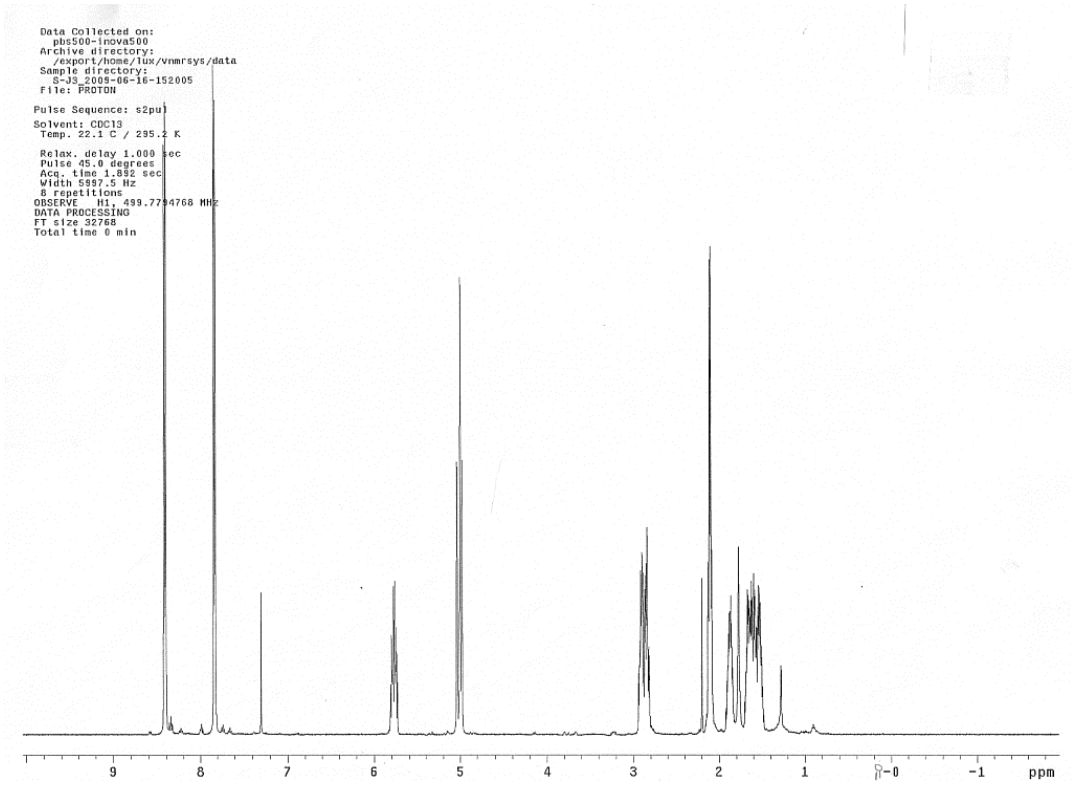

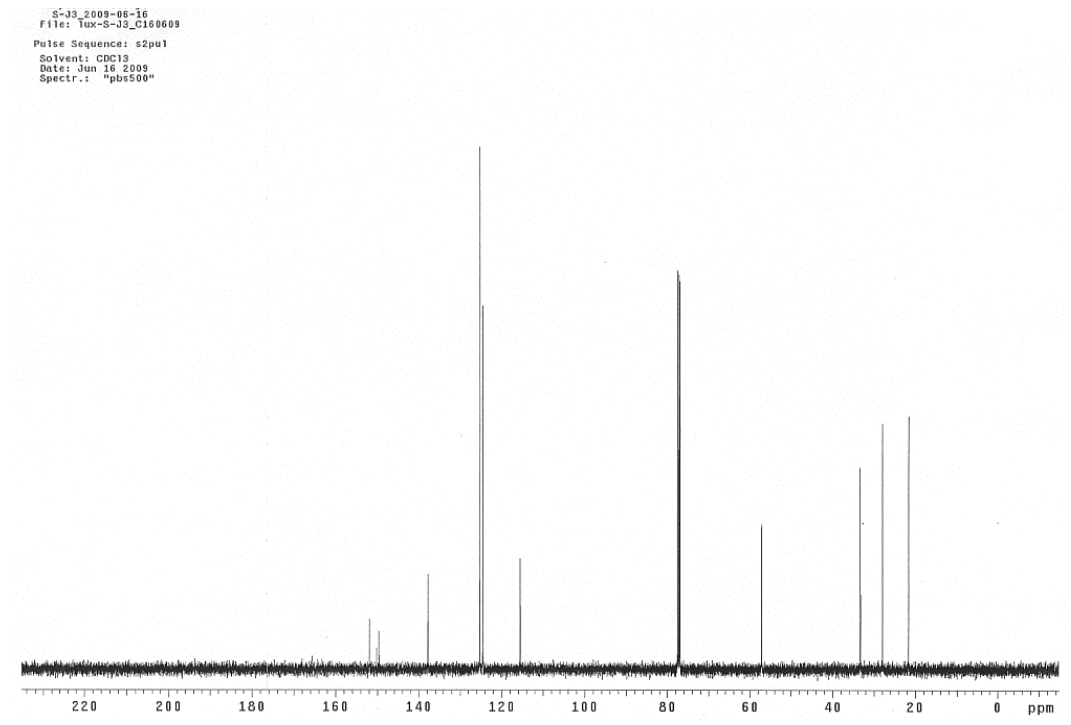

(*E*)-Benzyl but-2-enoate ((*E*)-4i)

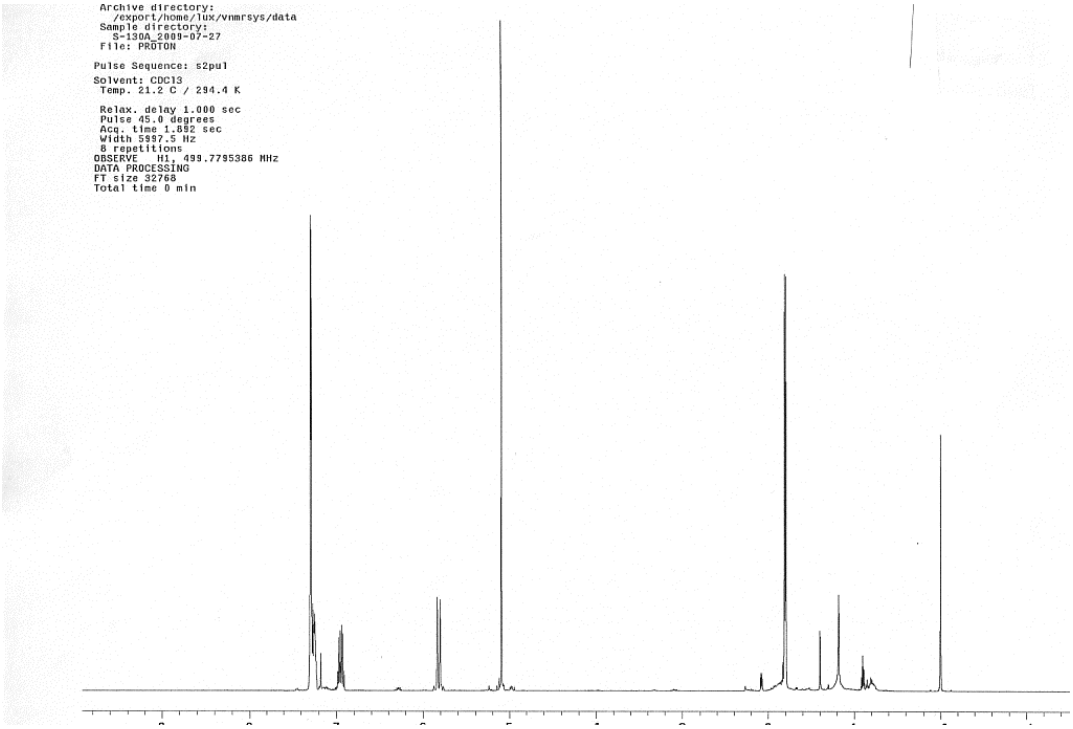

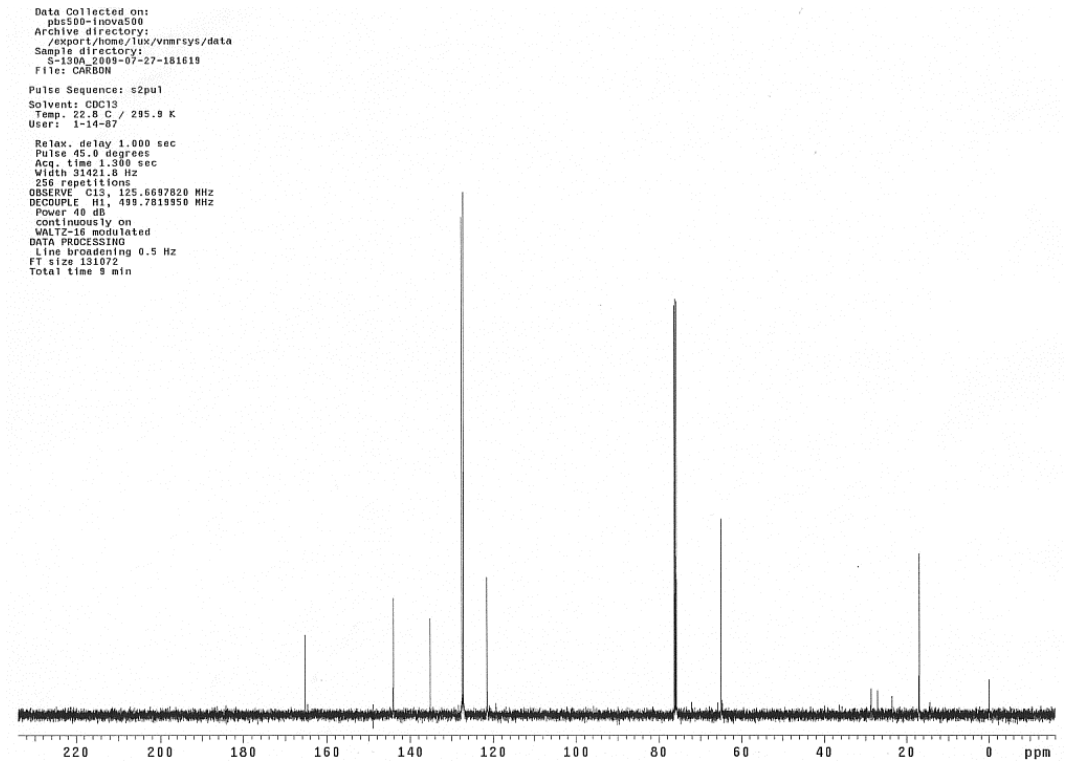

Benzyl 3-methylbut-2-enoate (4j)

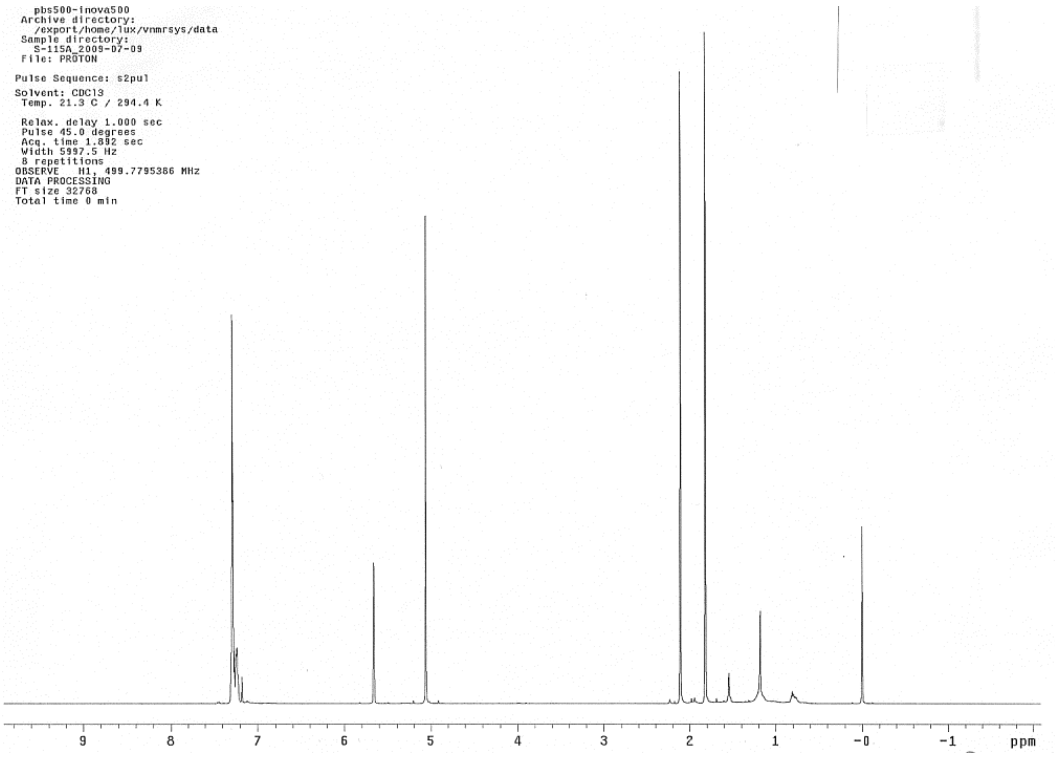

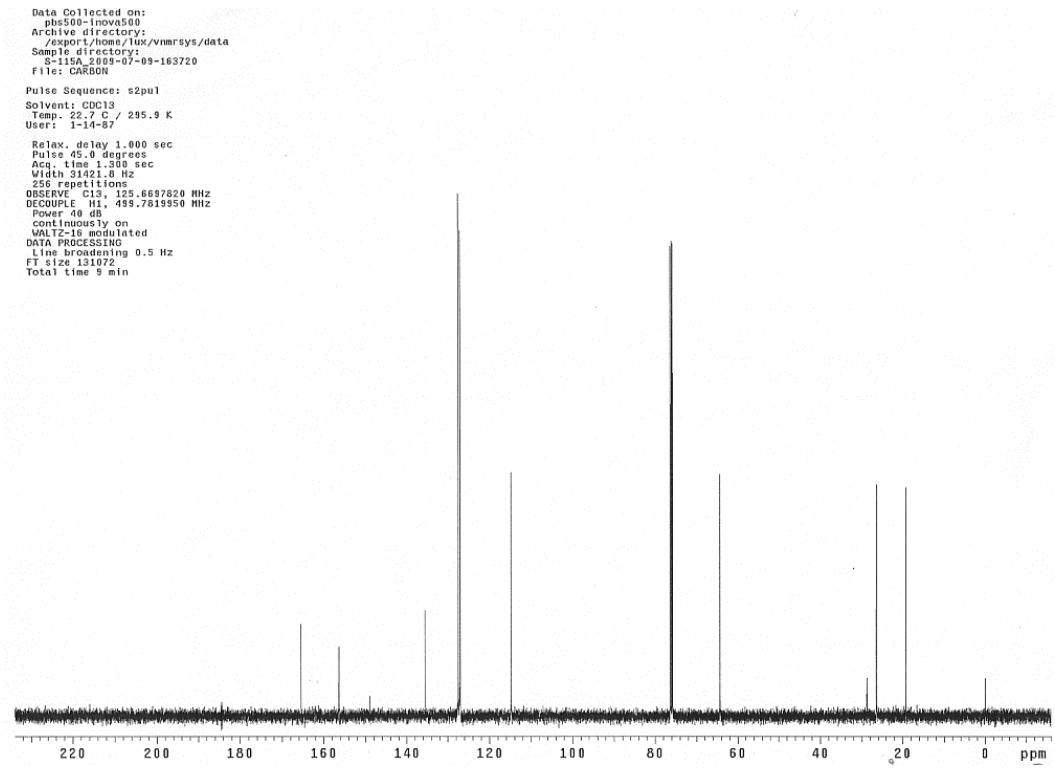

(*E*)-Benzyl cinnamate ((*E*)-4k)

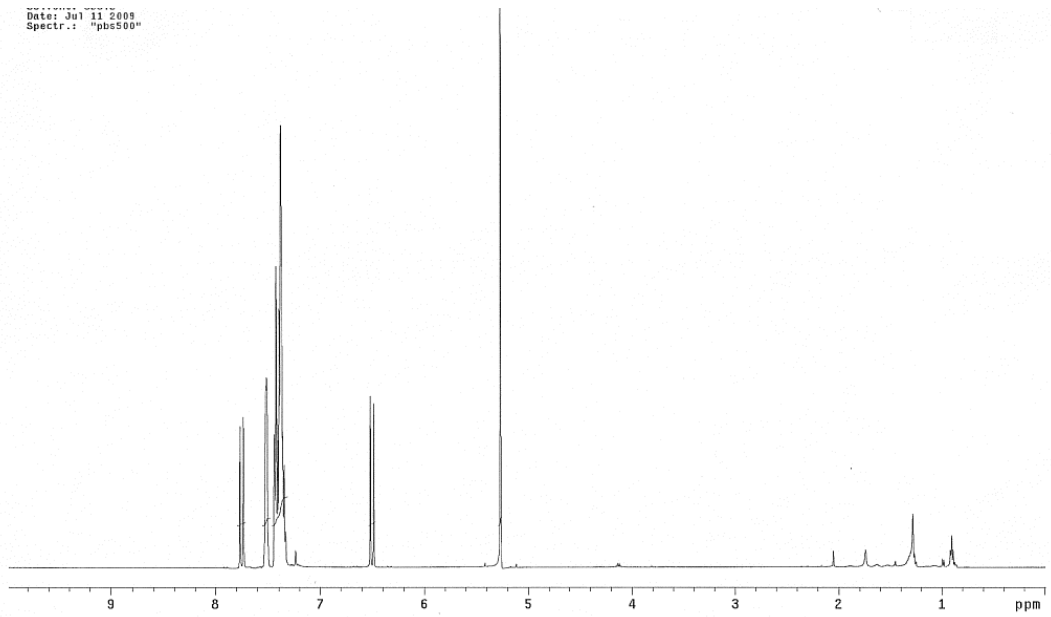

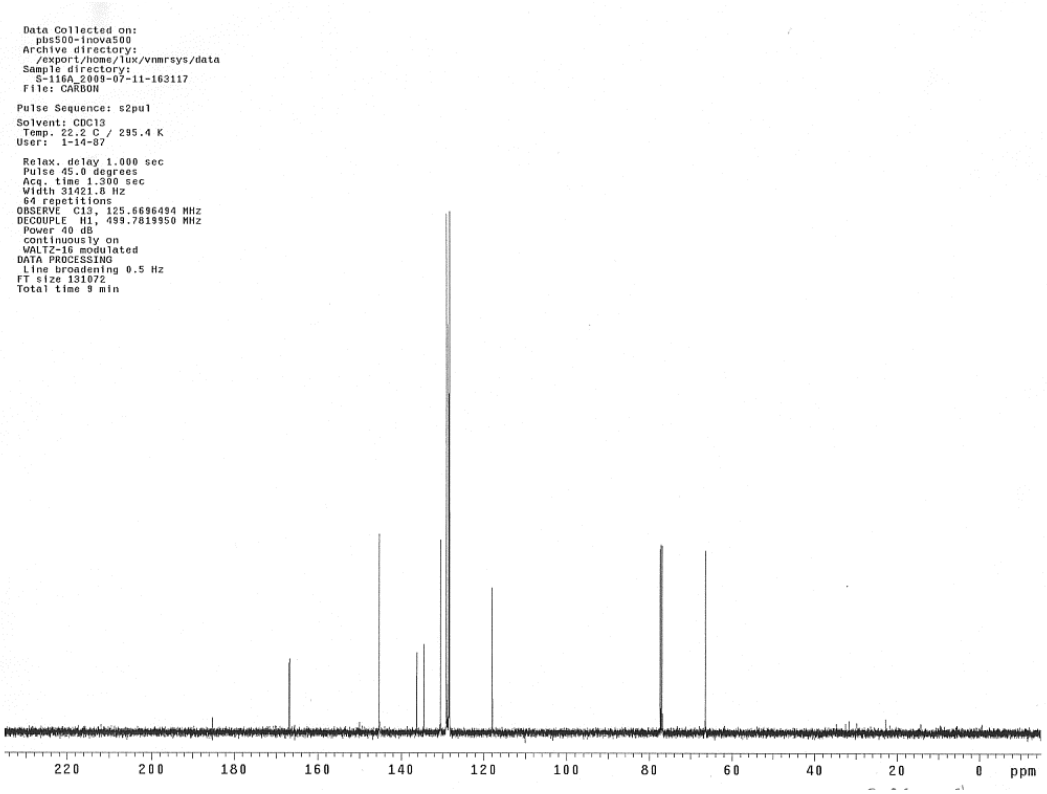

Benzyl hexenoate 4m

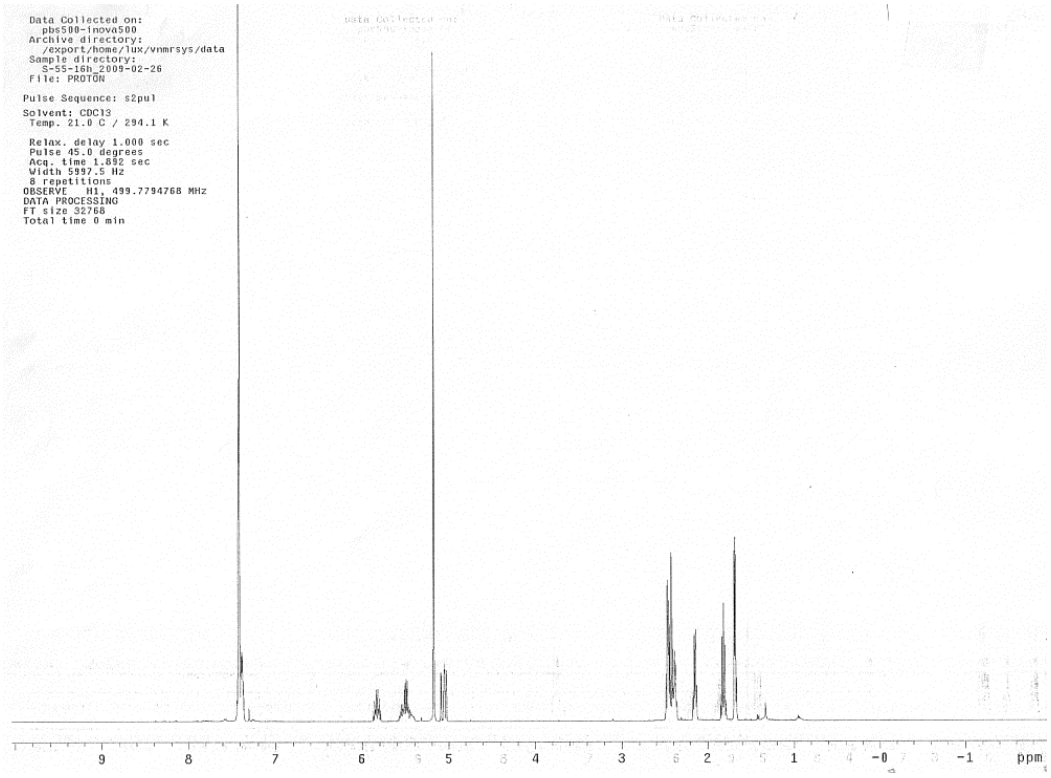

2-Phenylhex-5-ynoic acid (9)

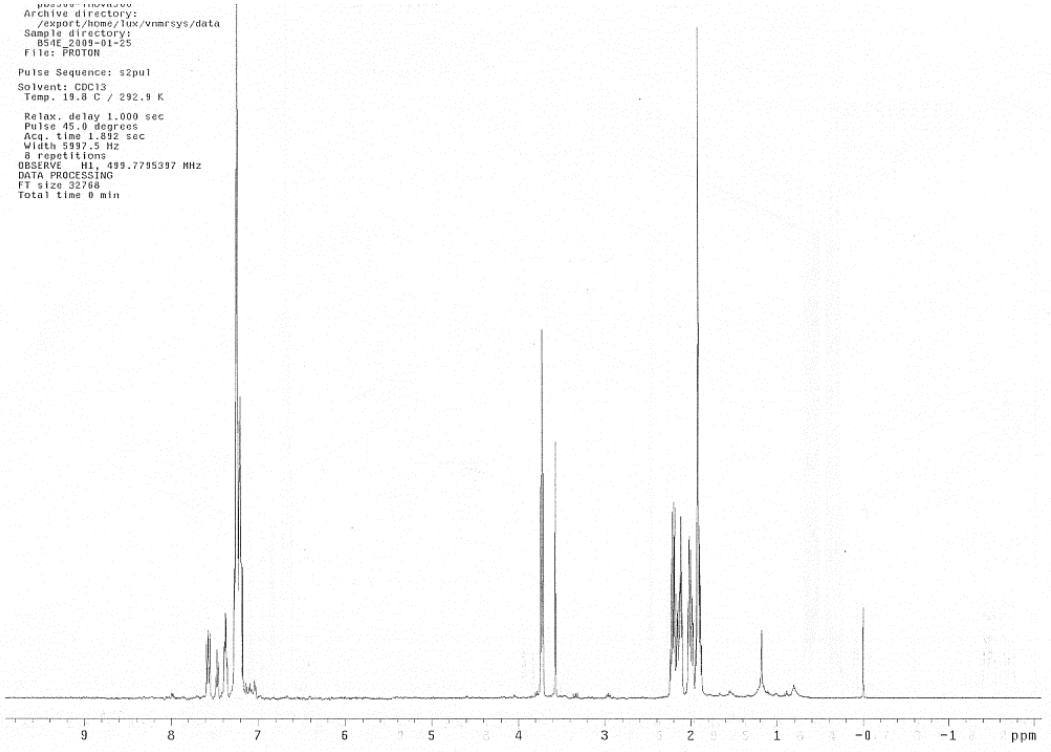

(*E*)-6-(Bromomethylene)-tetrahydro-3-phenylpyran-2-one (6)

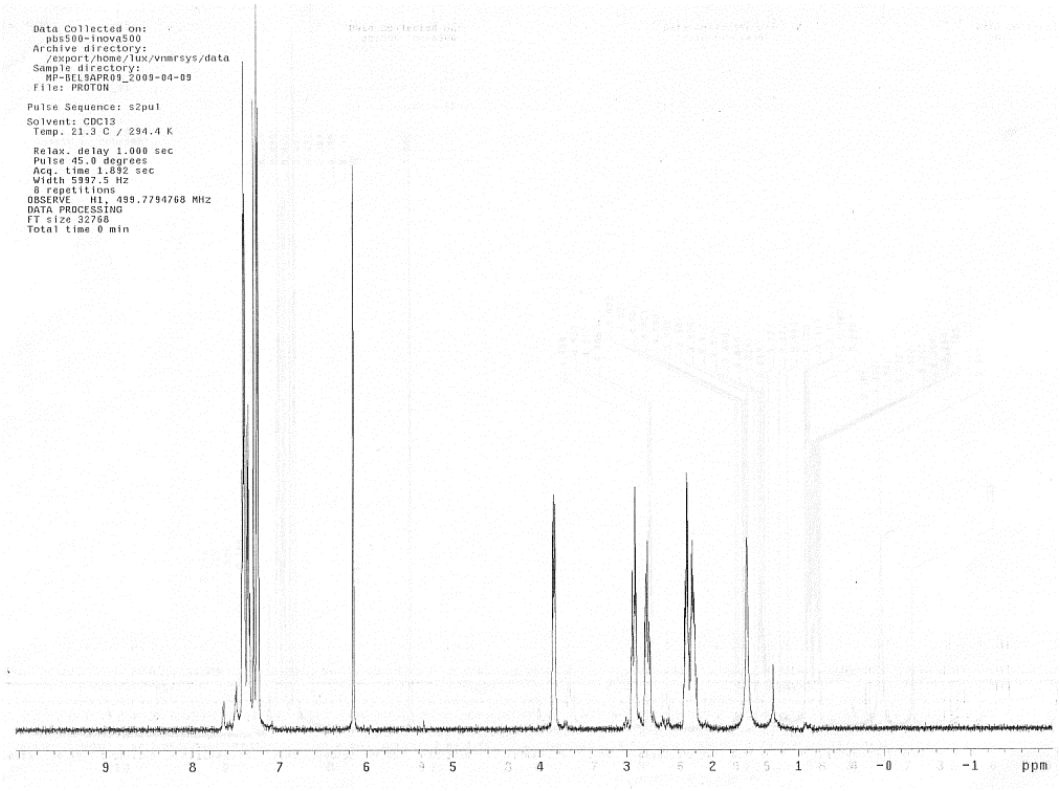

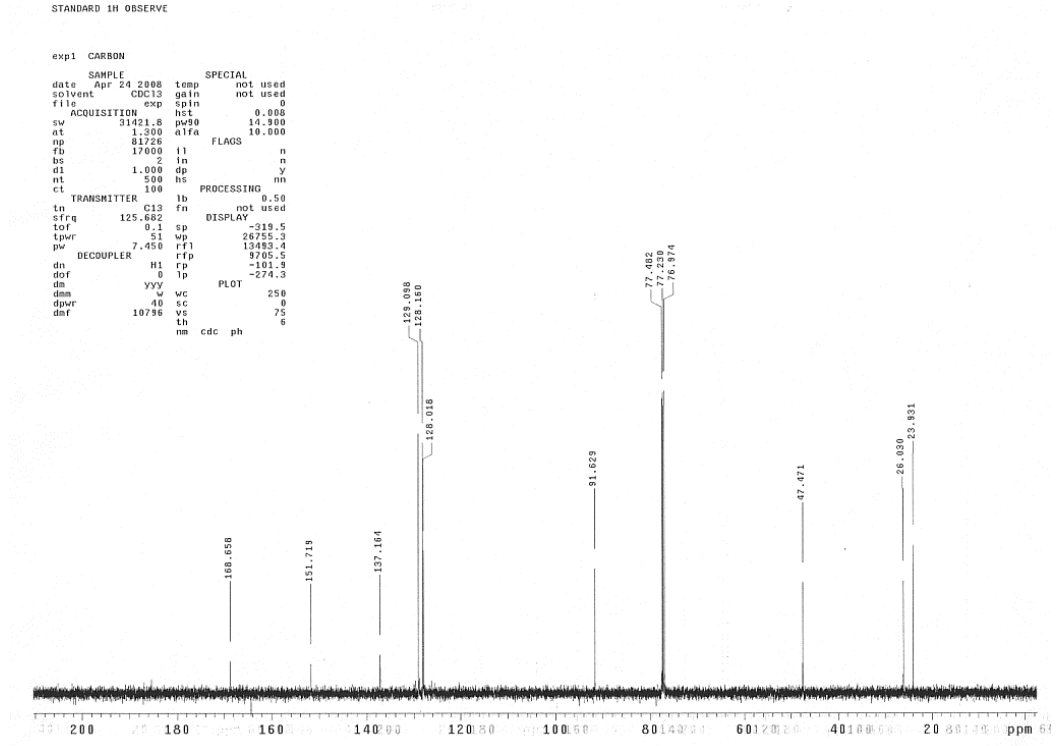

Methyl 2-(9,10-dihydro-9,10-dioxoanthracen-5-yl)acetate (11)

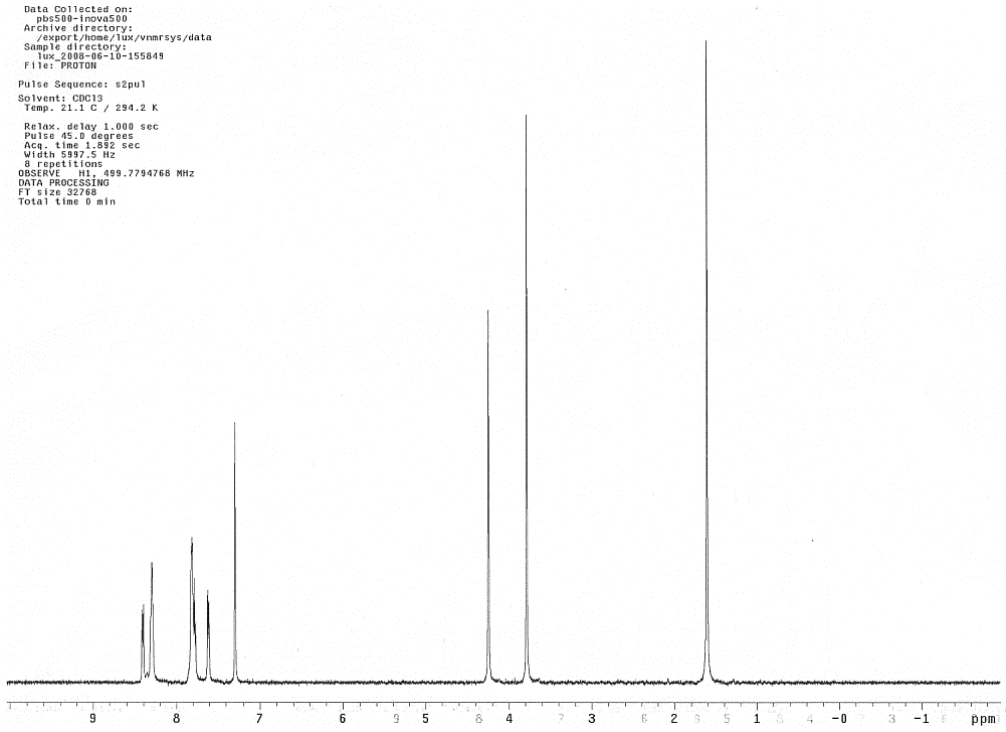

2-(Anthracen-5-yl)acetic acid (13)

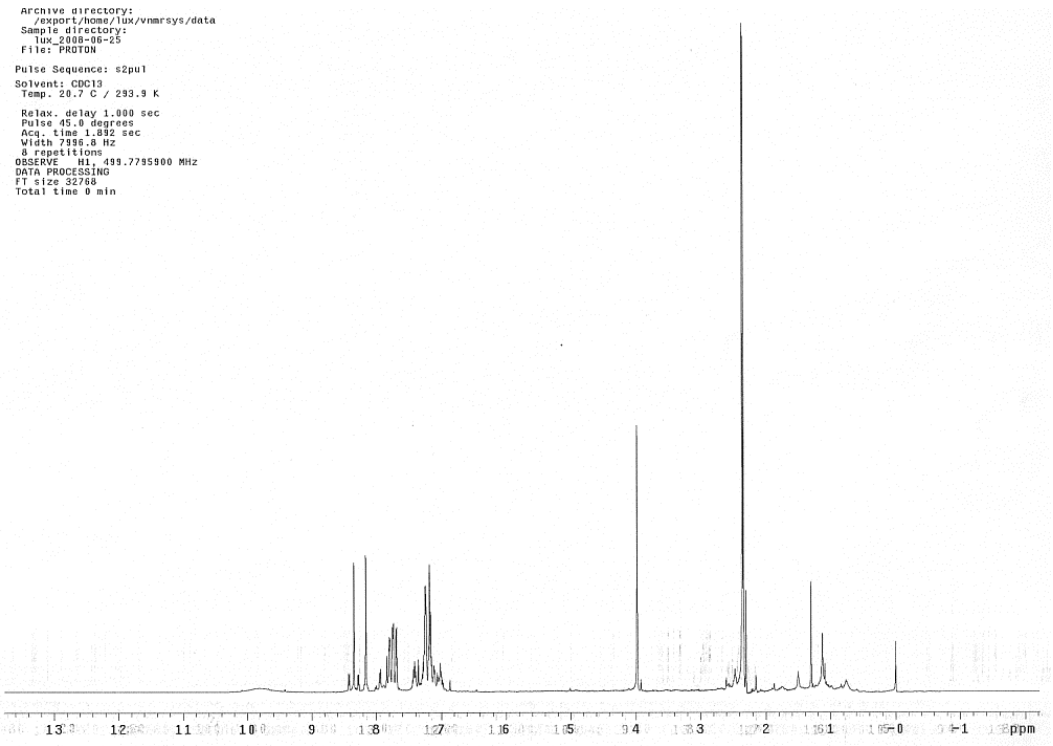

tert-Butyl 2-(prop-2-ynyloxy)acetate (15)

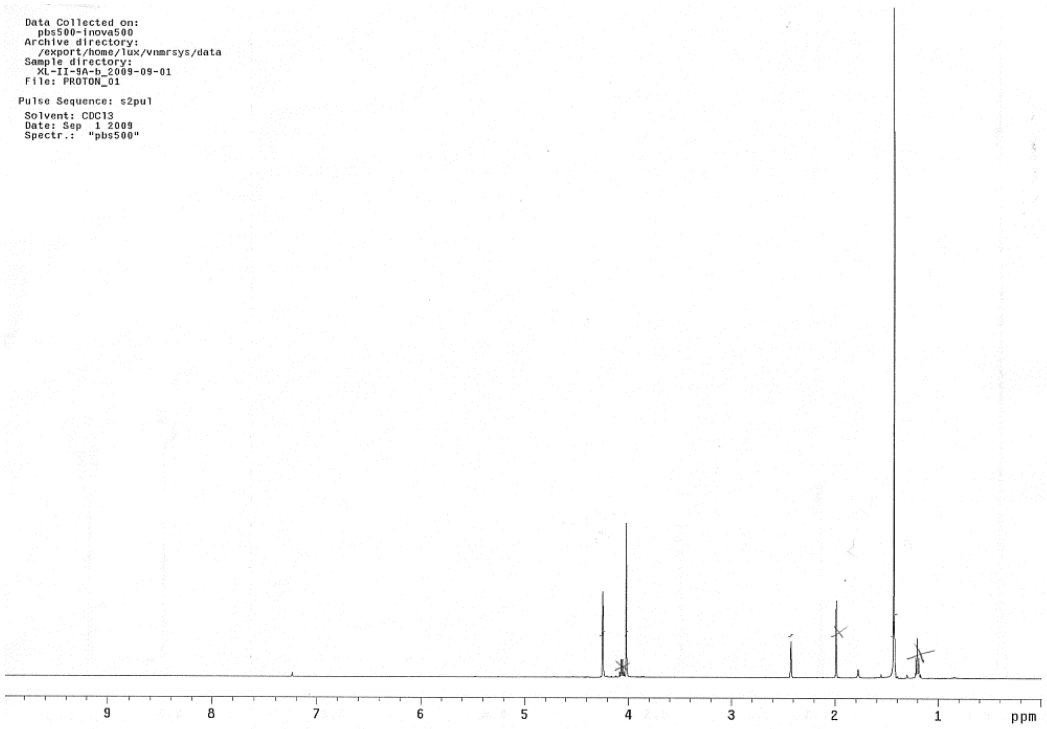

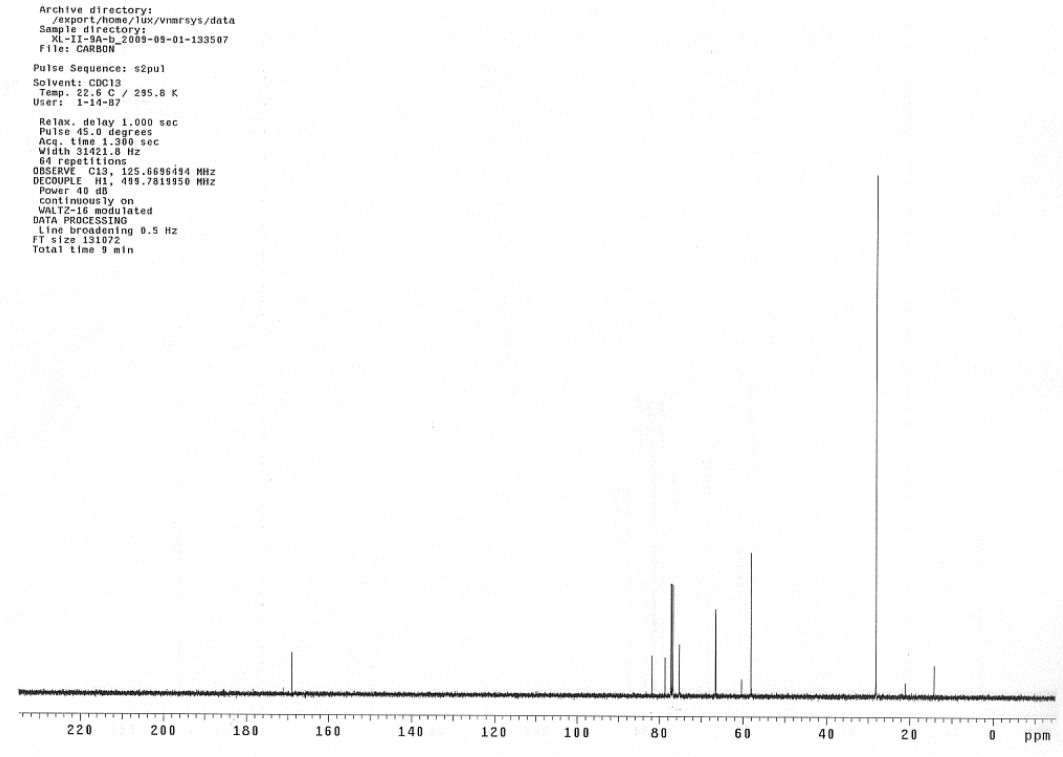

2-(Prop-2-ynyloxy)acetic acid (16)

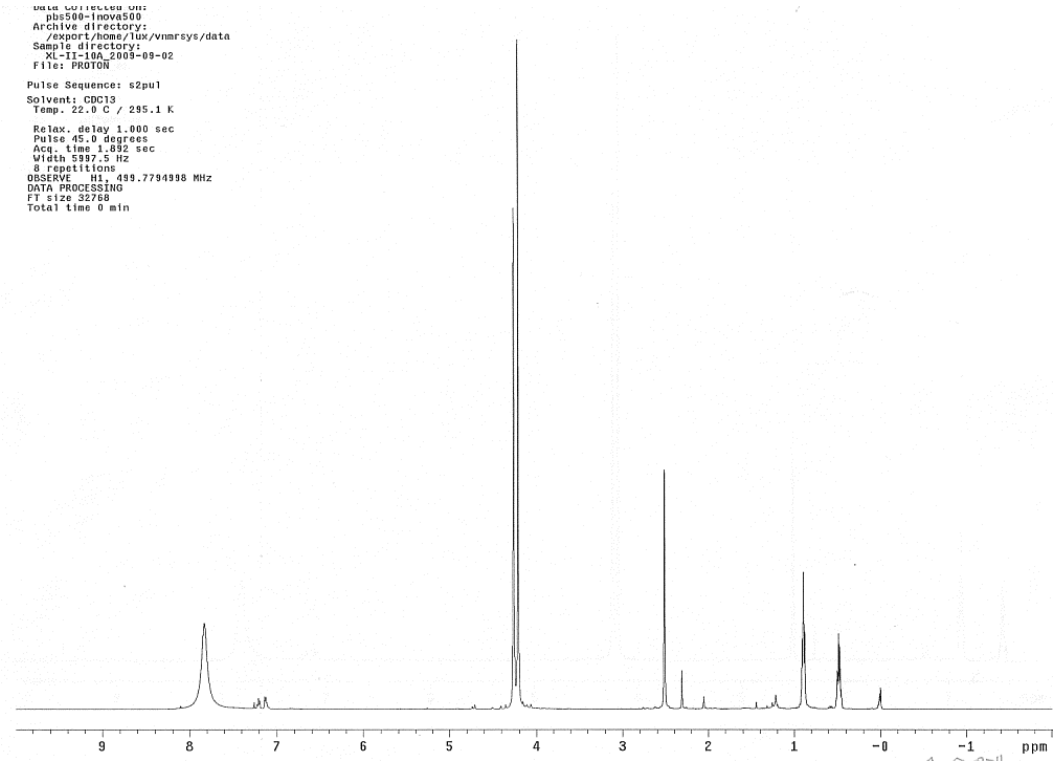

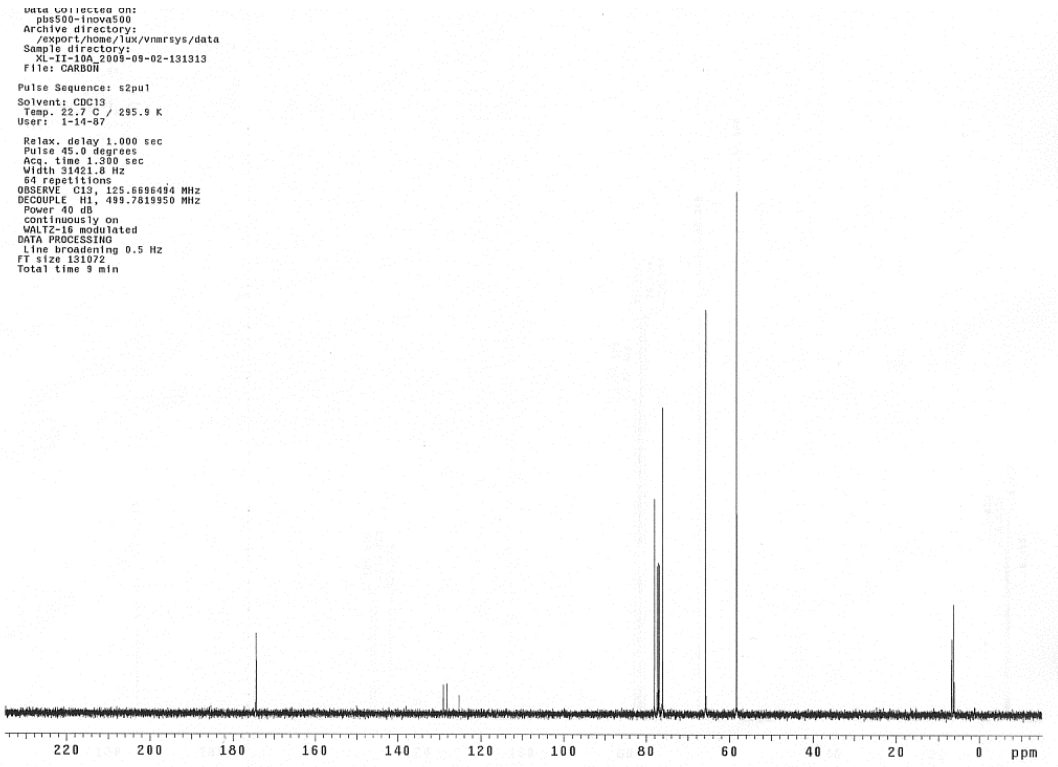

APPENDIX B

N-Benzyl-2,2-dimethyl thiazolidine-4-carboxylic acid (2e)

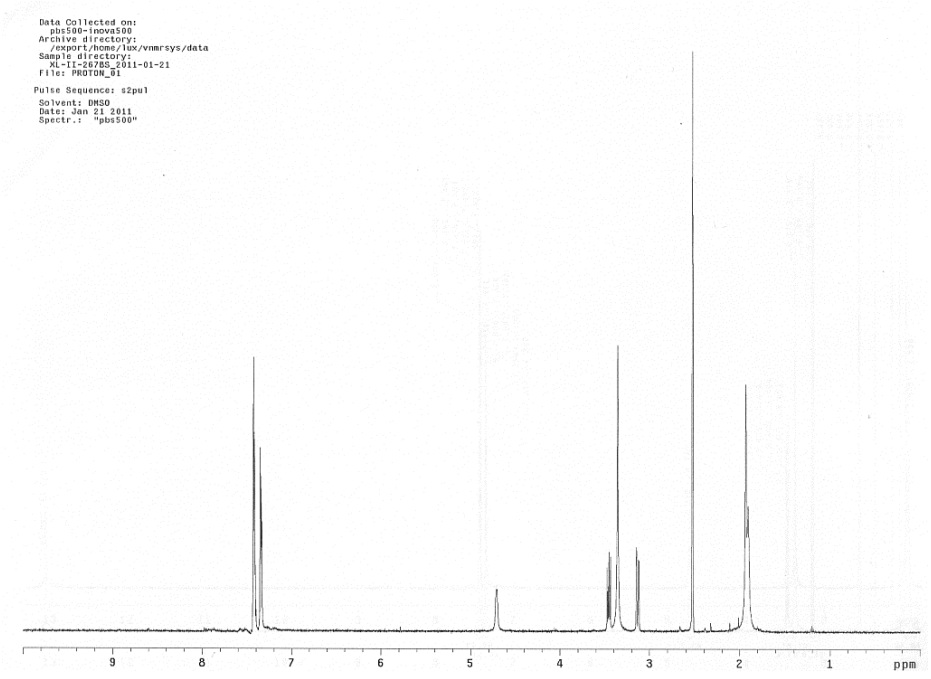

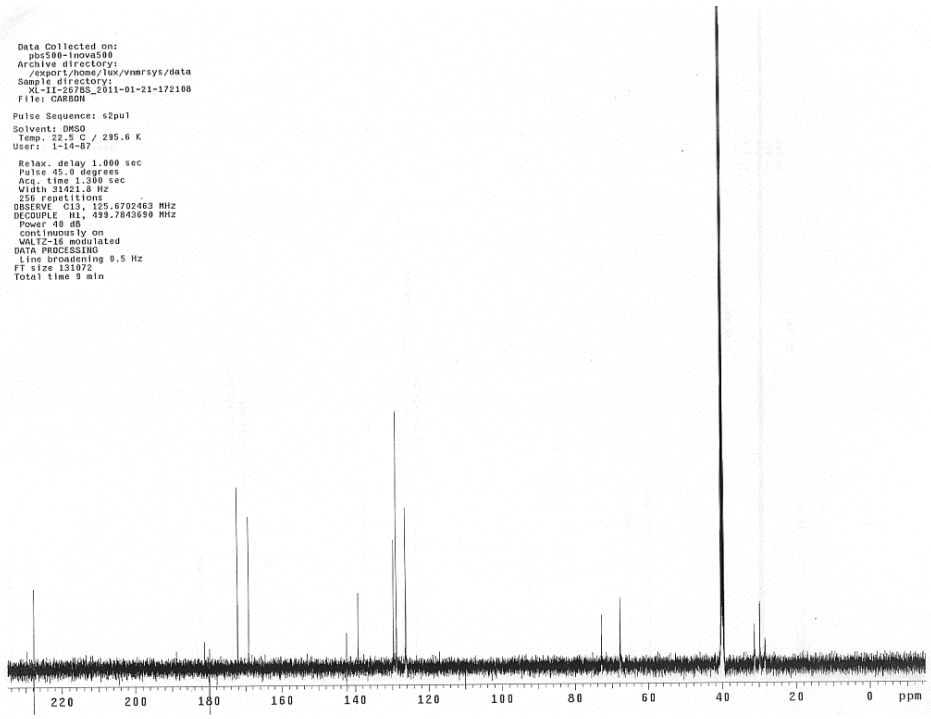

(*R*)-*N*-(Benzyloxy)-3-formyl-2,2-dimethylthiazolidine-4-carboxamide (9e)

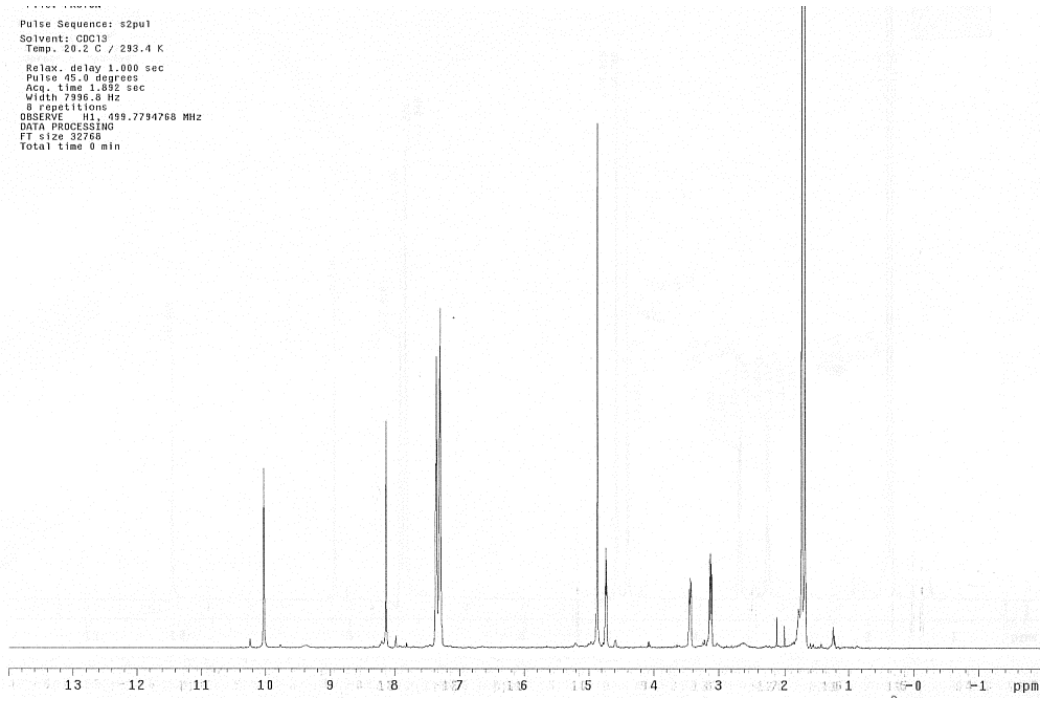

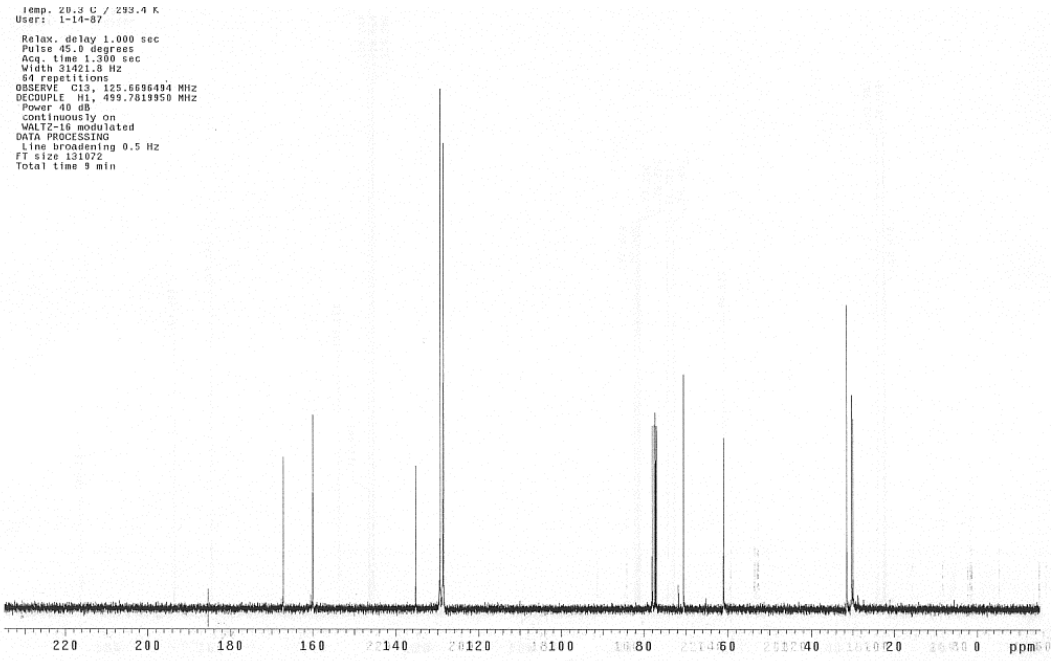

(*R*)-Benzyl 2-((3-benzoyl-2,2-dimethylthiazolidine-4-carboxamido)oxy)acetate (9k)

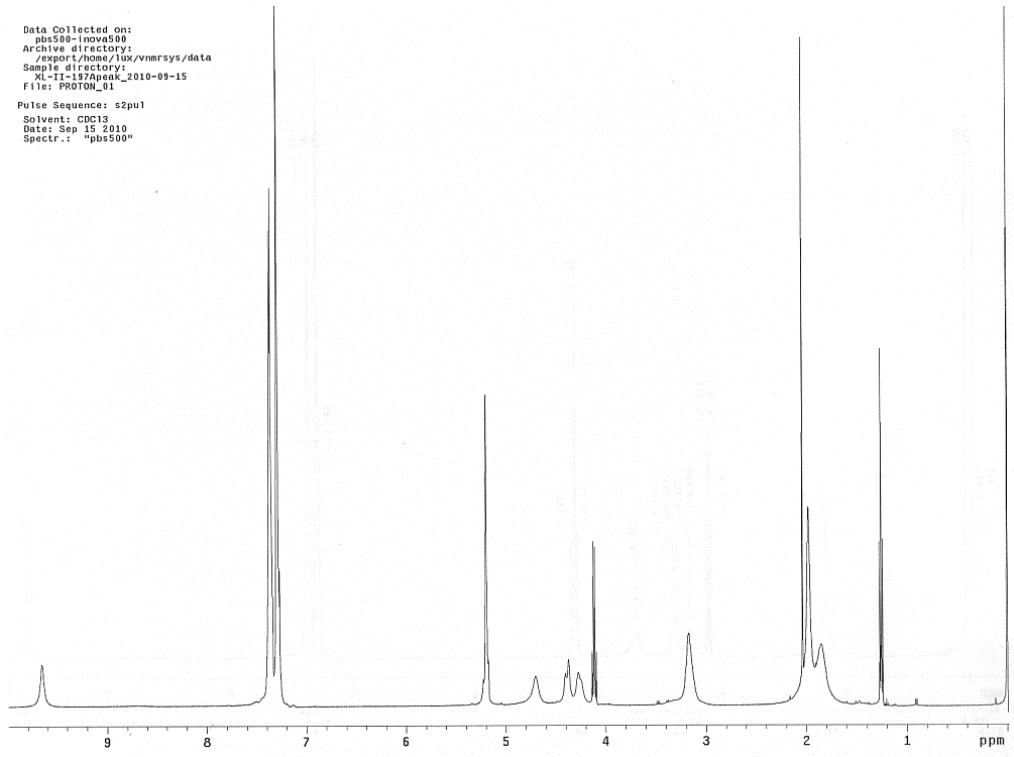

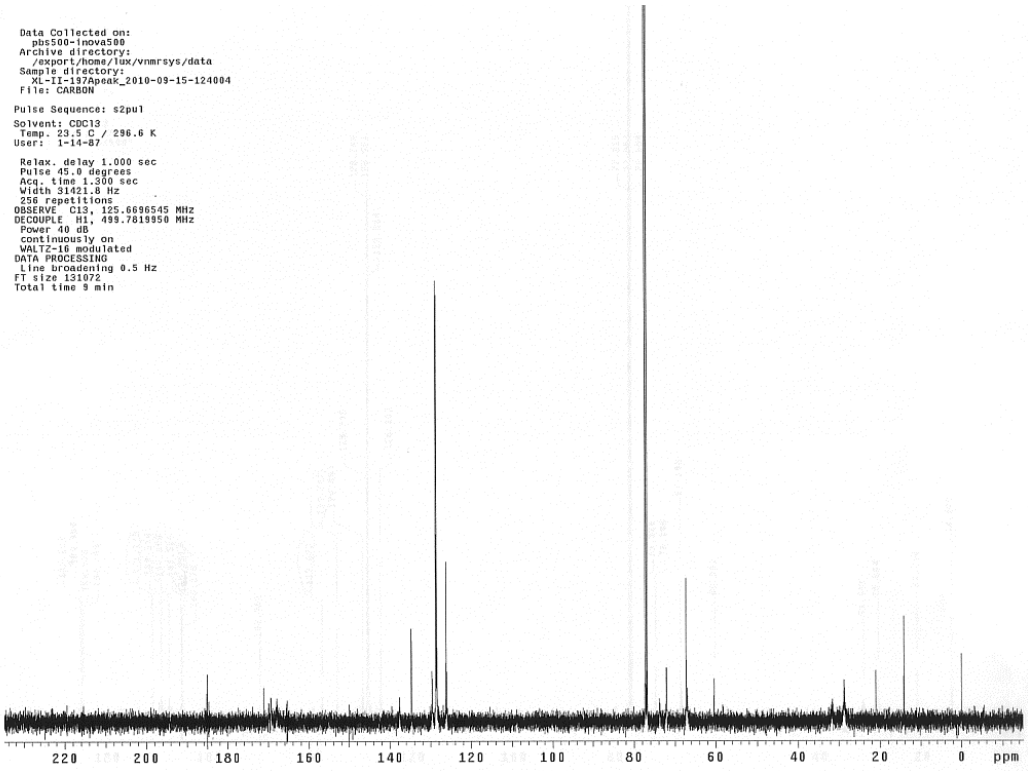

(*R*)-3-Benzoyl-*N*-(benzyloxy)-2,2-dimethylthiazolidine-4-carboxamide (9l)

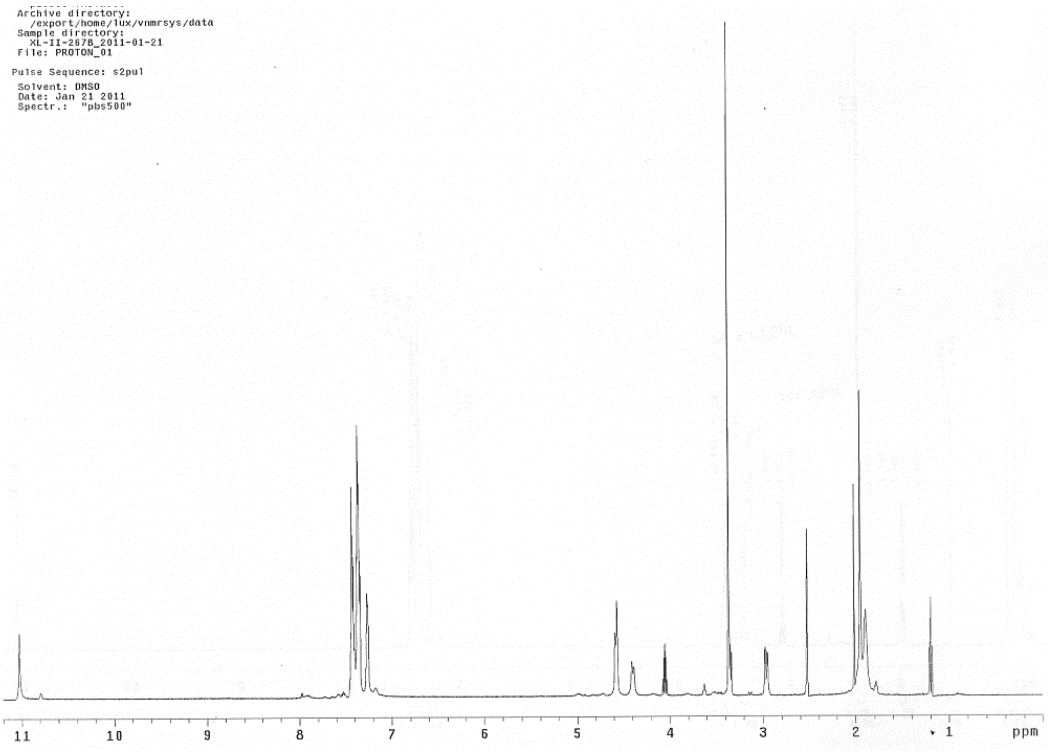

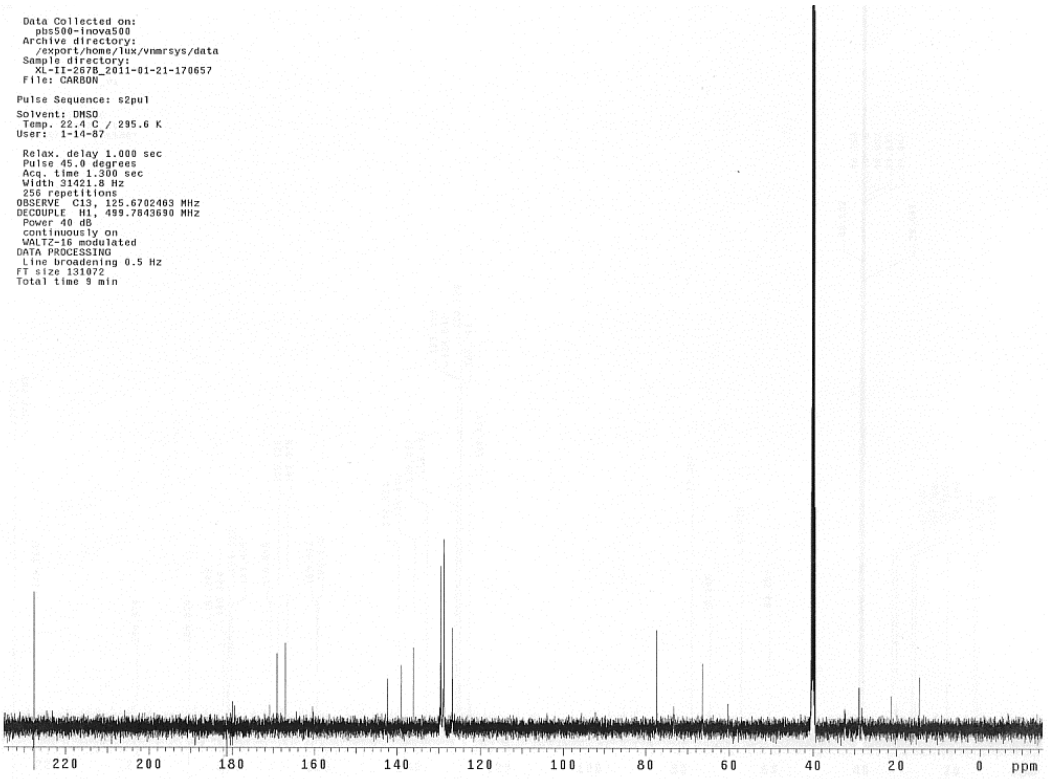

(*R*)-3-Benzoyl-*N*-methoxy-2,2-dimethylthiazolidine-4-carboxamide (9m)

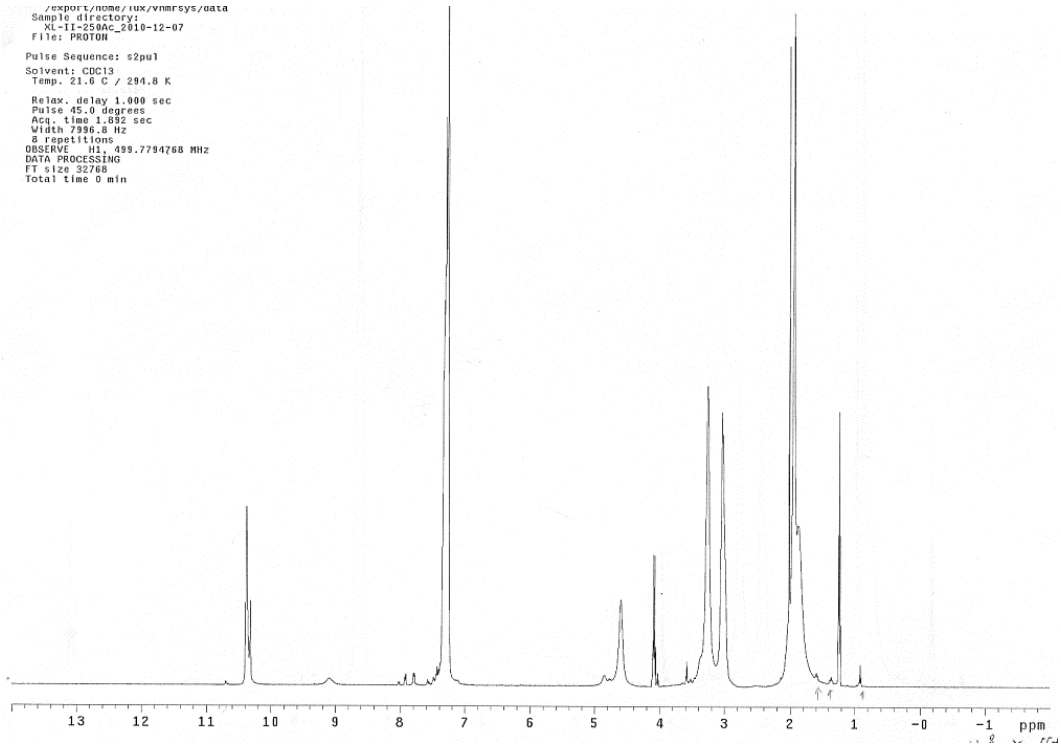

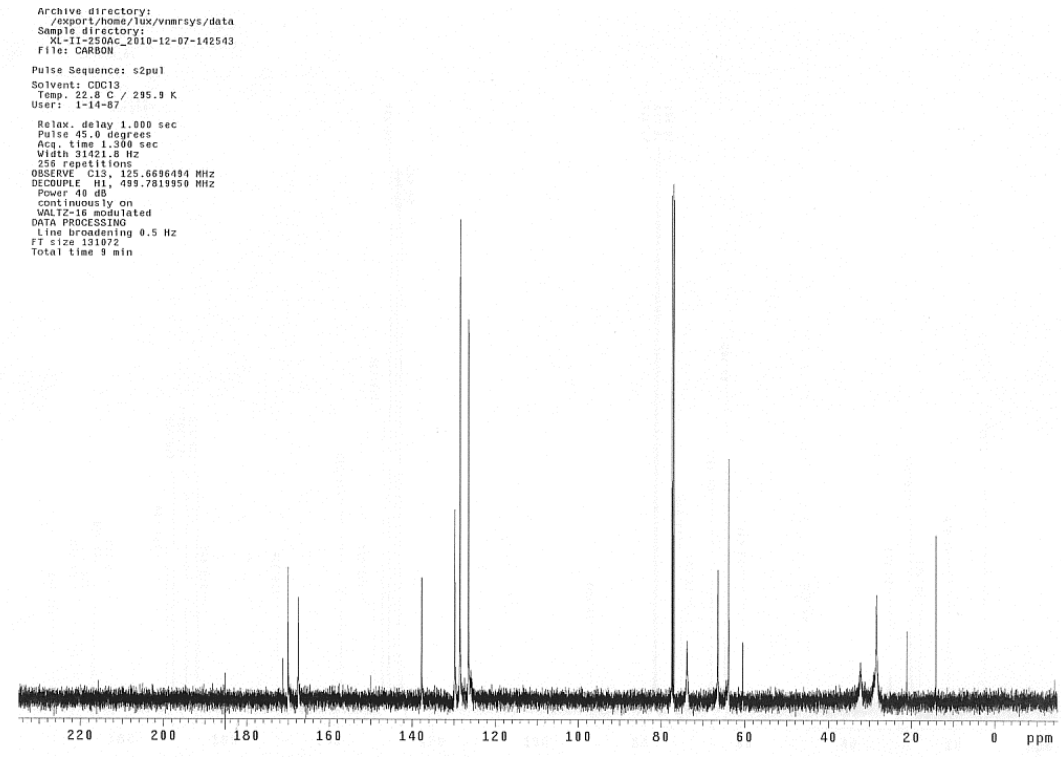

Benzyl 2-(((4*R*,5*S*)-3-benzoyl-5-hydroxy-2,2-dimethylthiazolidine-4 carboxamido)-oxy)acetate (10h)

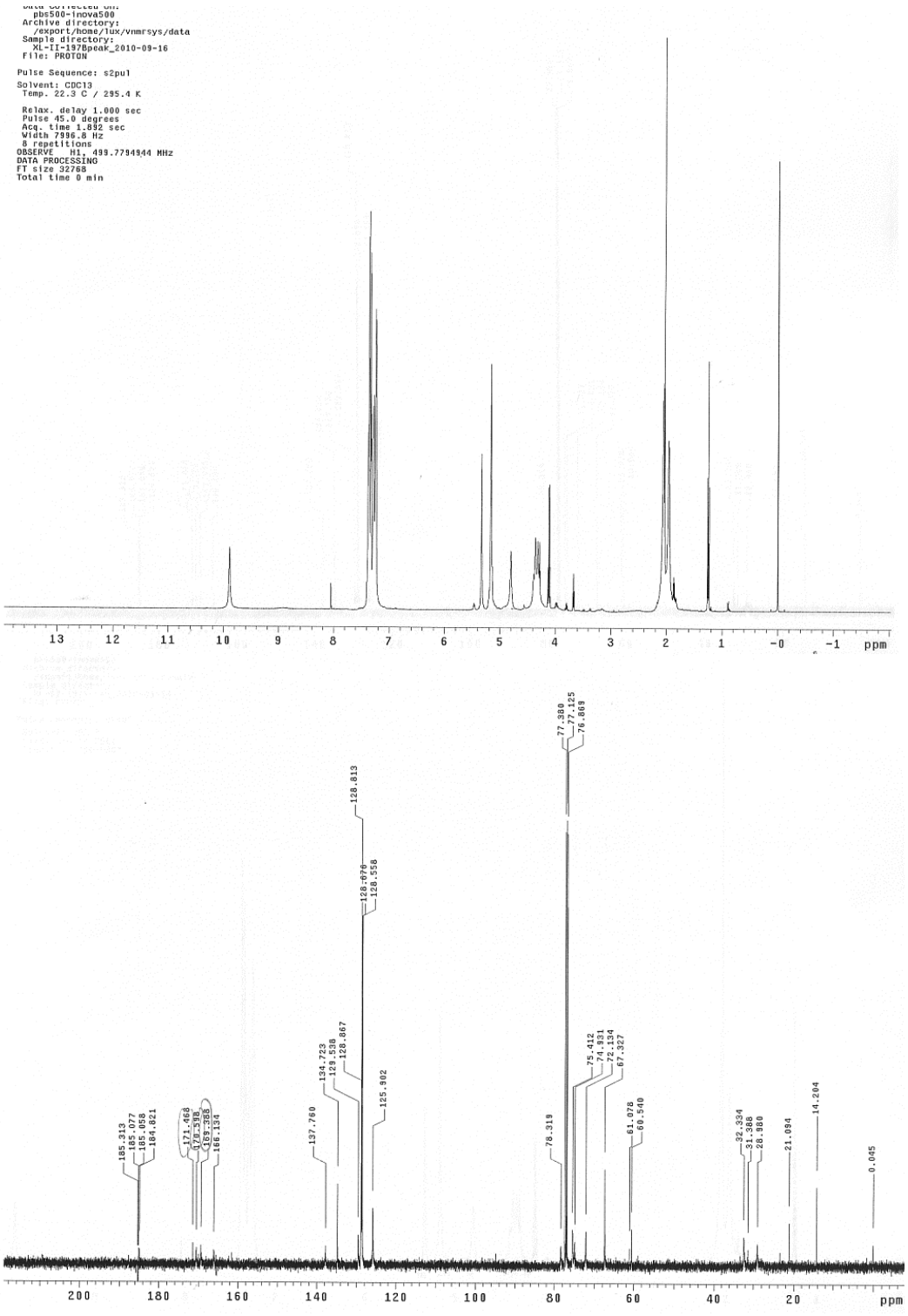

(4*R*,5*S*)-*N*-(Benzyloxy)-3-formyl-5-hydroxy-2,2-dimethylthiazolidine-4-carboxamide (10a)

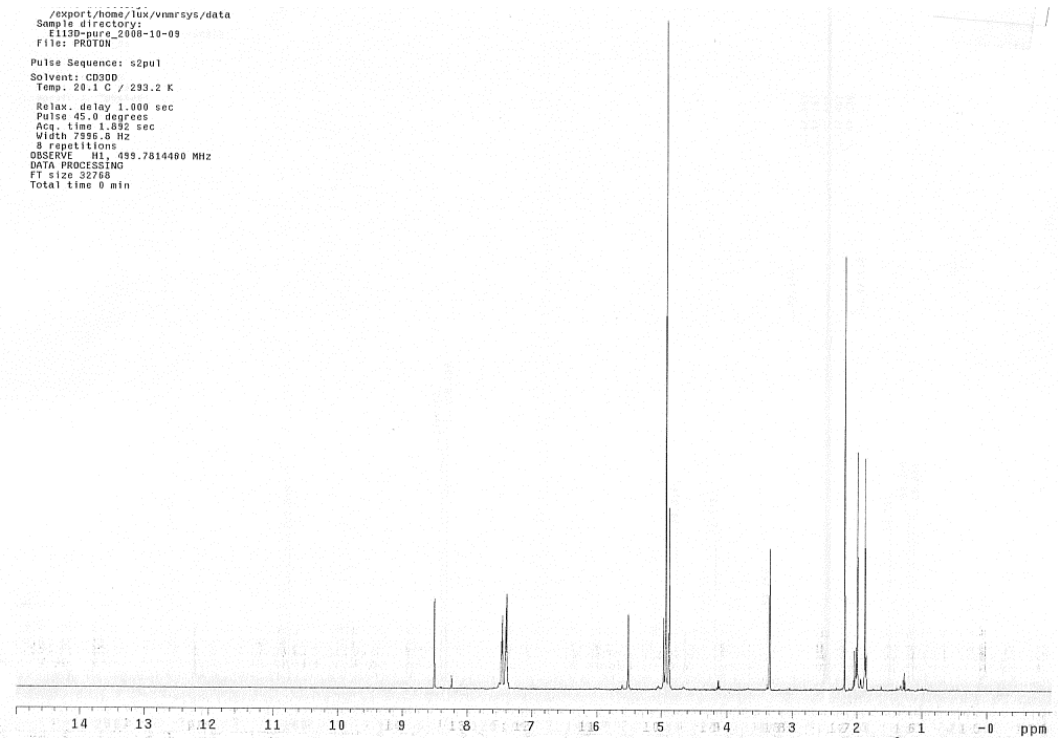

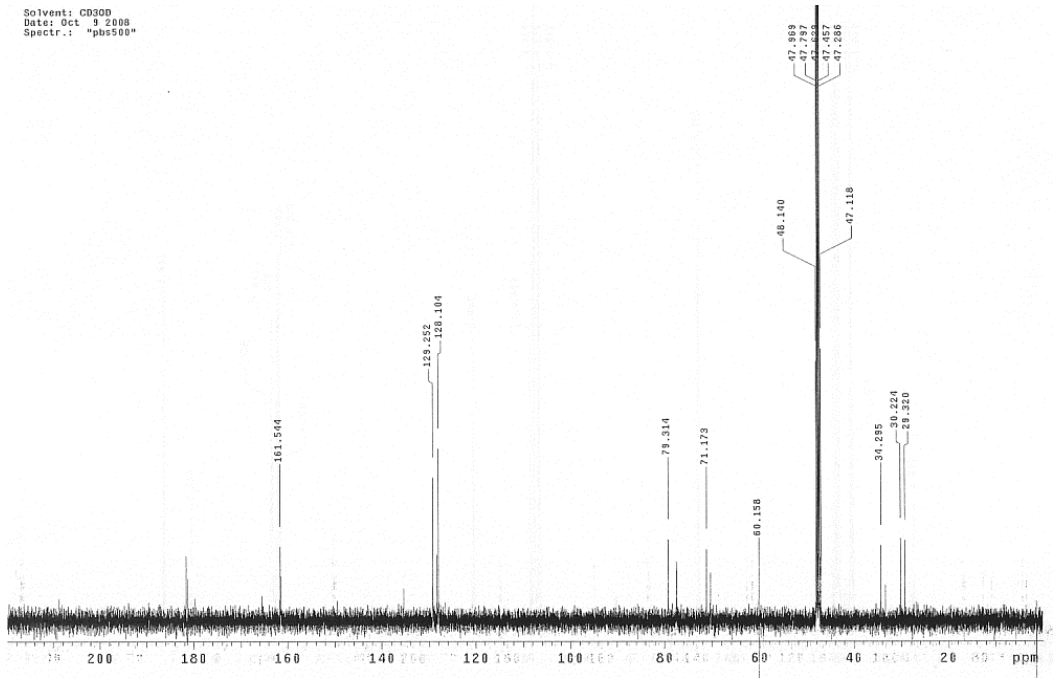

(4*R*,5*S*)-*N*-Acetoxy-5-hydroxy-2,2-dimethyl-3-(2-phenoxyacetyl)thiazolidine-4-carboxamide (10f)

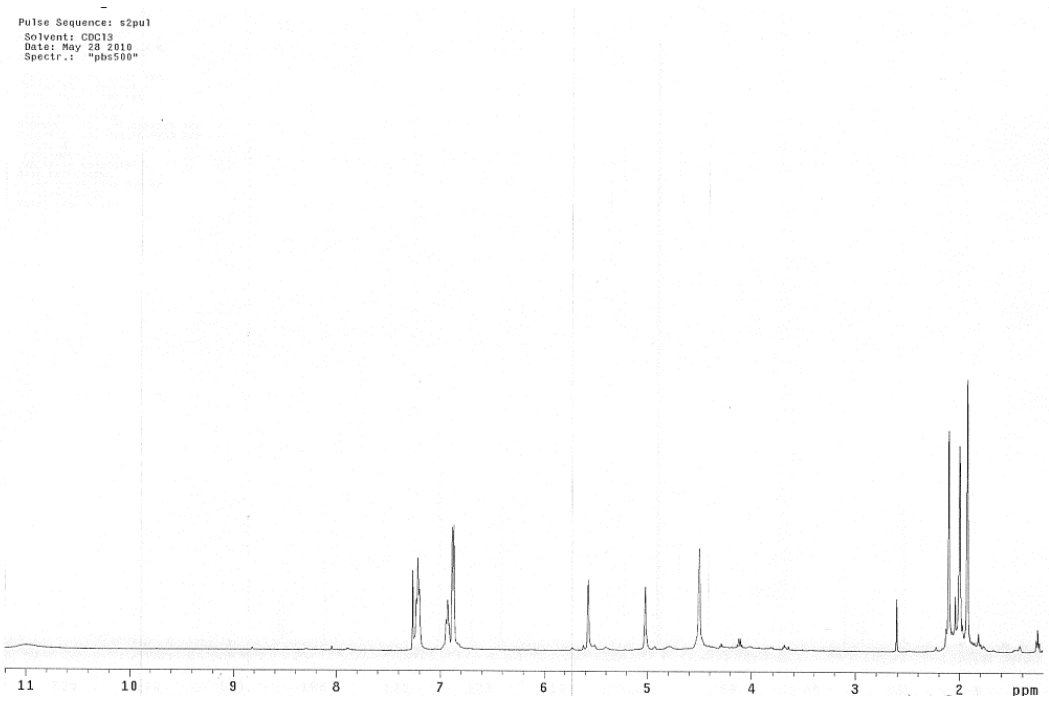

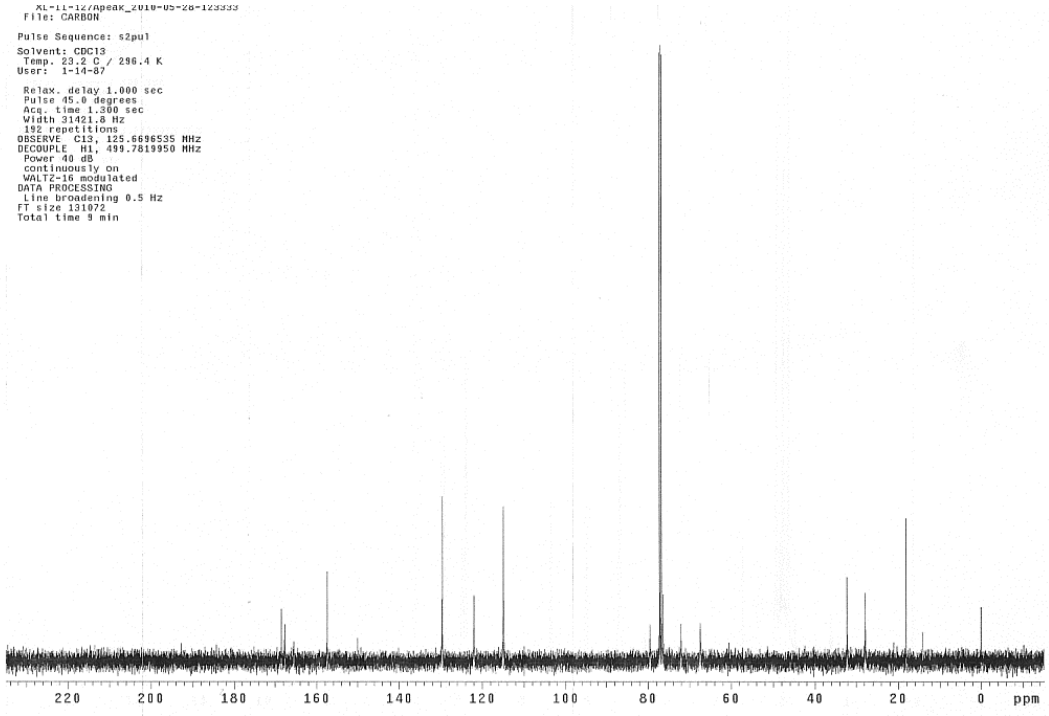

***tert*-Butyl 2-(((4*R*,5*S*)-5-hydroxy-2,2-dimethyl-3-(2-phenoxyacetyl)thiazolidine-4-car-boxamido)oxy)-acetate (10g)**

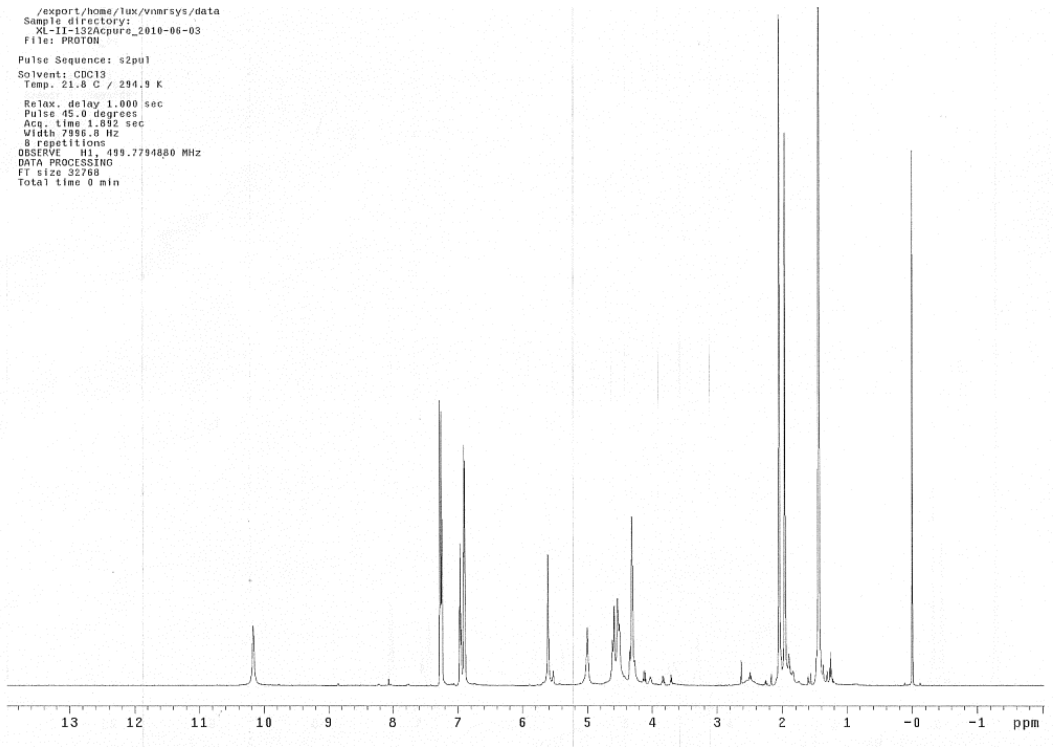

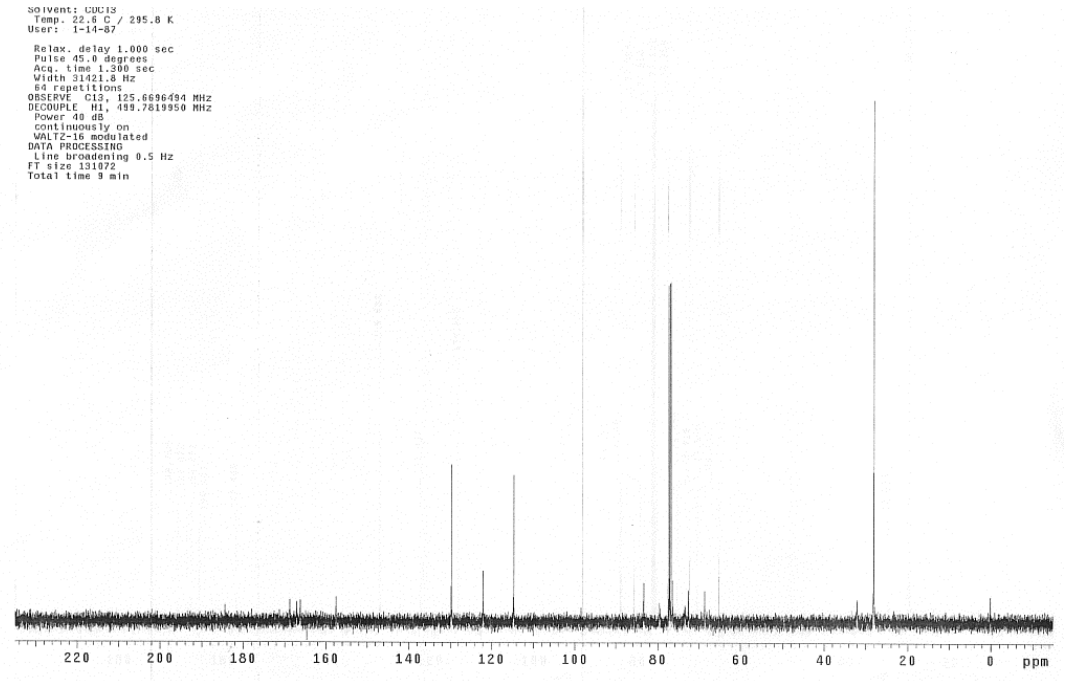

(4*R*,5*S*)-3-Benzoyl-*N*-(benzyloxy)-5-hydroxy-2,2-dimethylthiazolidine-4-carboxamide (10i)

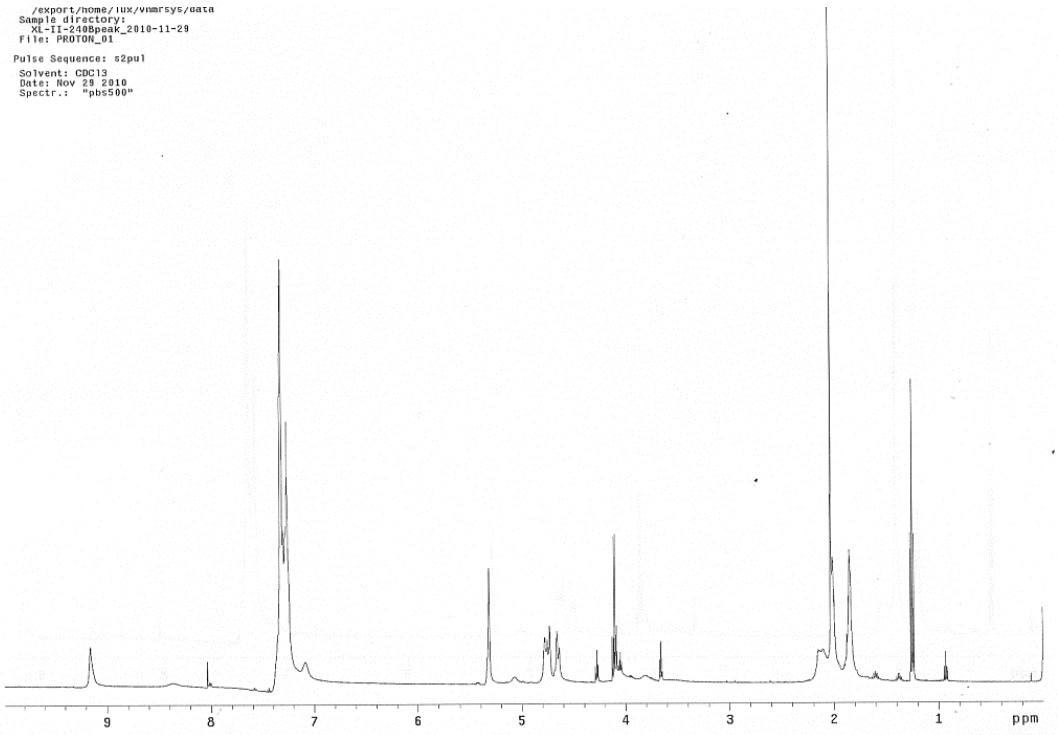

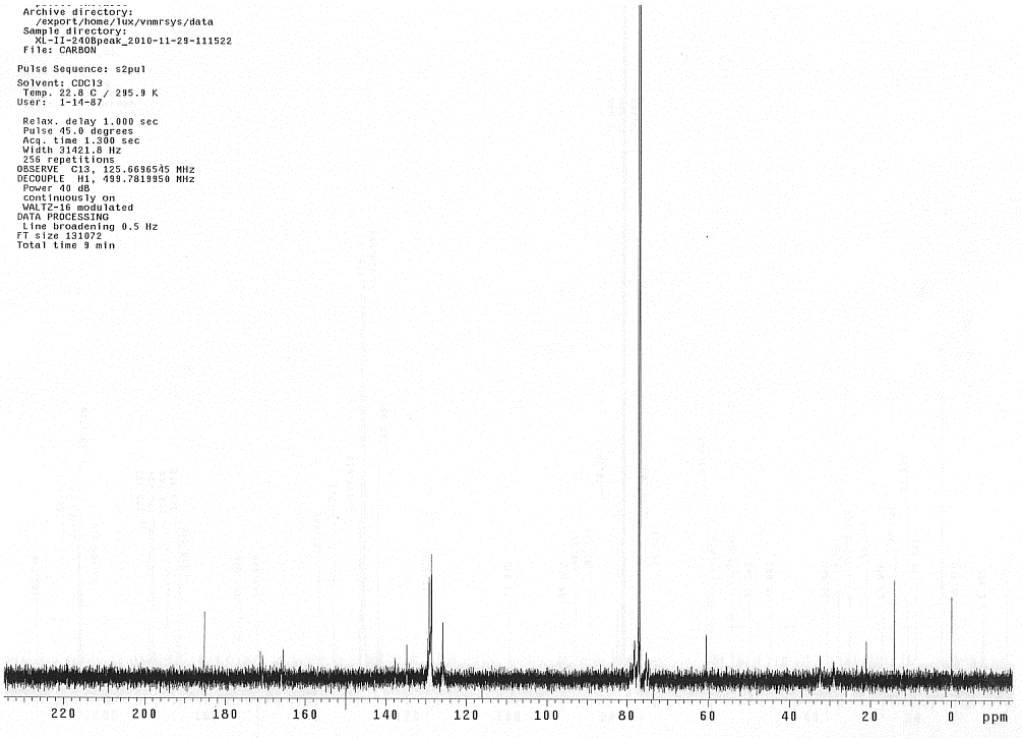

(1*R*,5*R*)-Benzyl 6-(2-(benzyloxy)-2-oxoethoxy)-3,3-dimethyl-7-oxo-4-thia-2,6-diazabi-cyclo[3.2.0]heptane-2-carboxylate (14c)

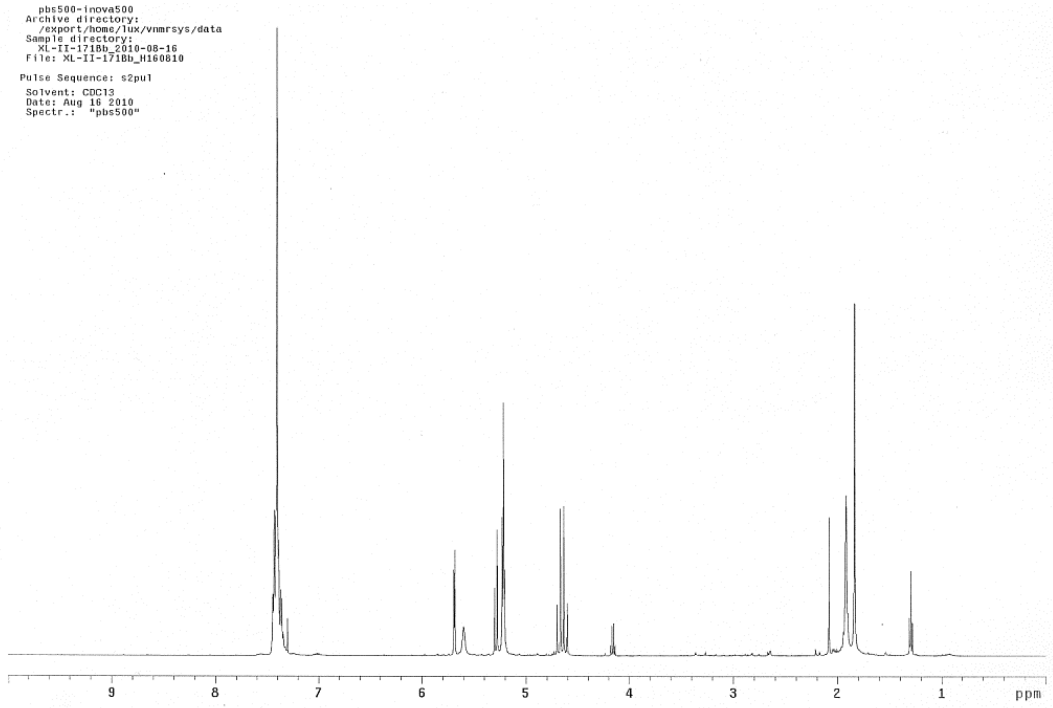

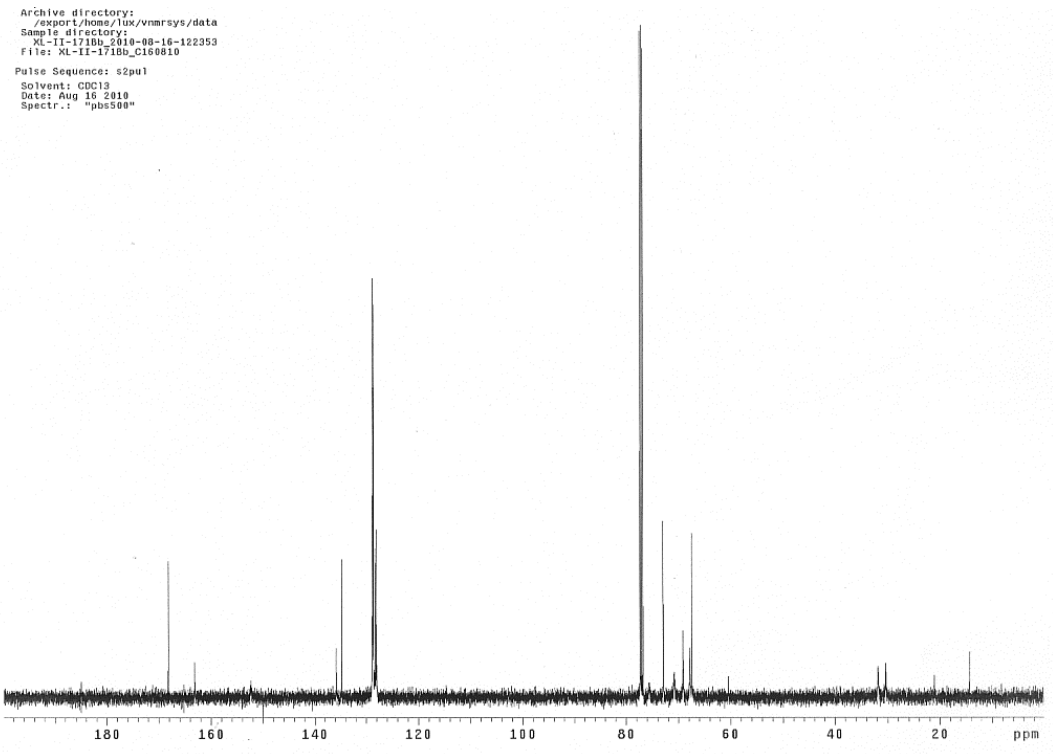

(1*R*,5*R*)-6-(Benzyloxy)-3,3-dimethyl-7-oxo-4-thia-2,6-diazabicyclo[3.2.0]heptane-2-carbaldehyde (14d)

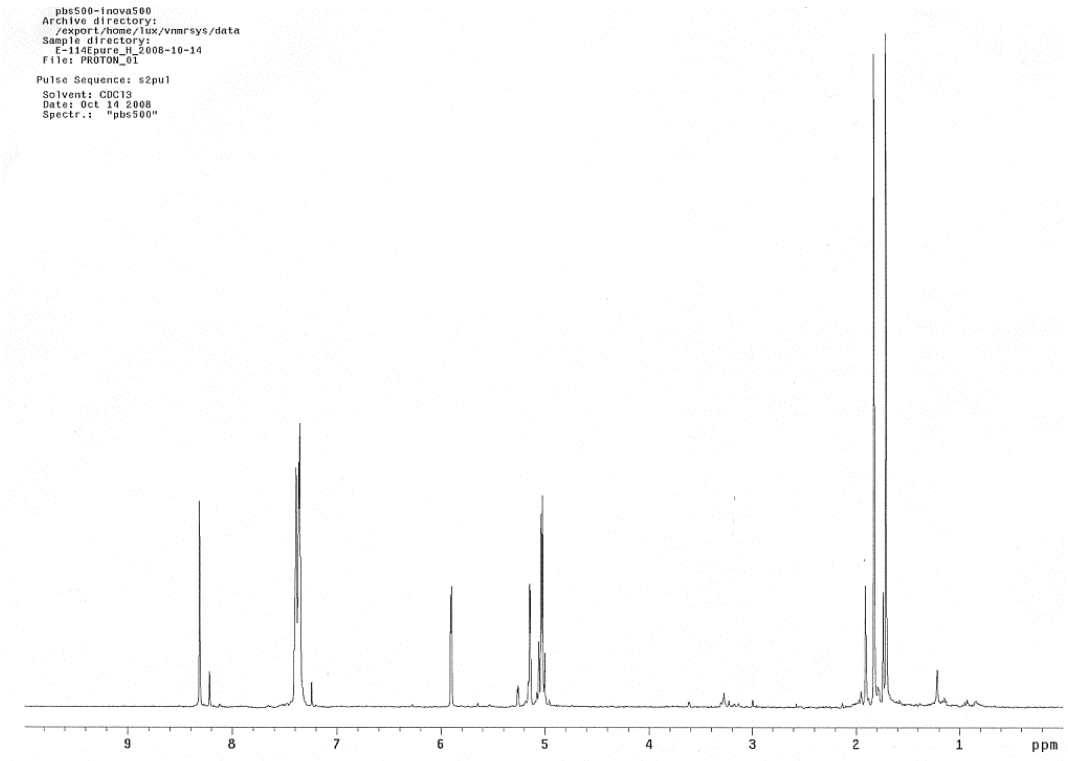

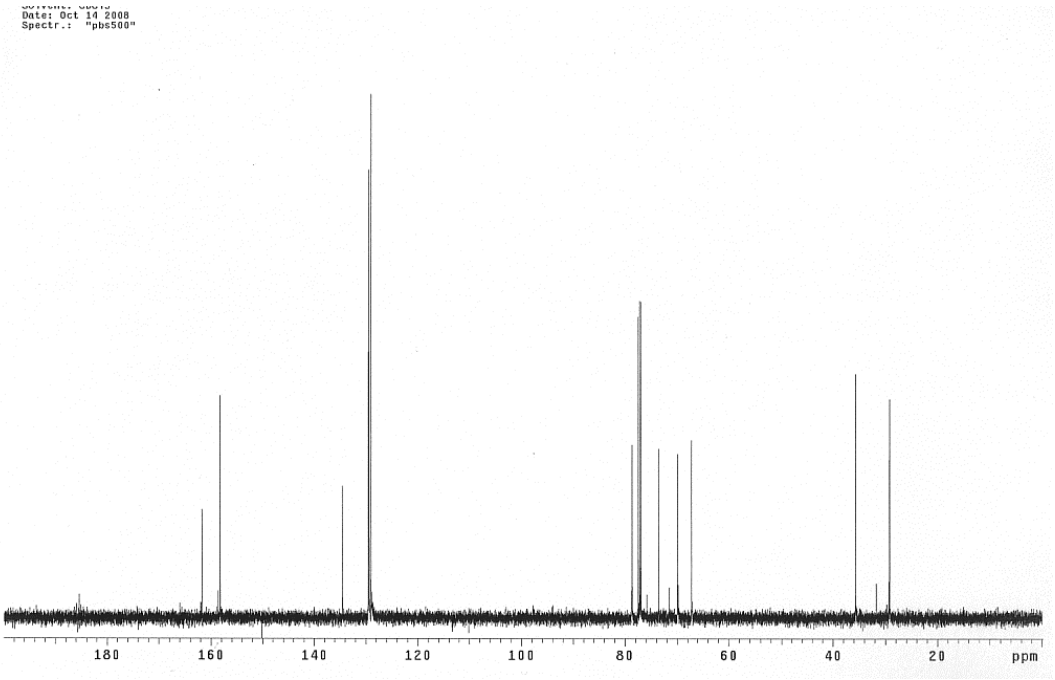

***tert*-Butyl 2-(((1*R*,5*R*)-3,3-dimethyl-7-oxo-2-(2-phenoxyacetyl)-4-thia-2,6-diazabicyclo[3.2.0]heptan-6-yl)oxy)-acetate (14f)**

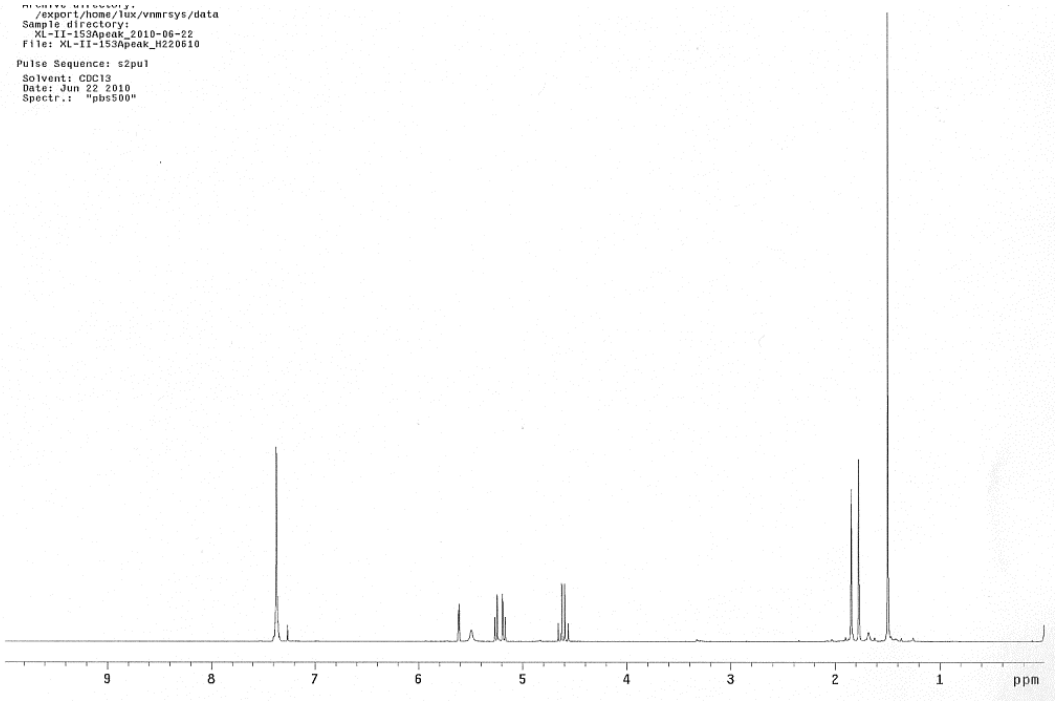

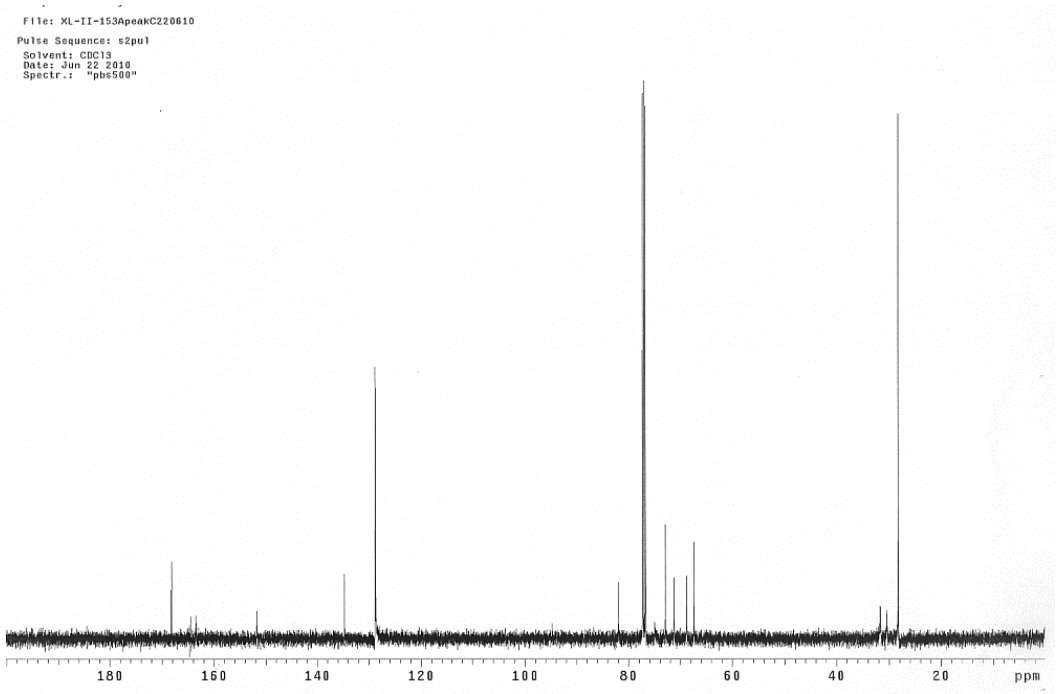

Benzyl 2-(((1*R*,5*R*)-2-benzoyl-3,3-dimethyl-7-oxo-4-thia-2,6-diazabicyclo[3.2.0]heptan-6-yl)oxy)acetate (14h)

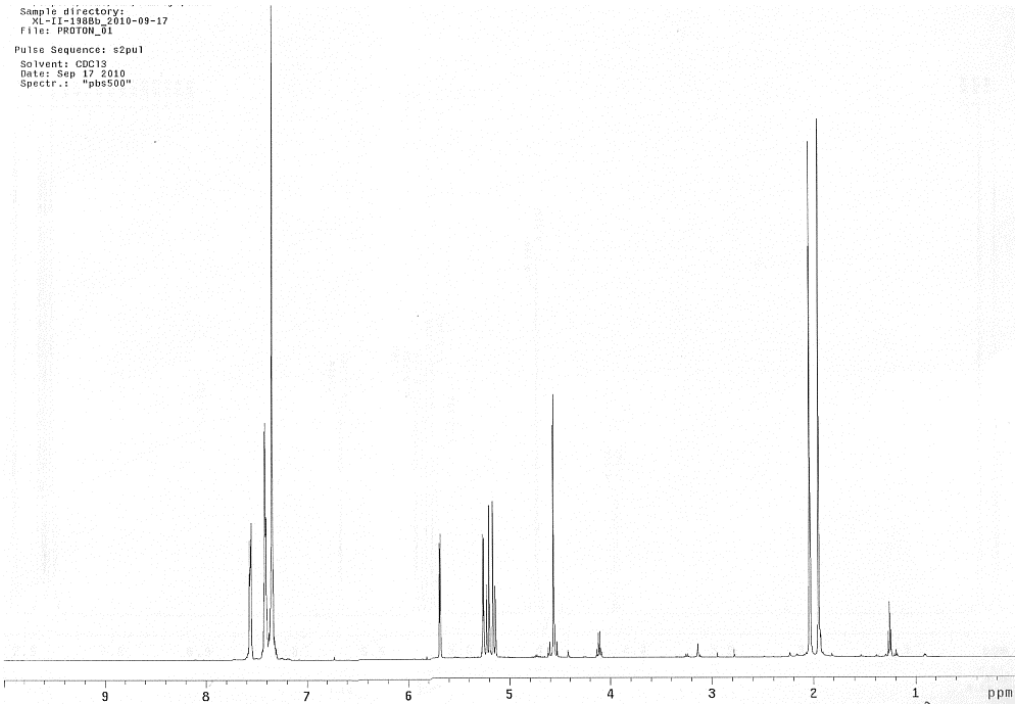

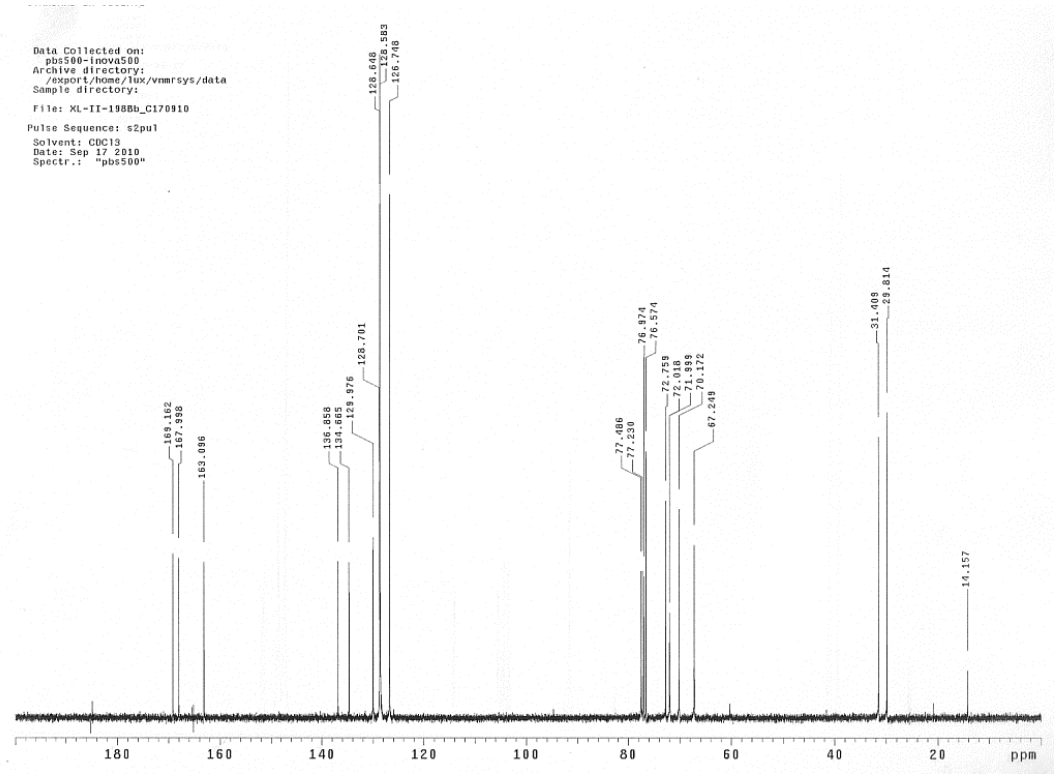

(1*R*,5*R*)-2-Benzoyl-6-(benzyloxy)-3,3-dimethyl-4-thia-2,6-diazabicyclo[3.2.0]heptan-7-one (14i)

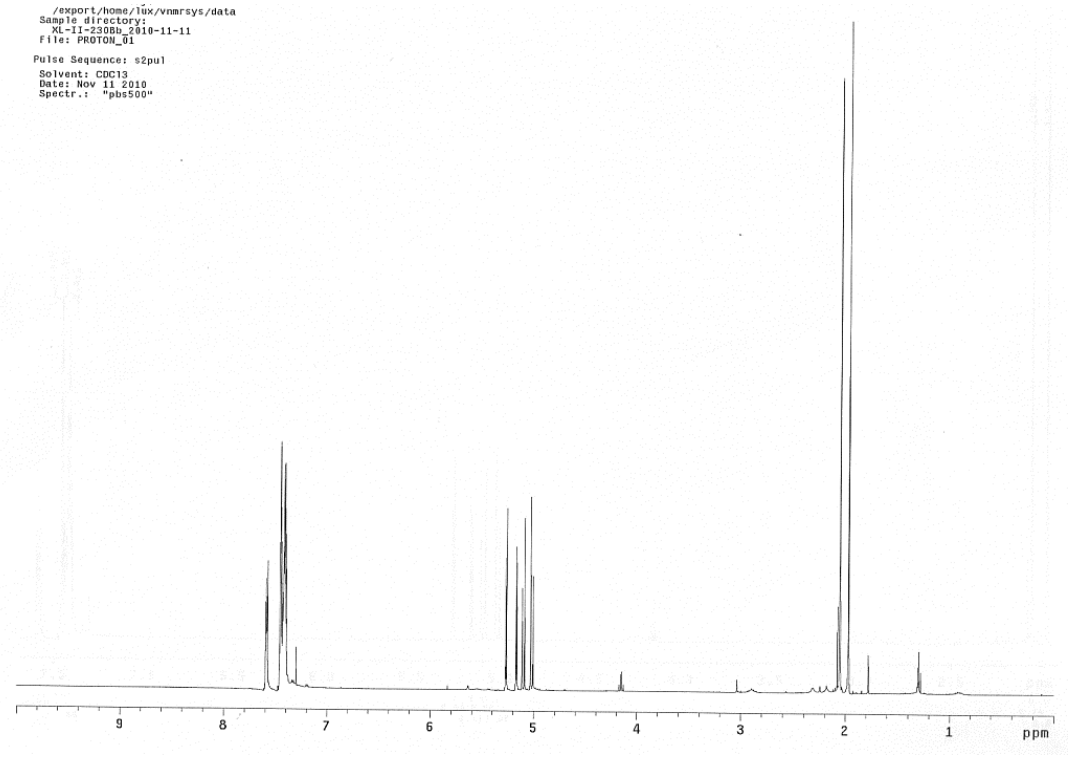

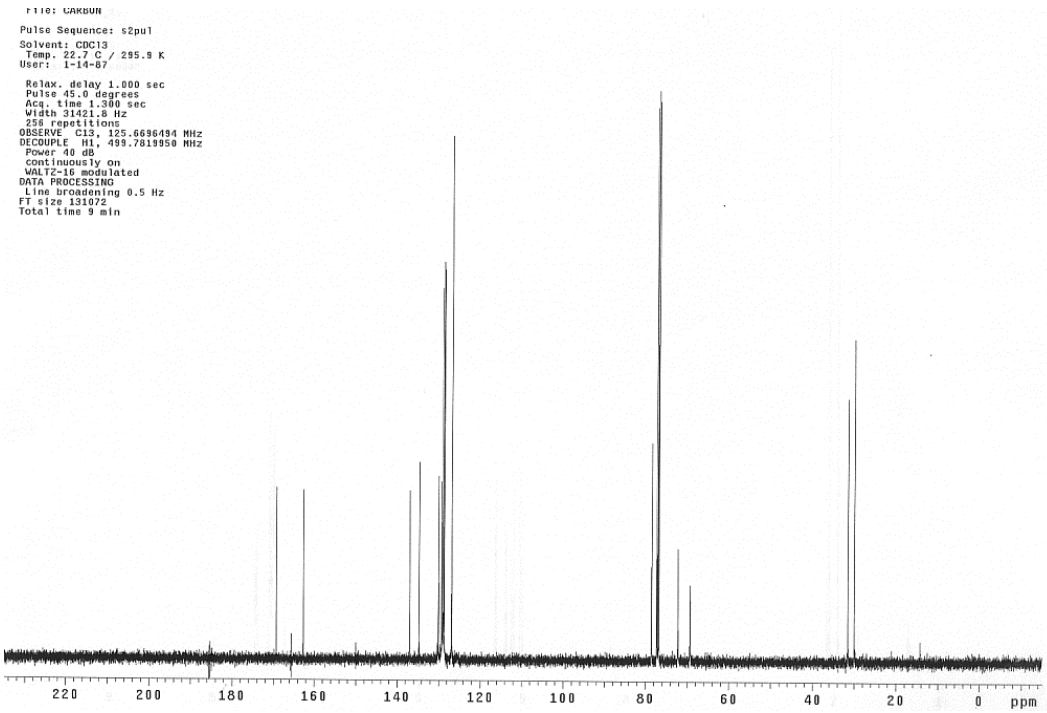

(1*R*,5*R*)-2-Benzoyl-6-methoxy-3,3-dimethyl-4-thia-2,6-diazabicyclo[3.2.0]heptan-7-one (14j)

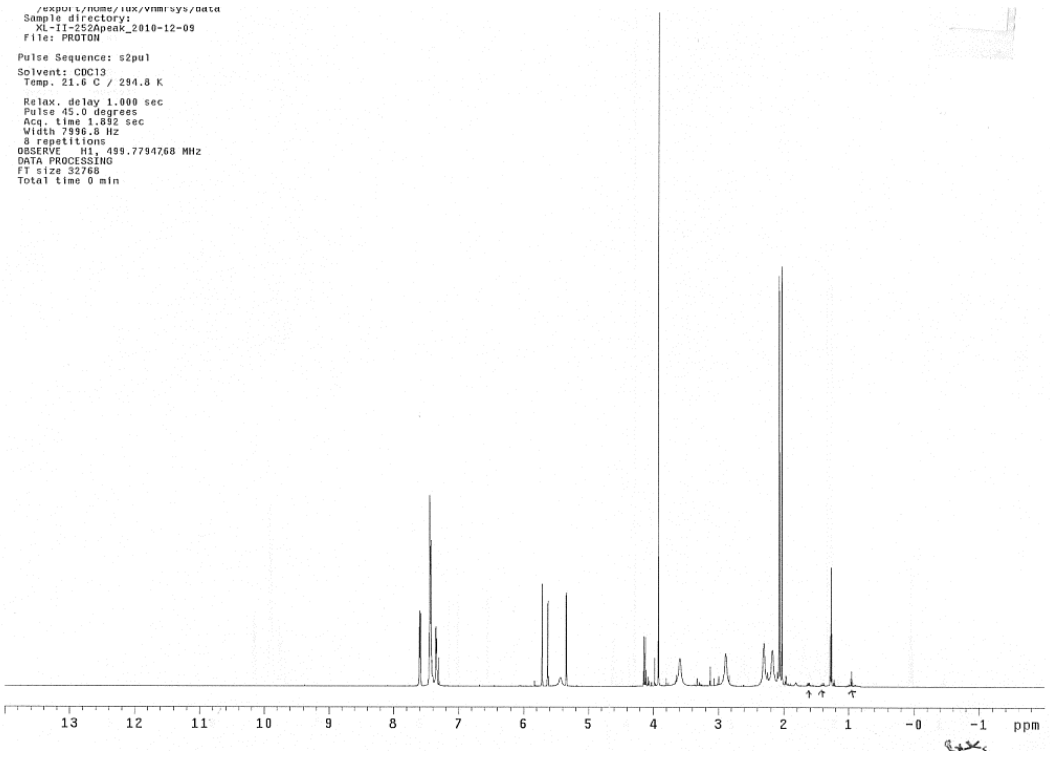

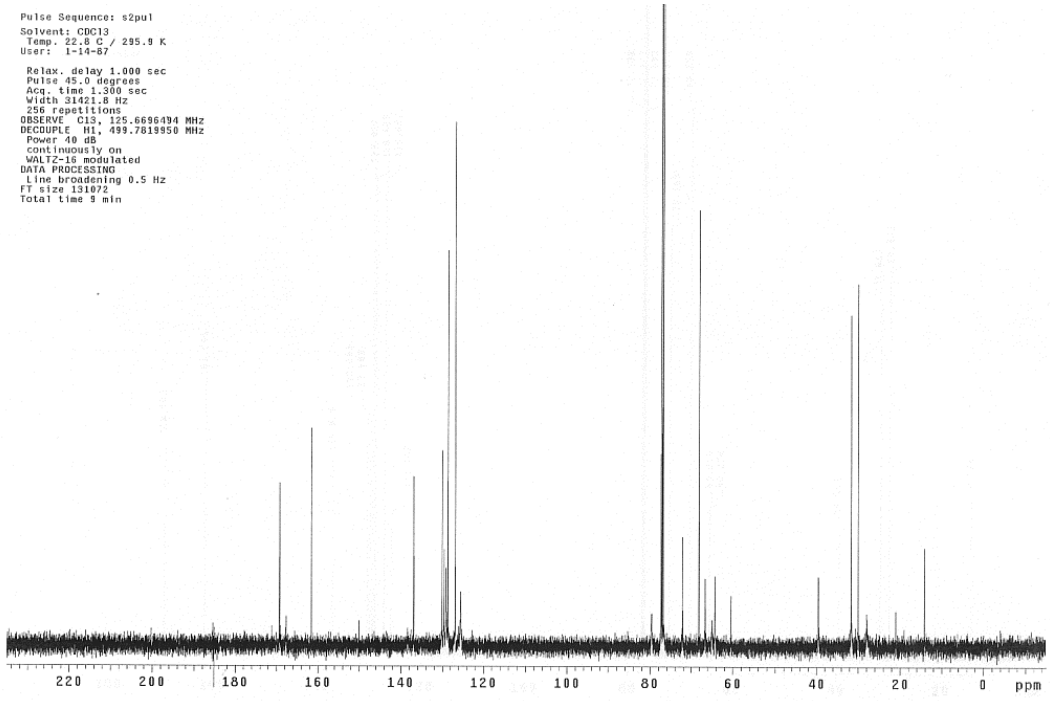

***SS*-((2*R*,3*R*)-3-Benzamido-1-(benzyloxy)-4-oxoazetidin-2-yl) *O*-methyl carbon-(dithioperoxoate) (15b)**

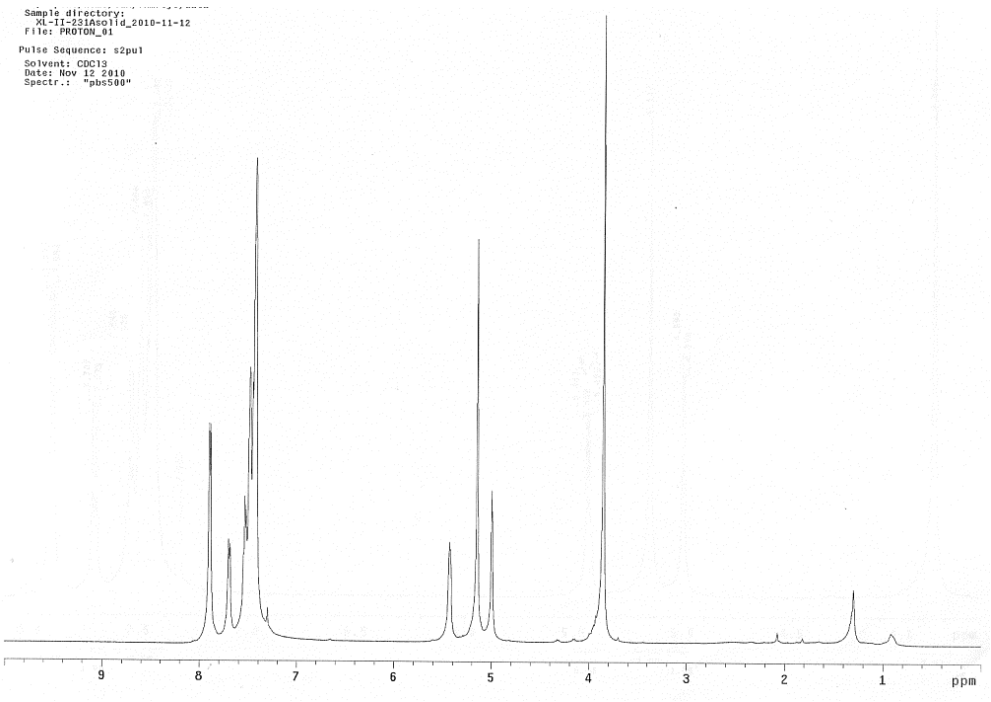

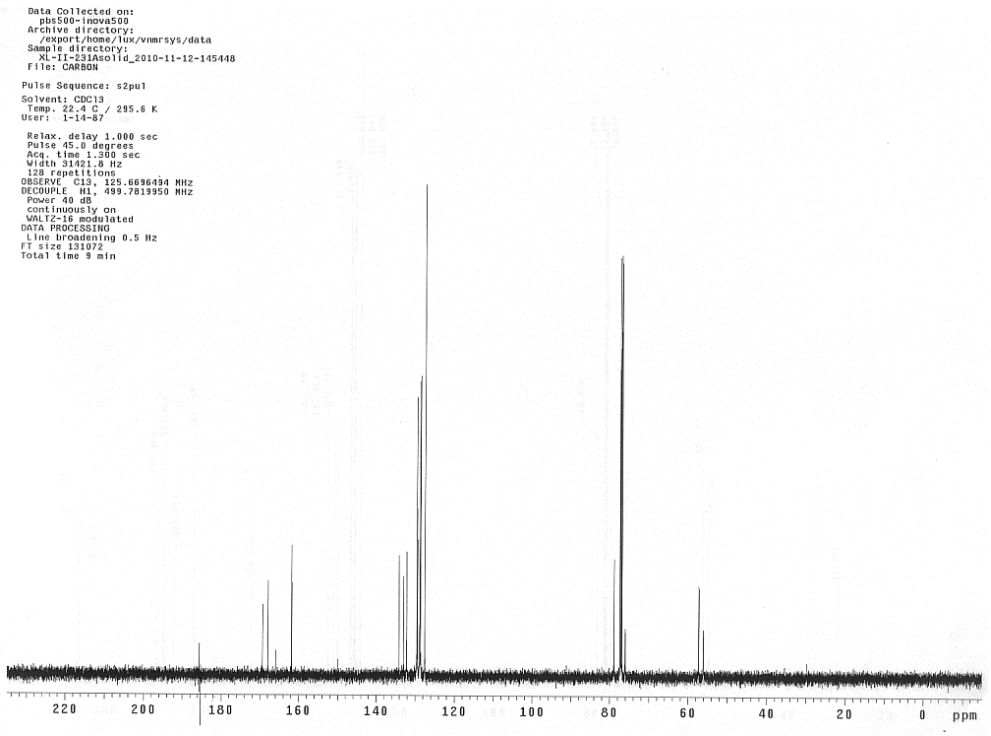

(1*R*,5*R*)-2-Benzoyl-3,3-dimethyl-4-thia-2,6-diazabicyclo[3.2.0]heptan-7-one (17)

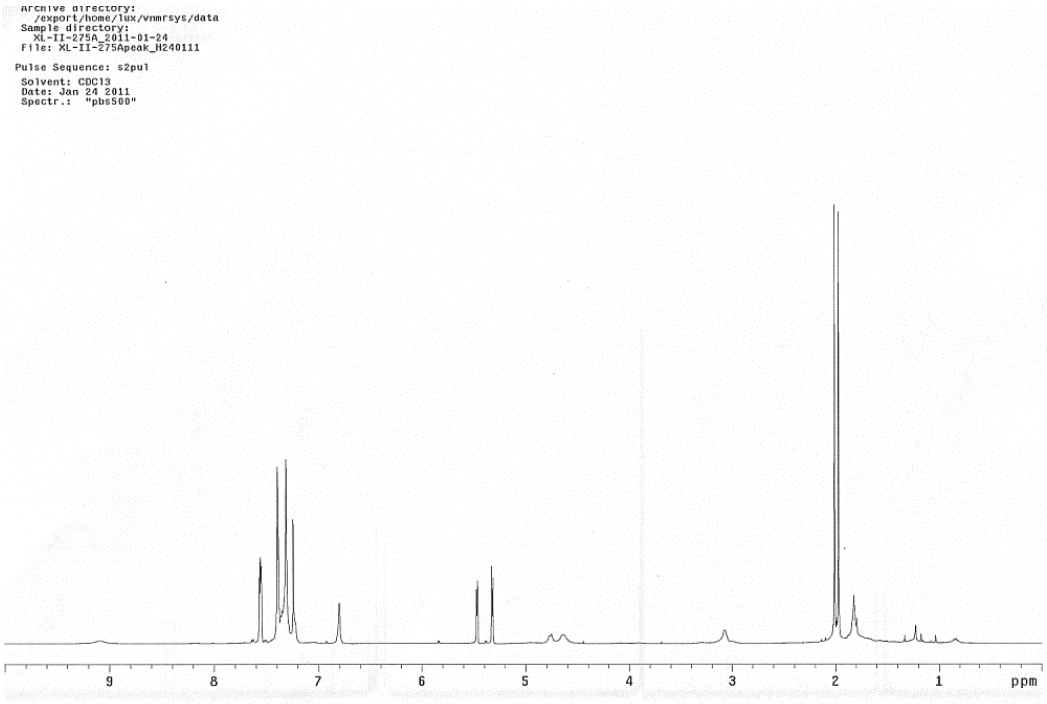

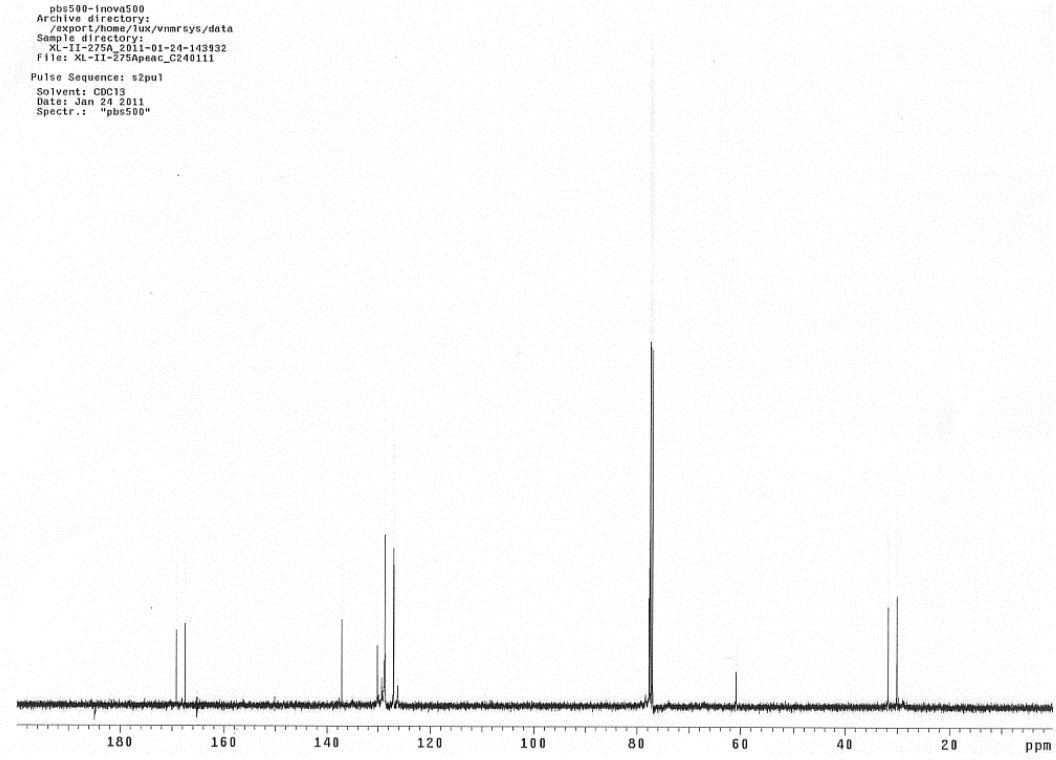

***SS*-((2*R*,3*R*)-3-Benzamido-4-oxoazetidin-2-yl) *O*-methyl carbon-(dithioperoxoate) (16)**

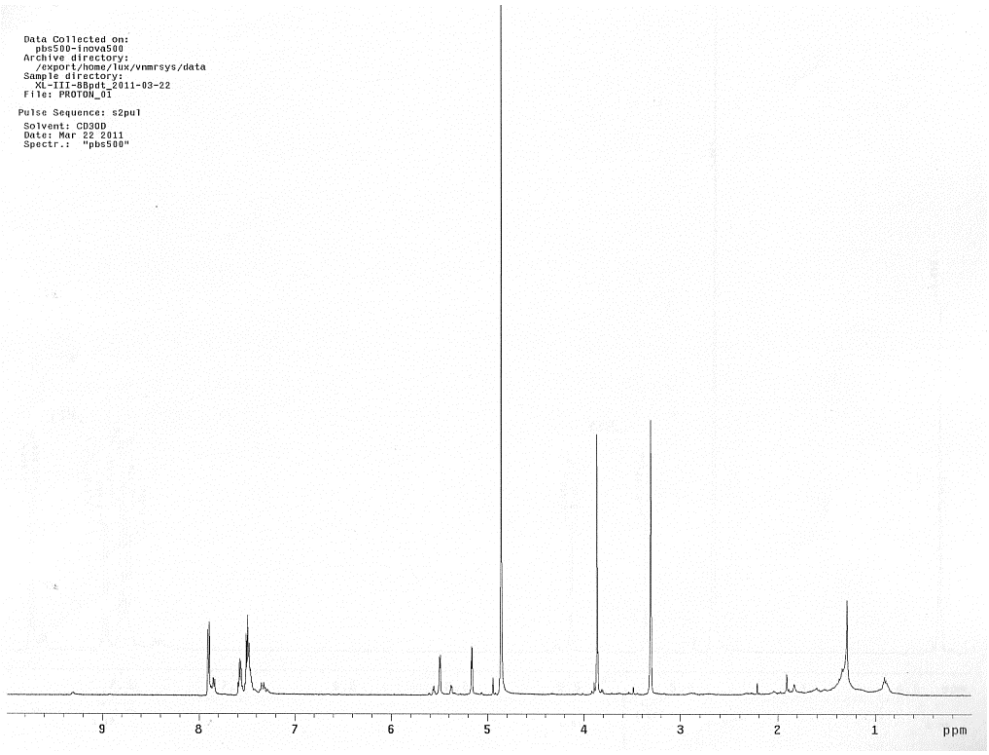

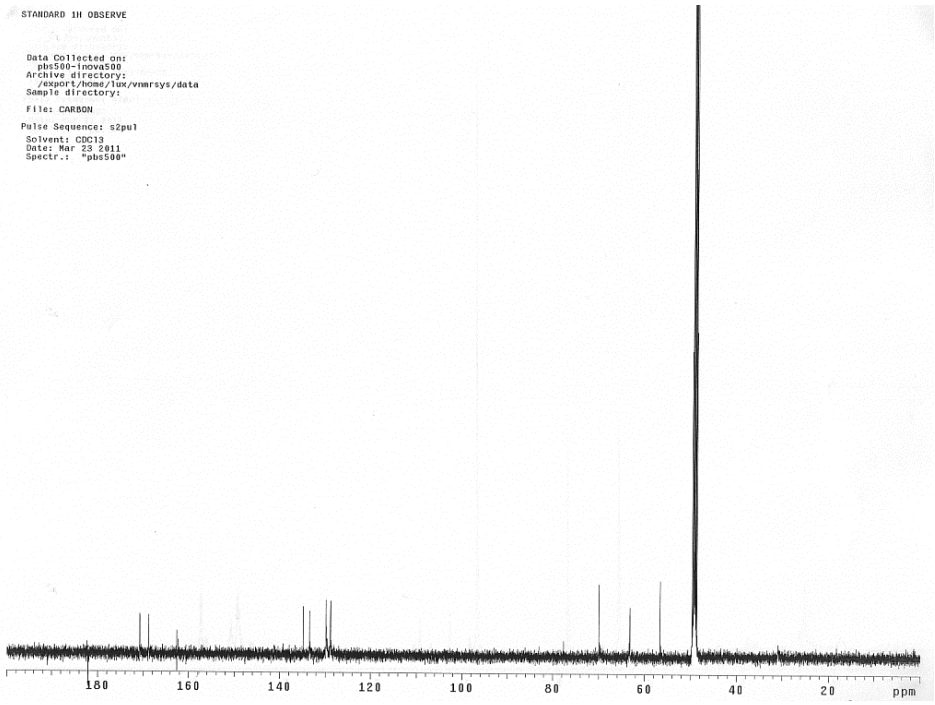

APPENDIX C

10-(1-Decyloxy-1H-benzotriazole)triphenylphosphonium bromide (3)

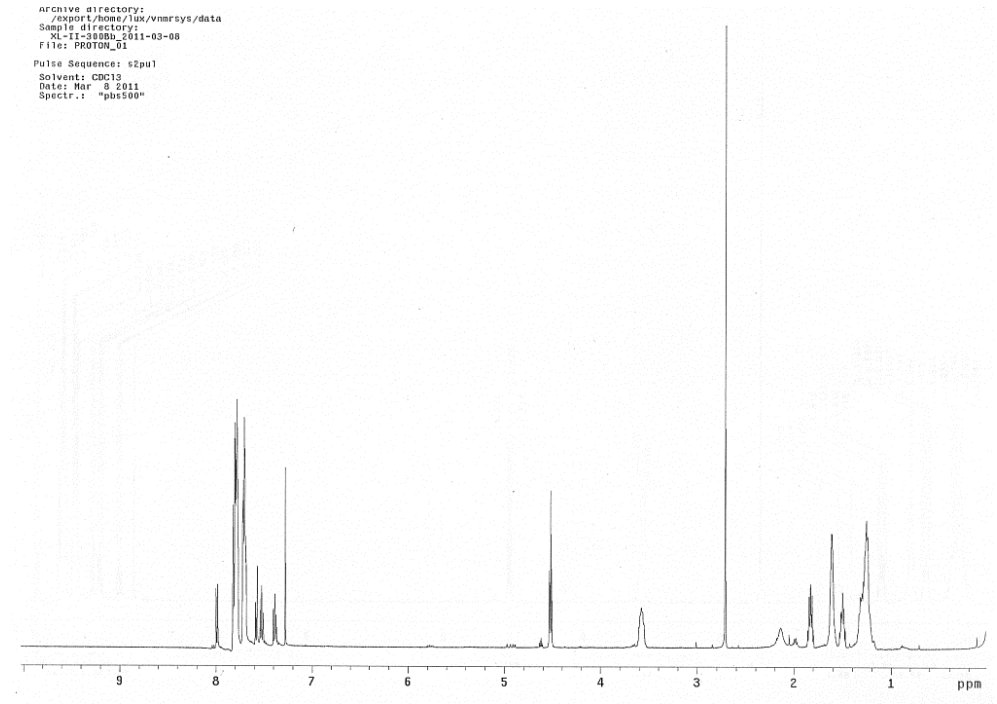

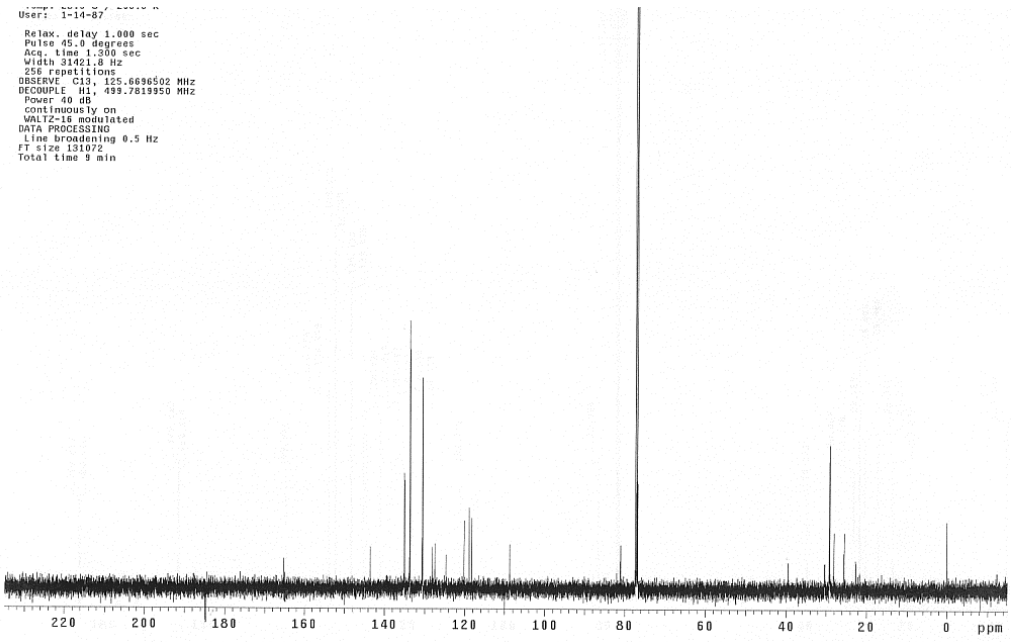

10-(1-Decyloxy-pyrrolidine-2,5-dione)triphenylphosphonium bromide (7)

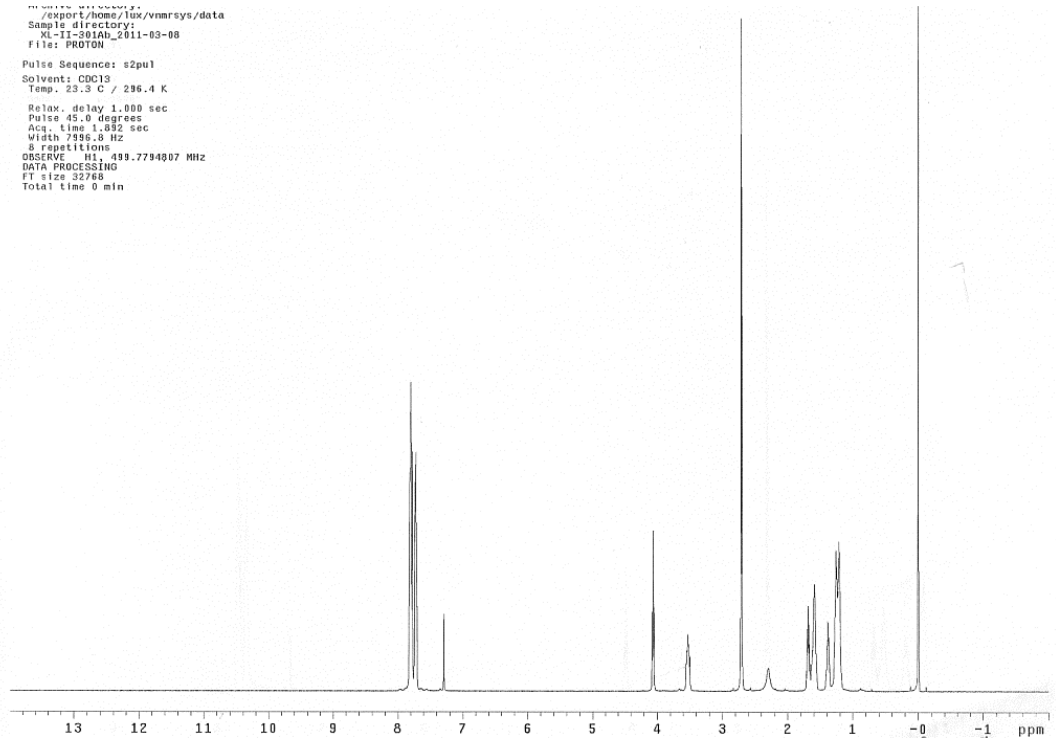

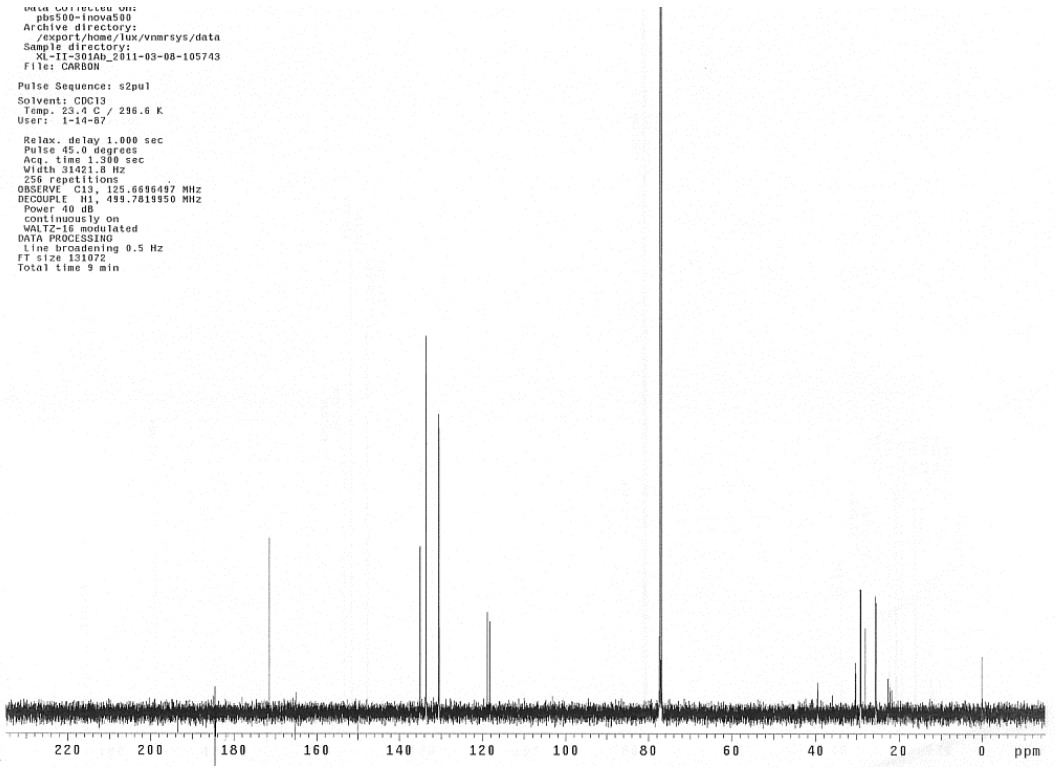

2-(10-Hydroxydecyl)isoindoline-1,3-dione (9a)

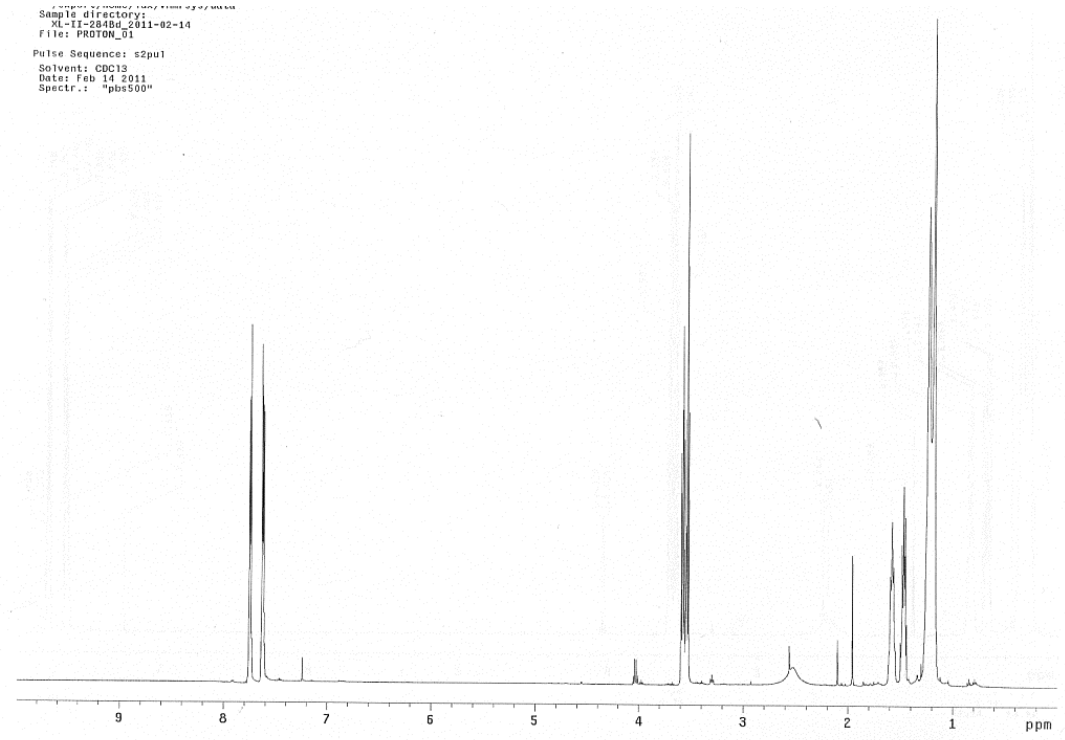

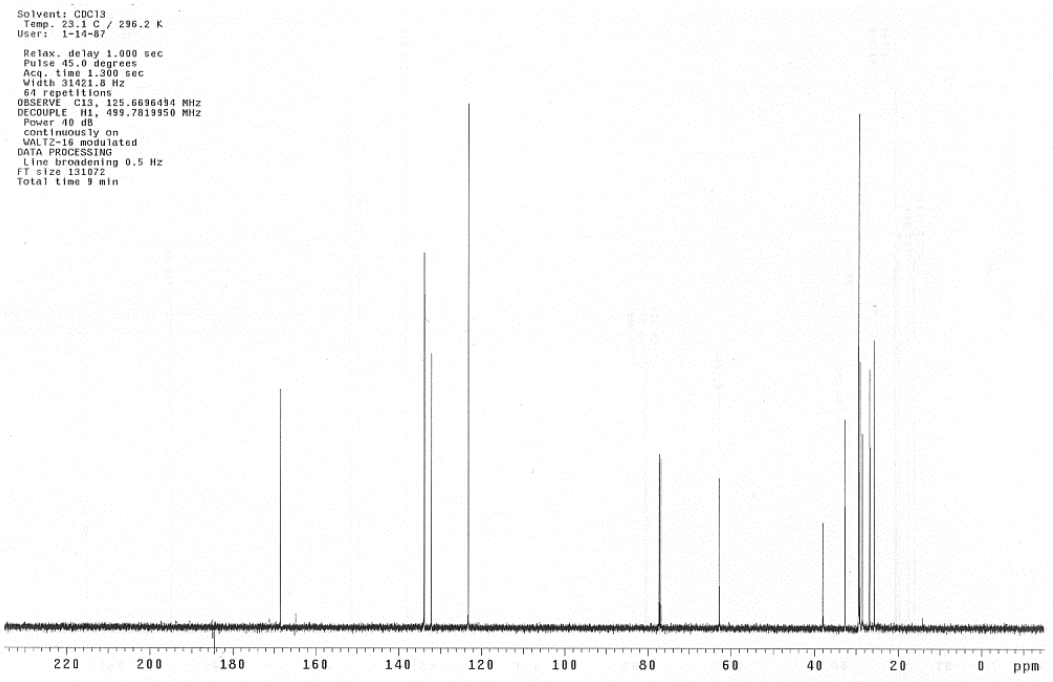

10-(1,3-Dioxoisoindolin-2-yl)decyl methanesulfonate **(10a)**

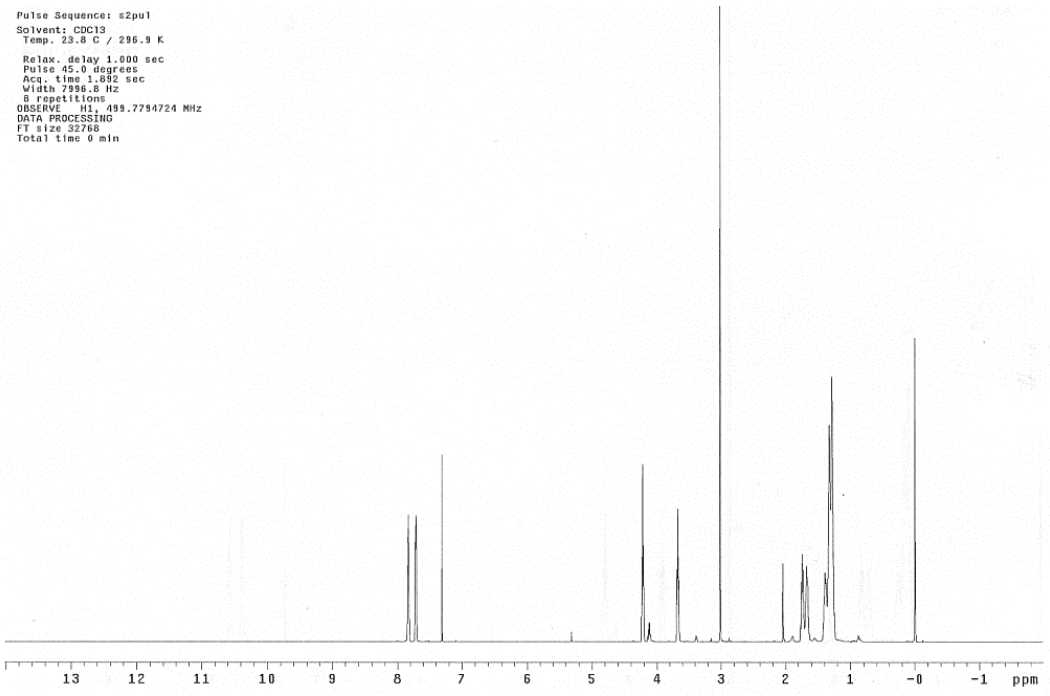

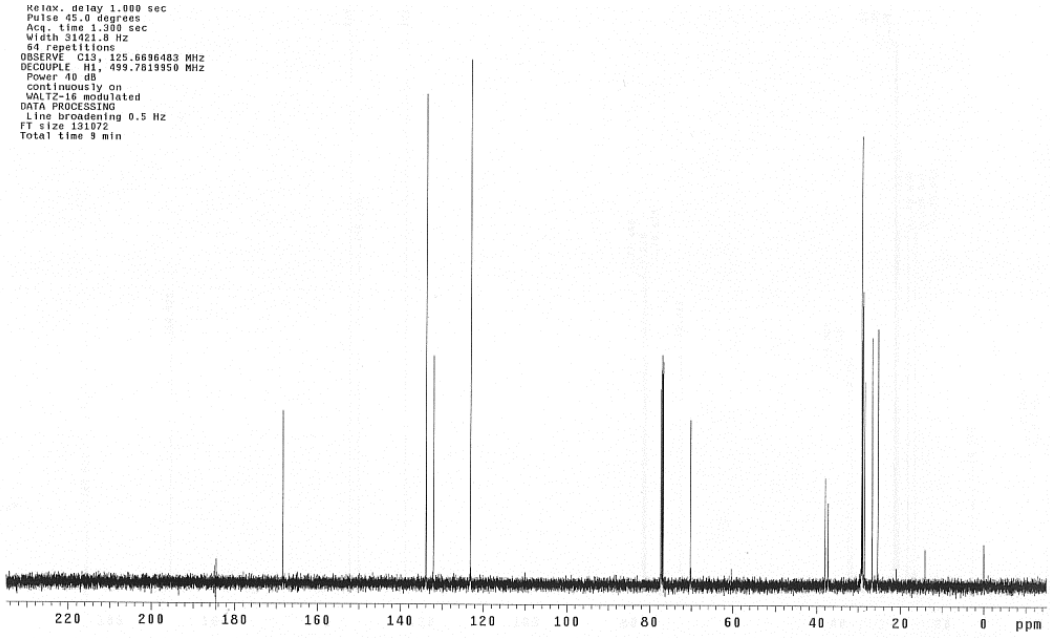

(10-(1,3-Dioxoisoindolin-2-yl)decyl)triphenylphosphonium methanesulfonate (11a)

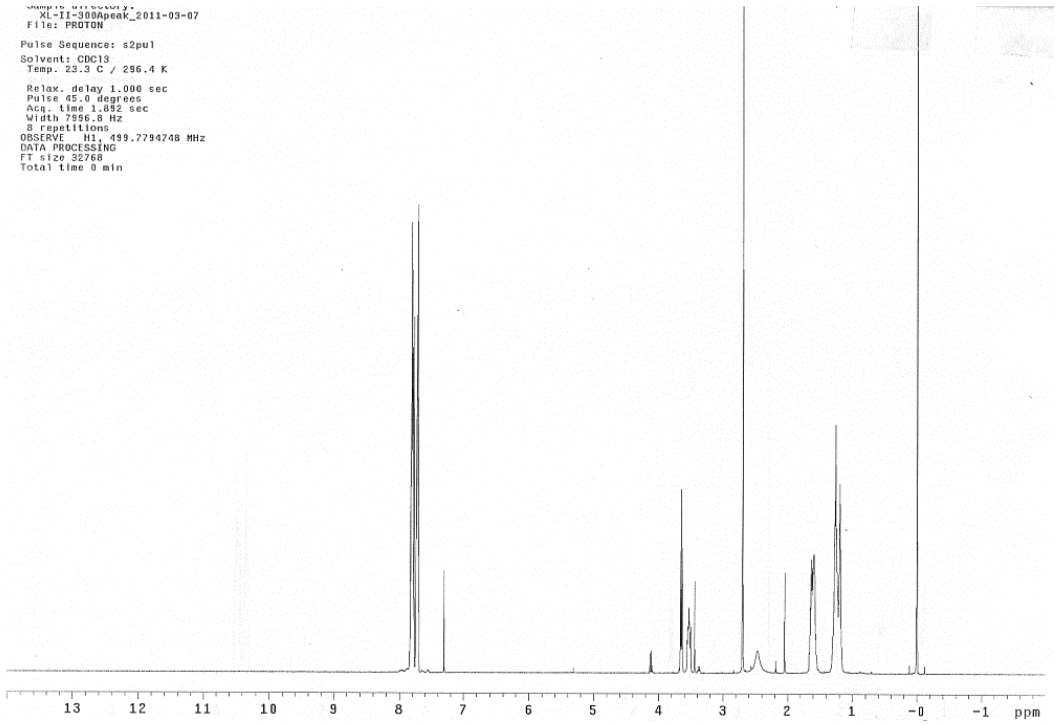

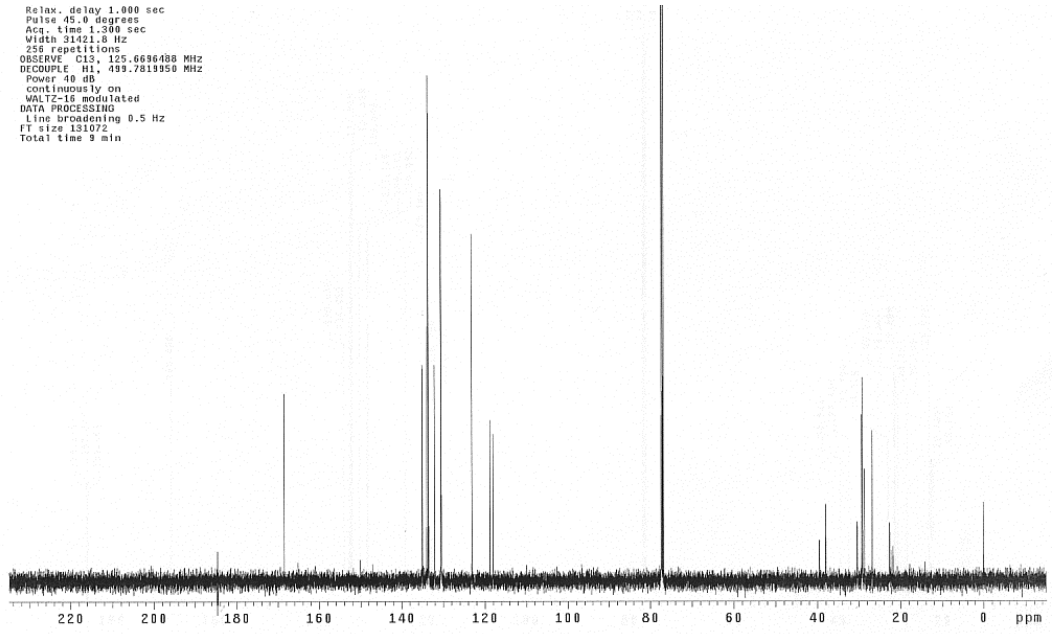

Tribenzyl(10-(1,3-dioxoisoindolin-2-yl)decyl) phosphonium methanesulfonate (11e)

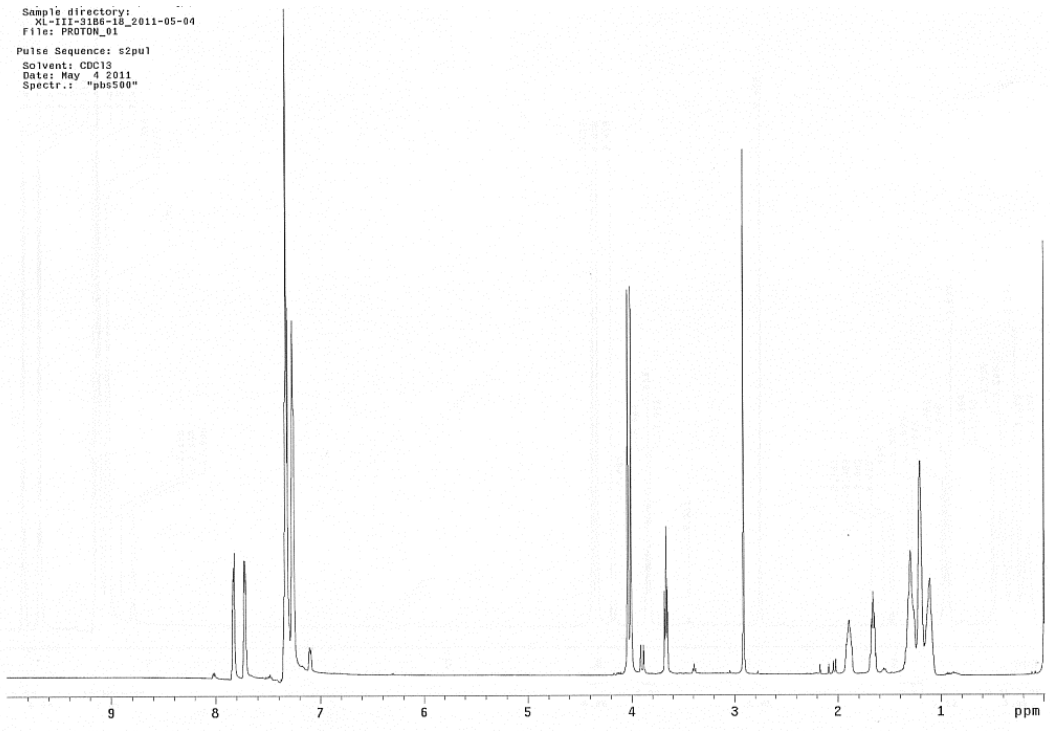

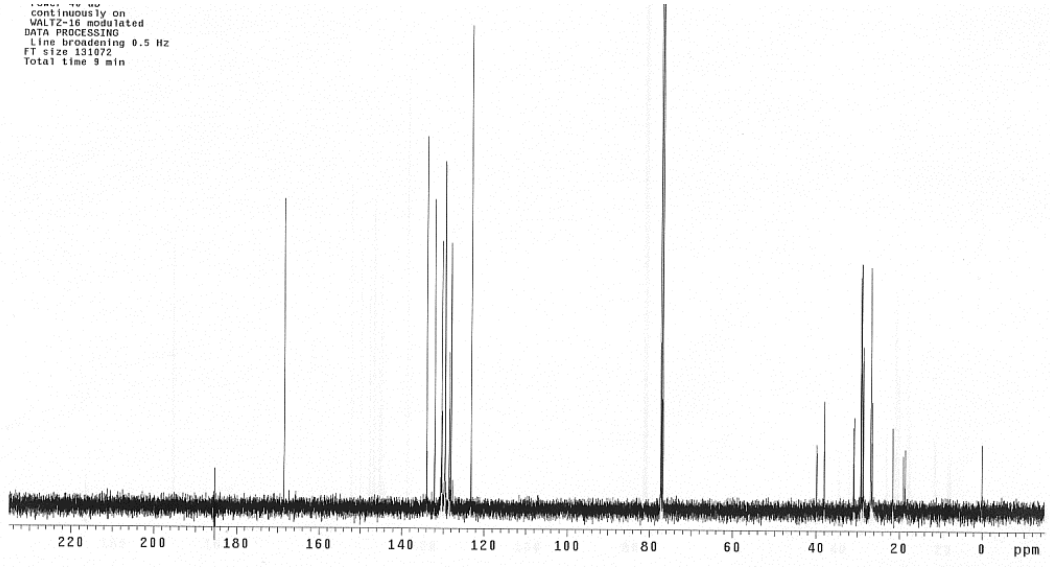

Tricyclohexyl(10-(1,3-dioxoisoindolin-2-yl)decyl) phosphonium methanesulfonate (11f)

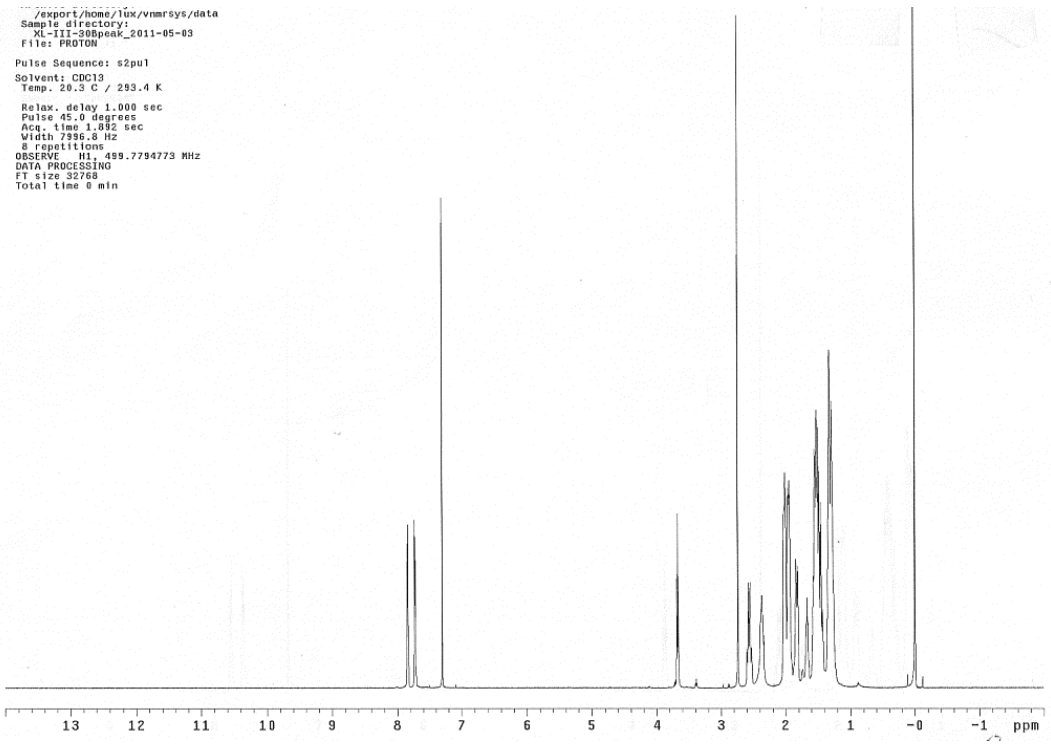

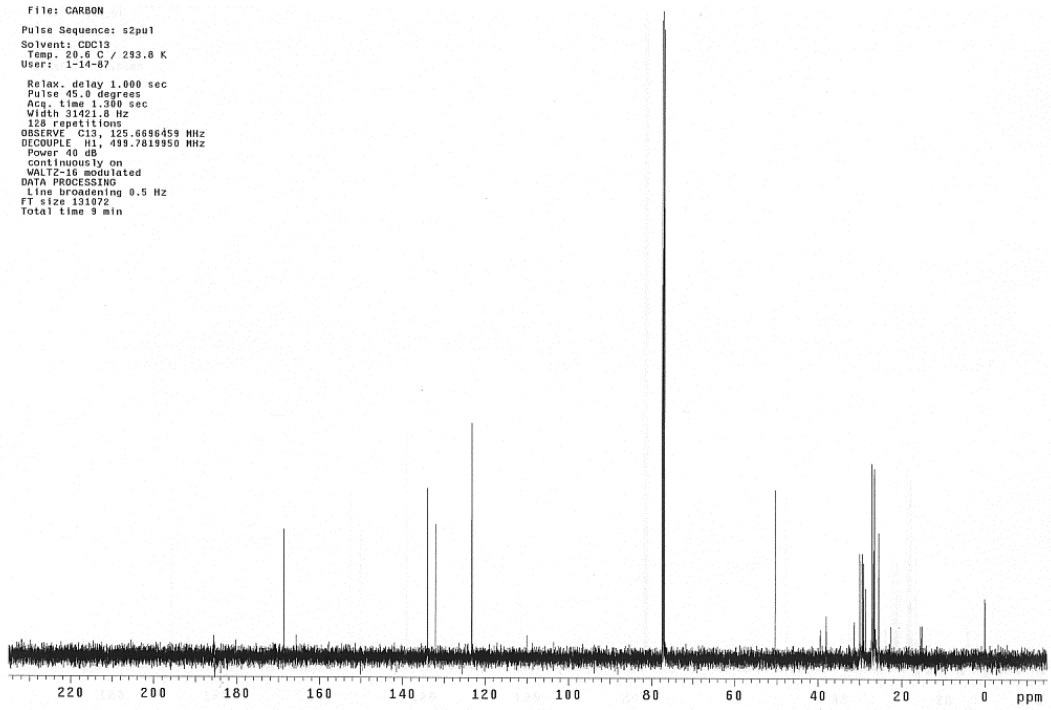

(10-(1,3-Dioxoisoindolin-2-yl)decyl)*tris*(4-methoxyphenyl)phosphonium methanesulfonate (11g)

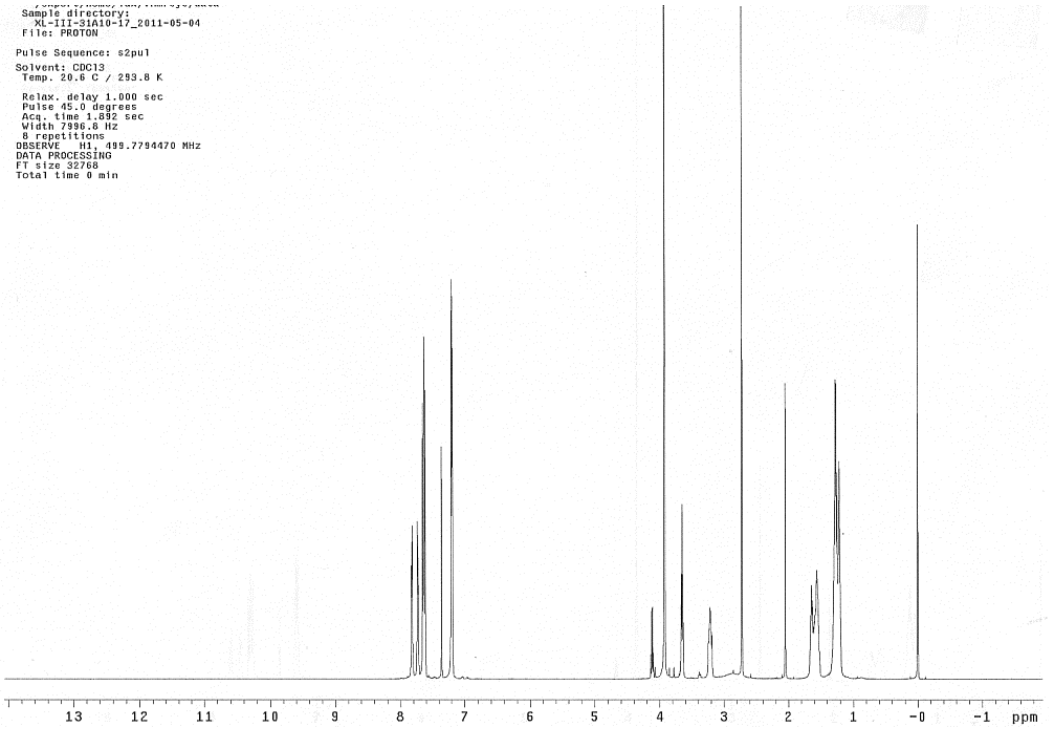

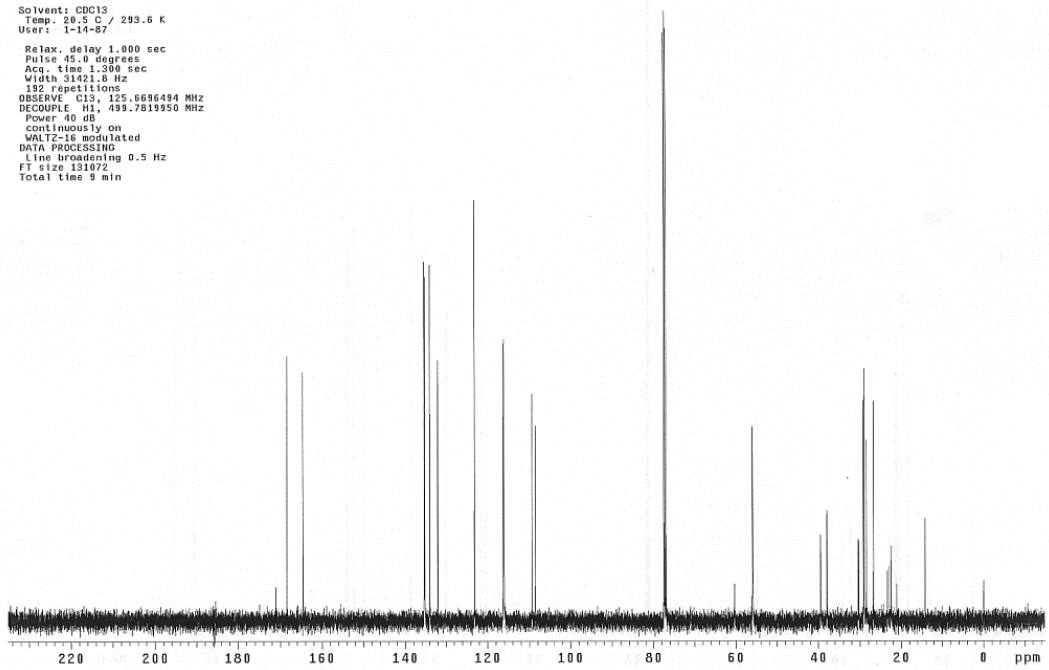

2-(2-Hydroxyethylamino)naphthalene-1,4-dione (13a)

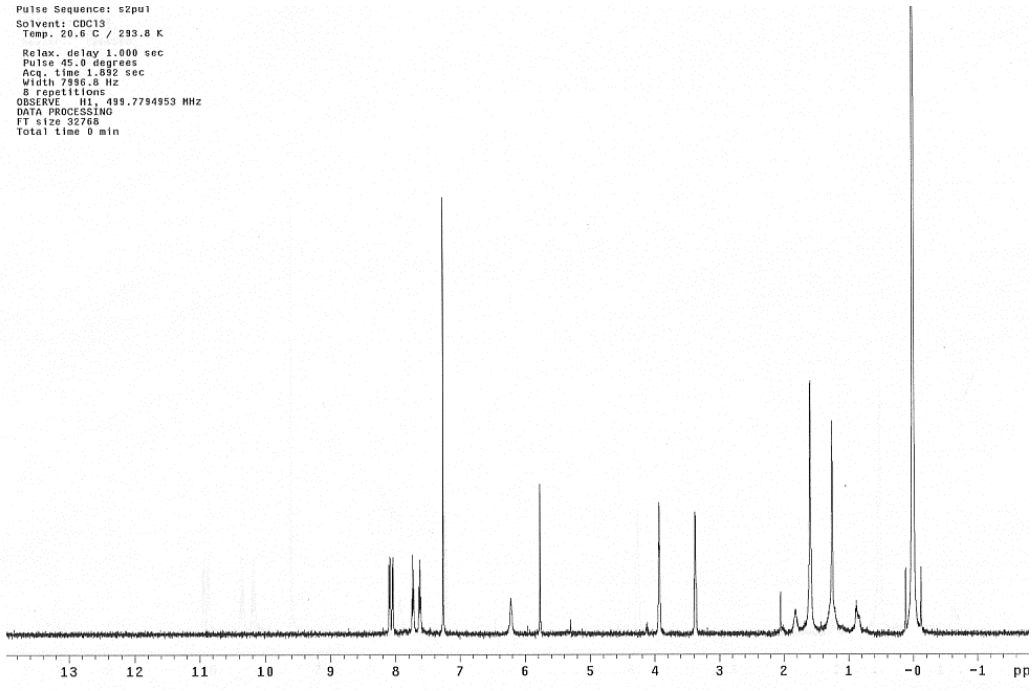

2-(10-Hydroxydecylamino)naphthalene-1,4-dione (13b)

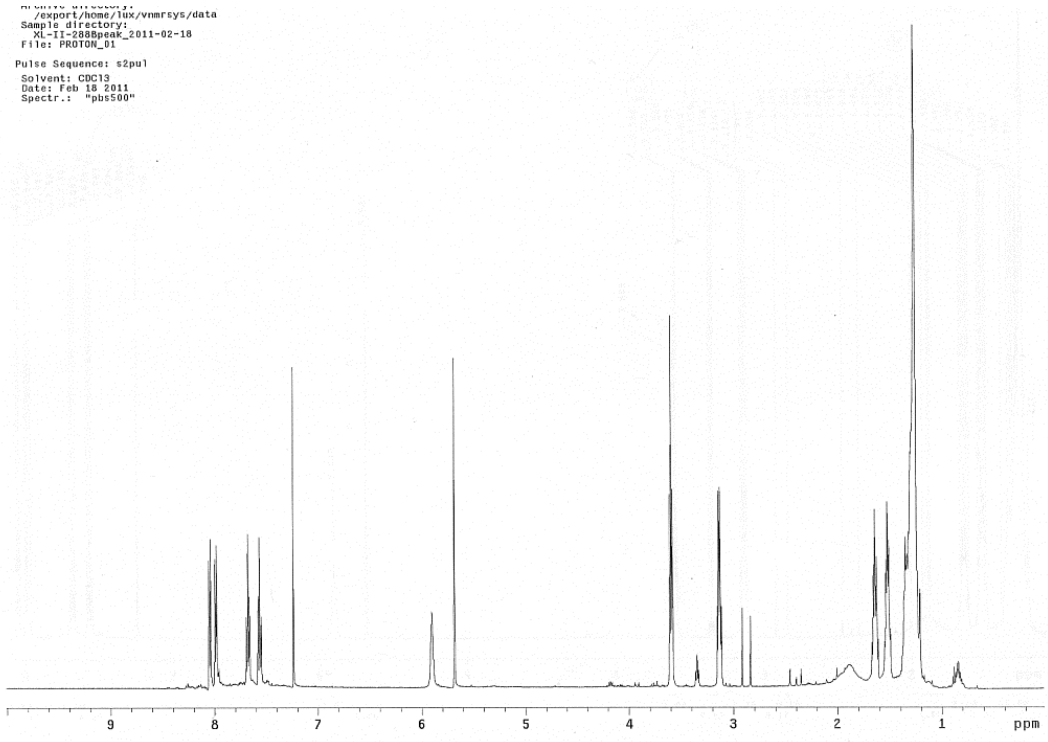

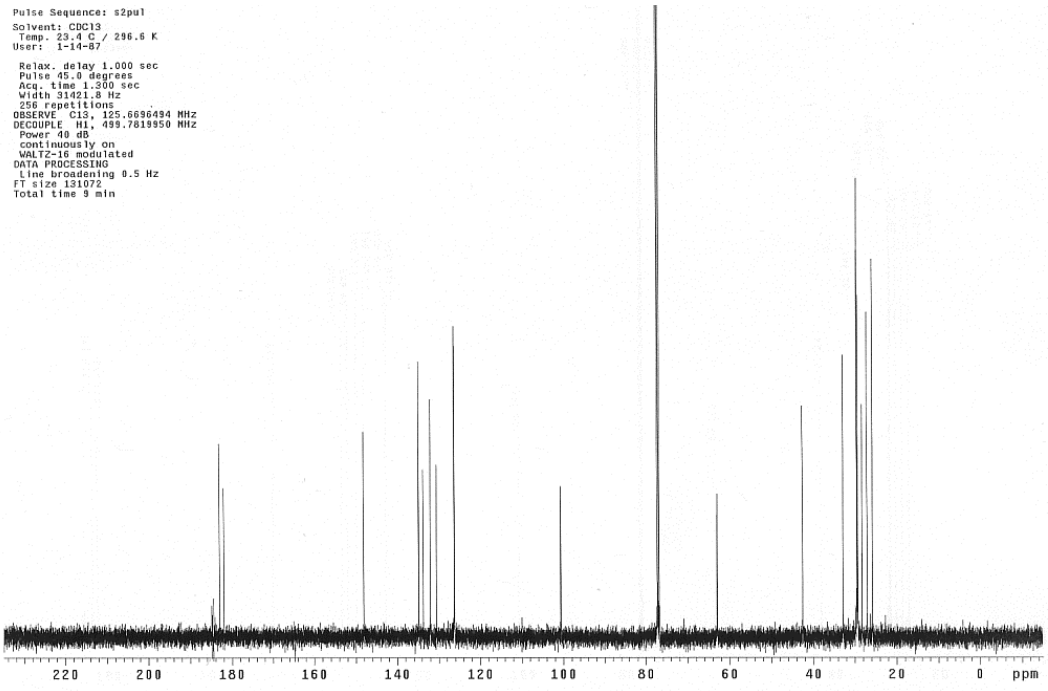

2-((1,4-Dioxo-1,4-dihydronaphthalen-2-yl)amino)ethyl methanesulfonate (14a)

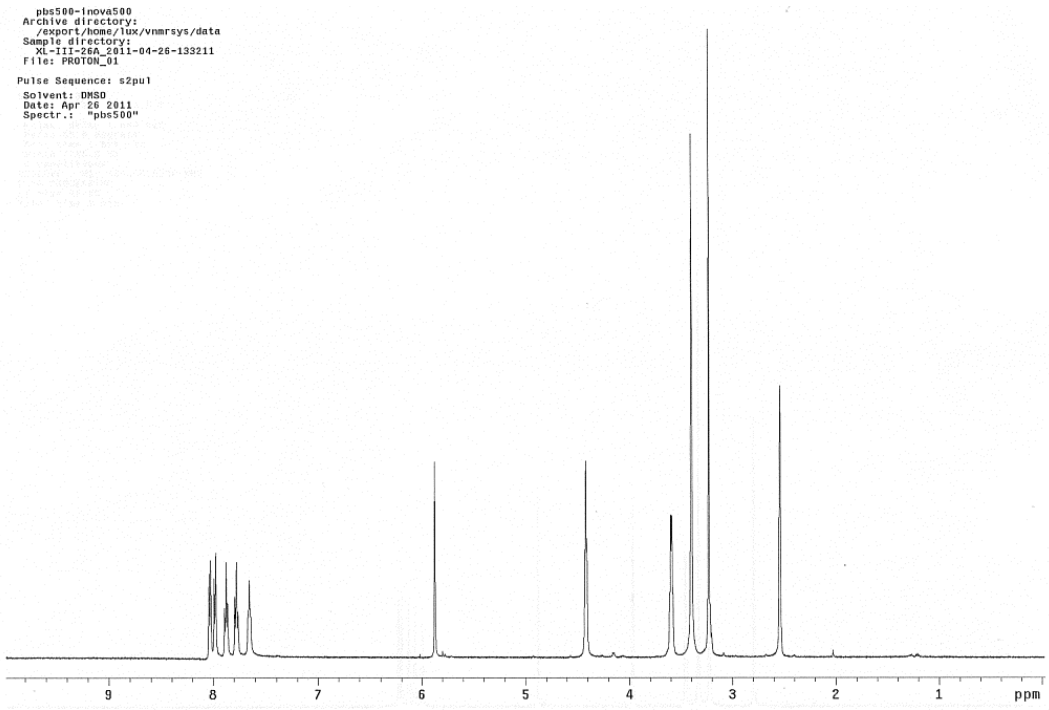

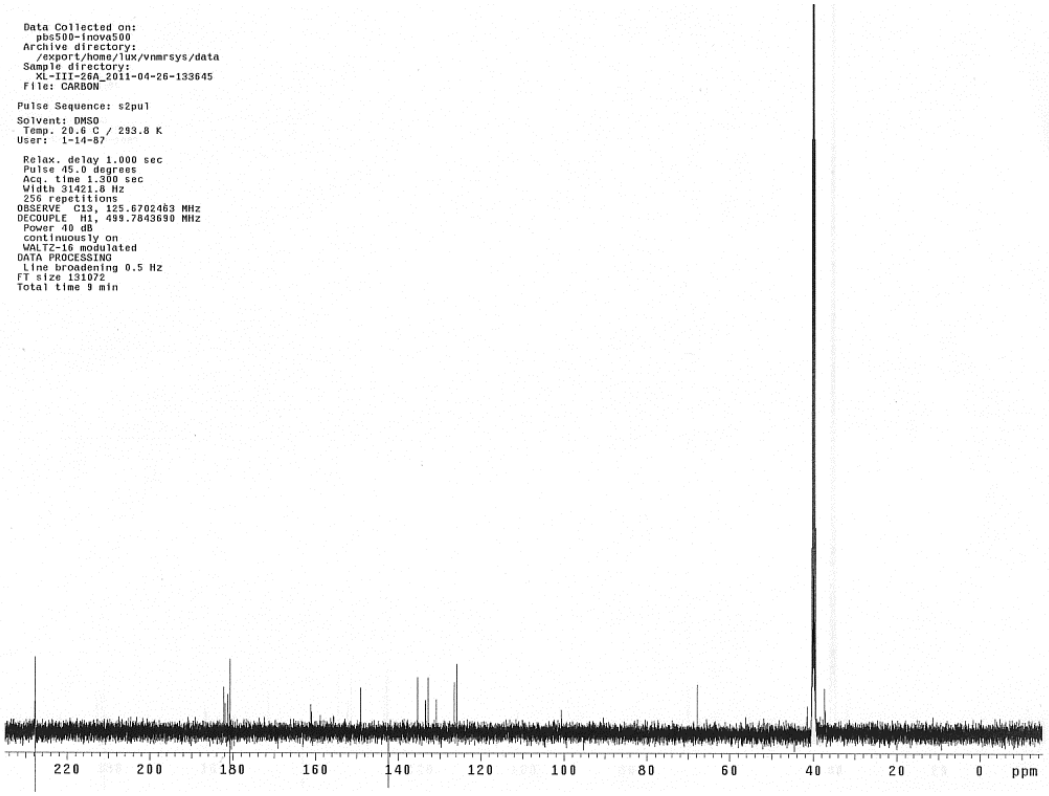

10-(1,4-Dihydro-1,4-dioxonaphthalen-3-ylamino)decyl methanesulfonate (14b)

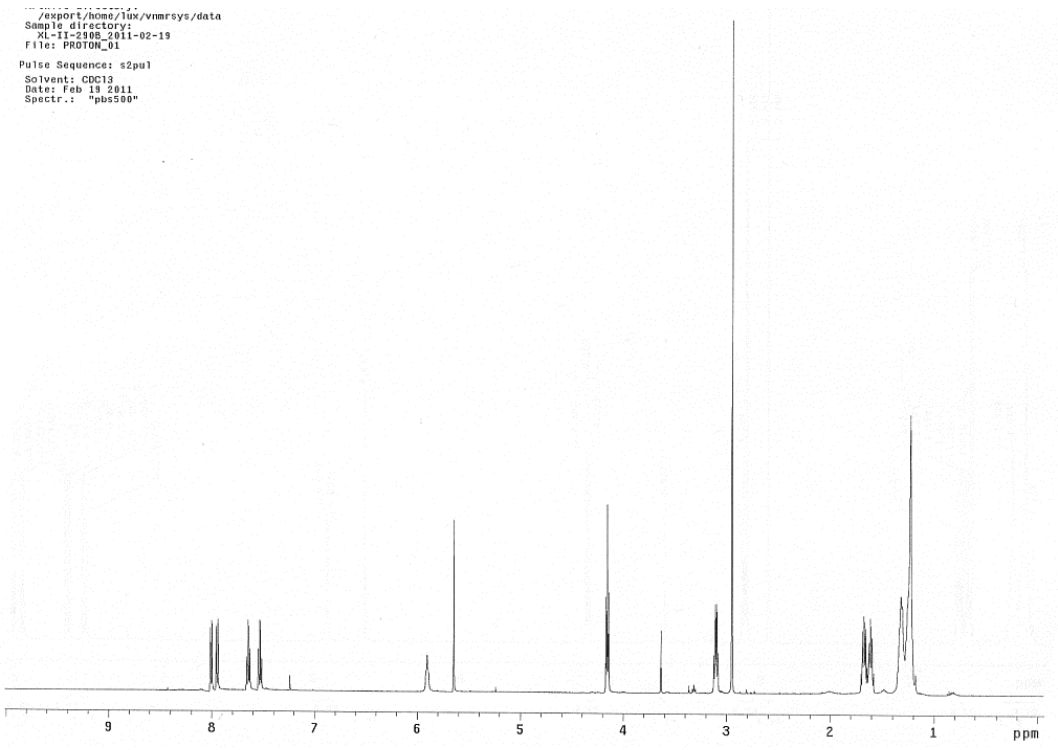

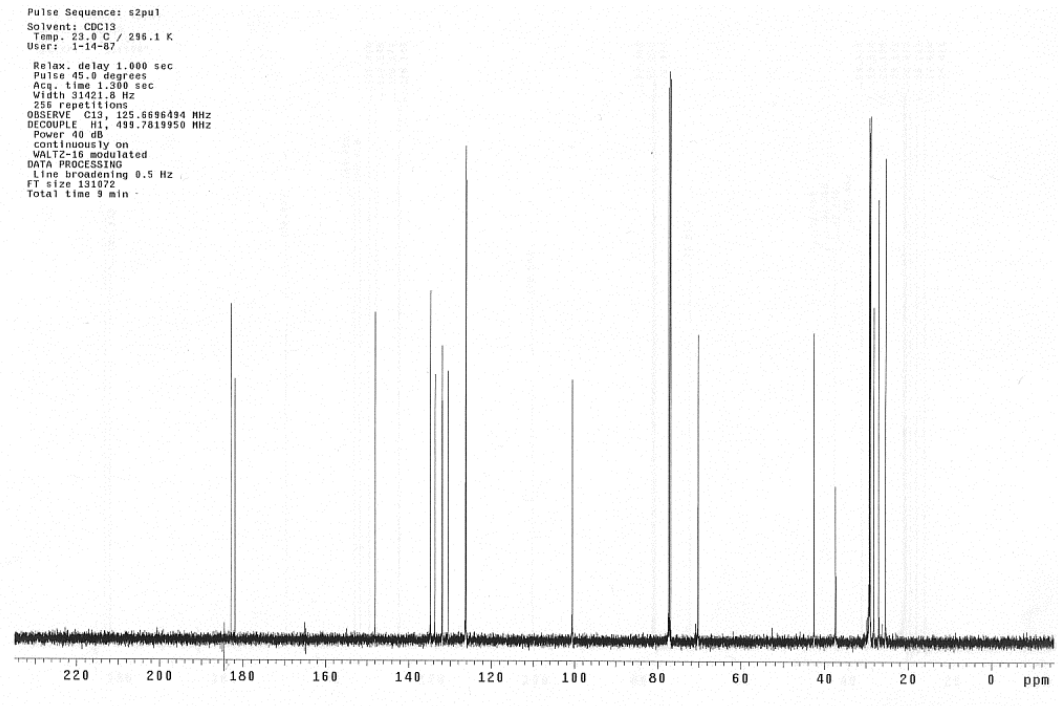

(2-(1,4-Dihydro-1,4-dioxonaphthalen-3-ylamino)ethyl)triphenylphosphonium methanesulfonate (15a)

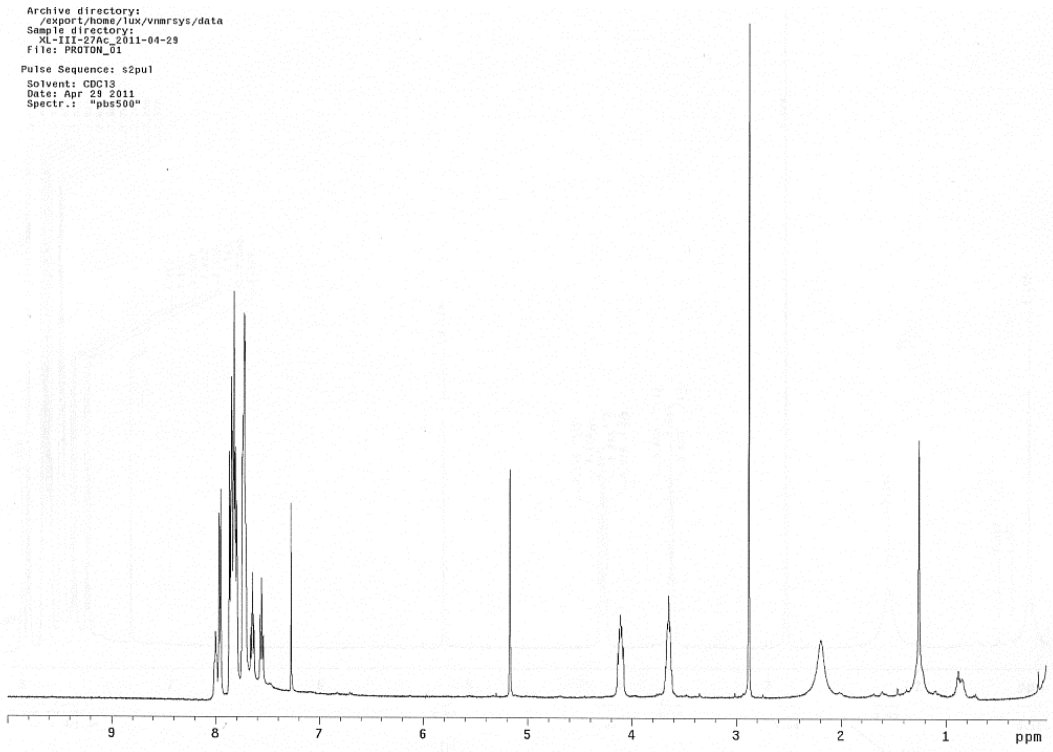

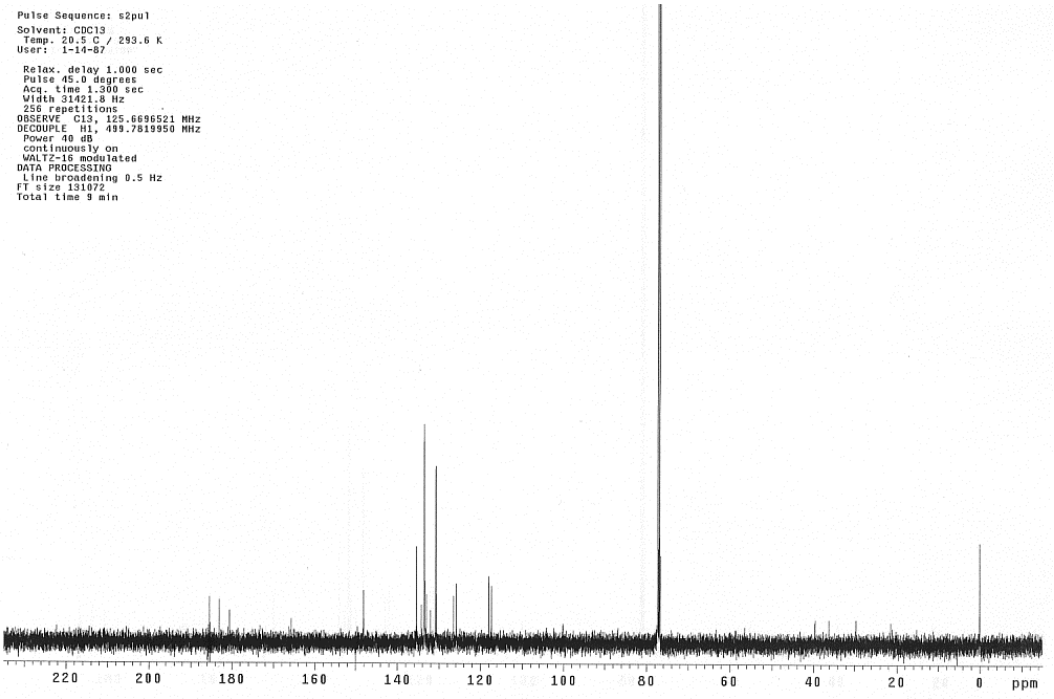

(10-(1,4-Dihydro-1,4-dioxonaphthalen-3-ylamino)decyl)*tris*(4-fluorophenyl)-phosphonium methanesulfonate (15b)

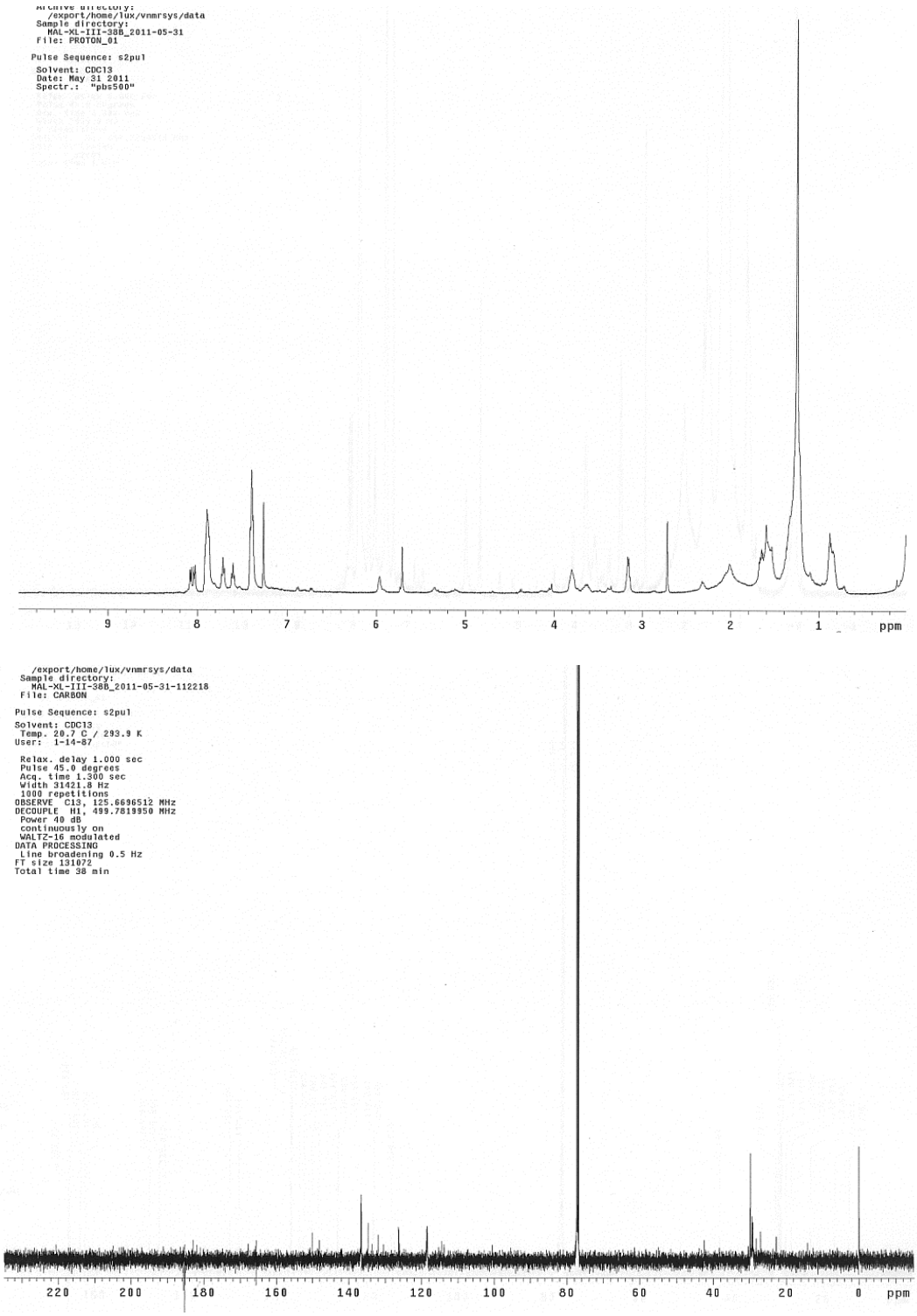

(10-(1,4-Dihydro-1,4-dioxonaphthalen-3-ylamino)decyl)tribenzyl-phosphonium methanesulfonate (15c)

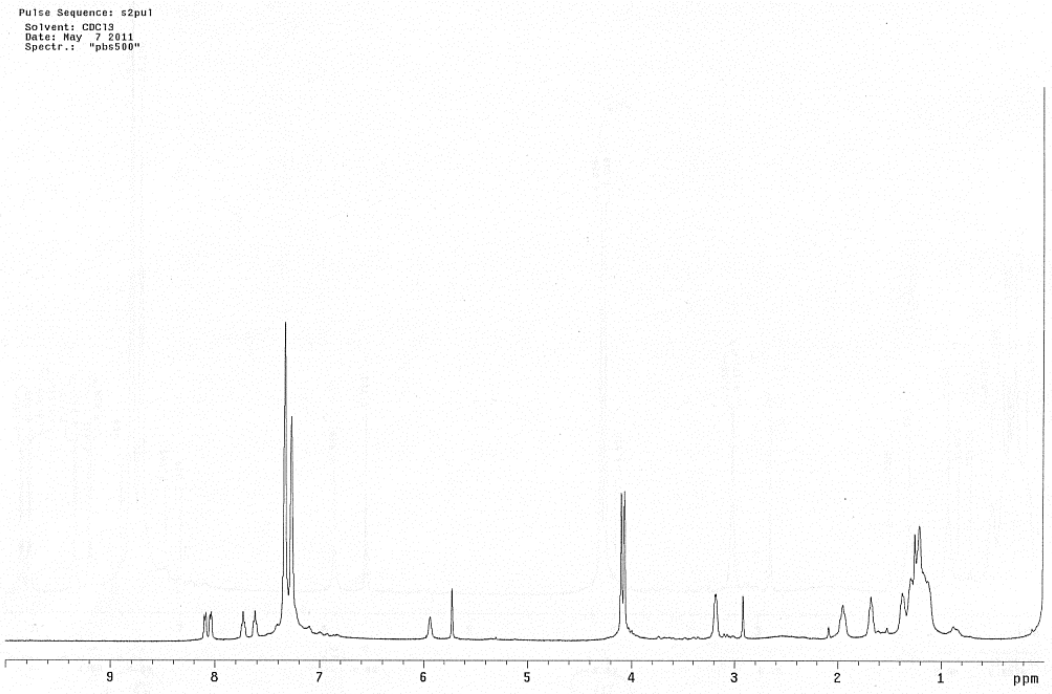

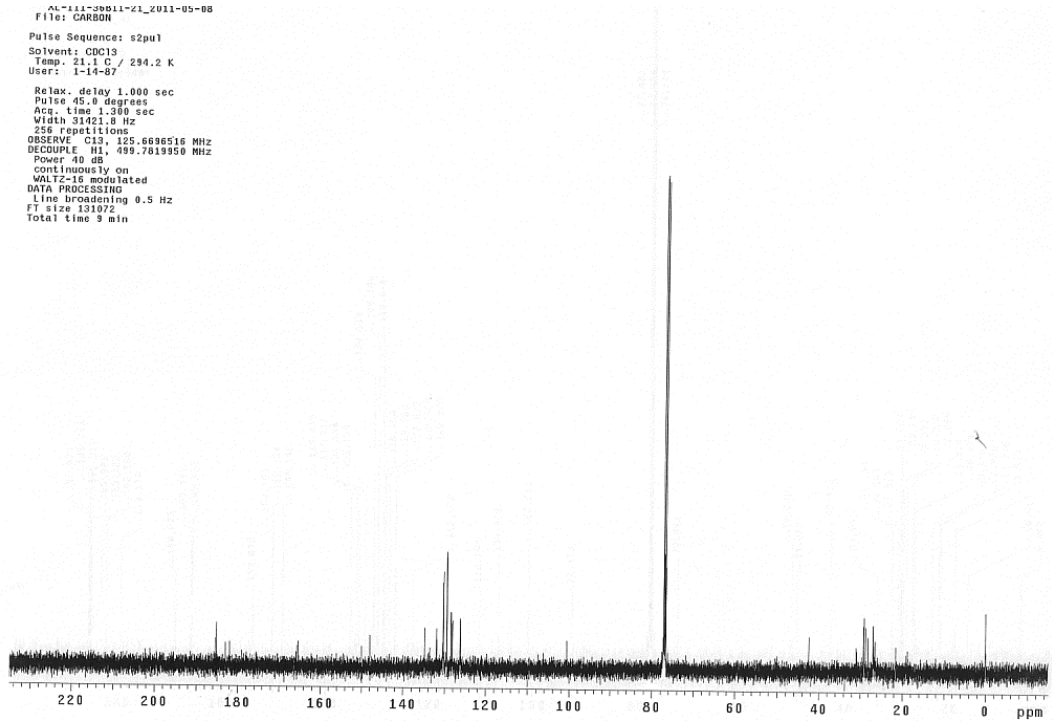

(10-(1,4-Dihydro-1,4-dioxonaphthalen-3-ylamino)decyl)*tris*(4-methoxyphenyl)phosphonium methanesulfonate (15d)

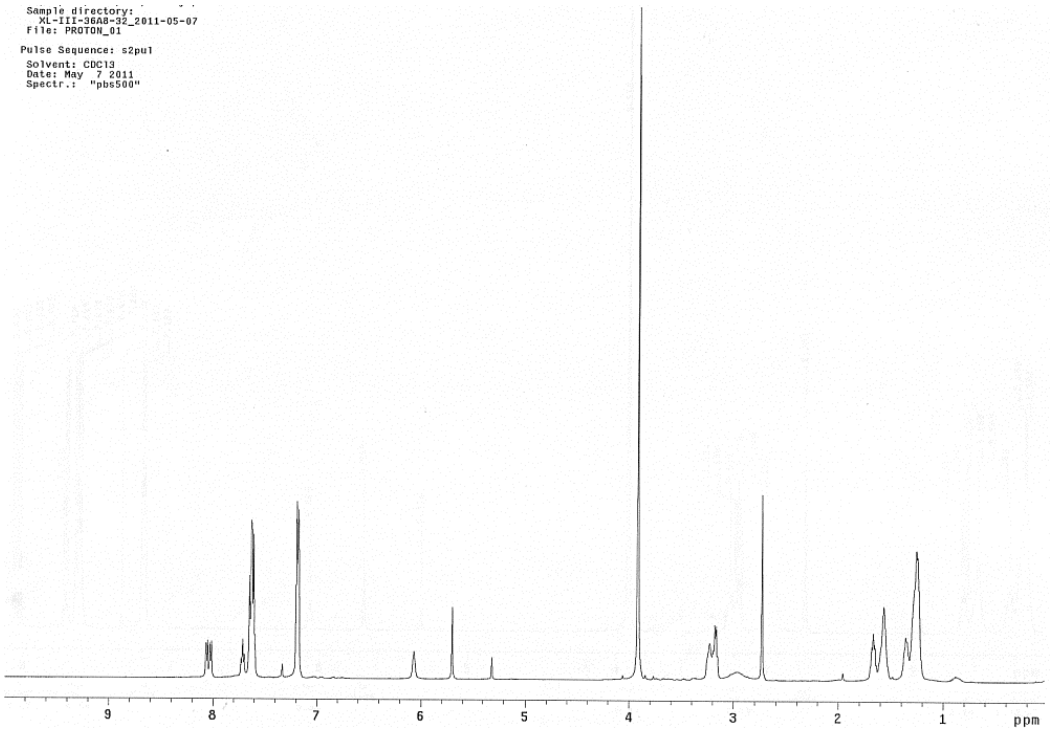

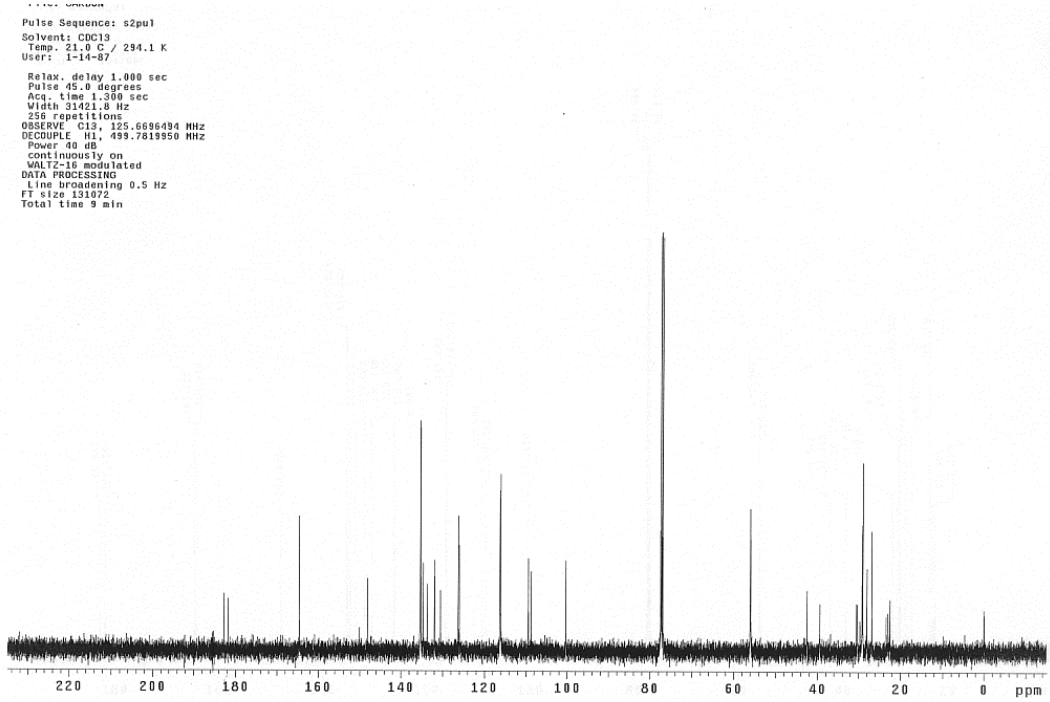

(10-(1,4-Dihydro-1,4-dioxonaphthalen-3-ylamino)decyl)triphenylphosphonium methanesulfonate (15e)

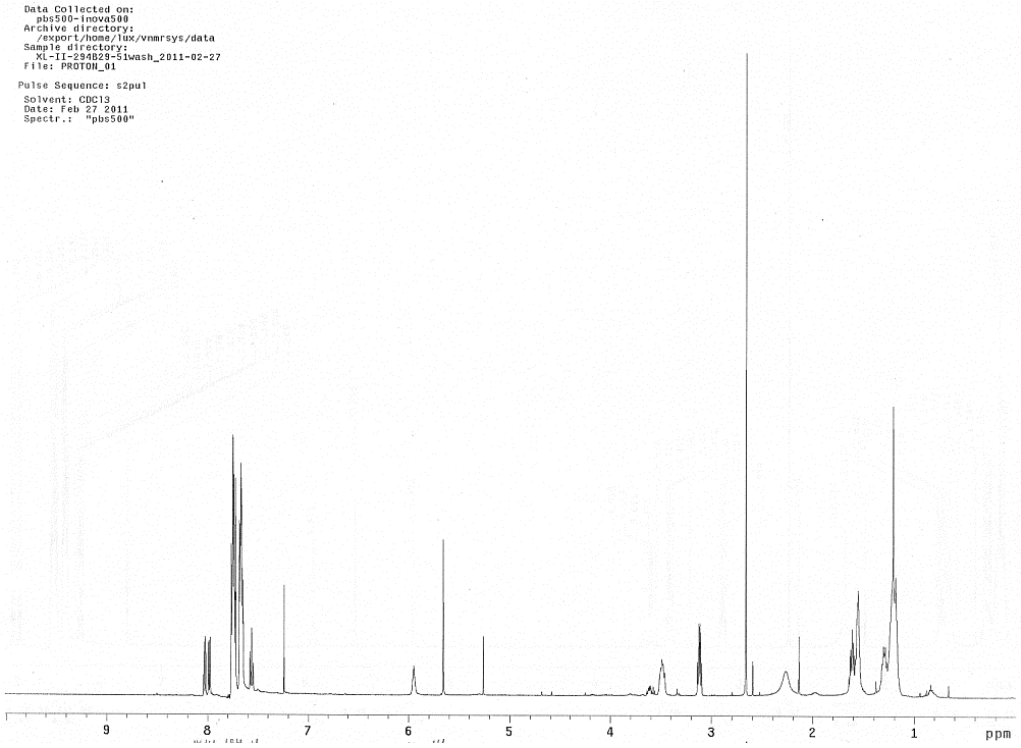

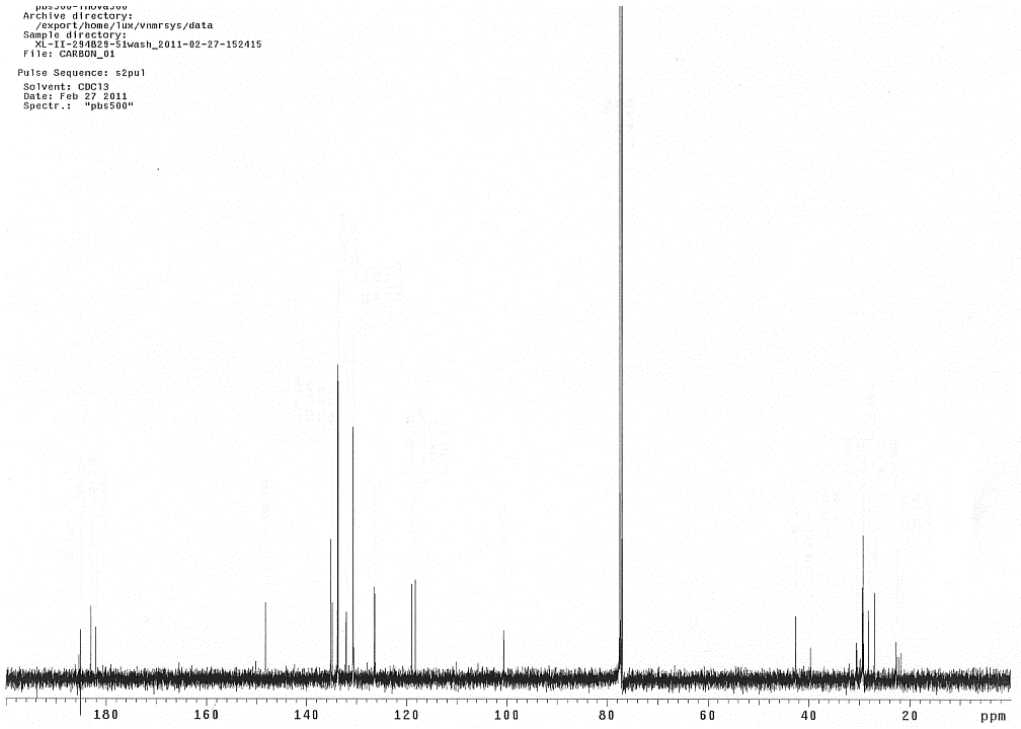

(10-(1,4-Dihydro-1,4-dioxonaphthalen-3-ylamino)decyl)tricyclohexyl-phosphonium methanesulfonate (15f)

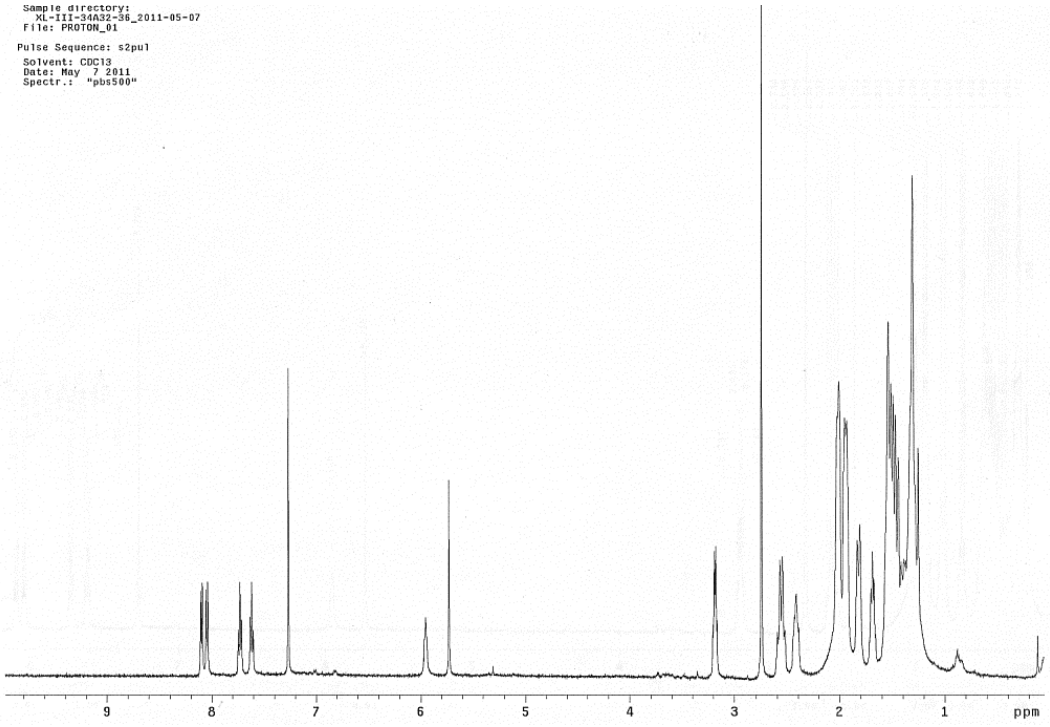

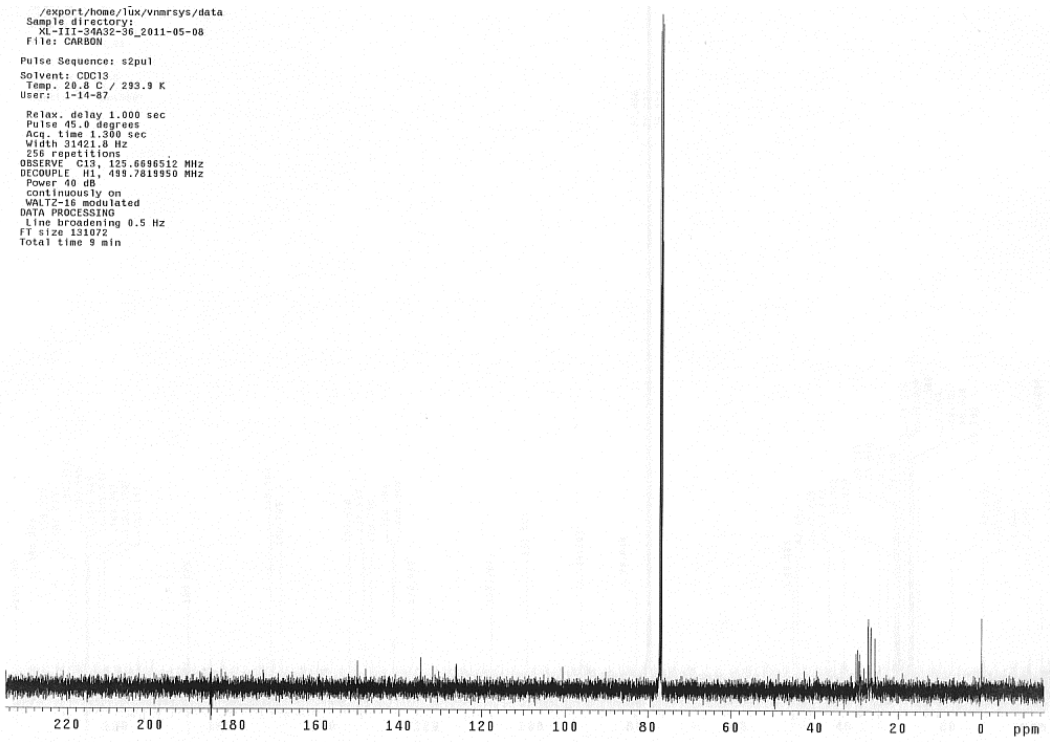

2-(Chloromethyl)-3-methylnaphthalene-1,4-dione (20)

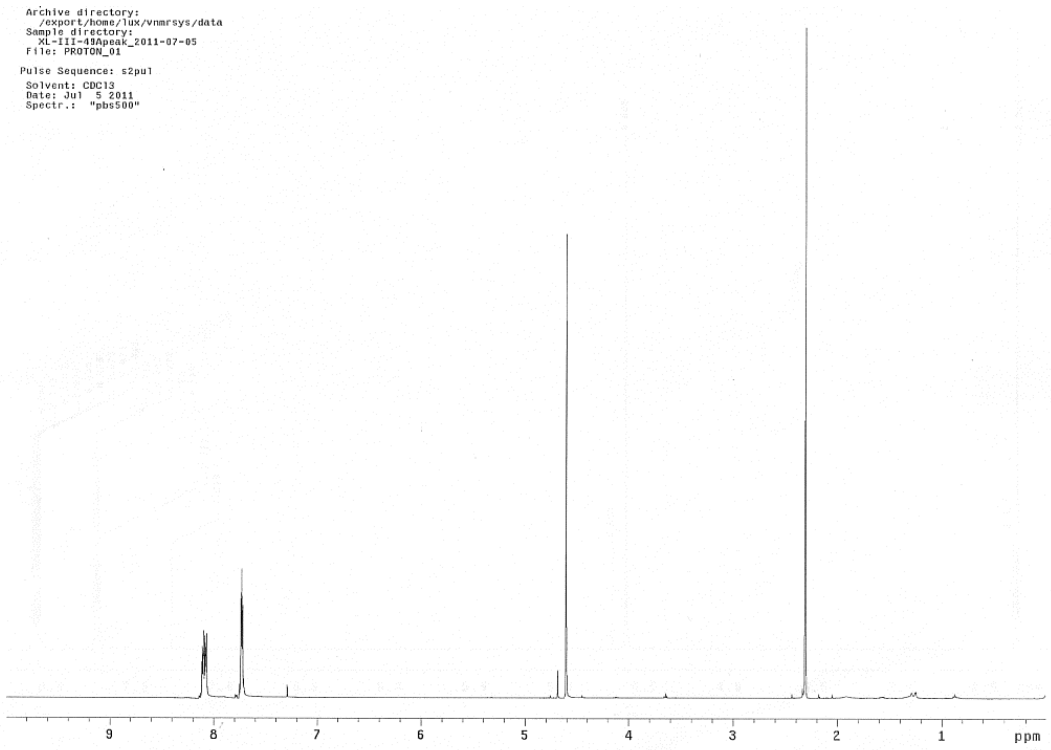

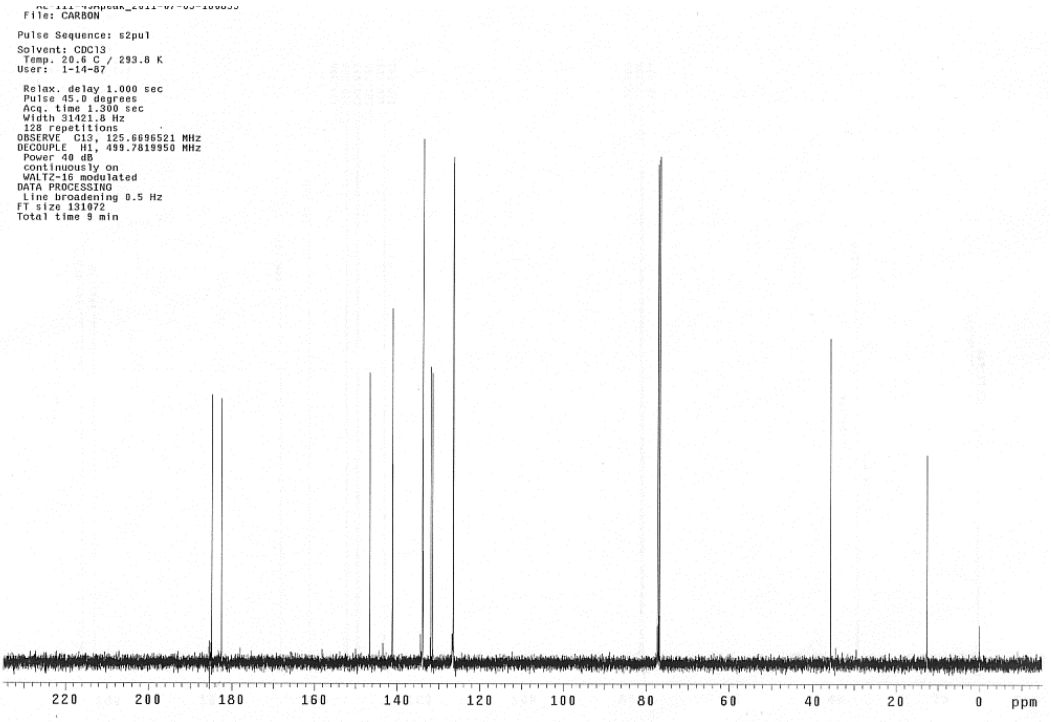

((3-Methyl-1,4-dioxo-1,4-dihydronaphthalen-2-yl)methyl)triphenylphosphonium chloride (21)

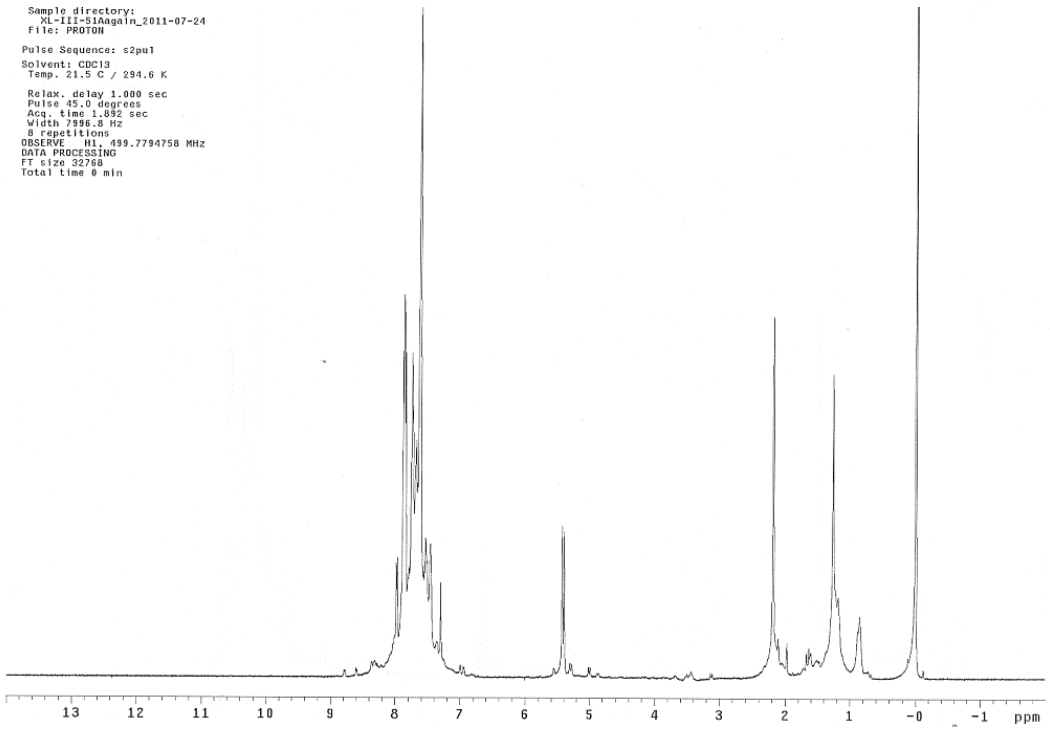

1α-(10-Bromodecyl)naphtho[2,3-β]oxirene-2,7(1α*H*,7α*H*)-dione (23c)

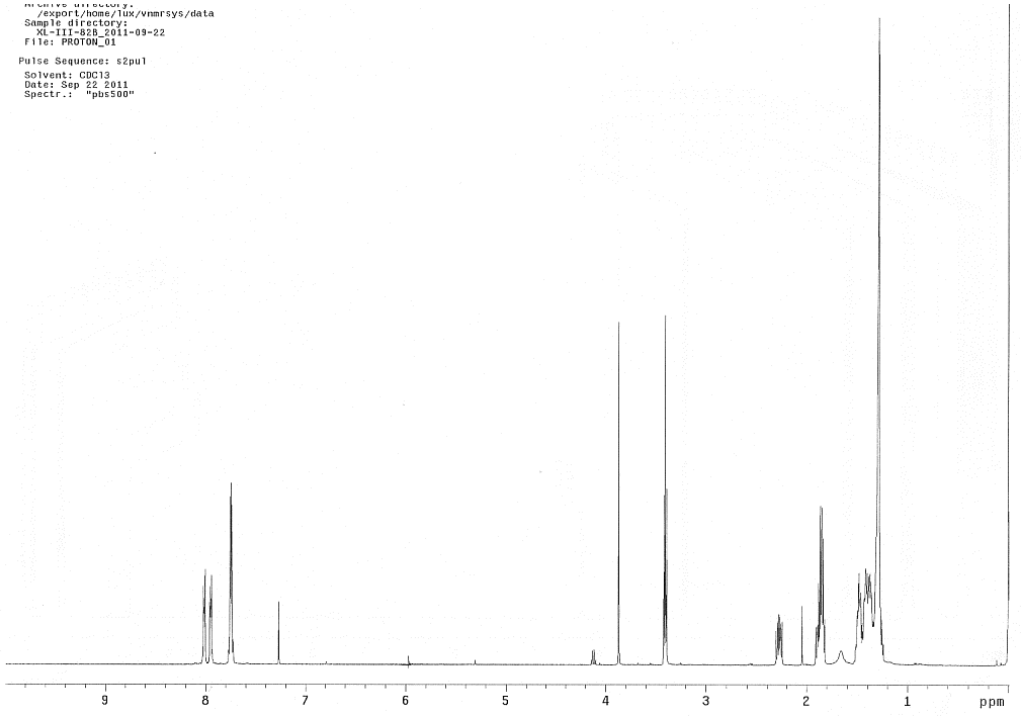

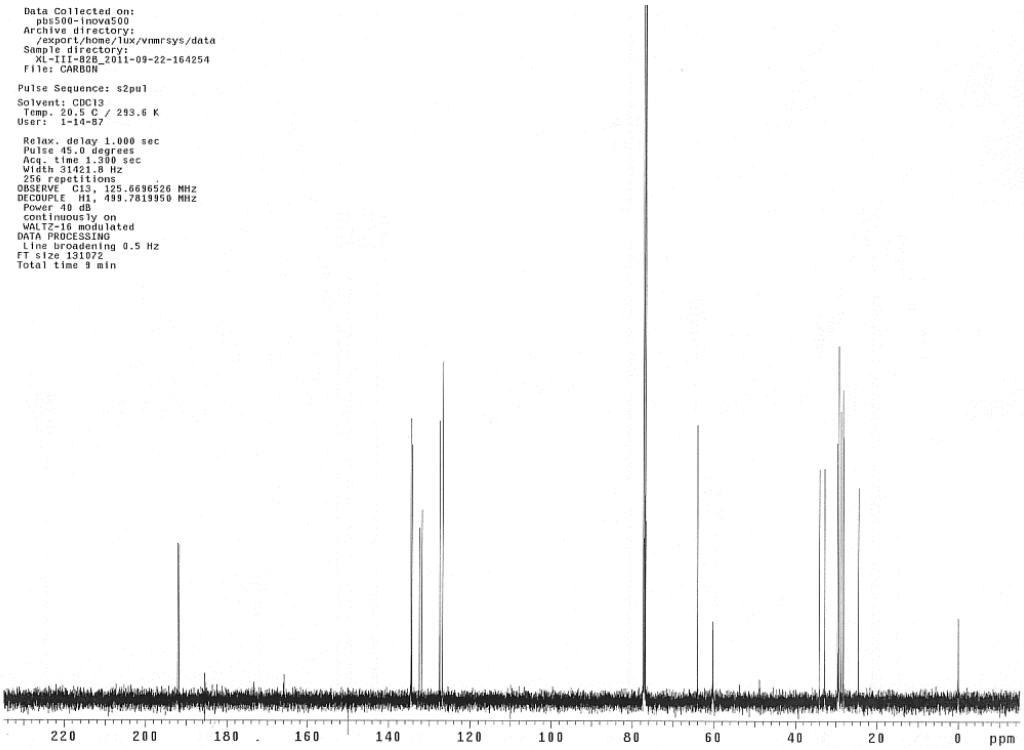

2-(Bromodecyl)-3-hydroxynaphthalene-1,4-dione (24c)

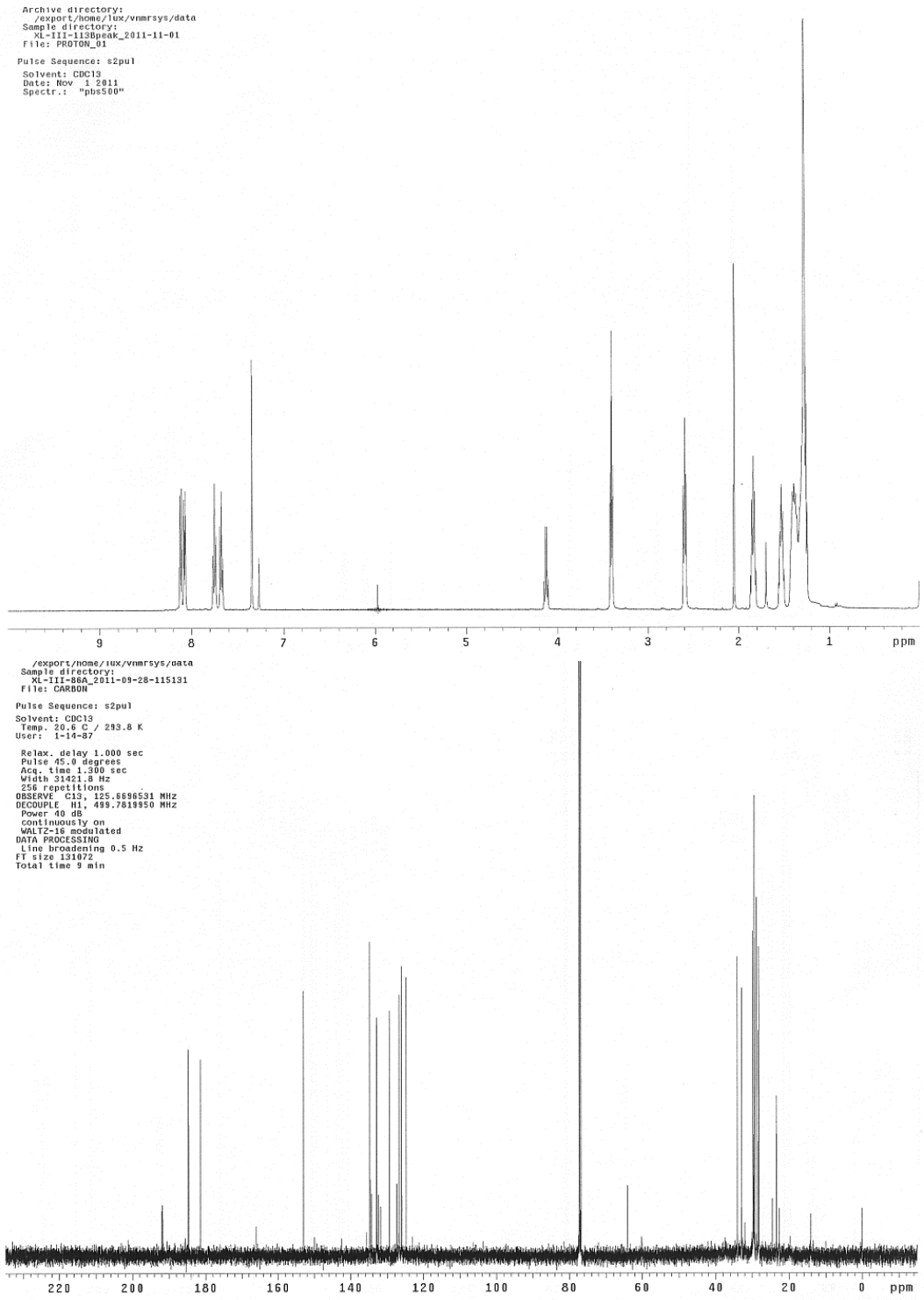

3-(10-Bromodecyl)-1,4-dioxo-1,4-dihydronaphthalen-2-yl acetate (25c)

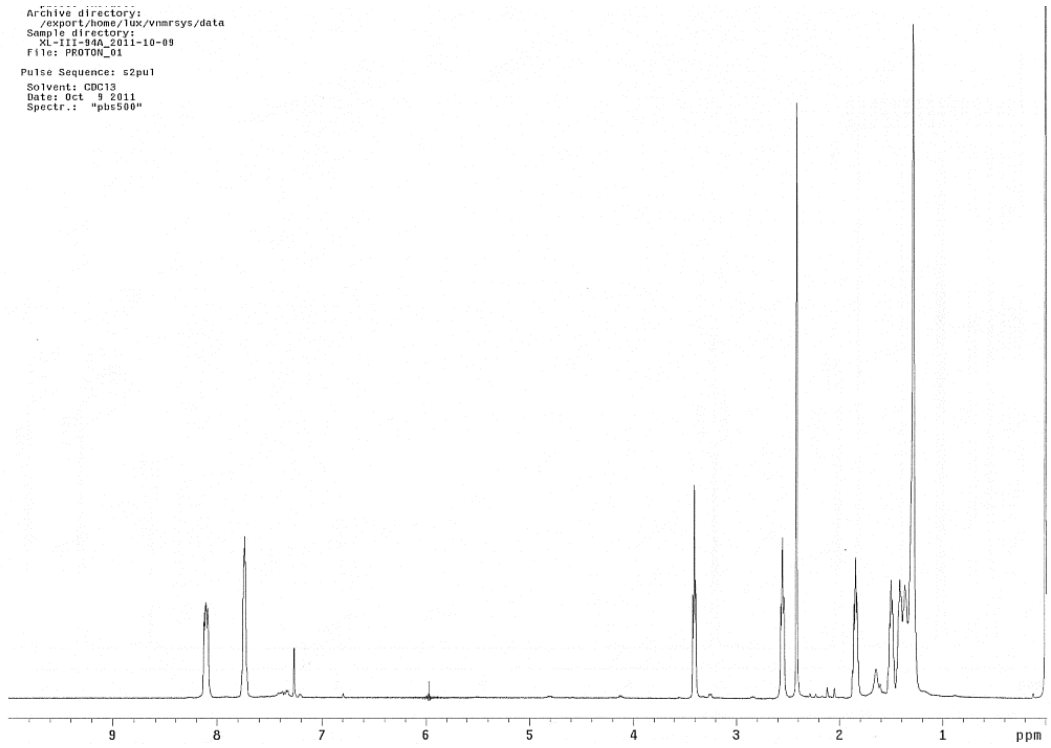

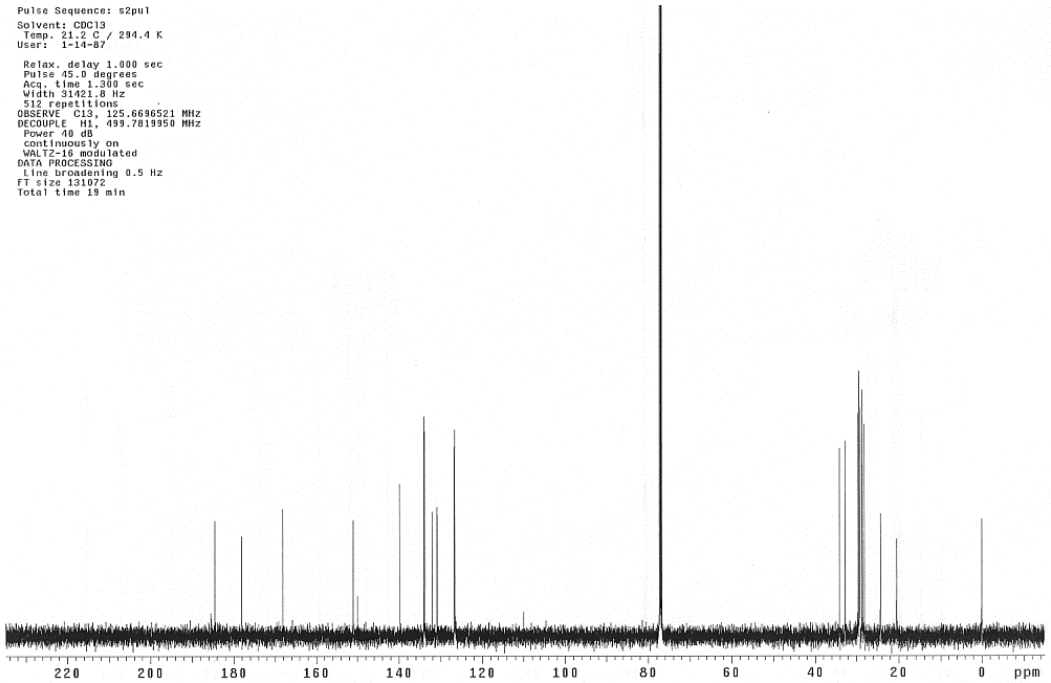

(10-(3-Acetoxy-1,4-dioxo-1,4-dihydronaphthalen-2-yl)decyl)triphenylphosphonium bromide (26a)

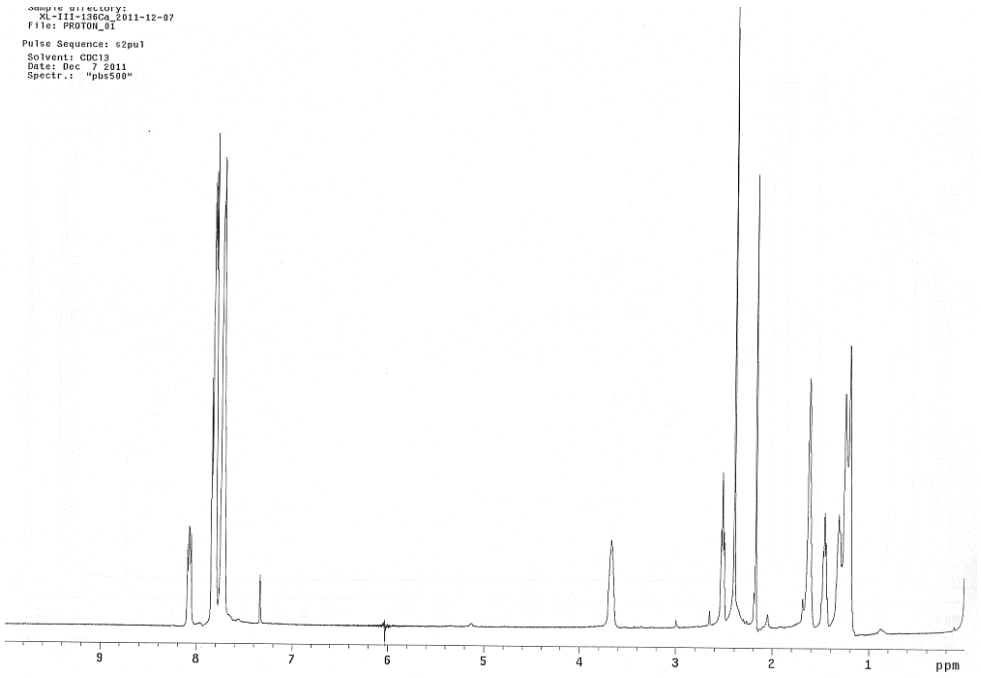

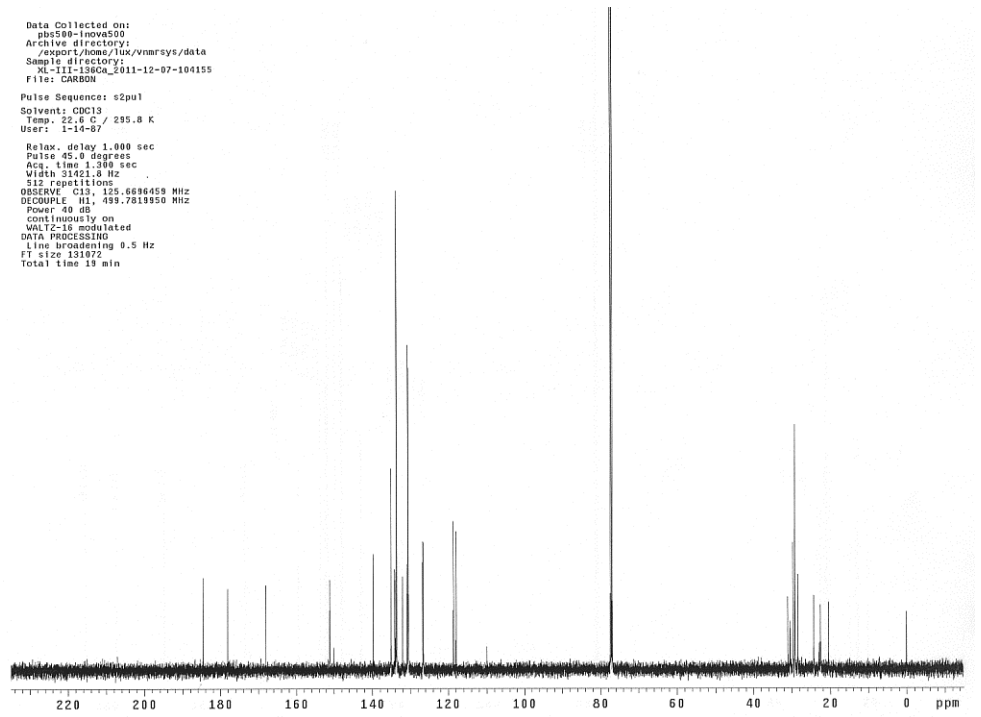

(4-(10-(3-Acetoxy-1,4-dioxo-1,4-dihydronaphthalen-2-yl) phenyl)bromodecyloxy)triphenylphosphonium bromide (29)

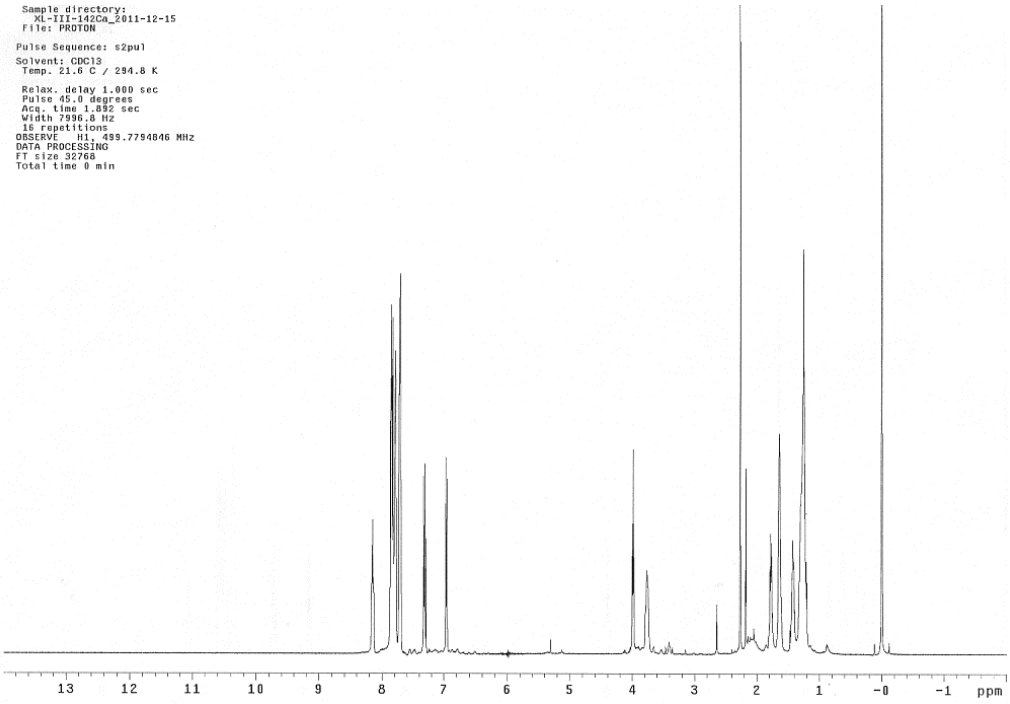

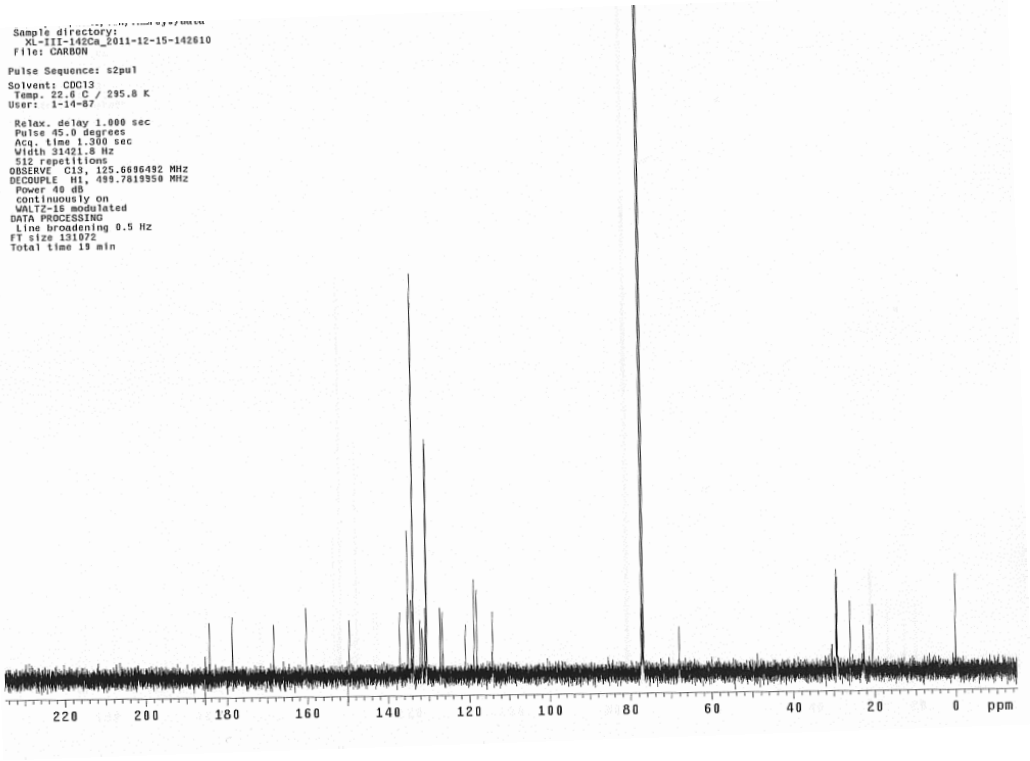

(10-(3-Hydroxy-1,4-dioxo-1,4-dihydronaphthalen-2-yl)decyl)triphenylphosphonium bromide (27a)

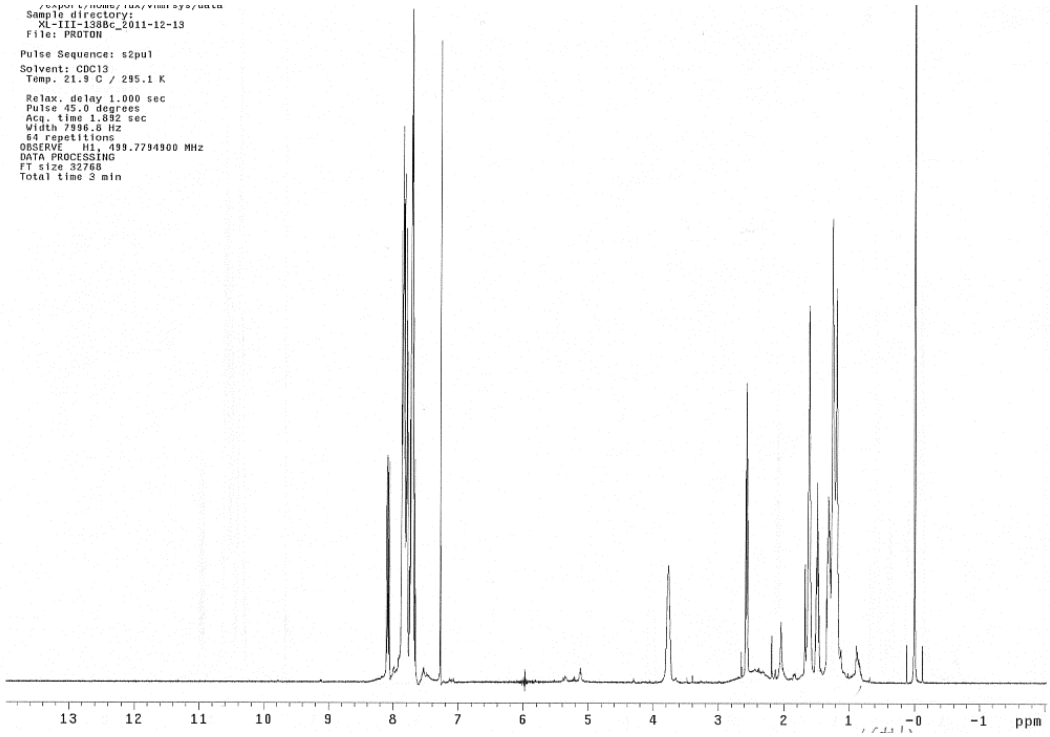

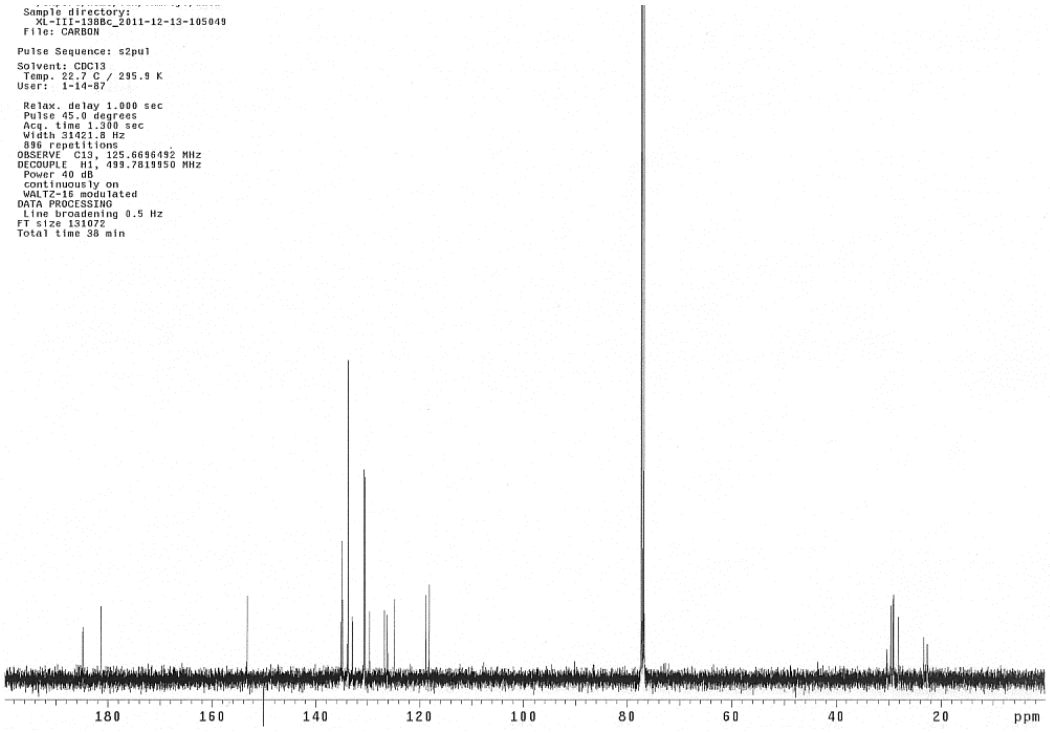

(10-(3-Hydroxy-1,4-dioxo-1,4-dihydronaphthalen-2-yl)decyl)tributylphosphonium bromide (27b)

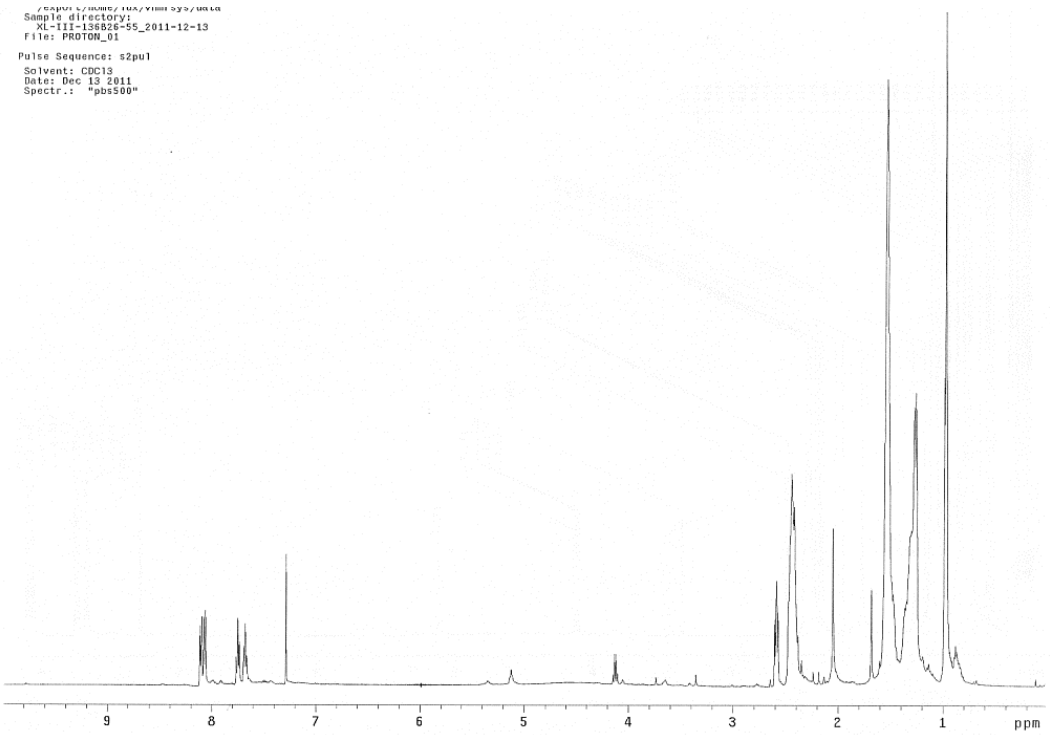

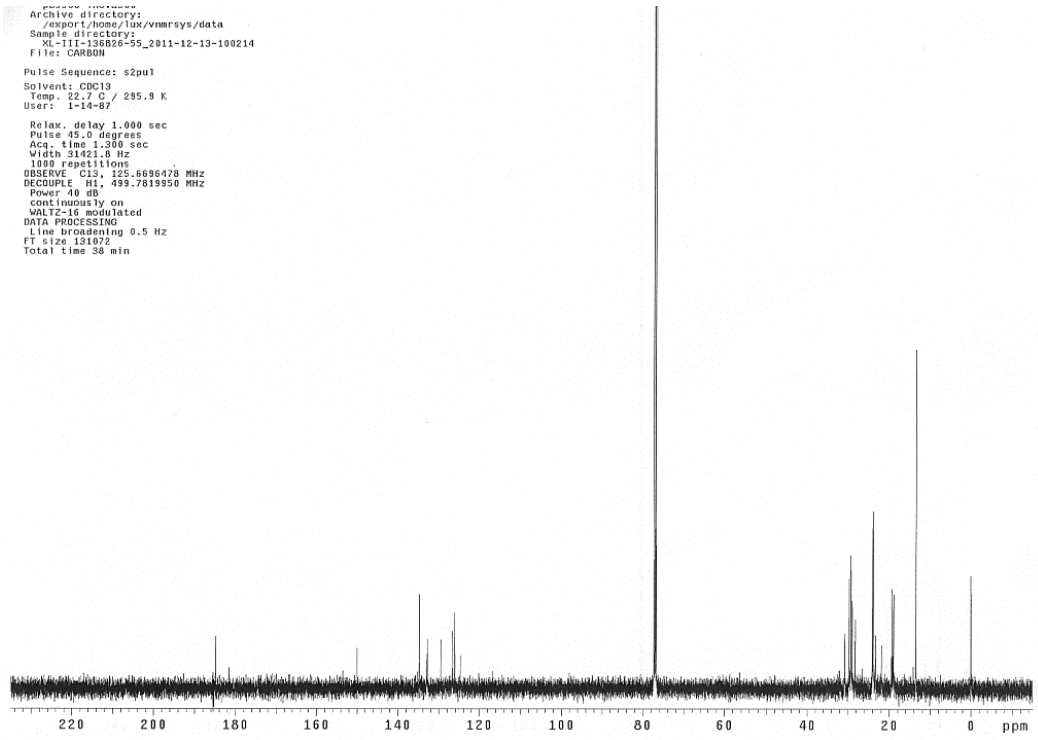

(10-(3-Hydroxy-1,4-dioxo-1,4-dihydronaphthalen-2-yl)decyl)tribenzylphosphonium bromide (27c)

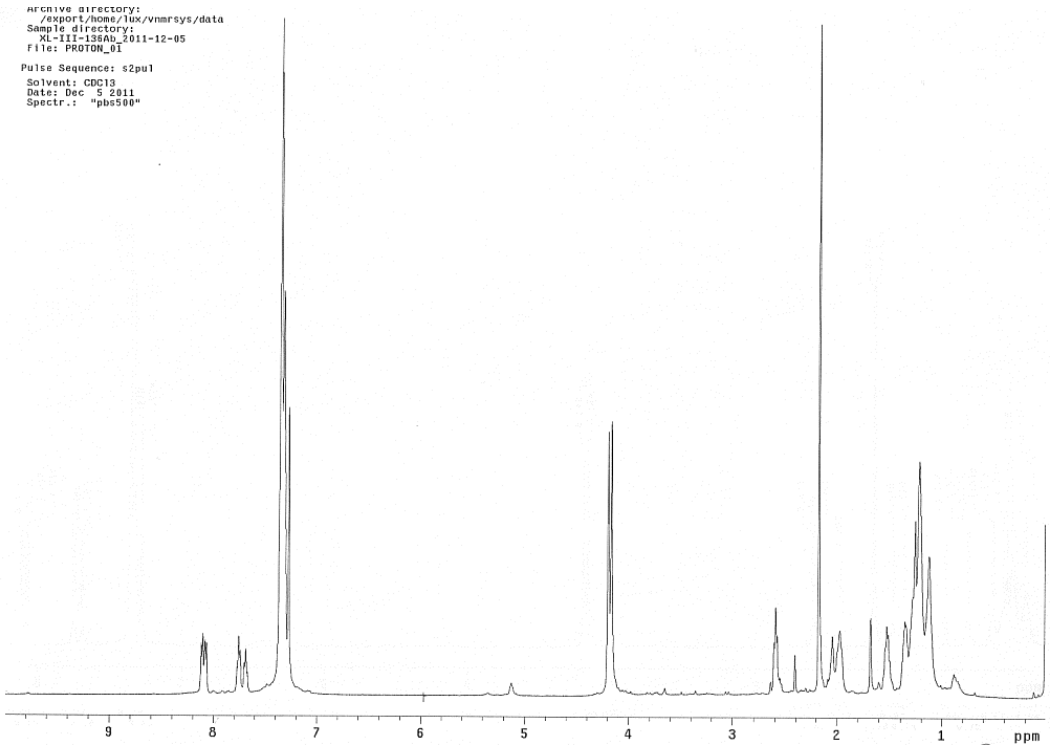

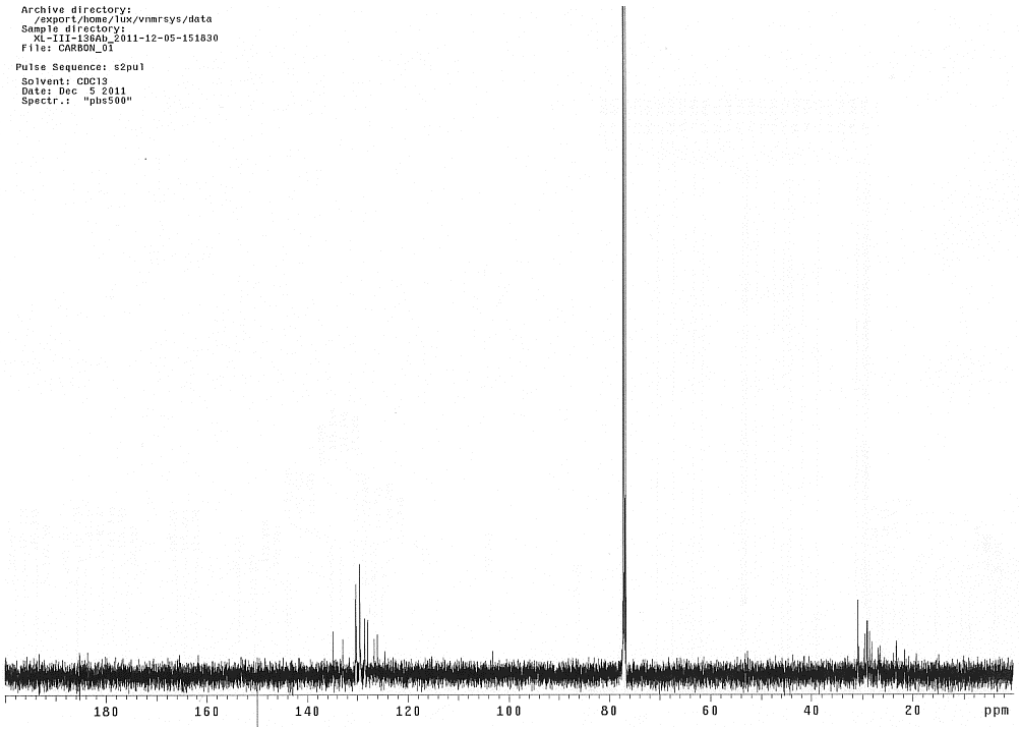

(4-(10-(3-Hydroxy-1,4-dioxo-1,4-dihydronaphthalen-2-yl)-phenyl)bromodecyloxy)triphenylphosphonium bromide (30)

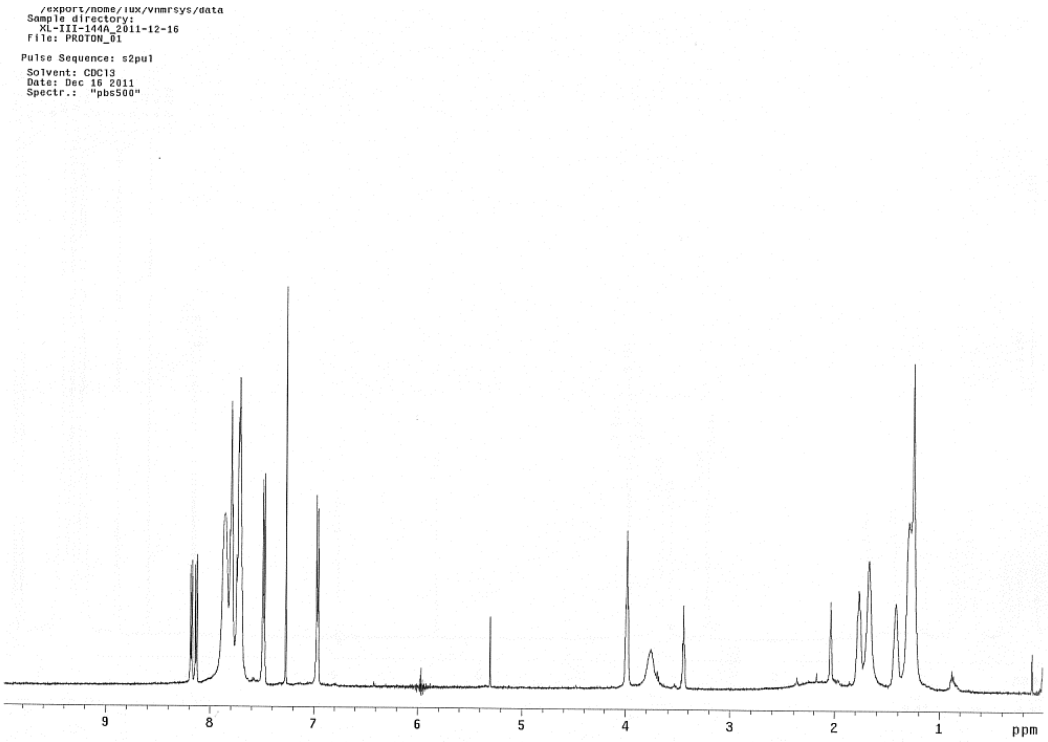

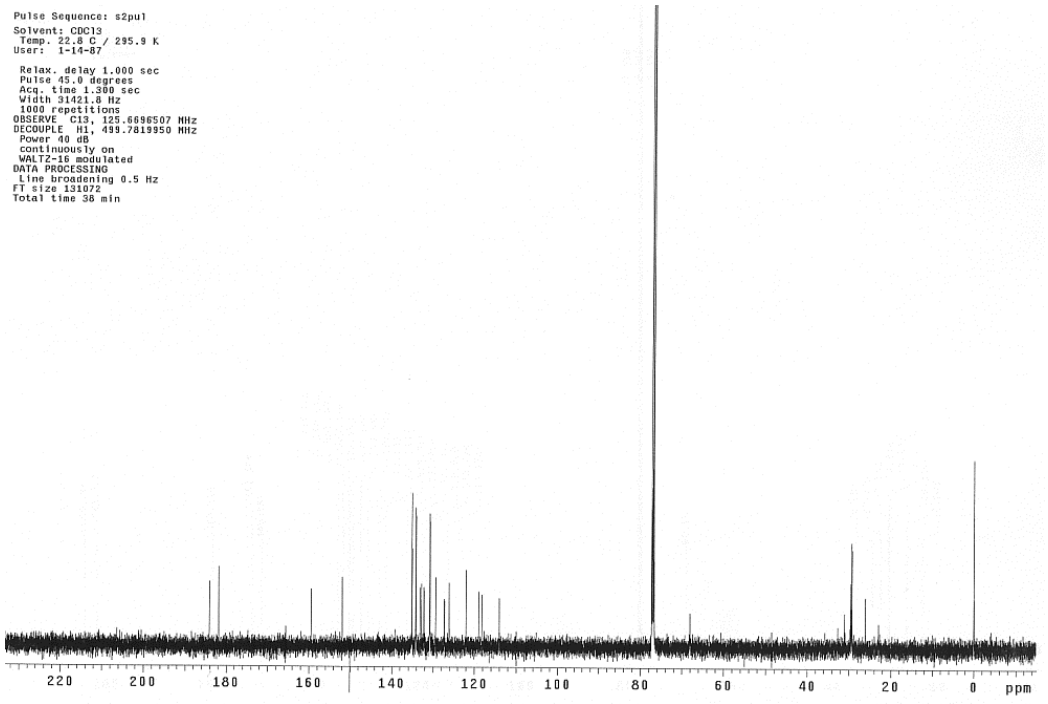

2-(4-Chlorobenzyl)-3-(6-bromohexyloxy)naphthalene-1,4-dione (34a)

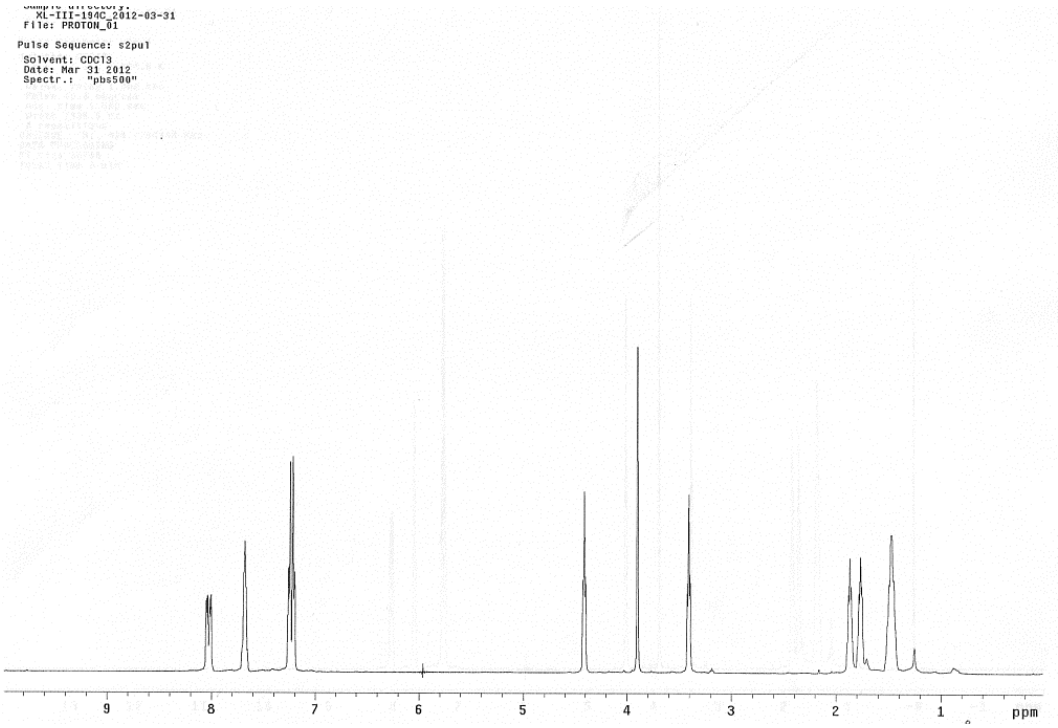

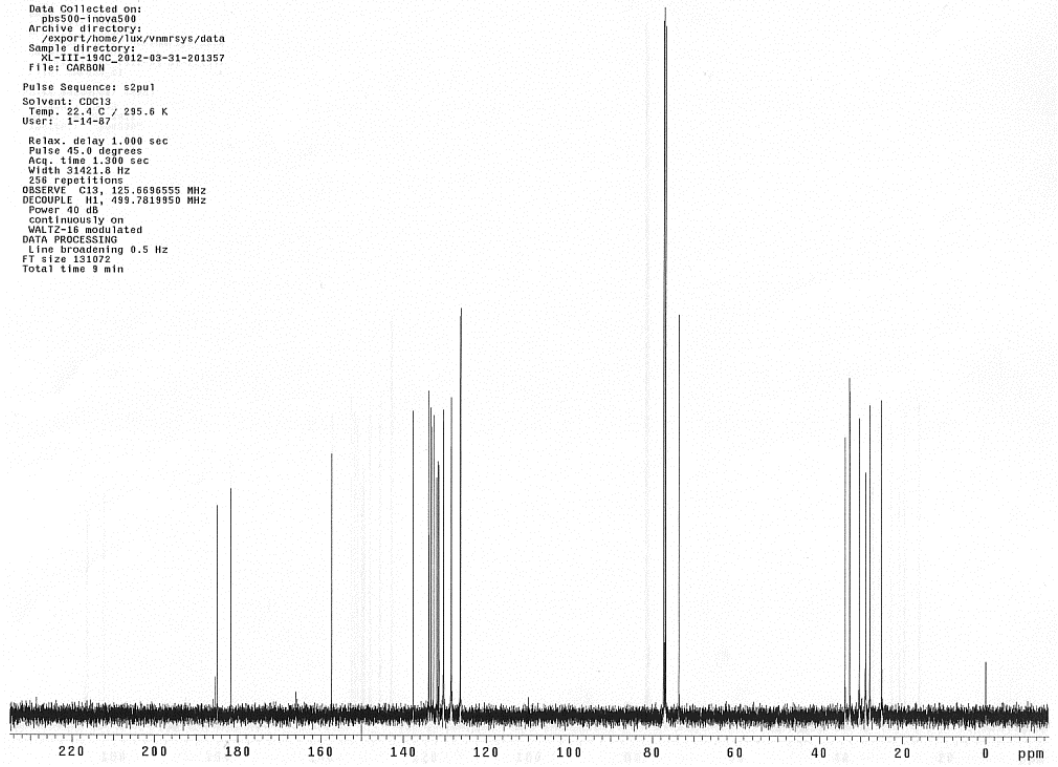

2-Methyl-3-propoxynaphthalene-1,4-dione (34b)

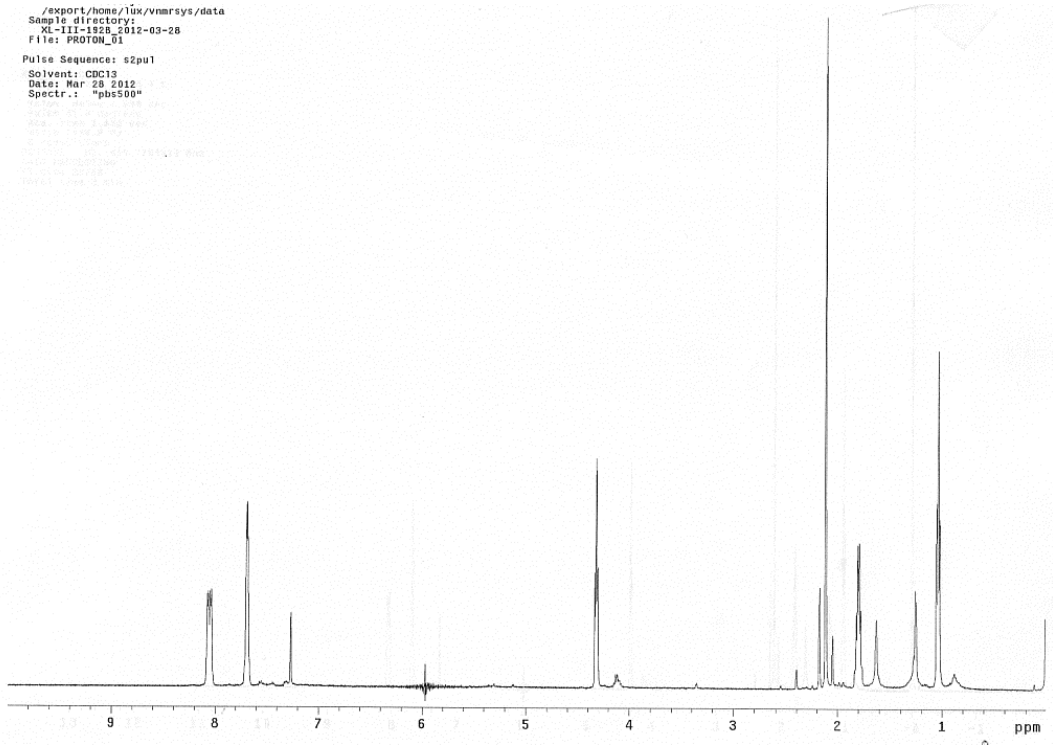

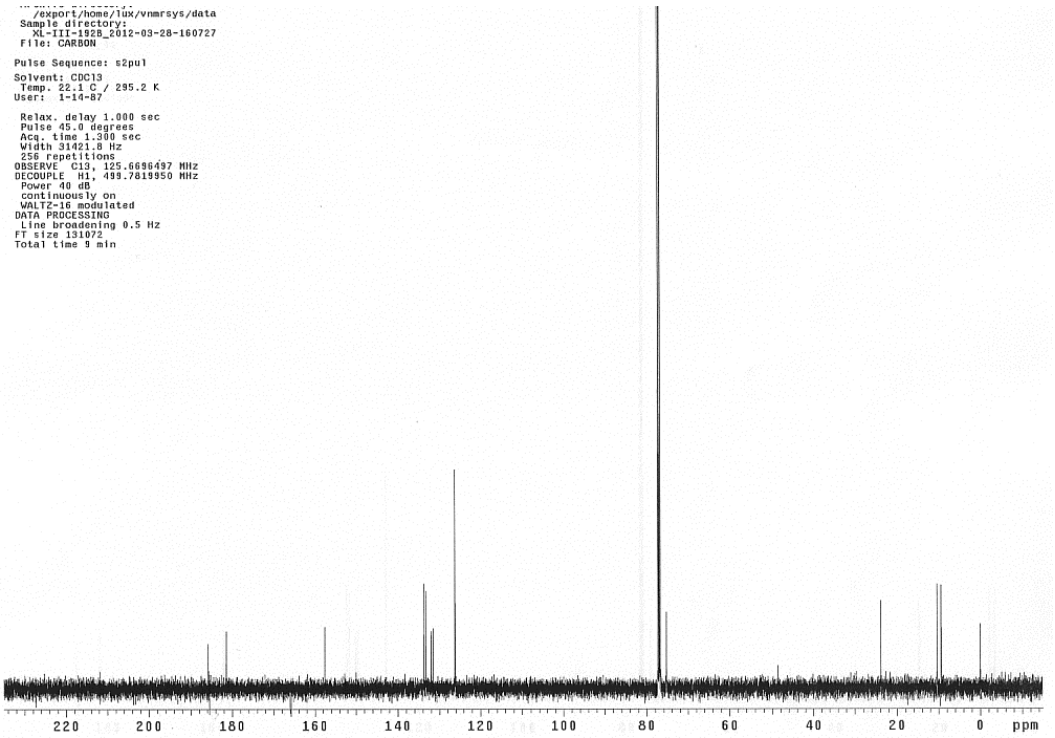

2-Butoxy-3-methylnaphthalene-1,4-dione (34c)

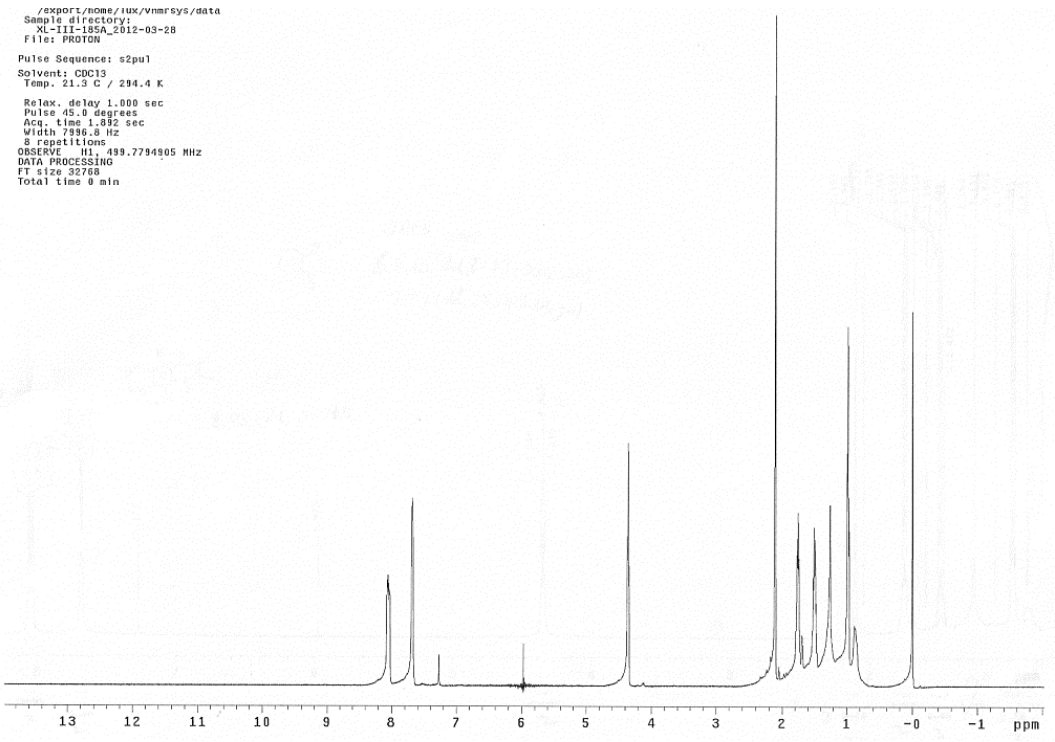

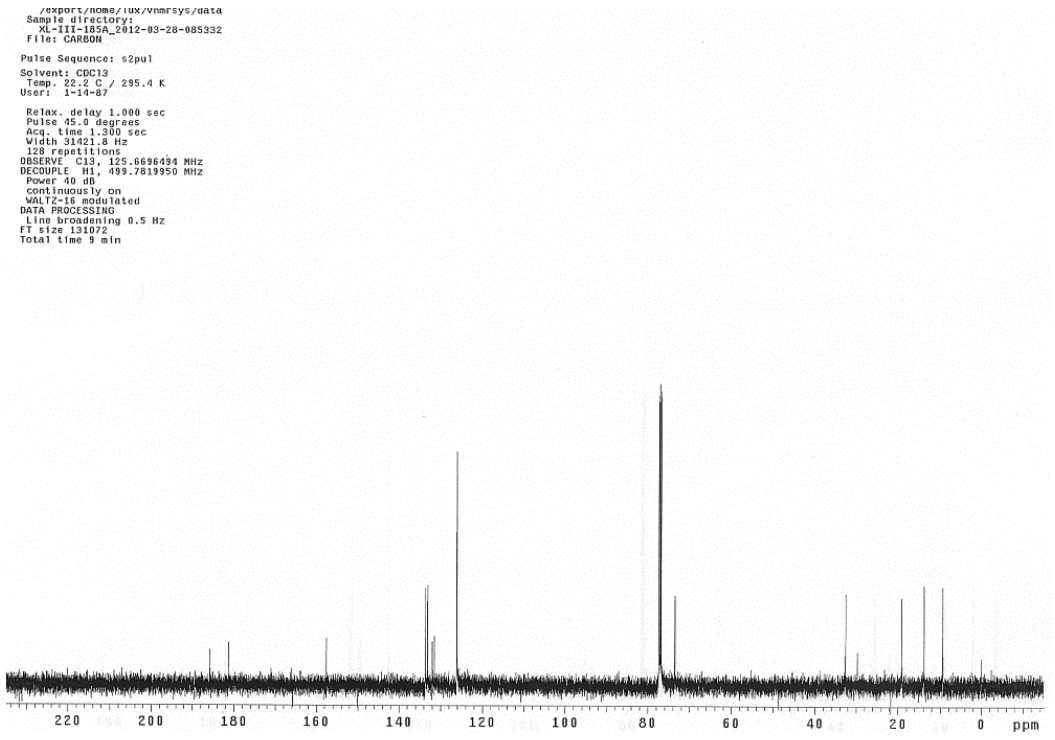

2-Isopropoxy-3-methylnaphthalene-1,4-dione (34d)

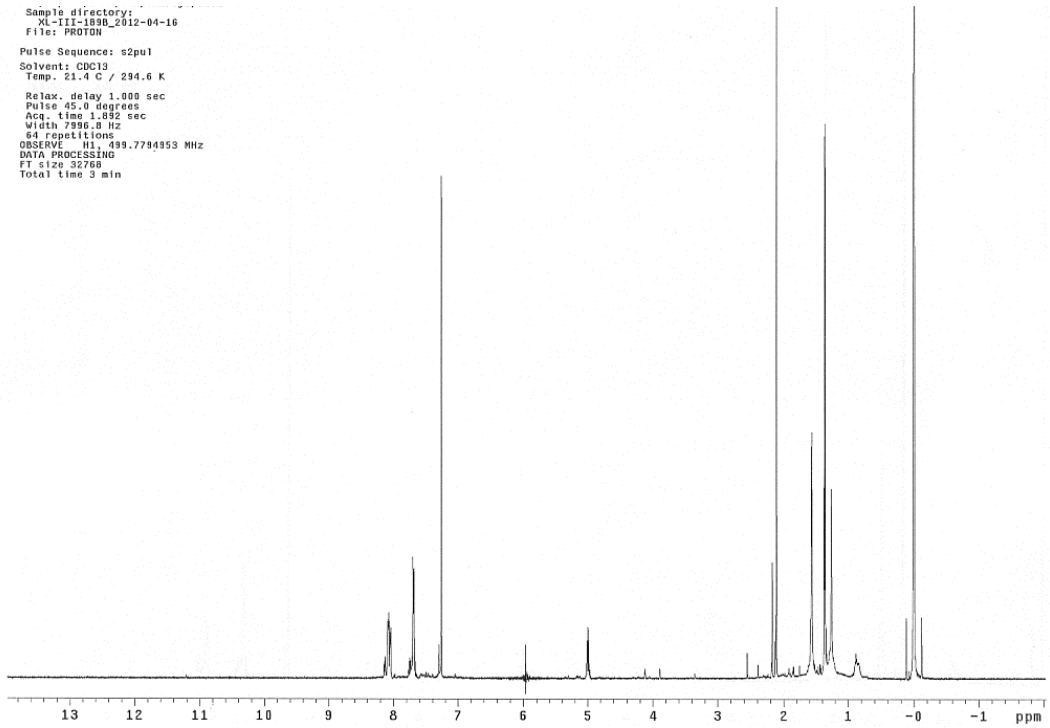

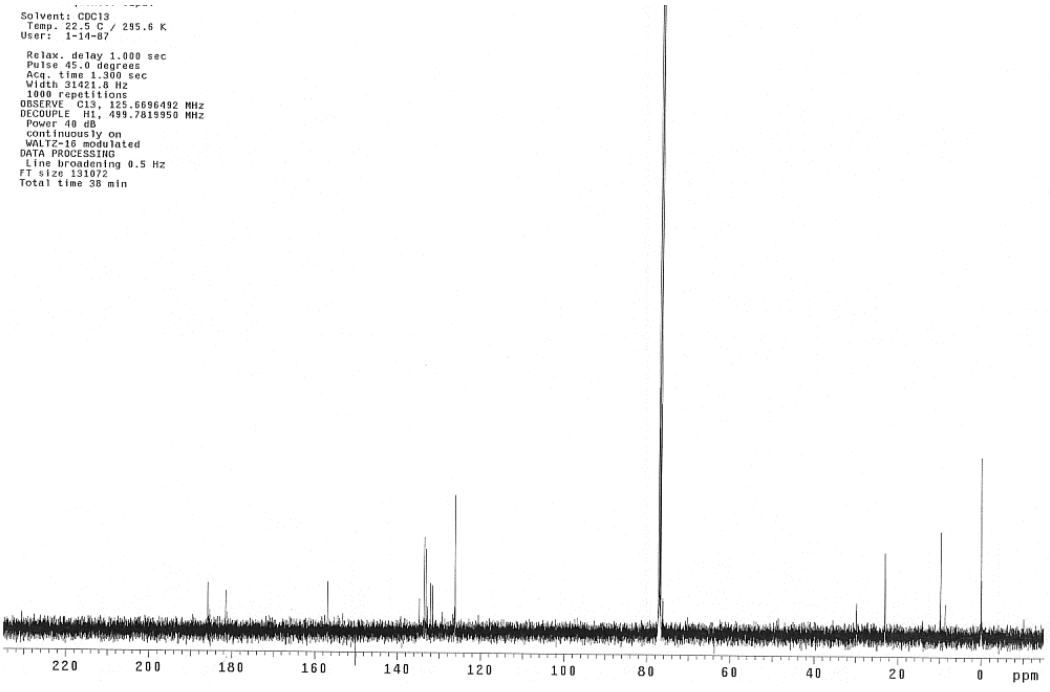

2-(3-Bromopropoxy)-3-cyclohexylnaphthalene-1,4-dione (34g)

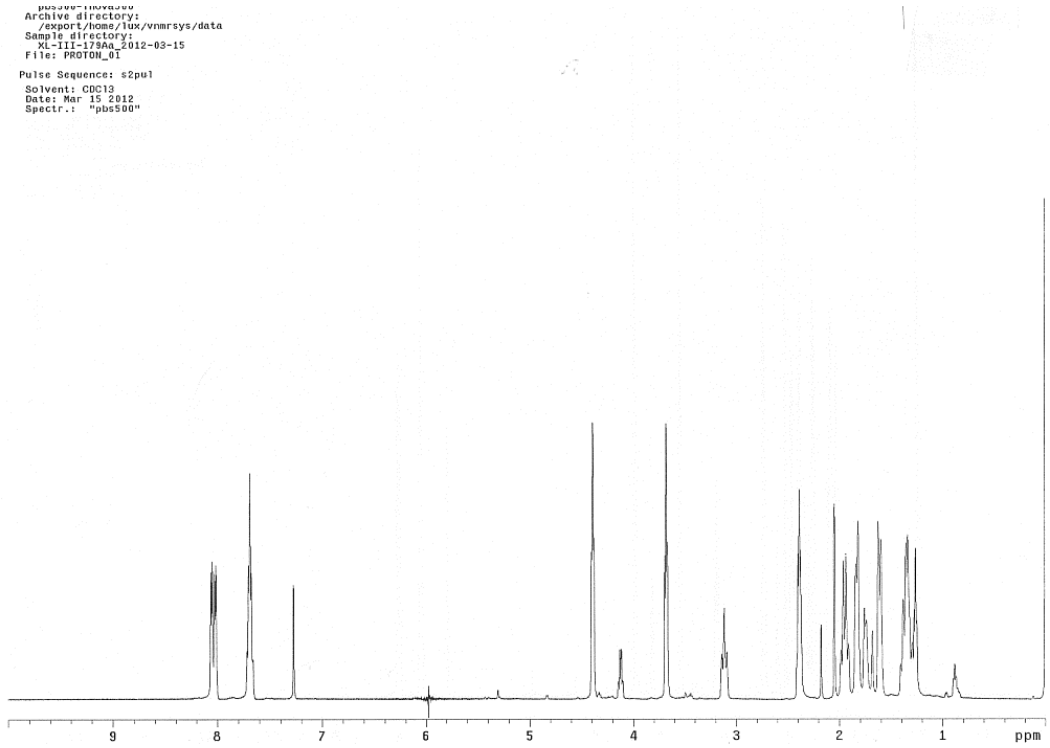

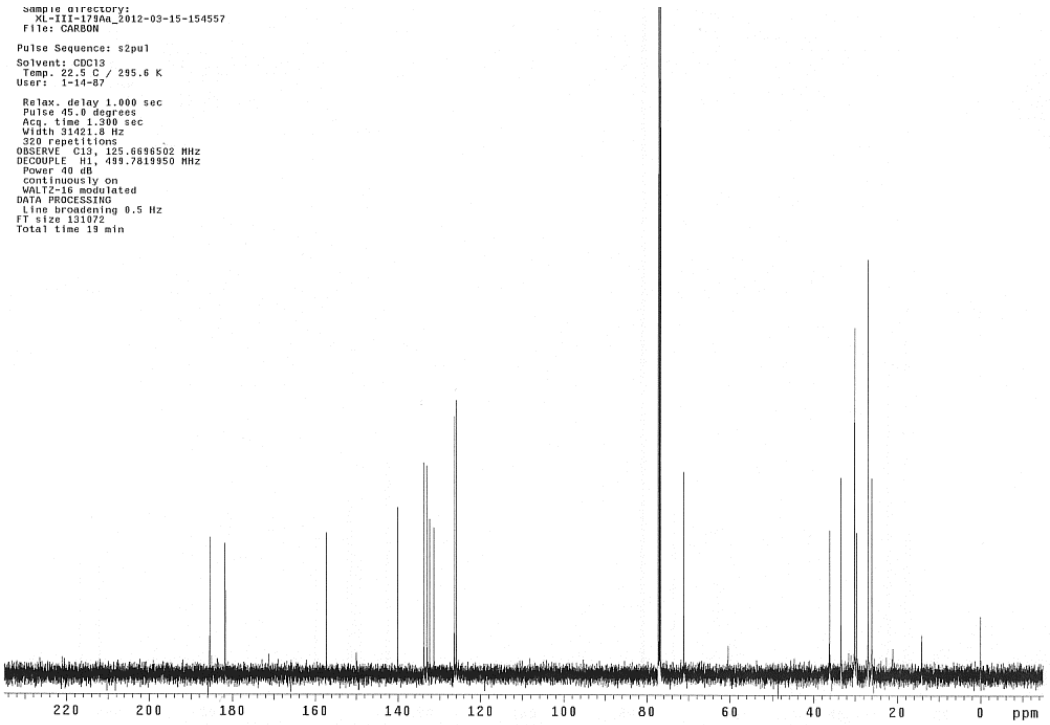

2-Benzyl-3-propoxynaphthalene-1,4-dione (34i)

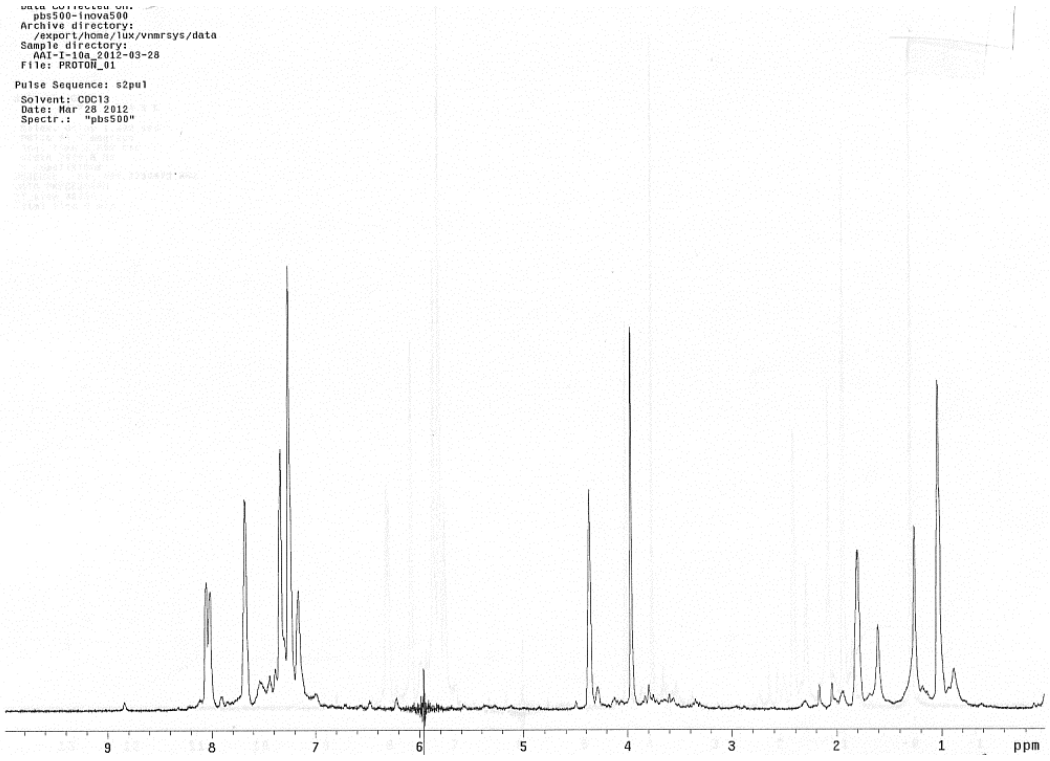

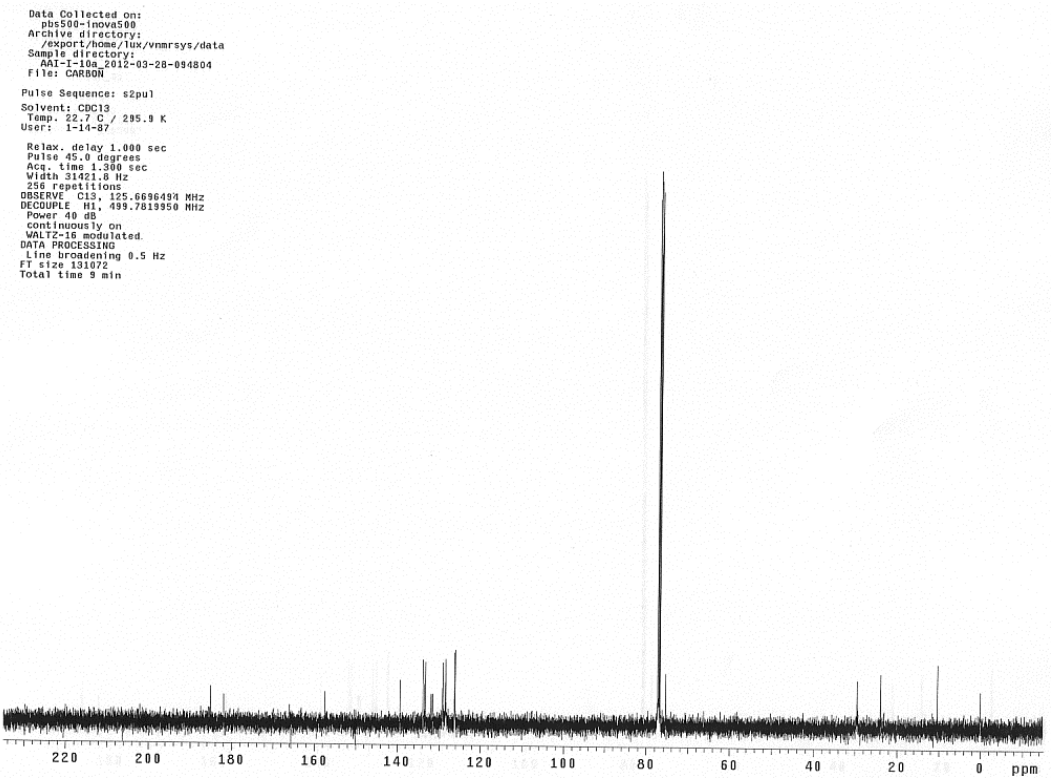

2-((6-Bromohexyl)oxy)-3-cyclohexylnaphthalene-1,4-dione (34h)

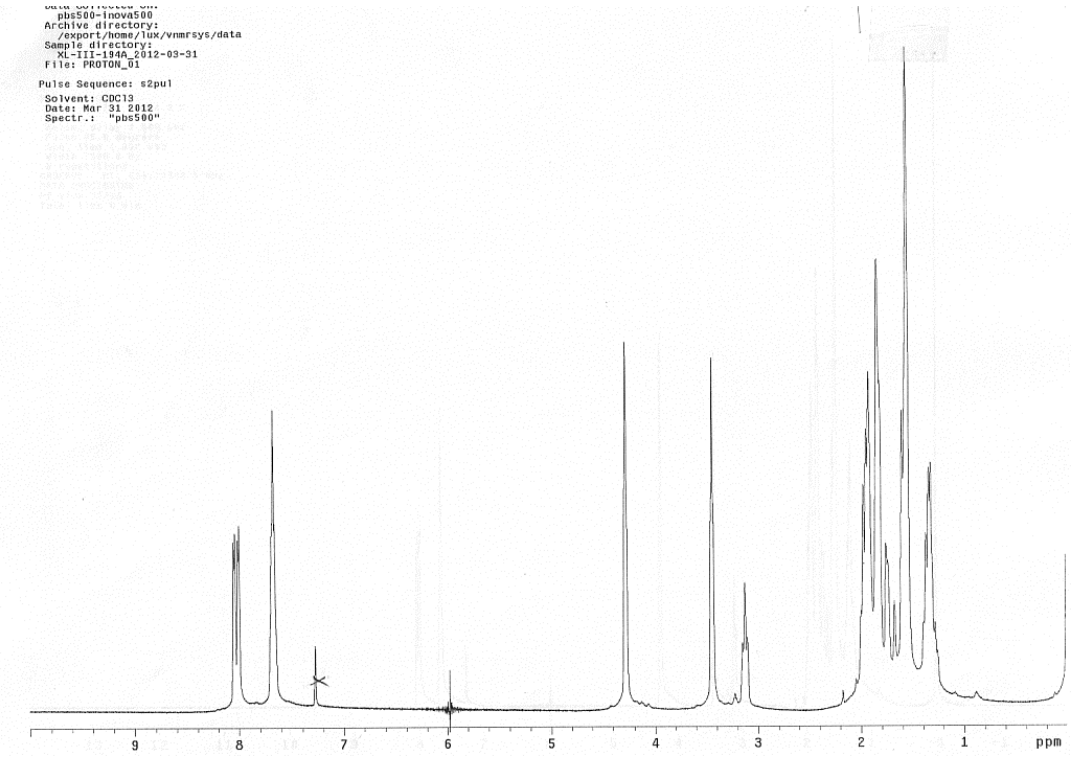

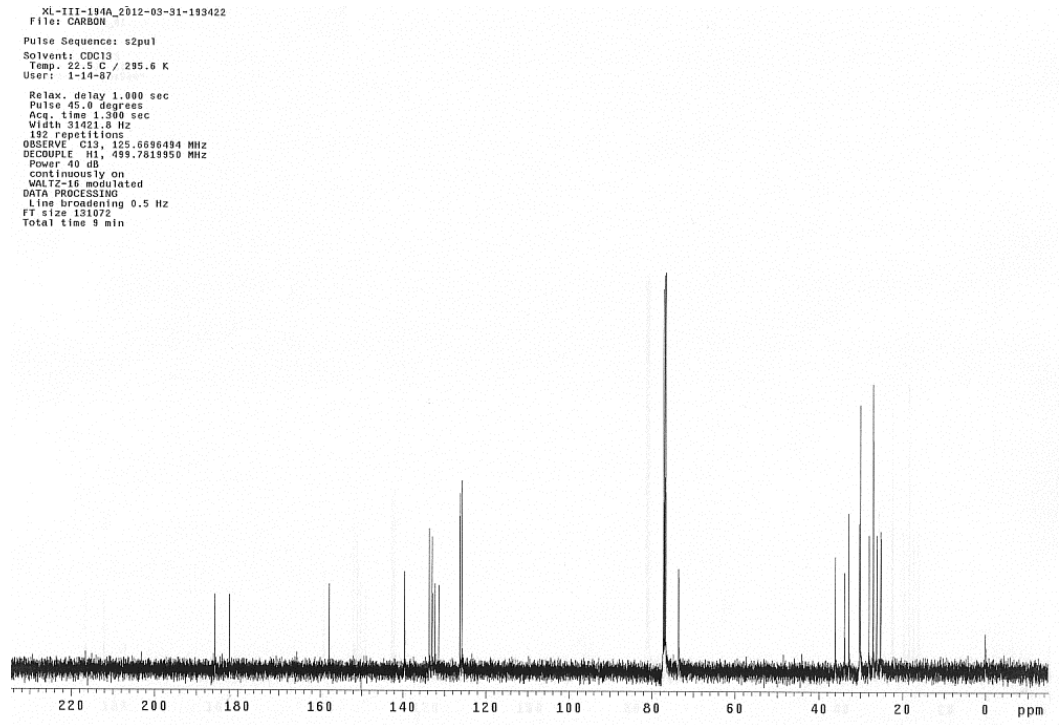

2-Benzyl-3-((6-bromohexyl)oxy)naphthalene-1,4-dione (34j)

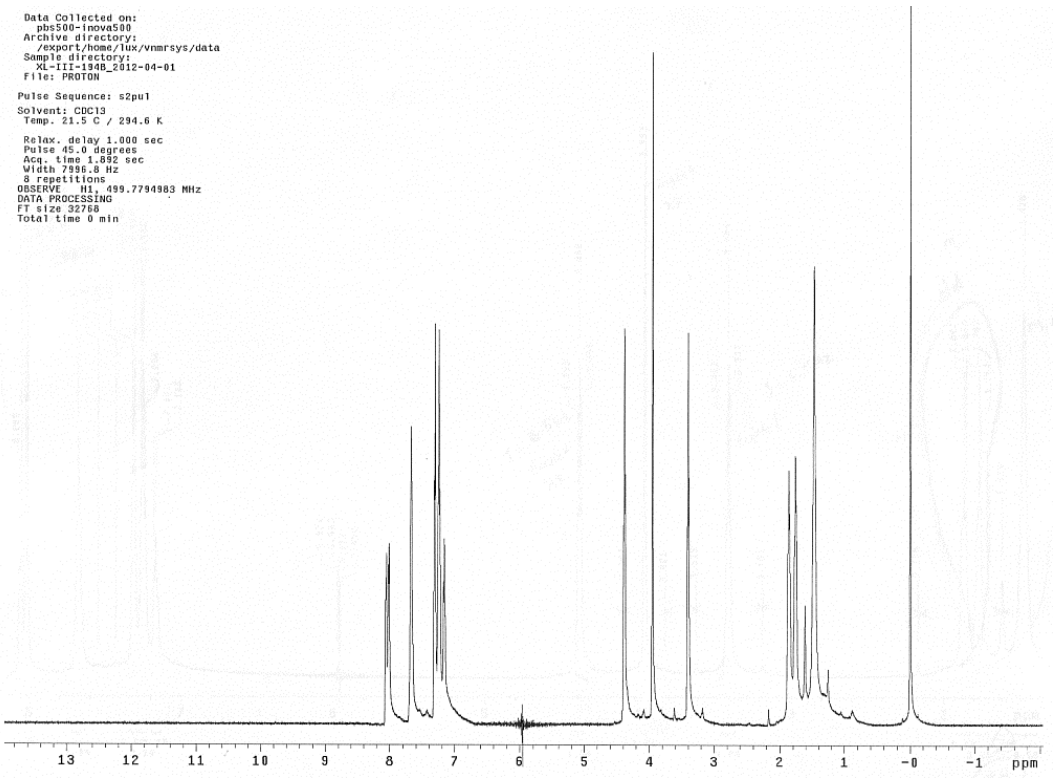

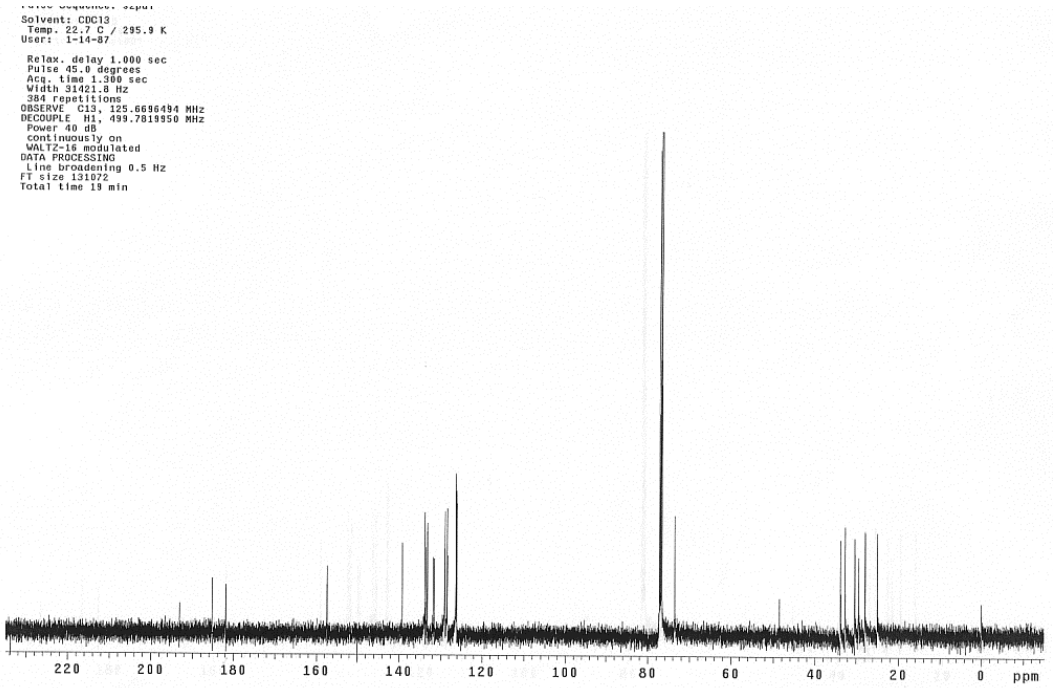

2-(3-Bromopropoxy)-3-chloronaphthalene-1,4-dione (34k)

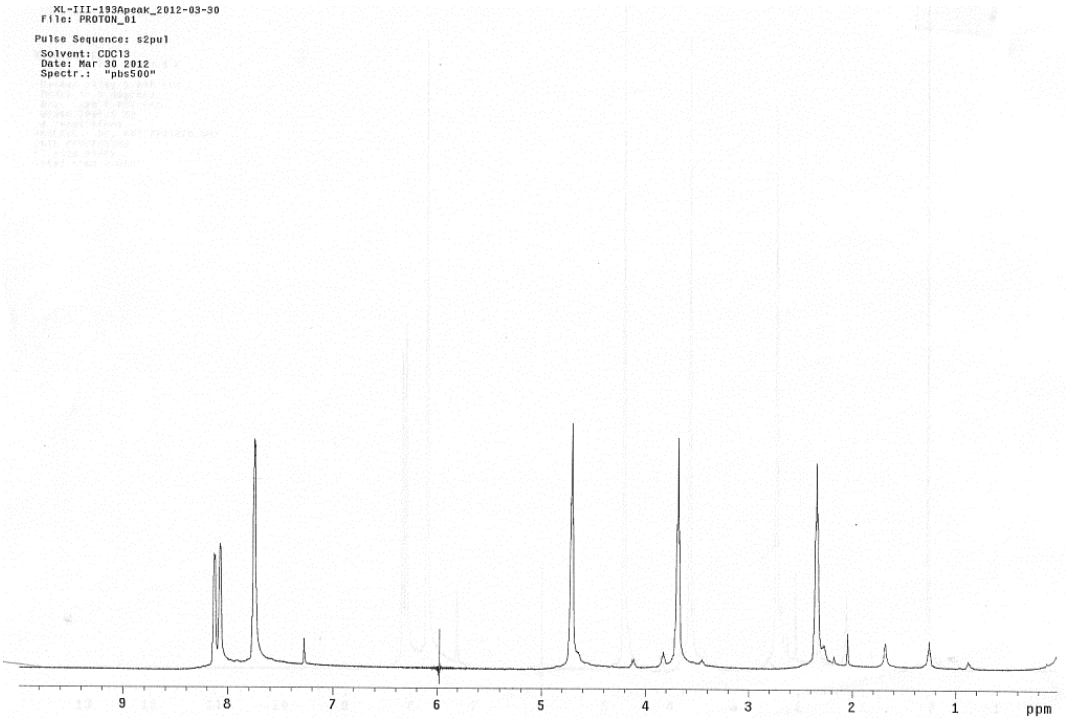

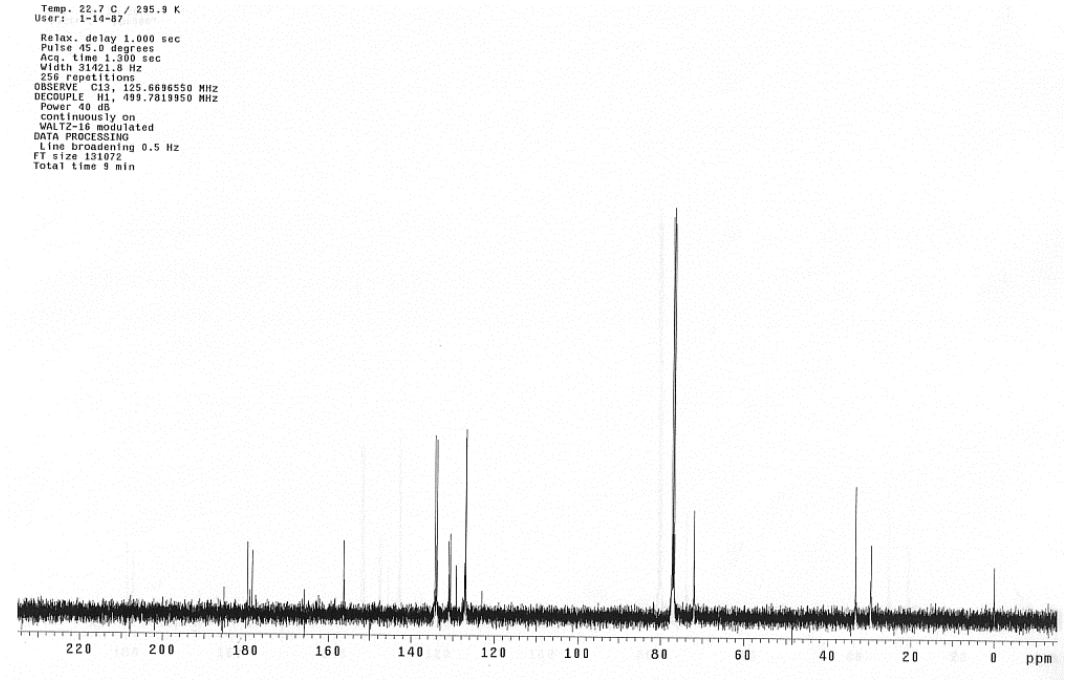

2-(6-Bromohexyloxy)-3-chloronaphthalene-1,4-dione (34l)

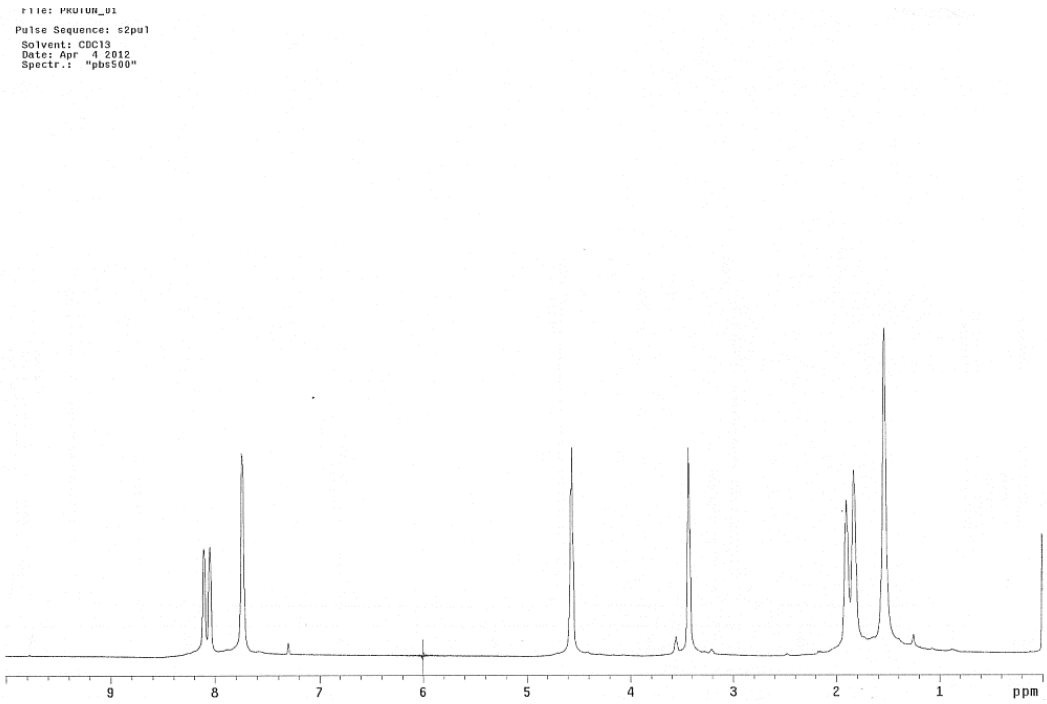

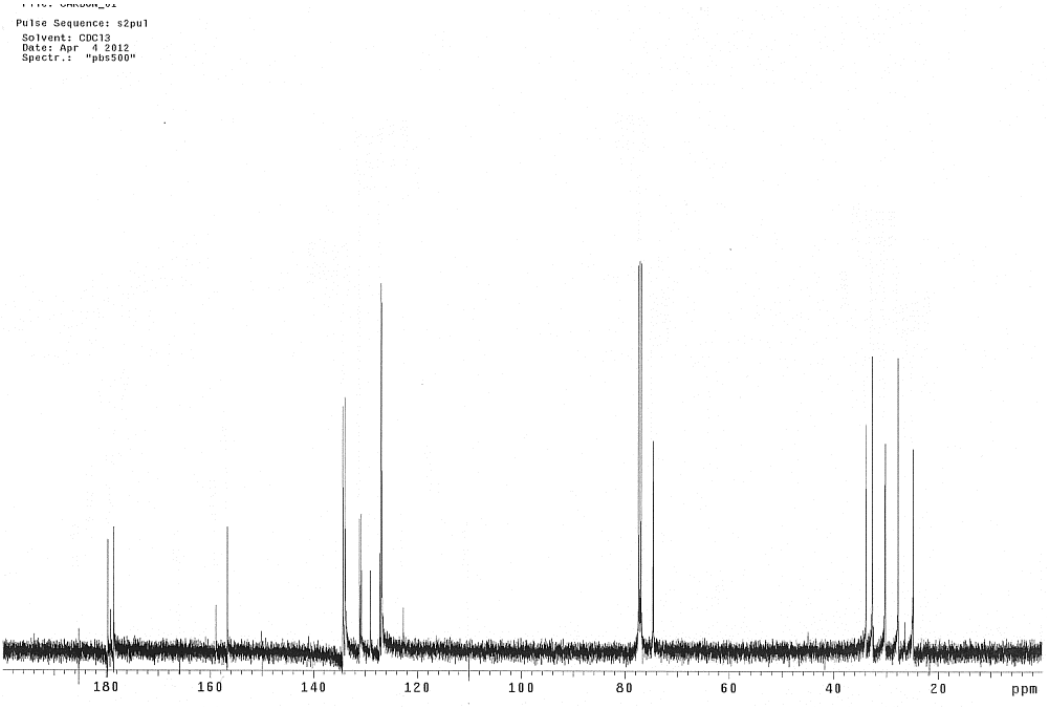

2-Propoxynaphthalene-1,4-dione (34m)

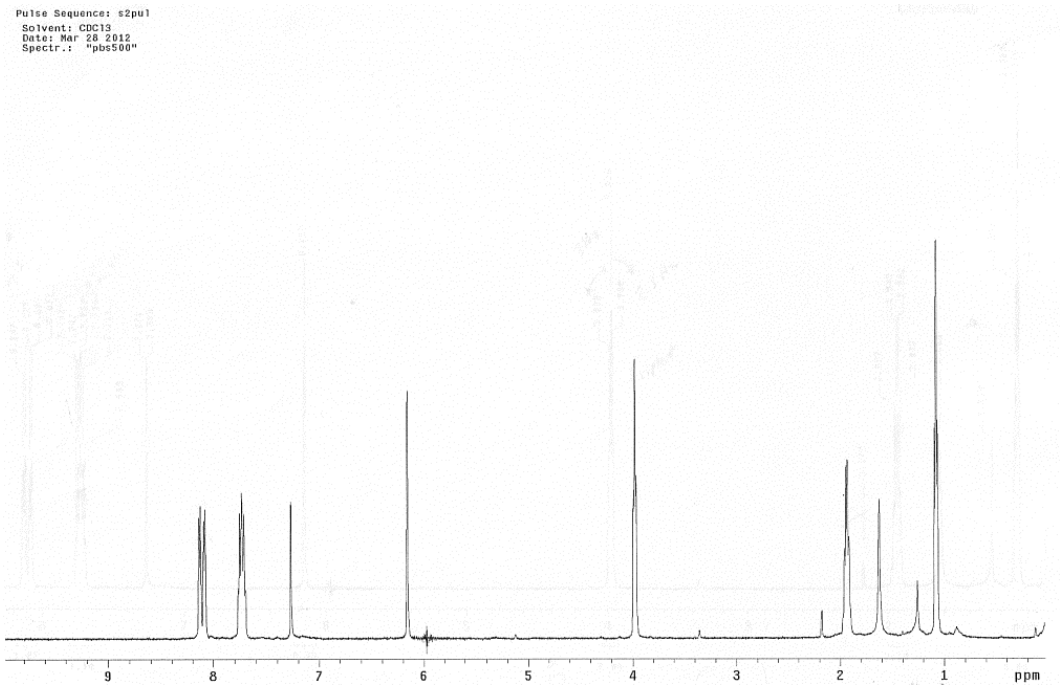

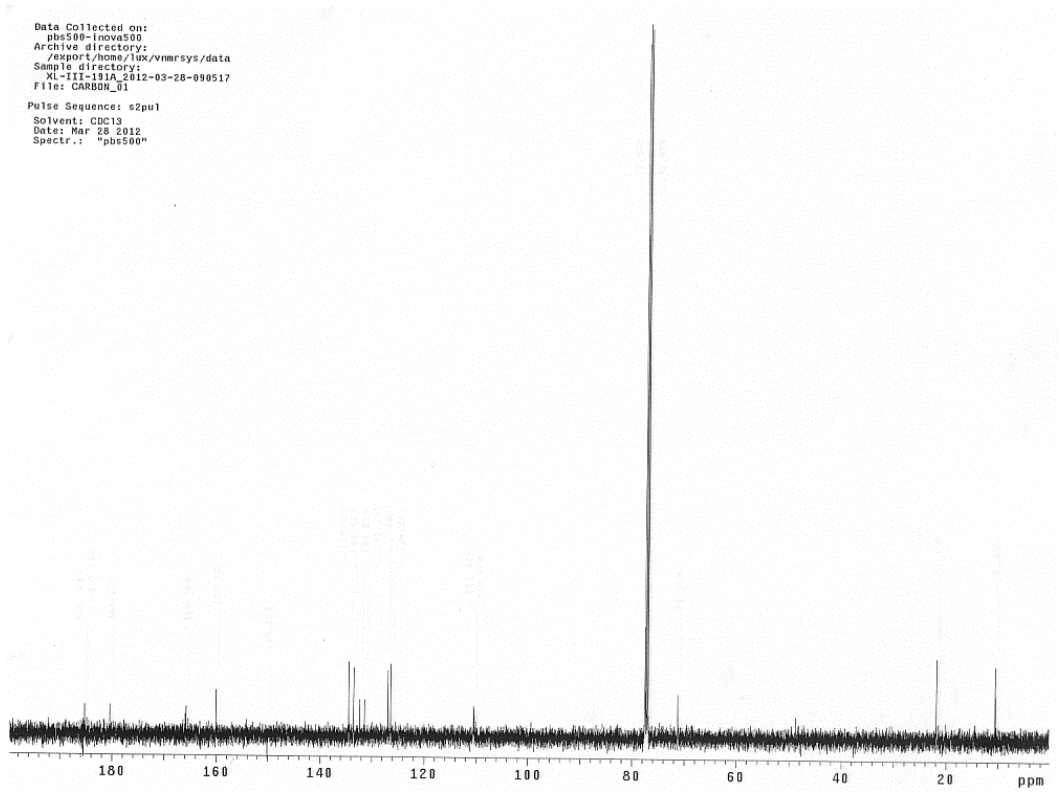

2-(6-Bromohexyloxy)naphthalene-1,4-dione (31a)

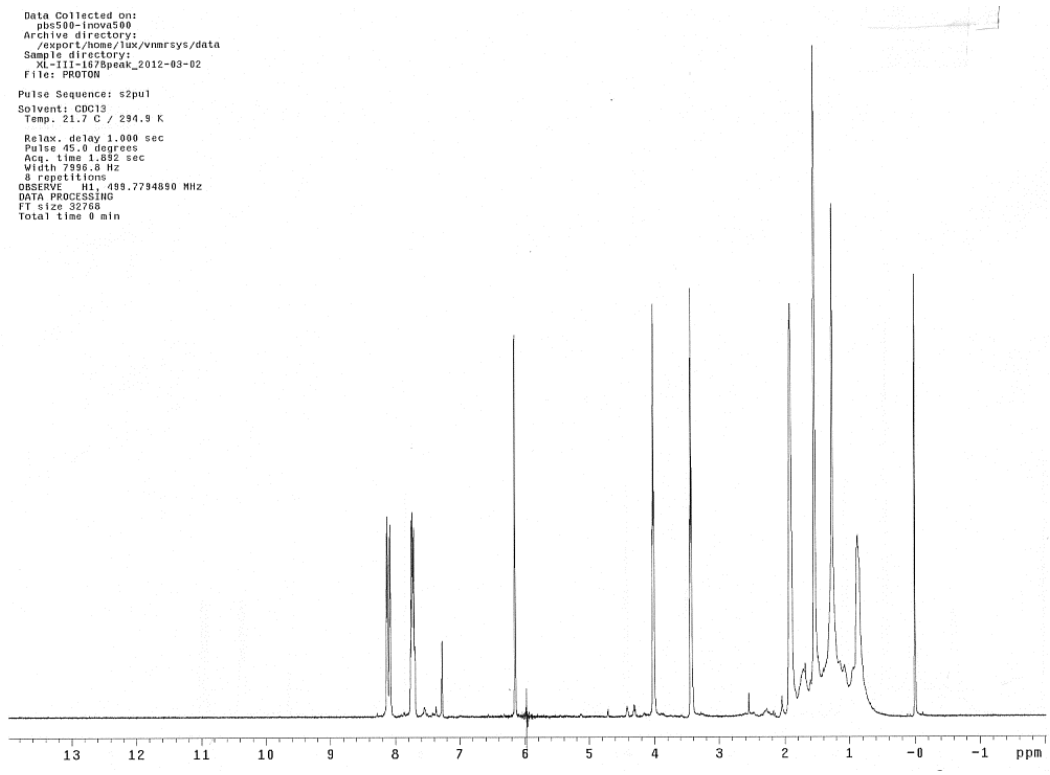

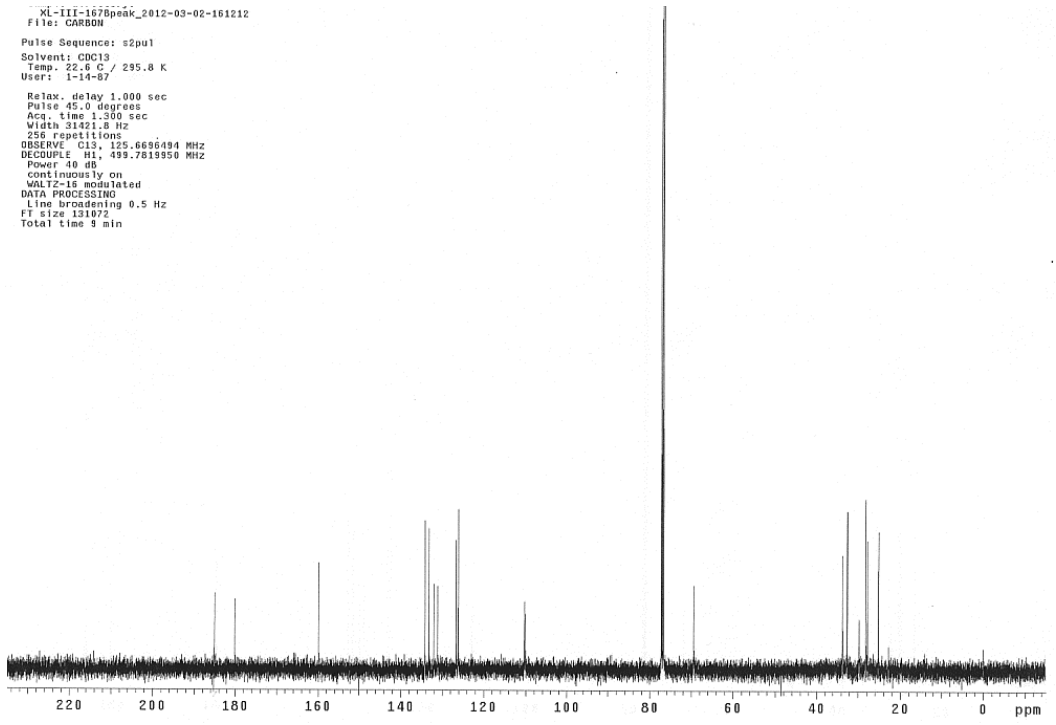

2-(3-Bromopropoxy)naphthalene-1,4-dione (31b)

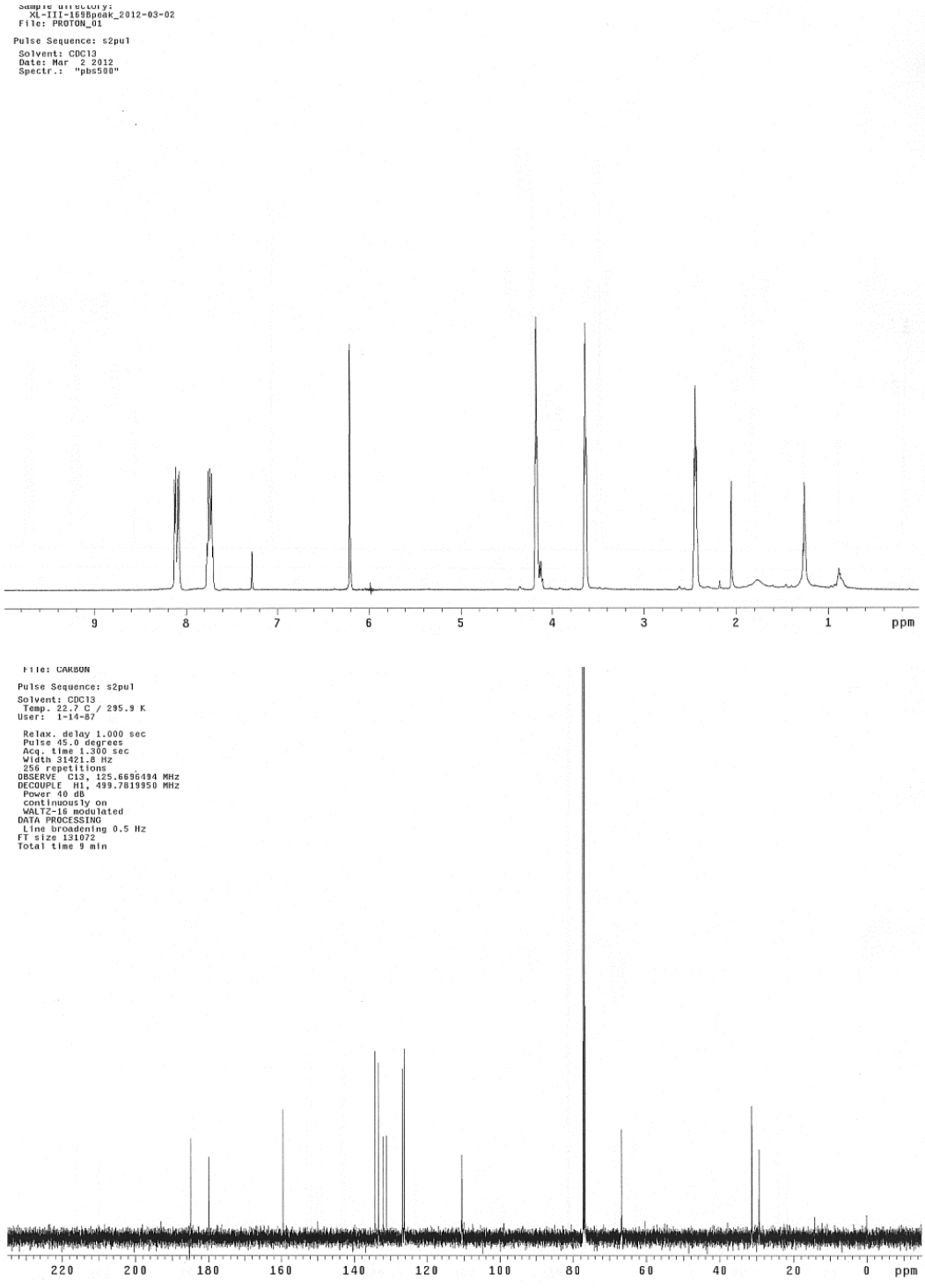

2-(4-(Bromomethyl)benzyloxy)naphthalene-1,4-dione (**31c**)

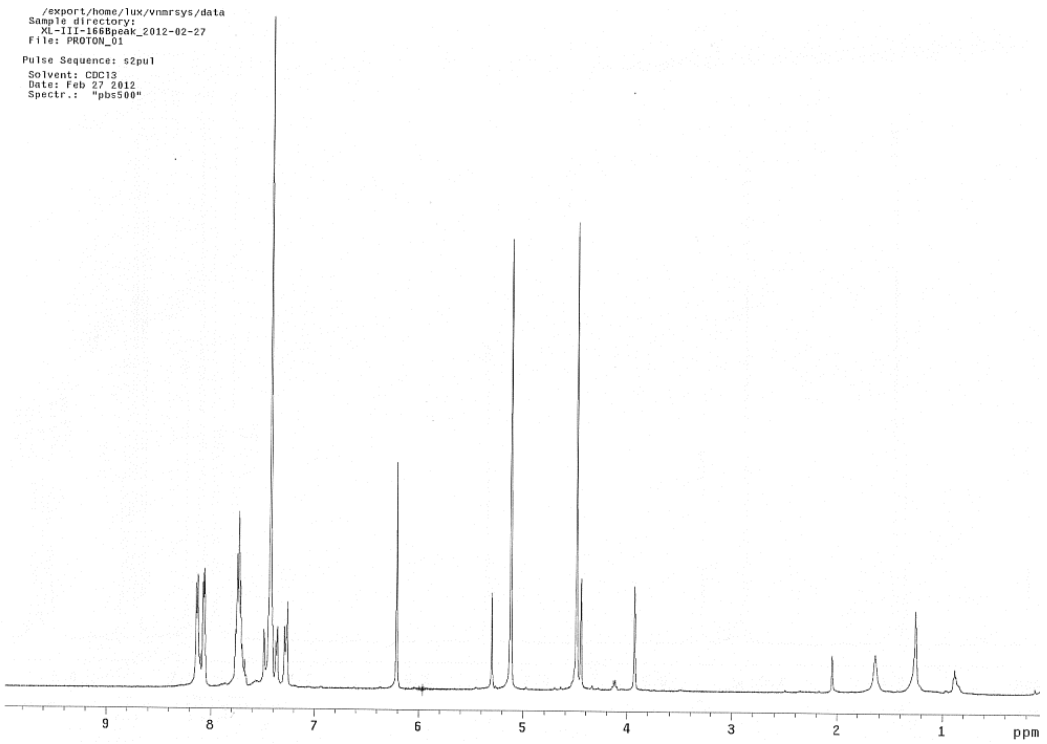

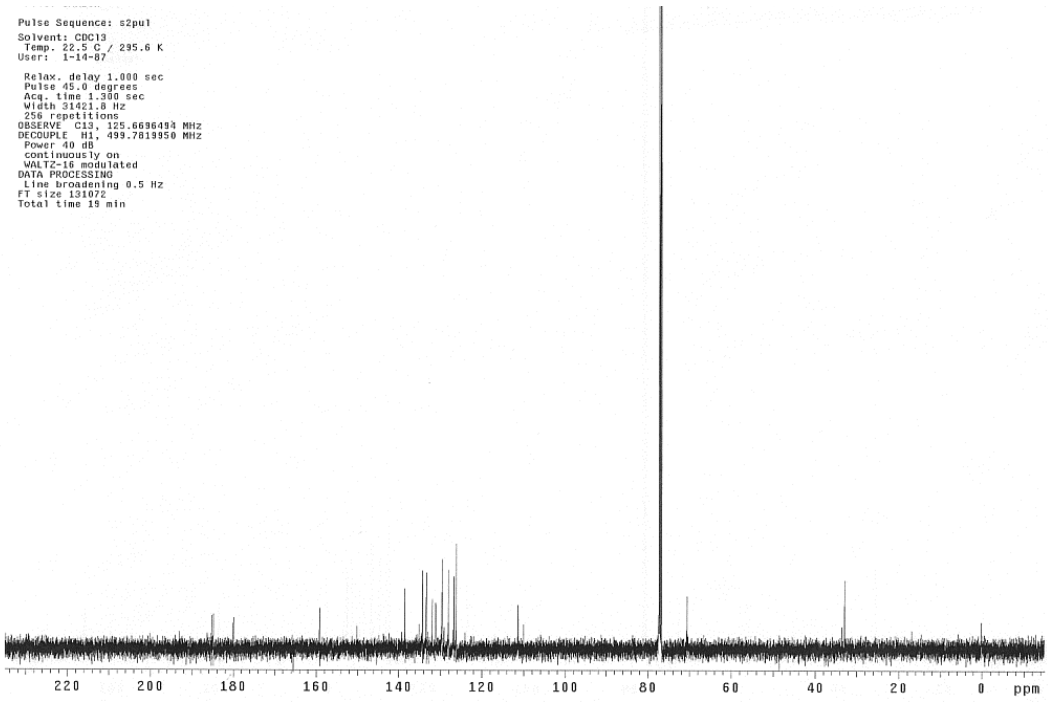

2-(3-Bromopropoxy)-3-(4-chlorobenzyl)naphthalene-1,4-dione (31e)

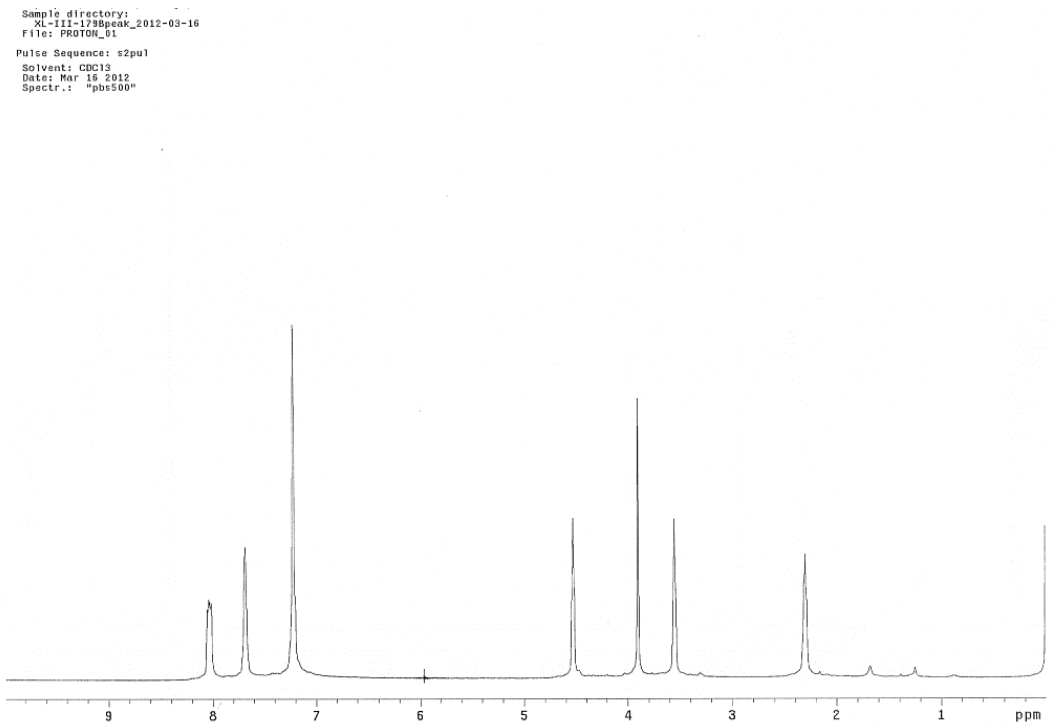

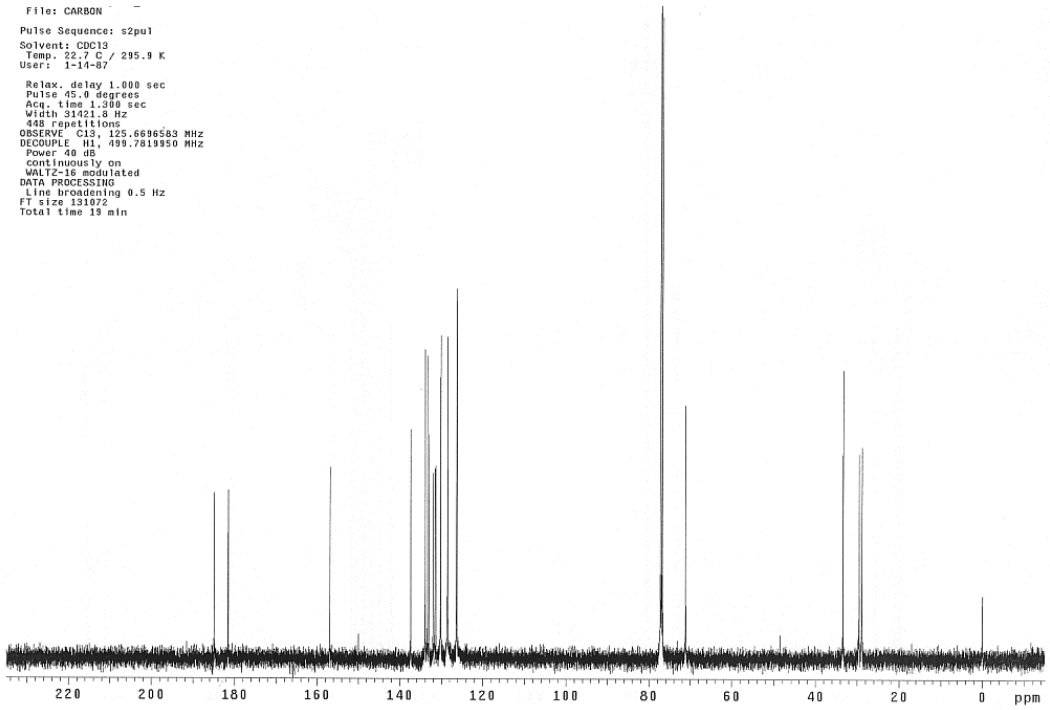

10-(2-Oxy-3-methylnaphthalene-1,4-dione)decyl triphenylphosphonium bromide (40)

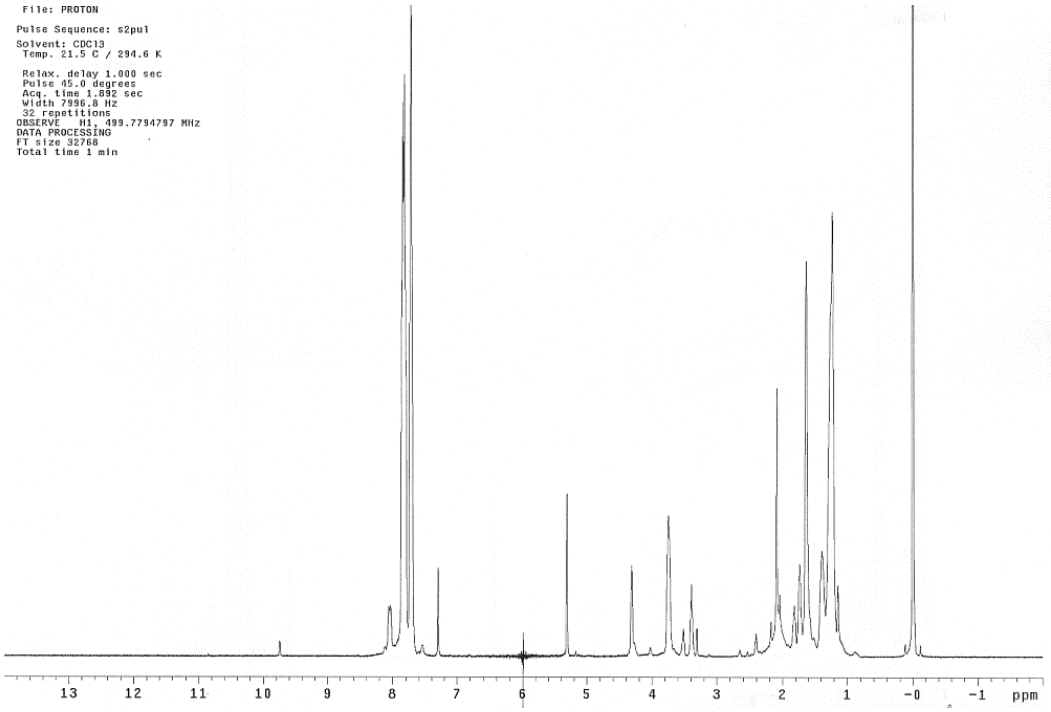

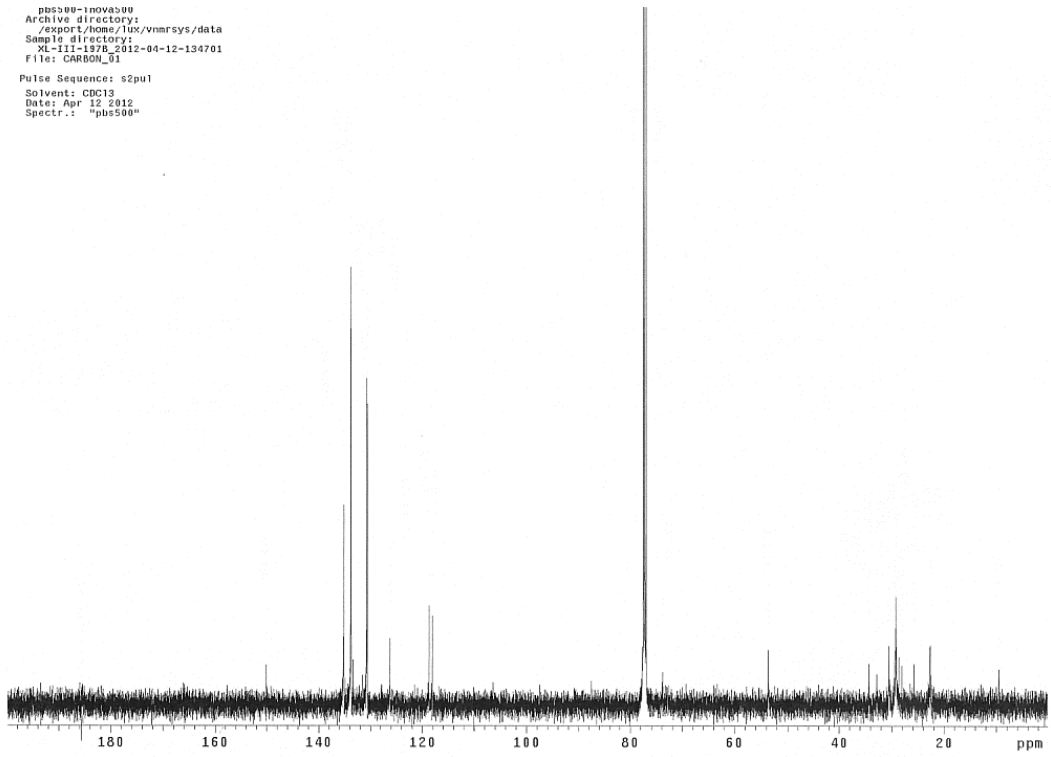

3-(2-Oxy-3-(4-chlorobenzyl)naphthalene-1,4-dione)propyl triphenylphosphonium bromide (35)

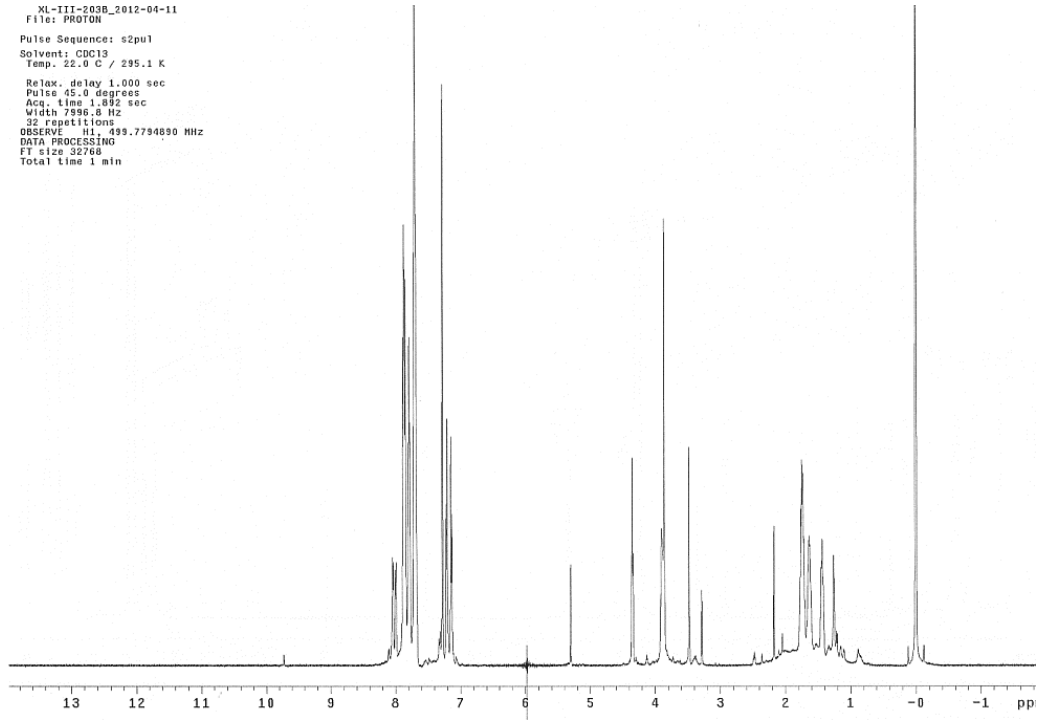

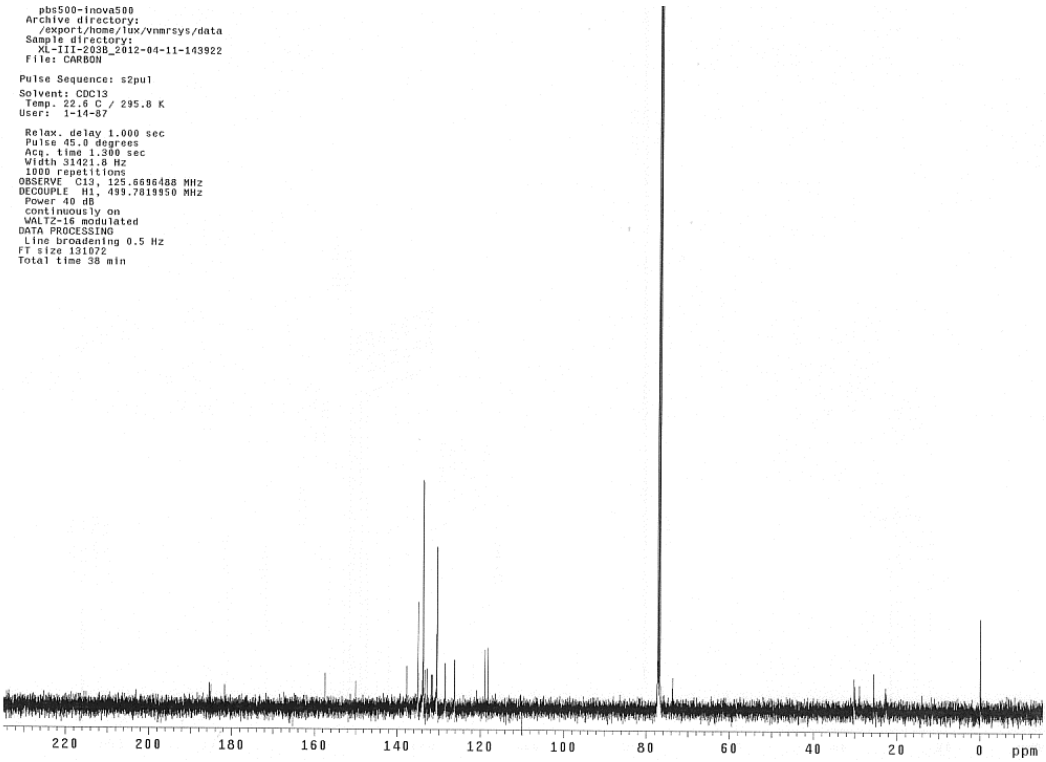

6-(2-Oxy-3-benzylnaphthalene-1,4-dione)hexyl triphenylphosphonium bromide (41)

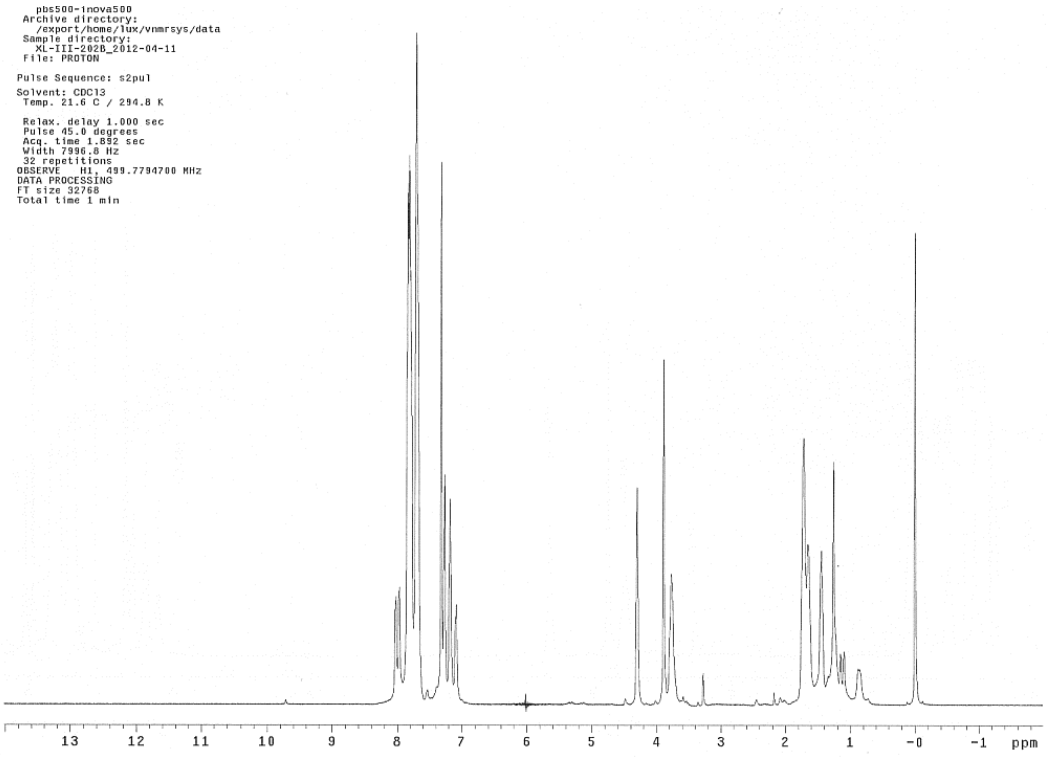

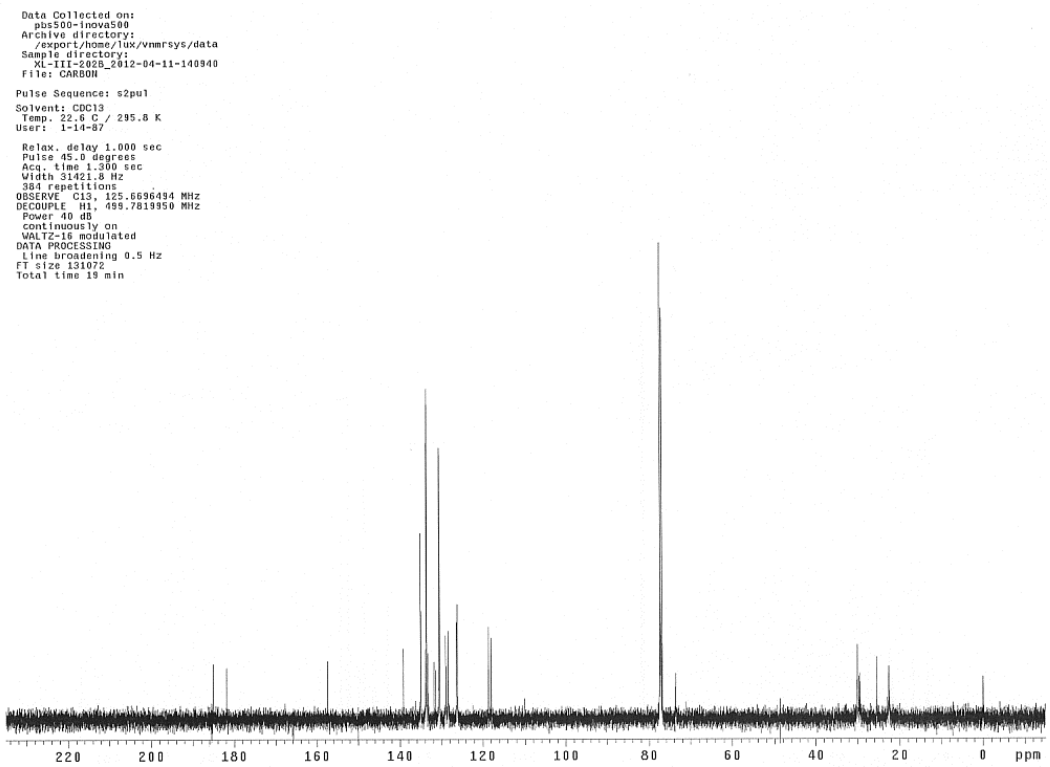

3-(2-Oxy-3-benzylnaphthalene-1,4-dione)propyl triphenylphosphonium bromide (42)

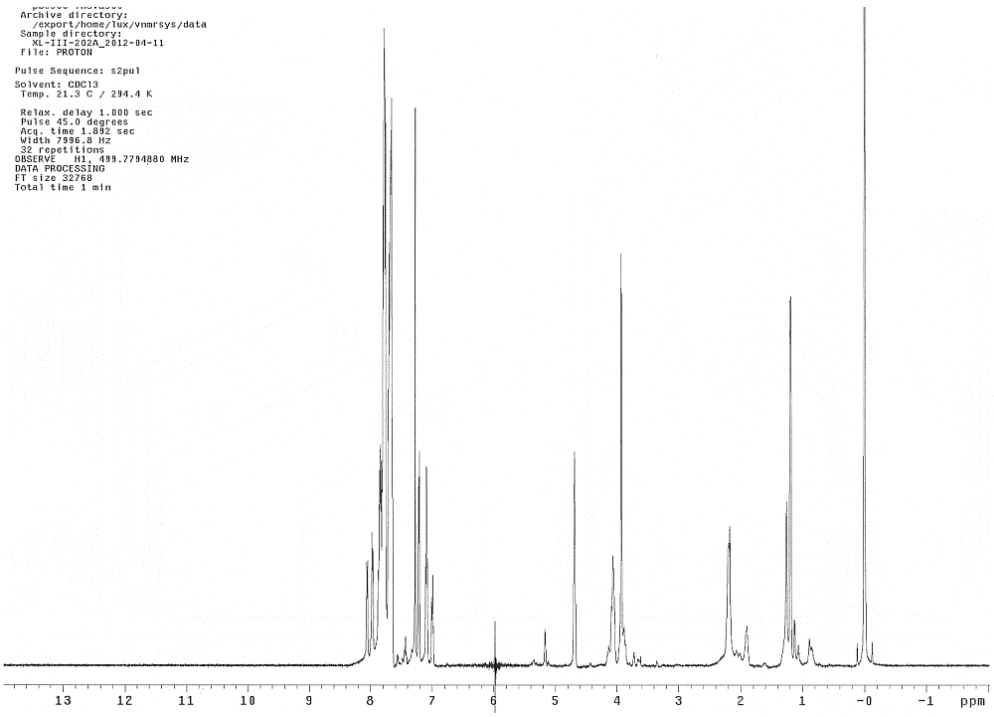

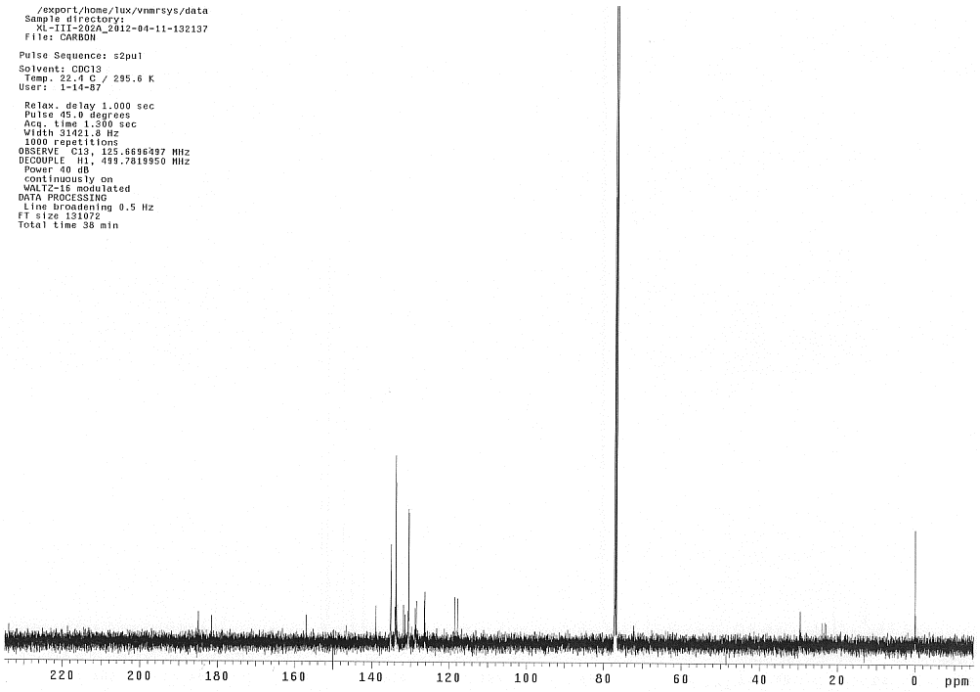

6-(2-Oxy-3-cyclohexylnaphthalene-1,4-dione)hexyl triphenylphosphonium bromide (43)

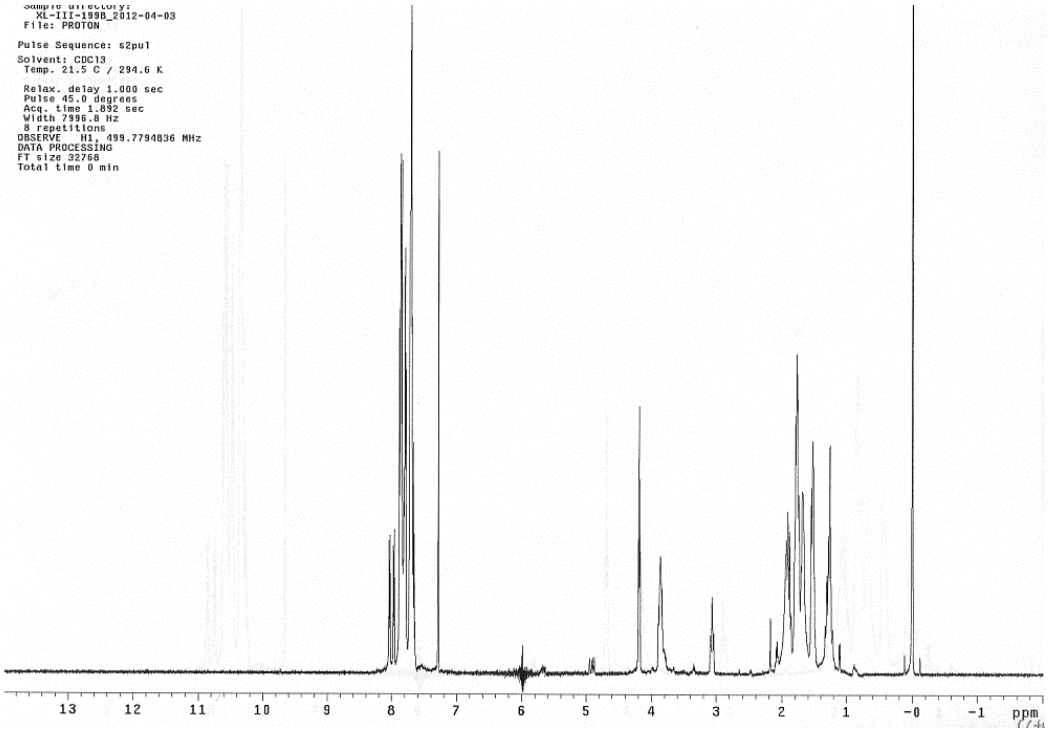

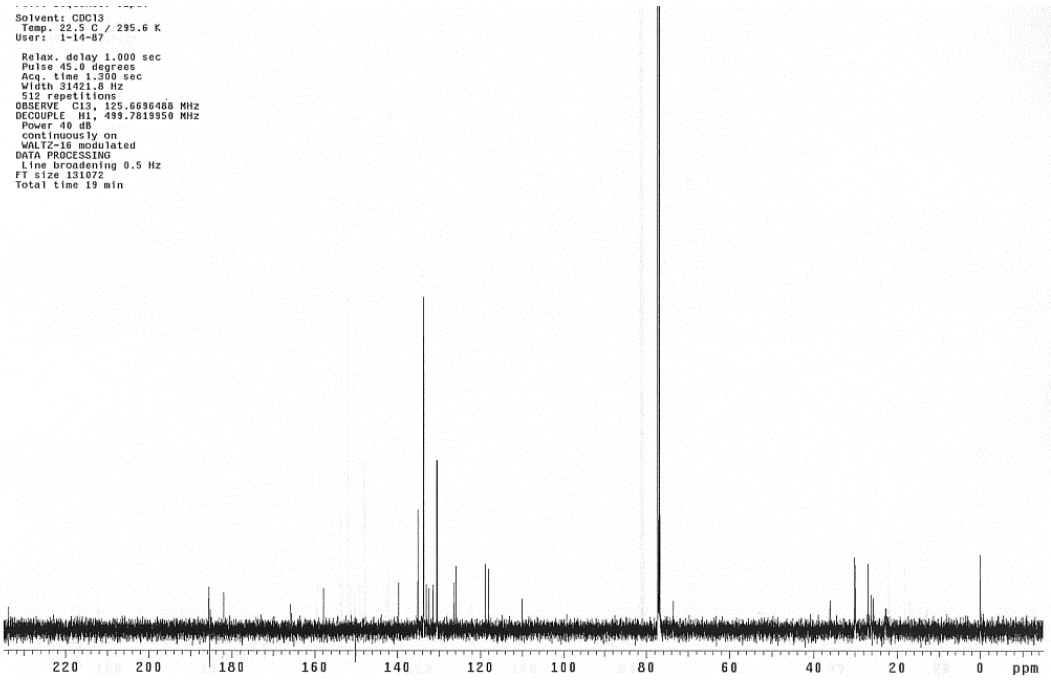

3-(2-Oxy-3-cyclohexylnaphthalene-1,4-dione)propyl triphenylphosphonium bromide (44)

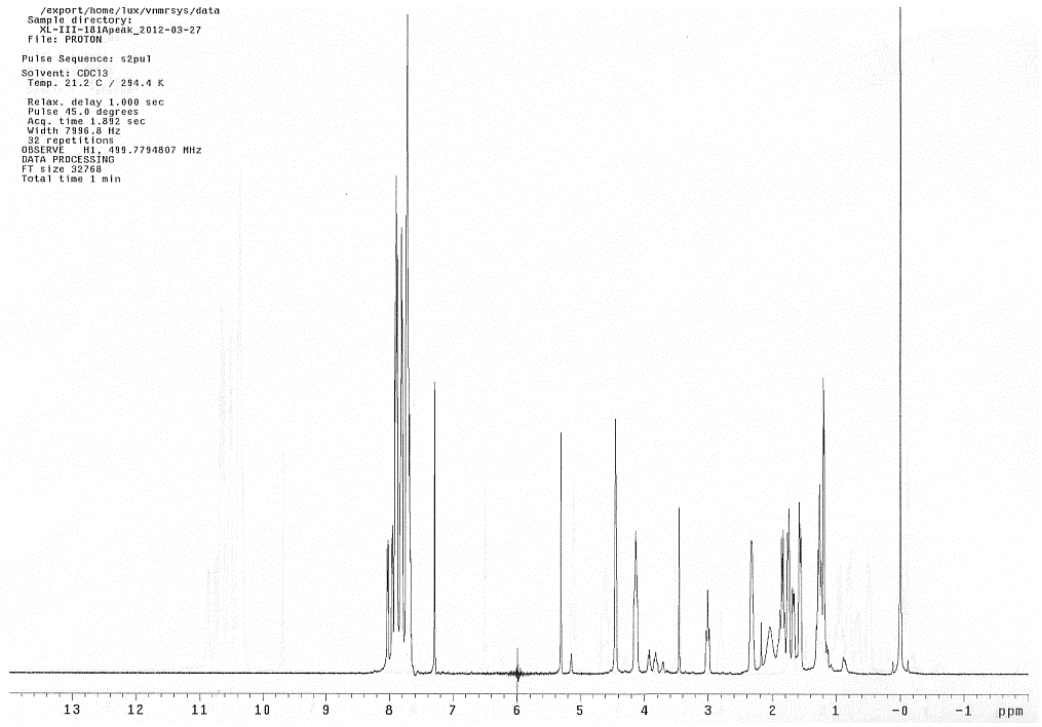

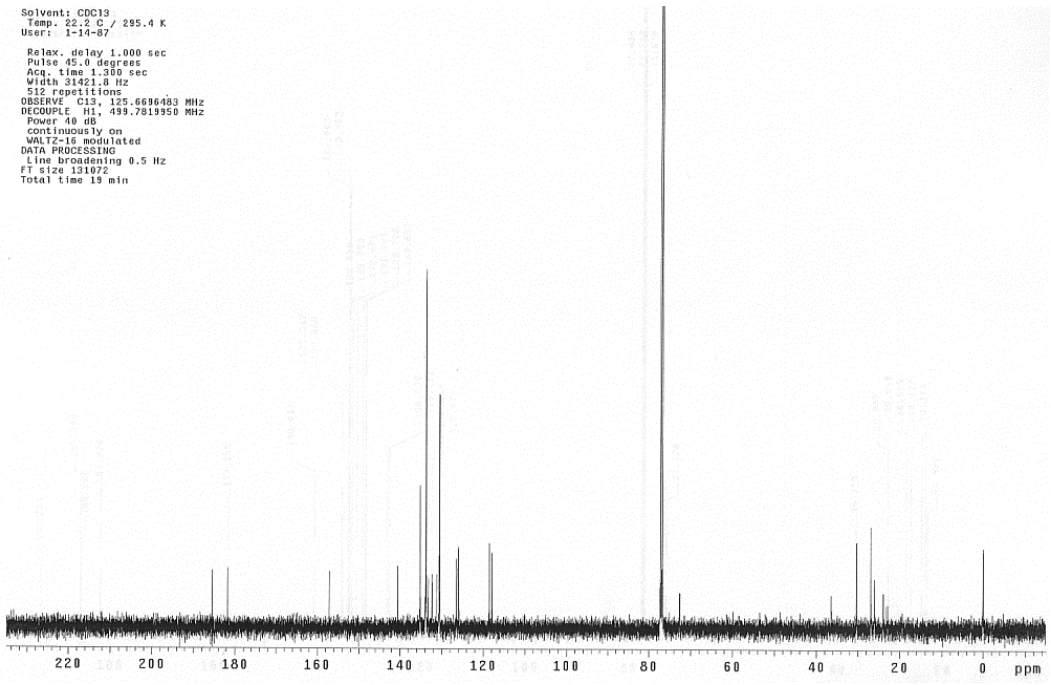

3-(2-Oxynaphthalene-1,4-dione)propyl triphenylphosphonium bromide (32b)

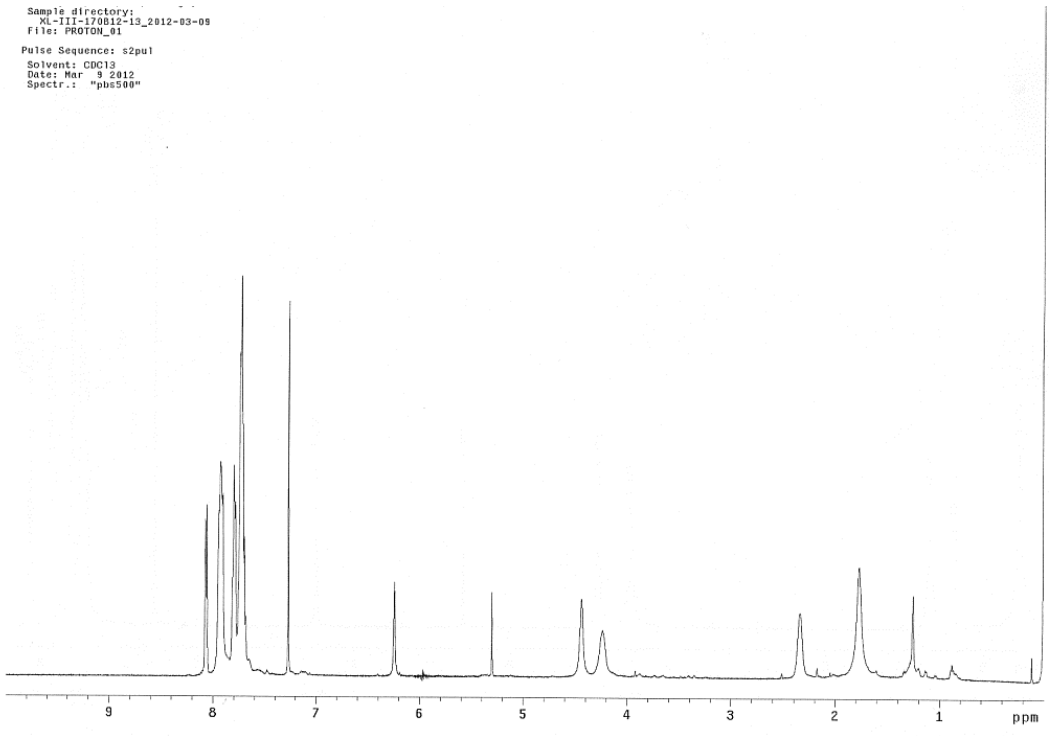

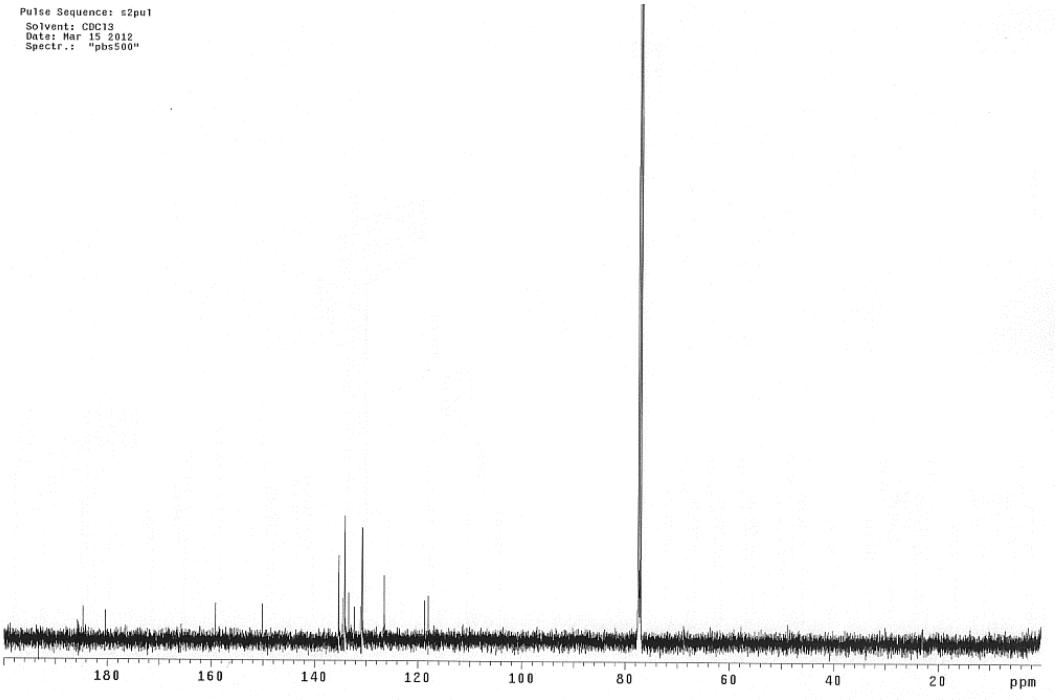

6-(2-Oxynaphthalene-1,4-dione)hexyl triphenylphosphonium bromide (32a)

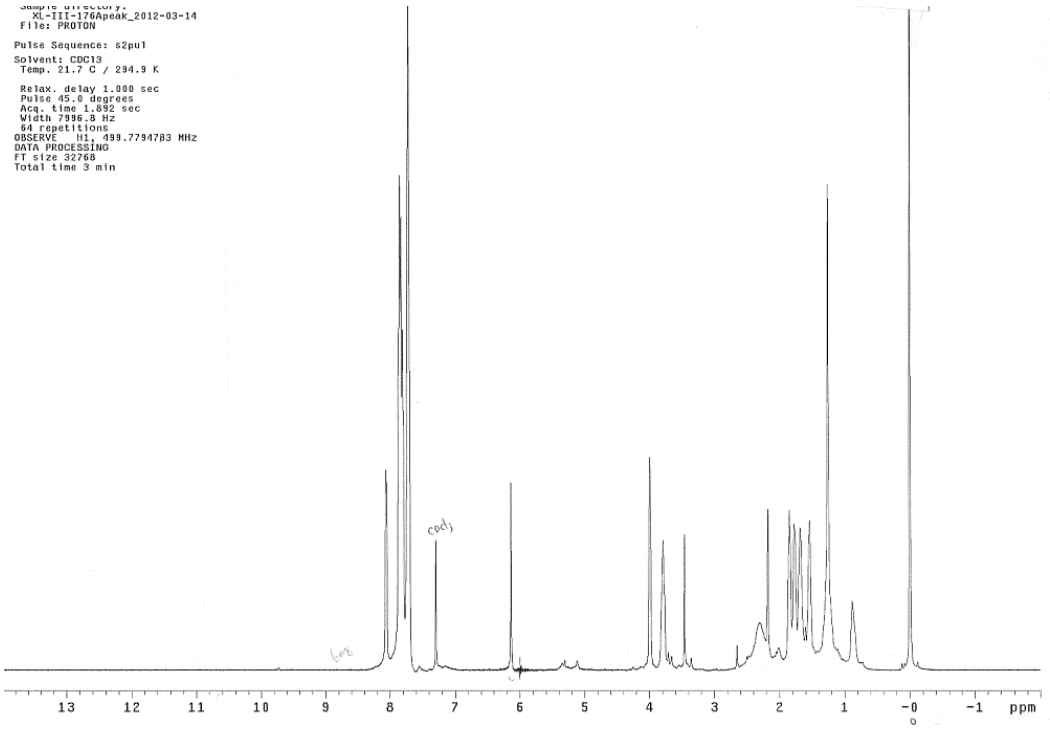

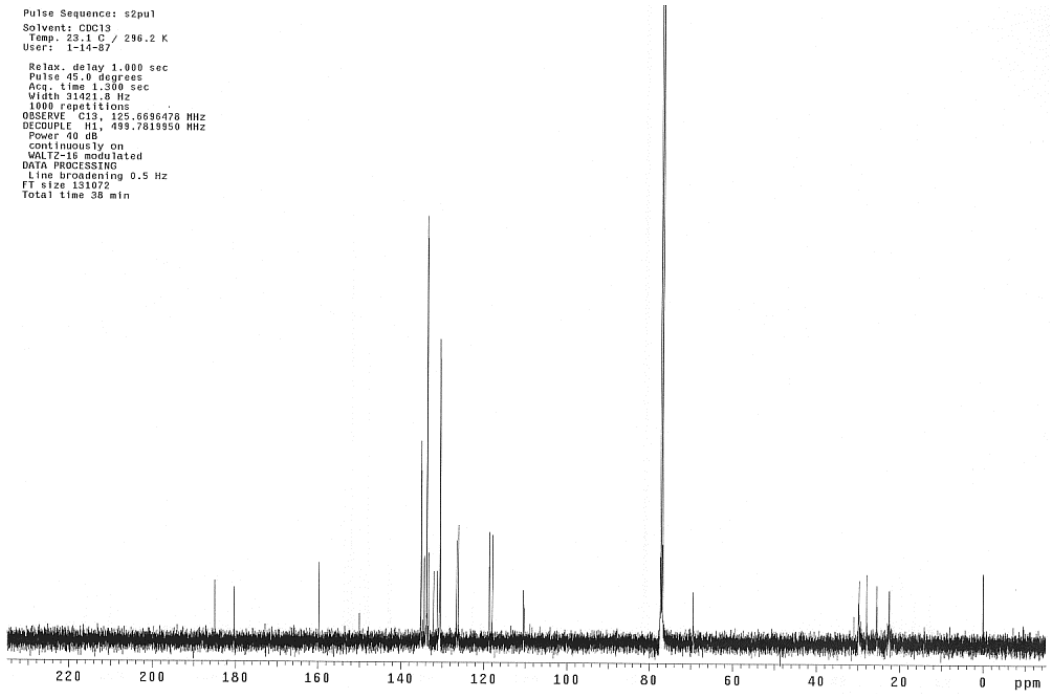

3-(2-Oxy-3-(4-methoxyphenyl)naphthalene-1,4-dione)propyl triphenylphosphonium bromide (47)

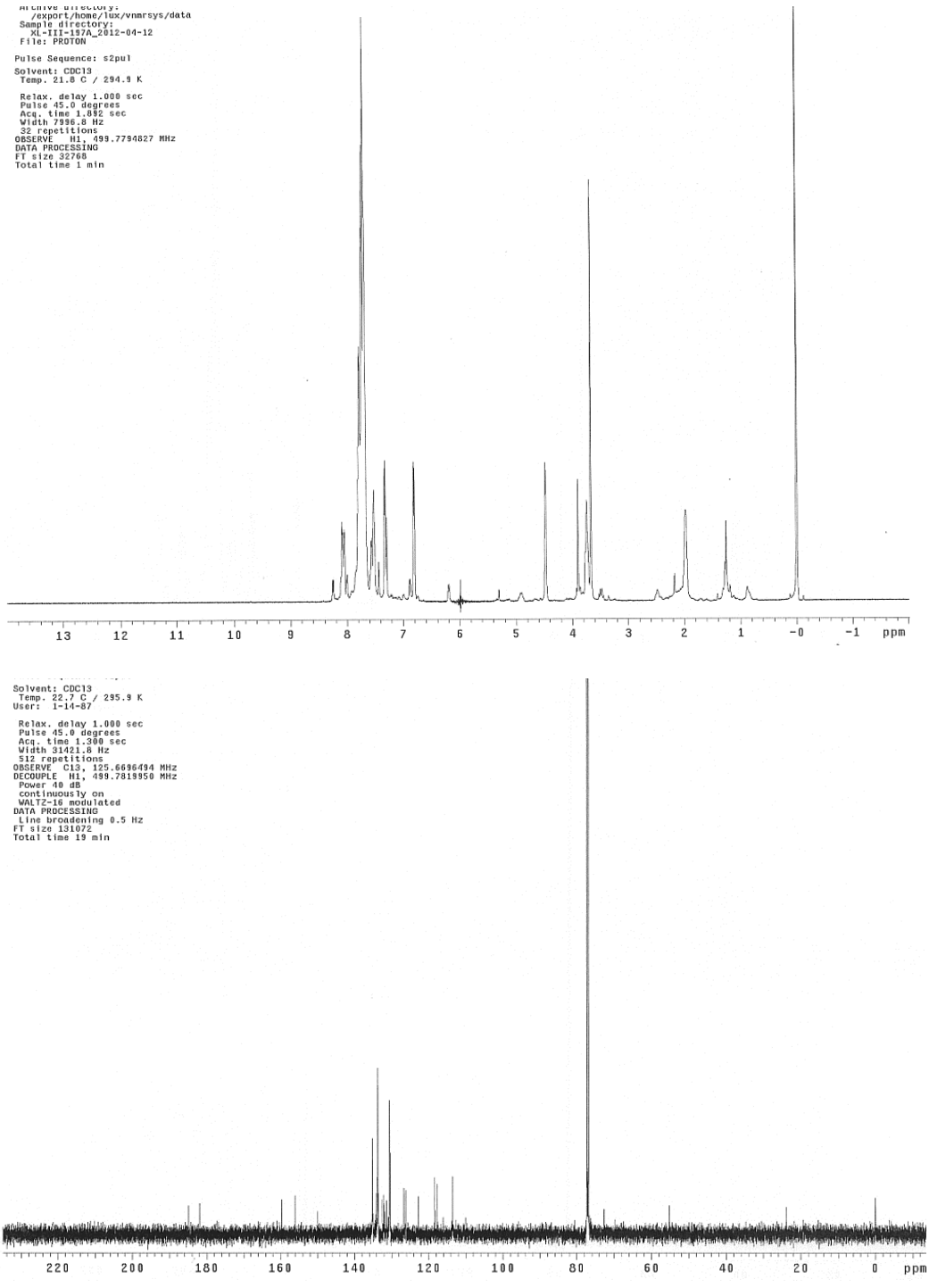

APPENDIX D

Hemolysis determination

Step 1. Preparation of red blood cell (RBC) suspension.

Whole blood (purchased, 10 ml per testing tube, keep at 4 ºC) was washed with phosphate buffered saline (PBS, pH 7.4) solution and centrifuged (2,500 rpm, 10 min at room temperature), and the supernatant was discarded. Repeated this until the supernatant was colorless. RBCs were then resuspended in PBS solution and used within 48 h (for example, as shown in the figure, 10 x 10^9 in 10 ml).

Step 2.1 Preparation of Stock Solution (10 µM).

(see graphed procedure two page later)

Step 2.2 Preparation of Test Solution with different concentrations.

(see graphed procedure two page later)

Step 3. Test/ Measurement.

RBCs (around 0.5 x 10^8 per testing tube) were incubated with increasing concentrations (12.5 µM and 25.0 µM, final concentrations) of tested compounds, previously dissolved in the minimum required quantity of DMSO or MeOH (to a final organic solvent concentration of 0.5 %), for 1 h at 37 ºC.

Step 4. Calculation/Analysis:

Hemolysis was determined by spectrophotometric measurements at 540 nm. The percentage of hemolysis of human RBC was determined by the formula

$$\% \text{ hemolysis} = \frac{(C-B)-(A-B)}{(C-B)} \times 100$$

in which A = hemolysis of the sample;

B = 100 % hemolysis = RBCs with 0.1 % (wt/vol) Triton X-100;

C = 0 % hemolysis = RBCs with PBS solution.

The assays were carried out in triplicate.

Graphed procedure (Hemolytic toxicity)

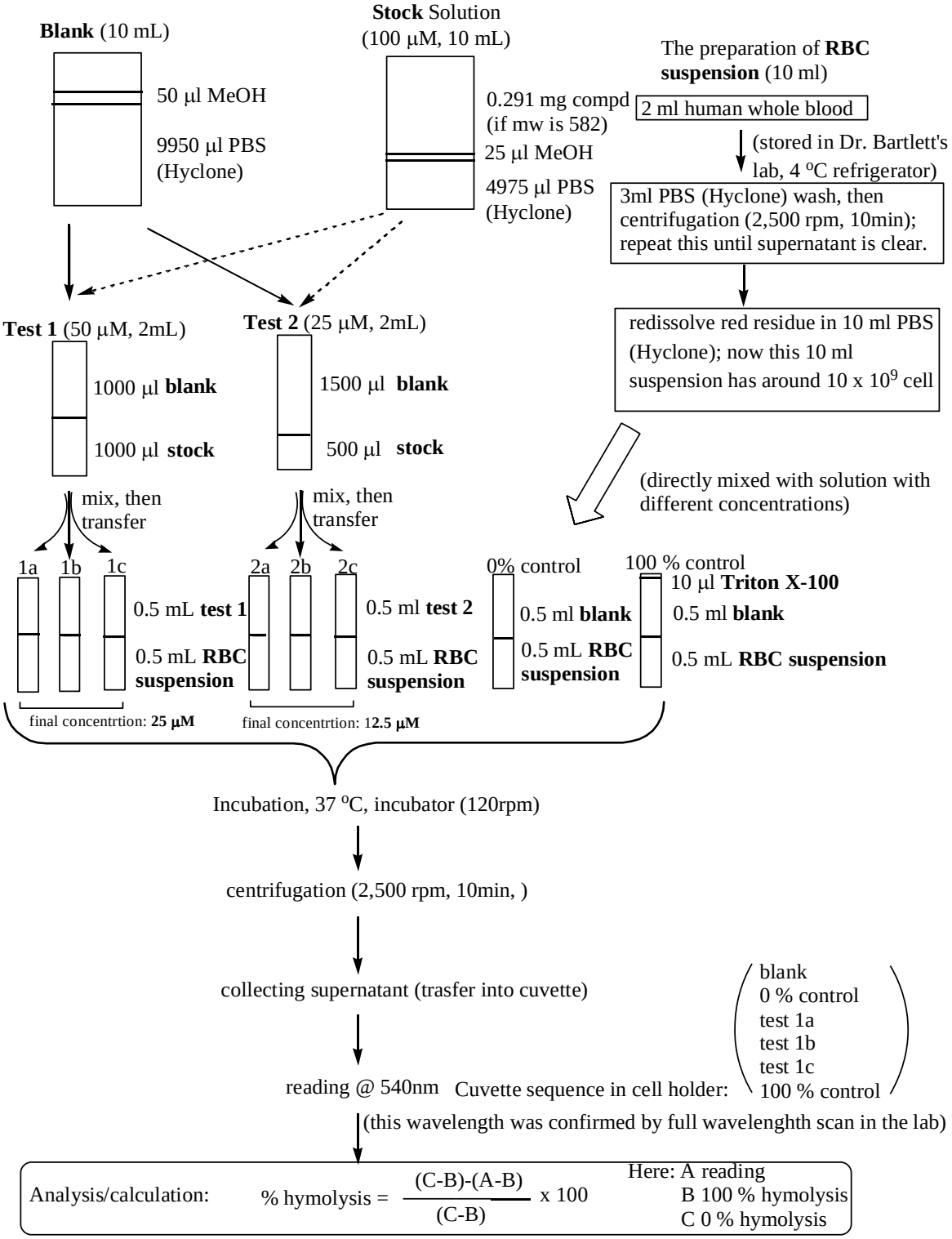

P.S. MeOH can be changed to DMSO if the test compound has bad solubility.

APPENDIX E

Partition coefficient determination

The Log $D_{pH7.4}$ of compounds were determined in octanol-buffer system by shaking flask method at 25 ºC.

Step 1. Preparation:

a. Clean and thoroughly rinse the flask with distilled water and methanol.

b. Prepare 1 ml of stock solution in 1-octanol (around 0.05 mg/ml).

c. 500 µl of the stock solution was mixed with exactly equal volume of phosphate buffer solution (500 µl, pH 7.4), vortex for 1 min.

d. The organic layer was then centrifuged at 5,000 rpm at 25 ºC for 5 min.

e. Repeat step b-d two times.

Step 2. Measurement:

a. The concentration of the organic layer and the stock solution were analyzed by a UV-Visible light spectrophotometer.

b. Here the proper wavelength of each compound (based on the π to π* transition of aromatic systems and the resulting maximum wavelength are: 274 nm for the triphenylphosphine group and 240 nm for the 1,3-dioxoisoindolin-2-yl unit) was determined by full wavelength scan.

c. After determining the wavelength, the fixed wavelength scan was performed.

d. Each value (reading) was also repeated in triplicate. Cuvette sequence in cell holder: (**octanol** for blanking)/(**stock octanol** solution)/(**octanol solution after shaking**/mixing)

Step 3. Analysis:

The Log *D* value was then calculated by the logarithm of the ratio of concentrations of deionized solute in 1-octanol to aqueous solution.

$$\text{Log } D \text{ oct/water} = \log \left(\frac{1}{\frac{[\text{solute}]\text{stock}}{[\text{solute}]\text{octanol}} - 1} \right)$$